



**HAL**  
open science

# Transfert d'hydrogène asymétrique catalysé par des métaux de transition : synthèse énantiosélective d'hétérocycles et de $\alpha$ -méthoxy $\beta$ -hydroxy esters

Bin He

► **To cite this version:**

Bin He. Transfert d'hydrogène asymétrique catalysé par des métaux de transition : synthèse énantiosélective d'hétérocycles et de  $\alpha$ -méthoxy  $\beta$ -hydroxy esters. Autre. Université Paris sciences et lettres, 2020. Français. NNT : 2020UPSLC005 . tel-03261579

**HAL Id: tel-03261579**

**<https://pastel.hal.science/tel-03261579>**

Submitted on 15 Jun 2021

**HAL** is a multi-disciplinary open access archive for the deposit and dissemination of scientific research documents, whether they are published or not. The documents may come from teaching and research institutions in France or abroad, or from public or private research centers.

L'archive ouverte pluridisciplinaire **HAL**, est destinée au dépôt et à la diffusion de documents scientifiques de niveau recherche, publiés ou non, émanant des établissements d'enseignement et de recherche français ou étrangers, des laboratoires publics ou privés.

**THÈSE DE DOCTORAT**  
**DE L'UNIVERSITÉ PSL**

Préparée à Chimie ParisTech

**Transition-metal catalyzed asymmetric transfer  
hydrogenation: enantioselective synthesis of  
heterocycles and  $\alpha$ -methoxy  $\beta$ -hydroxy esters**

Soutenue par

**Bin HE**

Le 16 Octobre 2020

Ecole doctorale n° 406

**Chimie moléculaire Paris  
Centre**

Spécialité

**Chimie Moléculaire**

Composition du jury :

Emmanuelle, SCHULZ DR, Université Paris-Sud	<i>Président</i>
Catherine, GUILLOU DR, Université de Paris-Saclay	<i>Rapporteur</i>
Thomas, POISSON Prof., INSA de Rouen	<i>Rapporteur</i>
Amandine, GUÉRINOT MdC, ESPCI Paris	<i>Examineur</i>
Phannarath, PHANSAVATH MdC, Chimie ParisTech	<i>Co-directeur de thèse</i>
Virginie, VIDAL DR, Chimie ParisTech	<i>Directeur de thèse</i>







*Dedicated to my beloved parents and my wife*



*“First they ignore you.  
Then they ridicule you.  
And then they attack you  
and want to burn you.  
And then they build monuments to you.”*

*—Nicholas Klein*



# Acknowledgements

This thesis was conducted at Chimie ParisTech - PSL University, at the Institute of Chemistry for Life and Health Science (i-CLeHS) in the team Catalysis, Synthesis of Biomolecules and Sustainable Development led by Dr Virginie Vidal, under the supervision of Dr Virginie VIDAL, CNRS Research Director and Dr Phannarath PHANSAVATH, Associate Professor.

My sincere thanks to Dr **Catherine GUILLOU**, CNRS Research Director at the Institut de Chimie des Substances Naturelles (ICSN), and Prof. **Thomas POISSON** at the INSA Rouen, for having accepted to be rapporteurs for my thesis. I also thank Dr **Amandine GUÉRINOT**, Associate Professor at ESCPI Paris and Dr. **Emmanuelle SCHULZ**, CNRS Research Director at the Université Paris-Saclay for having taken the time to examine this thesis work.

I appreciated and cherished this PhD career so much given by my two dear supervisors **Virginie** and **Pocki**. They afforded me the chance to do my PhD in Paris such a beautiful city that I yearned for since my childhood. They afforded me the chance to study in this prestigious and the No.1 university in France -- L'Université PSL (Paris Sciences & Lettres). They afforded me the chance to do chemistry in such a well equipped, safe and clean lab, in Chimie ParisTech – PSL. They led me into a whole new chemical field that I have never touched before – Asymmetric Transfer Hydrogenation, then they showed me the magical metal—Rh which I worked on in my whole three years of PhD. Thank them for providing all the good chemicals and analytical equipments I need. I still remember **Pocki** launched some reactions with me that I can't succeed by myself and she taught me how to use the polarimeter to measure the rotation value of my products. She is a good teacher, she knows how to make students accept new knowledge; she is a knowledgeable chemist as well, she did total synthesis before; she is a kind lady meanwhile, she helped me deal with many administrative documents especially on ADUM. Even if **Virginie** was busy, we still have a meeting about my work every week; she was always serious with students but she also played jokes with us and celebrated with us when we obtained good results. I still remembered the conversation when I got two publications, she said “you already have enough results for your PhD so you can rest at home for your left time of PhD”. Thanks to her serious attitude about chemical research work which guided me to fruitful results and taught me how to treat science honestly in my future research career. Another important thing I want to thank is her encouragement which really supported me to finish my PhD, the

sentence “you are the best” really make me cheer up when I felt tired or lost. As we recently met COVID-19, I had to finish my last project and thesis, Virginie and Pocki came to the lab every week to give me guidance, and once I finished lab work late, the institution must be closed, we had to discuss in the courtyard of the institution. PhD life is exhausting everywhere, but thanks to their accompany it became colourful. Words are not enough to express my feelings for them for three years’ PhD life. I just want to say that if God gives me another chance to choose, I will still choose to come to Paris and become again the student of **Virginie** and **Pocki**.

I would like to thank all the members of the laboratory that I have been able to meet during these three years. Thank **Fei YE** to introduce me to my supervisors. Then I want to thank **Longsheng ZHENG** who came to the airport to pick me up when I first arrived Paris. When I arrived in the lab, **Longsheng** helped me so much, he was a kind brother to me. In the lab, he taught me how to use HPLC, SFC and guided me how to synthesize the Rh complex. In life, he often invited me to share his dishes and took me to visit interesting sights of Paris. After one year, came two other Chinese friends—**Yantao WANG** and **Deyang ZHAO**. We had a happy time, I missed the time we always went to crous for lunch. Then **Yantao**’s wife came to Paris too, we had a barbecue in his house. **Longsheng** and **Yantao** finished their PhD and went back to China to continue academic research. I was happy for them but I also felt a bit lonely with **Deyang**. **Deyang** is my longest friend who has been with me for the longest time during the three years. He is also a nice brother to me, he has a good temper and make me feel very comfortable to talk with him. I can’t count how many times we went to restaurant or made home parties together, I neither can’t remember how many activities we played together. Anyway he became my closest friend.

Of course, I would like to thank all my French labmates as well. **Ayman SELMANI**, a doctor who is one year older than me, often played jokes with me and always helped me answer my phone calls which were spoken by French. He is a hard working guy with fruitful results as well. **Johanne LING**, PhD in the same class as me, as she can understand a little Chinese and just sit next to me, I often asked her help to translate some documents and she was always glad to help me. She became more talkative after drinking and we often talked about the different culture between China and France. **Anne WESTERMEYER**, PhD in the same class as me, she is a strong girl and high EQ girl, she always gave me sweet smile that made me feel warm. Ever since I watched her play the cello and paint, I have always thought she was an artist who was delayed by chemistry. She obtained good results during PhD, but I just thought she can get

more shining achievements if being an artist. And thanks for the last company during my PhD after the break out of COVID-19. **Ricardo MOLINA BETANCOURT** is a smart boy, a PhD two years younger than me, he likes drinking, smoking and “Sichuan” food. I enjoyed the time we went to drink and eat at Chinese restaurant. I wish him an interesting PhD life. I also want to thank **Maxime VITALE**, he is a humorous guy with knowledgeable chemistry, he is the supervisor of Johanne and also a friend to our students. He is generous in giving help, he helped me a lot about my computer problems and he also helped me purified one product once. I enjoyed the time we ate in “Burger King” and discussing academic problems during lunch time. I am glad to meet **Christine TRAN**, a post-doctoral, she is a nice and beautiful girl. Now, she became a lecturer in another university, I am happy for her and I hope she works successfully in the future. Thanks to **Sylvain DARSEES**, Aymane’s supervisor, a knowledgeable chemist, we didn’t talk a lot but I can feel his kindness to me. His magical laughter impressed me deeply. Thanks to **Mansour HADDAD** for helping me find chemicals. Thanks to **Frédéric EMENEGGER**, a kind technician working in my lab who gave me a French made knife. Thanks to **Franck GIRARD**, who always carried chemicals and reagents for our students silently, and handled some trivial matters. Thanks to **Tahar AYAD**, his humor gave me a lot of fun.

Besides, I was glad to meet the friends from other labs. I was glad to talk with **Lidie ROUSSEAU**, **Hugo FOUILLOUX**, **Nancy SOLIMAN**, **Pascal MATTON** and **Capucine MAHE**. And I also thank the CSC students in my institution, we often discussed CSC policy together.

I would like also to thank **Lise-Marie CHAMOREAU** and **Geoffrey GONTARD** for the X-ray analysis. Thanks to **Cécile FOSSE** for her incredible work in mass spectrometry. Thanks to **Cédric PRZYBYLSKI** for the HRMS analysis. I also want to thank my tutors of “Comité de suivi de thèse”, Dr. **Sylvain ROLAND** and Dr. **Virginie MANSUY**, for their comments and advices on my work during my PhD.

Many thanks to my friends **Sining LI** and **Wei CHEN** who helped and supported me in my daily life when I arrived in Villejuif in the beginning. They are my nice and beautiful neighbors, they helped me dealing with OFII, CAF and the documents for my wife’s Visa. Thanks for the beautiful gift for me and my wife. I miss the time when we had parties, barbecue, travelling and watching World Football Cup 2018. I hope Sining works well in Sichuan. Wei has her own career now, I really appreciate Wei’s strength and independence, I hope she can catch her goal

soon. I believe her language education company will become bigger and bigger. Special thanks when Wei called 15 and sent me to the hospital when I was heavily sick. I also thank very much **Hua QIAN** and **Rong**, they always offered me and my wife so much delicious food and took us to visit so many beautiful seaside cities—Deauville, Le Mont-Saint-Michel and Saint-Malo.

The last and the most important people are my family. I deeply thank my parents, thanks for their understanding and tolerance, without their solid backing, I can't continue what I want to do. Especially, I often felt guilty and sad for mum, you sacrificed so much for me, but I can't serve you when you were sick, I also know that you pretend to be happy so that I can work in Paris with peace of mind. No matter what, I can't make up for what I owe you. All I can do is go back home often and I hope I can have more time to accompany with you after I come back to China. I also deeply thank my wife and my mother in law, thank them for their support for my PhD study in Paris. Thanks to my lovely and beautiful wife who gave up her job and came to Paris to stay with me and take care of me. Thank you for doing all the boring house work for me. When you were in Paris, I can have hot dinner immediately when I arrived home after work; after dinner, we walked through the park until sunset. You like viewing natural scenery, then we visited almost all the forests in Paris and near Paris, we went to the beaches of Étretat, Deauville, Le Mont-Saint-Michel and Saint-Malo. We also had sweet memories in Disneyland, in the boat on the Seine river and Christmas market. Besides, we traveled to Germany, Netherlands, Luxembourg and Belgium as well which was a short and wonderful journey. Your company was like adding a spoonful of honey to my life in Paris. Thank you for appearing in my life, walking into my heart and I really cherish you.

Finally, I would like to give a special acknowledgement to China Scholarship Council for a three years' fellowship in Paris. Without the powerful financial support I can't live in Paris and I would like to go back to China for serving my country with my knowledge obtained in Paris.





## Table of Contents

<b>Abbreviation .....</b>	<b>5</b>
<b>R ésum é.....</b>	<b>10</b>
<b>General introduction.....</b>	<b>35</b>
<b>Part A: Recent Developments on Transition Metal-Catalyzed Asymmetric Transfer Hydrogenation (ATH) of Ketones.....</b>	<b>38</b>
<b>1. Theoretical background on asymmetric transfer hydrogenation.....</b>	<b>38</b>
1.1 Introduction to asymmetric transfer hydrogenation.....	38
1.1.1 Mechanisms .....	40
1.1.2 Ligands.....	42
1.1.3 Noyori's bifunctional catalysts .....	44
1.1.4 General mechanism .....	44
1.1.5 Origins of enantioselectivity.....	47
1.1.6 Other catalysts for asymmetric transfer hydrogenation .....	49
1.1.7 The various hydrogen sources .....	53
<b>2. Reaction scope: catalysts and chiral ligands.....</b>	<b>59</b>
2.1 Ruthenium catalysts.....	59
2.1.1 Aminoalcohols as ligands .....	59
2.1.2 Diamines as ligands .....	60
2.1.3 Phosphorus containing ligands .....	67
2.1.4 Sugar containing ligands .....	70
2.1.5 Sulfur containing ligands .....	72
2.1.6 Heterocyclic ligands.....	72
2.1.7 Other type of chiral Ru complexes.....	73
2.2 Tandem reactions using Ruthenium catalysts .....	74
2.3 ATH of functionalized ketone derivatives with Ruthenium catalysts .....	78
2.4 Rhodium catalysts .....	95
2.5 Iridium catalysts .....	98

2.6 Iron catalysts .....	105
2.7 Manganese catalysts .....	107
2.8 Osmium catalyst .....	110
<b>3. Applications in total synthesis .....</b>	<b>111</b>
<b>4. Immobilized catalysts.....</b>	<b>115</b>
<b>5. Conclusions .....</b>	<b>118</b>
<b>Part B: ATH of heterocyclic ketones .....</b>	<b>120</b>
<b>1. Rhodium-Catalyzed Asymmetric Transfer Hydrogenation of 4-Quinolone Derivatives .....</b>	<b>120</b>
1.1 Introduction.....	120
1.1.1 Biological interest of enantiopure tetrahydroquinolin-4-ols derivatives .....	120
1.1.2 Different synthetic pathways for enantiopure tetrahydroquinolin - 4-ols...	121
1.2 Results and discussion.....	124
1.2.1 Synthesis of ( <i>R,R</i> ) and ( <i>S,S</i> )-enantiomers of rhodium complex C86 .....	124
1.2.2 Synthesis of aryl <i>tert</i> -butyl 4-oxoquinoline-1(4H)-carboxylates.....	125
1.2.3 Optimisation of the reaction conditions .....	126
1.2.4 Substrate scope .....	131
1.2.5 Determination of the absolute configuration .....	133
1.2.6 Scale up experiment.....	134
1.2.7 Post-functionalization .....	134
1.2.8 Synthesis of ( <i>S</i> )- <i>tert</i> -butyl4-hydroxy-3,4-dihydroquinoline-1(2H)- carboxylate .....	135
1.2.9 Mechanism .....	136
1.2.10 Origin of enantioselectivity .....	137
1.3 Conclusion .....	137
<b>2. Rhodium-Catalyzed Asymmetric Transfer Hydrogenation of 2-aryl-2,3-dihydroquinolin-4(1H)-one Derivatives .....</b>	<b>139</b>
2.1 Introduction.....	139
2.2 Results and discussion.....	140

2.2.1 Synthesis of 2-aryl-2,3-dihydroquinolin-4(1H)-ones.....	140
2.2.2 Optimisation of the reaction conditions with 2-phenyl-2,3-dihydroquinolin-4(1H)-one.....	141
2.2.3 Synthesis of 1-acetyl-2-aryl-2,3-dihydroquinolin-4(1H)-one derivatives .....	143
2.2.4 Optimisation of the reaction conditions with 1-acetyl-2-phenyl-2,3-dihydroquinolin-4(1H)-one.....	144
2.2.5 Kinetic experiment .....	146
2.2.6 Substrate scope .....	148
2.2.7 Kinetic resolution selectivity factor .....	152
2.2.8 Scale-up experiment .....	153
2.3 Conclusion .....	153
<b>3. Rh-Mediated Asymmetric Transfer Hydrogenation of 3-Substituted Chromones: an Efficient Route to Enantioenriched cis 3-Hydroxymethyl Chroman-4-ol Derivatives through Dynamic Kinetic Resolution .....</b>	<b>155</b>
3.1 Introduction.....	155
3.1.1 Biological interest of chromanoid and flavanoid derivatives .....	155
3.1.2 Different synthetic pathways to enantiomerically enriched chromanols and flavanols .....	156
3.2 Results and discussion.....	162
3.2.1 Synthesis of 3-substituted chromones.....	162
3.2.2 Optimisation of the reaction conditions .....	163
3.2.3 Kinetic experiment .....	168
3.2.4 Dynamic kinetic experiment .....	169
3.2.5 Substrate scope .....	170
3.2.6 Determination of the absolute configuration.....	172
3.2.7 Scale up experiment.....	173
3.2.8 Post-functionalization .....	173
3.2.9 Origin of the enantio- and diastereoselectivities.....	174
3.3 conclusion.....	175
<b>Part C: ATH of <math>\alpha</math>-methoxy <math>\beta</math>-ketoesters via dynamic kinetic resolution.....</b>	<b>176</b>

<b>1. Rh(III)-Catalyzed Asymmetric Transfer Hydrogenation of <math>\alpha</math>-Methoxy <math>\beta</math>-Ketoesters through DKR in 2-MeTHF and Water: Toward a Greener Procedure.....</b>	<b>176</b>
1.1 Introduction.....	176
1.1.1 Biological interest of 1,2- diol derivatives.....	176
1.1.2 Different synthetic pathways for 1,2-diol derivatives .....	177
1.2 Results and discussion.....	179
1.2.1 Synthesis of aryl $\alpha$ -methoxy $\beta$ -keto esters.....	179
1.2.2 Synthesis of a new Rh(III)-TsDPEN-based tethered complex.....	182
1.2.3 Optimisation of the reaction conditions.....	183
1.2.4 Substrate scope in 2-MeTHF .....	187
1.2.5 Optimisation of the reaction conditions in water.....	190
1.2.6 Substrate scope in water.....	192
1.2.7 Mechanism .....	195
1.2.8 Origin of enantioselectivity and diastereoselectivity.....	196
1.3 Conclusion .....	197
<b>General conclusion .....</b>	<b>198</b>
<b>Experimental part .....</b>	<b>201</b>
<b>1. General informations .....</b>	<b>201</b>
1.1 Purification of solvents and reagents.....	201
1.2 Chromatography .....	201
1.3 Analysis.....	201
<b>2. Description of the synthesized products.....</b>	<b>202</b>
2.1 Index of the synthesized products .....	202
2.2 Description of the synthesis processes and detailed data.....	225

## Abbreviation

	Ac	Acetate
	AIBN	2,2'-Azobis(2-methylpropionitrile)
	ALK	Anaplastic lymphoma kinase
<b>A</b>	Ar	Aromatic
	ATH	Asymmetric transfer hydrogenation
	atm	Atmosphere
	[ $\alpha$ ]	Specific rotation
	$\beta$ -LG	Beta-lactoglobulin
	BMS	Bristol-Myers Squibb
<b>B</b>	Bn	Benzyl
	Boc	<i>Tert</i> -butoxycarbonyl
	Bu	Butyl
	Bz	Benzoyl
	Cat.	Catalyst
	Cbz	Carboxybenzyl
	°C	Celsius degree
	CDC	Cross-dehydrogenative coupling
<b>C</b>	CDI	1,1'-Carbonyldiimidazole
	CIL	Chiral ionic liquids
	Cod	Cycloocta-1,5-diene
	Cp	Cyclopentadienyl
	Cp*	Pentamethylcyclopentadienyl
	Cy	Cyclohexyl
	DABCO	1,4-Diazabicyclo[2.2.2]octane
	DCC	Dicyclohexylcarbodiimide
<b>D</b>	DCD	D édoublement cin étique dynamique
	DCE	1,2-Dichloroethane
	DDQ	2,3-Dichloro-5,6-dicyano- <i>p</i> -benzoquinone
	de	Diastereomeric excess

	DHPD	5,6-Dihydrophenanthridine
	DIPA	Diisopropylamine
	DKR	Dynamic kinetic resolution
	DMAP	4-Dimethylaminopyridine
	DMAPA	Dimethyl aminopropyl acrylamide
	DMC	Dimethylcarbonate
	DMF	<i>N,N</i> -Dimethylformamide
	DMP	Dess-Martin periodinane
	DMSO	Dimethyl sulfoxide
	DPEN	1,2-Diphenylethylenediamine
	dr	Diastereomeric ratio
	DIODMA	<i>N</i> <sup>4</sup> , <i>N</i> <sup>4</sup> , <i>N</i> <sup>5</sup> , <i>N</i> <sup>5</sup> ,2,2-hexamethyl-4,5-bis-(aminomethylene)-1,3-dioxolane
	δ	Chemical shift
	ee	Enantiomeric excess
<b>E</b>	equiv	Equivalent
	Et	Ethyl
<b>F</b>	FDA	US Food and Drugs Administration
	g	Gramme
<b>G</b>	gem	Geminal
	GPR	G-protein coupled receptor
	h	Hour
	IBX	2-Iodobenzoic acid
	HIV	Human immunodeficiency virus
<b>H</b>	HMDS	Hexamethyldisilazane
	HMSN	Hollow mesoporous silica nanospheres
	HPLC	High performance liquid chromatography
	HRMS	High resolution mass spectra
<b>I</b>	IC <sub>50</sub>	Half maximal inhibitory concentration

	<i>i</i> Bu	<i>Iso</i> -butyl
	<i>i</i> Pr	<i>Iso</i> -propyl
	IPA	<i>Iso</i> -Propanol
	IR	Infrared radiation
	IUPAC	International Union of Pure and Applied Chemistry
<b>K</b>	k	Rate constant
	KR	Kinetic resolution
	L*	Chiral ligand
<b>L</b>	LDA	Lithium diisopropylamide
	Lit.	Literature
	MW	Molecular weight
	MCM	Mobil composition of matter
	Me	Methyl
<b>M</b>	2-MeTHF	2-Methyltetrahydrofuran
	min	Minute
	MMP	Macromolecular polymers
	m.p.	Melting point
	Ms	Methylsulfonyl
	NMDA	<i>N</i> -methyl-D-aspartate
	NMR	Nuclear magnetic resonance
	<i>J</i> : coupling constant	
	<i>s</i> : singulet	
	<i>d</i> : doublet	
	<i>t</i> : triplet	
	<i>q</i> : quadruplet	
	<i>quint</i> = quintuplet,	
	<i>sext</i> = sextuplet,	
	<i>hept</i> = heptuplet,	



	<i>m</i> :	multiplet
	<i>br</i> :	broad
	NADH	Dihyronicotinamide adenine dinucleotide
	NADPH	Dihyronicotinamide-adenine dinucleotide phosphate
	Pd/C	Palladium on activated charcoal
	PEG	Polyethylene glycol
	Ph	Phenyl
	pH	Hydrogen ion concentration
<b>P</b>	PHOX	Phosphinooxazolines
	P*P	Chiral diphosphine
	ppm	Parts per million
	Pr	Propyl
	P <sub>R</sub> , P <sub>S</sub>	Product enantiomers
	PTSA	<i>para</i> -Toluenesulfonic acid
<b>Q</b>	Quant.	Quantitative
	rt	Room temperature
<b>R</b>	R <sub>f</sub>	Retention factor
	rac	Racemic
	ROS1	a receptor tyrosine kinase
	SFC	Supercritical Fluid Chromatography
<b>S</b>	SpiroPAP	Spiro pyridine aminophosphine
	Synphos	6,6'-Bis(diphenylphosphino)-2,2',3,3'-tetrahydro-5,5'-Bibenzo[b][1,4]dioxine
	S <sub>R</sub> , S <sub>S</sub>	Substrate enantiomers
	T	Temperature
<b>T</b>	t	Time
	TAPS	Tetraarylphosphonium salts
	TBS	<i>tert</i> -Butyldimethylsilyl

TCCA	Trichloroisocyanuric acids
<i>t</i> Bu	<i>tert</i> -Butyl
TEOS	Tetraethoxysilane
Tf	Triflate
TH	Transfer hydrogenation
THA	Transfert d'hydrogène asymétrique
THF	Tetrahydrofuran
THIQ	Tetrahydroisoquinoline
TLC	Thin layer chromatography
TMS	Trimethylsilyl
TIPS	Triisopropylsilyl
TOF	Turnover frequency
Ts	Toluenesulfonyl
<i>t<sub>R</sub></i>	Retention time
<b>U</b> UV	Ultraviolet
<b>V</b> VMAT-2	Vesicular monoamine transporter type 2
VCD	Vibrational Circular Dichroism
<b>W</b> wt%	Percentage by weight



# RÉSUMÉ

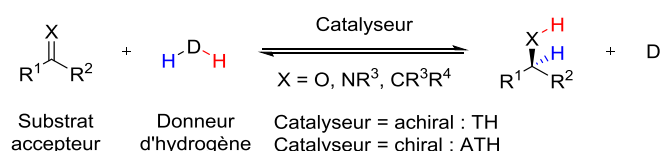




## Résumé

### Partie A: Développements récents sur le transfert d'hydrogène asymétrique de cétones catalysé par des métaux de transition.

Ce chapitre présente un rappel sur le transfert d'hydrogène asymétrique (THA) de composés insaturés catalysé par des complexes de métaux de transition (Schéma 1).



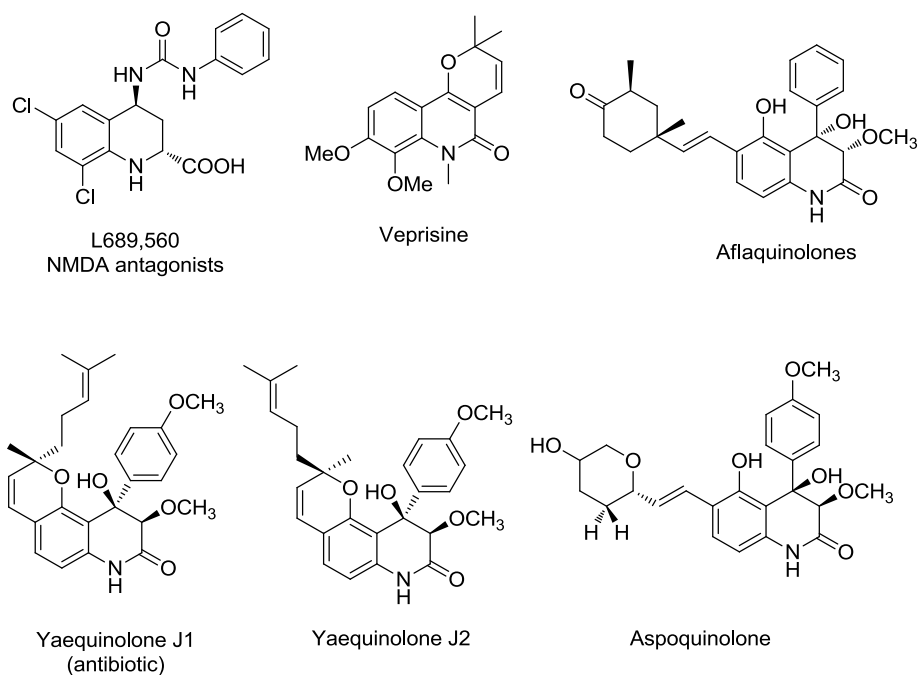
### Schéma 1

Les différents complexes utilisés dans ce type de réactions sont présentés, ainsi que les différentes sources d'hydrogène et le mécanisme général est discuté. De nombreux exemples de réactions de transfert d'hydrogène asymétrique de cétones illustrent cette partie.

### Partie B: Transfert d'hydrogène asymétrique d'(hétéro)arylcétones

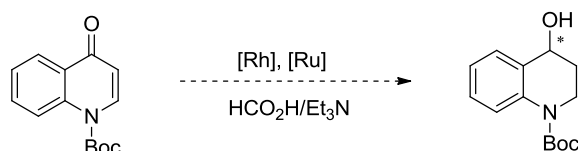
#### 1. Transfert d'hydrogène asymétrique d'(hétéro)arylcétones catalysé par des complexes de rhodium.

Les alcools benzyliques chiraux et leurs dérivés sont des motifs importants pour la synthèse de produits chimiques, pharmaceutiques et agrochimiques, car le groupement hydroxyle peut être facilement fonctionnalisé pour accéder à des intermédiaires polyvalents (Figure 1). Par conséquent, des efforts considérables ont été déployés pour développer des procédés stéréosélectifs efficaces et économes en atomes pour obtenir ces composés. Parmi ces derniers, les dérivés tétrahydroquinolin-4-ols énantio-purs constituent une cible attrayante en raison de leurs activités biologiques prometteuses et de leur utilisation à grande échelle comme intermédiaires synthétiques pour des candidats médicaments.



**Figure 1**

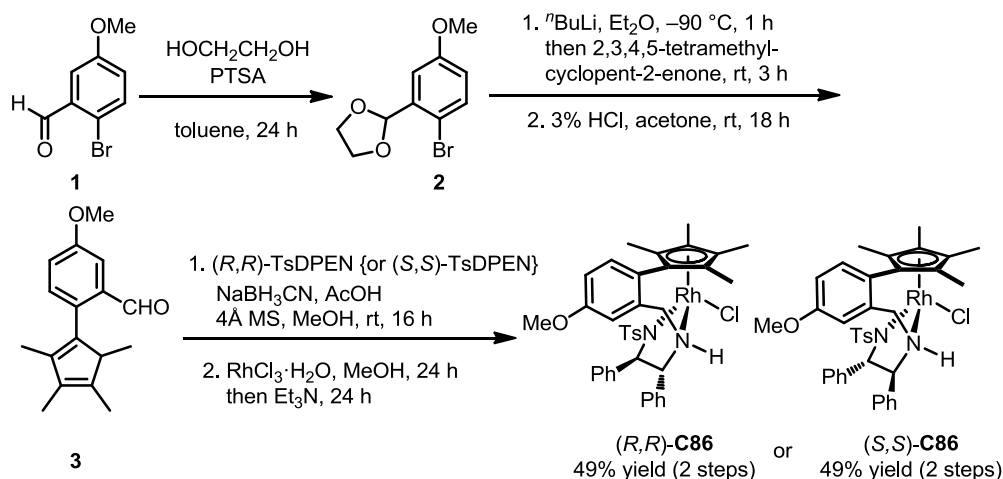
Il existe peu de méthodologies pour accéder aux dérivés tétrahydroquinolin-4-ols énantiomériquement enrichis mettant en jeu la réduction de cétones. En ce qui concerne le transfert d'hydrogène asymétrique (THA) du 1(4H)-*tert*-butyl carboxylate de 4-oxoquinoline, aucun exemple n'a été rapporté à notre connaissance. Notre projet s'est donc centré sur la réduction asymétrique conjuguée des liaisons C=C et C=O du motif quinolone (Schéma 2).



**Schéma 2**

Pour cette étude, nous avons préparé les deux énantiomères du complexe de rhodium **C86** en utilisant la procédure précédemment développée dans notre groupe. Les complexes diastéreo- et énantiomériquement purs (*R,R*)-**C86** et (*S,S*)-**C86** ont été isolés après chromatographie éclair sous forme de solides orange (Schéma 3).





## Schéma 3

Pour cette étude, différents substrats dérivés du 1(4H)-*tert*-butyl carboxylate de 4-oxoquinoline ont été préparés en une étape selon une procédure écrite. Ainsi, en présence de dicarbonate de di-*tert*-butyle, de triéthylamine et de DMAP, des dérivés de 4-quinolinol diversement substitués ont été convertis en précurseurs **4a-m** pour la réaction de transfert d'hydrogène asymétrique (THA) avec des rendements isolés de 50 à 84% (Figure 2).

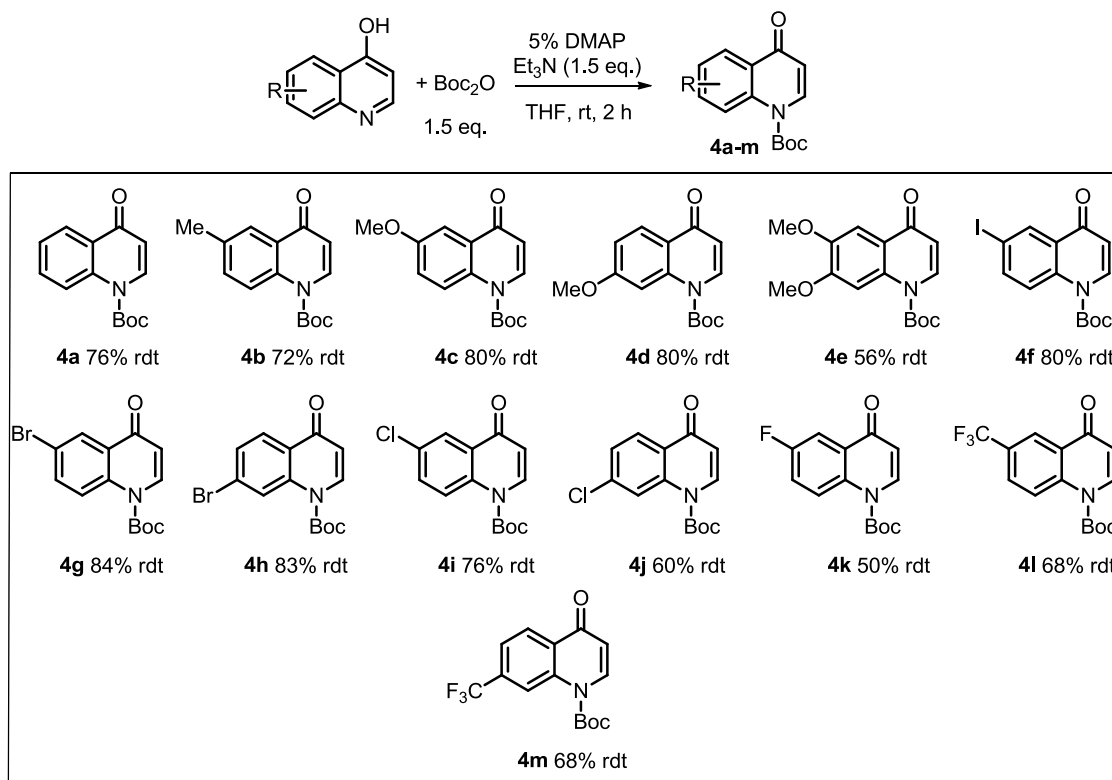


Figure 2

Le 1(4H)-*tert*-butyl carboxylate de 4-oxoquinoline **4a** a été choisi comme substrat modèle pour l'étude des différents paramètres (tels que la température, le solvant, la concentration, la source d'hydrogène, la charge catalytique) de la réaction de transfert d'hydrogène asymétrique en utilisant des complexes de rhodium et de ruthénium. Les

conditions optimales retenues sont: **C86** (1.0 mol %) comme pré-catalyseur, HCO<sub>2</sub>H/Et<sub>3</sub>N (5:2) (4.0 éq.) comme source d'hydrogène, dans le dichlorométhane (1.0 M) à 30 °C.

**Tableau 1.** Optimisation des conditions de réaction du THA de **4a**<sup>a</sup>

**C86**

**C87**

**C88**

**C89**

**C2**

Entrée	Catalyseur	Solvant	Rendement <sup>[b]</sup> (%)	ee <sup>[c]</sup> (%)
1	<b>C86</b>	CH <sub>2</sub> Cl <sub>2</sub>	83	>99
2	<b>C87</b>	CH <sub>2</sub> Cl <sub>2</sub>	76	>99
3	<b>C88</b>	CH <sub>2</sub> Cl <sub>2</sub>	67	>99
4	<b>C89</b>	CH <sub>2</sub> Cl <sub>2</sub>	41	>99
5	<b>C2</b>	CH <sub>2</sub> Cl <sub>2</sub>	--	--
6	<b>C86</b>	toluene	67	>99
7	<b>C86</b>	Et <sub>2</sub> O	63	>99
8	<b>C86</b>	THF	59	>99
9	<b>C86</b>	CH <sub>3</sub> CN	64	>99
10	<b>C86</b>	DMF	22	>99
11	<b>C86</b>	Me-THF	36	>99
12	<b>C86</b>	DMC	63	>99
13	<b>C86</b>	TBME	69	>99

<sup>a</sup> Conditions de réaction: **4a** (0.5 mmol), catalyseur (1.0 mol%), HCO<sub>2</sub>H/Et<sub>3</sub>N (5:2) (170 μL, 4.0 equiv), Solvant (0.5 mL), 30 °C. <sup>b</sup> Rendement isolé. <sup>c</sup> Déterminé par analyse SFC.

Avec ces conditions optimisées, nous avons ensuite étudié l'étendue de la réaction avec une série de composés **4b-m** (Figure 3). Le THA des composés **4b-d** ayant des groupes électrodonneurs sur le cycle aromatique conduit à une excellente énantioselectivité (>99% ee) avec des rendements de 50-79%, tandis que le produit **5e** présentant deux groupements méthoxy a été isolé avec un rendement de 23%. Pour les substrats **4f-m** portant des groupements électroattracteurs tels que des atomes de brome, iode, chlore, fluor ou un groupement trifluorométhyle, la réaction conduit à d'excellentes énantioinductions (jusqu'à >99% ee) et des rendements de 64-73%. La configuration absolue de l'alcool **5f** a été attribuée sans ambiguïté comme étant (*R*) par analyse cristallographique par diffraction des rayons X. Par analogie, nous supposons que les autres produits réduits suivent la même tendance.

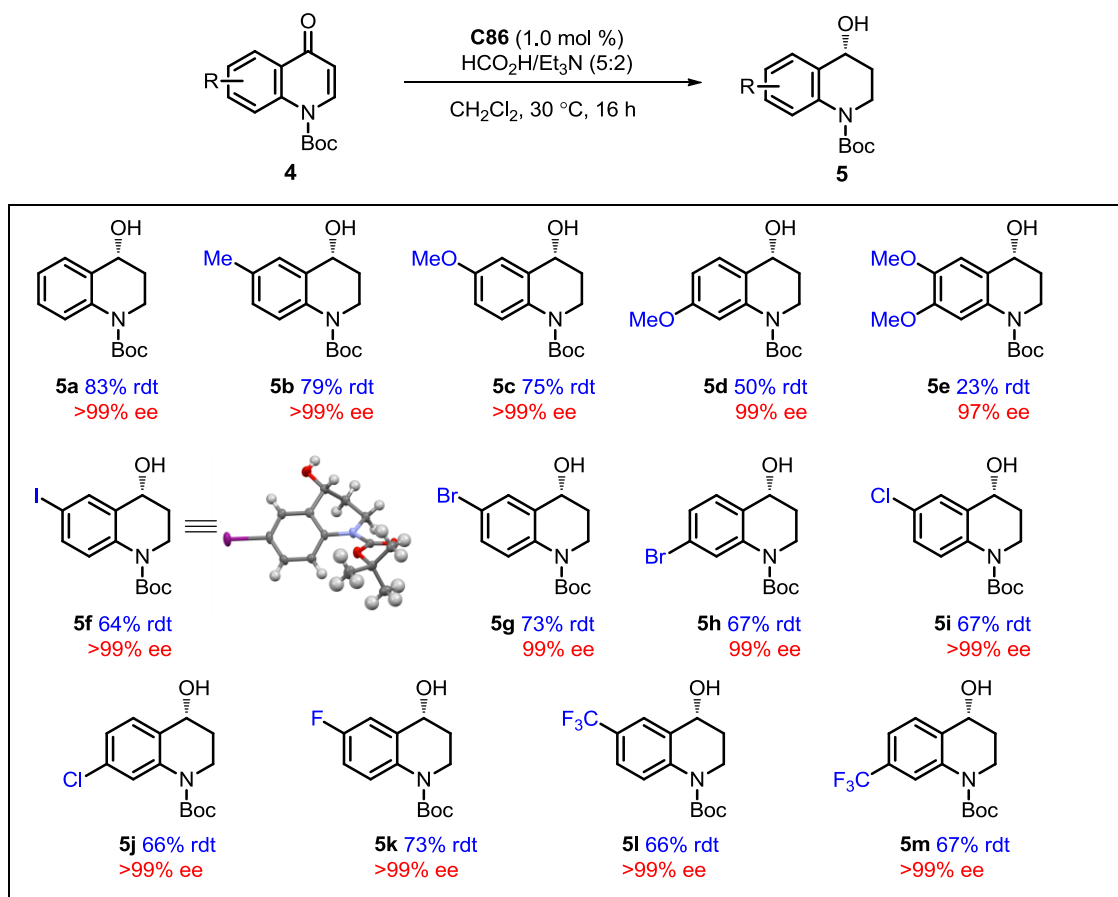


Figure 3

Une montée en échelle réalisée sur le composé **4a** (1.1 g, 4.5 mmol) conduit aux mêmes rendement et ee que sur une échelle de 0.5 mmol (81%, >99% ee), montrant l'efficacité de la réaction. Par ailleurs, l'alcool (*S*)-**5a'** a été préparé en utilisant le complexe énantiomère (*S,S*)-**C86** au lieu de l'isomère (*R,R*)-**C86** et le composé (*S*)-**5a'** a été obtenu avec un rendement et une énantiosélectivité comparables à ceux observés pour l'alcool (*R*)-**5a** (Schéma 4).

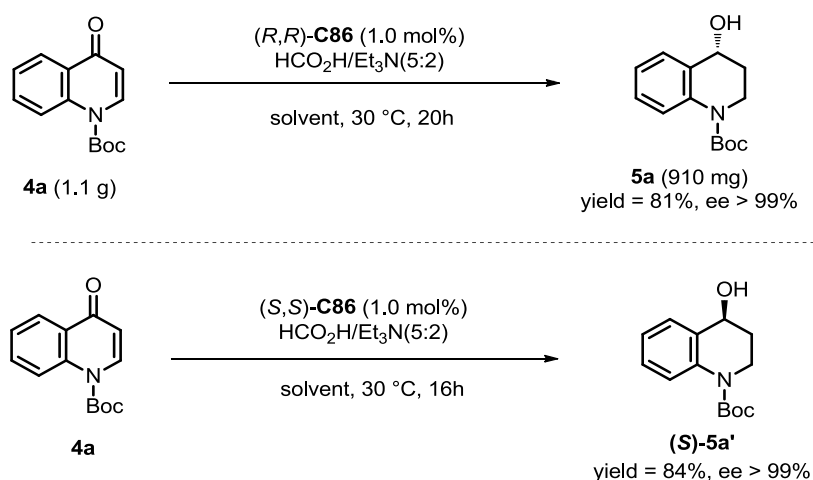


Schéma 4

Il est à noter que les divers alcools chiraux **5** peuvent être facilement fonctionnalisés

pour accéder à des dérivés 1,2,3,4-tétrahydroquinoléne-4-ol diversément substitués (Schéma 5). Ainsi, le composé *O*-allyle **9**, facilement obtenu à partir de **5a** pourrait ensuite être davantage fonctionnalisé par exemple par une réaction de méthylation croisée. Une réaction de couplage croisé catalysée au Pd a été effectuée sur **5g**, qui après *O*-silylation a été soumise à une réaction de Suzuki-Miyaura en présence de Pd(OAc)<sub>2</sub>, cataCXium A, K<sub>2</sub>CO<sub>3</sub> et d'acide phénylboronique, pour fournir le produit correspondant **7** avec un rendement de 98%. Enfin, une réaction de Mitsunobu sur **5a** a permis l'introduction d'un substituant phthalimide sur l'hétérocycle.

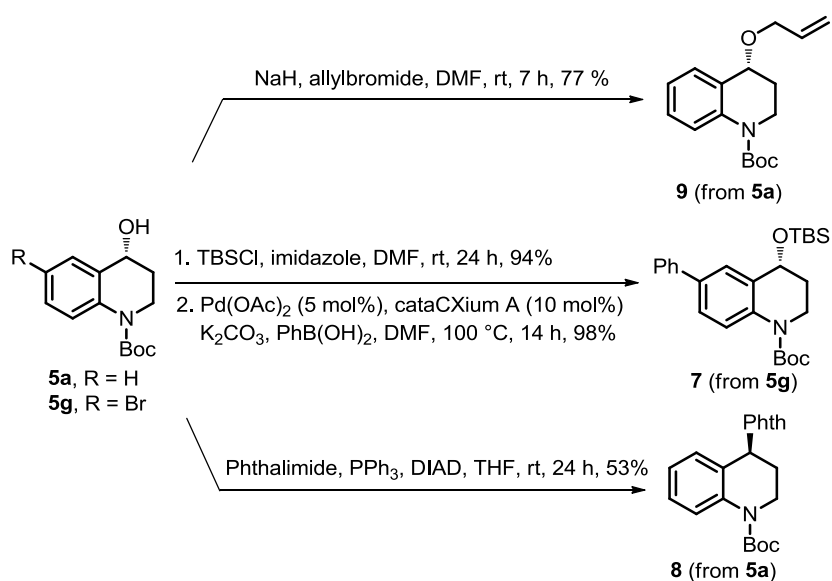


Schéma 5

## 2. Transfert d'hydrogène asymétrique catalysé par le rhodium de dérivés de la 2-aryl-2,3-dihydroquinoléne-4(1H)-one

Après avoir étudié l'élution de dérivés de la 4-quinolone, nous avons choisi d'examiner la réduction asymétrique d'hétérocycles plus fonctionnalisés pour la formation en une seule étape de deux centres stéréogènes. Ainsi, le dédoublement cinétique de dérivés de la 2-aryl-2,3-dihydroquinoléne-4(1H)-one a été étudié par transfert d'hydrogène asymétrique (Schéma 6).

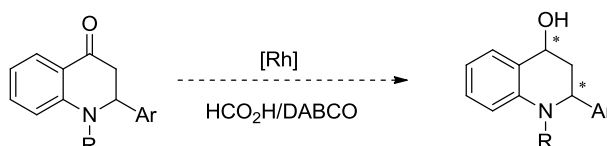
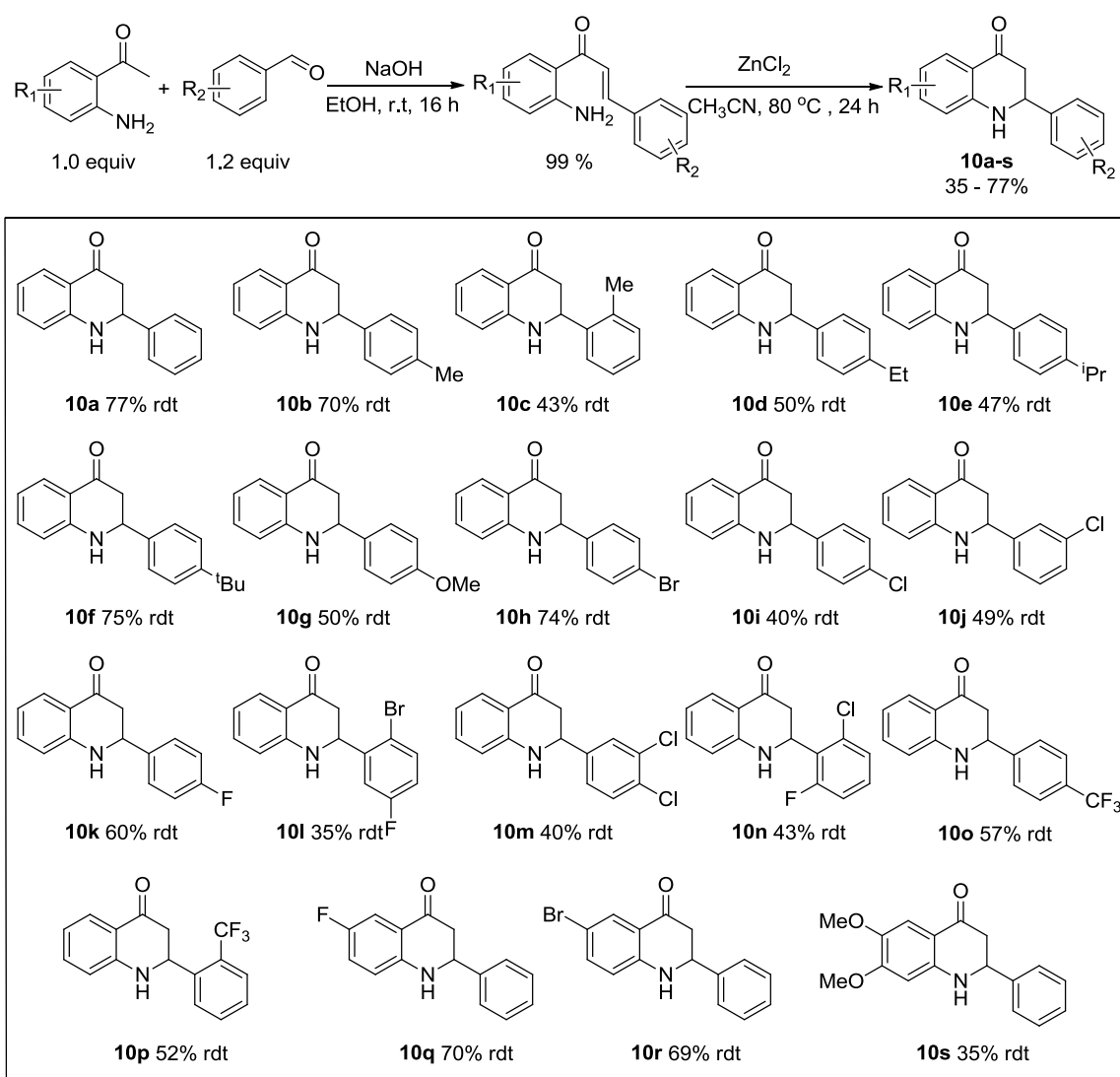


Schéma 6

Pour cette étude, les substrats 2-aryl-2,3-dihydroquinoléne-4(1H)-ones **1** ont d'abord été préparés en deux étapes selon des procédures décrites. Dans une première étape, la

condensation aldolique de 2-aminoacétophénone variées sur divers benzaldéhydes conduit aux énone correspondantes de manière quantitative. Après évaporation du solvant, les produits intermédiaires bruts sont directement engagés dans l'étape suivante qui permet la cyclisation de l'aniline sur l'énone assistée par  $\text{ZnCl}_2$ , pour former les structures 2-aryl-2,3-dihydroquinoléine-4(1H)-ones souhaitées avec des rendements de 35-77% (Figure 4).

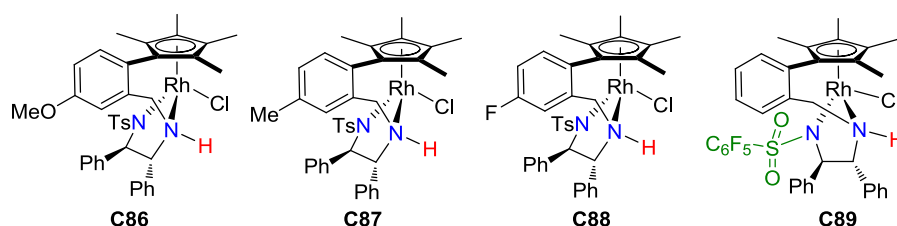
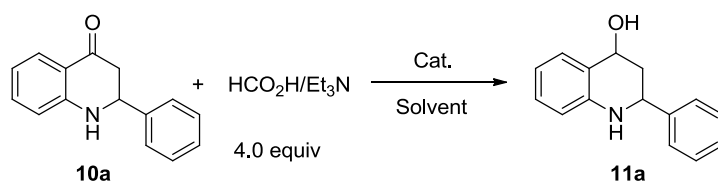


**Figure 4** Préparation de 2-aryl-2,3-dihydroquinoléine-4(1H)-ones

Disposant d'une gamme variée de 2-aryl-2,3-dihydroquinoléine-4(1H)-ones, l'optimisation des paramètres de la réaction de transfert d'hydrogène asymétrique a été effectuée sur la 2-phényl-2,3-dihydroquinoléine-4(1H)-one **10a** comme substrat standard. Différents complexes de rhodium ont été examinés en présence du mélange azéotropique  $\text{HCO}_2\text{H}/\text{Et}_3\text{N}$  (5:2) comme source d'hydrogène dans divers solvants. Les meilleurs résultats sont obtenus avec le complexe **C86** dans  $\text{CH}_3\text{CN}$  avec un rendement de 51% et un excès

énantiomérique de 99% (Tableau 2, entrée 6). Cependant, il s'est avéré que le produit **11a** résultant de la réduction se dégradait partiellement lors de la purification par chromatographie éclair sur gel de silice. Nous avons donc décidé pour la suite de l'étude de protéger l'atome d'azote et de déterminer les conditions optimales sur les substrats résultants.

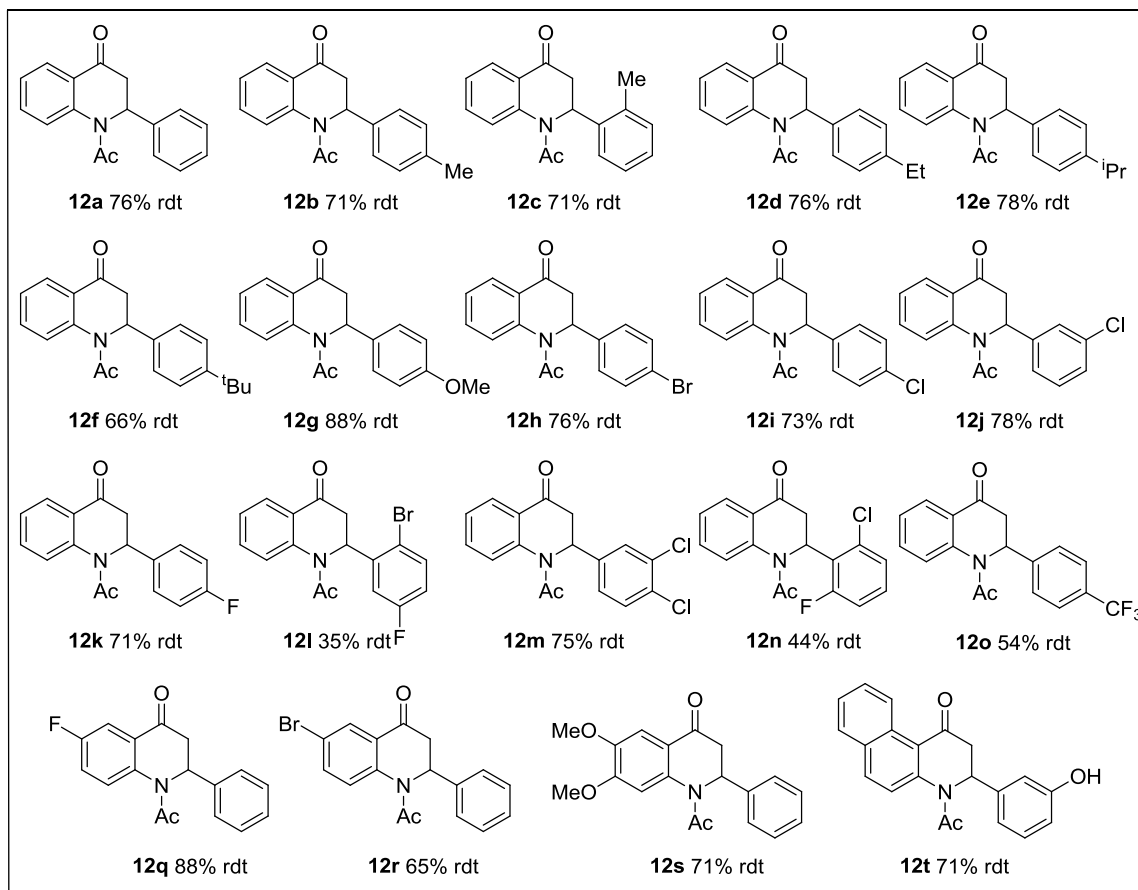
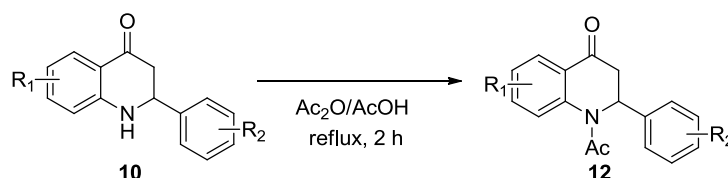
**Tableau 2 Optimisation des conditions réactionnelles pour le THA de 10a<sup>a</sup>**



Entrée	Catalyseur	Solvant	Rendement <sup>[b]</sup> (%)	de <sup>[c]</sup> (%)	ee <sup>[d]</sup> (%)
1	<b>C86</b>	CH <sub>2</sub> Cl <sub>2</sub>	57	87	94
2	<b>C87</b>	CH <sub>2</sub> Cl <sub>2</sub>	46	43	93
3	<b>C88</b>	CH <sub>2</sub> Cl <sub>2</sub>	41	73	92
4	<b>C89</b>	CH <sub>2</sub> Cl <sub>2</sub>	49	89	93
5	<b>C86</b>	CH <sub>3</sub> OH	56	8	99
6	<b>C86</b>	CH <sub>3</sub> CN	51	99	99

<sup>a</sup> Conditions de réaction: **10a** (0.4 mmol), catalyseur (1.0 mol%), HCO<sub>2</sub>H/Et<sub>3</sub>N (5:2) (136 μL, 4 equiv), CH<sub>2</sub>Cl<sub>2</sub> (1.0 mL), 30 °C. <sup>b</sup> Rendement isolé <sup>c</sup> Déterminé par RMN <sup>1</sup>H du produit brut. <sup>d</sup> Déterminé par analyse SFC.

Ainsi diverses 1-acétyl-2-aryl-2,3-dihydroquinolin-4(1H)-ones **12** substituées par des groupements électrodonneurs et électroattracteurs ont été obtenues avec des rendements isolés de 35-88% par acétylation au reflux d'un mélange Ac<sub>2</sub>O/AcOH des composés **10** (Figure 5).



**Figure 5** Préparation de 1-acétyl-2-aryl-2,3-dihydroquinolin-4(1H)-ones

L'optimisation des paramètres de la réaction de transfert d'hydrogène asymétrique (catalyseur, solvant, charge catalytique, source d'hydrogène) a été effectuée sur le composé **12a** et les meilleurs résultats sont obtenus dans les conditions suivantes: **C86** (0.1 mol%) comme pré-catalyseur, HCO<sub>2</sub>H/DABCO(2:1) (2.0 équivalents) comme donneur d'hydrogène, CH<sub>3</sub>CN (0.4 M) à température ambiante.

Dans ces conditions de réaction optimisées, le doublement cinétique par THA a été effectué sur une série de dérivés de la 2-aryl-2,3-dihydroquinolin-4(1H)-one (**12b-g**, **12s**) diversément substitués (Figure 6). Tous les substrats portant divers substituants électrodonneurs et électroattracteurs sur les différentes positions du noyau phényle ont conduit aux alcools correspondants sous forme d'un seul diastéréoisomère avec de bons rendements, et des énantiosélectivités atteignant jusqu'à >99 % ee. Les cétones énantioériquement enrichies quant à elles ont été obtenues avec des rendements de 47-50% et d'excellentes énantiosélectivités (98-> 99 % ee). Enfin, une réduction de **12a** à l'échelle du gramme a permis

d'obtenir le produit souhaité **13a** avec un rendement de 49 % et un ee de 99 %, le substrat chiral **12a'** étant obtenu avec un rendement de 50 % et un ee de 98 %.

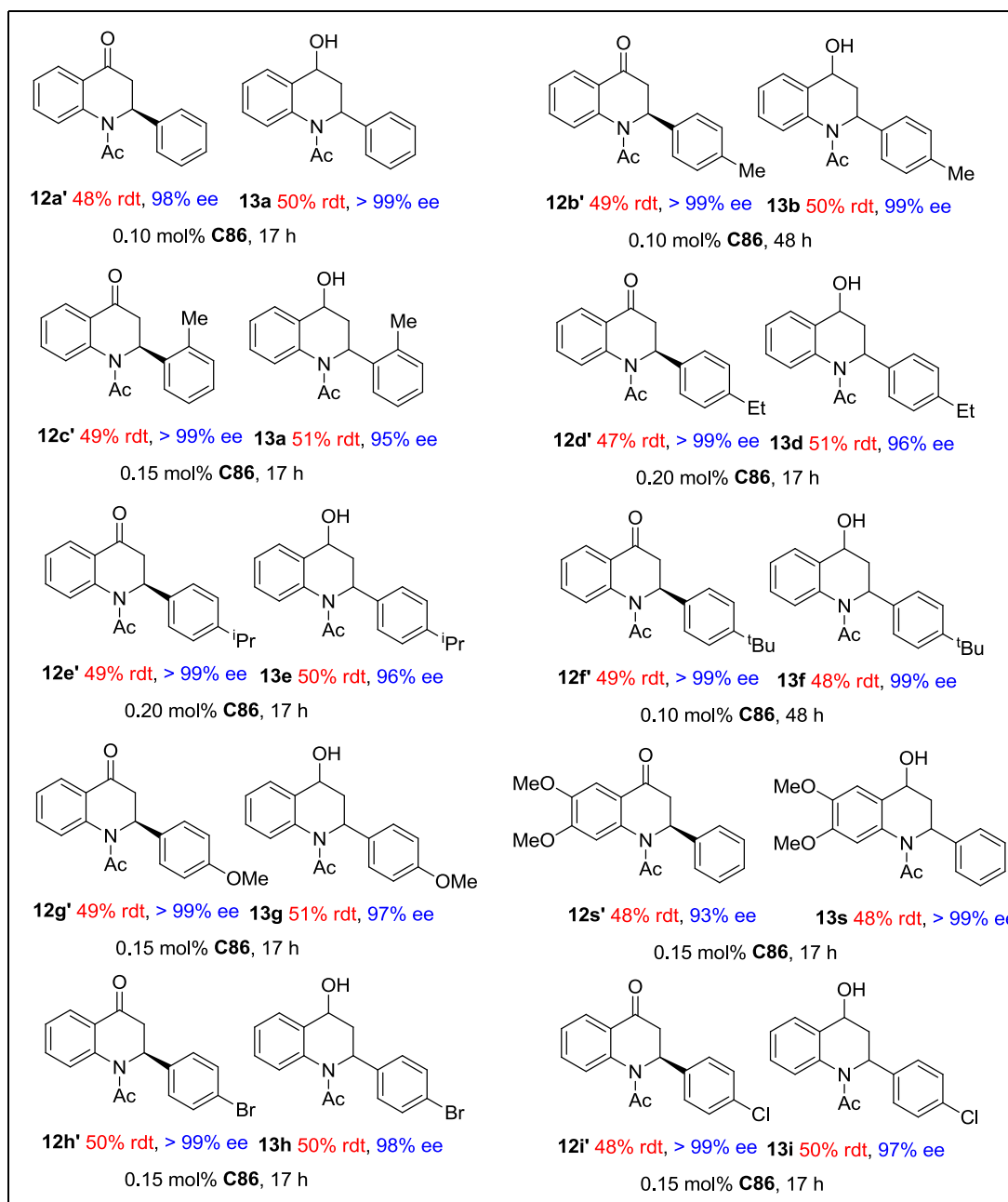
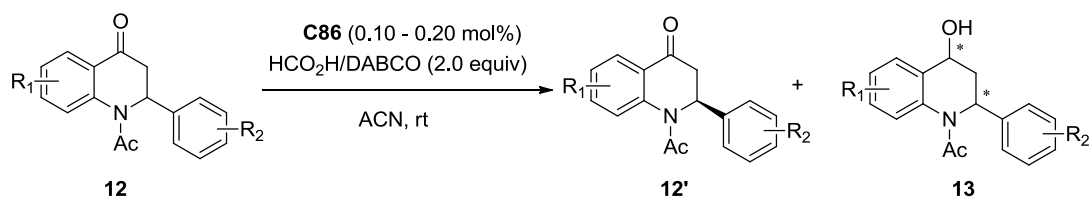


Figure 6



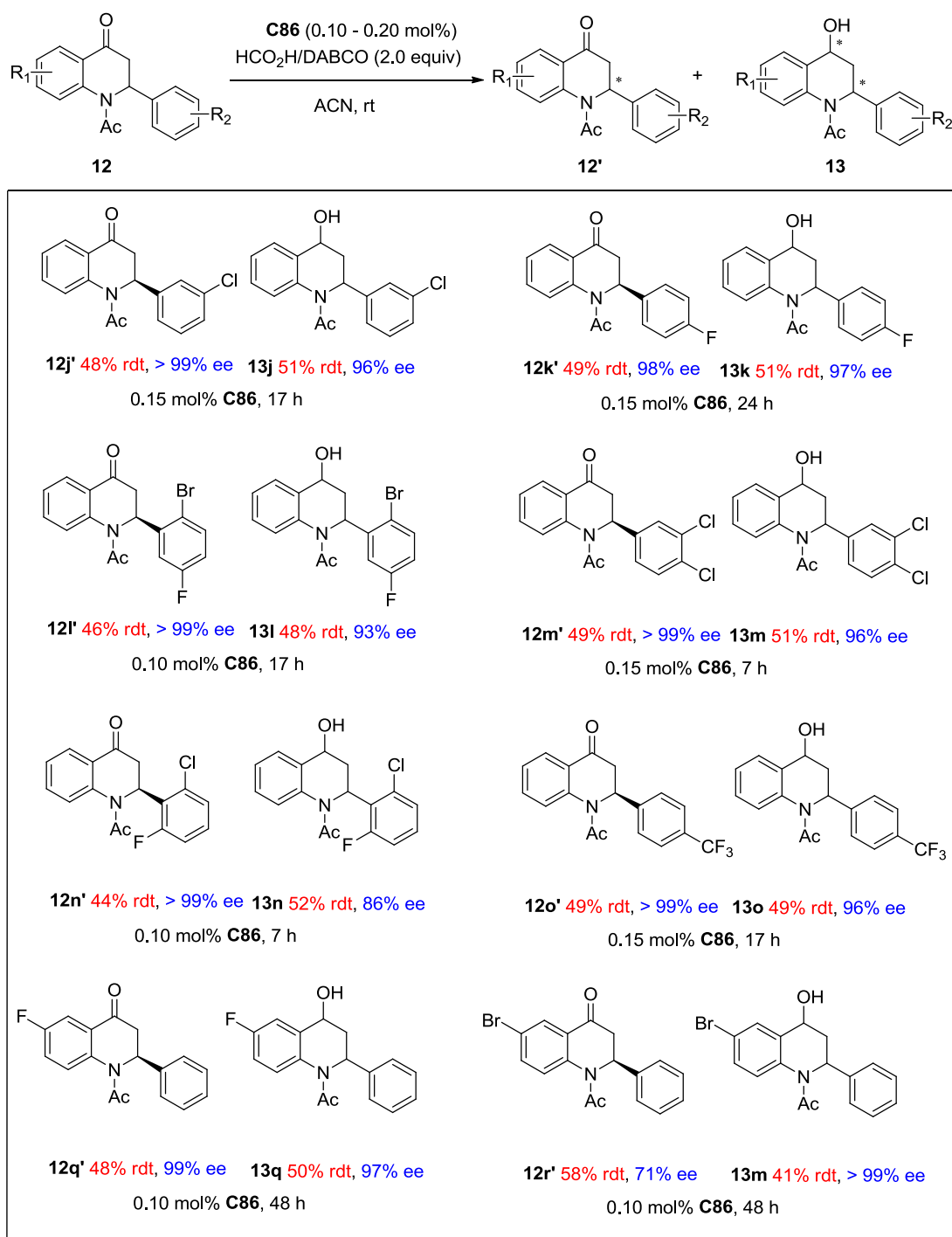


Figure 6 (Suite)

### 3. Transfert d'hydrogène asymétrique catalysé au rhodium/d'équilibre cinétique dynamique: accès stéréosélectif aux dérivés 3-hydroxyéméthyl-3-ol *cis*

Les chromanoïdes et les flavanoïdes présentent des motifs de base que l'on retrouve dans de nombreux produits naturels possédant des activités pharmacologiques et biologiques, notamment des propriétés antitumorales, antibactériennes, antioxydantes ou antiœstrogéniques (Figure 7). Il est par conséquent intéressant de disposer de voies d'accès efficaces et économiques à ces motifs.

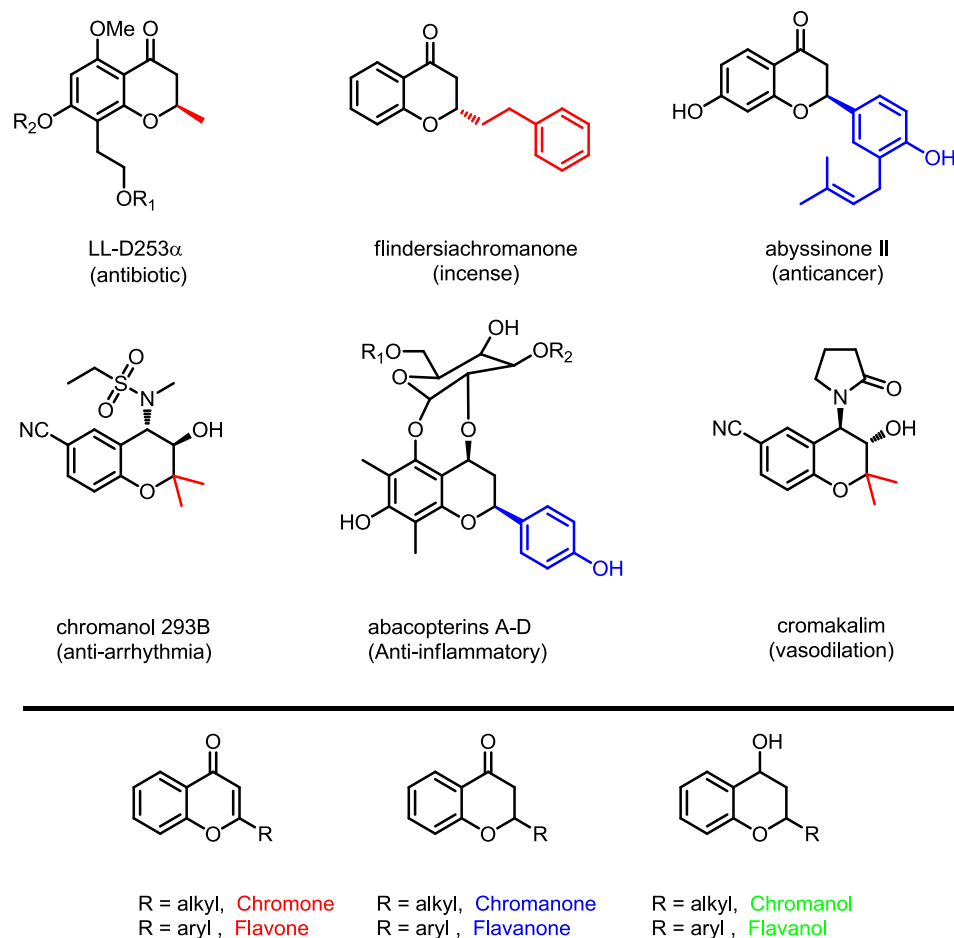


Figure 7

Dans ce contexte, un accès direct vers les chromanols 3-substitués énantiomériquement enrichis repose sur la réduction asymétrique de chroman-4-ones 3-substitués. Toutefois, à notre connaissance, seuls deux exemples de telles transformations, utilisant une réaction d'hydrogénation asymétrique, ont été décrits. En ce qui concerne le transfert d'hydrogène asymétrique (THA) de chromones 3-substitués, aucun exemple n'était décrit. Nous avons ainsi étudié la réaction de THA catalysée au rhodium de dérivés de 3-formylchromone conduisant aux 3-hydroxyméthyl chromanols correspondants par un processus de doublement cinétique dynamique (DCD) (Schéma 7).

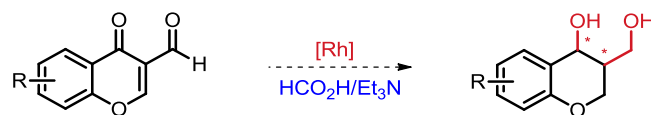


Schéma 7

Dans le cadre de cette étude, nous avons synthétisé quatre chromones 3-substitués (**14c**, **i**, **j**). Ces composés ont été facilement préparés en une seule étape à partir d'*o*-hydroxy-acétophénone (1.0 éq.) et d'oxychlorure de phosphore (5.0 éq.) dans le DMF avec des rendements de 18% à 78% (Figure 8).

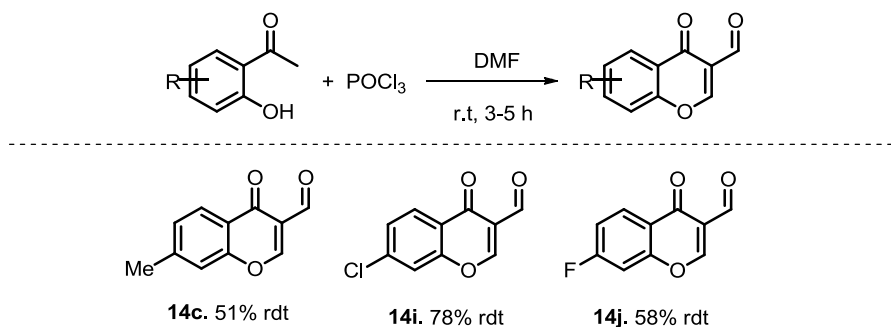
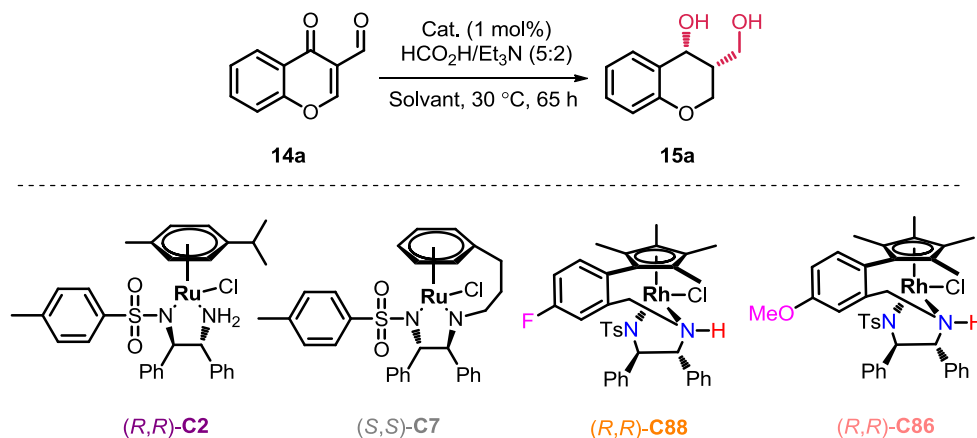


Figure 8

Pour l'étude de la réaction de THA/DCD, la 3-formylchromone **14a** a été choisie comme substrat modèle pour l'optimisation des paramètres réactionnels. Divers complexes de ruthénium et de rhodium ont été étudiés pour cette transformation qui a été effectuée en présence de 5.0 éq. du mélange azéotropique HCO<sub>2</sub>H/Et<sub>3</sub>N (5:2) comme source d'hydrogène dans différents solvants à 30 °C. Comme le montre le Tableau 2, c'est le complexe de rhodium (*R,R*)-**C86** qui a donné le meilleur rendement (62%) dans le dichlorométhane.

Tableau 3 Dépistage des pré-catalyseurs et des solvants pour l'HTA de **14a**<sup>a</sup>

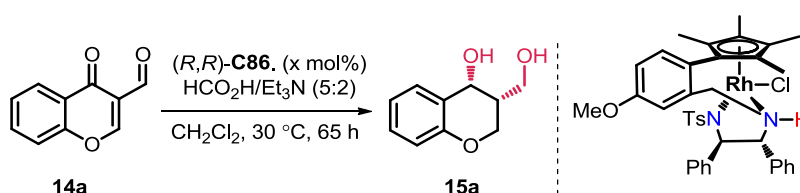
Entrée	Catalyseur	Solvant	Rendement <sup>[b]</sup> (%)	d.r. <sup>[c]</sup> (cis/trans)	ee <sub>cis</sub> <sup>[d]</sup> (%)
1	( <i>R,R</i> )- <b>C2</b>	CH <sub>2</sub> Cl <sub>2</sub>	--	--	--
2	( <i>S,S</i> )- <b>C7</b>	CH <sub>2</sub> Cl <sub>2</sub>	44	67:33	95
3	( <i>R,R</i> )- <b>C88</b>	CH <sub>2</sub> Cl <sub>2</sub>	28	96:4	99
4	( <i>R,R</i> )- <b>C86</b>	CH <sub>2</sub> Cl <sub>2</sub>	62	97:3	99
5	( <i>R,R</i> )- <b>C86</b>	toluene	28	94:6	97
6	( <i>R,R</i> )- <b>C86</b>	Et <sub>2</sub> O	38	91:9	99
7	( <i>R,R</i> )- <b>C86</b>	CH <sub>3</sub> CN	56	98:2	98
8	( <i>R,R</i> )- <b>C86</b>	dioxane	42	96:4	97
9	( <i>R,R</i> )- <b>C86</b>	DMF	52	97:3	98

10 (R,R)- **C86** 2-MeTHF 37 95:5 97

<sup>a</sup>Conditions: **14a** (0.5 mmol), Cat. (1 mol%), Solvant (1.5 mL), HCO<sub>2</sub>H/Et<sub>3</sub>N (5:2) (212 μL), 30 °C. La réaction a été surveillée par TLC ou <sup>1</sup>H NMR. <sup>b</sup> Rendement isolé <sup>c</sup> Déterminé par RMN <sup>1</sup>H du produit brut. <sup>d</sup> Déterminé par analyse SFC.

L'influence de la charge catalytique, de la quantité de mélange azéotrope HCO<sub>2</sub>H/Et<sub>3</sub>N (5:2) et de la concentration a ensuite été examinée. Les conditions optimisées, conduisant à un rendement en **15a** de 84% et de très bonnes diasté- et énantiosélectivités (98:2 rd, 99% ee) ont été établies comme suit: (R,R)- **C86** (0.5 mol%), HCO<sub>2</sub>H/Et<sub>3</sub>N (5:2) (7.0 éq.), CH<sub>2</sub>Cl<sub>2</sub> (1.0 M) à 30 °C.

Tableau 4 D épistage d'autres conditions pour l'THA de **1a**<sup>a</sup>

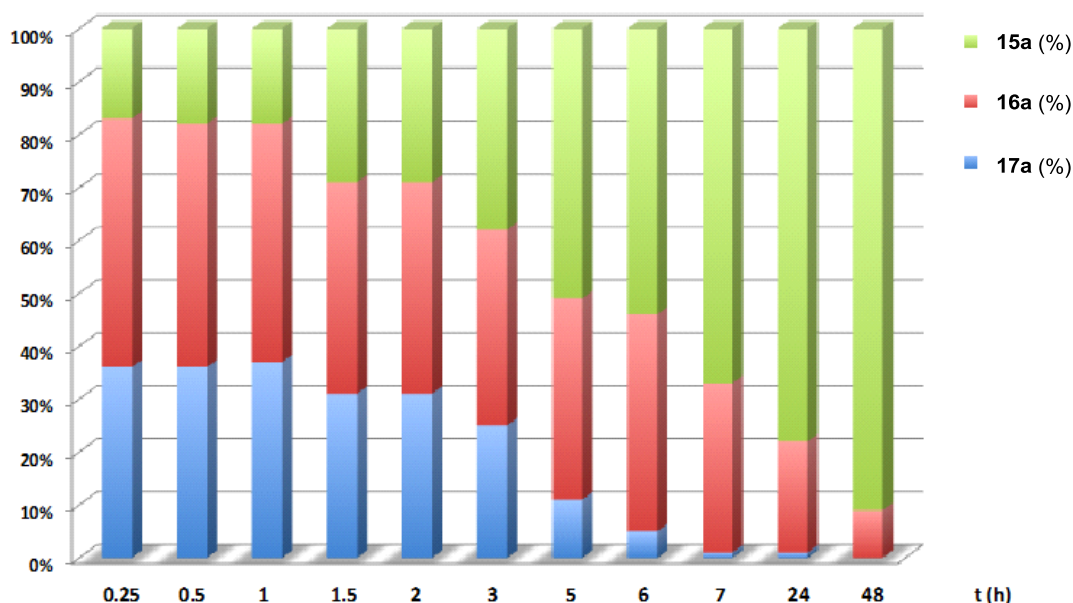
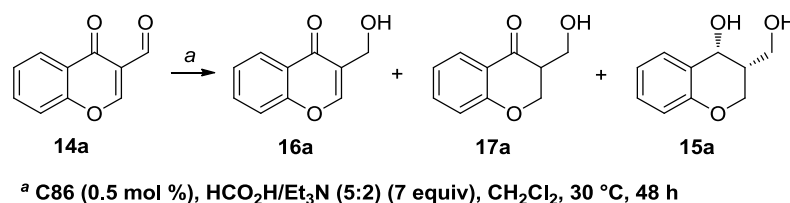


Entrée	S/C	FA/TEA (5:2) (éq.)	CH <sub>2</sub> Cl <sub>2</sub> (mL)	Rendement <sup>[b]</sup> (%)	d.r. <sup>[c]</sup> (cis/trans)	ee <sub>cis</sub> <sup>[d]</sup> (%)
1	100	5.0	1.5	62	97:3	99
2	200	5.0	1.5	62	97:3	99
3	1000	5.0	1.5	47	99:1	99
4	200	3.0	1.5	26	90:10	98
5	200	7.0	1.5	74	97:3	99
6	200	10.0	1.5	67	98:2	99
7	200	7.0	2.0	72	97:3	99
8	200	7.0	1.0	79	97:3	99
9	200	7.0	0.5	84	98:2	99
10	200	7.0	0	73	98:2	99

<sup>a</sup>Conditions: **14a** (0.5 mmol), (R,R)-**C86** (x mol%), CH<sub>2</sub>Cl<sub>2</sub> (x mL), HCO<sub>2</sub>H/Et<sub>3</sub>N (5:2) (x μL), 30 °C. La réaction a été surveillée par TLC ou <sup>1</sup>H NMR. <sup>b</sup> Rendement isolé <sup>c</sup> Déterminé par RMN <sup>1</sup>H du produit brut. <sup>d</sup> Déterminé par analyse SFC.

Des études de suivi de la réaction de transfert d'hydrogène asymétrique de **14a** dans les conditions optimisées ont été réalisées (Figure 9). Après 0.25 h de réaction, le produit de départ est totalement consommé et la formation des produits **15a**, **16a** et **17a** est observée. Il est à noter que le diol résultant de la réduction de la cétone sur l'intermédiaire **16a** n'a pas été détecté dans cette étude. Il semble que la réduction de l'aldéhyde et de la liaison C=C sur **14a** soit rapide,

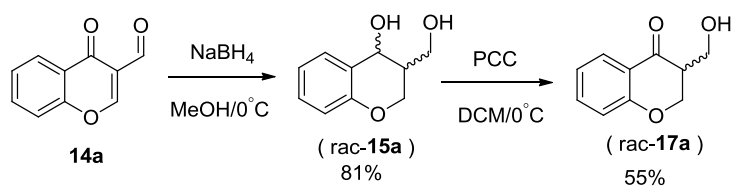
produisant un mélange des composés **16a** et **17a** avec une proportion cumulée de 80% avec **15a** après 0.25 h de réaction. La quantité de l'intermédiaire **17a** diminue ensuite rapidement, avec seulement des traces détectées après 7 h et la consommation complète de **14a** est obtenue après 48 h. Il convient de noter que lorsque la réaction est arrêtée après 0.25 h, l'intermédiaire **17a** présent dans le milieu réactionnel est sous forme de mélange racémique, indiquant ainsi que la réaction se déroule dans des conditions de doublement cinétique dynamique.



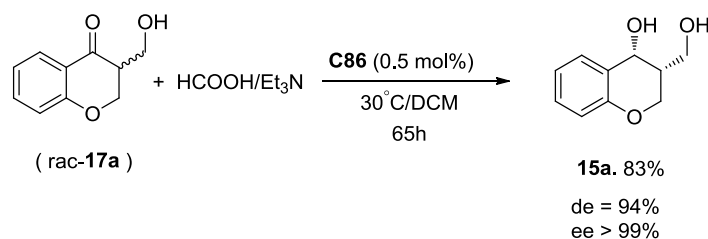
**Figure 9**

Par ailleurs, pour confirmer que le THA de **14a** procède *via* un doublement cinétique dynamique, un échantillon de produit racémique **17a** a été préparé et soumis aux conditions optimisées de réaction. La réduction de **14a** avec le borohydrure de sodium dans le méthanol donne **15a** avec un rendement de 81%. Ce dernier est ensuite sélectivement oxydé en hydroxycétone désirée en présence de PCC avec un rendement de 55%. Le produit racémique **17a** a ensuite été soumis aux conditions de réaction standard et a conduit au produit attendu **15a** avec les mêmes rendement (83%), diastéréosélectivité (97:3 dr) et énantiosélectivité (99% ee) que ceux obtenus en utilisant **14a** comme produit de départ, ce qui démontre qu'un DCD se produit pour cette réaction (Schéma 8).

**a.** Preparation of rac-17a



**b.** Reduction of rac-17a under the standard conditions



**Schéma 8**

Avec ces conditions optimisées en main, l'étendue de la réaction a ensuite été étudiée avec une série de 3-formyl chromones **14a-m** portant divers substituants électrodonneurs ou électroattracteurs sur le noyau phényle (Figure 10). Tous les substrats utilisés ont conduit aux diols *cis* correspondants avec de bons rendements, des diastéréosélectivités élevées et d'excellentes énantiosélectivités. Les configurations absolues des diols **15a** et **15g** ont été attribuées sans ambiguïté comme étant (*R,R*) par analyse cristallographique par diffraction des rayons X. Par analogie, nous supposons que les autres produits réduits suivent la même tendance.

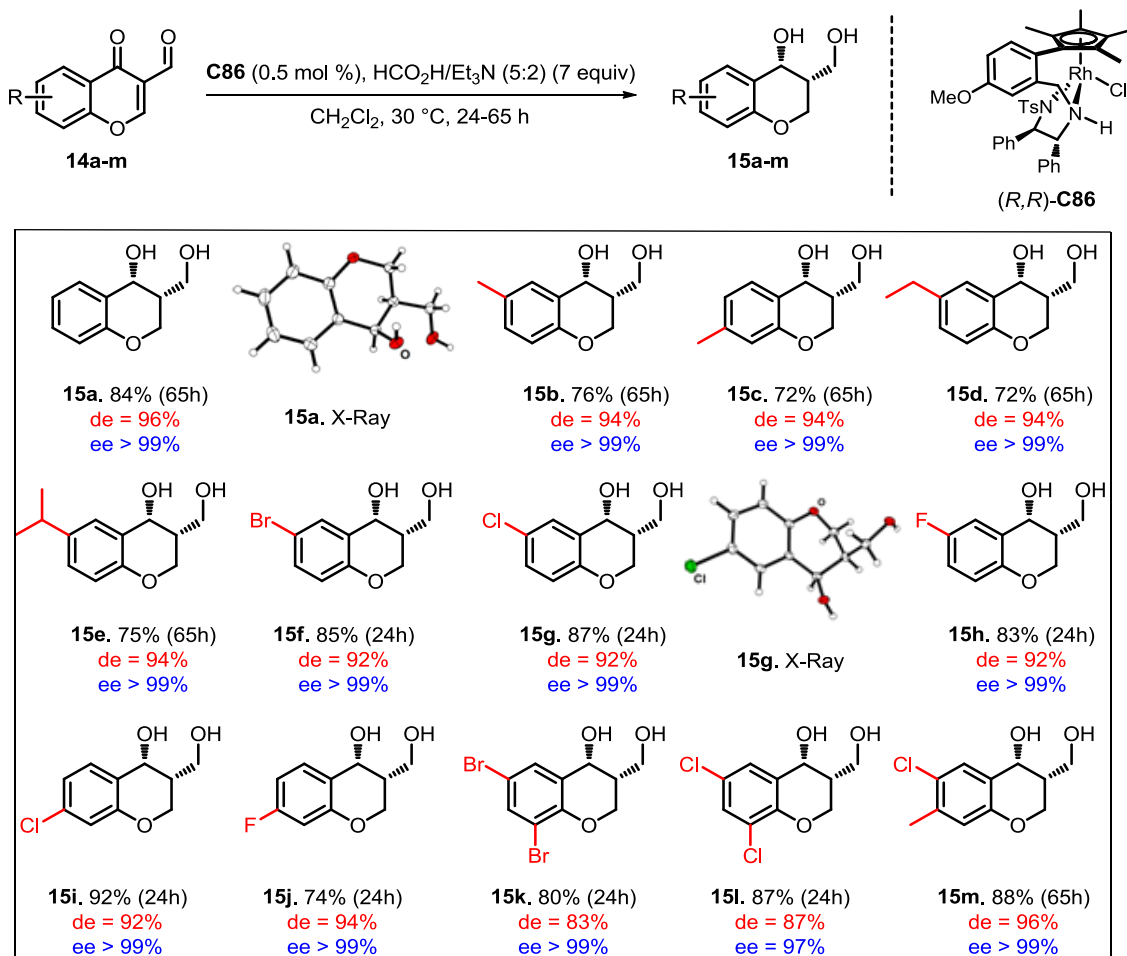


Figure 10

Par ailleurs, une réduction dans les conditions standard du composé **14g** à l'échelle du gramme a permis d'obtenir le produit souhaité **15g** avec un rendement de 81% et des valeurs élevées de dr et de ee (Schéma 9). De plus, la post-fonctionnalisation des composés **15f** et **15g** a été réalisée. Après la protection à l'acétonide de **15f**, les dérivés biaryles **19** et **20** ont été facilement préparés avec de très bons rendements par couplage de Suzuki-Miyaura en utilisant Pd(OAc)<sub>2</sub>, cataCXium A, K<sub>2</sub>CO<sub>3</sub> et l'acide phényl- ou 4-méthoxyphénylboronique, respectivement. Enfin, le diol **15g** a été facilement converti en aminoalcool **23** en 3 étapes par une réaction de Mitsunobu.

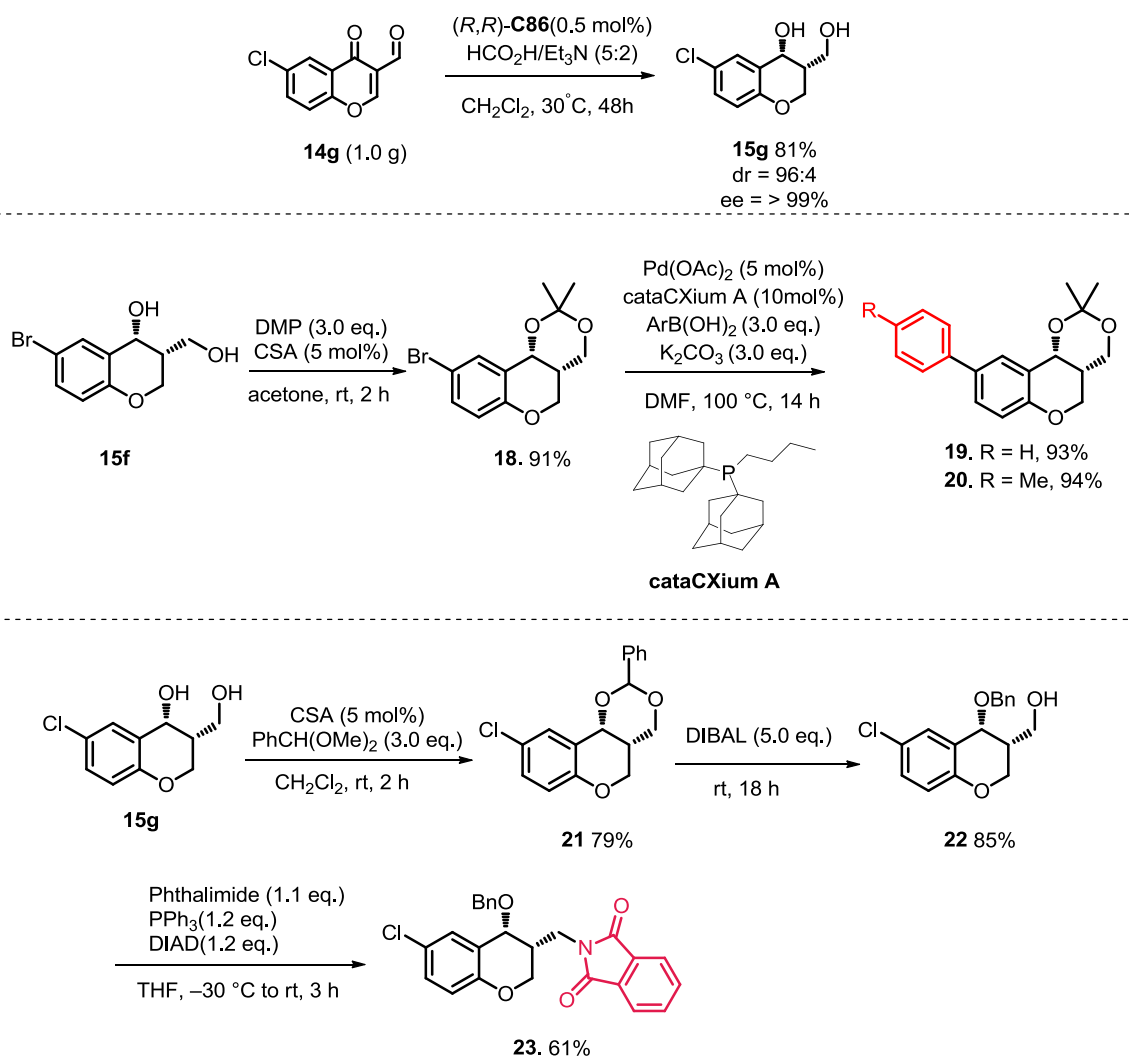


Schéma 9

En résumé, le transfert d'hydrogène asymétrique catalysé au rhodium des chromones 3-formyle semble être un outil efficace pour la synthèse de dérivés *cis* 3-hydroxyméthyl-chromanol. Cette méthode présente plusieurs avantages par rapport aux quelques exemples d'hydrogénation asymétrique précédemment décrits. Le complexe Rh(III)-développé au laboratoire permet la réduction dans des conditions douces en utilisant une faible charge catalytique, fournissant les composés réduits avec de bons rendements et d'excellentes diastéréo- et énantioselectivités (jusqu'à 98:2 dr, jusqu'à >99% ee). De plus, l'utilité de cette méthode a été démontrée par l'efficacité de la réaction réalisée avec **14g** à l'échelle du gramme. Enfin, les 3-hydroxyméthyl chromanols synthétisés dans le cadre de cette étude peuvent servir de plate-forme pour des fonctionnalisations ultérieures afin d'accéder à des dérivés de chromanol diversement substitués.

### Partie C: Transfert d'hydrogène asymétrique de $\beta$ -cétosters $\alpha$ -substitués



## 1. Transfert d'hydrogène asymétrique/DCD de $\alpha$ -méthoxy $\beta$ -cétoesters catalysé au rhodium dans le 2-MeTHF et l'eau: vers une procédure plus verte

Les diols 1,2 chiraux sont des motifs structuraux importants que l'on trouve dans un certain nombre de molécules naturelles et biologiquement actives, comme par exemple les dérivés de la silymarine, un antagoniste d' $\alpha_{1A}$ -adréno-récepteur, la (*S,S*)-réboxétine, des inhibiteurs sélectifs de la recapture de la norépinéphrine (sNRI), les polycéides ou les alcaloïdes. Ces motifs trouvent par ailleurs de nombreuses applications en synthèse organique en tant que ligands chiraux ou auxiliaires chiraux (Figure 11).

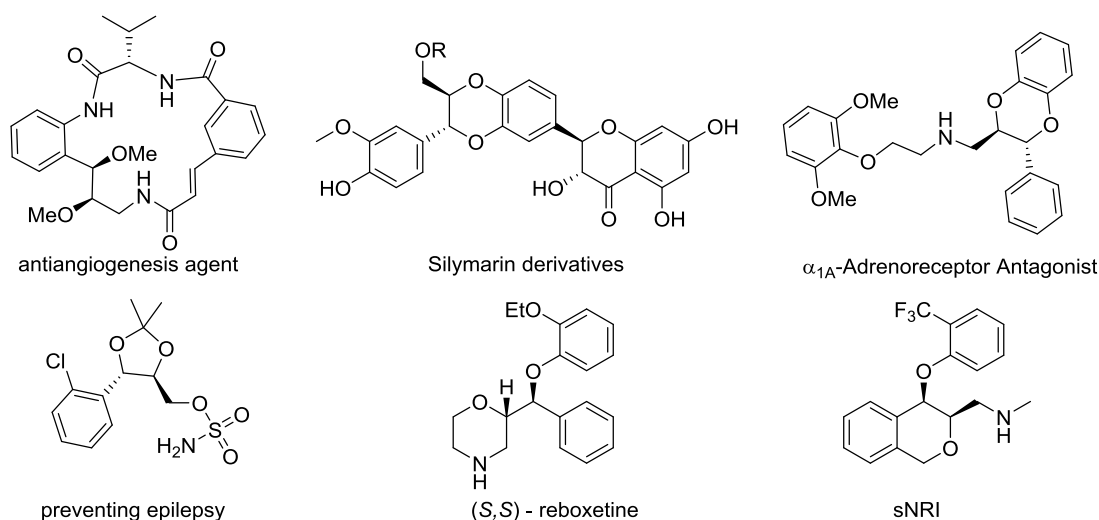


Figure 11

Par conséquent, le développement de nouvelles méthodologies catalytiques diastéréo- et énantiosélectives pour accéder à des diols-1,2 monodifférenciés énantiomériquement purs avec une stéréosélectivité élevée et avec une économie d'atomes maximale est primordial. Suite aux résultats obtenus précédemment dans l'équipe sur la réaction de THA/DCD catalysé au Ru de  $\alpha$ -alkoxy  $\beta$ -cétoesters, nous avons étudié cette transformation en utilisant des complexes Rh et plus particulièrement un nouveau complexe possédant une agrafe carbonée, pour évaluer leurs performances catalytiques (Schéma 10).

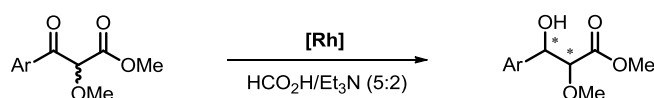


Schéma 10

Pour cette étude, nous avons d'abord préparé une série de  $\beta$ -cétoesters **24a-m** selon les méthodes A ou B données ci-dessous (Figure 12).

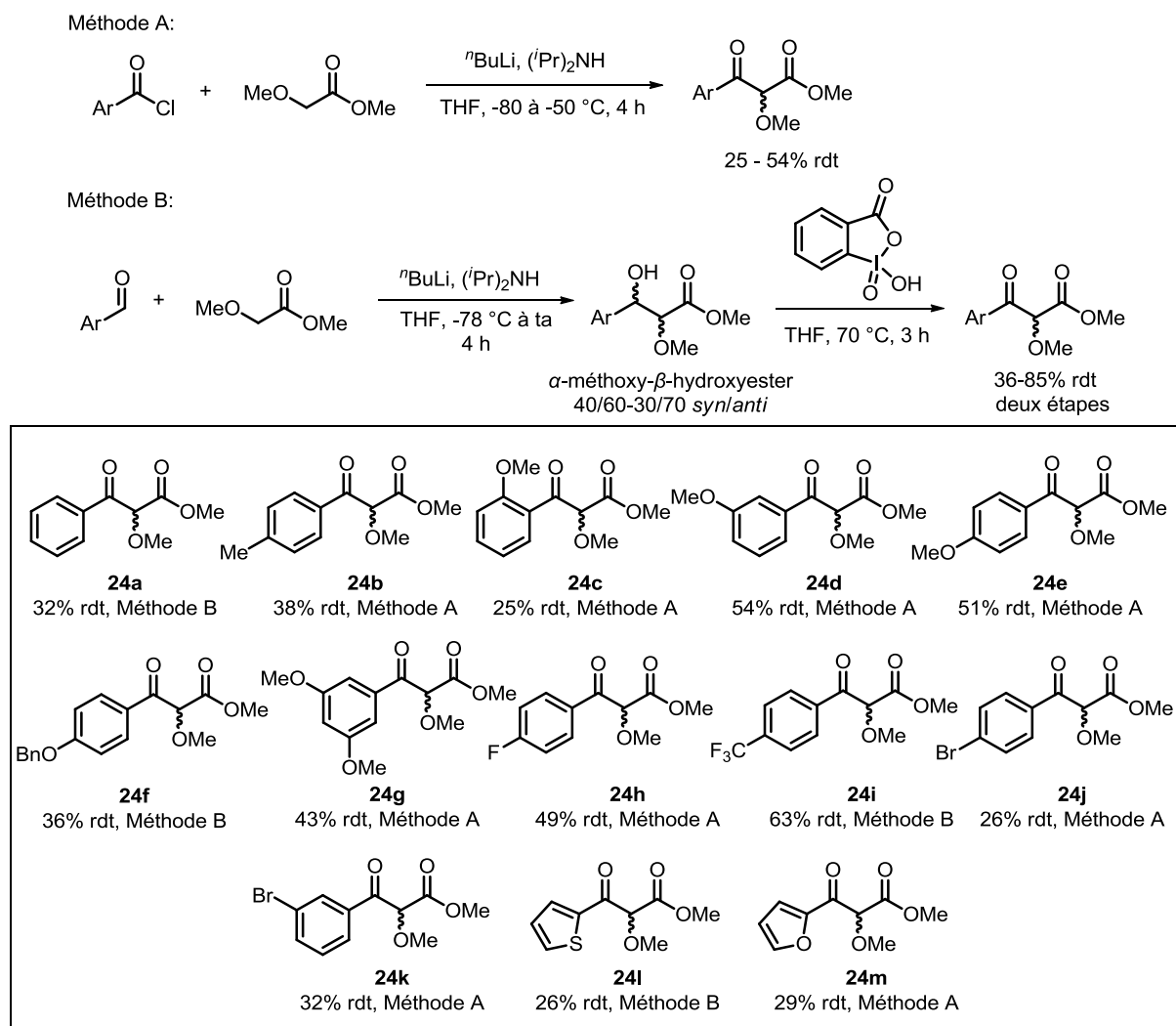
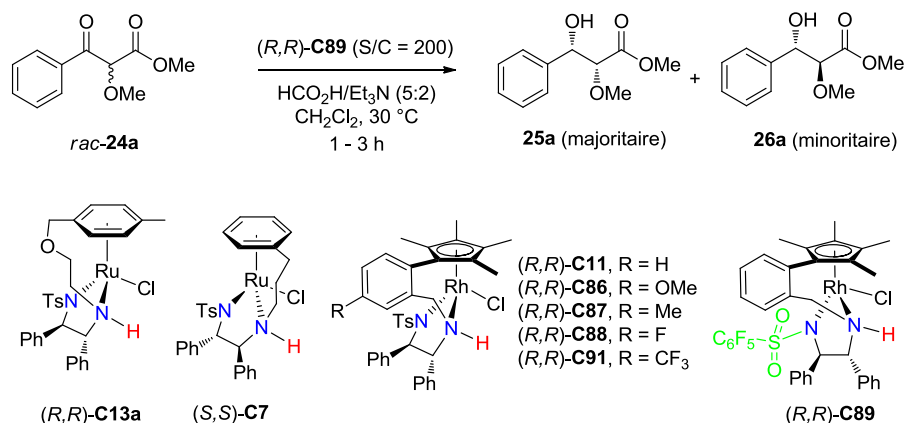


Figure 12

Pour l'étude de la réaction de THA/DCD, le composé **24a** a été choisi comme substrat modèle et différents complexes de ruthénium ou de rhodium ont été testés en présence de  $\text{HCO}_2\text{H}/\text{Et}_3\text{N}$  (5:2) comme source d'hydrogène dans le dichlorométhane à 30 °C. D'après les résultats regroupés dans le Tableau 5, les meilleurs résultats en termes de diasté- et énantiosélectivités (93:7 dr, 99% ee) sont obtenus avec le complexe de rhodium **C89** précédemment synthétisé au laboratoire.

Tableau 5. Influence des pré-catalyseurs

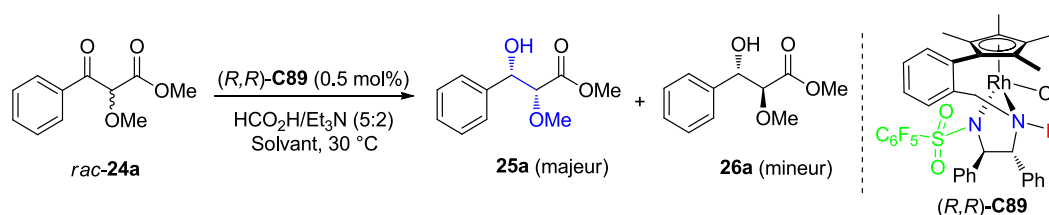


Entrée	Catalyseur	Temps (h)	Rendement (%)	dr	ee <sub>syn</sub> (%) <sup>d</sup>
1	$(R,R)\text{-C}13a$	20	85	85:15	99
2 <sup>e</sup>	$(S,S)\text{-C}7$	14	85	70:30	-97
3	$(R,R)\text{-C}86$	1	91	91:9	99
4 <sup>f</sup>	$(R,R)\text{-C}86$	22	90	88:12	99
5	$(R,R)\text{-C}87$	1	89	91:9	99
6	$(R,R)\text{-C}88$	3	89	91:9	99
7	$(R,R)\text{-C}91$	3	92	89:11	99
8	$(R,R)\text{-C}89$	3	94	93:7	99
9	$(R,R)\text{-C}11$	1	89	91:9	99

<sup>a</sup> Conditions: **24a** (0.8 mmol), [Rh] ou [Ru] (0.5 mol%), HCO<sub>2</sub>H/Et<sub>3</sub>N (5:2) (2.0 équiv.), CH<sub>2</sub>Cl<sub>2</sub> (4.0 mL, 0.2 M), 30 °C, conversion complète. <sup>b</sup> Rendement isolé pour **25a** et **26a**. <sup>c</sup> Déterminé par RMN <sup>1</sup>H du produit brut. <sup>d</sup> Déterminé par analyse HPLC ou SFC. <sup>e</sup> Enantiomère *ent*-**25a** majoritaire. <sup>f</sup> Réaction effectuée à 0 °C.

L'influence du solvant a ensuite été étudiée, et compte tenu des résultats observés, nous avons privilégié l'utilisation du 2-MeTHF comme solvant vert pour le reste de cette étude (Tableau 6). Les conditions de réaction optimisées ont été fixées comme suit: **24a** (0.8 mmol), complexe  $(R,R)\text{-C}89$  (0.5 mol%), HCO<sub>2</sub>H/Et<sub>3</sub>N (5:2) (2.0 équiv.), 2-MeTHF (4.0 mL), 30 °C.

**Tableau 6. Influence du solvant<sup>a</sup>**



Entrée	Solvant	Temps	Conv. (%) <sup>b</sup>	Rendement	dr ( <b>25a:26a</b> ) <sup>b</sup>	ee <sub>syn</sub> (%) <sup>d</sup>
--------	---------	-------	------------------------	-----------	------------------------------------	------------------------------------

## Résumé

---

1	CH <sub>2</sub> Cl <sub>2</sub>	3	100	94	93:7	99
2	CH <sub>3</sub> CN	72	46.5	42	94:6	99
3	Toluene	6	100	88	95:5	99
4	<i>i</i> PrOH	6	100	87	94:6	99
5	<i>i</i> Pr <sub>2</sub> O	22	75	68	86:14	99
6	EtOAc	3	100	93	96:4	99
7	THF	10	100	95	97:3	99
8	THF	5	100	95	95:5	99
9	2-MeTHF	5	100	93	97:3	99
10	DMC <sup>e</sup>	3	100	92	95:5	99
11	neat	6	100	93	81:19	99

<sup>a</sup> Conditions: **24a** (0.8 mmol), (*R,R*)-**C89** (0.5 mol%), HCO<sub>2</sub>H/Et<sub>3</sub>N (5:2) (2.0 équiv.), solvant (4.0 mL, 0.2 M), 30 °C, réaction suivie par CCM. <sup>b</sup> Déterminé par RMN <sup>1</sup>H du produit brut. <sup>c</sup> Rendement isolé pour **25a** et **26a**. <sup>d</sup> Déterminé par analyse HPLC ou SFC. <sup>e</sup> DMC = Dimethyl carbonate.

---

L'étendue de la réaction de THA/DCD de  $\beta$ -methoxy  $\beta$ -c $\alpha$ oesters catalysée par le complexe (*R,R*)-**C89** a ensuite été étudiée pour une série d'aryl c $\alpha$ ones différemment substitués **24a-k** portant des substituants électrodonneurs ou électroaccepteurs sur le cycle aromatique. De très bonnes diasté- et énantio-sélectivités sont généralement observées avec des rendements de bons à élevés. Il est intéressant de noter que les substrats h $\alpha$ roaromatiques **24l-m** conduisent à des diasté- et énantio-sélectivités quasi parfaites (99:1 dr) et à d'excellentes énantio-sélectivités (Figure 13).

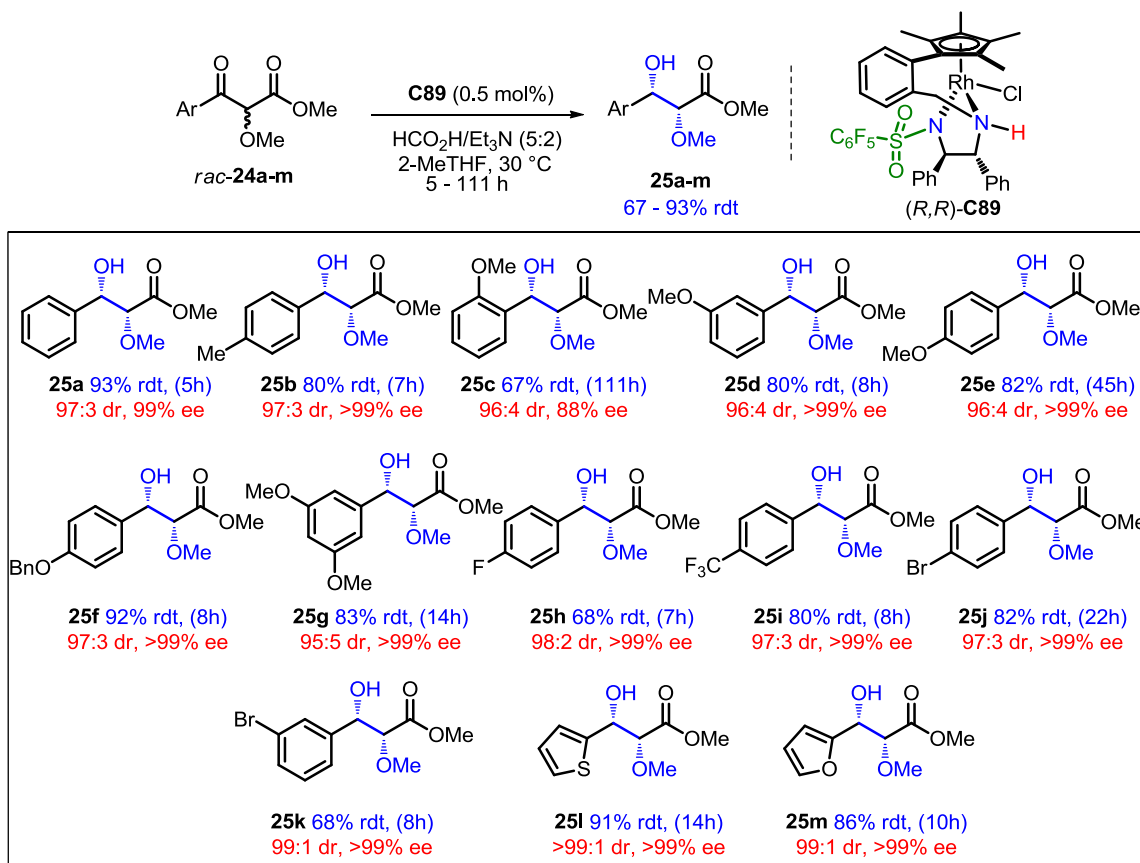
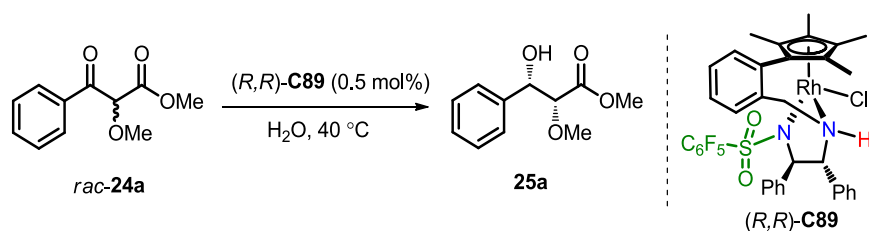
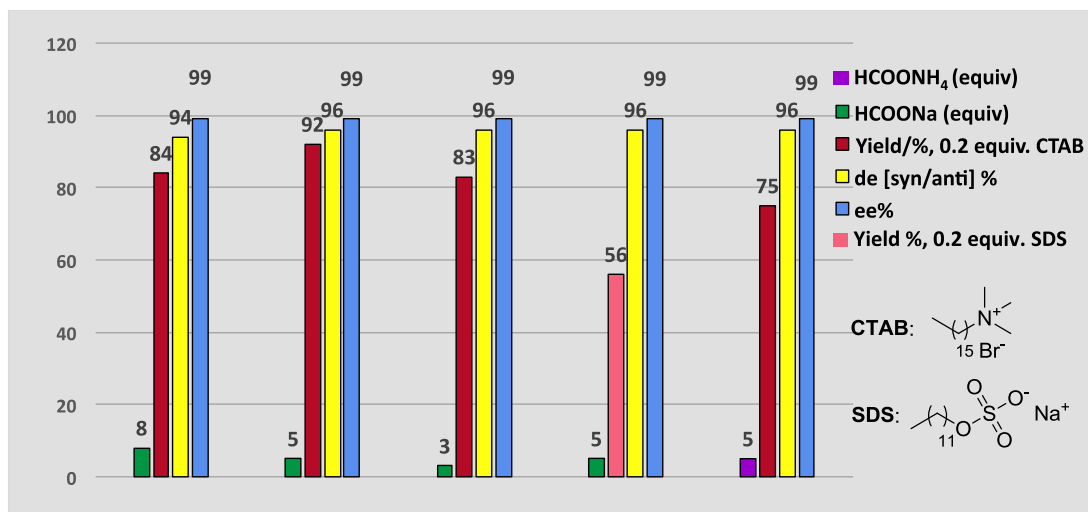


Figure 13

Dans l'optique de développer des procédures plus respectueuses de l'environnement, nous avons ensuite cherché à effectuer cette réaction en milieu aqueux (Figure 14). Ainsi, après avoir étudié la source d'hydrogène et le tensioactif utilisé dans l'eau, nous avons établi les conditions optimales comme suit: **24a**, **(R,R)**-**C89** (S/C 200),  $\text{HCO}_2\text{Na}$  (5.0 éq.),  $\text{H}_2\text{O}$ , CTAB (0.2 éq.), 40 °C.





**Figure 14. Optimisation des conditions réactionnelles dans l'eau à 40 °C avec (R,R)-C89**

Avec ces conditions optimisées en main, nous avons ensuite étudié l'étendue de la réaction de THA/DCD catalysée au Rh de  $\alpha$ -méthoxy  $\beta$ -c éoesters avec une série d'aryl c étones diversement substitués **24b-m** (Figure 15). Les composés **24b-g** contenant des substituants méthyle, méthoxy ou benzyloxy sur le noyau benzénique en position *meta* ou *para* ont conduit à des niveaux élevés de diastérosélectivité (de 96:4 à 98:2 dr), avec d'excellentes énantiosélectivités (>99% ee) observés dans tous les cas. Les substrats **24h-k** contenant des groupes électroattracteurs sur le noyau aryle, tels que des substituants fluoro, trifluorométhyl ou bromo, ont donné des rendements de 73% à 97%, des niveaux élevés de diastérosélectivité (95:5 à 98:2 dr) et d'excellentes énantioinductions (>99% ee). De plus, les substrats hétéroaromatiques **24k-l** ont conduit à de bons rendements (88% et 98%), une *syn* diastérosélectivité presque parfaite (>99:1 dr) et d'excellentes énantiosélectivités (>99% ee).

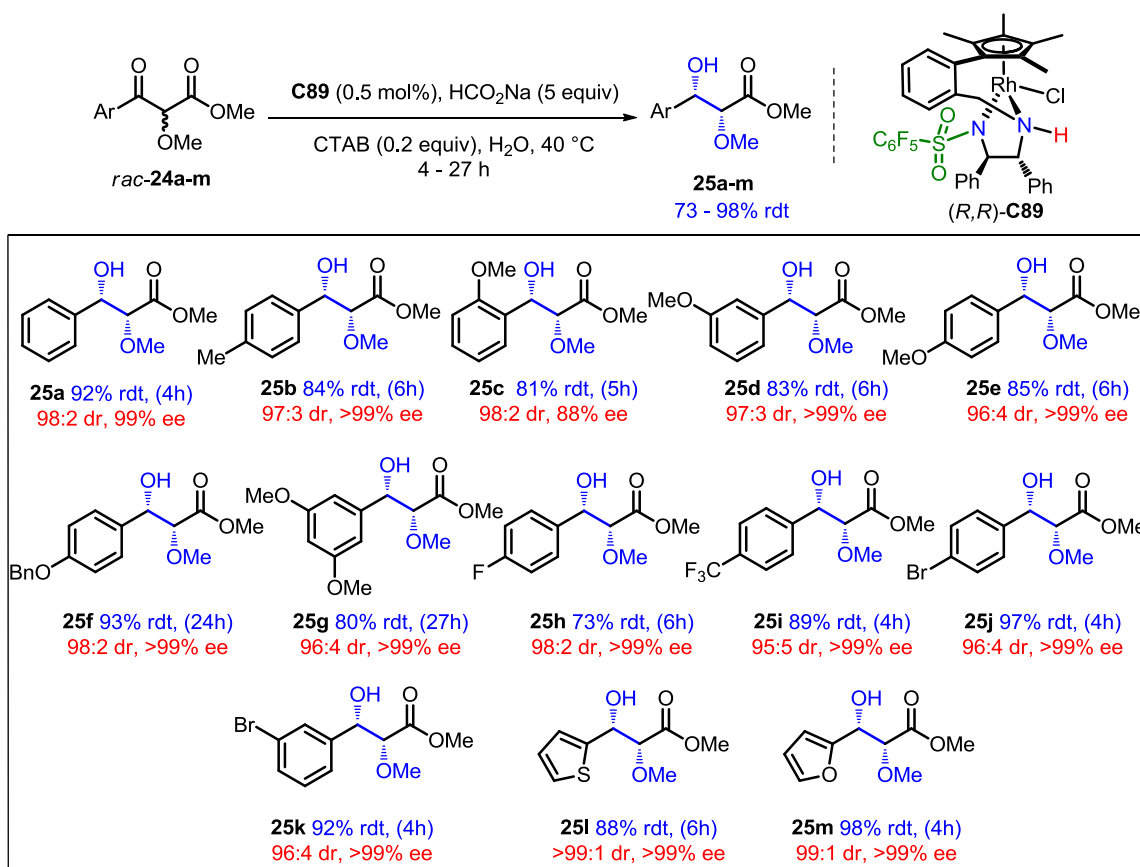


Figure 15

En conclusion, un nouveau catalyseur de rhodium comportant un ligand pentafluorobenzènesulfonyl-DPEN a été utilisé de manière efficace pour le transfert d'hydrogène asymétrique de composés  $\alpha$ -méthoxy  $\beta$ -étoesters en présence de  $\text{HCO}_2\text{H}/\text{Et}_3\text{N}$  (5:2) dans un solvant vert 2-MeTHF, ou en présence de  $\text{HCO}_2\text{Na}$  dans l'eau. Cette réaction de THA catalytique permet d'accéder à des dérivés  $\beta$ -hydroxyesters monodifférenciés avec de bons rendements (jusqu'à 98%), une excellente diastéosélectivité (jusqu'à >99:1 rd) et d'excellentes énantiosélectivités (jusqu'à >99% ee) *via* un processus de dédoublement cinétique dynamique, et s'effectue dans l'eau selon un protocole expérimental très facile à mettre en œuvre.





# **General Introduction**



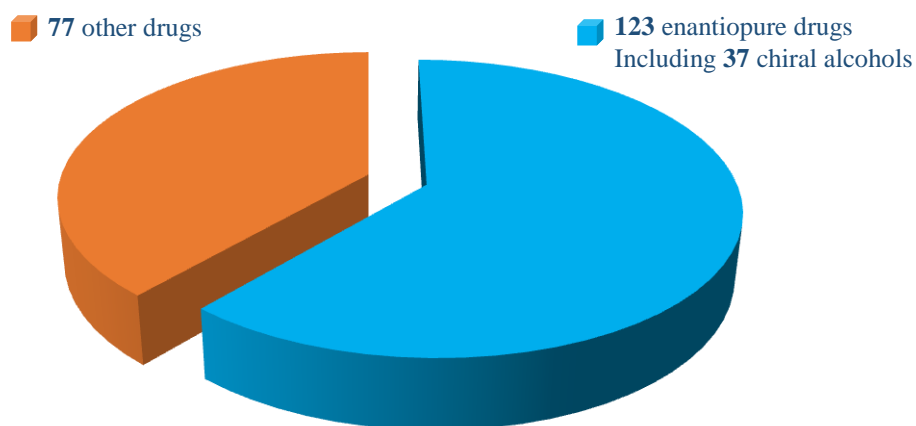


## General introduction

Chirality is now one major topic in academic research as well as in pharmaceutical development. Accounting for their significant work in chirally catalysed hydrogenation and chirally catalysed oxidation reactions, the 2001 Nobel Prize in Chemistry has been awarded to three scientists: W. S. Knowles, K. B. Sharpless and R. Noyori, for their development of asymmetric synthesis using chiral catalysts in the production of single enantiomer drugs or chemicals. Thanks to a wide range of new technologies for chiral separation, US Food and Drug Administration (FDA) recommends the assessments of each enantiomer activity for racemic drugs in body and promotes the development of new chiral drugs as single enantiomers.<sup>1</sup>

Because the use of enantiomerically pure drugs has numerous advantages, such as: (i) an improvement of the therapeutic index through increased potency and selectivity and decreased side-effects; (ii) a faster onset of action; (iii) a reduced propensity for drug-drug interactions, and (iv) the exposition of the patient to a lower dosage, 15 racemate drugs have been successfully switched to the single-enantiomer version from 1994 to 2011.<sup>2</sup>

It is worth noting that among the top 200 pharmaceutical products by prescriptions in 2010, the major part (60%) are chiral molecules under their enantiomerically pure form with 30% of the latter having alcohol moieties.



### Top 200 Pharmaceutical Products by Prescriptions in 2010<sup>3</sup>

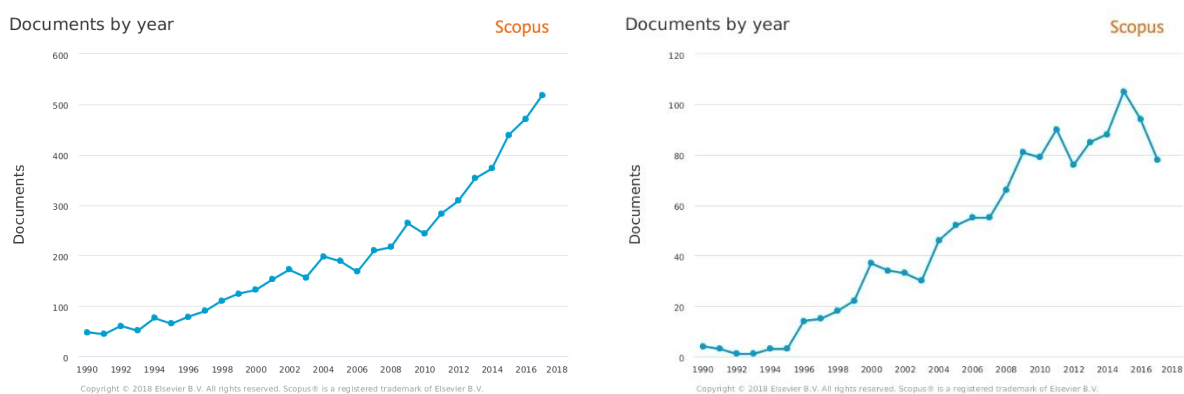
Therefore, the development of efficient synthetic approaches to access these optically

<sup>1</sup> Nguyen, L. A.; He, H.; Pham-Huy, C. *J. Biomed. Sci.* **2006**, *2*, 85.

<sup>2</sup> Calcaterra, A.; D'Acquarica, I. *J. Pharm. Biomed. Anal.* **2018**, *147*, 323.

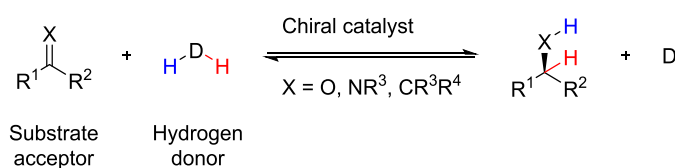
<sup>3</sup> McGrath, N. A.; Brichacek, M.; Njardarson, J. T. *J. Chem. Educ.* **2010**, *87*, 1348.

active alcohols is highly desired. To this end, one of the most direct methods relies on asymmetric reduction of carbonyl compounds to prepare secondary chiral alcohols and in this field, asymmetric hydrogenation (AH) and asymmetric transfer hydrogenation (ATH) appear as powerful tools. By searching the topics “transfer hydrogenation” and “asymmetric transfer hydrogenation” from 1990 to 2017 in Scopus, we can see the trend of yearly publications for both TH and ATH is generally increasing.



(left: TH; right: ATH)

In this manuscript, we will more particularly focus on ATH. Transfer hydrogenation (TH) can be described as the reduction of an unsaturated acceptor substrate (such as ketone, imine or alkene) with the aid of a hydrogen donor  $DH_2$  in the presence of a catalyst. The hydrogen donor  $DH_2$  is then converted into a dehydrogenated by-product D. When chirality is introduced during the reaction by using a chiral catalyst, this process is called asymmetric transfer hydrogenation (ATH).



A broad range of hydrogen donors, typically alcohols, formic acid and its salt can be used, thus avoiding handling of molecular hydrogen. Therefore, asymmetric transfer hydrogenation has received considerable attention because this technology is considered as one of the most powerful, practical, and versatile tools especially to access chiral alcohols and amines in organic synthesis.

Although a number of catalysts have been developed for ATH, the development of more efficient catalysts and new applications using known catalysts are still ongoing.

One aim of this thesis work was to develop new catalytic systems for the ATH of

ketones. Thus, the preparation and evaluation of catalytic performance of a new family of rhodium (III) complexes will be described.

Chiral alcohols bearing multiple stereocenters are important building blocks in pharmaceuticals and natural products. In this manuscript, we will study the ATH reaction combined with a dynamic kinetic resolution (DKR) process of heterocycle ketones and racemic  $\alpha$ -methoxy  $\beta$ -ketoesters to access enantiomerically enriched heterocycle alcohol and diol derivatives.

**PART A:**

**Recent Developments on Transition  
Metal-Catalyzed ATH of Ketones**



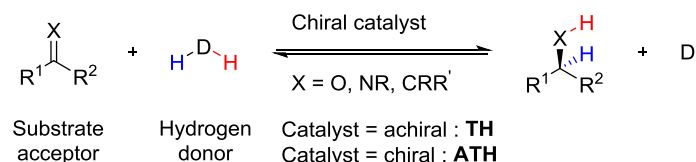


## Part A: Recent Developments on Transition Metal-Catalyzed Asymmetric Transfer Hydrogenation (ATH) of Ketones

### 1. Theoretical background on asymmetric transfer hydrogenation

#### 1.1 Introduction to asymmetric transfer hydrogenation

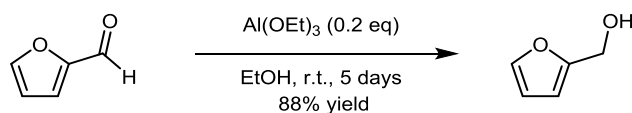
Transfer hydrogenation (TH) can be described as the transfer of a hydride ion and a proton from a hydrogen donor to an unsaturated acceptor substrate. The hydrogen donor  $DH_2$  is then converted into a dehydrogenated by-product D. The reaction is facilitated by a catalyst that will promote the hydride transfer. When a chiral catalyst is used, the reaction is named asymmetric transfer hydrogenation (ATH) (Scheme 1).<sup>4</sup>



**Scheme 1**

This technology has many advantages over traditional hydrogenation reactions. Indeed, it does not require the use of hydrogen gas and high pressure equipment, thus limiting the risks in terms of safety and also in terms of cost.

Historically, the first homogeneous hydrogen transfer reaction was described in 1925, when Meerwein and Schmidt reported the reduction of furfural using an aluminum alkoxide as Lewis acid and ethanol as the hydrogen source (Scheme 2).<sup>5</sup>



**Scheme 2**

This reaction, later known as the Meerwein-Ponndorf-Verley (MPV) reduction, saw its scope broadened thanks to the work of Verley,<sup>6a</sup> Ponndorf<sup>3b</sup> and Lund.<sup>3c</sup> In 1937, Oppenauer

<sup>4</sup> (a) Andersson, P. G.; Munslow, I. J. *Modern Reduction Methods*, Wiley, **2008**, p135. (b) De Vries, J. G.; Elsevier, C. J. *Handbook of Homogeneous Hydrogenation*, Wiley, **2007**, p.585 and p.1215.

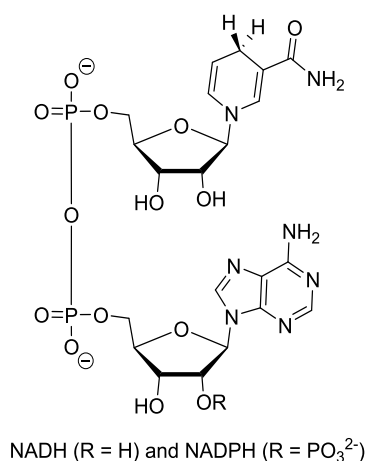
<sup>5</sup> Meerwein, H.; Schmidt, R. *Justus Liebigs Ann. Chem.* **1925**, *444*, 221.

<sup>6</sup> (a) Verley, A. *Bull. Soc. Chim. Fr.* **1925**, *37*, 537. (b) Ponndorf, W. *Angew. Chem.* **1926**, *39*, 138. (c) Lund, H. *Ber. Dtsch. Chem. Ges.* **1937**, *70*, 1520.

studied the reverse reaction, *i.e.* the oxidation reaction.<sup>7</sup> These reactions were subsequently improved with the use of other types of alkoxymetals.<sup>8</sup> The main disadvantage of these two reactions lies in the low catalytic activity obtained with these Lewis acids. Therefore, the introduction of transition metal catalysts for this type of reaction has emerged as a major advantage in ATH.

Mitchell *et al.* reported, in 1964, the reduction of cyclohexanone using the hexachloroiridic acid catalyst  $\text{H}_2\text{IrCl}_6$  in an isopropanol/water solution.<sup>9</sup> The introduction of the Wilkinson catalyst  $[\text{RhCl}(\text{PPh}_3)_3]$  for hydrogen transfer reactions in 1966 also contributed to these advances. Although designed for hydrogenation in the presence of molecular hydrogen, this catalyst has been used extensively in hydrogen transfer catalyzed reactions.<sup>10</sup>

In nature, hydrogen transfer occurs when metabolites are reduced within biological systems. The catalysts responsible for hydrogen transfer are called enzymatic dehydrogenases and are assisted by cofactors that facilitate the transfer of electrons, such as NADH or NADPH (Scheme 3).



Scheme 3

The following bibliographical part will cover the transition metal-catalyzed ATH of ketones.<sup>11</sup>

<sup>7</sup> Oppenauer, R. V. *Recl. Trav. Chim. Pays-Bas* **1937**, 56, 137.

<sup>8</sup> (a) Namy, J. L.; Soupe, J.; Collin, J.; Kagan, H. B. *J. Org. Chem.* **1984**, 49, 2045. (b) Okano, T.; Matsuoka, M.; Konishi, H.; Kiji, J. *Chem. Lett.* **1987**, 181. (c) Campbell, E. J.; Zhou, H.; Nguyen, S. T. *Org. Lett.* **2001**, 3, 2391. (d) Ooi, T.; Miura, T.; Itagaki, Y.; Ichikawa, H.; Maruoka, K. *Synthesis* **2002**, 279. (e) Liu, Y.-C.; Ko, B.-T.; Huang, B.-H.; Lin, C.-C. *Organometallics* **2002**, 21, 2066.

<sup>9</sup> Haddad, Y. M. Y.; Henbest, H. B.; Husbands, J.; Mitchell, T. R. B. *Proc. Chem. Soc.* **1964**, 361.

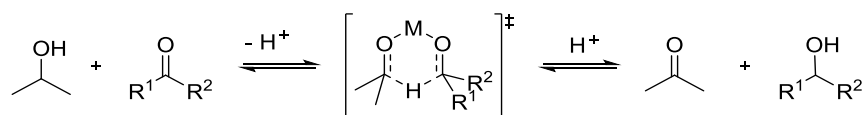
<sup>10</sup> Osborn, J. A.; Jardine, F. H.; Young, J. F.; Wilkinson, G. *J. Chem. Soc. A* **1966**, 1711.

<sup>11</sup> (a) Noyori, R.; Hashiguchi, S. *Acc. Chem. Res.* **1997**, 30, 97. (b) Palmer, M. J.; Wills, M. *Tetrahedron: Asymmetry* **1999**, 10, 2045. (c) Everaere, K.; Mortreux, A.; Carpentier, J.-F. *Adv. Synth. Catal.* **2003**, 345, 67.

### 1.1.1 Mechanisms

Hydrogen transfer can be carried out according to two type of mechanisms<sup>12</sup> depending on the nature of the metal and ligands:

- *Direct transfer mechanism*: this proceeds via a complex in which the donor and the acceptor are linked to the metal. By coordinating with the metal, the hydride acceptor will be activated and thus the nucleophilic attack of the hydride is facilitated. The spatial proximity of the two entities will also facilitate a concerted mechanism via a six-centered transition state without involving a metal-hydride intermediate. This mechanism is not limited to transition metals since this mechanism is proposed for the Meerwein-Ponndorf-Verley reduction (Scheme 4).



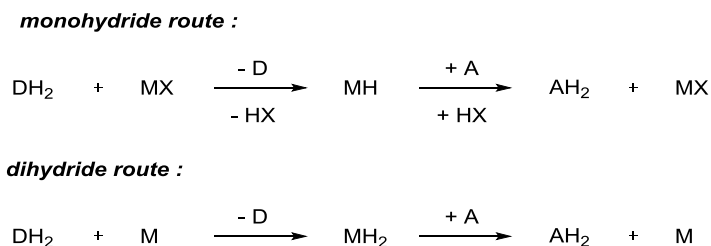
**Scheme 4**

- *Indirect transfer mechanism (hydride pathway)*: this mechanism first involves the transfer of a hydride from a donating molecule to the metal catalyst, leading to the formation of a metal hydride. The hydride is then transferred from the metal centre to the accepting substrate. Thus, the privileged precatalysts with a metal center bearing a strong affinity to hydride, such as ruthenium, rhodium and iridium, follow this type of mechanism. The Lewis acidity of these metals is too weak to sufficiently activate direct hydrogen transfer catalysis and, conversely, the affinity of aluminium (III) to

(d) Gladiali, S.; Alberico, E. *Chem. Soc. Rev.* **2006**, *35*, 226. (e) Ikariya, T.; Blacker, A. J. *Acc. Chem. Res.* **2007**, *40*, 1300. (f) Blacker, A. J., In *Handbook of Homogeneous Hydrogenation*; de Vries, J. G.; Elsevier, C. J., Ed.; Wiley-VCH, Weinheim **2007**, 1215. (g) Wang, C., Wu, X., Xiao, J., *Chem. Asian J.* **2008**, *3*, 1750. (h) Ikariya, T., *Bull. Chem. Soc. Jpn.* **2011**, *84*, 1. (i) Zheng, C., and You, S.-L., *Chem. Soc. Rev.*, **2012**, *41*, 2498. (j) Bartoszewicz, A., Ahlsten, N., Martín-Matute, B., *Chem. Eur. J.* **2013**, *19*, 7274. (k) Slagbrand, T., Lundberg, H., Adolfsson, H., *Chem. Eur. J.* **2014**, *20*, 16102. (l) Slagbrand, T.; Lundberg, H.; Adolfsson, H. *Chem. Eur. J.* **2014**, *20*, 16102. (m) Štefane, B.; Požgan, F. *Catal. Rev.* **2014**, *56*, 82. (n) Foubelo, F.; Nájera, C.; Yus, M. *Tetrahedron: Asymmetry* **2015**, *26*, 769. (o) Wang, D.; Astruc, D. *Chem. Rev.* **2015**, *115*, 6621. (p) Li, Y.-Y., Yu, S.-L., Shen, W.-Y., Gao, J.-X., *Acc. Chem. Res.* **2015**, *48*, 2587. (q) G. Nedden, H.; Zanotti-Gerosa, A.; Wills, M. *Chem. Rec.* **2016**, *16*, 2623. (r) Ayad, T.; Phansavath, P.; Ratovelomanana-Vidal, V. *Chem. Rec.* **2016**, *16*, 2754. (s) Matuška, O., Kindl, M., Kačer, P., in *New Advances in Hydrogenation Process*. Ravanchi, T. M. Ed.; InTech:Croatia; **2017**, p. 37. (t) Matsunami, A., and Kayaki, Y., *Tetrahedron Lett.* **2018**, *59*, 504. (u) Whittlesey, M. K., in *N-Heterocyclic Carbenes in Catalytic Organic Synthesis 1*. Nolan, S. P. Ed.; Science and Synthesis; **2018**, p. 285; (v) Zhang, Z., Butt, N. A., Zhou, M., Liu, D., Zhang, W., *Chin. J. Chem.* **2018**, *36*, 443 and references therein.

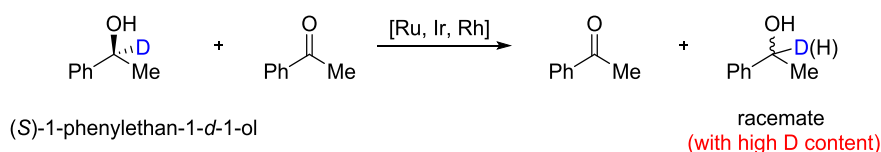
<sup>12</sup> (a) Bäckvall, J.-E. *J. Organomet. Chem.* **2002**, *652*, 105. (b) Clapham, S. E.; Hadzovic, A.; Morris, R. H. *Coord. Chem. Rev.* **2004**, *248*, 2201. (c) Samec, J. S. M.; Bäckvall, J.-E.; Andersson, P. G.; Brandt, P. *Chem. Soc. Rev.* **2006**, *35*, 237.

hydride anion is too low to catalyse indirect hydrogen transfer. For this type of mechanism, a monohydride and a dihydride pathway are possible (Scheme 5).

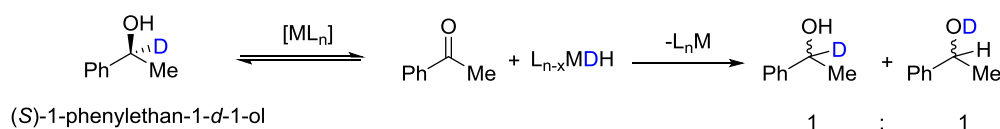


Scheme 5

To well-understand the mono- or dihydride mechanisms for metal-catalyzed transfer reactions, Bäckvall *et al.* have designed an experiment for metal-catalyzed hydrogen transfer reactions.<sup>13</sup> To demonstrate the monohydride mechanism, first, they utilized enantiomerically pure  $\alpha$ -deuterated (*S*)-phenylethanol in the presence of acetophenone with an achiral metal complex as a catalyst precursor. By monitoring and analyzing the deuterium level in the  $\alpha$  position of racemized phenylethanol, they observed that using most of metal catalysts, such as iridium, rhodium and ruthenium complexes, resulted in high deuterium content during the racemized reaction. The results revealed that the nature of the metal as well as that of the ligands were important for the type of mechanism, which could be classified as a monohydride mechanism (Scheme 6). In addition, another experiment has been performed to investigate the dihydride mechanism, which is to racemize an optically active  $\alpha$ -deuterated (*S*) - phenylethanol (Scheme 7). If the catalysts follow the dihydride mechanism, the deuterium will be equally distributed between carbon and oxygen (C–D : O–D = 1 : 1).



Scheme 6

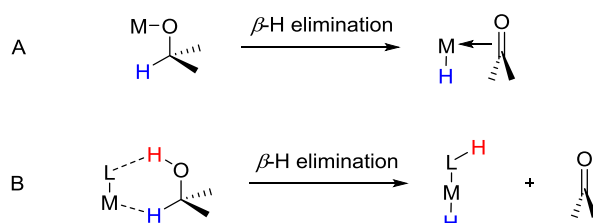


Scheme 7

In addition, there are two types of catalysts operating according to a monohydride

<sup>13</sup> (a) Laxmi, Y. R. S.; Bäckvall, J.-E. *Chem. Commun.* **2000**, 611. (b) Pàmies, O.; Bäckvall, J. E. *Chem. Eur. J.* **2001**, *7*, 5052.

mechanism: those for which the transfer of hydride takes place in the inner sphere of the metal, *i.e.* there will be a direct interaction between the hydrogen donor and the metal during the formation of the hydride metal (Scheme 8, **A**) and those for which the transfer takes place outside the internal sphere of the metal, *i.e.* there will be no direct coordination of the donor on the metal (Scheme 8, **B**).<sup>12c</sup>



Scheme 8

After this short description of the different possible mechanisms for asymmetric transfer hydrogenation, we will focus on the ligands that can be used with transition metals, and will pay a particular attention to the bifunctional ligands developed by the Noyori's group.

### 1.1.2 Ligands

Numerous ligands can be used for ATH, associated with transition metals such as iridium, rhodium or ruthenium. Their structures are quite diverse, such as bidentate, tridentate or tetradentate. The following section is a non-exhaustive description of selected ligands used for ATH of acetophenone as a point of comparison (Scheme 9).<sup>11b</sup>

Generally, chiral diphosphines such as DIOP<sup>14</sup> **L1** led to moderate conversions and enantioselectivities under high temperature conditions.<sup>15</sup> Phenanthroline-derived ligands such as **L2** showed low to moderate enantioselectivities for transfer hydrogenation of acetophenone.<sup>16</sup> The introduction of the tetrahydro-bis(oxazole) **L3** ligand by Pfaltz and co-workers<sup>17</sup> allowed moderate to good enantioselectivities for different aromatic ketones. Tridentate ligands *P,N,P* **L7**<sup>18</sup>, *N,N,N* **L8**<sup>19</sup> or *N,P,N* **L9**<sup>20</sup> were used by Zhang's group leading

<sup>14</sup> (a) Dang, T. P.; Kagan, H. B. *J. Chem. Soc. D*, **1971**, 7, 481. (b) Kagan, H. B.; Dang, T. P. US3798241, **1974**.

<sup>15</sup> (a) Bianchi, M.; Matteoli, U.; Menchi, G.; Frediani, P.; Pratesi, S.; Piacenti, F.; Botteghi, C. *J. Organomet. Chem.* **1980**, 198, 73. (b) Krause, H. W.; Bhatnagar, A. K. *J. Organomet. Chem.* **1986**, 302, 265. (c) Spogliarich, R.; Kašpar, J.; Graziani, M.; Morandini, F. *J. Organomet. Chem.* **1986**, 306, 407. (e) Khai, B. T.; Arcelli, A. *Tetrahedron Lett.* **1996**, 37, 6599. (f) Barbaro, P.; Bianchini, C.; Togni, A. *Organometallics* **1997**, 16, 3004.

<sup>16</sup> (a) Botteghi, C.; Chelucci, C.; Chessa, G.; Delogu, G.; Gladiali, S.; Soccolini, F. *J. Organomet. Chem.* **1986**, 304, 217. (b) Gladiali, S.; Pinna, L.; Delogu, G.; De Martin, S.; Zassinovich, G.; Mestroni, G. *Tetrahedron: Asymmetry* **1990**, 1, 635.

<sup>17</sup> Müller, D.; Umbricht, G.; Weber, B.; Pfaltz, A. *Helv. Chim. Acta* **1991**, 74, 232.

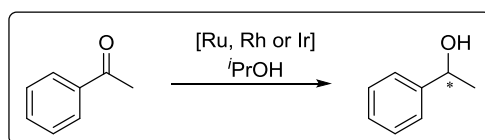
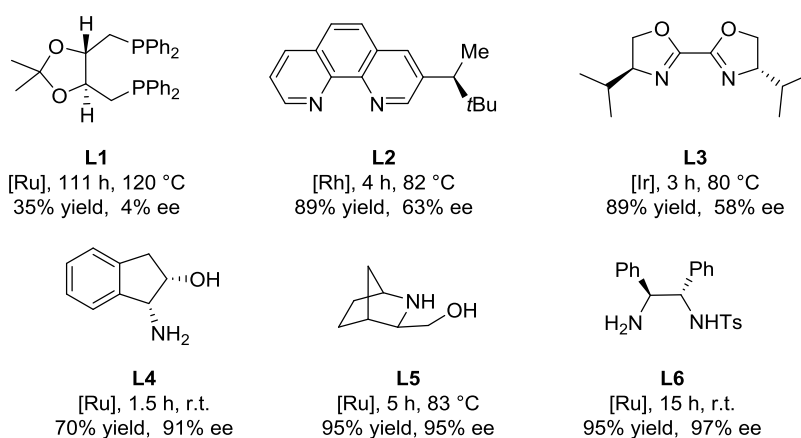
<sup>18</sup> Jiang, Q.; Van Plew, D.; Murtuza, S.; Zhang, X. *Tetrahedron Lett.* **1996**, 37, 797.

<sup>19</sup> Jiang, Y.; Jiang, Q.; Zhang, X. *J. Am. Chem. Soc.* **1998**, 120, 3817.

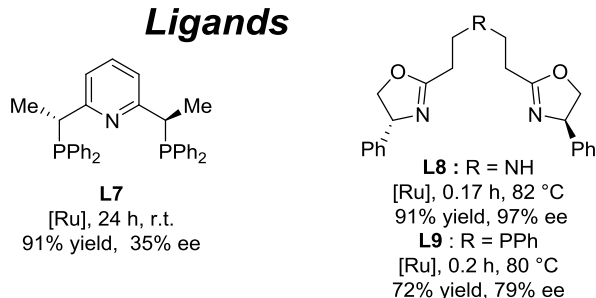
to weak to excellent enantioselectivities. Tetradentate ligands such as **L10** and **L11** have been developed.<sup>21</sup> These examples of tridentate or tetradentate ligands have demonstrated the crucial role of the NH group on the reactivity and stereoselectivity.<sup>22</sup> Indeed, ligands with an NH group such as **L8** or **L10** showed an acceleration effect in reactivity as well as better stereoselectivities as compared to ligands without an NH group such as **L9** or **L11** (Scheme 9).

Effective ligands in terms of catalytic performance and substrate compatibility are 1,2-aminoalcohols<sup>23</sup> such as **L4**,<sup>24</sup> **L5**,<sup>25</sup> and the monotosylated diamine **L6** developed by Noyori's group<sup>26</sup> (Scheme 9).

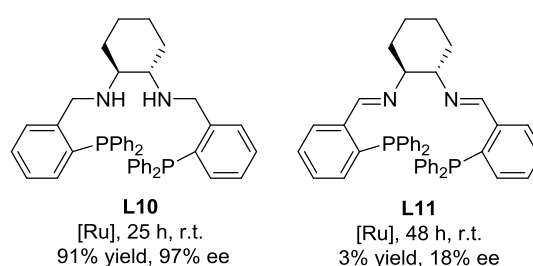
### Bidentate Ligands



### Tridentate Ligands



### Tetradentate Ligands



Scheme 9

<sup>20</sup> Jiang, Y.; Jiang, Q.; Zhu, G.; Zhang, X. *Tetrahedron Lett.* **1997**, *38*, 215.

<sup>21</sup> Gao, J.; Ikariya, T.; Noyori, R. *Organometallics* **1996**, *15*, 1087.

<sup>22</sup> Zhao, B.; Han, Z.; Ding, K. *Angew. Chem. Int. Ed.* **2013**, *52*, 4744.

<sup>23</sup> Takehara, J.; Hashiguchi, S.; Fujii, A.; Inoue, S.; Ikariya, T.; Noyori, R. *Chem. Commun.* **1996**, 233.

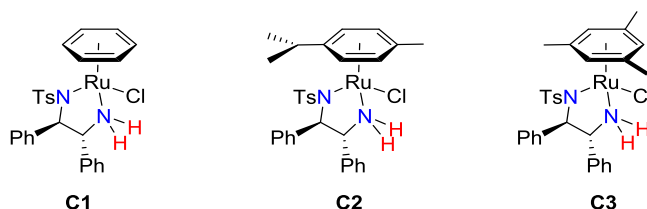
<sup>24</sup> Palmer, M.; Walsgrove, T.; Wills, M. *J. Org. Chem.* **1997**, *62*, 5226.

<sup>25</sup> Alonso, D. A.; Guijarro, D.; Pinho, P.; Temme, O.; Andersson, P. G. *J. Org. Chem.* **1998**, *63*, 2749.

<sup>26</sup> Hashiguchi, S.; Fujii, A.; Takehara, J.; Ikariya, T.; Noyori, R. *J. Am. Chem. Soc.* **1995**, *117*, 7562.

### 1.1.3 Noyori's bifunctional catalysts

The importance of the basic NH group on the ligand led Noyori's group to develop bifunctional metal-ligand catalysts **C1–C3** (Scheme 10).<sup>11a,27</sup>



Scheme 10

### 1.1.4 General mechanism

The proposed mechanism for the ATH of ketone derivatives catalyzed by the complexes developed by Noyori and Ikariya involves a concerted transfer of the proton and hydride from the catalytic species mono-hydride [RuH( $\eta^6$ -arene)((*R,R*)-TsDPEN)] **A** to the substrate via a cyclic six-center transition state **B** to release the desired alcohol, and the 16-electron Ru (II) intermediate [Ru( $\eta^6$ -arene)((*R,R*)-TsDPEN)] **C** (Scheme 11).

The NH unit forms a hydrogen bond with the oxygen atom of the carbonyl group which stabilizes the transition state **B**. Therefore, the presence of the NH group within the ligand core is of great importance for obtaining good bifunctional catalytic performances. Indeed, the use of *N,N*-dimethyl ligands led to ruthenium complexes which proved to be totally inactive as catalysts.<sup>11a</sup>

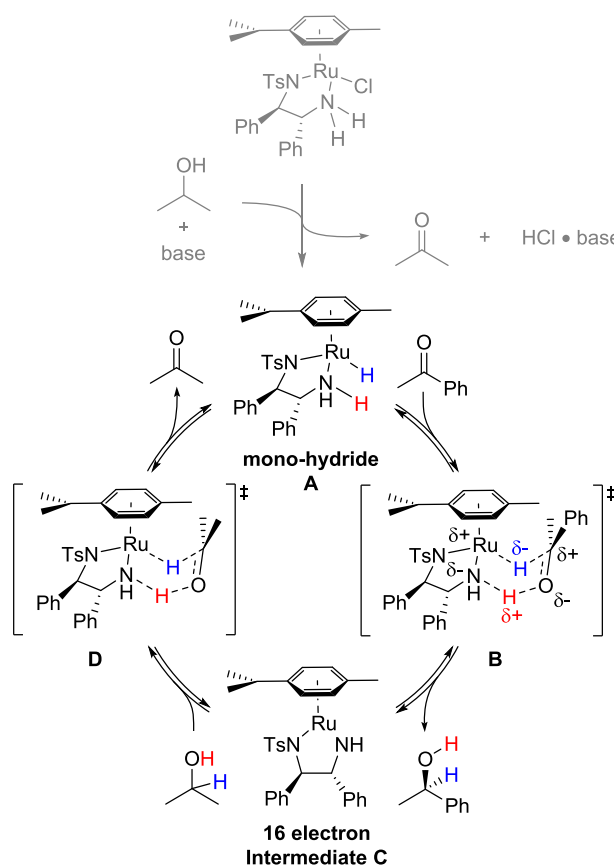
The proton and hydride originating from isopropanol are then delivered to the complex **C**, via a six-center cyclic transition state **D**, respectively to the amine and the metal, to release acetone and regenerate the initial catalytic Ru (II) species [RuH( $\eta^6$ -arene)((*R,R*)-TsDPEN)] **A** mono-hydride (Scheme 11).

This mechanism has been confirmed by numerous studies (chemical, theoretical and kinetic). Indeed, complexes **A** and **C** have been isolated, characterized and successfully tested

<sup>27</sup> (a) Fujii, A.; Hashiguchi, S.; Uematsu, N.; Ikariya, T.; Noyori, R. *J. Am. Chem. Soc.* **1996**, *118*, 2521. (b) Haack, K.-J.; Hashiguchi, S.; Fujii, A.; Ikariya, T.; Noyori, R. *Angew. Chem. Int. Ed.* **1997**, *36*, 285. (c) Matsumura, K.; Hashiguchi, S.; Ikariya, T.; Noyori, R. *J. Am. Chem. Soc.* **1997**, *119*, 8738. (d) Noyori, R.; Ohkuma, T. *Angew. Chem. Int. Ed.* **2001**, *40*, 40. (e) Noyori, R.; Yamakawa, M.; Hashiguchi, S. *J. Org. Chem.* **2001**, *66*, 7931. (f) Noyori, R. *Angew. Chem. Int. Ed.* **2002**, *41*, 2008. (g) Ikariya, T.; Murata, K.; Noyori, R. *Org. Biomol. Chem.* **2006**, *4*, 393.

in catalysis.<sup>27b</sup> Several theoretical studies<sup>27f,28</sup> confirmed that the 6-center transition state was the lowest energy transition state.

Detailed structural analyzes of the catalyst and reaction intermediates showed that the effective catalytic species was the 16-electron complex  $[\text{Ru}(\eta^6\text{-arene})((R,R)\text{-TsDPEN})]$  **C**. In particular, it shows a Ru-N bond length comprised between a single bond and a triple bond.<sup>27b</sup> Because of the nature of this Ru-N bond, this electron-deficient complex readily dehydrogenates isopropanol to deliver the ruthenium monohydride complex  $[\text{RuH}(\eta^6\text{-arene})((R,R)\text{-TsDPEN})]$  **A** as a single diastereoisomer.



Scheme 11

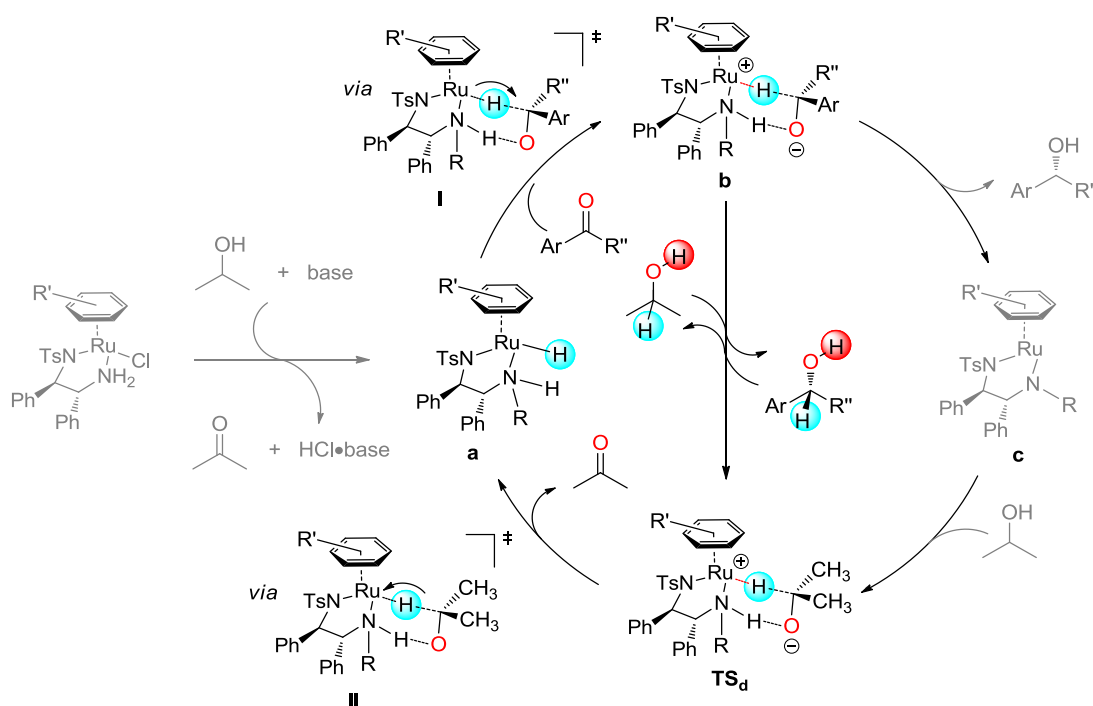
Throughout the catalytic process, the stereochemistry on the metal center is thus preserved and the carbonyl compound is activated without interacting directly with the metal center. It is therefore a hydrogen transfer mechanism named as "outer sphere" because the ketone substrate and the hydride donor remain outside the coordination sphere of the metal.

<sup>28</sup> (a) Alonso, D. A.; Brandt, P.; Nordin, S. J. M.; Andersson, P. G. *J. Am. Chem. Soc.* **1999**, *121*, 9580. (b) Yamakawa, M.; Ito, H.; Noyori, R. *J. Am. Chem. Soc.* **2000**, *122*, 1466. (c) Petra, D.; Reek, J.; Handgraaf, J.; Meijer, E.; Dierkes, P.; Kamer, P.; Brussee, J.; Schoemaker, H.; van Leeuwen P. W. N. M. *Chem. Eur. J.* **2000**, *6*, 2818. (d) Dub, P. A.; Ikariya, T. *J. Am. Chem. Soc.* **2013**, *135*, 2604.



In 2003, the Casey's group studied the kinetic isotopic effect of the dehydrogenation of isopropanol by the Ru (II) catalytic intermediate of  $[\text{Ru}(\eta^6\text{-}p\text{-cymene})((S,S)\text{-TsDPEN})]$  and found that both hydride transfer and proton transfer occur simultaneously and reversibly,<sup>29</sup> which is consistent with the bifunctional concerted mechanism *via* a six-center transition state suggested by Noyori and co-workers.

However, Dub and Gordon's group proposed in 2016 a revised catalytic cycle for the ATH of aromatic ketones in propan-2-ol using the Noyori–Ikariya (pre)catalyst. First, as proposed in early studies, the oxidation state of the metal does not change during the catalytic reaction and the ketone derivatives are indeed reduced within the outer sphere, *i.e.* without initial coordination of the substrate to the metal. However, this reduction proceeds *via* a one-bond type hydride ( $\text{H}^-$ ) transfer to generate the ion-pair intermediate (complex **b**, Scheme 12). The corresponding transition state ( $\text{TS}_d$ ) has been found to be the enantio- and typically rate-determining step (Scheme 12).<sup>28d,30</sup>



Scheme 12

For the transfer hydrogenation process with the Noyori–Ikariya's catalyst in isopropanol, there are two pathways to neutralize the anion of the ion-pair product **b** ("starting" branching point) and regenerate the catalyst. The latter proceeds *via* a one-bond type C–H proton plus two

<sup>29</sup> Casey, C. P.; Johnson, J. B. *J. Org. Chem.* **2003**, *68*, 1998.

<sup>30</sup> Dub, P. A.; Gordon, J. C. *Dalton Trans.* **2016**, *45*, 6756.

electron transfer from the isopropoxide anion to the cation within the ion-pair of type **d** (“closing” branching point), Scheme 12. In this process, the hydrogen atom is repolarized as follows  $H^+ \rightarrow H^-$ . In one pathway, the source of the proton that neutralizes the anion in **b** is the ligand, thus the N–H ligand is chemically non-innocent. This mechanism for ketone reduction can be denoted as a step-wise metal–ligand bifunctional in order to explain the difference with the conventional mechanism, which is concerted and realized only in the gas-phase. In the second path, the source of the proton used to neutralize the anion in **b** is propan-2-ol, therefore the N–H ligand is chemically innocent in this case. This is the same type of  $H^-/H^+$  outer-sphere hydrogenation, except that the source of the proton used to neutralize the anion is now a protic solvent molecule. The crossover of these two reaction pathways is possible and likely takes place in all transfer hydrogenation processes catalyzed by bifunctional catalysts. Although the relative contribution of each mechanism is computationally intractable,<sup>28d</sup> the neutralization of the anion within ion-pair **b** by a protic solvent seems to be more probable, especially with increasing reaction medium polarity, *e.g.*, if the reaction is carried out in more polar formic acid or water.<sup>28d</sup> In fact, Car–Parrinello molecular dynamics studies of Meijer<sup>31</sup> suggest that the catalytic reaction in water<sup>32,33</sup> proceeds exclusively or largely through, what we call here a  $H^-/H^+$  outer-sphere hydrogenation mechanism.

### 1.1.5 Origins of enantioselectivity

The enantioselectivity of ATH for aromatic ketones catalyzed by the Noyori-Ikariya complex originates from the stabilization of the favorable transition state through multiple C–H $\cdots\pi$  electrostatic interactions<sup>28d,34</sup> between the electron-deficient proton of the arene attracted by the ruthenium metal center and the electron-enriched carbons of the aromatic ring of the substrate, as well as from the destabilization of the unfavorable diastereomeric transition state via lone pair(s)– $\pi$  repulsion<sup>35</sup> between the SO<sub>2</sub> group and the  $\pi$ -cloud of the approaching aromatic ketone as shown in Scheme 13.

---

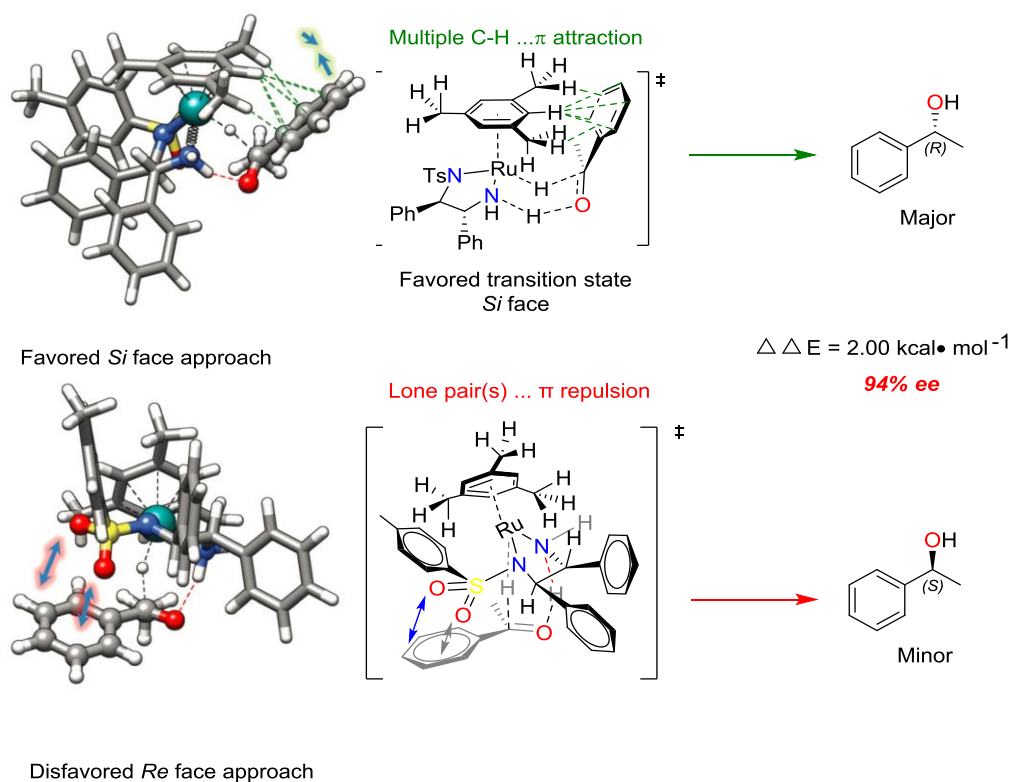
<sup>31</sup> Pavlova, A.; Meijer, E. J. *ChemPhysChem* **2012**, *13*, 3492.

<sup>32</sup> Wu, X.; Liu, J.; Di Tommaso, D.; Iggo, J. A.; Catlow, C. R. A.; Bacsa, J.; Xiao, J. *Chem. Eur. J.* **2008**, *14*, 7699.

<sup>33</sup> Tanis, S. P.; Evans, B. R.; Nieman, J. A.; Parker, T. T.; Taylor, W. D.; Heasley, S. E.; Herrinton, P. M.; Perrault, W. R.; Hohler, R. A.; Dolak, L. A.; Hesterf, M. R.; Seest, E. P. *Tetrahedron: Asymmetry* **2006**, *17*, 2154.

<sup>34</sup> Matsuoka, A.; Sandoval, C. A.; Uchiyama, M.; Noyori, R.; Naka, H. *Chem. Asian J.* **2015**, *10*, 112.

<sup>35</sup> Mooibroek, T. J.; Gamez, P.; Reedijk, J. *CrystEngComm* **2008**, *10*, 1501.



Scheme 13

Wills group undertook a comparative study<sup>36</sup> to understand the importance of the following parameters:

- The *anti* diamine configuration of the diamine
- The disubstitution of the diamine
- Which stereogenic center is involved in the asymmetric induction?

The results are gathered in the table below (Table 1).

Table 1. Ru-catalyzed ATH of acetophenone

Entry	Ligand	Time	Conv./ %	Ee/%
1	<b>I</b>	22 h	100	98 ( <i>R</i> )
2	<b>II</b>	220 h	32	70 ( <i>S</i> )
3	<b>III</b>	48 h	95	69 ( <i>S</i> )
4	<b>IV</b>	13 days	46	33 ( <i>R</i> )

<sup>36</sup> Hayes, A.; Clarkson, G.; Wills, M. *Tetrahedron: Asymmetry* **2004**, *15*, 2079.

Based on experimental results, better stereoselectivities are obtained when the diamine is disubstituted (Entries 1 and 2 vs. entries 3 and 4). When the ligand **II** presents a (*R,S*)-configuration, a reversed configuration for 1-phenyl-ethanol is observed (Entries 1 and 2). If the ligand has only one stereogenic center, the alcohol will have the same configuration as the ligand (Entries 3 and 4). However, when the ligand has two stereogenic centers, the alcohol will follow the stereochemistry of the stereocenter bearing the tosylated amine (Entries 1 and 2). Therefore, the chirality of the final product seems to be determined by the absolute configuration of the tosylated amine.

### 1.1.6 Other catalysts for asymmetric transfer hydrogenation

The excellent performances of the Noyori-Ikariya ruthenium(II) precatalysts **C1-C3** have prompted other research groups to develop different types of ruthenium complexes, as well as rhodium and iridium precatalysts containing an NH group (Scheme 14, 15, selected examples).

In 2002, Zhou's group described the **C4** complex with a chiral tetrahydroquinolinyl-oxazoline ligand for ATH of aromatic ketones with moderate enantioselectivities (46–83%) (Scheme 14).<sup>37</sup>

Since 2004, Wills *et al.* introduced various ruthenium complexes (**C5**, **C7**<sup>38</sup>, **C6**,<sup>39</sup> **C8**<sup>40</sup> and **C9**<sup>41</sup>), as well as rhodium precatalysts (**C10**,<sup>42a</sup> **C11**,<sup>42b</sup> **C12**<sup>43</sup>) in which the aminoalcohol or diamine unit is linked to the arene with an alkyl or a benzyl tether. These diamine containing complexes are more stable thanks to a three-point anchorage to the metal constraining the free rotation of the arene ring and allowing control of the spatial positions of the substituents on the complex. For example, the tethered complex **C7** gave excellent conversions and enantioselectivities, with shorter reaction time than the untethered Noyori's complex **C3** in the

---

<sup>37</sup> Zhou, Y.-B.; Tang, F.-Y.; Xu, H.-D.; Wu, X.-Y.; Ma, J.-A.; Zhou, Q.-L. *Tetrahedron: Asymmetry* **2002**, *13*, 469.

<sup>38</sup> (a) Hannedouche, J.; Clarkson, G. J.; Wills, M. *J. Am. Chem. Soc.* **2004**, *126*, 986. (b) Cheung, F. K. K.; Hayes, A. M.; Hannedouche, J.; Yim, A. S. Y.; Wills, M. *J. Org. Chem.* **2005**, *70*, 3188.

<sup>39</sup> Hayes, A. M.; Morris, D. J.; Clarkson, G. J.; Wills, M. *J. Am. Chem. Soc.* **2005**, *127*, 7318.

<sup>40</sup> (a) Cheung, F. K.; Lin, C.; Minissi, F.; Crivillé, A. L.; Graham, M. A.; Fox, D. J.; Wills, M. *Org. Lett.* **2007**, *9*, 4659. (b) Cheung, F. K.; Hayes, A. M.; Morris, D. J.; Wills, M. *Org. Biomol. Chem.* **2007**, *5*, 1093. (c) Soni, R.; Jolley, K. E.; Clarkson, G. J.; Wills, M. *Org. Lett.* **2013**, *15*, 5110.

<sup>41</sup> Martins, J. E. D.; Morris, D. J.; Tripathi, B.; Wills, M. *J. Organomet. Chem.* **2008**, *693*, 3527.

<sup>42</sup> (a) Cross, D. J.; Houson, I.; Kawamoto, A. M.; Wills, M. *Tetrahedron Lett.* **2004**, *45*, 843. (b) Matharu, D. S.; Morris, D. J.; Kawamoto, A. M.; Clarkson, G. J.; Wills, M. *Org. Lett.* **2005**, *7*, 5489.

<sup>43</sup> (a) Matharu, D. S.; Morris, D. J.; Clarkson, G. J.; Wills, M. *Chem. Commun.* **2006**, 3232. (b) Matharu, D. S.; Martins, J. E. D.; Wills, M. *Chem. Asian J.* **2008**, *3*, 1374.

ATH of ketones<sup>44</sup> (Scheme 14).

In 2011, Ikariya's group demonstrated the effectiveness of ruthenium catalysts (**C13a** and **C13b**) bearing an ether tether for the ATH of various aromatic ketones with 84–99% ee.<sup>45</sup> In 2013, Mohar's group reported a series of sulfonamide tethered ruthenium complexes,<sup>46</sup> such as **C14**, which has been demonstrated to be active in the ATH of aromatic ketones with high yields and enantioselectivities (Scheme 14).

To fulfill the principles of green chemistry,<sup>47</sup> an immobilized version of the ruthenium(II) precatalyst (**C15**) has been synthesized.<sup>48</sup> Similarly, water-soluble ruthenium (**C16**) and iridium (**C17**) catalysts have been prepared by Deng's<sup>49</sup> and Carreira's<sup>50</sup> groups, enabling the reduction of  $\alpha$ -functionalized acetophenones, and  $\beta$ -ketoesters in the presence of sodium formate and/or formic acid in water with excellent enantioselectivities up to 99%. In most cases, the stereoselectivities observed in water were better than those obtained using formic acid/triethylamine azeotropic mixture in an organic solvent (Scheme 14).

<sup>44</sup> Morris, D. J.; Hayes, A. M.; Wills, M. J. *Org. Chem.* **2006**, *71*, 7035.

<sup>45</sup> (a) Touge, T.; Hakamata, T.; Nara, H.; Kobayashi, T.; Sayo, N.; Saito, T.; Kayaki, Y.; Ikariya, T. *J. Am. Chem. Soc.* **2011**, *133*, 14960. (b) Ikariya, T. *Bull. Chem. Soc. Jpn.* **2011**, *84*, 1. (c) Parekh, V.; Ramsden, J. A.; Wills, M. *Catal. Sci. Technol.* **2012**, *2*, 406.

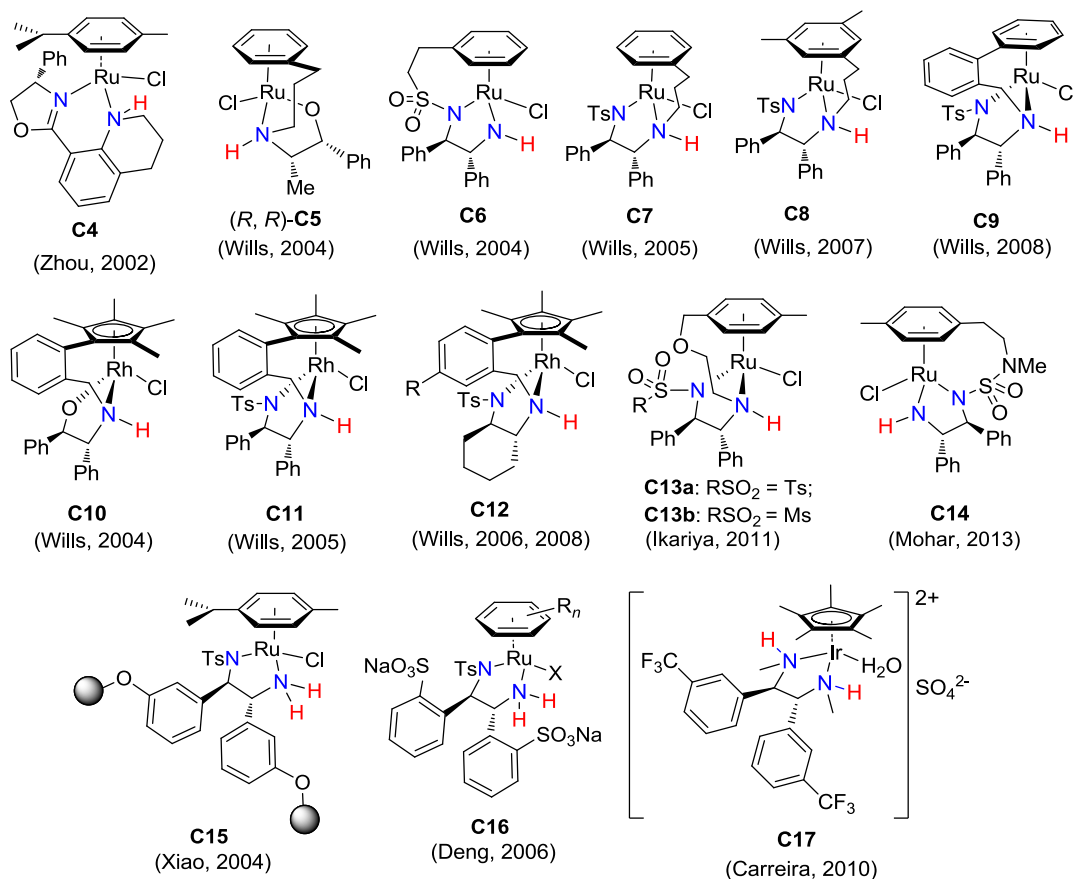
<sup>46</sup> (a) Kišić, A.; Stephan, M.; Mohar, B. *Org. Lett.* **2013**, *15*, 1614. (b) Kišić, A.; Stephan, M.; Mohar, B. *Adv. Synth. Catal.* **2014**, *356*, 3193.

<sup>47</sup> Anastas, P. T.; Warner, J. C. *Green Chemistry: Theory and Practice*, Oxford University Press: New York, **1998**, p.30.

<sup>48</sup> (a) Li, X.; Wu, X.; Chen, W.; Hancock, F. E.; King, F.; Xiao, J. *Org. Lett.* **2004**, *6*, 3321. (b) Li, X.; Chen, W.; Hems, W.; King, F.; Xiao, J. *Tetrahedron Lett.* **2004**, *45*, 951.

<sup>49</sup> Wu, J.; Wang, F.; Ma, Y.; Cui, X.; Cun, L.; Zhu, J.; Deng, J.; Yu, B. *Chem. Commun.* **2006**, 1766.

<sup>50</sup> (a) Soltani, O.; Ariger, M. A.; Vázquez-Villa, H.; Carreira, E. M. *Org. Lett.* **2010**, *12*, 2893. (b) Vázquez-Villa, H.; Reber, S.; Ariger, M. A.; Carreira, E. M. *Angew. Chem. Int. Ed.* **2011**, *50*, 8979. (c) Ariger, M. A.; Carreira, E. M. *Org. Lett.* **2012**, *14*, 4522.



Scheme 14

Ruthenium and rhodium precatalysts with a diamino-phosphine ligand have been successfully used by the Baratta's (**C18**),<sup>51</sup> Morris's (**C19**)<sup>52</sup> and Mikami's (**C20**)<sup>53</sup> groups for the ATH of various ketones (Scheme 15).

Metallacycles such as **C21**<sup>54</sup> or **C22**<sup>55</sup> were shown to be active and enantioselective for the reduction of prochiral ketones (Scheme 15).

The rhodium (**C23**) and iridium (**C24**) analogues of the Noyori's ruthenium catalyst also displayed excellent activities for ATH of aromatic ketones (84–99% ee).<sup>56</sup> The Lin and Xu's group reported that ruthenium catalysts with an unsymmetric diamine ligand such as **C25**

<sup>51</sup> (a) Baratta, W.; Chelucci, G.; Herdtweck, E.; Magnolia, S.; Siega, K.; Rigo, P. *Angew. Chem. Int. Ed.* **2007**, *46*, 7651.

<sup>52</sup> Guo, R.; Elpelt, C.; Chen, X.; Song, D.; Morris, R. H. *Chem. Commun.* **2005**, 3050.

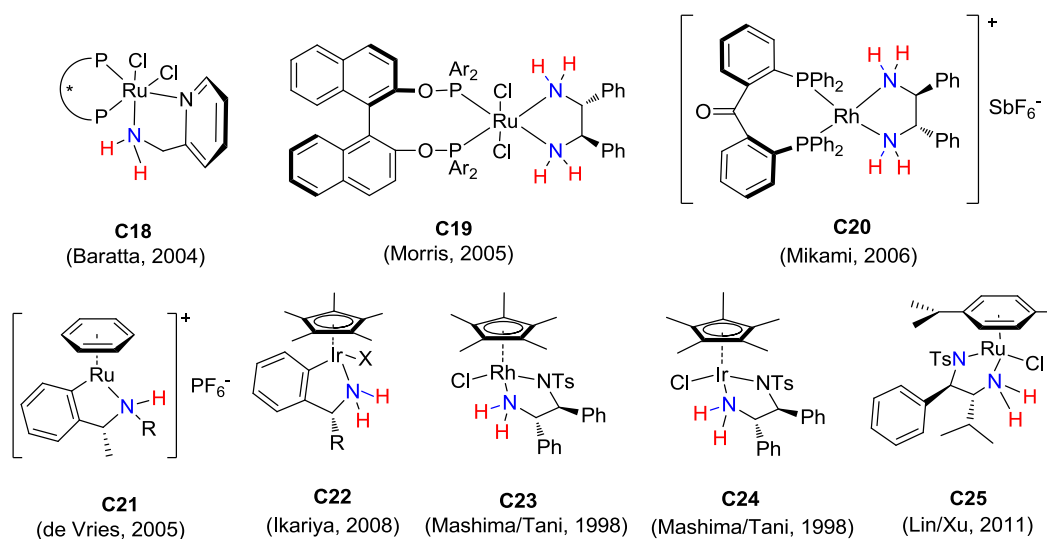
<sup>53</sup> Mikami, K.; Wakabayashi, K.; Yusa, Y.; Aikawa, K. *Chem. Commun.* **2006**, 2365.

<sup>54</sup> Sortais, J.; Ritleng, V.; Voelklin, A.; Holuigue, A.; Smail, H.; Barloy, L.; Sirlin, C.; Verzijl, G. K. M.; Boogers, J. A. F.; de Vries, A. H. M.; de Vries, J. G.; Pfeffer, M. *Org. Lett.* **2005**, *7*, 1247.

<sup>55</sup> Arita, S.; Koike, T.; Kayaki, Y.; Ikariya, T. *Organometallics* **2008**, *27*, 2795.

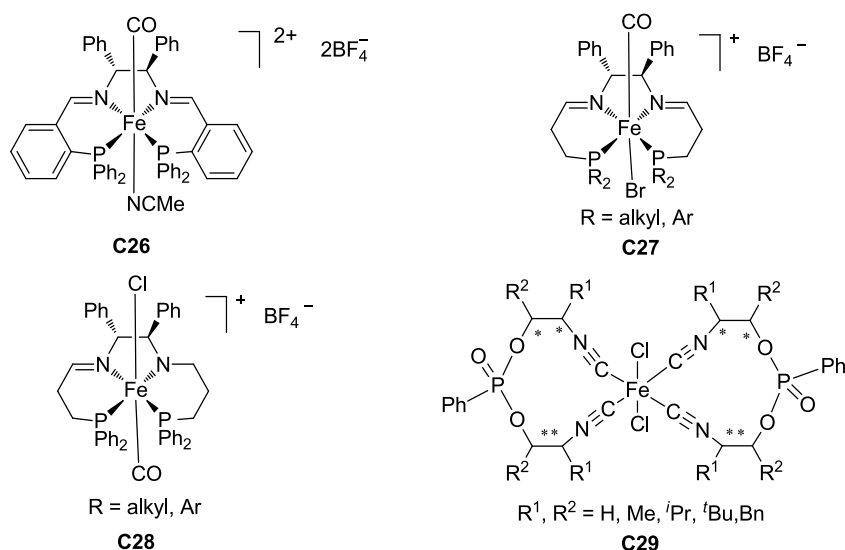
<sup>56</sup> (a) Mashima, K.; Abe, T.; Tani, K. *Chem. Lett.* **1998**, 1199. (b) Mashima, K.; Abe, T.; Tani, K. *Chem. Lett.* **1998**, 1201.

induce excellent enantioselectivities<sup>57</sup> (Scheme 15).



**Scheme 15**

Iron catalysts such as **C26**,<sup>58</sup> **C27**,<sup>59</sup> **C28**<sup>60</sup> and **C29**<sup>61</sup> have also been successfully used for the ATH of ketones (Scheme 16).



<sup>57</sup> Zhang, B.; Wang, H.; Lin, G.; Xu, M. *Eur. J. Org. Chem.* **2011**, 4205.

<sup>58</sup> (a) Meyer, N.; Lough, A. J.; Morris, R. H. *Chem. Eur. J.* **2009**, *15*, 5605. (b) Morris, R. H. *Chem. Soc. Rev.* **2009**, *38*, 2282. (c) Mikhailine, A. a; Maishan, M. I.; Lough, A. J.; Morris, R. H. *J. Am. Chem. Soc.* **2012**, *134*, 12266. (d) Gopalaiah, K. *Chem. Rev.* **2013**, *113*, 3248. (e) Riener, K.; Haslinger, S.; Raba, A.; Högerl, M. P.; Cokoja, M.; Herrmann, W. a; Kühn, F. E. *Chem. Rev.* **2014**, *114*, 5215.

<sup>59</sup> (a) Lagaditis, P. O.; Lough, A. J.; Morris, R. H. *J. Am. Chem. Soc.* **2011**, *133*, 9662. (b) Sues, P. E.; Lough, A. J.; Morris, R. H. *Organometallics* **2011**, *30*, 4418. (c) Sues, P. E.; Demmans, K. Z.; Morris, R. H. *Dalton Trans.* **2014**, 43,7650.

<sup>60</sup> (a) Mikhailine, A.; Lough, A. J.; Morris, R. H. *J. Am. Chem. Soc.* **2009**, *131*, 1394. (b) Zuo, W.; Tauer, S.; Prokopchuk, D. E.; Morris, R. H. *Organometallics* **2014**, *33*, 5791; (c) Zuo, W.; Lough, A. J.; Li, Y. F.; Morris, R. H. *Science* **2013**, *342*, 1080.

<sup>61</sup> Naik, A.; Maji, T.; Reiser, O. *Chem. Commun.* **2010**, 4475.

## Scheme 16

## 1.1.7 The various hydrogen sources

## 1.1.7.1 Short description

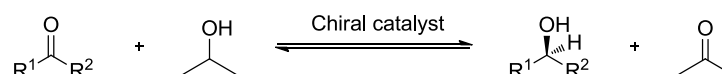
By definition,<sup>4</sup> hydrogen transfer is a reaction in which two hydrogens of a hydrogen donor (other than molecular hydrogen) are transferred to an acceptor substrate. Theoretically, the hydrogen donor could be any compound that can transfer its hydrogens in the presence of a catalyst and under appropriate conditions. Another requirement is that the hydrogen donor must have an affinity with the catalytic center, but this affinity should not be too strong once the hydrogen transfer has been effected. The choice of the hydrogen donor therefore depends on a number of parameters such as the type of reaction (Meerwein-Ponndorf-Verley or Oppenauer reaction catalyzed by a transition metal), its solubility in the reaction medium or its ability to dissolve all the reagents, its influence on the equilibrium of the reaction, the nature of the molecule obtained after dehydrogenation, the nature of the functional group to be reduced, the temperature of the reaction, *etc.*

## 1.1.7.2 Examples of hydrogen donors

*In this section, we will only focus on the sources of hydrogen used for the reduction of ketones. Isopropanol and formic acid (and its salts) are the most frequently used sources of hydrogen for hydrogen transfer because of their low cost and low toxicity.*

Isopropanol:

When isopropanol is used as a reducing agent, the dehydrogenation product is acetone, a non-toxic compound, making the reduction reaction reversible, which is the main disadvantage of using this donor. This is why a large excess is often necessary to shift the equilibrium of the reaction. Isopropanol is often used as a solvent because of the stability of the catalysts in this solvent, which results in excellent conversions (Scheme 17).

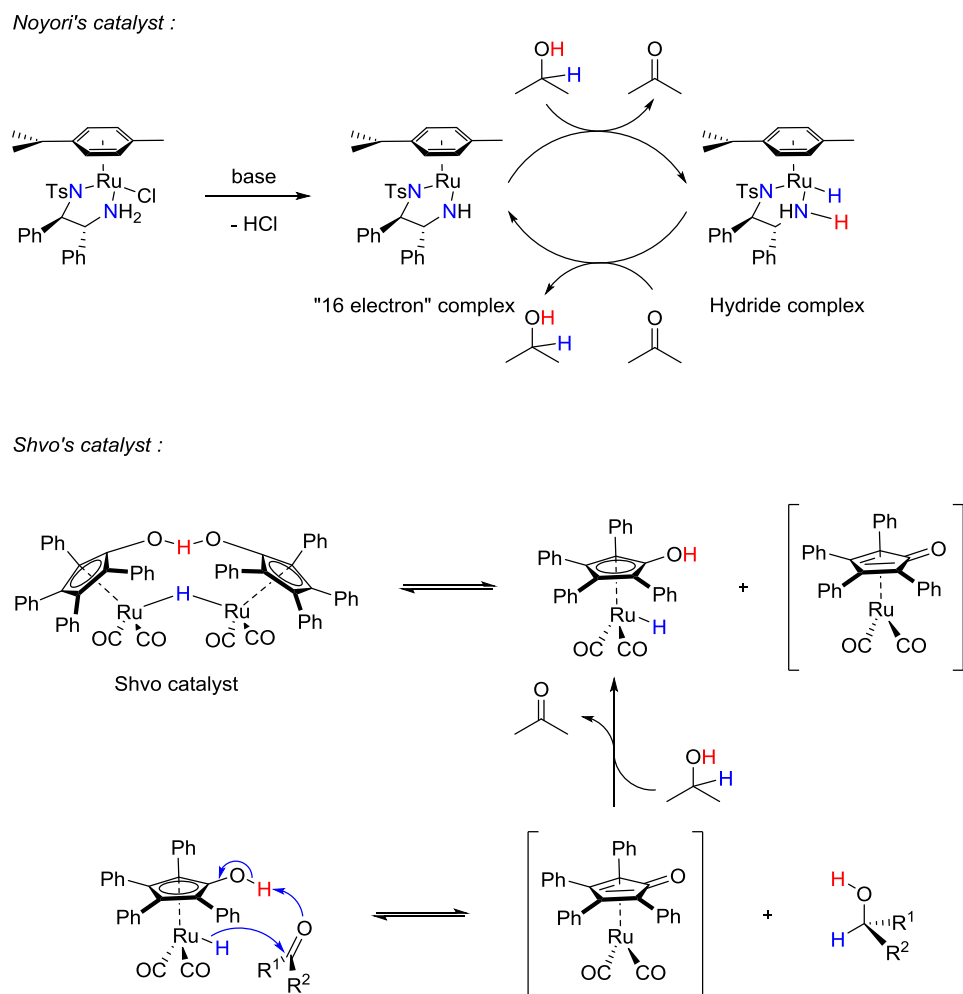


Scheme 17

When isopropanol is used as a hydrogen donor, it is necessary to use a base (alkoxide or hydroxide salt) to allow the formation of the 16-electron complex via a dissociative mechanism ( $\text{S}_{\text{N}}1\text{CB}$ ). The required quantity of base depends on the nature of the catalyst. For example, for



the Shvo's catalyst,<sup>62</sup> there is no need to use a base whereas for the Noyori catalyst, two equivalents per metal atom are required (Scheme 18).



Scheme 18

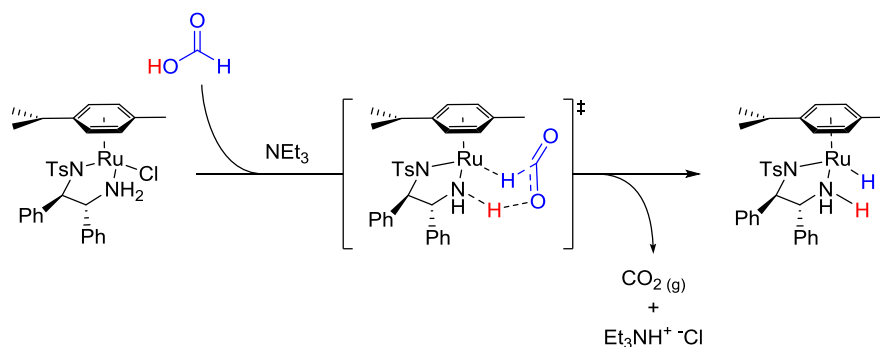
The presence of this base can also create secondary reactions and promote racemization. Although reactions with chiral ruthenium catalysts give satisfactory results in isopropanol in terms of reactivity and selectivity<sup>11a</sup> the major disadvantage is its reversibility, leading to a limited conversion. Because of this reversibility, a dramatic decrease in the enantiomeric excess of the products is observed during long-term exposure of the reaction mixture to the catalyst.

Other alcohols such as methanol or ethanol may be used but are generally less effective than secondary alcohols (in terms of the sum of  $\delta$  inductive electronic effects) and the aldehydes formed may interfere with the reaction medium although these are volatile.

<sup>62</sup> (a) Shvo, Y.; Czarkie, D.; Rahamim, Y.; Chodosh, D. F. *J. Am. Chem. Soc.* **1986**, *108*, 7400. (b) Menashe, N.; Shvo, Y. *Organometallics* **1991**, *10*, 3885. (c) Menashe, N.; Salant, E.; Shvo, Y. *J. Organomet. Chem.* **1996**, *514*, 97. (d) Casey, C. P.; Singer, S. W.; Powell, D. R.; Hayashi, R. K.; Kavana, M. *J. Am. Chem. Soc.* **2001**, *123*, 1090. (e) Conley, B. L.; Pennington-Boggio, M. K.; Boz, E.; Williams, T. J. *Chem. Rev.* **2010**, *110*, 2294.

Formic acid and its salts:

Formic acid and its salts are the hydrogen donors of choice for the reduction of carbonyl compounds. Indeed, the dehydrogenation product is CO<sub>2</sub> gas making the reaction irreversible and under kinetic control.<sup>27a,63</sup> When formic acid is used, it is necessary to use a base such as triethylamine to deprotonate the formic acid and release the formate ion required for the formation of the metal hydride (Scheme 19).



Scheme 19

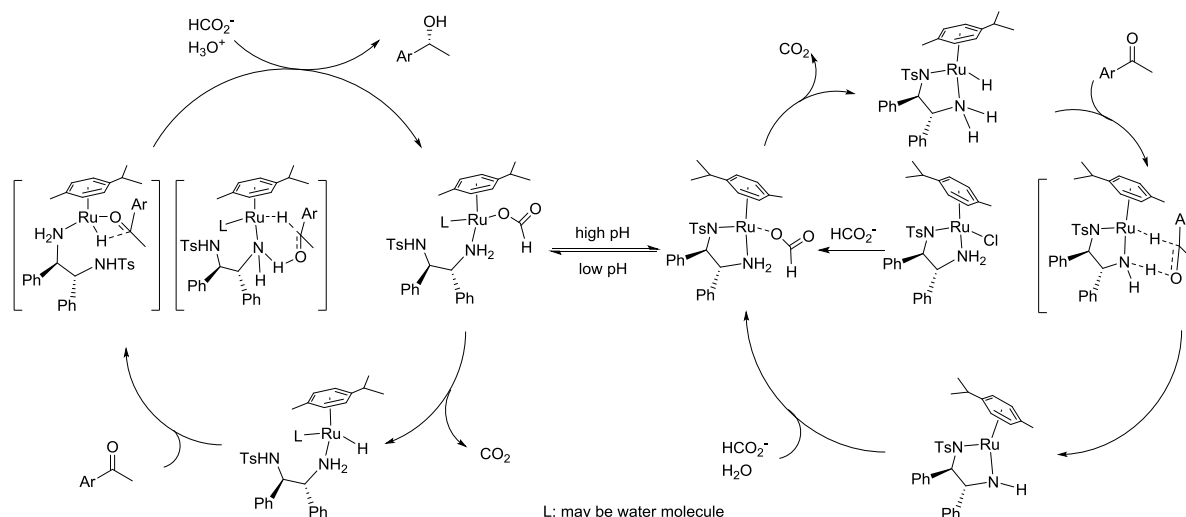
In addition, the azeotropic mixture HCOOH/Et<sub>3</sub>N (5/2) is commercially available, soluble in various solvents and is the most frequently used. Xiao *et al.* showed that this azeotropic mixture could also be used in water. They observed that the enantioselectivity of the ATH catalyzed by the Noyori's complex [RuCl( $\eta^6$ -*p*-cymene)((*R,R*)-TsDPEN)] formed *in situ* was dependent on the pH of the medium. At pH > 7, high catalytic activities and high enantioselectivities were obtained, resulting from two competitive catalytic cycles (Scheme 20) depending on the pH value of the solution.<sup>64</sup> Other research groups studied the influence of the formic acid/triethylamine ratio and concluded that the ratios leading to the best reactivity and selectivity were 0.2/1 and 1/1.<sup>65</sup> Finally, Zhang's group reported that the formic acid/DIPEA mixture (5/2) provided the best enantioselectivity compared to other chiral and nonchiral tertiary amines for asymmetric hydrogen transfer of  $\alpha$ -ketopantolactam (Scheme 21).<sup>66</sup>

<sup>63</sup> Koike, T.; Ikariya, T. *Adv. Synth. Catal.* **2004**, *346*, 37.

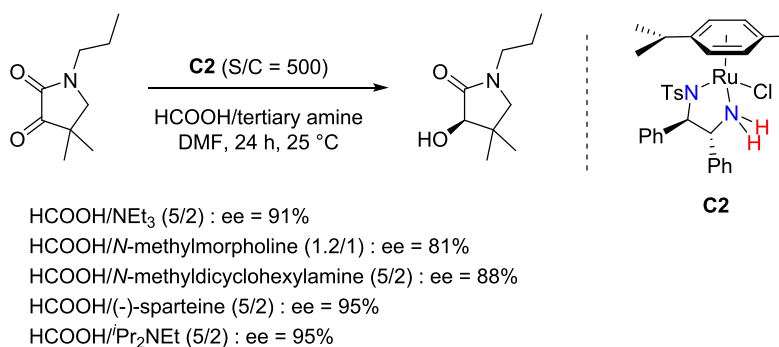
<sup>64</sup> (a) Wu, X.; Li, X.; King, F.; Xiao, J. *Angew. Chem. Int. Ed.* **2005**, *44*, 3407. (b) Zhou, X.; Wu, X.; Yang, B.; Xiao, J. *J. Mol. Catal. A Chem.* **2012**, *357*, 133.

<sup>65</sup> (a) Tanaka, K.; Katsurada, M.; Ohno, F.; Shiga, Y.; Oda, M.; Miyagi, M.; Takehara, J.; Okano, K. *J. Org. Chem.* **2000**, *65*, 432. (b) Miyagi, M.; Takehara, J.; Collet, S.; Okano, K. *Org. Process Res. Dev.* **2000**, *4*, 346. Also see the reference on ATH of imines: (c) Shende, V. S.; Deshpande, S. H.; Shingote, S. K.; Joseph, A.; Kelkar, A. A. *Org. Lett.* **2015**, *17*, 2878.

<sup>66</sup> Zhang, J.; Blazecka, P. G.; Bruendl, M. M.; Huang, Y. *J. Org. Chem.* **2009**, *74*, 1411.



Scheme 20



Scheme 21

The azeotropic mixture  $\text{HCOOH}/\text{Et}_3\text{N}$  (5/2) has an acidic pH and its value depends on the solvent used. However, this acidity can be a disadvantage since some complexes can decompose under acidic conditions.

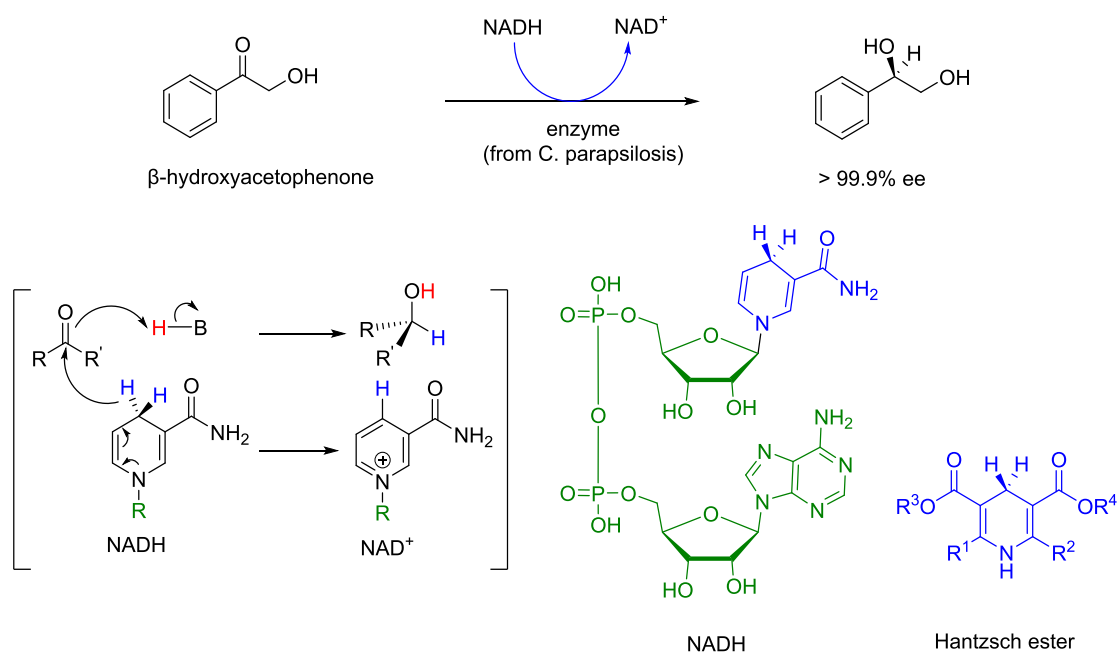
Finally, formic acid salts are also used as hydrogen donors. In particular, sodium formate ( $\text{HCOONa}$ ) is very often used for ATH in water.<sup>31,67</sup>

### Hantzsch ester:

Inspired by the way nature achieves asymmetric reductions, chemists have developed a biomimetic approach to asymmetric hydrogen transfer using Hantzsch ester<sup>68 a-b</sup> as the hydrogen donor and thus mimicking the role of  $\text{NADH}$ <sup>68 c-d</sup> (Scheme 22).

<sup>67</sup> (a) Wu, X.; Li, X.; Hems, W.; King, F.; Xiao, J. *Org. Biomol. Chem.* **2004**, *2*, 1818. (b) Wu, X.; Xiao, J. *Chem. Commun.* **2007**, 2449. (c) Wu, X.; Li, X.; Zanotti-Gerosa, A.; Pettman, A.; Liu, J.; Mills, A. J.; Xiao, J. *Chem. Eur. J.* **2008**, *14*, 2209.

<sup>68</sup> (a) Hantzsch, A. *Ber. Dtsch. Chem. Ges.* **1881**, *14*, 1637. (b) Hantzsch, A. *Justus Liebigs Ann. Chem.* **1882**, 215, 1. (c) Nie, Y.; Xu, Y.; Mu, X. Q. *Org. Process Res. Dev.* **2004**, *8*, 246. (d) Wang, S.; Nie, Y.; Xu, Y.; Zhang, R.; Ko, T.-P.; Huang, C.-H.; Chan, H.-C.; Guo, R.-T.; Xiao, R. *Chem. Commun.* **2014**, *50*, 7770.



**Scheme 22**

The use of Hantzsch ester for organocatalyzed reduction of C=C, C=N or C=O bonds has grown particularly rapidly in recent years.<sup>69</sup>

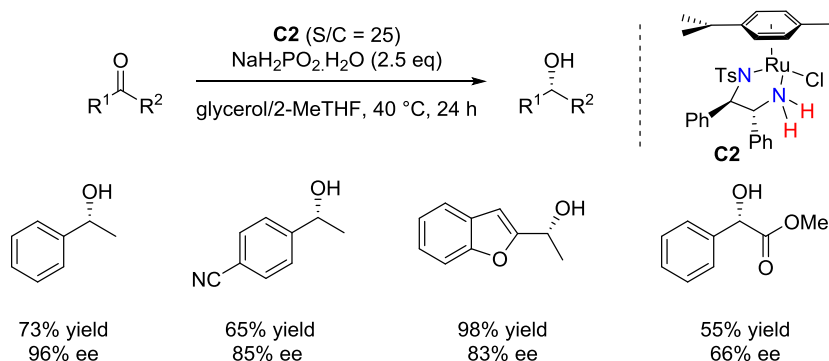
However, its application for the metal-catalyzed ATH has few precedents in the literature because it is not atom-economical. In addition, the resulting dehydrogenated product causes purification issues.

Other donors:

In 2013, Lemaire *et al.* used  $\text{NaH}_2\text{PO}_2 \cdot \text{H}_2\text{O}$  as a hydrogen donor for the ATH of a wide range of ketones catalyzed by the Noyori's complex  $[\text{RuCl}(\eta^6\text{-}p\text{-cymene})((R,R)\text{-TsDPEN})]$  **C2** in a glycerol/2-MeTHF biphasic system (Scheme 23).<sup>70</sup>

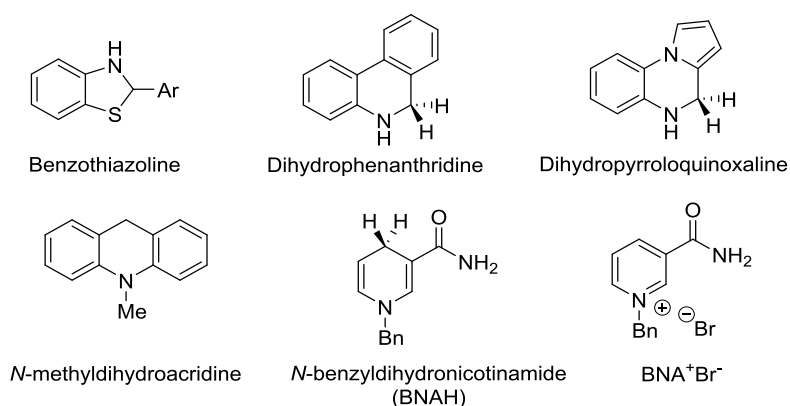
<sup>69</sup> (a) Ouellet, S. G.; Walji, A. M.; MacMillan, D. W. C. *Acc. Chem. Res.* **2007**, *40*, 1327. (b) Rueping, M.; Dufour, J.; Schoepke, F. R. *Green Chem.* **2011**, *13*, 1084. (c) Zheng, C.; You, S. *Chem. Soc. Rev.* **2012**, *41*, 2498 and references therein.

<sup>70</sup> Guyon, C.; Méta y, E.; Duguet, N.; Lemaire, M. *Eur. J. Org. Chem.* **2013**, 5439.



Scheme 23

The hydrogen donors shown in Scheme 24 are used mostly for organocatalyzed reduction of C=N bonds. Their structures are always based on NADH biomimetic approach. Examples include benzothiazoline derivatives,<sup>71</sup> dihydrophenanthridine (DHPD),<sup>72</sup> dihydropyrroloquinoxaline<sup>73</sup> or dihydronicotinamide.<sup>74</sup>



Scheme 24

For example, Connon's group proposed an organocatalyst bearing the hydrogen donor (MNA<sup>+</sup>Br<sup>-</sup>: methylnicotinamide) part and the substrate activating fragment (thiourea) for the transfer hydrogenation of 1,2-diketones in the presence of sodium dithionate as a co-reductant for 'cofactor' generation/recycling. However, this approach suffers from a racemization problem due to a long reaction time (Scheme 25).<sup>75</sup>

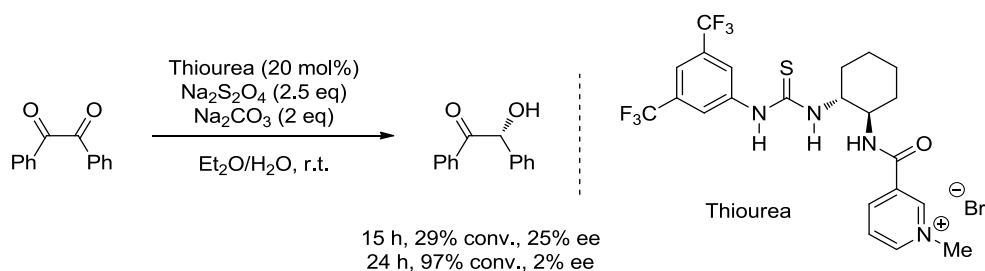
<sup>71</sup> Henseler, A.; Kato, M.; Mori, K.; Akiyama, T. *Angew. Chem. Int. Ed.* **2011**, *50*, 8180.

<sup>72</sup> Lu, L.-Q.; Li, Y.; Junge, K.; Beller, M. *Angew. Chem. Int. Ed.* **2013**, *52*, 8382.

<sup>73</sup> Chen, Z.-P.; Chen, M.-W.; Guo, R.-N.; Zhou, Y.-G. *Org. Lett.* **2014**, *16*, 1406.

<sup>74</sup> Xu, H.-J.; Liu, Y.-C.; Fu, Y.; Wu, Y.-D. *Org. Lett.* **2006**, *8*, 3449.

<sup>75</sup> Procuranti, B.; Connon, S. *J. Chem. Commun.* **2007**, 1421.

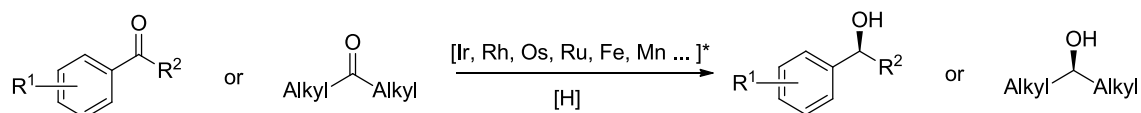


Scheme 25

After describing the general principles of asymmetric transfer hydrogenation reaction (mechanisms, bifunctional metal-ligand catalysis, hydrogen donors), the next section will address some recent developments on metal-catalyzed asymmetric transfer hydrogenation of ketones from 2015 to 2020 in terms of new metal precatalysts, and their application to synthetic chemistry.

## 2. Reaction scope: catalysts and chiral ligands

Different transition metals (Ru, Rh, Ir, Fe, Os, Mn) in combination with a number of chiral ligands bearing coordinating heteroatoms (N, O, P, S) have been developed and investigated in asymmetric transfer hydrogenation of aromatic or aliphatic ketones (Scheme 26).



Scheme 26

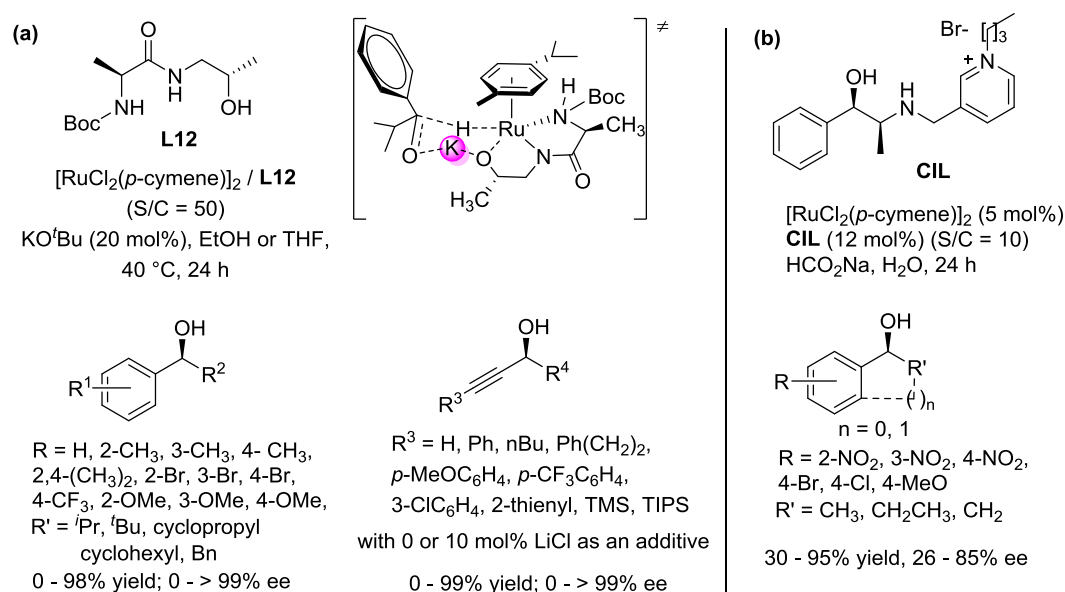
### 2.1 Ruthenium catalysts

#### 2.1.1 Aminoalcohols as ligands

Chiral aminoalcohols are one type of the most common used ligands in asymmetric transfer hydrogenation and have been well documented in the literature. Developing novel chiral aminoalcohols as ligands is still ongoing, because they are easily available from natural or unnatural chiral amino acids.

Adolfsson *et al.* reported, in 2015, a Ru(II) complex bearing a chiral amino acid derived ligand **L12** formed *in situ* for ATH of a series of challenging sterically hindered aryl ketones using EtOH/KO<sup>t</sup>Bu system as a hydrogen donor to provide the chiral alcohols with high

conversions and enantioselectivities.<sup>76</sup> The same group reported in 2015 the use of the above catalytic system with different ratios of KO<sup>t</sup>Bu/LiCl for ATH of various propargylic ketones to give the corresponding propargylic alcohols, in most cases, with yields up to 99% and with excellent enantioselectivities >90% (Scheme 27a).<sup>77</sup> A new type of hydrophilic chiral ionic liquid (CIL) bearing amino alcohol unit was developed and coordinated with [RuCl<sub>2</sub>(*p*-cymene)]<sub>2</sub> precursor for ATH of simple ketones to yield moderate to high enantioselectivities. However, recovery experiments showed the limited reactivity of these systems because of the catalyst leaching (Scheme 27b).<sup>78</sup>



Scheme 27

### 2.1.2 Diamines as ligands

Based on commercially available norephedrine, several unsymmetrical vicinal diamine ligands **L13** were prepared and evaluated in combination with [RuCl<sub>2</sub>(*p*-cymene)]<sub>2</sub>, [RhCl<sub>2</sub>Cp\*]<sub>2</sub>, [IrCl<sub>2</sub>Cp\*]<sub>2</sub> for ATH of acetophenone with sodium formate as the hydrogen source in aqueous phase (Scheme 28a).<sup>79</sup> Moreover, simple unsymmetric monotosylated 1,3-diamines **L14** were developed and combined with [RuCl<sub>2</sub>(*p*-cymene)]<sub>2</sub> for the ATH of phenones to give the corresponding alcohols in low to moderate ee (0–63%) (Scheme 28b).<sup>80</sup>

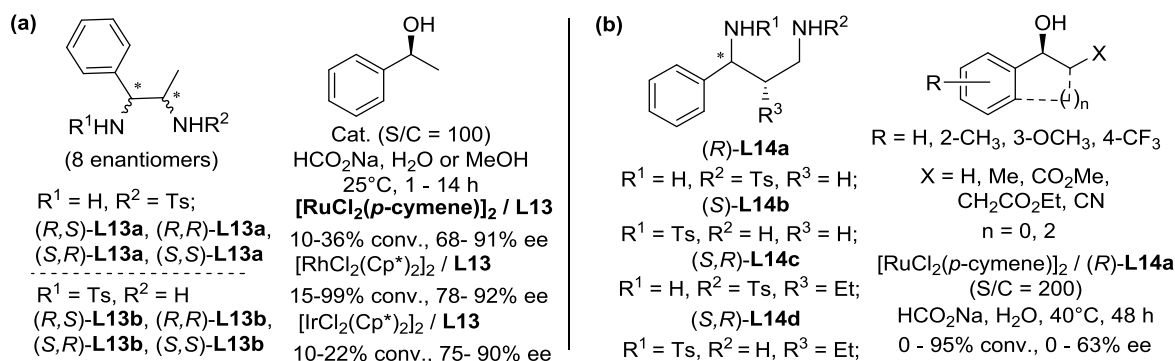
<sup>76</sup> Slagbrand, T.; Kivijärvi, T.; Adolfsson, H. *ChemCatChem* **2015**, *7*, 3445.

<sup>77</sup> Shatskiy, A.; Kivijärvi, T.; Lundberg, H.; Tinnis, F.; Adolfsson, H. *ChemCatChem* **2015**, *7*, 3818.

<sup>78</sup> Vasiloiu, M.; Gaertner, P.; Zirbs, R.; Bica, K. *Eur. J. Org. Chem.* **2015**, 2374.

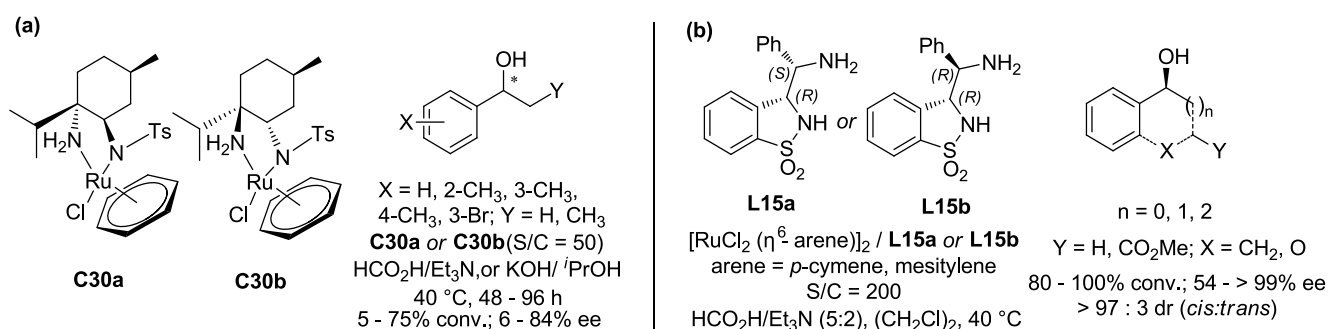
<sup>79</sup> Deshpande, S. H.; Shende, V. S.; Shingote, S. K.; Chakravarty, D.; Puranik, V. G.; Chaudhari, R. V.; Kelkar, A. *RSC Adv.* **2015**, *5*, 51722.

<sup>80</sup> Facchetti, G.; Gandolfi, R.; Fusè, M.; Zerla, D.; Cesarotti, E.; Pellizzoni, M.; Rimoldi, I. *New J. Chem.* **2015**, *39*, 3792.



Scheme 28

Chiral monotosylated diamines based on natural (–)-menthol were synthesized and used to form Ru(II) complexes **C30**. These complexes catalyzed the ATH of simple aromatic ketones with  $HCO_2H/Et_3N$  or  $KOH/iPrOH$  as the hydrogen source to generate chiral alcohols with moderate activities and good enantioselectivities (up to 84% ee) (Scheme 29a).<sup>81</sup> In 2016, Mohar *et al.* developed a new type of diamine ligands **L15** used in Ru(II)-catalyzed ATH of simple aryl ketones as well as cyclic aryl ketones using  $HCO_2H/Et_3N$  as hydrogen source under mild conditions to furnish the corresponding alcohols in 54–99% yields and up to 99% enantioselectivities (Scheme 29b).<sup>82</sup>



Scheme 29

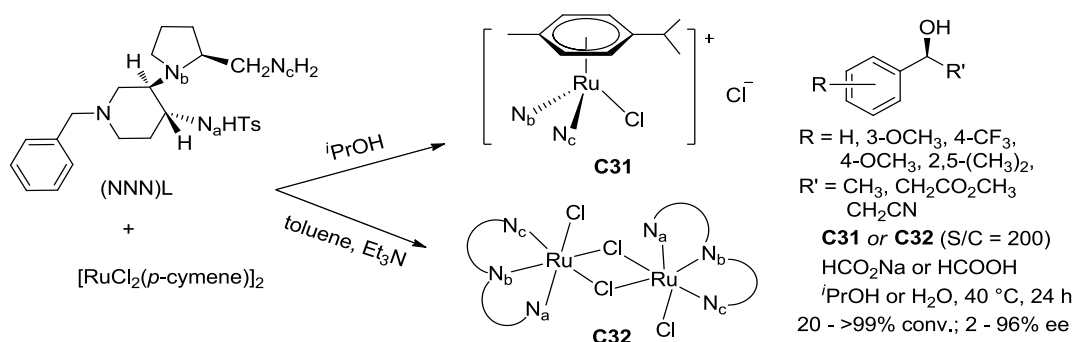
A novel (*N,N,N*) chiral ligand was prepared and combined with  $[RuCl_2(*p*-cymene)]_2$  to form bidentate complex **C31** and tridentate complex **C32**. The catalytic activity of these complexes in ATH of aromatic ketones largely depended on the reaction conditions and the substituents on the ketones (Scheme 30).<sup>83</sup>

<sup>81</sup> Roszkowski, P.; Maurin, J. K.; Czarnocki, Z. *Tetrahedron Lett.* **2018**, *59*, 2184.

<sup>82</sup> Rast, S.; Modéc, B.; Stephan, M.; Mohar, B. *Org. Biomol. Chem.* **2016**, *14*, 2112.

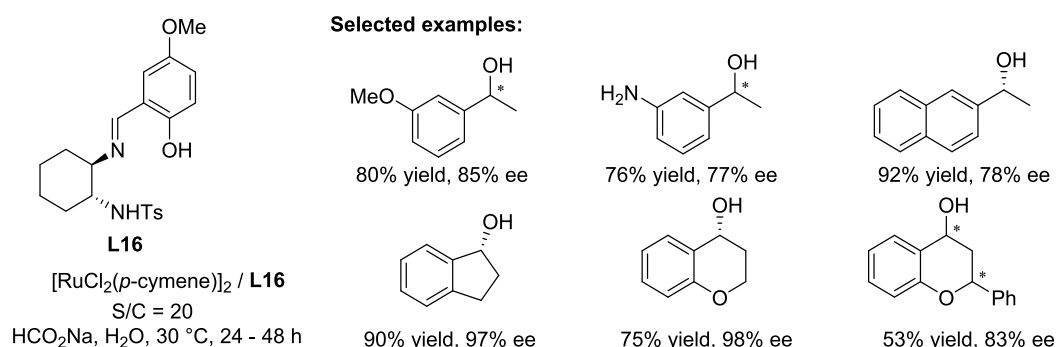
<sup>83</sup> Pellegrino, S.; Facchetti, G.; Gandolfi, R.; Fusè, M.; Erba, E.; Rimoldi, I. *Can. J. Chem.* **2018**, *96*, 40.





Scheme 30

A number of hemisalen type ligands **L16** were prepared and evaluated with  $[\text{RuCl}_2(p\text{-cymene})]_2$  complex for ATH of acetophenone in water. Chiral cyclohexyl diamine based hemisalen ligand displayed high catalytic activity and was investigated for the reduction of a broad range of ketones to deliver the corresponding alcohols in yields ranging from 53 to 92% and ee values from 77 to 97% (Scheme 31).<sup>84</sup>

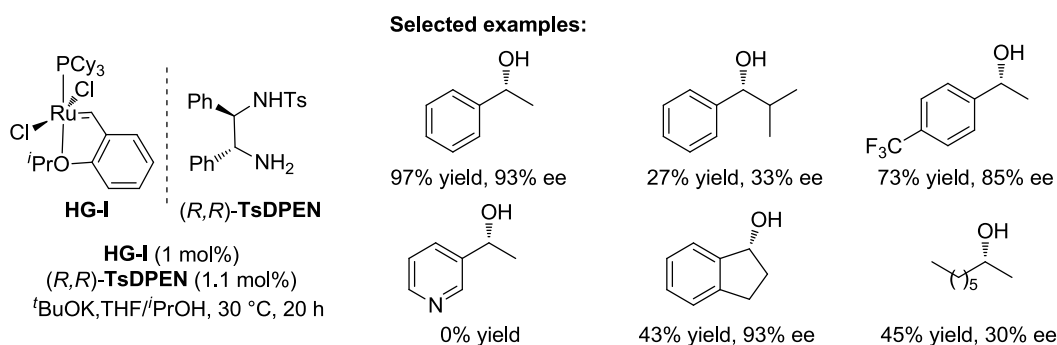


Scheme 31

The 1<sup>st</sup> generation Hoveyda-Grubbs metathesis catalyst in association with (*R,R*)-TsDPEN ligand was successfully evaluated in the ATH of simple aromatic ketones in the presence of  $i\text{PrOH}$  as a hydrogen donor. High activities and enantioselectivities (up to 97% ee) were obtained in the ATH of several ketones. Moreover, a tandem reaction including metathesis reaction and ketone transfer reduction was achieved (Scheme 32).<sup>85</sup>

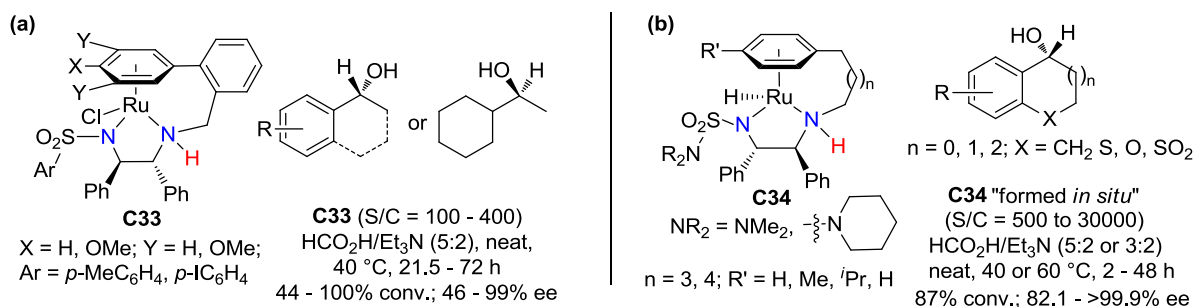
<sup>84</sup> Boukachabia, M.; Aribi-Zouioueche, L.; Riant, O. *J. Organomet. Chem.* **2018**, 868, 95.

<sup>85</sup> Renom-Carrasco, M.; Gajewski, P.; Pignataro, L.; de Vries, J. G.; Piarulli, U.; Gennari, C.; Lefort, L. *Adv. Synth. Catal.* **2016**, 358, 515.



Scheme 32

A new family of benzyl-tethered Ru(II)/arene/TsDPEN complexes **C33** was developed through a direct arene-exchange process. These complexes were applied in the ATH of a broad range of ketones to generally provide the chiral alcohols in high conversions and enantioselectivities up to 99% (Scheme 33a).<sup>86</sup> In 2015, Mohar *et al.* reported a new series of 3<sup>rd</sup> generation *ansa*-Ru(II) complexes **C34** bearing a sulfamoylamino (NSO<sub>2</sub>N) moiety (Scheme 33b).<sup>87</sup>



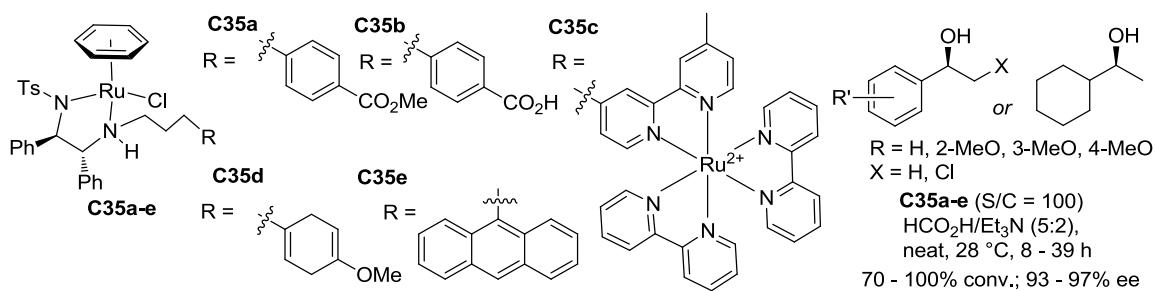
Scheme 33

In 2015, Wills *et al.* developed a number of Ru(II)(benzene)/*N*-alkyl-TsDPEN complexes **C35a–e** and evaluated their catalytic activities and enantioinductions for the ATH of acetophenone. They used **C35a** and **C35b** for the ATH of a broad range of ketone derivatives by using HCO<sub>2</sub>H/Et<sub>3</sub>N under mild conditions to give 1-phenyl ethanol in high conversions and ees (Scheme 34).<sup>88f</sup>

<sup>86</sup> (a) Soni, R.; Jolley, K. E.; Gosiewska, S.; Clarkson, G. J.; Fang, Z.; Hall, T. H.; Treloar, B. N.; Knighton, R. C.; Wills, M. *Organometallics* **2018**, *37*, 48. (b) Knighton, R. C.; Vyas, V. K.; Mailey, L. H.; Bhanage, B. M.; Wills, M. *J. Organomet. Chem.* **2018**, *875*, 72.

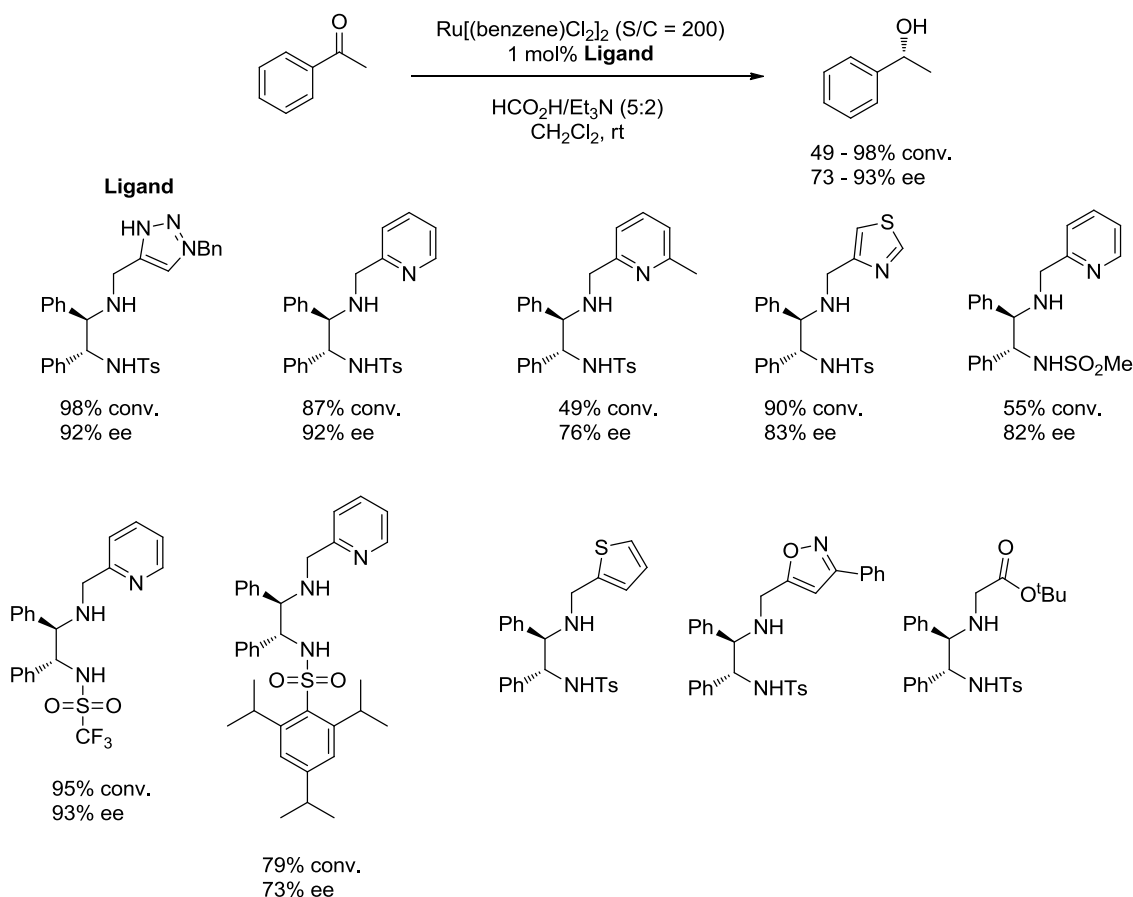
<sup>87</sup> (a) Kišić, A.; Stephan, M.; Mohar, B. *Adv. Synth. Catal.* **2015**, *357*, 2540. (b) Hodgkinson, R.; Jurčič, V.; Nedden, H.; Blackaby, A.; Wills, M. *Tetrahedron Lett.* **2018**, *59*, 930.

<sup>88</sup> (a) Soni, R.; Hall, T. H.; Morris, D. J.; Clarkson, G. J.; Owen, M. R.; Wills, M. *Tetrahedron Lett.* **2015**, *56*, 6397. Also see previous work : (b) Koike, T.; Ikariya, T. *Adv. Synth. Catal.* **2014**, *346*, 37; (c) Koike, T.; Ikariya, T. *J. Organomet. Chem.* **2007**, *692*, 408. (d) Martins, J. E. D.; Clarkson, G. J.; Wills, M. *Org. Lett.* **2009**, *11*, 847; (e) Martins, J. E. D.; Contreras Redondo, M. A.; Wills, M. *Tetrahedron: Asymmetry* **2010**, *21*, 2258; (f) Zammit, C.



Scheme 34

In 2019, the same group developed TsDPEN bidentate and tridentate ligands containing different heterocyclic groups on the amine nitrogen atom. They prepared a range of ruthenium complexes using TsDPEN type ligands and tested their catalytic properties on the asymmetric transfer hydrogenation of aryl alkyl ketones. Some catalysts afforded excellent conversions and enantioselectivities. (Scheme 35)<sup>89</sup>



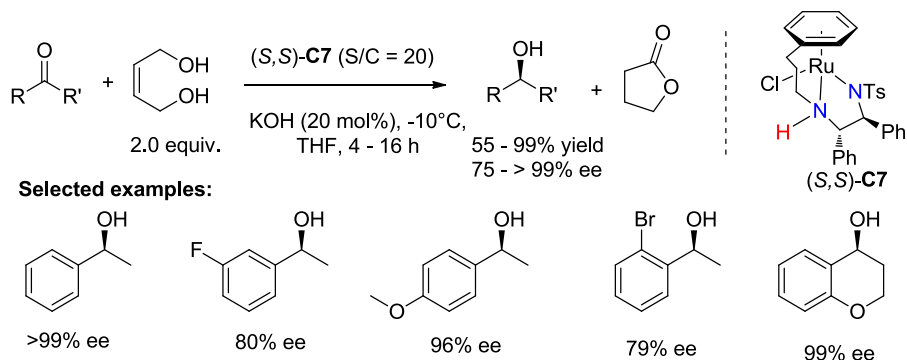
Scheme 35

In 2015, Wakeham *et al.* described a new approach by using *cis*-1,4-butanediol as a

M.; Wills, M. *Tetrahedron: Asymmetry* **2013**, *24*, 844.

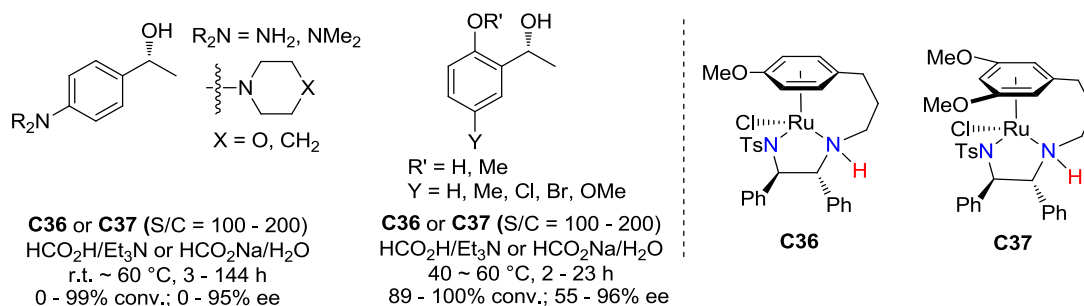
<sup>89</sup> Barrios-Rivera, J.; Xu, Y.; Wills, M. *Org. Lett.* **2019**, *21*, 7223.

hydrogen donor with Wills' catalyst (*S,S*)-**C7** in the ATH of simple aryl ketones to yield the chiral alcohols in 75 to 99% ee values (Scheme 36).<sup>90</sup>



Scheme 36

Considering the ATH of challenging electron-rich aromatic ketones, the two tethered Ru(II) complexes **C36** and **C37** were investigated in the presence of HCO<sub>2</sub>H/Et<sub>3</sub>N or aqueous sodium formate as the hydrogen source, and exhibited efficient catalytic activities. For the aniline ketones, the reaction worked well in aqueous sodium formate; whereas for *ortho*-methoxy substituted ketones, a HCO<sub>2</sub>H/Et<sub>3</sub>N system exhibited high performance (Scheme 37).<sup>91</sup>



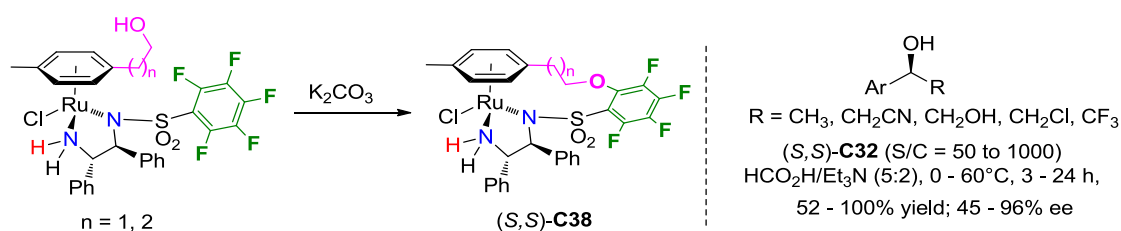
Scheme 37

In 2018, Kayaki and coworkers presented a concise approach for the synthesis of new oxy-tethered ruthenium complexes **C38**, which were effective for the ATH of aromatic ketones. The key step involves a defluorinative etherification reaction to construct an oxy-tether arising from an intramolecular nucleophilic substitution of a perfluorinated phenylsulfonyl substituent. The resulting tethered complexes exhibited high catalytic activity and selectivity for ATH of functionalized aromatic ketones. Their superior catalytic performances relative to the

<sup>90</sup> Wakeham, R. J.; Morris, J. A.; Williams, J. M. J. *ChemCatChem* **2015**, *7*, 4039.

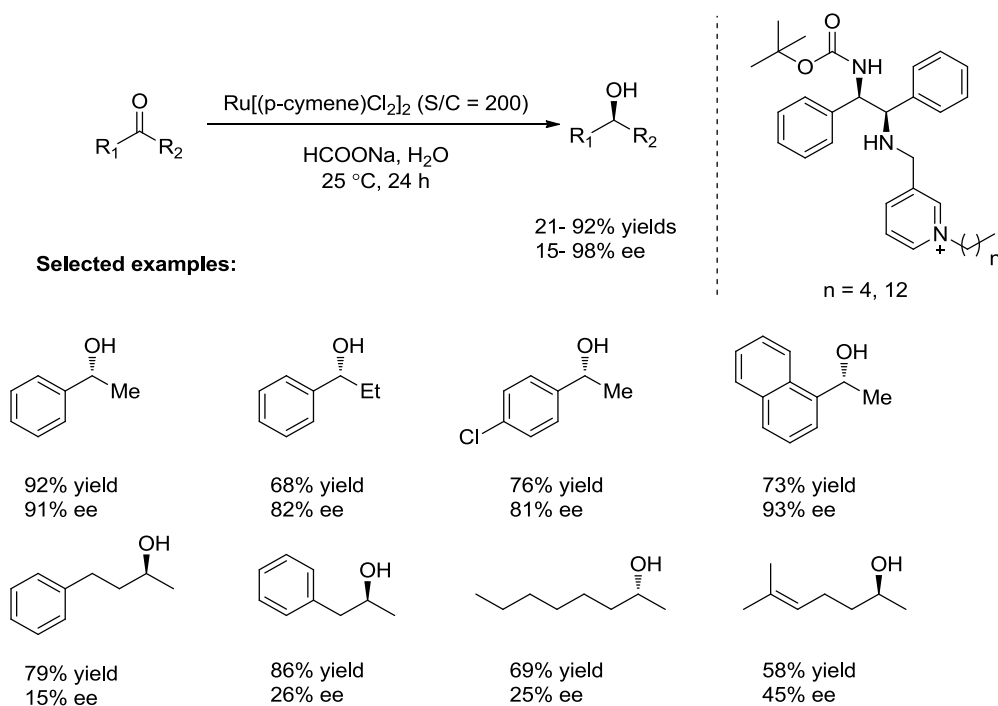
<sup>91</sup> Soni, R.; Hall, T. H.; Mitchell, B. P.; Owen, M. R.; Wills, M. J. *Org. Chem.* **2015**, *80*, 6784.

nontethered prototype complex owe to the robustness and rigidity of the tether (Scheme 38).<sup>92</sup>



**Scheme 38**

In 2019, Bica *et al.* designed several novel ion-tagged chiral ligands for Ru-catalyzed asymmetric transfer hydrogenation (ATH) of prochiral ketones, which were based on (*R,R*)-1,2-diphenylethylene diamine (DPEN) as structural motif. As for the ionic nature of the ligands, the preformed chiral ruthenium-complex was readily soluble in water, allowing the ATH of ketones to be performed in water along with sodium formate as the hydrogen source. A series of aliphatic and aromatic ketones were reduced with excellent isolated yields up to 92% and enantioselectivities up to 98% (Scheme 39).<sup>93</sup>



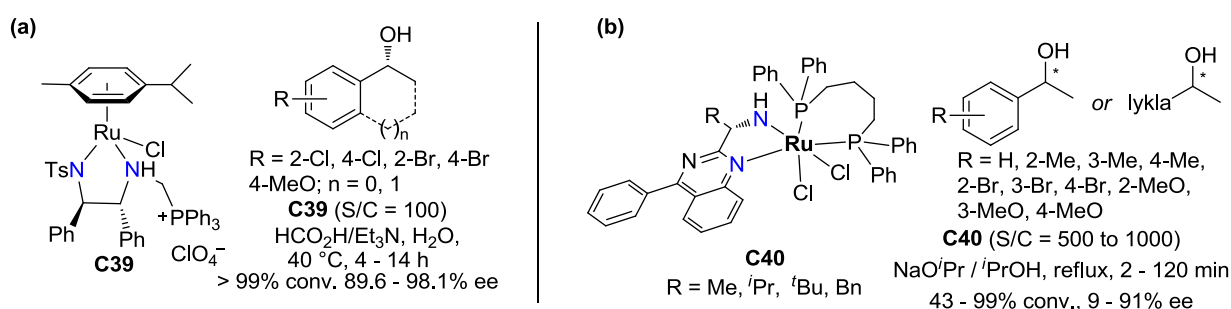
**Scheme 39**

<sup>92</sup> Matsunami, A.; Ikeda, M.; Nakamura, H.; Yoshida, M.; Kuwata, S.; Kayaki, Y. *Org. Lett.* **2018**, *20*, 5213.

<sup>93</sup> Pálvölgyi, Á. M.; Bitai, J.; Zeindhofer, V.; Schröder, C.; Bica, K. *ACS Sustainable Chem. Eng.* **2019**, *7*, 3414

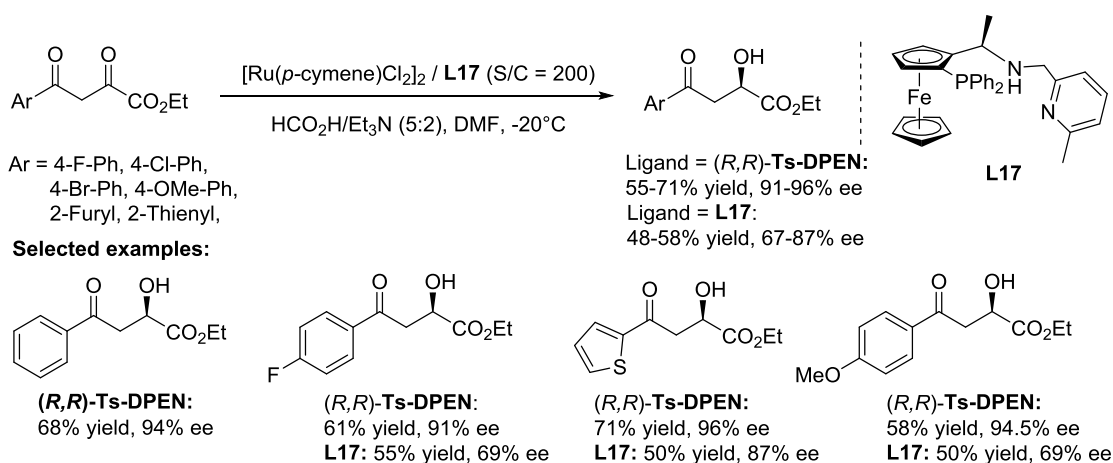
## 2.1.3 Phosphorus containing ligands

A Noyori-Ikariya tetraarylphosphonium salt (TAP)-supported catalyst **C39** was reported for ATH of aryl ketones in water with  $\text{HCO}_2\text{H}/\text{Et}_3\text{N}$  as a hydrogen donor. Additionally, the supported catalyst could be recycled 5 times after simple manipulation with good results (Scheme 40a).<sup>94</sup> A series of *N,N*-containing quinazoline-based Ru(II) complexes **C40** were developed and proved to be efficient in ATH of ketones with  $\text{NaO}^i\text{Pr}/^i\text{PrOH}$  as the hydrogen source. For aryl ketones, up to 91 % enantioselectivities were obtained, whereas alkyl alkyl ketones were reduced with lower ee values (33–52%) (Scheme 40b).<sup>95</sup>



Scheme 40

A convenient approach to access chiral  $\alpha$ -hydroxy- $\gamma$ -keto-butyrates was described by using a Ru(II) catalyst with chiral ferrocene-based *P,N,N* ligand **L17** for the ATH of the corresponding ketones in the presence of  $\text{HCO}_2\text{H}/\text{Et}_3\text{N}$  as a hydrogen source. Meanwhile, chiral TsDPEN ligand has been evaluated to provide the products in 55–71% yields with 91–96% ee (Scheme 41).<sup>96</sup>



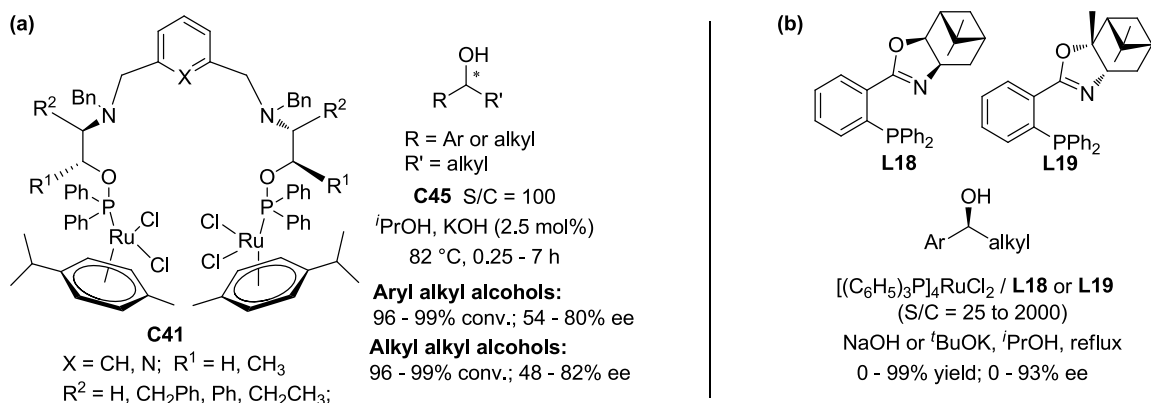
<sup>94</sup> Zimbron, J. M.; Dauphinais, M.; Charette, A. B. *Green Chem.* **2015**, *17*, 3255.

<sup>95</sup> Kucukturkmen, C.; Agac, A.; Eren, A.; Karakaya, I.; Aslantas, M.; Celik, O.; Ulukanli, S.; Karabuga, S. *Catal. Commun.* **2016**, *74*, 122.

<sup>96</sup> Mo, Y.-Z.; Nie, H.-F.; Lei, Y.; Zhang, D.-X.; Li, X.-Y.; Zhang, S.-Y.; Wang, Q.-F. *RSC Adv.* **2016**, *6*, 33126.

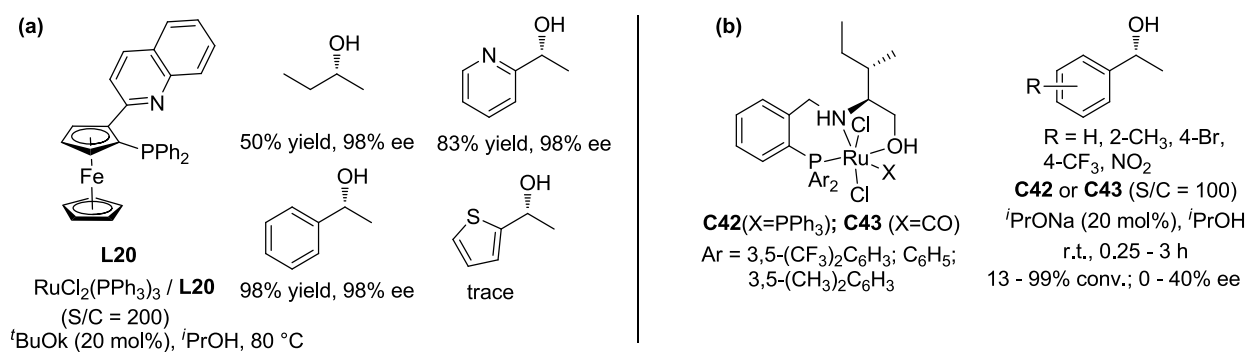
## Scheme 41

A series of binuclear Ru(II) precatalysts was prepared and used for ATH of aryl methyl ketones and alkyl alkyl ketones to furnish the corresponding alcohols in high conversions and moderate to high enantioselectivities (Scheme 42a).<sup>97</sup> In 2017, Krzemiński *et al.* reported a new type of terpene derived PHOX ligands **L18**, **L19** and their application in the presence of [Ru(PPh<sub>3</sub>)<sub>4</sub>Cl<sub>2</sub>] complex for ATH of aromatic ketones to give chiral alcohols in moderate to high yields and enantioselectivities (Scheme 42b).<sup>98</sup>



## Scheme 42

New planar chiral ferrocene *P,N*-ligands **L20** were designed and evaluated with RuCl<sub>2</sub>(PPh<sub>3</sub>)<sub>2</sub> complex in the ATH of acetophenone to give (*R*)-1-phenyl ethanol in high yield (98%) and excellent ee. Heteroaryl methyl ketones and alkyl alkyl ketones were also investigated using RuCl<sub>2</sub>(PPh<sub>3</sub>)<sub>2</sub>/**L20** to provide the chiral alcohols up to 98% yields and up to 98% ees (Scheme 43a).<sup>99</sup>



## Scheme 43

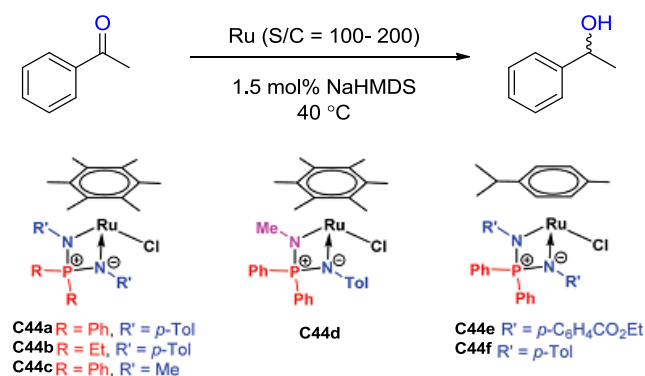
<sup>97</sup> Karakaş, D. E.; Aydemir, M.; Durap, F.; Baysal, A. *Inorg. Chim. Acta* **2018**, *471*, 430.

<sup>98</sup> Kmiecik, A.; Krzemiński, M. P. *Tetrahedron: Asymmetry* **2017**, *28*, 467.

<sup>99</sup> Utepova, I. A.; Serebrennikova, P. O.; Streltsova, M. S.; Musikhina, A. A.; Fedorchenko, T. G.; Chupakhin, O. N.; Antonchick, A. P. *Molecules* **2018**, *23*, 1311.

Several new chiral tridentate Ru(II)/*N,O,P* complexes **C42** and **C43** were synthesized and characterized. The precatalysts were investigated in ATH of simple aryl methyl ketones using NaO<sup>*i*</sup>Pr/<sup>*i*</sup>PrOH system as the hydrogen source to provide the corresponding chiral secondary alcohols. Although high catalytic activities (up to 99% yields) were observed for most of the substrates, the enantioselectivities were only moderate (up to 40% ee) (Scheme 43b).<sup>100</sup>

In 2020, Poli *et al* synthesized two new ruthenium complexes and did experiments with DFT calculations about ruthenium iminophosphonamide complexes containing different NPN ligands. They performed those (Arene)Ru(NPN) complexes **C44** (**a-f**) on the transfer hydrogenation of acetophenone and under basic conditions, they found after the precatalyst convert into the active ruthenium hydride species, the less sterically encumbering *p*-cymene ligand and the more electron-donating *N*-substituents favour the catalyst activity. Another point is that preliminary generation of the active RuH species strongly limits the overall stability of the catalytic system making it very sensitive to the quality of the solvent and the temperature. The experiment also revealed base is not necessary for the complexes with basic *N*-Me groups during the transfer hydrogenation reaction. The scheme below shows the reaction activity of the (Arene)Ru(NPN) complexes **C44** (Scheme 44).<sup>101</sup>



Precatalyst	Conversion, %						$k_{\text{obs}}$ , h <sup>-1</sup>
	$t_{\text{inc}}$ min	0.5 h	1 h	1.5 h	2 h	3 h	

<sup>100</sup> Altan, O.; Yilmaz, M. K. *J. Organomet. Chem.* **2018**, 861, 252.

<sup>101</sup> Kalsin, A. M.; Peganova, T. A.; Sinopalnikova, I. S.; Fedyanin, I. V.; Belkova, N. V.; Deydier, E.; Poli, R. *Dalton Trans.* **2020**, 49, 1473.



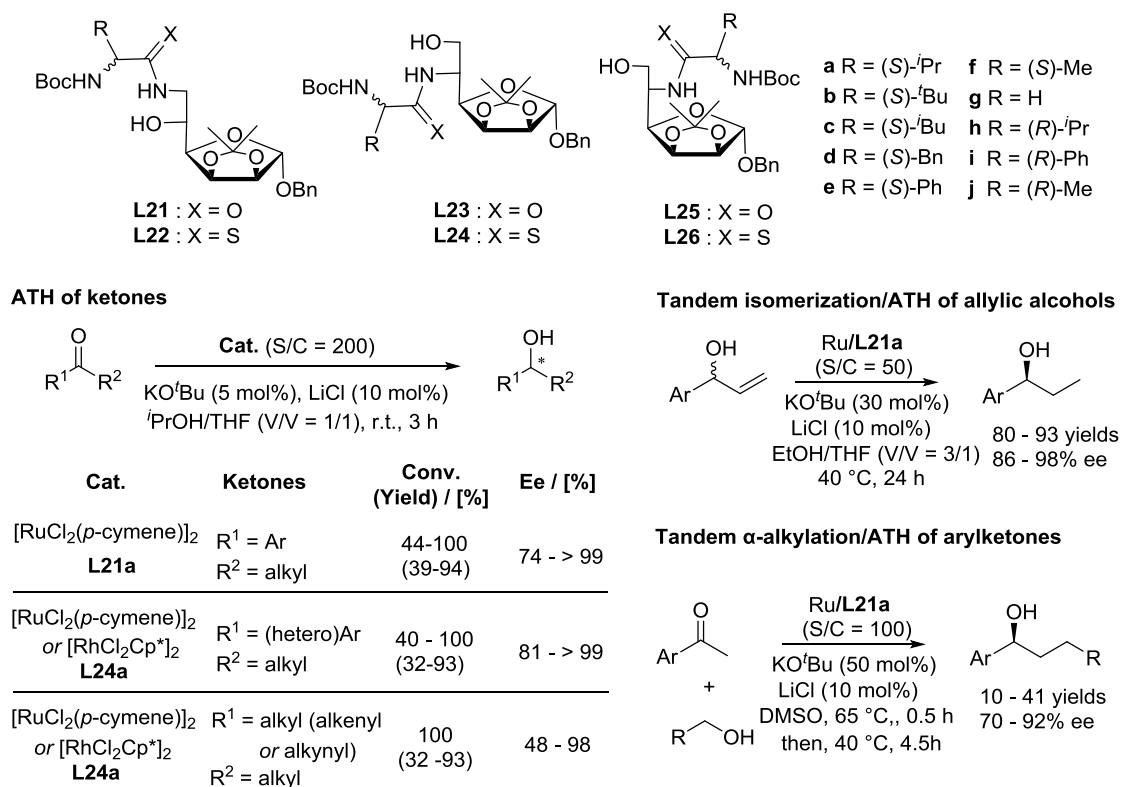
<b>C44a</b>	120	4.9	8.6	12.8	15	22.6	26.5	0.082
<b>C44b</b>	60	2.7	4.4	6.1	9.8	13.3	17.3	0.048
<b>C44c</b>	5	16.3	27.7	35.5	40.1	44.5	45.4	0.354
<b>C44d</b>	5	6.4	13.3	18.4	22.3	28.4	30.5	0.133
<b>C44e</b>	30	5.1	9.2	11.1	16.3	24.1	31.7	0.100
<b>C44f</b>	15	15.9	26.8	38.2	48	64.3	74.9	0.336

Scheme 44

### 2.1.4 Sugar containing ligands

A number of sugar-based hydroxyamide and thioamide ligands **L21–L26(a–j)** were prepared and evaluated with  $[\text{RuCl}_2(p\text{-cymene})]_2$  or  $[\text{RhCl}_2\text{Cp}^*]_2$  complexes for ATH of a wide variety of ketones, including more challenging trifluoromethyl ketones, propargylic and alkyl alkyl ketones. In general, when the optimized ligand was selected, excellent enantioselectivities (95 to >99% ee) were observed for a broad range of ketones. Moreover, tandem isomerization/ATH reactions of racemic allylic alcohols by using Ru/**L21a** yield chiral aryl alkyl alcohols in excellent ee. In addition, tandem  $\alpha$ -alkylation/ATH of arylketones with various primary alcohols was also investigated to release the corresponding chiral alcohols in good to high enantioselectivities (70–92%), albeit with low yields (10–41%) (Scheme 45).<sup>102</sup>

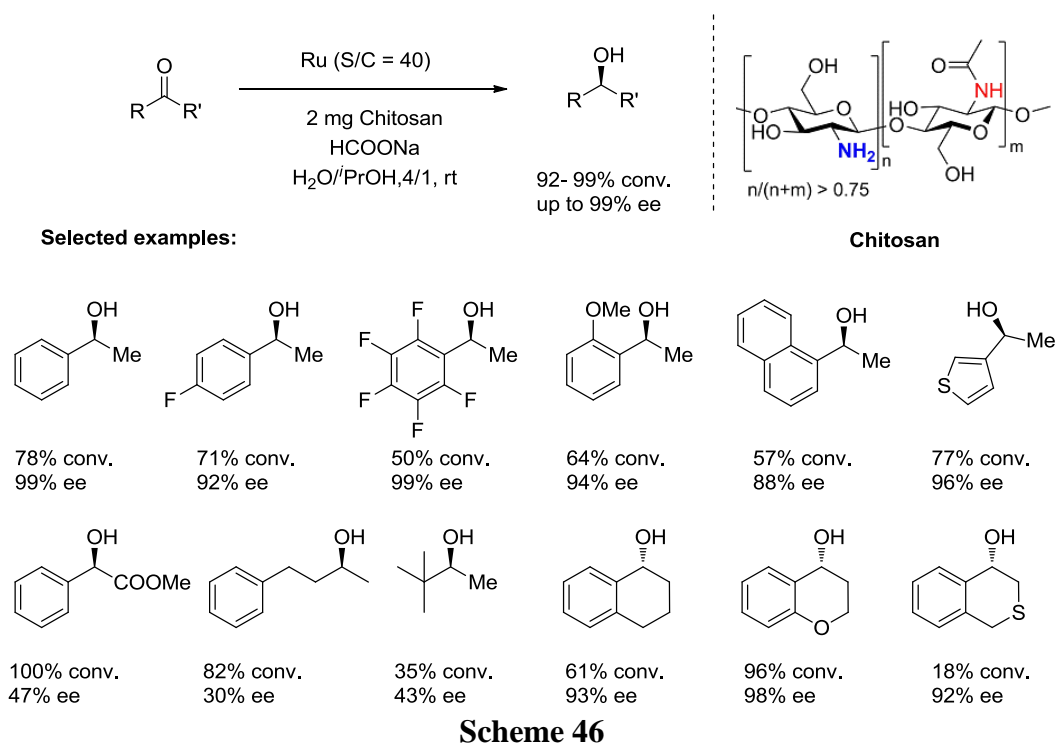
<sup>102</sup> (a) Margalef, J.; Slagbrand, T.; Tinnis, F.; Adolfsson, H.; Diéguez, M.; Pàmies, O. *Adv. Synth. Catal.* **2016**, *358*, 4006. (b) Margalef, J.; Pàmies, O.; Diéguez, M. *Tetrahedron Lett.* **2016**, *57*, 1301.



Scheme 45

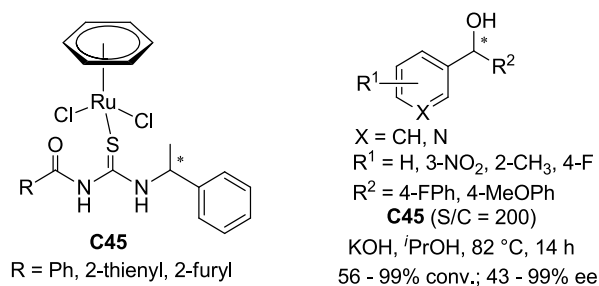
In 2019, Szöllősi and Kolcsár described a biocompatible, biodegradable chiral polymer ligand—chitosan, for ruthenium-catalyzed asymmetric transfer hydrogenation of prochiral ketones. Acetophenone derivatives were reduced to the corresponding 1-arylethanol in up to 86% ee and cyclic aryl ketones were hydrogenated in surprisingly high enantioselectivities over 90% ee. The chiral catalyst precursor prepared *ex situ* was examined by scanning electron microscopy, FT-mid- and -far-IR spectroscopy. In these complexes chitosan interacts with the metal through amino groups, however, in some species the role of the hydroxyl or even acetamido groups in bonding to the Ru could not be excluded (Scheme 46).<sup>103</sup>

<sup>103</sup> Szöllősi, G.; Kolcsár, V. J. *ChemCatChem*. **2019**, *11*, 820.



### 2.1.5 Sulfur containing ligands

A new type of chiral acyl/aryl thioureas containing [RuCl<sub>2</sub>( $\eta^6$ -benzene)] complexes **C45** were reported in 2015 and used in the ATH of aromatic ketones to access chiral aryl alcohols in moderate to excellent enantioselectivities (43–99%) (Scheme 47).<sup>104</sup>



**Scheme 47**

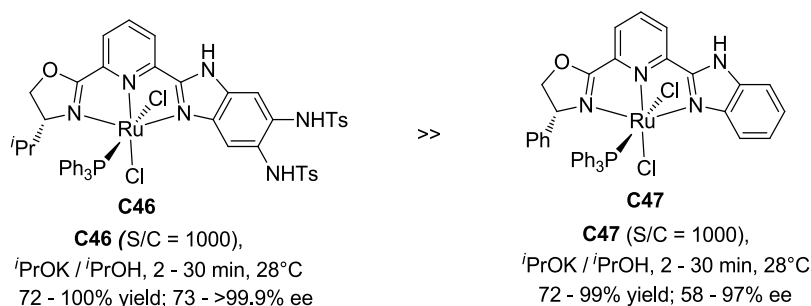
### 2.1.6 Heterocyclic ligands

In 2017, Yu *et al.* described a series of new Ru(II)-*N,N,N* complexes **C46** containing a chiral pincer type ligand with a chiral (NHTs)<sub>2</sub>-substituted imidazolyl-oxazolynyl-pyridine moiety. By comparison with the non-substituted Ru(II)-*N,N,N* complex **C47**,<sup>105</sup> a remarkable

<sup>104</sup> Mary Sheeba, M.; Preethi, S.; Nijamudheen, A.; Muthu Tamizh, M.; Datta, A.; Farrugia, L. J.; Karvembu, R. *Catal. Sci. Tech.* **2015**, *5*, 4790.

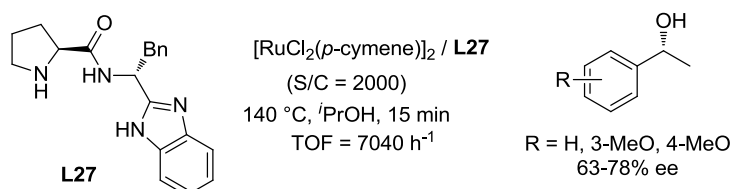
<sup>105</sup> Ye, W. J.; Zhao, M.; Du, W. M.; Jiang, Q. B.; Wu, K. K.; Wu, P.; Yu, Z. K. *Chem. Eur. J.* **2011**, *17*, 4737.

NHTs effect was observed for the (NHTs)<sub>2</sub>-substituted Ru(II)/*N,N,N* precatalyst **C46** in the ATH of ketones since higher enantiomeric excesses were obtained (Scheme 48).<sup>106</sup>



Scheme 48

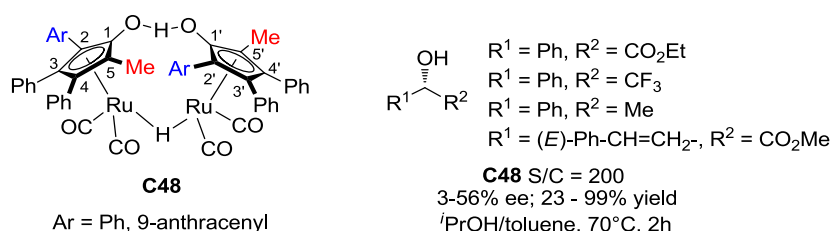
Chiral amino acid derived benzylimidazole **L27** was synthesized and evaluated in Ru(II)-catalyzed ATH of acetophenone to efficiently provide the chiral alcohols with ees ranging from 63 to 78% using a low catalyst loading (S/C = 2000) (Scheme 49).<sup>107</sup>



Scheme 49

### 2.1.7 Other type of chiral Ru complexes

A new type of planar chiral Shvo's catalysts with various substituents next to the Cp-OH moiety was prepared. The chiral Ru(II) complex **C48** bearing 9-anthracenyl- and methyl- next to Cp-OH ring was efficient for the enantioselective transfer hydrogenation of activated ketones, such as trifluoromethyl ketone,  $\alpha$ -keto ester, and  $\beta,\gamma$ -unsaturated  $\alpha$ -keto ester, providing the highest enantioselectivity (up to 56% ee) described so far for chiral Shvo's catalysts (Scheme 50).<sup>108</sup>



<sup>106</sup> Chai, H.; Liu, T.; Yu, Z.. *Organometallics* **2017**, 36, 4136.

<sup>107</sup> Li, X. -N.; Wang, L. -H.; Zhou, H. -Y.; Wang, J. -X. *Chin. J. Org. Chem.* **2016**, 36, 2175.

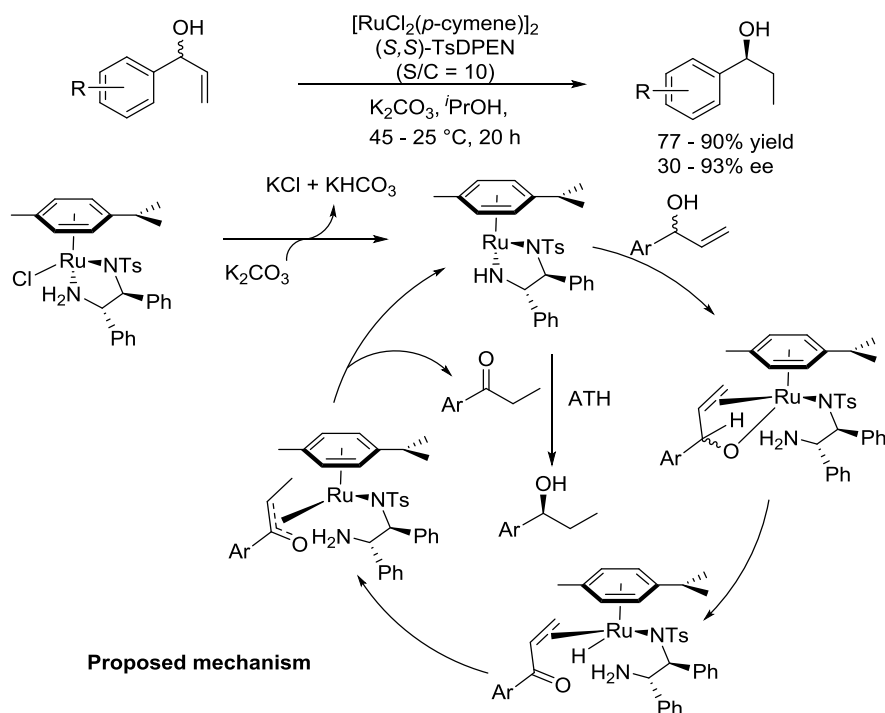
<sup>108</sup> Dou, X.; Hayashi, T. *Adv. Synth. Catal.* **2016**, 358, 1054.

## Scheme 50

A new type of artificial metalloenzymes was developed involving combination of several organometallic complexes  $\{[\text{RuCl}_2(\text{benzene})]_2, [\text{RuCl}_2(p\text{-cymene})]_2, [\text{RuCl}_2(\text{mesitylene})]_2, [\text{RhCl}_2\text{Cp}^*]_2, [\text{IrCl}_2\text{Cp}^*]_2\}$  with proteins (bovine  $\beta$ -lactoglobulin ( $\beta$ LG) or hen egg white lysozyme) as chiral macromolecular ligands. Among the protein-based metal complexes,  $[\text{RuCl}(\text{benzene})(\beta\text{LG})]$  complex displayed good catalytic activities and enantioselectivities for ATH of various aromatic ketones.<sup>109</sup>

## 2.2 Tandem reactions using Ruthenium catalysts

Sowa *et al.* reported the preparation of optically active secondary alcohols through a combined Ru-catalyzed isomerization<sup>110</sup>/ATH reaction. The corresponding alcohols were obtained in yields up to 97% with up to 93% enantiomeric excess (Scheme 51).<sup>111</sup>



Scheme 51

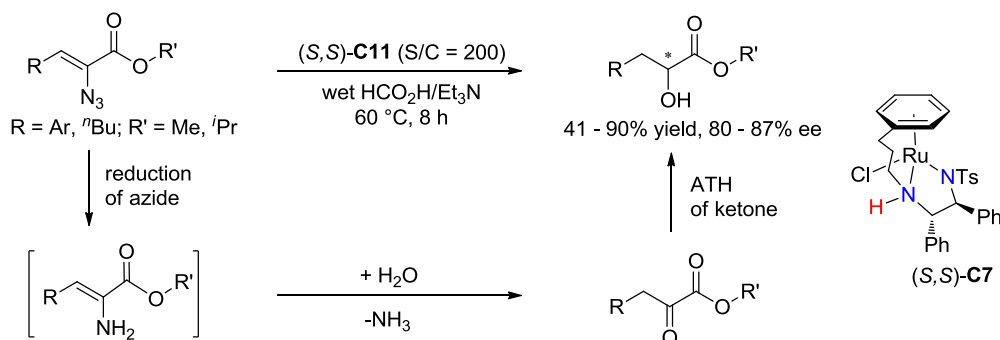
Another route was described to access chiral  $\alpha$ -hydroxy esters through reduction of  $\alpha$ -azido acrylates by using teth-Ru-TsDPEN complex (*S,S*)-**C7** as a catalyst in the presence of

<sup>109</sup> Cazares-Marinero, J. de J.; Przybylski, C.; Salmain, M. *Eur. J. Inorg. Chem.* **2018**, 1383.

<sup>110</sup> (a) Uma, R.; Crevisy, C.; Gree, R. *Chem. Rev.* **2003**, *103*, 27; (b) van der Drift, R. C.; Bouwman, E.; Drent, E. *J. Organomet. Chem.* **2002**, *650*, 1; (c) Arai, N.; Sato, K.; Azuma, K.; Ohkuma, T. *Angew. Chem. Int. Ed.* **2013**, *52*, 7500; (d) Mantilli, L.; Mazet, C. *Chem. Lett.* **2011**, *40*, 341; (e) Watson, A. J. A.; Atkinson, B. N.; Maxwell, A. C.; Williams, J. M. J. *Adv. Synth. Catal.* **2013**, *355*, 734.

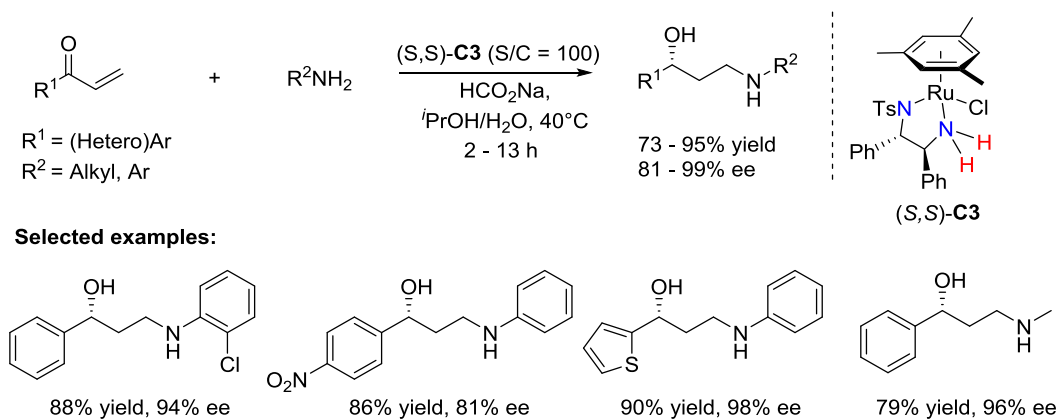
<sup>111</sup> Shoola, C. O.; DelMastro, T.; Wu, R.; Sowa, J. R. *Eur. J. Org. Chem.* **2015**, 1670.

wet  $\text{HCO}_2\text{H}/\text{Et}_3\text{N}$  as the hydrogen source. This three-step sequence includes azide reduction, enamine hydrolysis and ATH of ketones to deliver the products in good to excellent enantioselectivities (Scheme 52).<sup>112</sup>



Scheme 52

In 2017, Liu's group reported complex (S,S)-C3-catalyzed Michael-ATH tandem reaction for the one-pot transformation of a series of enones to efficiently access chiral (R)-secondary amino alcohols under mild conditions. This practical process produced the corresponding amino alcohols with 73–95% yields and up to 99% ees and provided another way for the synthesis of chiral antidepressants (Scheme 53).<sup>113</sup>

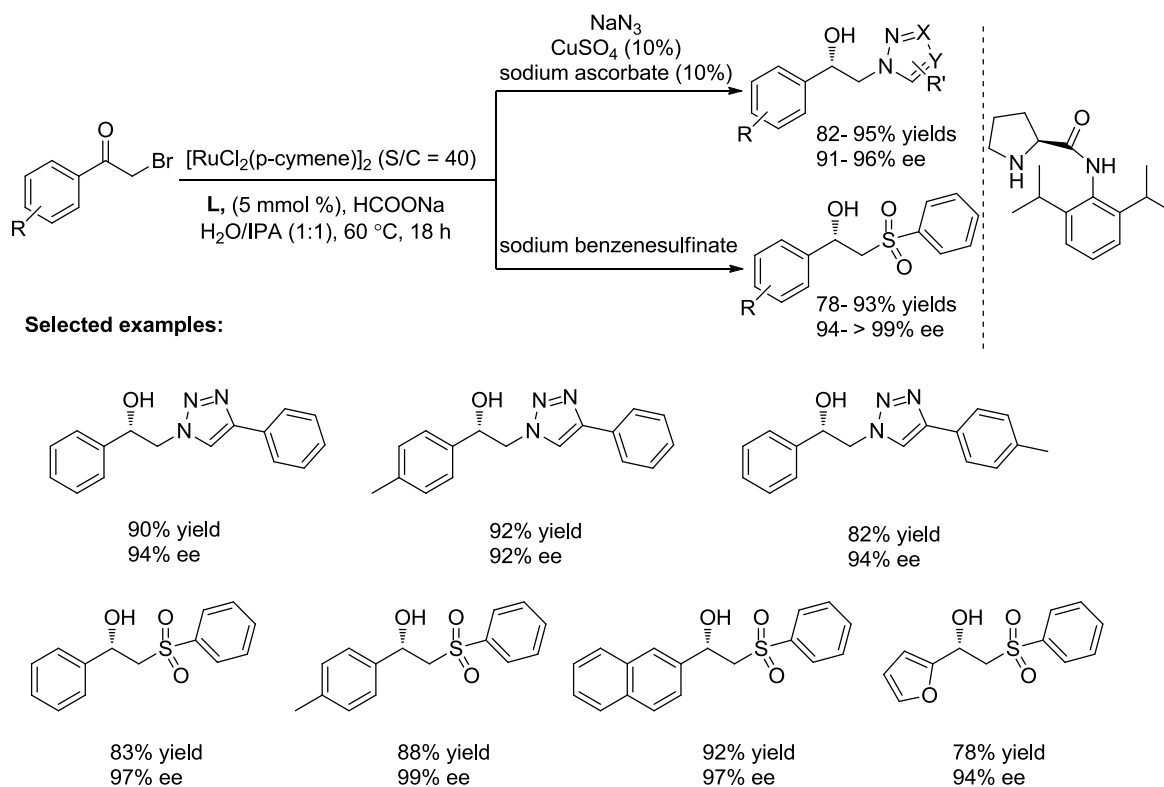


Scheme 53

In 2018, Bhanage *et al.* disclosed the synthesis of enantioenriched  $\beta$ -triazolylethanol and  $\beta$ -hydroxy sulfone derivatives by using ruthenium-catalyzed asymmetric transfer hydrogenation of the corresponding intermediate ketones. Their methodology involved asymmetric transfer hydrogenation of prochiral ketones and conversion of the resulting chiral alcohols to the  $\beta$ -triazolylethanol or  $\beta$ -hydroxy sulfone derivatives in a one pot procedure

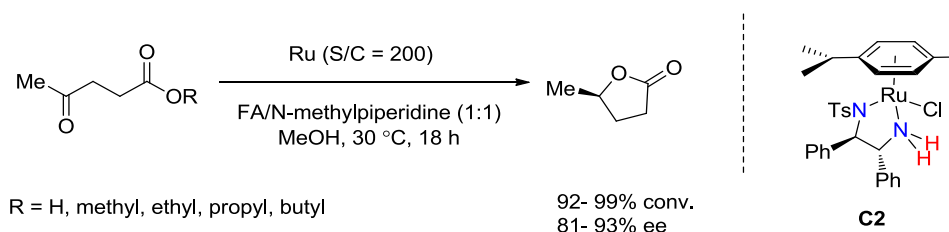
<sup>112</sup> Ji, Y.; Xue, P.; Ma, D.-D.; Li, X.-Q.; Gu, P.; Li, R. *Tetrahedron Lett.* **2015**, *56*, 192.

<sup>113</sup> Wu, L.; Jin, R.; Li, L.; Hu, X.; Cheng, T.; Liu, G. *A Org. Lett.* **2017**, *19*, 3047.

(Scheme 54).<sup>114</sup>

Scheme 54

Bhanage *et al.* presented in 2019 the first report of asymmetric transfer hydrogenation of levulinic acid derivatives to chiral  $\gamma$ -valerolactone (GVL) catalyzed by Noyori's type ruthenium catalyst (*R,R*)-**C2**. (*R*)-GVL was obtained with 99% conversion and 93% enantioselectivity (Scheme 55).<sup>115</sup>



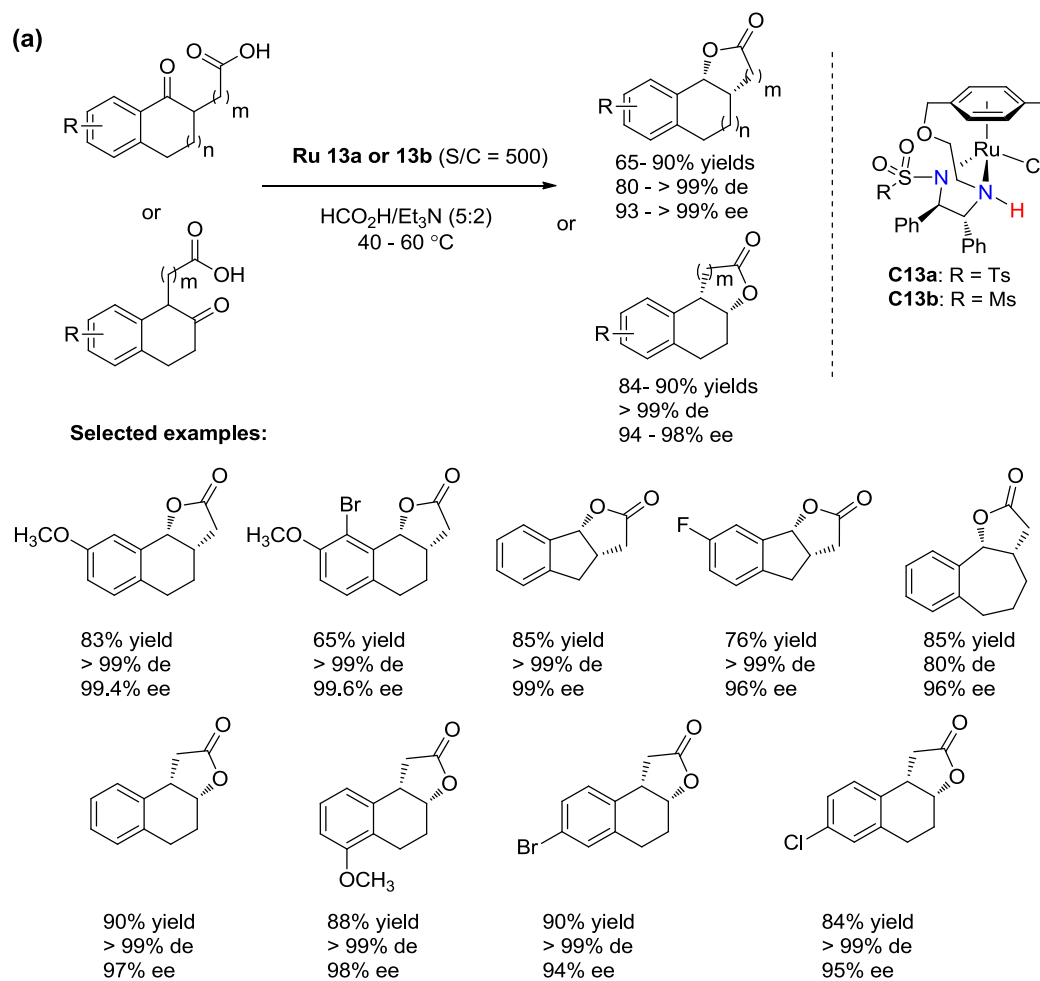
Scheme 55

In 2019, Kayaki *et al.* described the synthesis of chiral  $\gamma$ - and  $\delta$ -lactones containing multiple contiguous stereocenters through ATH of racemic keto acids in one pot. Their approach relies on (1) a DKR-ATH reaction mediated by oxo-tethered Ru(II) complexes and

<sup>114</sup> Vyas, V. K.; Srivastava, P.; Bhatt, P.; Shende, V.; Ghosh, P.; Bhanage, B. M. *ACS. Omega*. **2018**, *3*, 12737.

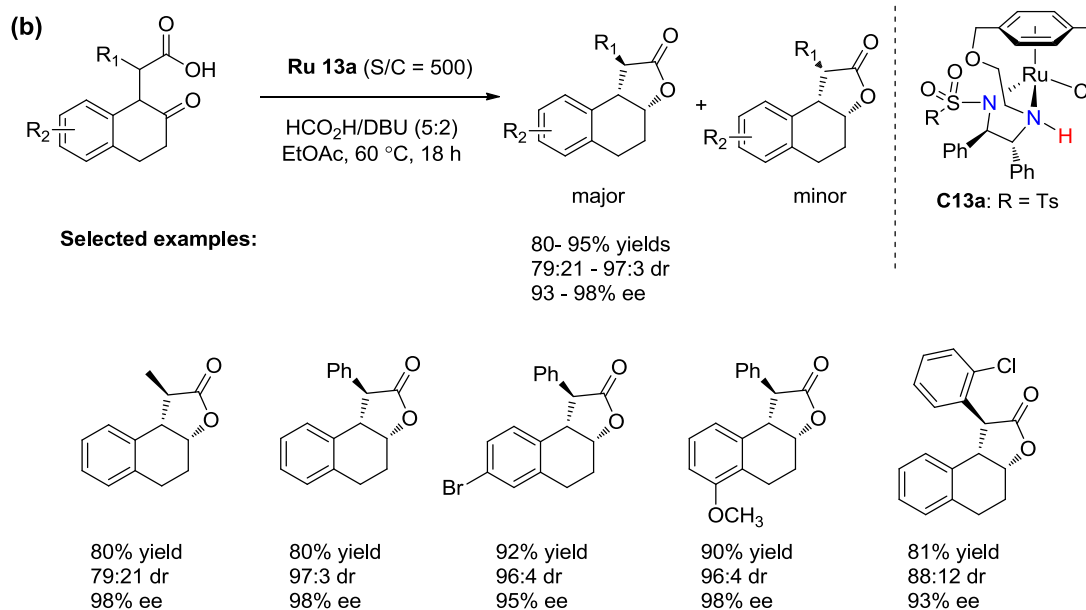
<sup>115</sup> Shende, V. S.; Raut, A. B.; Raghav, P.; Kelkar, A. A.; Bhanage, B. M. *ACS. Omega*. **2019**, *4*, 19491.

the subsequent *syn*-selective lactonization or (2) the combination of a DKR-ATH/lactonization sequence with asymmetric hydrogenation catalyzed by the chiral phosphine-Ru system (Scheme 56).<sup>116</sup>



<sup>116</sup> Touge, T.; Sakaguchi, K.; Tamaki, N.; Nara, H.; Yokozawa, T.; Matsumura, K.; Kayaki, Y. *J. Am. Chem. Soc.* **2019**, *141*, 16354.

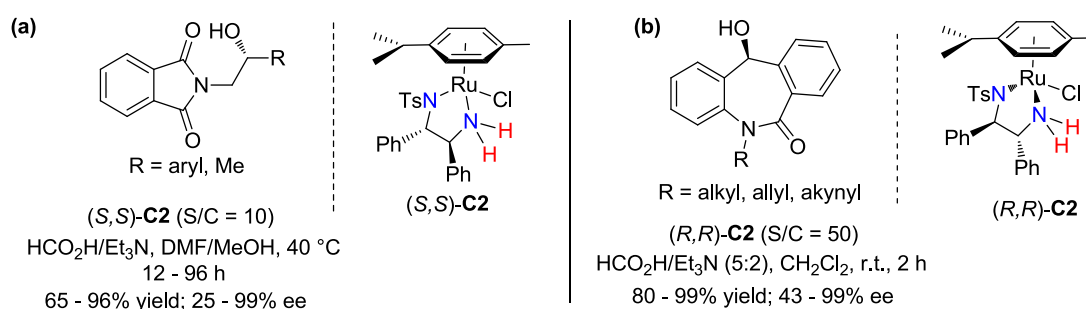




Scheme 56

## 2.3 ATH of functionalized ketone derivatives with Ruthenium catalysts

Liu *et al* reported, in 2015, complex (*S,S*)-**C2**-catalyzed ATH of  $\alpha$ -phthalimido ketones with the mixture of HCO<sub>2</sub>H/Et<sub>3</sub>N to yield the corresponding amino alcohols in high yields and excellent enantioselectivities (Scheme 57a).<sup>117</sup> In 2016, Bhanage *et al.* reported the use of complex **C2** in ATH of *N*-alkylated dibenzo [*b,e*]-azepine-6,11-dione by using HCO<sub>2</sub>H/Et<sub>3</sub>N (5:2) to provide the corresponding alcohols with moderate to excellent enantioselectivities. (43→ 99% ee) (Scheme 57b).<sup>118</sup>



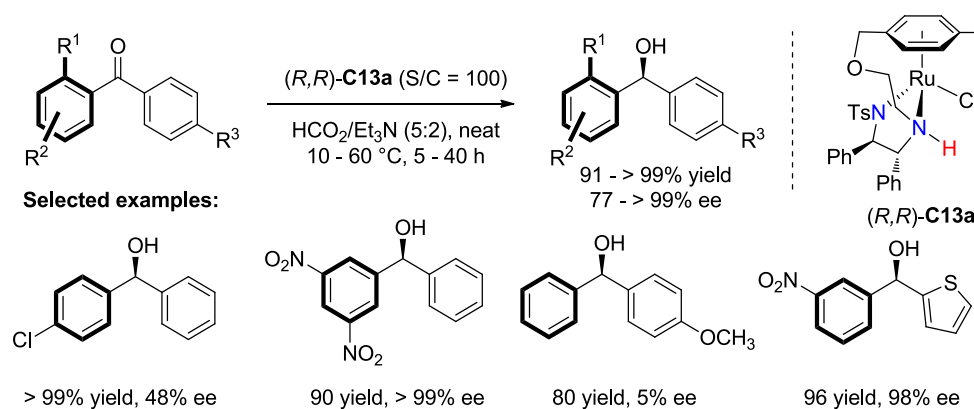
Scheme 57

Touge, Kayaki *et al.* first reported in 2016, an oxo-containing tethered Ru(II) complex (*R,R*)-**C13a** used in the ATH of a wide variety of unsymmetrical benzophenones to access chiral diarylmethanols with high yields (up to >99%) and enantioselectivities (up to > 99% ee).

<sup>117</sup> Xu, Z.; Li, Y.; Liu, J.; Wu, N.; Li, K.; Zhu, S.; Zhang, R.; Liu, Y. *Org. Biomol. Chem.* **2015**, *13*, 7513.

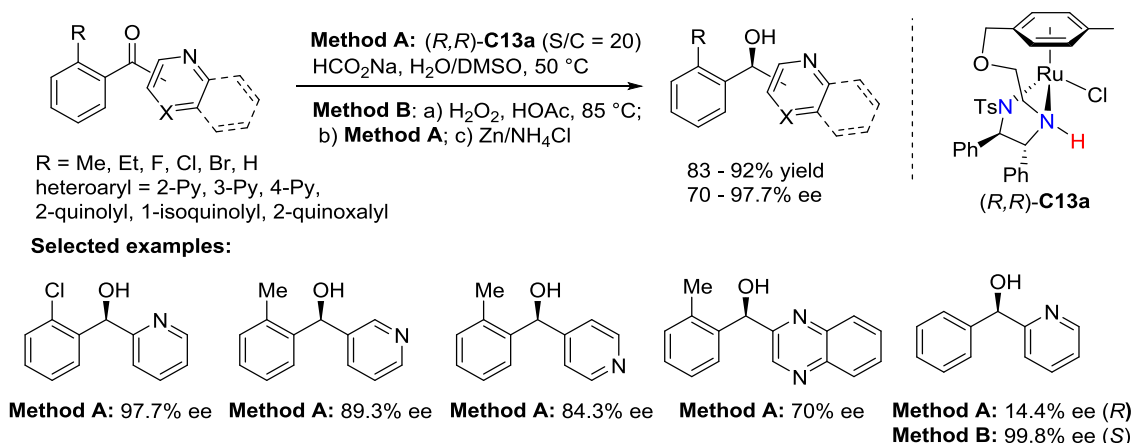
<sup>118</sup> Vyas, V. K.; Bhanage, B. M. *Org. Chem. Front.* **2016**, *3*, 614.

The high enantioinductions can be explained by the discrimination for substituents at the *ortho* position on the aryl group, as well as the differentiation between electron-poor and electron-rich arene rings (Scheme 58).<sup>119</sup>



Scheme 58

In 2017, Zhou *et al.* described an efficient approach to access a variety of chiral aryl *N*-heteroaryl methanols through commercially available bifunctional oxo-tethered ruthenium complex (*R,R*)-**C13a**-catalyzed ATH of the corresponding *ortho*- or non-*ortho*-substituted ketones in an aqueous solution, leading to the reduced products in high yields (83–92%) and enantioinductions (70–97.7% ee) (Scheme 59).<sup>120</sup>



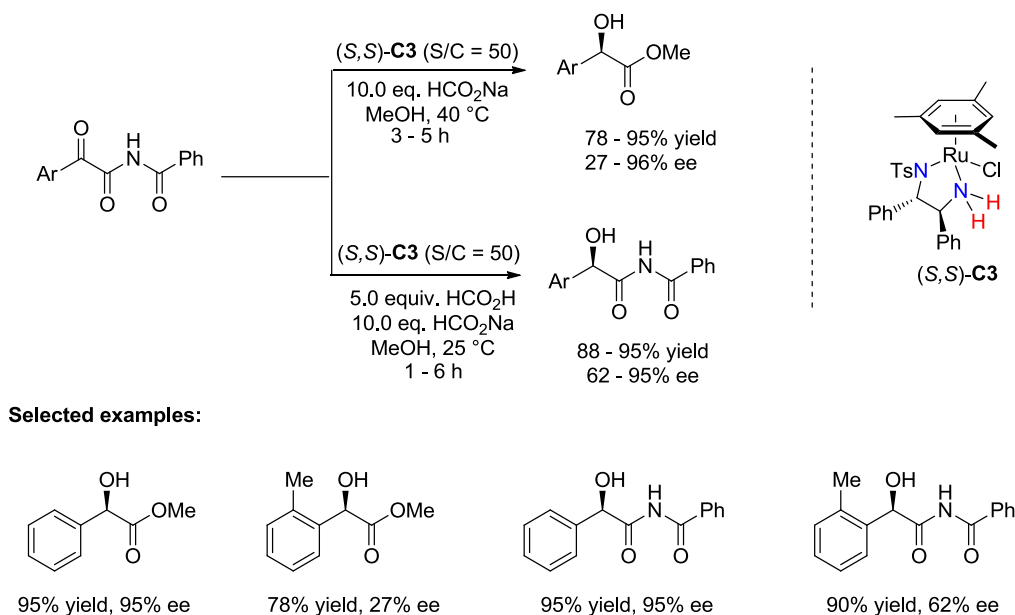
Scheme 59

In 2016, Liu *et al.* described ATH of  $\alpha$ -ketoimides catalyzed by Ru(II) complex (*S,S*)-**C3** to produce a wide variety of aromatic chiral  $\alpha$ -hydroxy imides (88–95% yield, 62–95% ee) or

<sup>119</sup> Touge, T.; Nara, H.; Fujiwhara, M.; Kayaki, Y.; Ikariya, T. *J. Am. Chem. Soc.* **2016**, *138*, 10084.

<sup>120</sup> Wang, B.; Zhou, H.; Lu, G.; Liu, Q.; Jiang, X. *Org. Lett.* **2017**, *19*, 2094.

$\alpha$ -hydroxy esters (78–95% yield, 27–96% ee) through a slight adjustment of the reaction conditions (Scheme 60).<sup>121</sup>

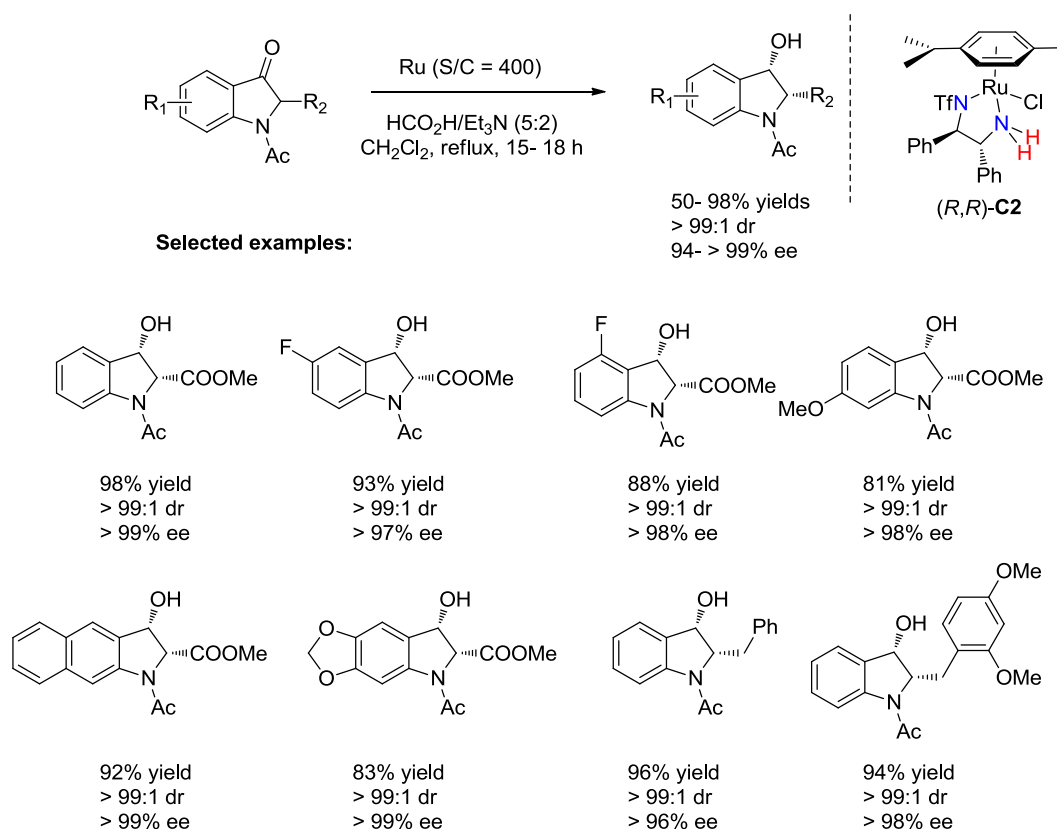


Scheme 60

In 2018, Wang *et al.* developed an asymmetric transfer hydrogenation of 3-oxindoline derivatives for the synthesis of *cis*-2-substituted-*N*-acetyl-3-hydroxyindolines through dynamic kinetic resolution. The reaction was catalyzed by Tf-DPEN-Ru catalyst (S/C = 400) with HCO<sub>2</sub>H/Et<sub>3</sub>N (5:2) azeotropic mixture as the hydrogen donor under mild conditions, and afforded the products in good yields with both high level of diastereoselectivities and enantioselectivities (Scheme 61).<sup>122</sup>

<sup>121</sup> Zhao, Q.; Zhao, Y.; Liao, H.; Cheng, T.; Liu, G. *ChemCatChem*. **2016**, *8*, 412.

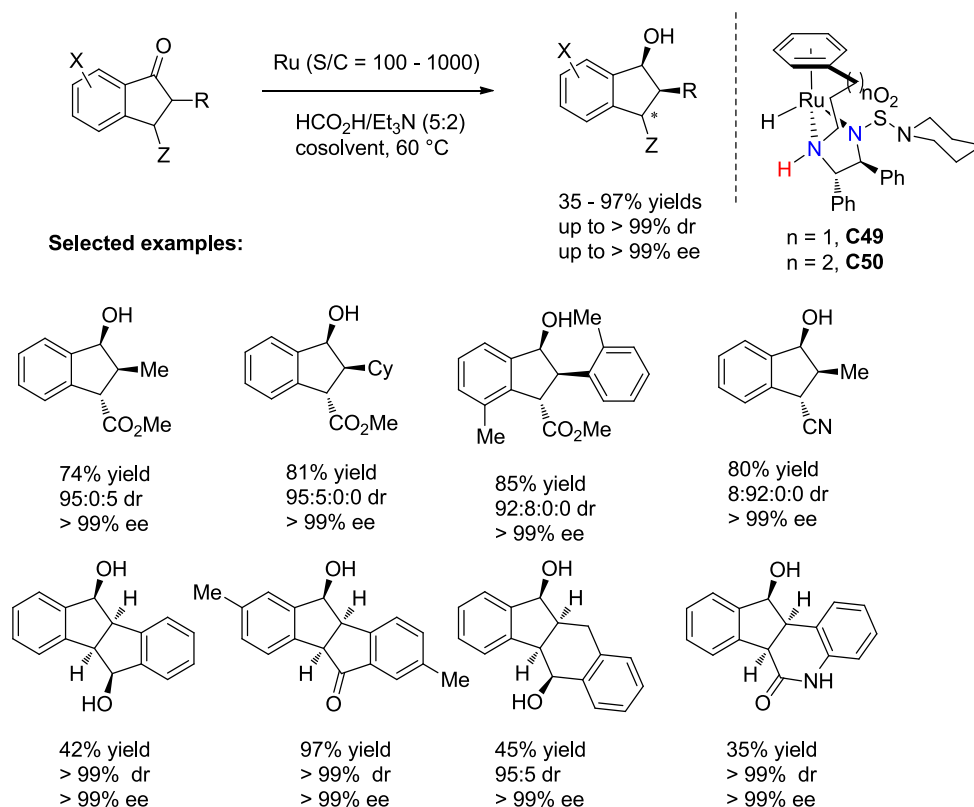
<sup>122</sup> Luo, Z.; Sun, G.; Zhou, Z.; Liu, G.; Luan, B.; Lin, Y.; Zhang, L.; Wang, Z. *Chem. Commun.* **2018**, *54*, 13503.



Scheme 61

Mohar *et al.* published a ruthenium-catalyzed asymmetric transfer hydrogenation of activated racemic 2,3-disubstituted 1-indanones to the corresponding chiral 2,3-disubstituted-1-indanols via dynamic kinetic resolution. Interestingly, their method also offered a practical access to a new class of conformationally rigid enantiopure 1,4-diols having four contiguous stereogenic centers. A number of alcohol products possessing multiple contiguous stereocenters were obtained in stereopure forms (Scheme 62).<sup>123</sup>

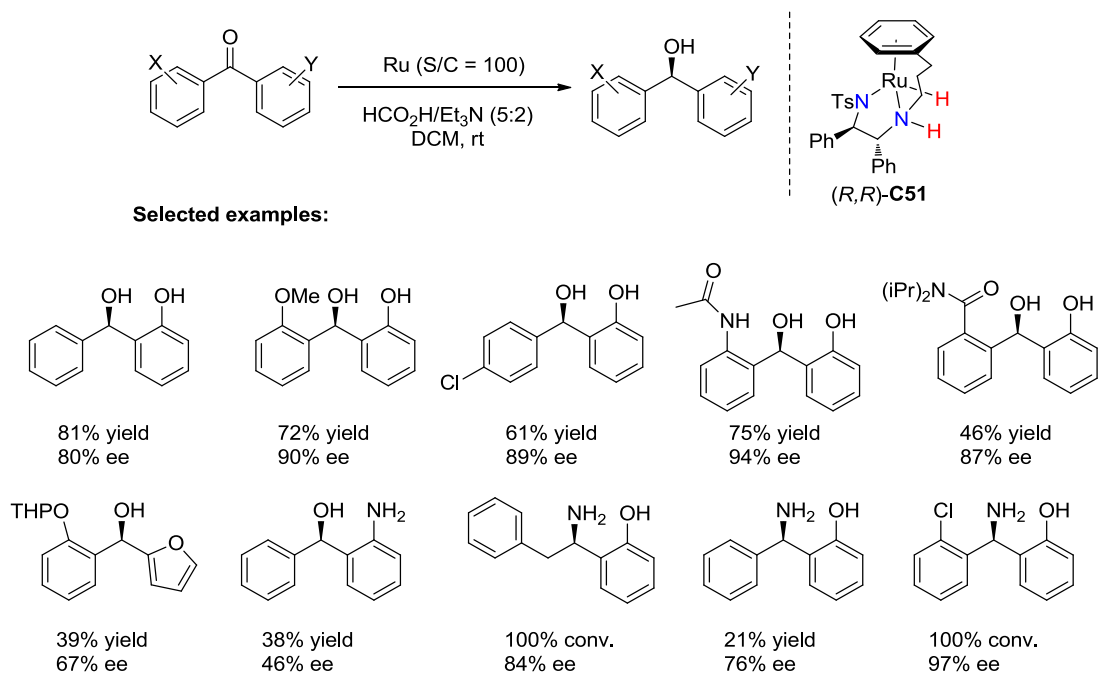
<sup>123</sup> Cotman, A. E.; Modéc, B.; Mohar, B. *Org. Lett.* **2018**, *20*, 2921.



Scheme 62

In 2020, Wills group reported an asymmetric transfer hydrogenation of *O*-hydroxyphenyl ketones. In their study, they tested different tethered and untethered ruthenium complexes with HCO<sub>2</sub>H/Et<sub>3</sub>N (5:2) azeotropic mixture as hydrogen donor. It turned out that the “3C-tethered” ruthenium complex (*R,R*)-**C51** gave the best yields with the highest enantioselectivities. It is worth noting that this method can also be applied to some imines derived from *o*-hydroxyphenyl ketones (Scheme 63).<sup>124</sup>

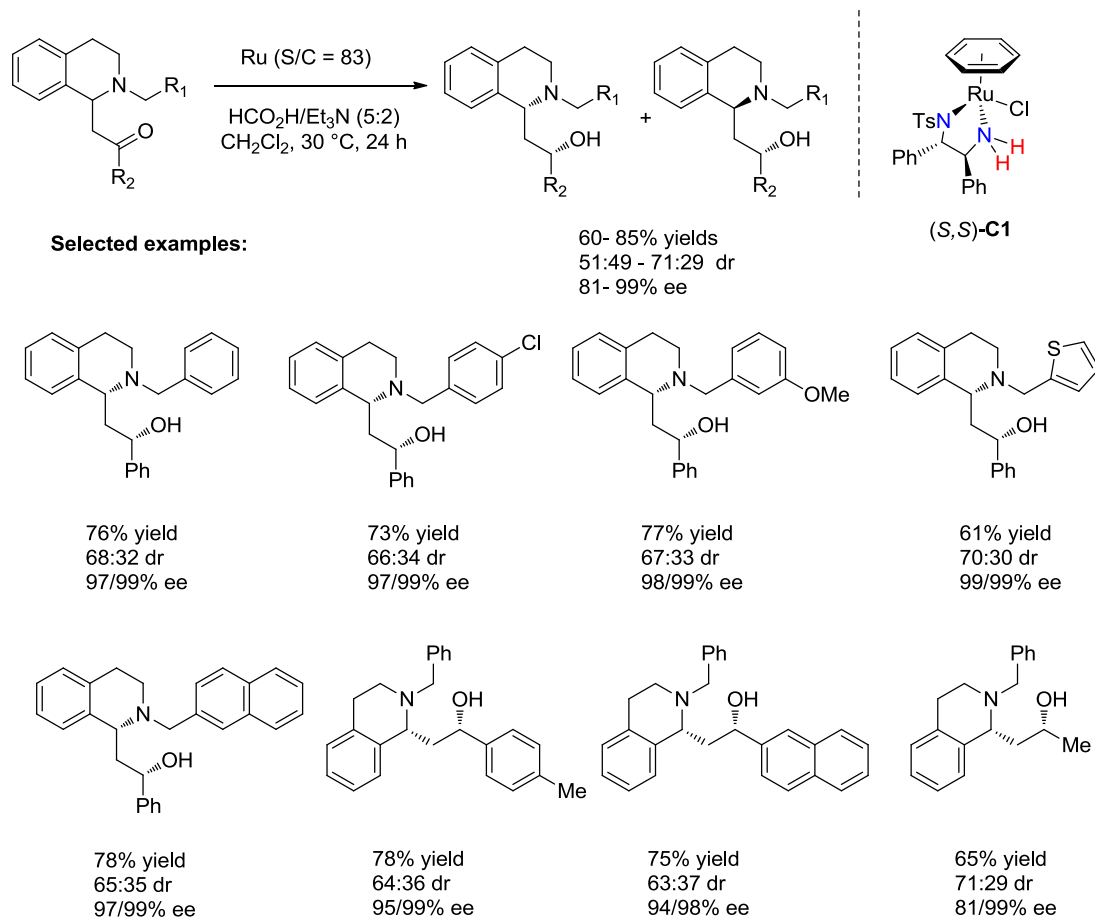
<sup>124</sup> Zheng, Y.; Clarkson, G. J.; Wills, M. *Org. Lett.* **2020**, *22*, 3717.



Scheme 63

In 2018, our group reported an efficient asymmetric synthesis of 2-(1,2,3,4-tetrahydro-1-isoquinolyl)ethanol derivatives, which were obtained from asymmetric transfer hydrogenation of ring-substituted  $\beta$ -amino ketones through dynamic kinetic resolution. This reaction proceeded under mild conditions in the presence of (*S,S*)-**C1** as catalyst and HCO<sub>2</sub>H/Et<sub>3</sub>N (5:2) as the hydrogen source, delivering a variety of *syn* 2-(1,2,3,4-tetrahydro-1-isoquinolyl) derivatives in good yields with excellent enantioselectivities (up to 99% ee) (Scheme 64).<sup>125</sup>

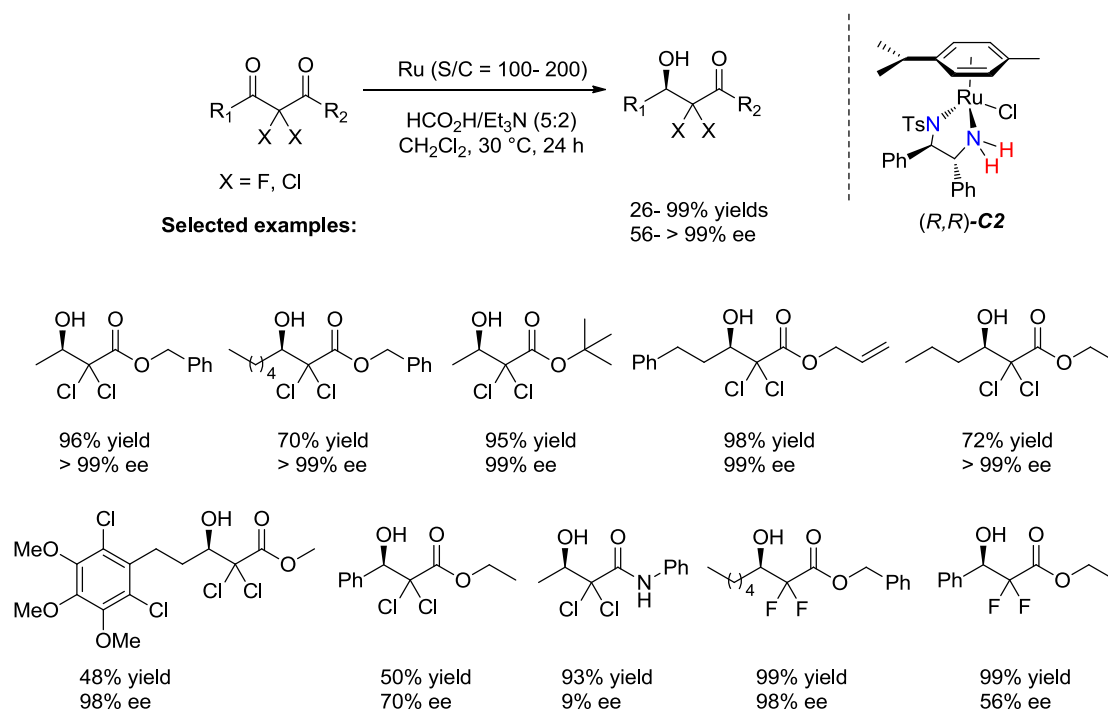
<sup>125</sup> Zheng, L. S.; Férard, C.; Phansavath, P.; Ratovelomanana-Vidal, V. *Org. Chem. Front.*, **2018**, *5*, 1366.



Scheme 64

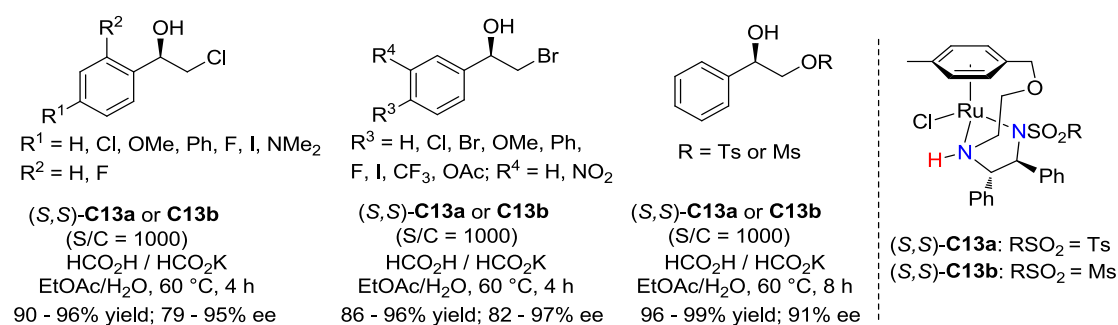
The same year, our group published another mild and convenient approach to prepare a series of  $\alpha,\alpha$ -dihalogeno  $\beta$ -hydroxy esters or amides. Highly enantioenriched  $\alpha,\alpha$ -dichloro or  $\alpha,\alpha$ -difluoro  $\beta$ -hydroxy esters and  $\beta$ -hydroxy amides were synthesized using Noyori's complex (*R,R*)-C2 by asymmetric transfer hydrogenation of the corresponding ketones with HCO<sub>2</sub>H/Et<sub>3</sub>N (5:2) azeotropic mixture as the hydrogen donor. A wide range of nonaromatic  $\alpha,\alpha$ -dihalogeno  $\beta$ -keto esters were reduced with high yields (up to 99%) and high level of enantioselectivities (up to >99% ee). Moreover, the ATH conditions can be performed on gram-scale as well, proving the usefulness of this method (Scheme 65).<sup>126</sup>

<sup>126</sup> Zheng, L. S.; Férard, C.; Phansavath, P.; Ratovelomanana-Vidal, V. *Org. Lett.* **2018**, *20*, 5107.



Scheme 65

In 2017, Kayaki, Yuki *et al.* developed an effective system for the ATH of  $\alpha$ -substituted (Br, Cl, OMs, OTs) aromatic ketone derivatives in the presence of (*S,S*)-**C13a** and (*S,S*)-**C13b** by using HCO<sub>2</sub>H/HCO<sub>2</sub>K in aqueous EtOAc to afford a wide variety of  $\alpha$ -substituted chiral secondary alcohols in high yields (86–98%) and good to excellent enantioselectivities (79–97% ee). The useful  $\alpha$ -functionalized chiral alcohols allow further transformations. This system is more practical and selective than previously reported approaches,<sup>127</sup> which led to byproducts (Scheme 66).<sup>128</sup>



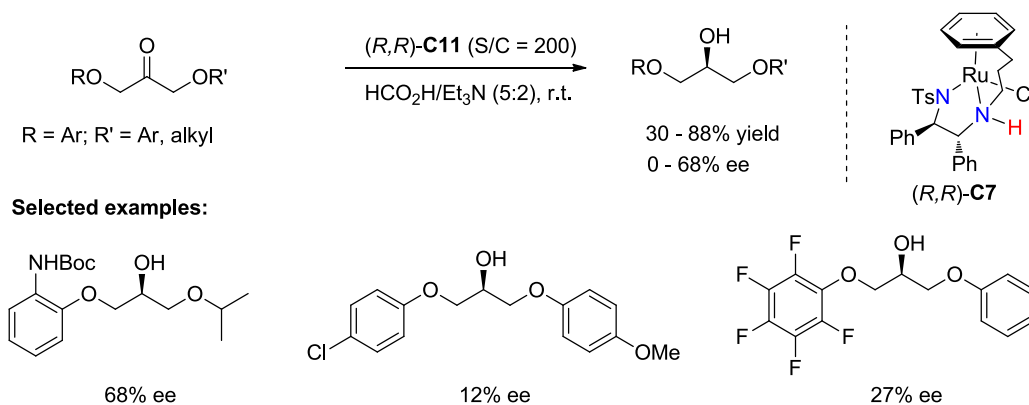
Scheme 66

<sup>127</sup> (a) Ma, Y.; Liu, H.; Chen, L.; Cui, X.; Zhu, J.; Deng, J. *Org. Lett.* **2003**, *5*, 2103. (b) Komiyama, M.; Itoh, T.; Takeyasu, T. *Org. Process Res. Dev.* **2015**, *19*, 315.

<sup>128</sup> Yuki, Y.; Touge, T.; Nara, H.; Matsumura, K.; Fujiwhara, M.; Kayaki, Y.; Ikariya, T. *Adv. Synth. Catal.* **2017**, *360*, 568.

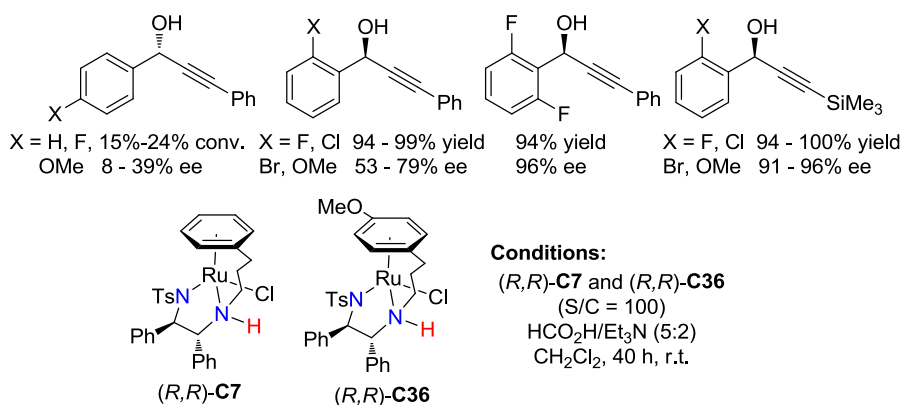


In 2017, Wills *et al.* reported the ATH of a number of propanones bearing aryloxy and alkoxy substituents at the 1- and 3-positions using the Ru(II)/TsDPEN tethered complex (*R,R*)-**C7**. The enantioselectivity of the reduction was highly dependent of the combination of steric and electronic effects for this challenging type of substrates, and ees up to 68% ee could be attained (Scheme 67).<sup>129</sup>



Scheme 67

A number of hindered aryl propargylic ketones were transformed into the corresponding chiral aryl propargylic alcohols in high yields and moderate to excellent enantioselectivities through an ATH process with tethered Ru(II) complexes (*R,R*)-**C7** and (*R,R*)-**C36** as catalysts in the presence of HCO<sub>2</sub>H/Et<sub>3</sub>N as the hydrogen source (Scheme 68).<sup>130</sup>



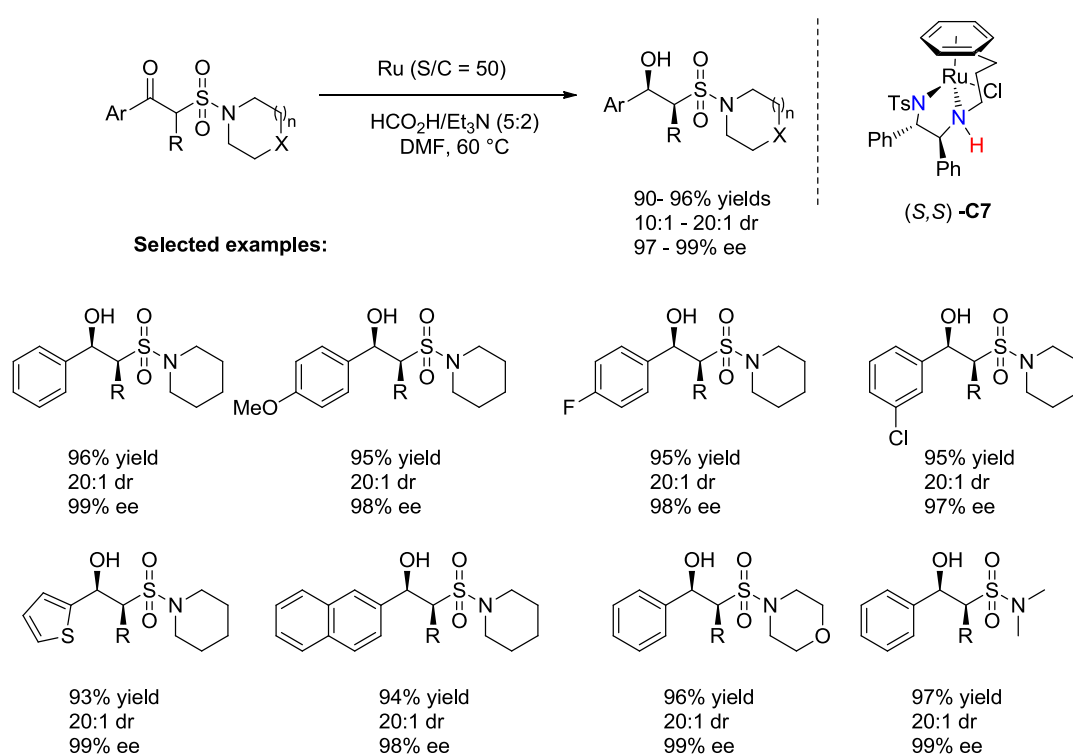
Scheme 68

In 2018, Lv and Zhang *et al.* published an efficient asymmetric transfer hydrogenation reaction for reduction of  $\alpha$ -sulfonamide- $\beta$ - ketones by using chiral Ru(II) complex (*S,S*)-**C7** as catalyst and HCO<sub>2</sub>H/Et<sub>3</sub>N azeotropic mixture as the hydrogen source under mild conditions. Their method afforded the corresponding syn  $\alpha$ -substituted  $\beta$ -hydroxy sulfonamides in good

<sup>129</sup> Forshaw, S.; Matthews, A. J.; Brown, T. J.; Diorazio, L. J.; Williams, L.; Wills, M. *Org. Lett.* **2017**, *19*, 2789.

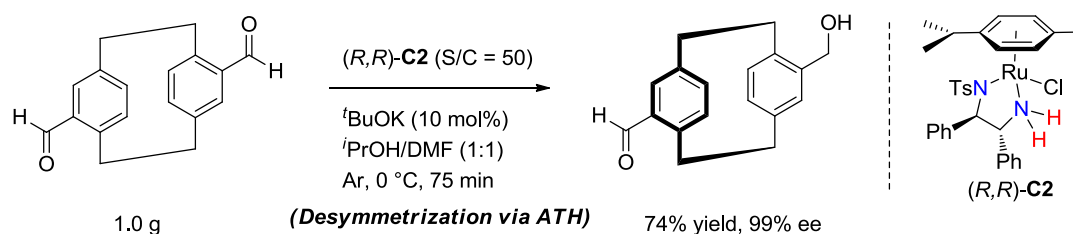
<sup>130</sup> Vyas, V. K.; Knighton, R. C.; Bhanage, B. M.; Wills, M. *Org. Lett.* **2018**, *20*, 975.

yields with high level of diastereo- and enantioselectivities upto 99% ee (Scheme 69).<sup>131</sup>



Scheme 69

In 2018, Benedetti and Micouin *et al.* reported the use of Noyori's catalyst (*R,R*)-C2 in the desymmetrization of a centrosymmetric pseudo-para-diformyl[2.2]paracyclophane via ATH. A monohydroxymethylated product was obtained in good yields and excellent enantioselectivities (up to 74% isolated yield and 99% ee) during the gram scale experiment without any significant loss in the reaction efficiency (Scheme 70).<sup>132</sup>



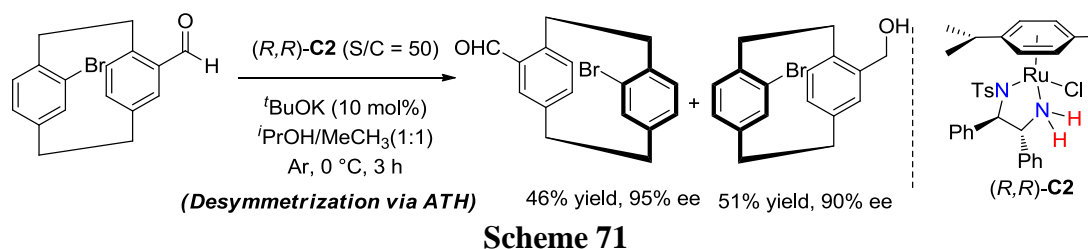
Scheme 70

The same group expanded the scope of the ATH reaction to polysubstituted [2.2]paracyclophanes. They focused their attention on halogenated derivatives, which include bromine atoms at different positions of the paracyclophane core. In 2019, they developed another method of asymmetric transfer hydrogenations to control the planar chirality of

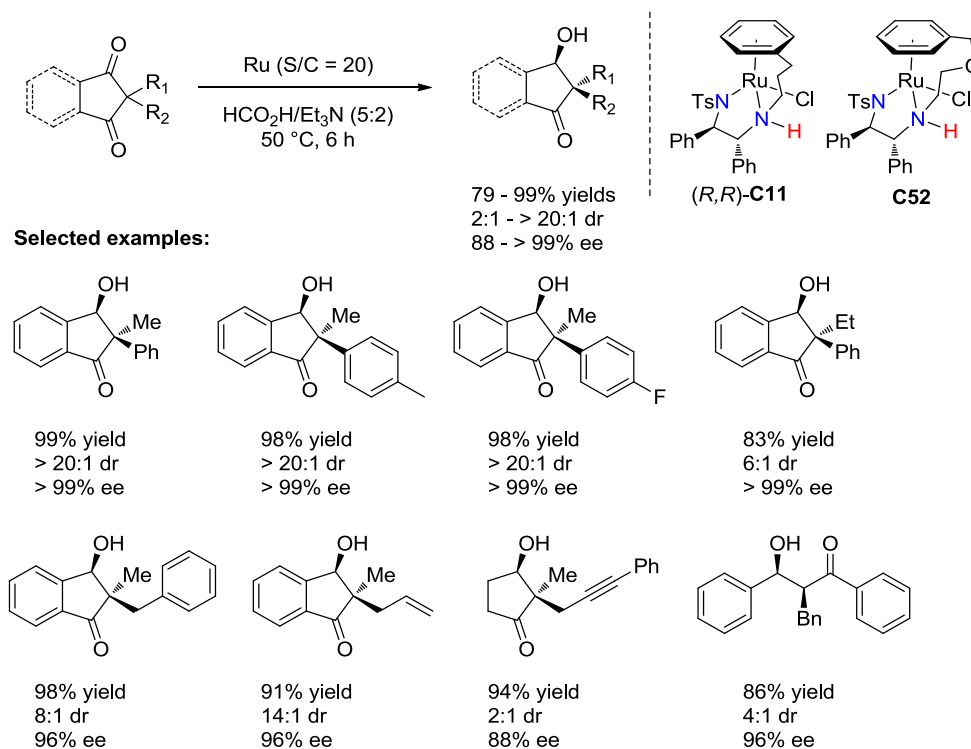
<sup>131</sup> Xiong, Z.; Pei, C.; Xue, P.; Lv, H.; Zhang, X. *Chem. Commun.* **2018**, 54, 3883.

<sup>132</sup> Delcourt, M.-L.; Felder, S.; Benedetti, E.; Micouin, L. *ACS Catal.* **2018**, 8, 6612.

[2.2]paracyclophanes via kinetic resolution (Scheme 71).<sup>133</sup>



In 2020, Zhou *et al.* developed a facile synthesis of chiral *cis*  $\beta$ -hydroxy ketones through hydrogenative desymmetrization of 1,3-cyclopentanediones catalyzed by ruthenium complexes. They used formic acid-triethylamine (5:2) azeotrope as both hydrogen donor and solvent, the reactions tolerated a wide range of substrates and led to excellent yields (up to 99%) with high diastereoselectivities (up to > 20:1) and enantioselectivities (up to > 99%). This simple operation can be performed on gram scale as well without loss of reactivity and enantioselectivity (Scheme 72).<sup>134</sup>

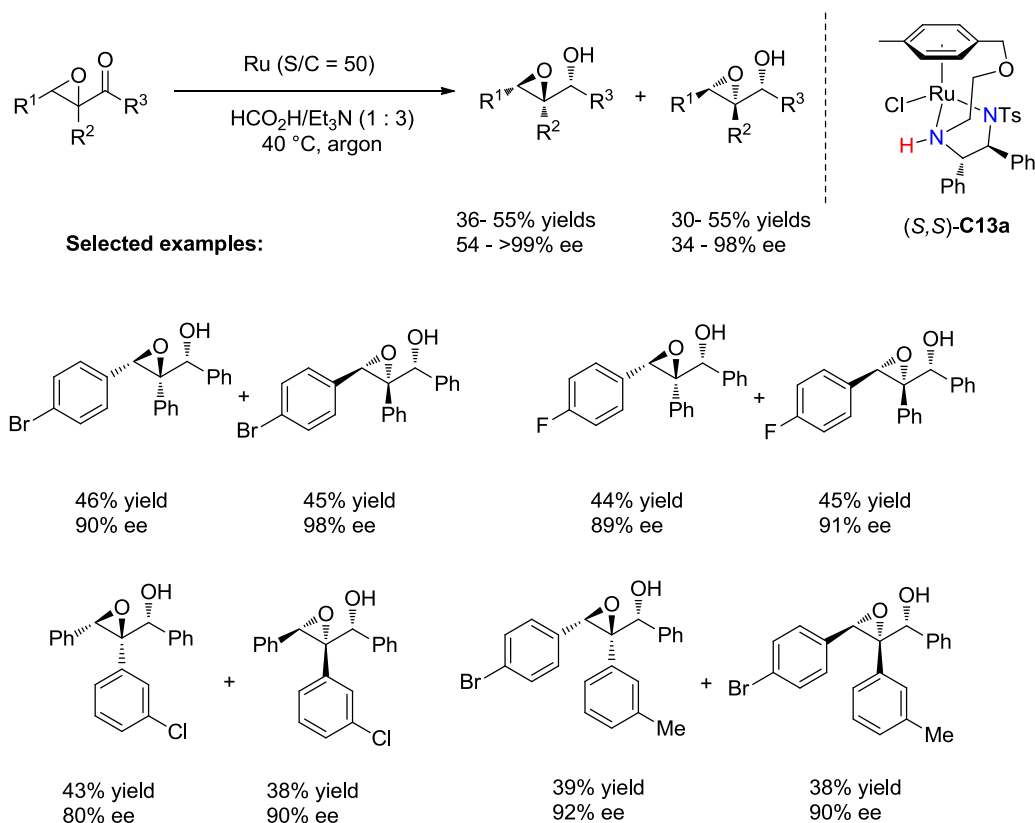


In 2019, Fang *et al.* reported the first example of ruthenium-catalyzed transfer hydrogenation of racemic epoxy ketones through the resolution technique of divergent RRM (Reaction on Racemic Mixture). The resolution technique of stereodivergent RRM is different

<sup>133</sup> Delcourt, M. L.; Felder, S.; Turcaud, S.; H. Pollok, C.; Merten, C.; Micouin, L.; Benedetti, E. *J. Org. Chem.* **2019**, *84*, 5369.

<sup>134</sup> Wang, H.; Zhao, Y.; Ding, Y-X.; Yu, C-B.; Zhou, Y-G. *Asian J. Org. Chem.* **2020**, *9*, 753

from the conventional classical kinetic resolution and displays 100% utilization of the starting materials and can produce two separable diastereomeric epoxy alcohols (Scheme 73).<sup>135</sup>

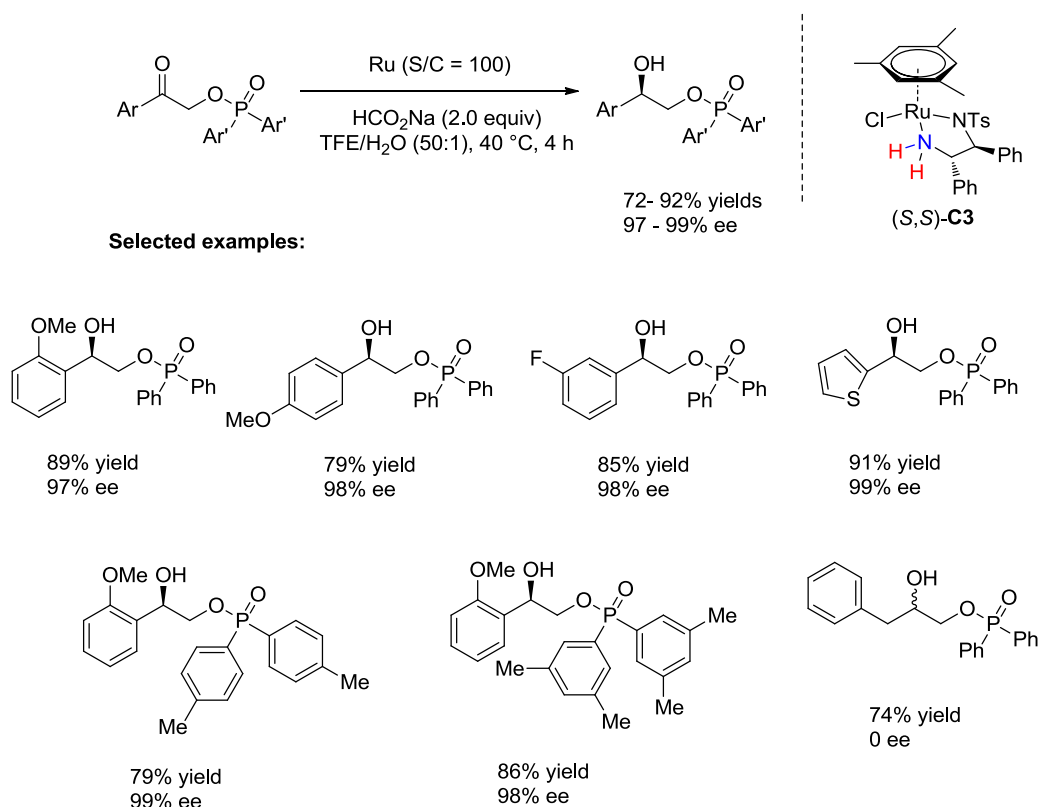


**Scheme 73**

Zhou *et al.* described an ATH of 2-oxo alkyl phosphinates catalyzed by commercially available ruthenium complex using sodium formate as a hydrogen source in an aqueous solution of 2,2,2-trifluoroethanol at 40 °C. A range of 2-hydroxyalkyl diarylphosphinates were prepared in good yields with 97–99% ee (Scheme 74).<sup>136</sup>

<sup>135</sup> Zhao, Z.; Bagdi, P. R.; Yang, S.; Liu, J.; Xu, W.; Fang, X. *Org. Lett.* **2019**, *21*, 5491.

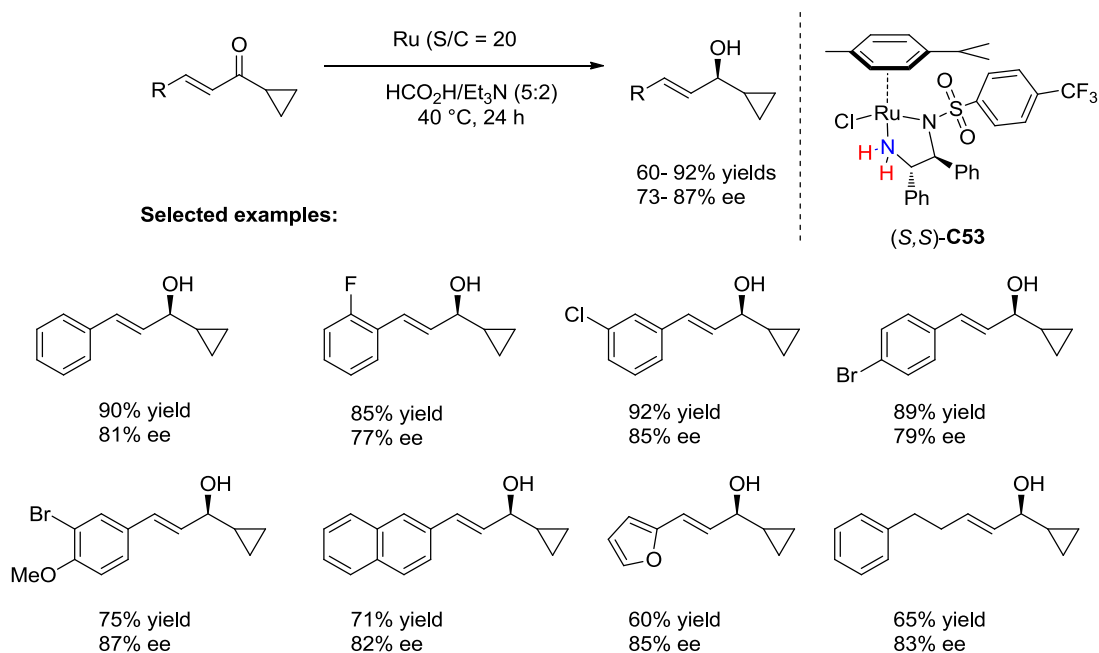
<sup>136</sup> Zhang, K.; Yang, Y.; Liu, H.; Liu, Q.; Lv, J.; Zhou, H. *Adv. Synth. Catal.* **2019**, *361*, 4106.



Scheme 74

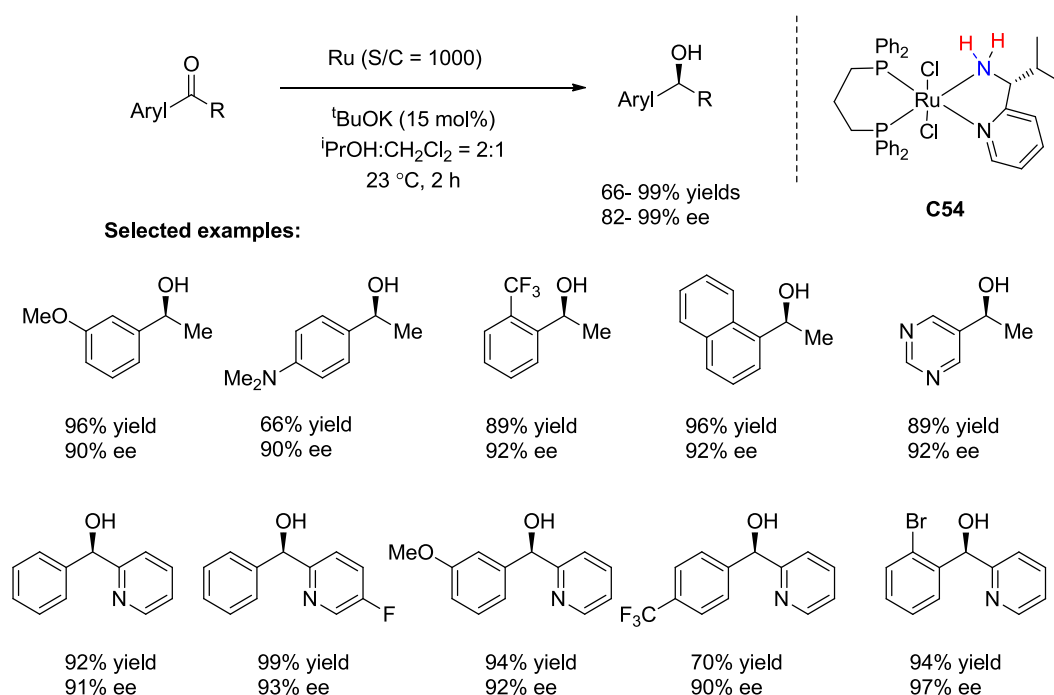
Lv *et al.* described a chemoselective asymmetric transfer hydrogenation of cycloalkyl vinyl ketones to prepare 1-cycloalkyl chiral allylic alcohols. The ATH reaction was catalyzed by a chiral diamine ruthenium complex **(S,S)-C53** with HCO<sub>2</sub>H/Et<sub>3</sub>N (5:2) azeotropic mixture as both a hydrogen source and solvent under mild conditions. A wide range of 1-cycloalkyl chiral allylic alcohols were obtained in good yields with good enantioselectivity up to 87% ee (Scheme 75).<sup>137</sup>

<sup>137</sup> Liu, S.; Cui, P.; Wang, J.; Zhou, H.; Liu, Q.; Lv, J. *Org. Biomol. Chem.* **2019**, *17*, 264.



Scheme 75

Xing *et al.* developed a new Ru-catalyst that features only a single stereogenic element and this new Ru-catalyst **C54** was demonstrated to be effective to attain high levels of stereoselectivity in the ATH over a broad range of ketone substrates, including aryl alkyl ketones and aryl *N*-heteroaryl ketones (Scheme 76).<sup>138</sup>

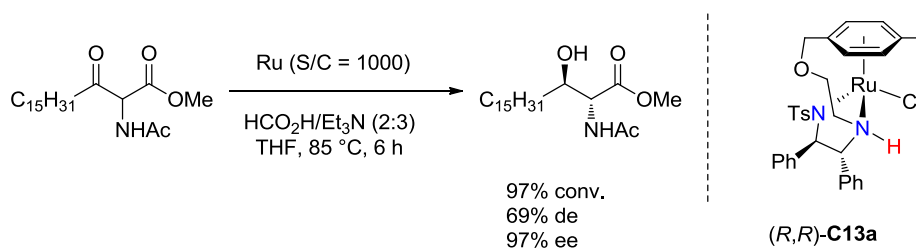


Scheme 76

In 2019, Saito *et al.* published the first example of ruthenium-catalyzed asymmetric transfer hydrogenation in a pipes-in-series flow reactor through dynamic kinetic resolution.

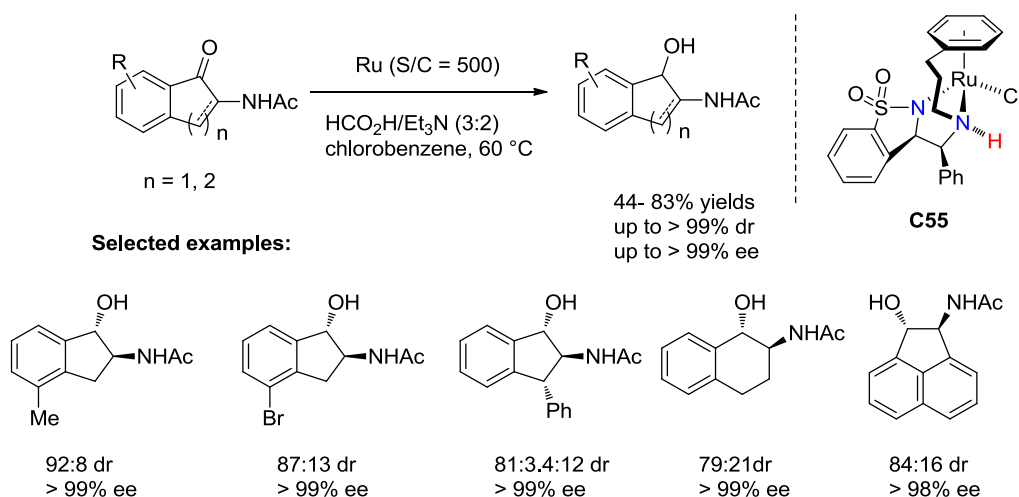
<sup>138</sup> Chen, F.; He, D.; Chen, L.; Chang, X.; W, Z. D.; Xu, C.; Xing, X. *ACS Catal.* **2019**, *9*, 5562.

Their method can be applied on >50 kg scale. And this process is an efficient synthetic route for an optically active ceramide compound (D-erythro-CER[NDS]) (Scheme 77).<sup>139</sup>



Scheme 77

The same year, Mohar *et al.* developed a new ansa-Ru(II) complex of an enantiomerically pure *syn*-*N,N*-ligand. This *ansa*-RuCl[*syn*-ULTAM-(CH<sub>2</sub>)<sub>3</sub>Ph] complex **C55** was used for the asymmetric transfer hydrogenation of  $\alpha,\beta$ -dehydro- $\alpha$ -acetamido and  $\alpha$ -acetamido benzocyclic ketones via dynamic kinetic resolution. The DFT calculations revealed that an atypical two-pronged substrate attractive stabilization engaging the commonly encountered CH/ $\pi$  electrostatic interaction and a new additional O=S=O  $\cdots$  HNAc H-bond hence favoring the trans-configured products (Scheme 78).<sup>140</sup>



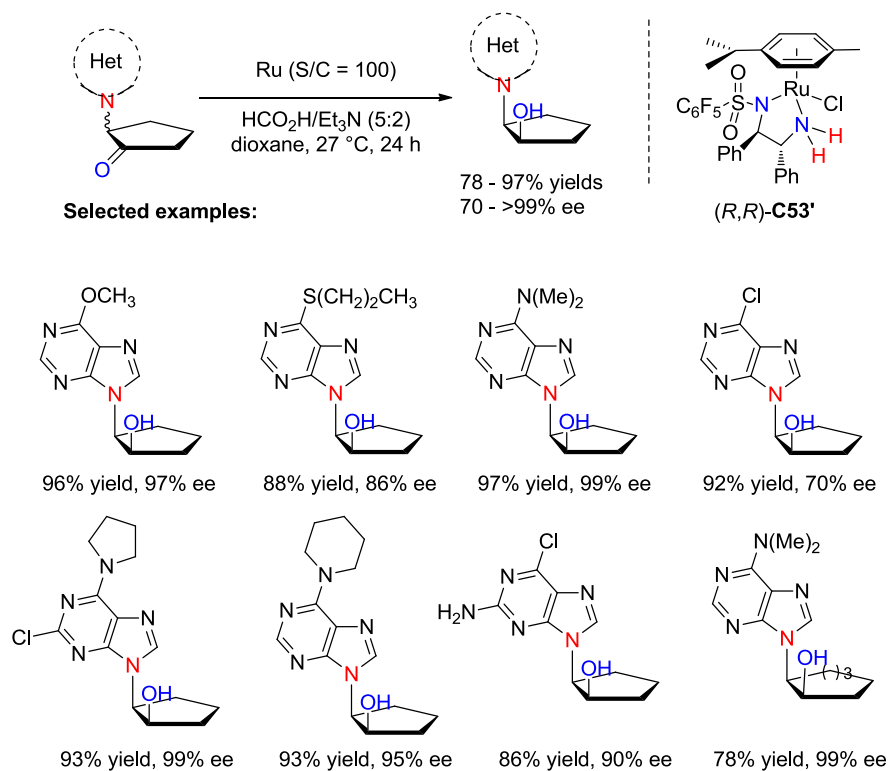
Scheme 78

Guo *et al.* developed the first example of asymmetric transfer hydrogenation via dynamic kinetic resolution of a broad range of rac- $\alpha$ -(purin-9-yl)cyclopentones. A number of cis- $\beta$ -(purin-9-yl)cyclopentanols were synthesized with up to 97% yield, >20:1 dr, and >99% ee. This method can be also applied as an efficient synthetic route to access various chiral carbocyclic nucleosides (Scheme 79).<sup>141</sup>

<sup>139</sup> Touge, T.; Kuwana, M.; Komatsuki, Y.; Tanaka, S.; Nara, H.; Matsumura, K.; Sayo, N.; Kashibuchi, Y.; Saito, T. *Org. Process Res. Dev.* **2019**, *23*, 452.

<sup>140</sup> Cotman, A. E.; Lozinsek, M.; Wang, B.; Stephan, M.; Mohar, B. *Org. Lett.* **2019**, *21*, 3644.

<sup>141</sup> Zhang, Y-M.; Zhang, Q-Y.; Wang, D-C.; Xie, M-S.; Qu, G-R.; Guo, H-M. *Org. Lett.* **2019**, *21*, 2998.

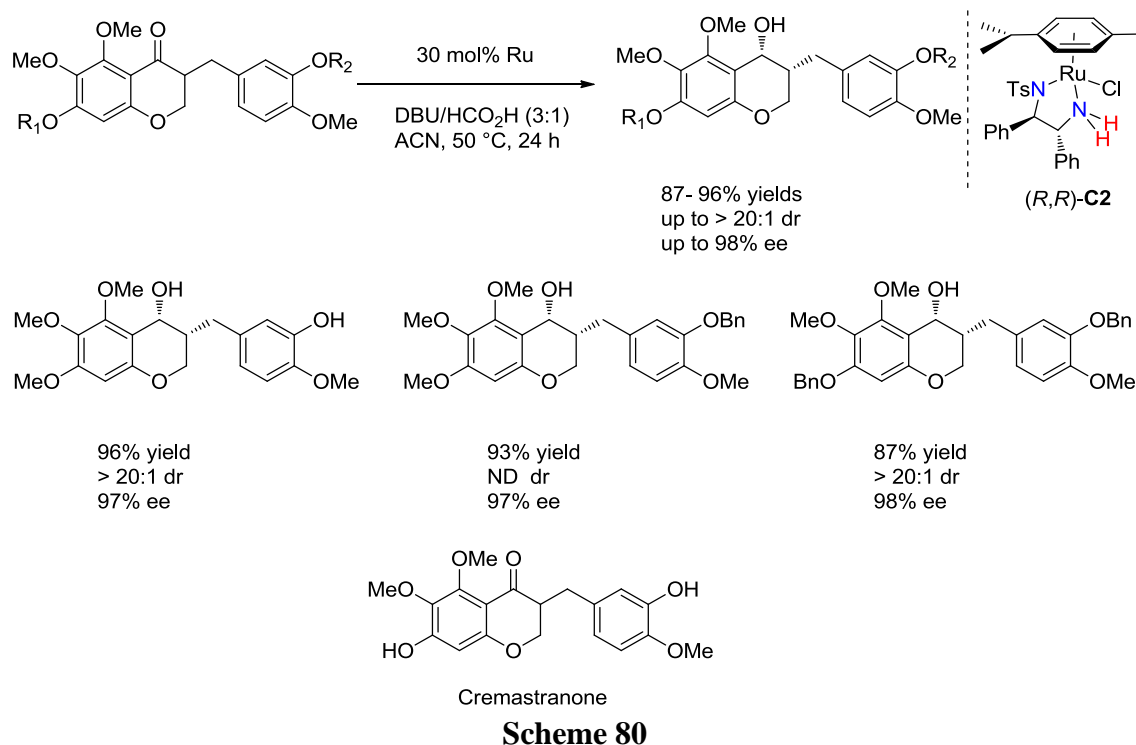


Scheme 79

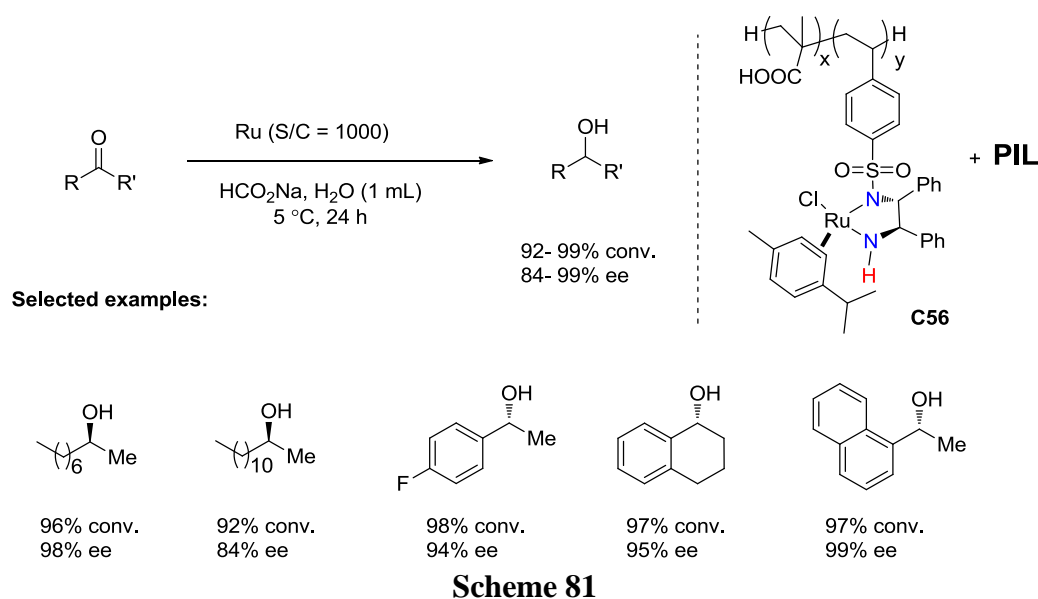
Seo *et al.* reported an asymmetric transfer hydrogenation of homoisoflavanones catalyzed by Noyori's ruthenium catalyst which proceeded in good yields with high diastereoselectivities and enantioselectivities. The reaction was used for the synthesis of the anti-angiogenic natural product – Cremastranone (Scheme 80).<sup>142</sup>

<sup>142</sup> Heo, M.; Lee, B.; Sishtla, K.; Fei, X.; Lee, S.; Park, S.; Yuan, Y.; Lee, S.; Kwon, S.; Lee, J.; Kim, S.; Corson, T. W.; Seo, S. Y. *J. Org. Chem.* **2019**, *84*, 9995.





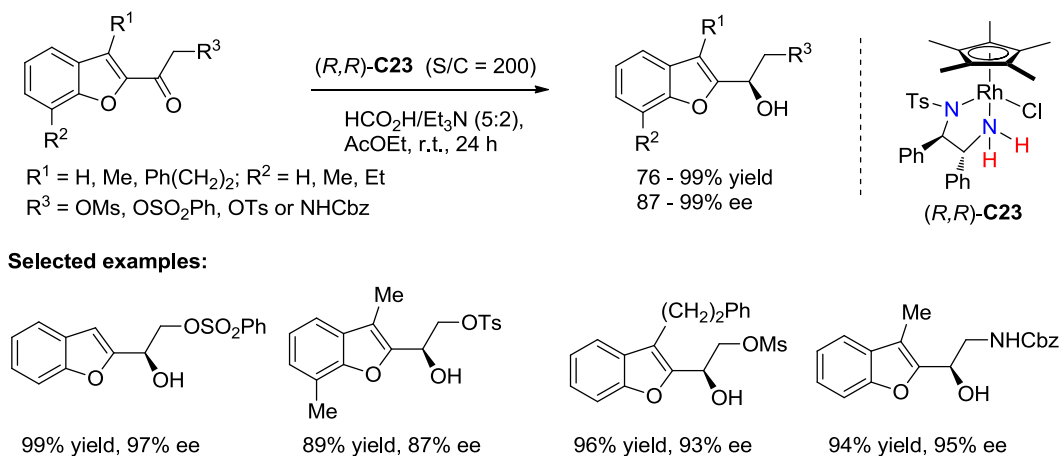
In 2020, Jia *et al.* developed a series of heterogeneous chiral ruthenium catalysts with a controllable hydrophobic surface. Based on a number of polymer ionic liquids (PILs) that contain coexisting Cl<sup>-</sup> and [NTf<sub>2</sub>]<sup>-</sup> anions, the Ru catalysts can be well dispersed as micelles in an aqueous solution, and enhance the adsorption of organic substrate, thereby significantly improving the reactivity in water. These Ru catalysts were successfully applied to the asymmetric transfer hydrogenation of ketones in water successfully and the heterogeneous chiral ruthenium catalysts could be simply recycled (Scheme 81).<sup>143</sup>



<sup>143</sup> Li, X.; Sun, Y.; Wang, S.; Jia, X. *ACS Appl. Polym. Mater.* **2020**, *2*, 1268.

## 2.4 Rhodium catalysts

In 2017, Tafelska-Kaczmarek *et al.* reported the use of [RhClCp\*(*R,R*)-TsDPEN] complex (*R,R*)-**C23** in the ATH of benzofuryl  $\alpha$ -sulfonyloxy ketones and *N*-protected  $\alpha$ -amino ketones by using HCO<sub>2</sub>H/Et<sub>3</sub>N (5:2) to give the corresponding alcohols in high yields and high enantioselectivities (Scheme 82).<sup>144</sup>

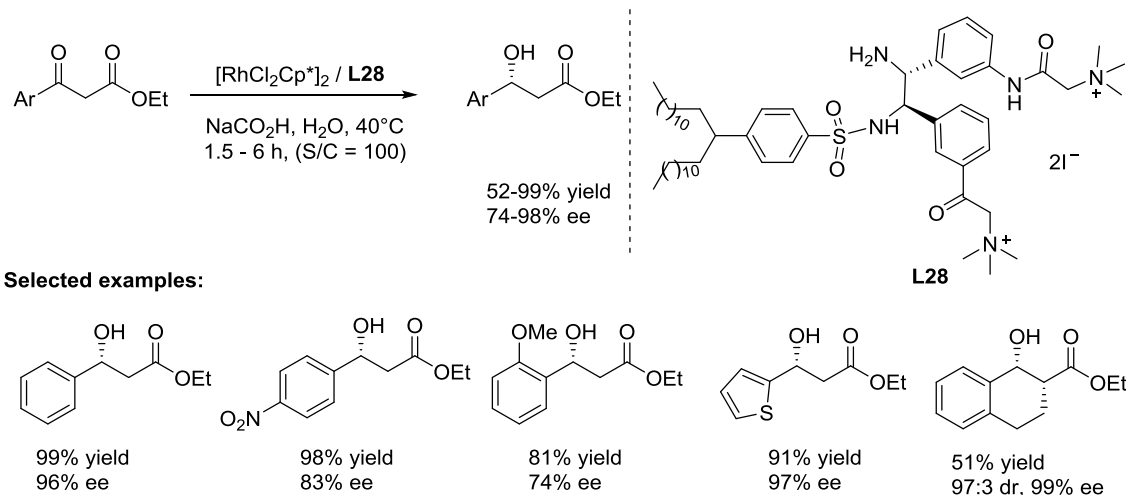


**Scheme 82**

In 2017, Deng *et al.* used [RhCl<sub>2</sub>Cp\*]<sub>2</sub> complex combined with a new chiral double-chain surfactant-type ligand **L28** to form the catalyst *in situ*, which can self-assemble into chiral vesicular aggregates in water. The catalyst was highly efficient for the ATH of various aromatic  $\beta$ -ketoesters, with yields from 52 to 99% and good to excellent enantioselectivities (74–99% ee). In addition, this double-chain surfactant-type catalyst could also be applied to the dynamic kinetic resolution of bicyclic  $\beta$ -ketoesters in water (Scheme 83).<sup>145</sup>

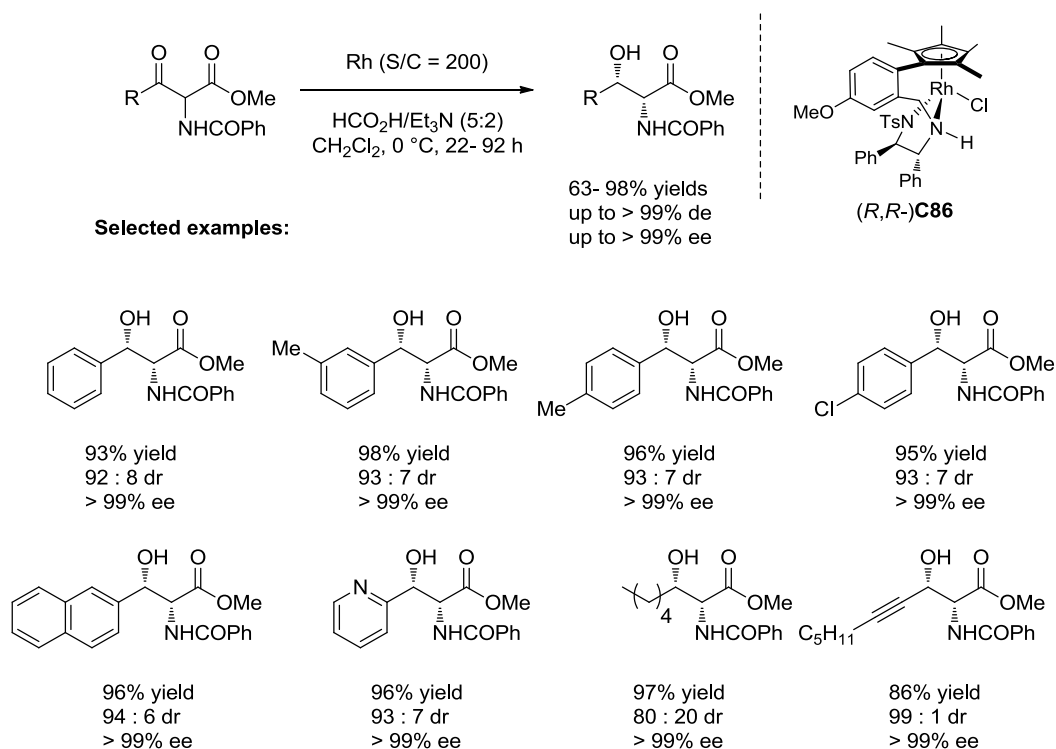
<sup>144</sup> Tafelska-Kaczmarek, A.; Krzemiński, M. P.; Ówiklińska, M. *Tetrahedron* **2017**, *73*, 3883.

<sup>145</sup> Li, J.; Lin, Z.; Huang, Q.; Wang, Q.; Tang, L.; Zhu, J.; Deng, J. *Green Chem.* **2017**, *19*, 5367.



Scheme 83

In 2018, our group designed a rhodium-catalyzed asymmetric transfer hydrogenation of  $\alpha$ -amido  $\beta$ -keto esters through dynamic kinetic resolution. It is an efficient tool for the synthesis of syn  $\alpha$ -benzoylamido  $\beta$ -hydroxy esters in good yields (63- 98%), high diastereomeric ratios ( up to > 99 : 1 dr), and excellent enantioselectivities ( up to > 99% ee) (Scheme 84).<sup>146</sup>

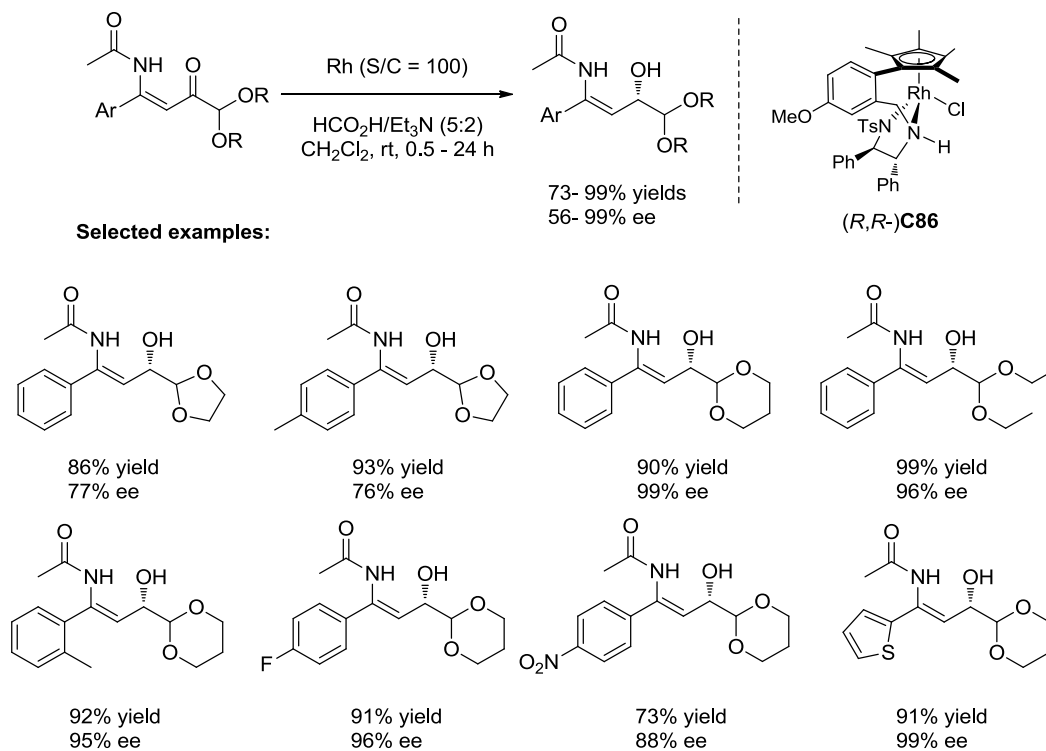


Scheme 84

In 2020, our group reported the first example of chemoselective and stereoselective reduction of  $\beta$ -keto- $\gamma$ -acetal enamides to the corresponding  $\beta$ -hydroxy- $\gamma$ -acetal enamides by rhodium catalyzed asymmetric transfer hydrogenation. In this case, an in-house developed

<sup>146</sup> Zheng, L. S.; Férard, C.; Phansavath, P.; Ratovelomanana-Vidal, V. *Chem. Commun.* **2018**, 54,283.

tethered rhodium complex was used as catalyst with HCO<sub>2</sub>H/Et<sub>3</sub>N (5:2) azeotropic mixture as hydrogen source, and the reaction was carried out in DCM at room temperature. A wide range of β-hydroxy-γ-acetal enamide derivatives were obtained in both high yields (73- 99%) and enantioselectivities (up to 99%). This method could be applied on gram-scale without decreasing of the yield or enantioselectivity (Scheme 85).<sup>147</sup>

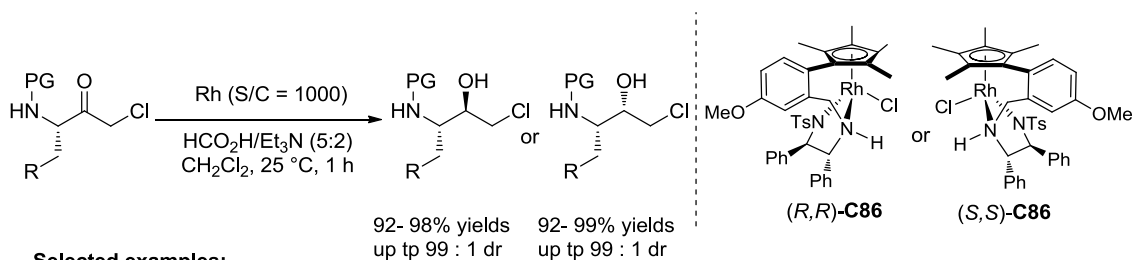


**Scheme 85**

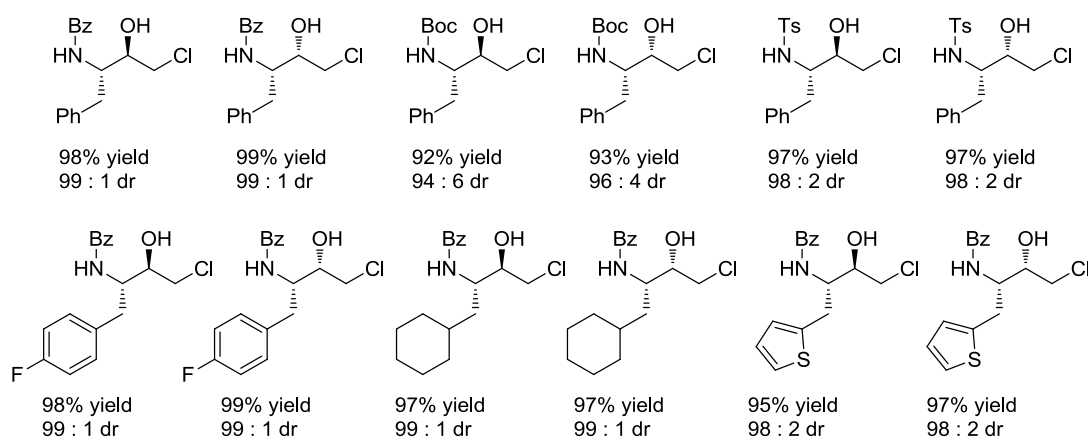
In 2020, Ratovelomanana-Vidal and Zhang *et al.* developed an asymmetric transfer hydrogenation on chiral α-aminoalkyl α'-chloro-methyl ketones catalyzed by rhodium complexes (*R,R*)-Rh and (*S,S*)-Rh. A number of chiral 3-amino-1-chloro-2-hydroxy-4-phenylbutanes were produced in excellent yields and dr (up to 99% yield, up to 99 : 1 dr) and importantly the reduced products were used to access key intermediates of HIV protease inhibitors atazanavir and saquinavir (Scheme 86).<sup>148</sup>

<sup>147</sup> Westermeyer, A.; Guillamot, G.; Phansavath, P.; Ratovelomanana-Vidal. V. *Org. Lett.* **2020**, *22*, 3911. (Highlighted in synfact. **2020**, *16*, 0815. Contributor(s): Lautens, M, Loup, J.)

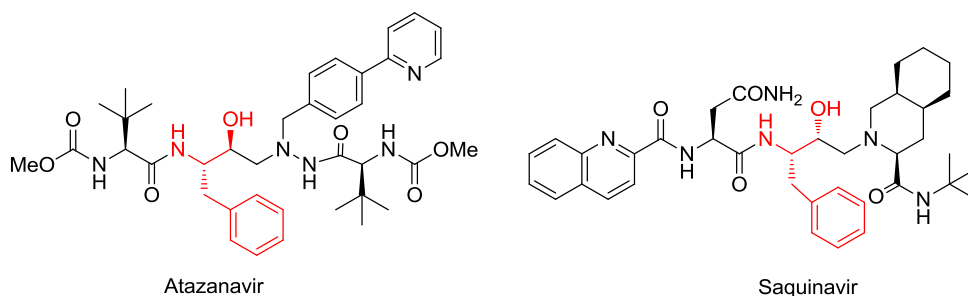
<sup>148</sup> Wang, F.; Zheng, L. S.; Lang, Q. W.; Yin, C.; Wu, T.; Phansavath, P.; Chen, G. Q.; Ratovelomanana-Vidal. V.; Zhang, X. *Chem. Commun.* **2020**, *56*, 3119.



Selected examples:



HIV protease inhibitors



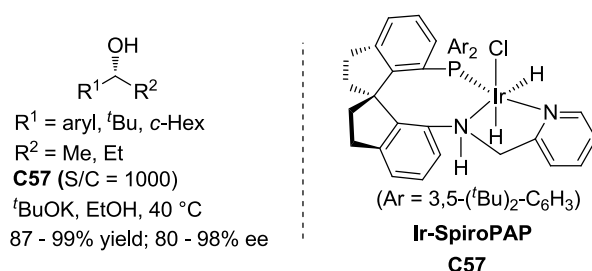
Scheme 86

## 2.5 Iridium catalysts

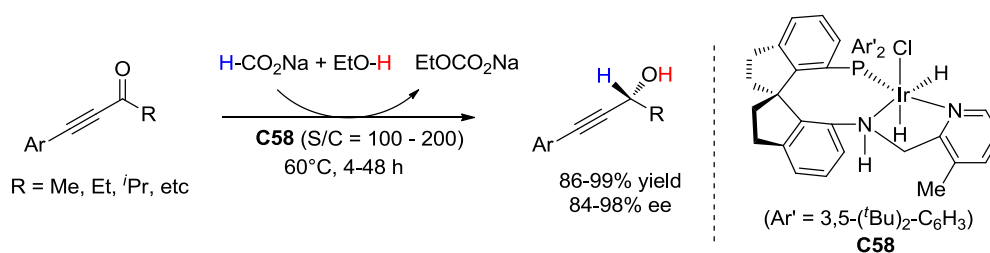
A chiral spiro iridium complex (**Ir-SpiroPAP**) **C57** was developed, by Zhou's group, for the ATH of various alkyl aryl ketones to provide chiral alcohols in high yields and excellent enantioselectivities (Scheme 87).<sup>149</sup> The same group synthesized an efficient iridium complex **C58** used in the ATH of alkynyl ketones to deliver optically active propargylic alcohols. By using sodium formate and ethanol, a broad range of alkynyl ketones were hydrogenated to provide a practical and sustainable approach to access enantioenriched propargylic alcohols

<sup>149</sup> Liu, W.-P.; Yuan, M.-L.; Yang, X.-H.; Li, K.; Xie, J.-H.; Zhou, Q.-L. *Chem. Commun.* **2015**, 51, 6123.

with up to 98% ee under base-free conditions (Scheme 88).<sup>150</sup>

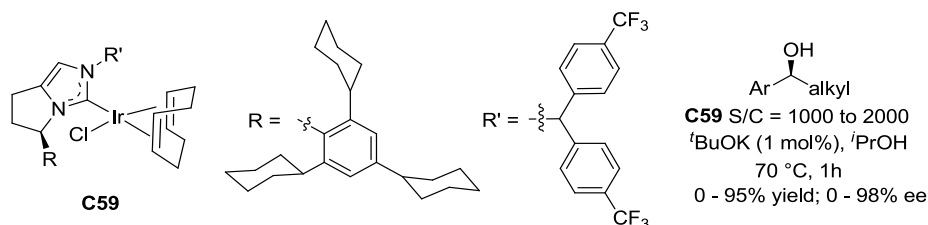


**Scheme 87**



**Scheme 88**

An air-stable and efficient NHC/Ir complex **C59** was developed for the asymmetric transfer hydrogenation of aryl alkyl ketones by using isopropanol as a hydrogen donor in the presence of  $^t\text{BuOK}$ . The enantioenriched alcohols were obtained in up to 95% yield and up to 98% ee (Scheme 89).<sup>151</sup>



**Scheme 89**

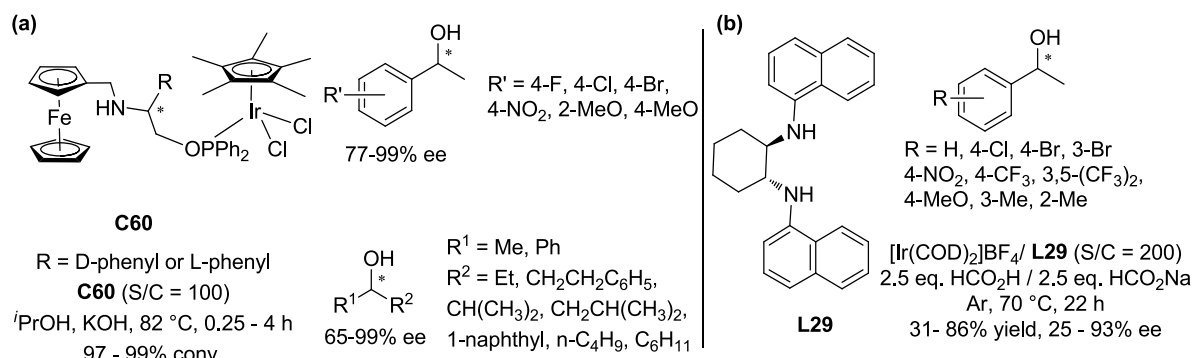
A series of ferrocenyl-phosphinite ligands was developed and used to prepare Ir(III) complexes **C60**. The latter were evaluated in the ATH of a wide range of ketones to provide the corresponding alcohols with high conversions (97–99%) and enantioselectivities ranging from 65 to 99% ee (Scheme 90a).<sup>152</sup> Chiral *N,N'*-diaryl-*trans*-1,2-diamino-cyclohexane ligand **L29** was prepared through Pd(II)-catalyzed dehydrogenative alkylation of chiral diamine with cyclohexanone derivative. Moreover, the chiral aryl diamine ligand **L29** was applied for the

<sup>150</sup> Zhang, Y.-M.; Yuan, M.-L.; Liu, W.-P.; Xie, J.-H.; Zhou, Q.-L. *Org. Lett.* **2018**, *20*, 4486.

<sup>151</sup> Yoshida, K.; Kamimura, T.; Kuwabara, H.; Yanagisawa, A. *Chem. Commun.* **2015**, *51*, 15442.

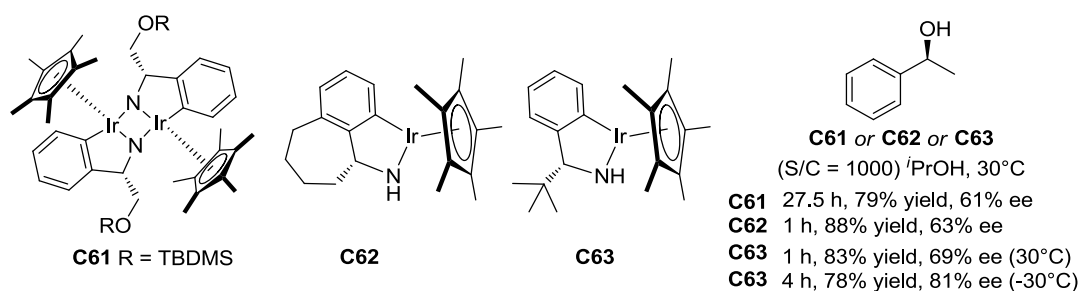
<sup>152</sup> Meriç, N.; Aydemir, M. *J. Organomet. Chem.* **2016**, *819*, 120.

Ir(III)-catalyzed ATH of a range of aromatic ketones with yields ranging from 96 to 100% and 52–86% ees (Scheme 90b).<sup>153</sup>



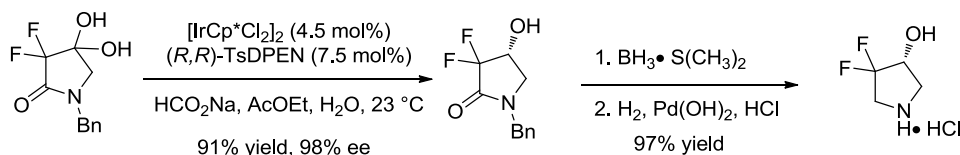
Scheme 90

In 2016, Ikariya *et al.* developed a series of new amido-bridged dinuclear Ir complex **C61** and mononuclear amido Ir complexes **C62** and **C63**, which were evaluated in the ATH of acetophenone to provide the corresponding alcohol with 61–69% ee values (Scheme 91).<sup>154</sup>



Scheme 91

A new route to (*R*)-4,4-difluoropyrrolidin-3-ol, an important building block in medicinal chemistry, was developed through ATH of *gem*-difluoro substituted benzylpyrroline-2,4-dione. The corresponding alcohol was obtained in high yield and 98% ee, and subsequent reduction/deprotection steps afforded the key product in good overall yield. This method avoids the use of potentially hazardous deoxofluorinating reagents and may be scalable (Scheme 92).<sup>155</sup>



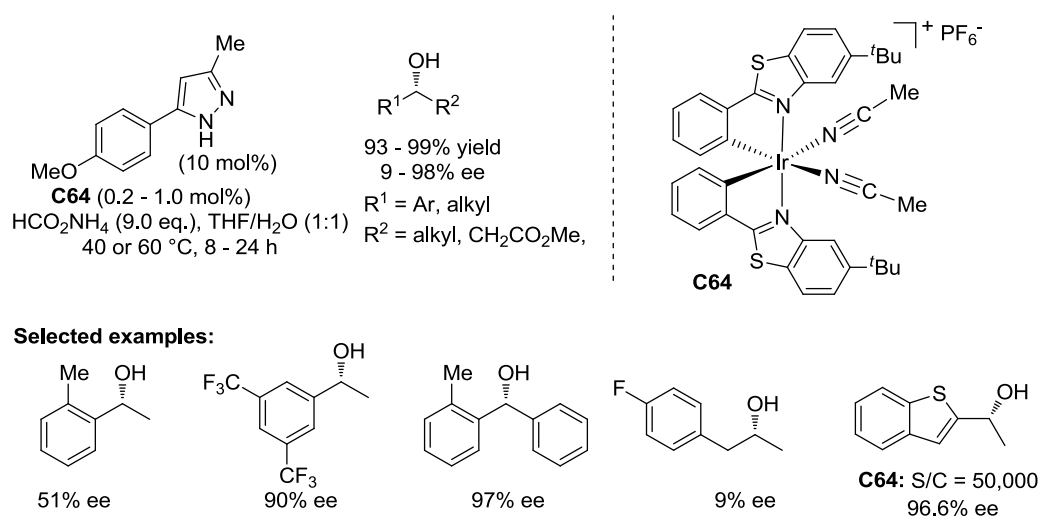
<sup>153</sup> El-Asaad, B.; Guicheret, B.; Méta, E.; Karamé, I.; Lemaire, M. *J. Mol. Catal. A. Chem.* **2016**, *411*, 196.

<sup>154</sup> Sato, Y.; Kayaki, Y.; Ikariya, T. *Chem. Asian J.* **2016**, *11*, 2924.

<sup>155</sup> Si, C.; Fales, K. R.; Torrado, A.; Frimpong, K.; Kaoudi, T.; Vandever, H. G.; Njoroge, F. G. *J. Org. Chem.* **2016**, *81*, 4359.

## Scheme 92

In 2016, Meggers, Gong *et al.* reported the ATH of a variety of (het)aryl and alkyl ketones using a bis-cyclometalated Ir(III) complex **C64** with metal-centered chirality in the presence of  $\alpha$ -substituted pyrazole as a co-ligand. 93–99% yields and 9–98% ees were obtained for the corresponding alcohols. A catalyst loading as low as S/C = 50,000 could be used (Scheme 93).<sup>156</sup> The same group reported, in 2018, several tandem processes by using different photoredox reactions, such as radical addition or radical conjugated addition, to generate ketone intermediates in sequence with the ATH to produce the corresponding enantioenriched alcohols (Scheme 94).<sup>157</sup>

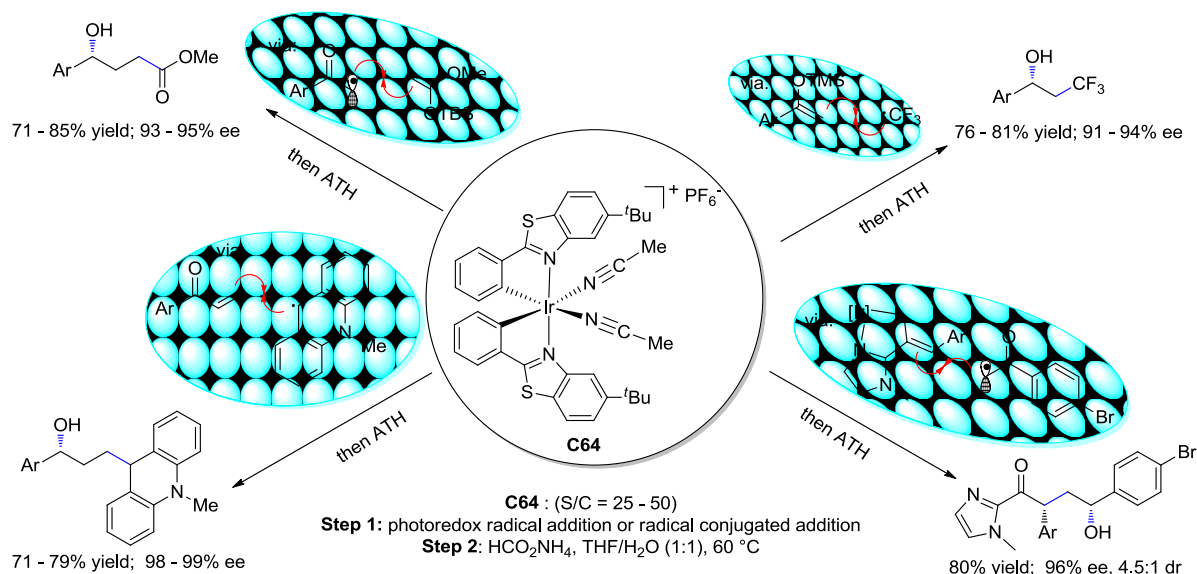


Scheme 93

<sup>156</sup> Tian, C.; Gong, L.; Meggers, E. *Chem. Commun.* **2016**, 52, 4207.

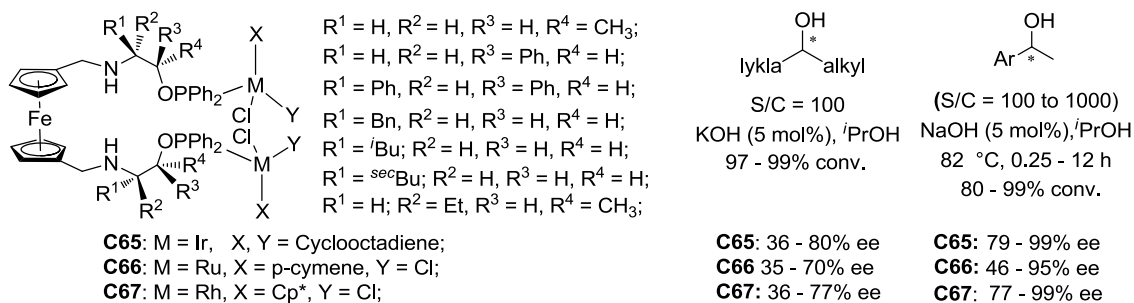
<sup>157</sup> Zhang, X.; Qin, J.; Huang, X.; Meggers, E. *Eur. J. Org. Chem.* **2018**, 571.





Scheme 94

A library of Ir(III) (**C65**), but also Ru(II) (**C66**) and Rh(III) (**C67**) precatalysts were generated from *C*<sub>2</sub>-symmetric ferrocenyl phosphinite ligands and these catalysts were evaluated in the ATH of a broad range of aromatic ketones in the presence of isopropanol as the hydrogen source. High conversions (97–>99%) and enantioselectivities ranging from 46 to 99% were obtained. Furthermore, more challenging alkyl alkyl ketones were also investigated and a broad range of chiral alkyl alcohols were obtained in moderate to high enantioselectivities (35–80% ees) (Scheme 95).<sup>158</sup>

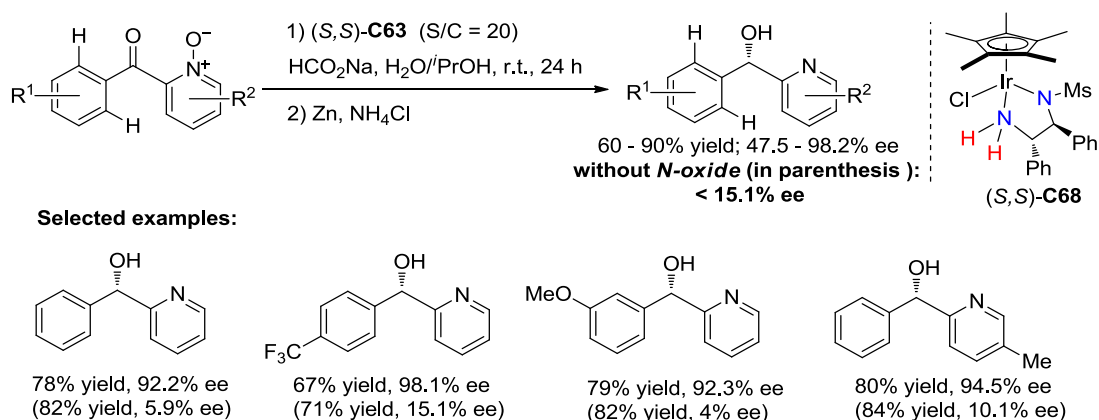


Scheme 95

Ir(III)-MsDPEN complex **C68** was used in the ATH of a range of non-*ortho*-substituted aryl *N*-heteroaryl ketones bearing *N*-oxide as a removable *ortho*-substituent. The reaction was conducted in the presence of sodium formate in aqueous isopropanol to provide the

<sup>158</sup> (a) Ak, B.; Aydemir, M.; Durap, F.; Meriç, N.; Baysal, A. *Inorg. Chim. Acta.* **2015**, *438*, 42. (b) Ak, B.; Durap, F.; Aydemir, M.; Baysal, A. *Appl. Organomet. Chem.* **2015**, *29*, 764. (c) Ak, B.; Aydemir, M.; Durap, F.; Meriç, N.; Elma, D.; Baysal, A. *Tetrahedron: Asymmetry* **2015**, *26*, 1307. (d) Durap, F.; Karakaş, D. E.; Ak, B.; Baysal, A.; Aydemir, M. *J. Organomet. Chem.* **2016**, *818*, 92. (e) Baysal, A.; Karakaş, D. E.; Meriç, N.; Ak, B.; Aydemir, M.; Durap, F. *Transit. Met. Chem.* **2017**, *42*, 365.

corresponding chiral aryl *N*-heteroaryl methanols in high yields and excellent enantioselectivities. This study showed that substrates not carrying an *N*-oxide functional group led to lower enantioselectivity (Scheme 96).<sup>159</sup>



**Scheme 96**

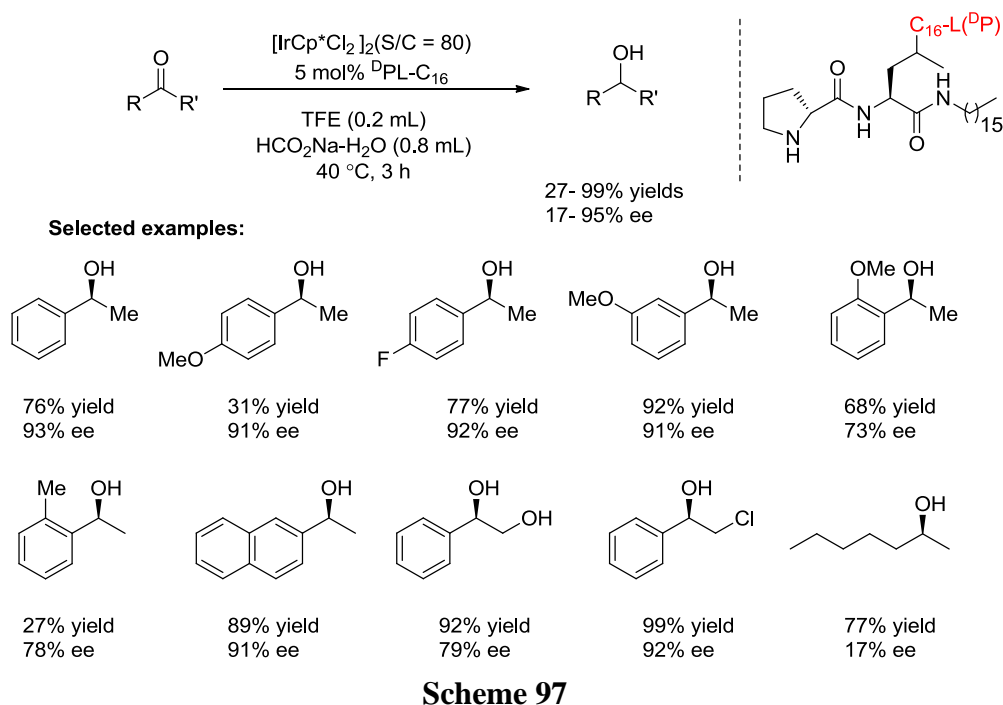
In 2018, Deng and Xiao *et al.* reported a selective approach to prepare *N,C*- or *N,O*-chelated Cp\*Ir(III) complex by reacting [Cp\*IrCl<sub>2</sub>]<sub>2</sub> with methyl (*S*)-2-phenyl-4,5-dihydrooxazole-4-carboxylate in the presence of NaOAc, depending on whether or not water was present in the reaction. Further investigation displayed that the enantioselectivity and the effective HCOOH/amine ratios were considerably influenced by the base additive. The above observations show the importance of ligand coordination mode and using the right base for the ATH reactions.<sup>160</sup>

In 2019, Korendovych *et al.* designed a semi-rational approach that utilizes self-assembly of short peptides for the preparation of highly efficient nanosized iridium catalysts for asymmetric transfer hydrogenation of a wide variety of substrates with sodium formate as hydrogen donor in aqueous solution. The designed peptides comprised of two amino acid residues spontaneously self-assemble in the presence of iridium ions to form supramolecular, vesicle-like nanoassemblies that promote asymmetric transfer hydrogenation of ketones in aqueous phase with good conversions and enantioselectivities (Scheme 97).<sup>161</sup>

<sup>159</sup> Liu, Q.; Wang, C.; Zhou, H.; Wang, B.; Lv, J.; Cao, L.; Fu, Y. *Org. Lett.* **2018**, *20*, 971.

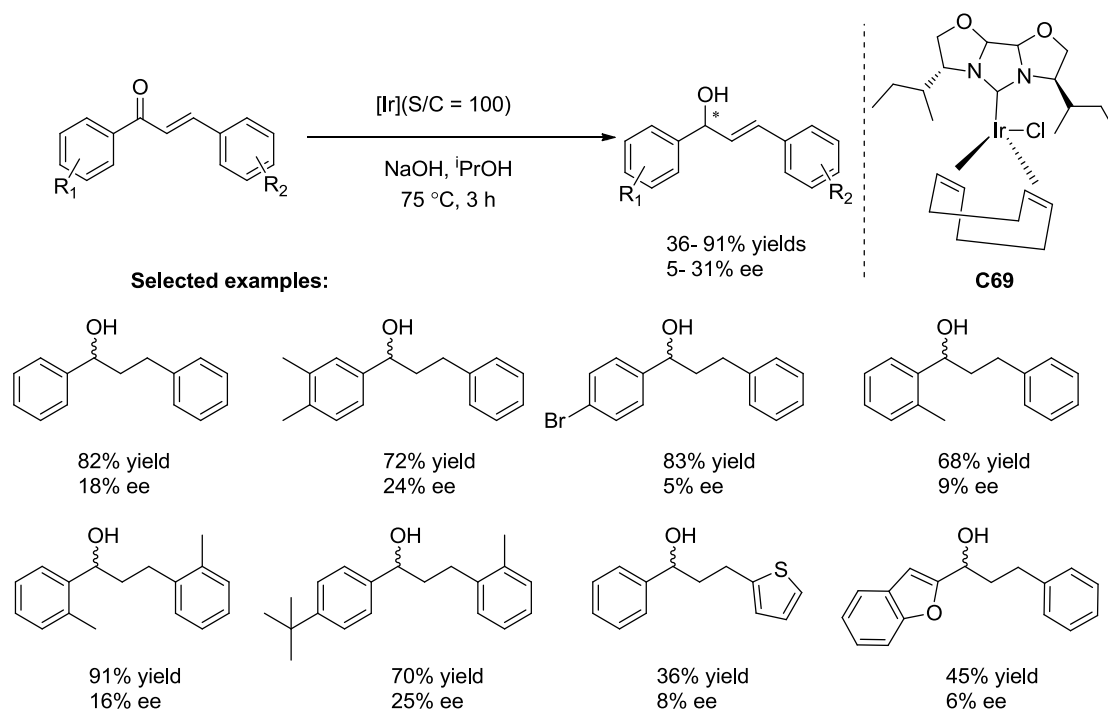
<sup>160</sup> Zhou, G.; Aboo, A. H.; Robertson, C. M.; Liu, R.; Li, Z.; Luzyanin, K.; Berry, N. G.; Chen, W.; Xiao, J. *ACS Catalysis* **2018**, 8020.

<sup>161</sup> Dolan, M. A.; Basa, P. N.; Zozulia, O.; Lengyel, Z.; Lebl, R.; Kohn, E. M.; Bhattacharya, S.; Korendovych, I. V. *ACS. Nano* **2019**, *13*, 9292.



Scheme 97

Ghosh *et al.* developed in 2109 an asymmetric transfer hydrogenation of  $\alpha$ ,  $\beta$ -unsaturated ketones catalyzed by a new Ir (NHC) complex **C69**. The reaction afforded 1,3-diaryl-propane-1-ol derivatives, in good yields but low enantioselectivities (5- 31% ee) (Scheme 98).<sup>162</sup>

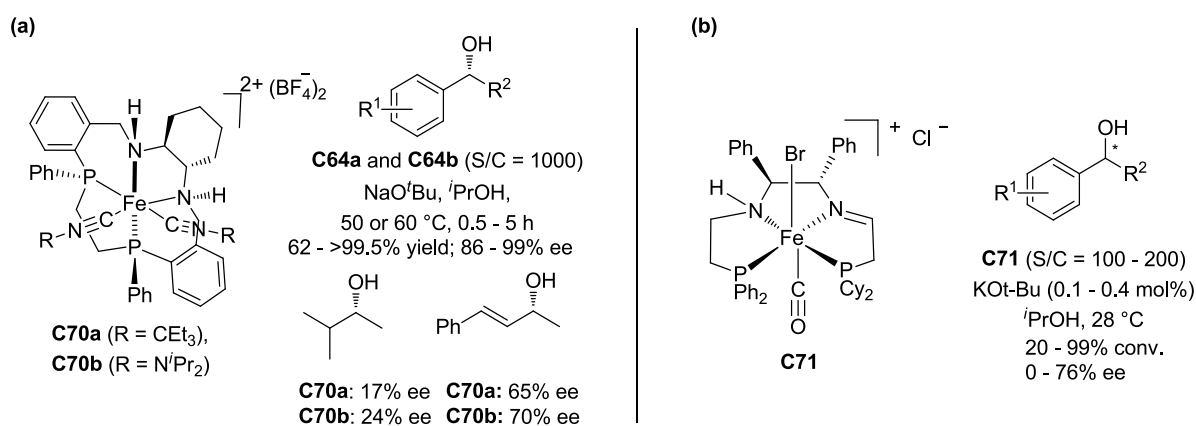


Scheme 98

<sup>162</sup> Ramasamy, B.; Prakasham, A. P.; Gangwar, M. K.; Ghosh, P. *ChemistrySelect*. 2019, 4, 357.

## 2.6 Iron catalysts

Iron as an inexpensive, non-toxic and environment friendly metal has already been studied with different types of  $C_2$ -symmetric macrocyclic  $N_2P_2$  and open-chain  $NPPN$  chiral ligands for ATH of aryl alkyl ketones, and challenging dialkyl ketones in highly catalytic activities with poor to high enantioselectivities,<sup>163</sup> and the design of novel efficient iron complexes is still ongoing. A well-defined bis(isonitrile) iron(II) complex **C70** containing a  $C_2$ -symmetric diamino  $(NH)_2P_2$  macrocyclic ligand was described. This Fe(II) complex exhibited effective catalytic activities (catalyst loading S/C = 1000) and excellent enantioselectivities for the ATH of a broad range of aromatic ketones (Scheme 99a).<sup>164</sup> Another type of Fe(II)/ $P-NH-N-P'$  complex **C71** was designed and examined in the ATH of various simple ketones in the presence of  $KO^tBu/iPrOH$ . The precatalyst displayed high catalytic activity (TON up to 4300) and excellent enantioselectivities (up to 99% ee) (Scheme 99b).<sup>165</sup> Complex **C71** was also investigated for the ATH of simple ketones in biphasic catalytic system employing water as the proton donor and potassium formate as the hydride source to provide enantioenriched alcohols with conversions up to 99% and good enantioselectivities up to 76% ee.<sup>166</sup>



Scheme 99

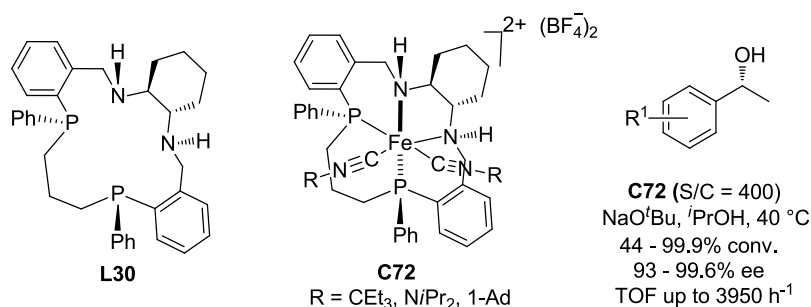
In 2016, Mezzetti *et al.* described iron complexes  $[Fe(CNR)_2((S_P, S_P, S_C, S_C)\text{-L30})](BF_4)_2$  **C72** wherein **L30** is a 15-membered  $(S_P, S_P, S_C, S_C)$ - $(NH)_2P_2$  macrocycle ligand bearing a propane-1,3-diyl bridge. The catalyst was evaluated for the ATH of a range of aromatic ketones in the presence of a base under mild conditions to provide enantioenriched alcohols (Scheme

<sup>163</sup> Bigler, R.; Huber, R.; Mezzetti, A. *Synlett* **2016**, 27, 831.

<sup>164</sup> Bigler, R.; Huber, R.; Mezzetti, A. *Angew. Chem. Int. Ed.* **2015**, 54, 5171.

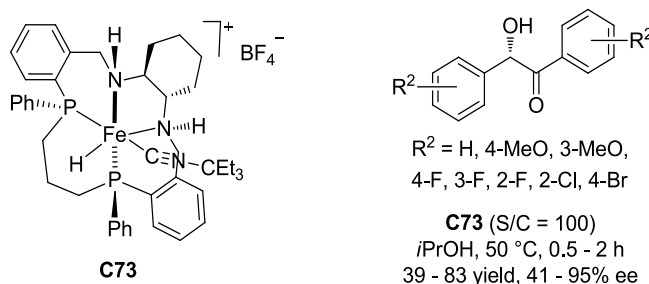
<sup>165</sup> Smith, S. A. M.; Morris, R. H. *Synthesis* **2015**, 47, 1775.

<sup>166</sup> Demmans, K. Z.; Ko, O. W. K.; Morris, R. H. *RSC Adv.* **2016**, 6, 88580.

100).<sup>167</sup>

Scheme 100

In 2017, they reported a hydride iron(II) complex **C73** which exhibited high selectivity in ATH of a number of benzils to access benzoin with acceptable yields (39–83%) and enantioinductions ranging from 41 to 95% (Scheme 101).<sup>168</sup>



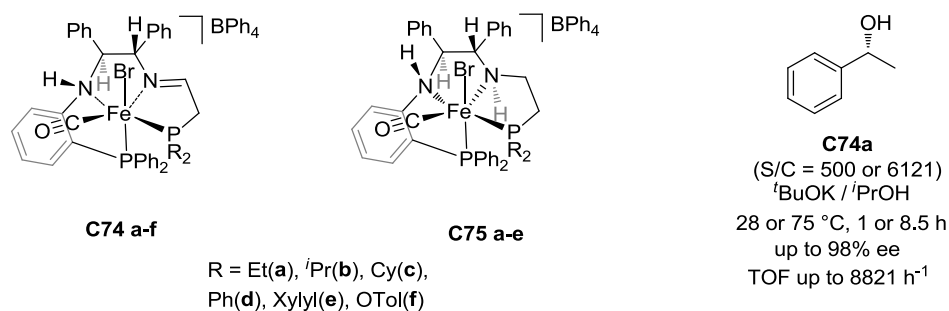
Scheme 101

In 2017, Morris *et al.* reported a series of novel *cis*- $\beta$  iron(II) precatalysts **C74a-f**, **C75a-e** bearing a *P,N,N,P'* pincer ligand with a bulky *ortho*-phenylene group and an imine or amine unit. In the ATH of acetophenone, *Cis*- $\beta$  iron(II)/*P,N,N,P* complexes **C75a-e** with an amine ligand displayed higher performances than the imine complexes **C74a-f**, leading to (*S*)-1-phenylethanol with excellent enantioselectivities (up to 98% ee). Furthermore, amine precatalyst **C74a** containing a PEt<sub>2</sub> part shows a more stable hydride species when activated compared to the other complexes, with powerful catalytic activity (TON = 8821) and high enantioselectivity in the reduction of acetophenone to (*S*)-1-phenylethanol (95% ee) (Scheme 102).<sup>169</sup>

<sup>167</sup> Bigler, R.; Huber, R.; Stöckli, M.; Mezzetti, A. *ACS Catal.* **2016**, *6*, 6455.

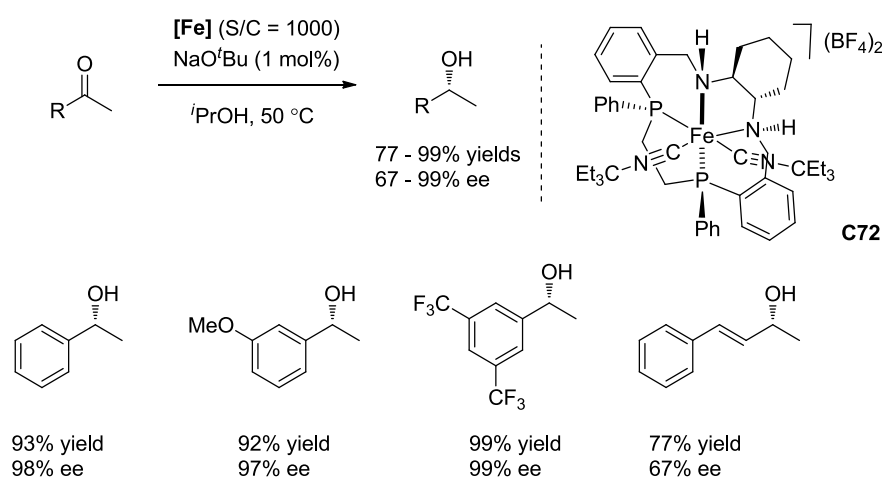
<sup>168</sup> De Luca, L.; Mezzetti, A. *Angew. Chem. Int. Ed.* **2017**, *56*, 11949.

<sup>169</sup> Demmans, K. Z.; Seo, C. S. G.; Lough, A. J.; Morris, R. H. *Chem. Sci.* **2017**, *8*, 6531.



Scheme 102

In 2019, Mezzetti *et al.* described the first study on the iron(II) catalyzed ATH of ketones that combines the experimental observation of on- and off-cycle species with a DFT study of the entire reaction profile and resting species on a real catalytic system (rather than a simplified model). They showed that the role of base in the asymmetric transfer hydrogenation of ketones catalyzed by dicationic N<sub>2</sub>P<sub>2</sub> macrocyclic complexes is to form the corresponding hydride complex, which is the active catalyst both after activation with base and under base-free conditions. They also proved the 2-propoxo and 1-phenylethanolato complexes as resting species of the catalytic cycle by NMR spectroscopy. The DFT calculations suggest the stability of the alkoxo complexes gives a significant contribution to the energetic span of the catalytic cycle. Their work brings more profound mechanistic understanding about ATH of ketones catalyzed by iron (Scheme 103).<sup>170</sup>



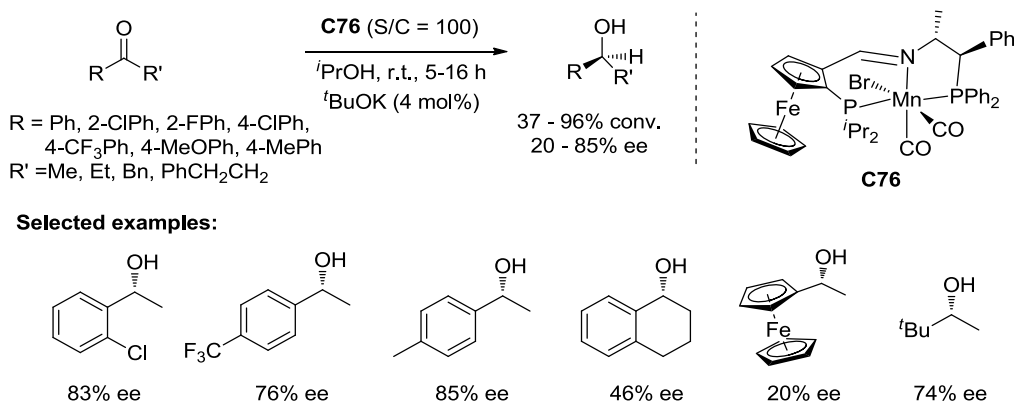
Scheme 103

## 2.7 Manganese catalysts

In 2017, Kirchner, Zirakzadeh *et al.* developed a new type of manganese complex

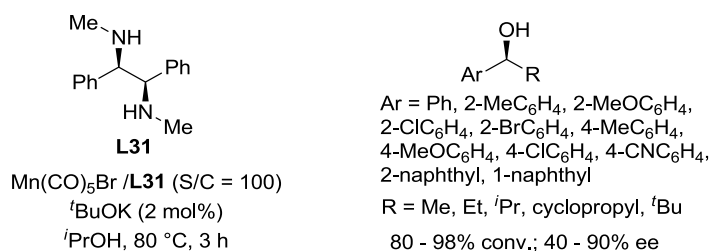
<sup>170</sup> De Luca, L; Passera, A; Mezzetti, A. *J. Am. Chem. Soc.* **2019**, *141*, 2545.

[Mn(PNP')(Br)(CO)<sub>2</sub>] **C76**. Complex **C76** displayed a good activity and low to high selectivity ranging from 20 to 85% ee for the ATH of aromatic ketones, albeit with low selectivities for 1-tetralone (46% ee) and acetylferrocene (20% ee) (Scheme 104).<sup>171</sup>



Scheme 104

Chiral diamine **L31** was used in combination with [Mn(CO)<sub>5</sub>Br] to form *in situ* the corresponding complex which was used in the ATH of ketones in the presence of <sup>t</sup>BuOK/<sup>i</sup>PrOH as the hydrogen source. The corresponding chiral alcohols were obtained in conversions up to 98% and enantioselectivities up to 90% (Scheme 105).<sup>172</sup>



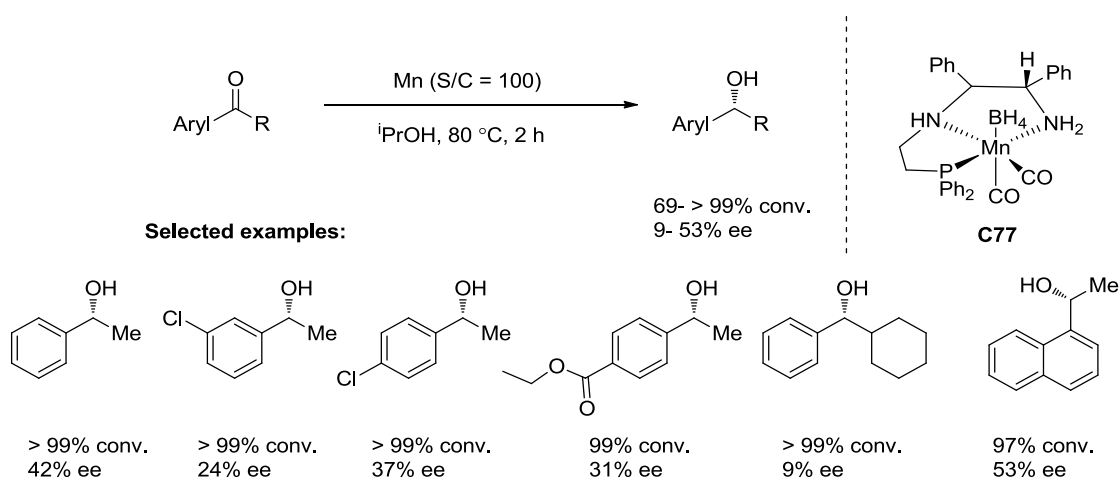
Scheme 105

In 2018, Morris *et al.* synthesized three new chiral manganese complexes. Among them the borohydride manganese complex was the most active for the ATH of ketone substrates. The reaction was carried out in <sup>i</sup>PrOH without other base additive and the conversions were high (up to 99%), however the enantioselectivities were moderate (up to 53% ee) (Scheme 106).<sup>173</sup>

<sup>171</sup> Zirakzadeh, A.; de Aguiar, S. R. M. M.; Stöger, B.; Widhalm, M.; Kirchner, K. *ChemCatChem* **2017**, *9*, 1744.

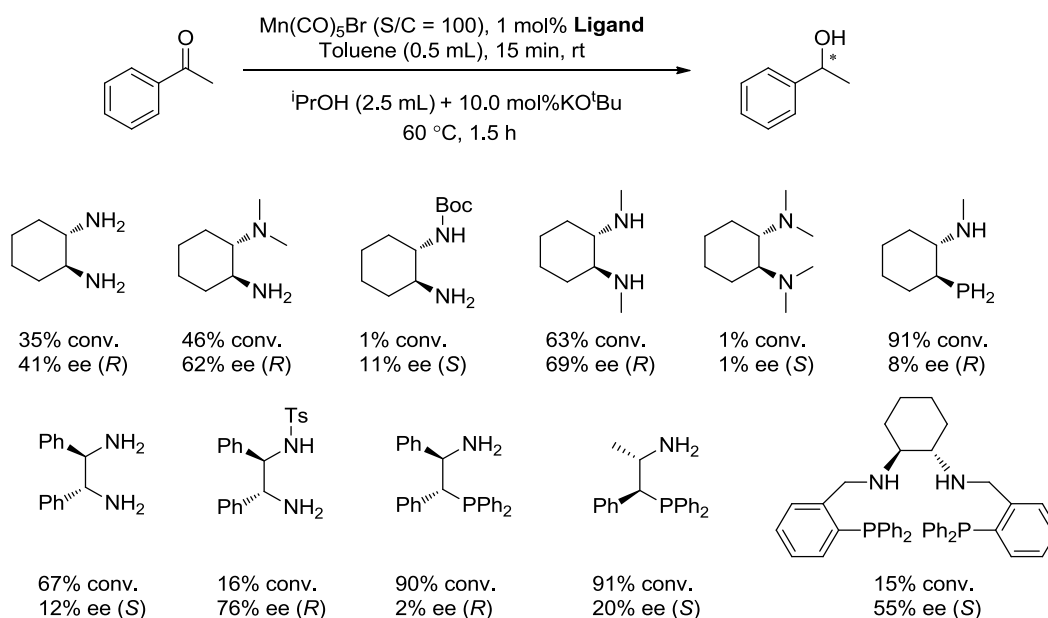
<sup>172</sup> Wang, D.; Bruneau-Voisine, A.; Sortais, J.-B. *Catal. Commun.* **2018**, *105*, 31 and references cited.

<sup>173</sup> Demmans, K. Z.; Olson, M. E.; Morris, R. H. *Organometallics*. **2018**, *37*, 4608.



Scheme 106

In 2019, Pidko *et al.* tested a series of chiral *N*-containing ligands in the Mn-catalyzed asymmetric transfer hydrogenation of acetophenone. The ligand screening showed the simple diamine ligands did not induce sufficient steric strain to give high enantioselectivity. The best enantioselectivity obtained was 76% ee with a low conversion of 16%. The authors did an extensive experimental and computational mechanistic study, the mechanistic insight and the recent applications of bidentate ligands containing a NHC group reveal that introduction of the strongly electron-donating but small bidentate ligand may result in highly active and selective second-generation Mn catalysts for asymmetric transfer hydrogenation of ketones (Scheme 107).<sup>174</sup>



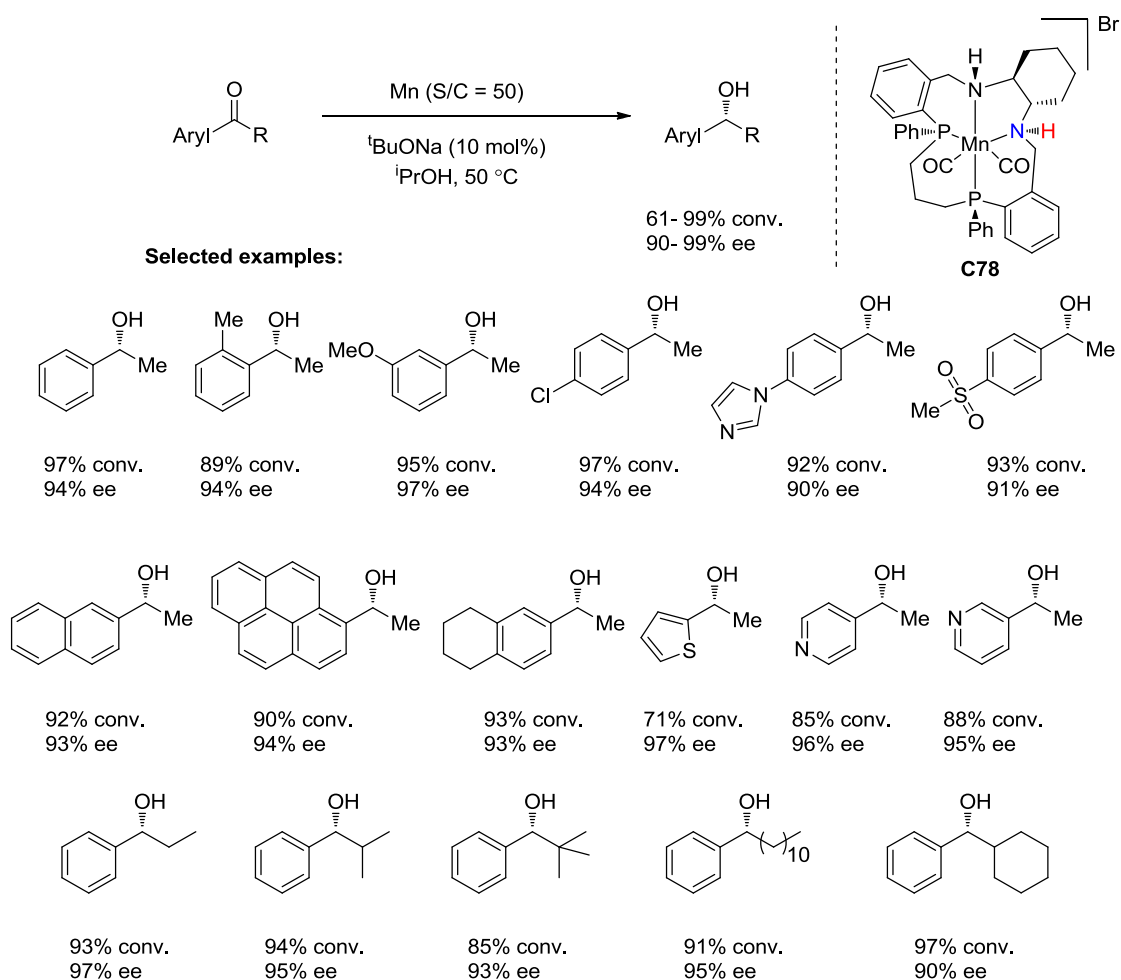
Scheme 107

In 2020, Mezzetti *et al.* designed a chiral (NH)<sub>2</sub>P<sub>2</sub> macrocyclic Mn(I) catalyst **C78** for

<sup>174</sup> Putten, R. V.; Filonenko, G. A.; Castro, A. G.; Liu, C.; Weber, M.; C.; Muller, Lefort, L.; Pidko, E. *Organometallics*. **2019**, *38*, 3187.



the ATH of a broad scope of aryl alkyl ketones. The attractive CH/ $\pi$  interactions between the Mn(I) catalyst and the substrate gave the reduced products in excellent enantioselectivities (90–99% ee) (Scheme 108).<sup>175</sup>



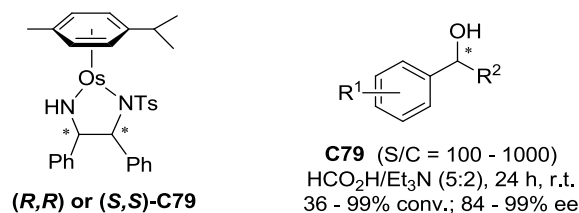
Scheme 108

## 2.8 Osmium catalyst

Based on Noyori-Ikariya's catalyst  $[\text{Ru}(\eta^6\text{-arene})(\text{TsDPEN})]$ , a novel type of [osmium(II)/arene/TsDPEN] complex **C79** was developed and evaluated in the ATH of simple aryl ketones in the presence of  $\text{HCO}_2\text{H}/\text{Et}_3\text{N}$ . Chiral alcohols were obtained with conversions up to 99% and enantioselectivities up to 99% (Scheme 109).<sup>176</sup>

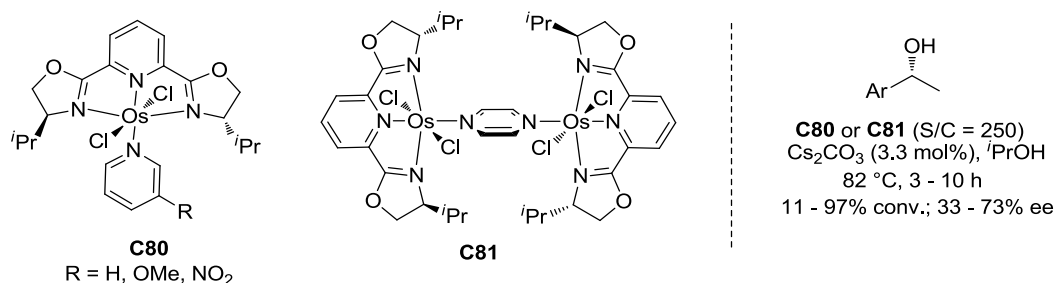
<sup>175</sup> Passera, A.; Mezzetti, A. *Angew. Chem. Int. Ed.* **2020**, *59*, 187.

<sup>176</sup> Coverdale, J. P. C.; Sanchez-Cano, C.; Clarkson, G. J.; Soni, R.; Wills, M.; Sadler, P. J. *Chem. Eur. J.* **2015**, *21*, 8043.



Scheme 109

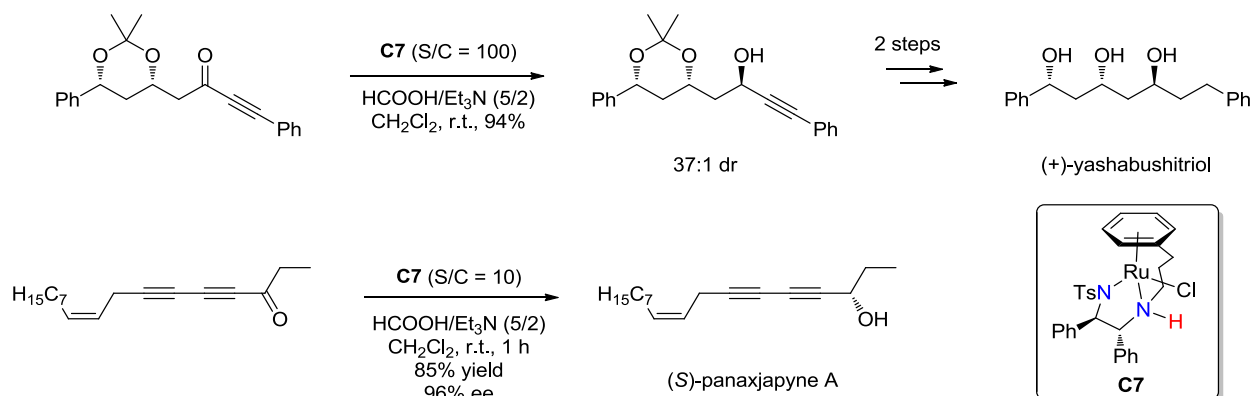
In 2018, Gamasa *et al.* reported various *trans*-[OsCl<sub>2</sub>(L){(*S,S*)-*i*Pr-pybox}] complexes, as well as the dinuclear complexes. The catalytic properties of osmium complexes **C80** and dinuclear complex [(OsCl<sub>2</sub>{(*S,S*)-*i*Pr-pybox})<sub>2</sub>(μ-N,N-C<sub>4</sub>H<sub>4</sub>N<sub>2</sub>)] **C81** have been evaluated in the ATH of a variety of aromatic ketones providing the corresponding (*R*)-benzylalcohols in conversions up to 97% and enantioselectivities up to 73% (Scheme 110).<sup>177</sup>



Scheme 110

### 3. Applications in total synthesis

The tethered complex **C7** described by Will *et al.* was used in the ATH of ketones for several total syntheses. Examples include the synthesis of (+)-yashabushitriol<sup>178</sup> and (*S*)-panaxjapyne A (Scheme 111).<sup>179</sup>



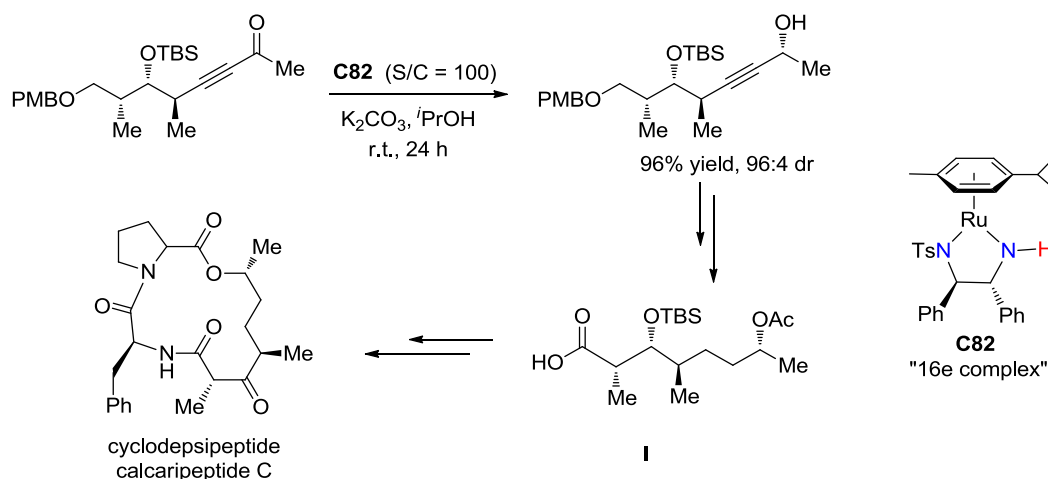
<sup>177</sup> de Julián, E.; Fernández, N.; Díez, J.; Lastra, E.; Gamasa, M. P. *Mol. Catal.* **2018**, 456, 75.

<sup>178</sup> (a) Fang, Z. A.; Clarkson, G. J.; Wills, M. *Tetrahedron Lett.* **2013**, 54, 6834. (b) Fang, Z.; Wills, M. *J. Org. Chem.* **2013**, 78, 8594.

<sup>179</sup> Fang, Z.; Wills, M. *Org. Lett.* **2014**, 16, 374.

## Scheme 111

Ru(II) complex **C82** was used in the ATH of a propargylic ketone bearing multiple stereocenters using *i*PrOH as the hydrogen source under mild conditions to produce the corresponding propargylic alcohol in 96% yield and 94:6 dr. The latter compound was transformed into the key carboxylic acid intermediate **I** for total synthesis of cyclodepsipeptide calcaripeptide C (Scheme 112).<sup>180</sup>

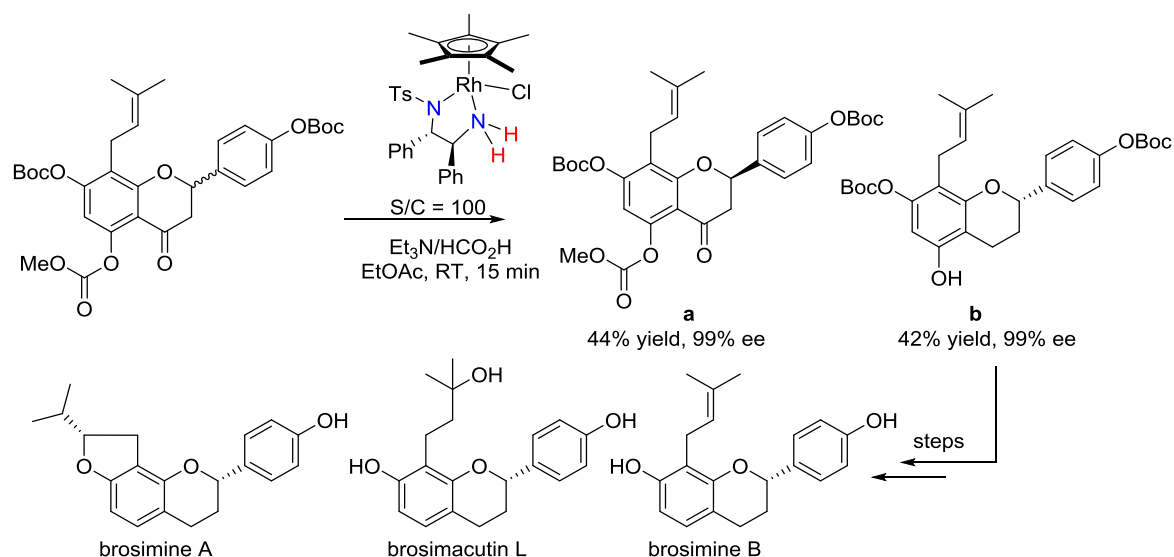


## Scheme 112

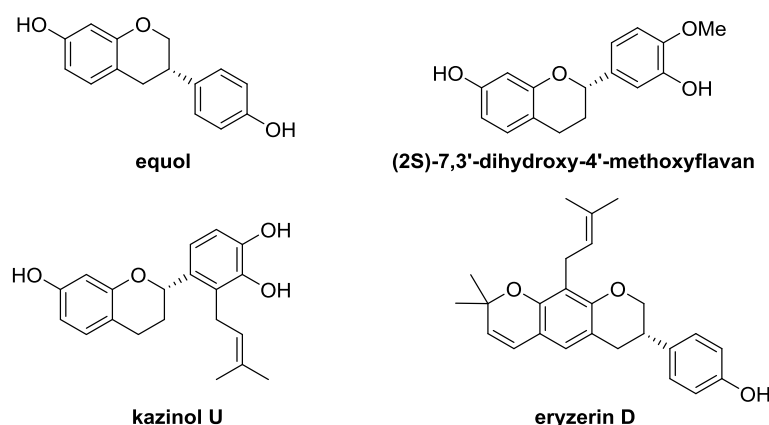
In 2016, Metz' group reported a concise and efficient method to access flavonoids brosimine A, brosimine B, and brosimacutin L, starting from commercially available racemic naringenin. The key step was a rhodium-catalyzed ATH/deoxygenation cascade reaction containing a kinetic resolution process to transform flavanone into flavans in high enantioselectivity. After several functional group interconversion reactions, the natural compounds were obtained with >99% ee (Scheme 113).<sup>181</sup>

<sup>180</sup> Kumaraswamy, G.; Narayanarao, V.; Raju, R. *Org. Biomol. Chem.* **2015**, *13*, 8487.

<sup>181</sup> Keßberg, A.; Metz, P. *Angew. Chem. Int. Ed.* **2016**, *55*, 1160.



The same group utilized this strategy of domino rhodium-catalyzed ATH/deoxygenation reaction to synthesize the key intermediates of kazinol U, (2*S*)-7,3'-dihydroxy-4'-methoxyflavan, equol and eryzerin D (Scheme 114).<sup>182,183</sup>

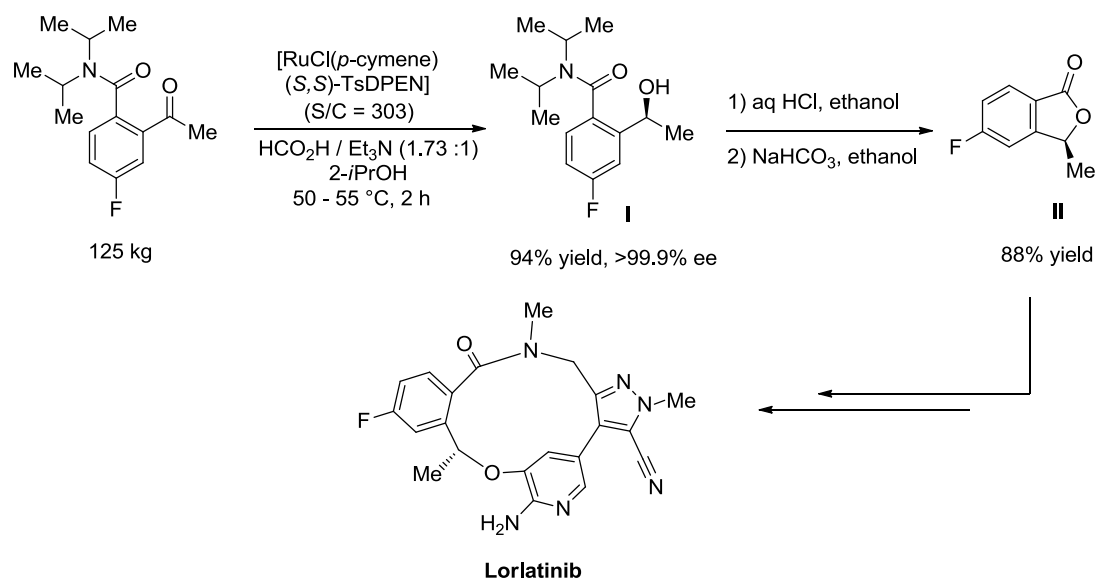


In 2017, Pfizer researchers reported an approach to (*S*)-5-fluoro-3-methylisobenzofuran-1(3*H*)-one, which is the key intermediate of Lorlatinib, an investigational medicine for inhibiting the anaplastic lymphoma kinase (ALK) and ROS1 proto-oncogene. The synthesis relied on the ATH of an *ortho*-diisopropylamide aromatic ketone using [RuCl(*p*-cymene)(*S,S*)-TsDPEN]. The reaction was performed on large scale (125 kg) and gave the corresponding (*S*)-alcohol (**I**) with 94% yield and >99.9% ee. Hydrolysis of the latter

<sup>182</sup> Keßberg, A.; Metz, P. *Org. Lett.* **2016**, *18*, 6500.

<sup>183</sup> Keßberg, A.; Lübken, T.; Metz, P. *Org. Lett.* **2018**, *20*, 3006.

allowed the formation of (*S*)-5-fluoro-3-methylisobenzofuran-1(*3H*)-one (**II**) in 88% yield (Scheme 115).<sup>184</sup>

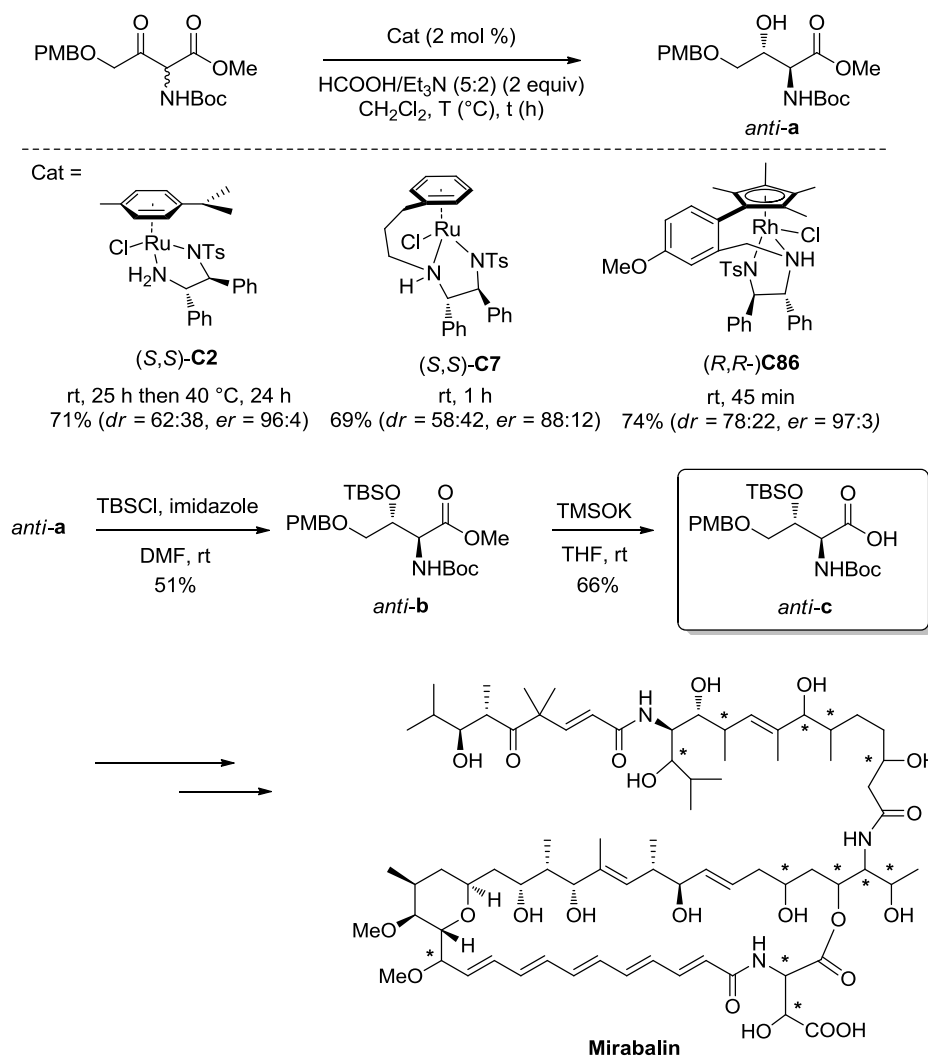


**Scheme 115**

In 2019, our group in collaboration with the group of J. Cossy used the ATH of ketones to perform an efficient asymmetric approach to the synthesis of mirabalin. In particular, ruthenium or rhodium-mediated asymmetric hydrogenation and transfer hydrogenation were used in combination with a dynamic kinetic resolution to control two contiguous stereocenters in a single step (Scheme 116).<sup>185</sup>

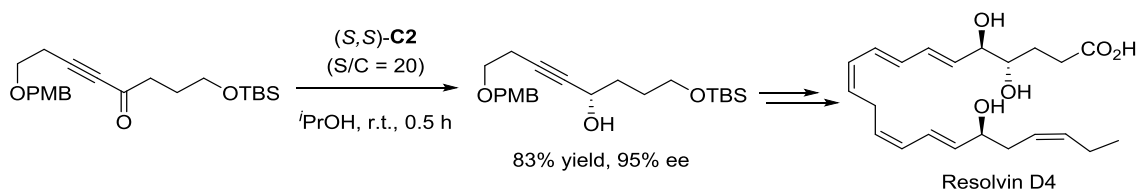
<sup>184</sup> Duan, S.; Li, B.; Dugger, R. W.; Conway, B.; Kumar, R.; Martinez, C.; Makowski, T.; Pearson, R.; Olivier, M.; Colon-Cruz, R. *Org. Process Res. Dev.* **2017**, *21*, 1340.

<sup>185</sup> Echeverria, P.-G., Pons, A., Prévost, S., Féraud, C., Cornil, J., Guérinot, A., Cossy, J.; Phansavath, P.; Ratovelomanana-Vidal, V. *Arkivoc*, **2019**, *4*, 44.



Scheme 116

A key intermediate for the total synthesis of Resolvin D4 was prepared through the ruthenium-catalyzed ATH of a propargylic ketone, with 83% yield and 95% ee (Scheme 117).<sup>186</sup>



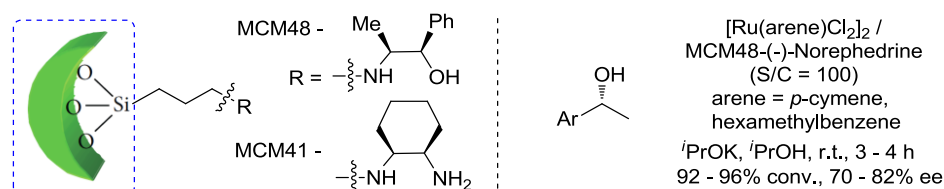
Scheme 117

## 4. Immobilized catalysts

Cubic mesoporous silica MCM41-supported chiral diamine and MCM-48

<sup>186</sup> Morita, M.; Kobayashi, Y. *J. Org. Chem.* **2018**, *83*, 3906.

silica-supported optically active (-)-norephedrine chiral amino alcohol were prepared and incorporated in Ru(II) complexes for the ATH of aromatic ketones in the presence of  $i$ PrOK/ $i$ PrOH as hydrogen source to provide the corresponding alcohols with good enantioselectivities. The supported catalysts could be reused for four times with the same high performance (Scheme 118).<sup>187</sup>



Scheme 118

In 2015, Abu-Reziq described the preparation of magnetically recoverable catalytic silica microcapsules. The catalytic activity of these microreactors was tested in the asymmetric transfer hydrogenation of ketones in an aqueous medium to provide chiral alcohols in high catalytic activities (90–99% conv.) and enantioselectivities (82–99% ee).<sup>188</sup>

In 2016, Reiser *et al.* reported magnetic ATH catalysts based on Noyori's catalyst  $[\text{RuCl}(\text{R,R})\text{-TsDPEN}]$ , which were assembled on organic/inorganic hybrids containing carbon-coated cobalt nanoparticles (Co/C) and different organic polymers.<sup>189</sup> Hou *et al.* developed a new type of reusable homogeneous catalyst  $\text{P}(\text{DMAPM}_{1,2}\text{-TsDPEN})\text{-Ru}_{0.74}$  catalyst which showed high levels of activity and enantioinduction in the ATH of the aromatic ketones and recycled for at least eight times without much loss of the catalytic activity.<sup>190</sup>

In 2016, Cheng, Liu *et al.* described a heterogeneous catalyst named  $\text{Imidazolium@Cp}^*\text{RhArDPEN@PMO}$ . The catalyst displayed high catalytic activity and excellent enantioselectivity in the ATH of  $\alpha$ -halo aromatic ketones and benzils in water, and can be recovered and recycled seven times without loss of its catalytic activity.<sup>191</sup> In 2017, the same group reported a mesoporous silica-based ruthenium/diamine-functionalized heterogeneous catalyst. The supported catalyst could be recovered and reused seven times.<sup>192</sup>

In 2016, Cheng *et al.* reported a fluorescence-marked core-shell structured

<sup>187</sup> (a) Sarkar, S. M.; Yusoff, M. M.; Rahman, M. L. *J. Chin. Chem. Soc.* **2015**, *62*, 177. (b) Sarkar, S. M.; Ali, M. E.; Rahman, M. L.; Mohd Yusoff, M. *J. Nanomater.* **2015**, ID381836

<sup>188</sup> Zoabi, A.; Omar, S.; Abu-Reziq, R. *Eur. J. Inorg. Chem.* **2015**, 2101.

<sup>189</sup> Eichenseer, C. M.; Kastl, B.; Pericàs, M. A.; Hanson, P. R.; Reiser, O. *ACS Sustain. Chem. Eng.* **2016**, *4*, 2698.

<sup>190</sup> Xie, Y.; Wang, M.; Wu, X.; Chen, C.; Ma, W.; Dong, Q.; Yuan, M.; Hou, Z. *ChemPlusChem* **2016**, *81*, 541.

<sup>191</sup> Zhou, F.; Hu, X.; Gao, M.; Cheng, T.; Liu, G. *Green Chem.* **2016**, *18*, 5651.

<sup>192</sup> Wang, J.; Wu, L.; Hu, X.; Liu, R.; Jin, R.; Liu, G. *Catal. Sci. Technol.* **2017**, *7*, 4444.

heterogeneous ruthenium catalyst. The catalyst can be recycled by following the tracks of fluorescent emission and reused at least six times without loss of the catalytic activity.<sup>193</sup> Liu *et al.* reported a new type of heterogeneous chiral catalyst synthesized by anchoring a chiral cinchona alkaloid ligand. The supported catalyst was stable and could be easily recovered and reused at least 4 times with no loss of enantioselectivity.<sup>194</sup> Badyrova *et al.* reported a series of Rh(I) nanoparticles. The colloidal Rh/(8*S*,9*R*)-(-)-cinchonidine nanoparticle was employed in the ATH of acetophenone.<sup>195</sup>

In 2017, Itsuno *et al.* developed a chiral main-chain polyamide containing an (*R,R*)-TsDPEN unit,<sup>196,197</sup> which was combined with [RuCl<sub>2</sub>(*p*-cymene)]<sub>2</sub> for the ATH of aromatic ketones.

A heterogeneous Rh catalyst was generated *in situ* through coordination between the metal precursor [RhCl<sub>2</sub>Cp\*]<sub>2</sub> and MMP@HMSN supported ligand. In addition, the supported catalyst could be easily recycled at least 4 times.<sup>198</sup>

In 2017, Liu developed a bifunctional heterogeneous catalyst **C83** through the immobilization of palladium nanoparticles with ethylene-bridged chiral ruthenium/diamine-functionalized periodic mesoporous organosilica. It could be used for the ATH–Sonogashira coupling one-pot enantioselective tandem reaction of 4-iodoacetophenone and ethynylbenzene at least seven times without loss of its catalytic activity (Scheme 119).<sup>199</sup>

---

<sup>193</sup> An, J.; Zhao, J.; Liu, G.; Cheng, T. *Sens. Actuators B Chem.* **2016**, *224*, 333.

<sup>194</sup> Lou, L.-L.; Li, S.; Du, H.; Zhang, J.; Yu, W.; Yu, K.; Liu, S. *ChemCatChem* **2016**, *8*, 1199.

<sup>195</sup> (a) Nindakova, L. O.; Badyrova, N. M.; Smirnov, V. V.; Kolesnikov, S. S. *J. Mol. Catal. A: Chem.* **2016**, *420*, 149. (b) Nindakova, L. O.; Badyrova, N. M.; Smirnov, V. V.; Strakhov, V. O.; Kolesnikov, S. S. *Russ. J. Gen. Chem.* **2016**, *86*, 1240.

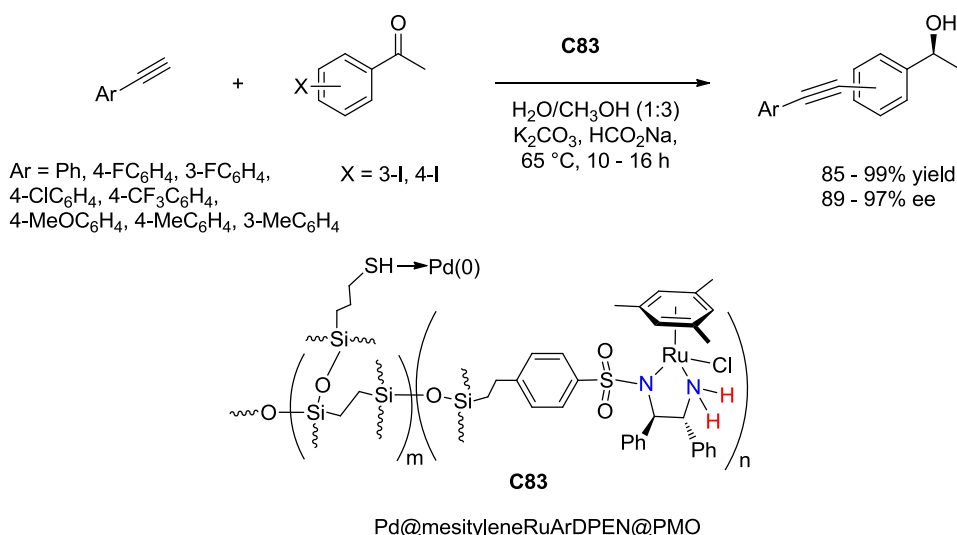
<sup>196</sup> Itsuno, S.; Takahashi, S. *ChemCatChem* **2017**, *9*, 385.

<sup>197</sup> Liu, P. N.; Deng, J. G.; Tu, Y. Q.; Wang, S. H. *Chem. Commun.* **2004**, 2070

<sup>198</sup> Jing, L.; Zhang, X.; Guan, R.; Yang, H. *Catal. Sci. Technol.* **2018**, *8*, 2304.

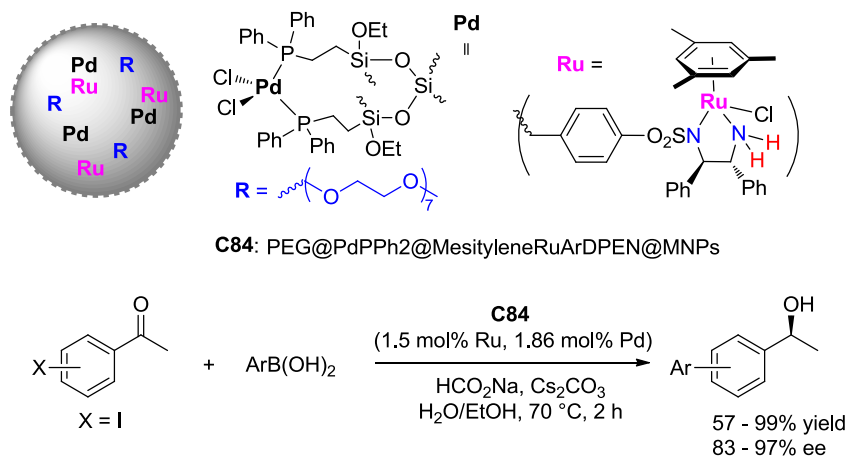
<sup>199</sup> Zhao, Y.; Jin, R.; Chou, Y.; Li, Y.; Lin, J.; Liu, G. *RSC Adv.* **2017**, *7*, 22592.





Scheme 119

Another type of bimetallic (Ru/Pd) supported catalyst **C84** bearing functionalized mesoporous silica, phosphine ligand and PEG was described. This catalyst allowed a one-pot tandem Suzuki cross-coupling and ATH reaction of iodoacetophenones and arylboronic acids in aqueous ethanol in high yields and excellent enantioinductions (up to 97% ee) (Scheme 120).<sup>200</sup>



Scheme 120

## 5. Conclusions

For asymmetric transfer hydrogenation in general, ruthenium complexes bearing tosyl diamine ligands (TsDPEN as the most commonly used diamine ligand) were widely evaluated and applied in organic synthesis chemistry. In the past few years, special attention has been paid

<sup>200</sup> Zhang, G.; Liu, R.; Chou, Y.; Wang, Y.; Cheng, T.; Liu, G. *Chemcatchem* **2018**, *10*, 1882.

to develop new transition metal complexes or new ligands. Usually (het)aryl ketones give high yields and excellent stereoselectivities in the ATH<sup>11</sup> and ATH/DKR<sup>201</sup> process, whereas aliphatic ketones generally yield lower conversions and enantioselectivities. In the context of sustainable chemistry, the design of efficient non-noble metal complexes has recently emerged as an attractive alternative. In addition, supported catalysts by modification of known Ru, Rh or Ir complexes are also welcome in academic research and will be possible for industrial process.

---

<sup>201</sup> For comprehensive reviews covering ATH/DKR, see: (a) Noyori, R.; Tokunaga, M.; Kitamura, M. *Bull. Chem. Soc. Jpn.* **1995**, *68*, 36. (b) Caddick, S.; Jenkins, K. *Chem. Soc. Rev.* **1996**, *25*, 447. (c) Ward, R. S. *Tetrahedron: Asymmetry* **1995**, *6*, 1475. (d) Sturmer, R. *Angew. Chem. Int. Ed.* **1997**, *36*, 1173. (e) El Gihani, M. T.; Williams, J. M. J. *Curr. Opin. Chem. Biol.* **1999**, *3*, 11. (f) Ratovelomanana-Vidal, V.; Genêt, J.-P. *Can. J. Chem.* **2000**, *851*, 846. (g) Huerta, F. F.; Minidis, A. B. E.; Bäckvall, J.-E. *Chem. Soc. Rev.* **2001**, *30*, 321. (h) Faber, K. *Chem. Eur. J.* **2001**, *7*, 5005. (i) Pàmies, O.; Bäckvall, J.-E. *Chem. Rev.* **2003**, *103*, 3247. (j) Pellissier, H. *Tetrahedron* **2003**, *59*, 8291. (k) Turner, N. J. *Curr. Opin. Chem. Biol.* **2004**, *8*, 114. (l) Vedejs, E.; Jure, M. *Angew. Chem. Int. Ed.* **2005**, *44*, 3974. (m) Martín-Matute, B.; Bäckvall, J.-E. *Curr. Opin. Chem. Biol.* **2007**, *11*, 226. (n) Pellissier, H. *Tetrahedron* **2008**, *64*, 1563. (o) Pellissier, H., *Tetrahedron* **2011**, *67*, 3769. (p) Xie, J.-H.; Zhou, Q.-L. *Aldrichimica Acta* **2015**, *48*, 33. (q) Echeverria, P.-G.; Ayad, T.; Phansavath, P.; Ratovelomanana- Vidal, V. *Synthesis* **2016**, *48*, 2523. (r) Bhat, V.; Welin, E. R.; Guo, X.; Stoltz, B. M. *Chem. Rev.* **2017**, *117*, 452. (s) Molina-Betancourt, R.; Echeverria, P.-G.; Ayad, T.; Phansavath, P.; Ratovelomanana- Vidal, V. *Synthesis* **2020** (accepted).



## **PART B: ATH of heterocyclic ketones**





## Part B: ATH of heterocyclic ketones

### 1. Rhodium-Catalyzed Asymmetric Transfer Hydrogenation of 4-Quinolone Derivatives

#### 1.1 Introduction

##### 1.1.1 Biological interest of enantiopure tetrahydroquinolin-4-ols derivatives

Chiral benzylic alcohols and their derivatives are important building blocks for the synthesis of chemical materials, pharmaceuticals, and agrochemicals, as the hydroxyl group can be easily functionalized, to access to versatile intermediates (Figure 1). Consequently, significant efforts have been displayed to develop efficient and atom-economical stereoselective processes to obtain such compounds.<sup>202</sup> Among these, enantiopure tetrahydroquinolin-4-ols are attractive targets due to their promising biological activities and wide-ranging use as synthetic intermediates for drug candidates.<sup>203</sup>

---

<sup>202</sup> (a) Bartoszewicz, A.; Ahlsten N.; Martín-Matute, B. *Chem. Eur. J.* **2013**, *19*, 7274. (b) Ahn, Y.; Ko, S.-B.; Kim, M.-J.; Park, J. *Coord. Chem. Rev.* **2008**, *252*, 647.

<sup>203</sup> (a) Matsubara, J.; Kitano, K.; Otsubo, K.; Kawano, Y.; Ohtani, T.; Bando, M.; Kido, M.; Uchida, M.; Tabusa, F. *Tetrahedron* **2000**, *56*, 4667; (b) Uchida, R.; Imasato, R.; Shiomi, K.; Tomoda, H.; Ohmura, S. *Org. Lett.* **2005**, *7*, 5701; (c) Scherlach, K.; Hertweck, C. *Org. Biomol. Chem.* **2006**, *4*, 3517; (d) Neff, S. A.; Lee, S. U.; Asami, Y.; Ahn, J. S.; Oh, H.; Baltrusaitis, J.; Gloer, J. B.; Wicklow, D. T. *J. Nat. Prod.* **2012**, *75*, 464, (e) H. I. Mosberg, L. Yeomans, A. A. Harland, A. M. Bender, K. Sobczyk-Kojiro, J. P. Anand, M. J. Clark, E. M. Jutkiewicz and J. R. Traynor. *J. Med. Chem.* **2013**, *56*, 2139.

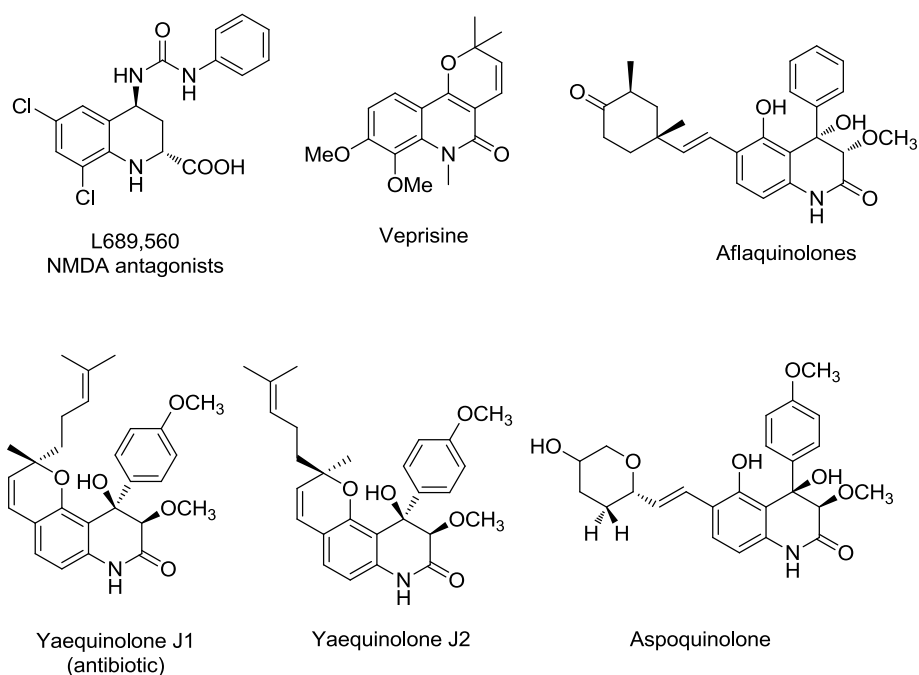


Figure 1

### 1.1.2 Different synthetic pathways for enantiopure tetrahydroquinolin-4-ols

Accordingly, quests for efficient routes to access these scaffolds are still underway. Although various methods allow the synthesis of enantiomerically enriched tetrahydroquinolin-4-ols, this motif can be conveniently prepared from the corresponding ketone through (*S*)-methyl-CBS-catalyzed reduction,<sup>204</sup> enzymatic asymmetric reduction<sup>205</sup> or asymmetric (transfer) hydrogenation.<sup>206, 207, 103</sup>

#### 1.1.2.1 (*S*)-Methyl-CBS-catalyzed reduction

In 2013, Traynor *et al.* described a new method to prepare opioid peptidomimetics. The total synthesis of the latter involved the preparation of an enantiopure tetrahydroquinolin-4-ol derivative. The authors used (*S*)-methyl-CBS as catalyst to reduce tert-butyl

<sup>204</sup> Mosberg, H. I.; Yeomans, L.; Harland, A. A.; Bender, A. M.; Sobczyk-Kojiro, K.; Anand, J. P.; Clark, M. J.; Jutkiewicz, E. M.; Traynor, J. R. *J. Med. Chem.* 2013, **56**, 2139.

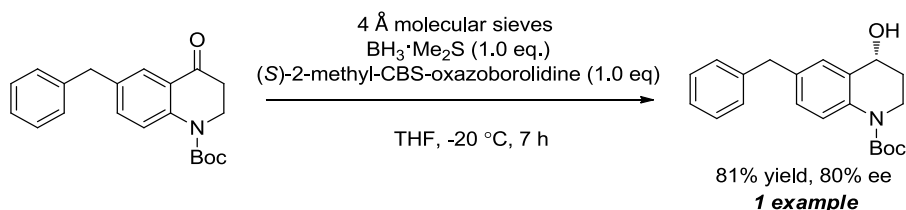
<sup>205</sup> Rowan, A. S.; Moody, T. S.; Howard, R. M.; Underwood, T. J.; Miskelly, I. R.; He, Y.; Wang, B. *Tetrahedron: Asymmetry* **2013**, **24**, 1369

<sup>206</sup> Masaki, O.; Akira, S.; Yoshikazu, M.; Muneki, K. European Patent, EP1944291A1, **2008**.

<sup>207</sup> Utsumi, N.; Tsutsumi, K.; Watanabe, M.; Murata, K.; Arai, N.; Kurono, N.; Ohkuma, T. *Heterocycles* **2010**, **80**, 141.



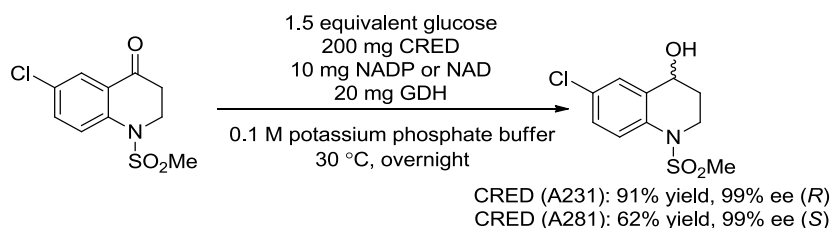
6-benzyl-4-oxo-3,4-dihydroquinoline-1(2H)-carboxylate to the corresponding chiral alcohol in the presence of an equivalent of  $\text{BH}_3 \cdot \text{Me}_2\text{S}$  in THF at  $-20\text{ }^\circ\text{C}$ . They obtained the (*R*)-tert-butyl 6-benzyl-4-hydroxy-3,4-dihydroquinoline-1(2H)-carboxylate with good yield (81%) and moderate enantioselectivity (80% ee) (Scheme 121).<sup>204</sup>



Scheme 121

### 1.1.2.2 Enzymatic asymmetric reduction

In 2013, Wang *et al.* established the enzymatic reduction of ketones using selectAZyme™ carbonyl reductase (CRED) technology to get highly enantioenriched secondary alcohols. 6-Chloro-1-(methylsulfonyl)-2,3-dihydroquinolin-4(1H)-one was reduced by using CRED, NADP or NAD, GDH, glucose as the hydrogen source and potassium phosphate buffer. When they chose A231 as carbonyl reductase (CRED), the corresponding alcohol was obtained in 91% yield with a good enantioselectivity (99% ee), whereas the use of A281 as CRED led to the opposite enantioenriched enantiomer (99% ee) in a lower yield (62%) (Scheme 122).<sup>205</sup>

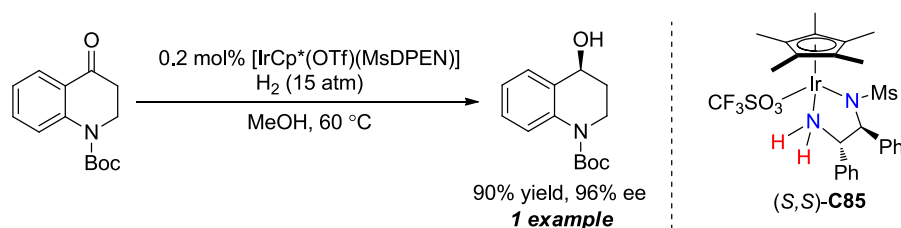


Scheme 122

### 1.1.2.3 Asymmetric (transfer) hydrogenation

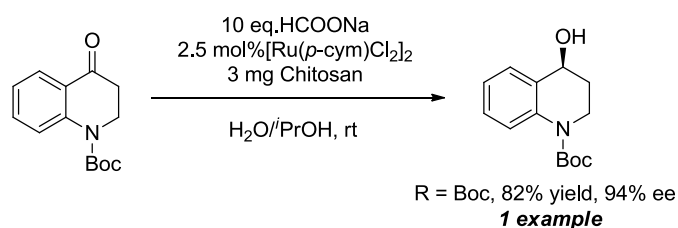
In 2010, Ohkuma *et al.* described the asymmetric hydrogenation of aromatic heterocyclic ketones by using  $[\text{IrCp}^*(\text{OTf})(\text{MsDPEN})]$  complex and methanol as solvent. They described the asymmetric hydrogenation of *tert*-butyl 4-oxo-3,4-dihydroquinoline-1(2H)-carboxylate with 0.2 mol% of  $[\text{IrCp}^*(\text{OTf})(\text{MsDPEN})]$  complex at  $60\text{ }^\circ\text{C}$  under 15 atm of hydrogen. High yield and enantioselectivity were obtained

high (90% yield, 96% ee) (Scheme 123).<sup>207</sup>



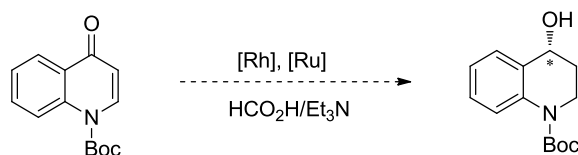
**Scheme 123**

In 2019, Szöllősi *et al.* disclosed the ruthenium(II)-catalyzed asymmetric transfer hydrogenation of *N*-heterocyclic ketones. They applied the reaction on the same substrate than Ohkuma, *tert*-butyl 4-oxo-3,4-dihydroquinoline-1(2*H*)-carboxylate. They used 2.5 mol% [Ru(*p*-cym)Cl<sub>2</sub>]<sub>2</sub> as a catalyst precursor with chitosan biopolymer as a ligand and sodium formate as the hydrogen source. The reaction was performed in a H<sub>2</sub>O/*i*PrOH (4:1) mixture, at room temperature and proceeded in 82% yield with 94% ee in 168 h (Scheme 124).<sup>103</sup>



**Scheme 124**

As shown above, there are a few methodologies to access enantiopure tetrahydroquinolin-4-ols derivatives, involving the reduction of the relevant ketones. However, as far as asymmetric transfer hydrogenation (ATH) of *tert*-butyl 4-oxoquinoline-1(4*H*)-carboxylate is concerned, no example has been reported to the best of our knowledge. So our project will focus on the conjugated asymmetric reduction of both C=C and C=O bonds on the quinolone scaffold (Scheme 125).

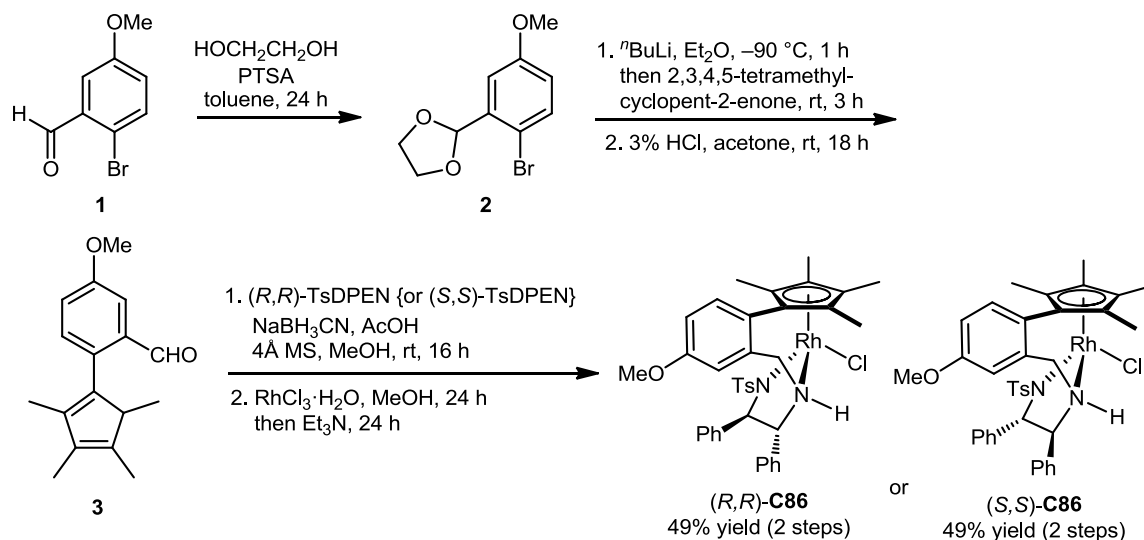


**Scheme 125**

## 1.2 Results and discussion

### 1.2.1 Synthesis of (*R,R*) and (*S,S*)-enantiomers of rhodium complex **C86**

For this study, we have prepared two enantiomers of the rhodium complex **C86** according to the procedure developed in our group.<sup>208</sup> These complexes were synthesized from 5-methoxy-2-(2,3,4,5-tetramethylcyclopenta-1,3-dien-1-yl)benzaldehyde **3**, which was obtained by protection of 2-bromo-5-methoxybenzaldehyde with glycol to 1,3-dioxolane derivative **2**, followed by treatment of compound **2** with <sup>n</sup>BuLi, and addition of 2,3,4,5-tetramethylcyclopent-2-enone to furnish the corresponding alcohol. The latter was then subjected to both deprotection of the aldehyde function and dehydration of the tertiary alcohol using 3% hydrochloric acid in acetone affording compound **3**. Subsequent reductive amination using (*R,R*)-TsDPEN or (*S,S*)-TsDPEN in the presence of sodium cyanoborohydride then delivered the corresponding diamine. The targeted complexes (*R,R*)-**C86** or (*S,S*)-**C86** were then obtained through heating the latter in refluxing methanol in the presence of rhodium(III) chloride followed by treatment with triethylamine. The complexes were isolated after flash chromatography as orange solids, respectively (Scheme 126).



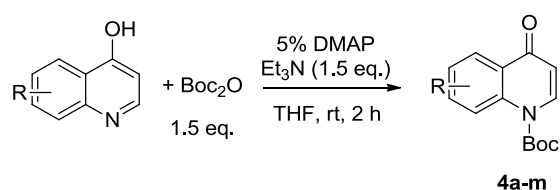
Scheme 126

<sup>208</sup> (a) Echeverria, P.-G.; Féraud, C.; Phansavath, P.; Ratovelomanana-Vidal, *Catal. Commun.* **2015**, *62*, 95.  
(b) Zheng, L.-S.; Llopis, Q.; Echeverria, P.-G.; Féraud, C.; Guillamot, G.; Phansavath, P.; Ratovelomanana-Vidal, V. *J. Org. Chem.* **2017**, *82*, 5607

### 1.2.2 Synthesis of aryl *tert*-butyl 4-oxoquinoline-1(4H)-carboxylates

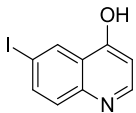
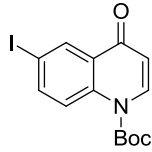
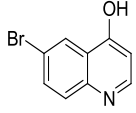
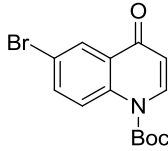
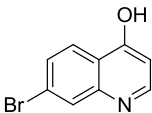
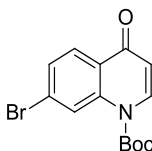
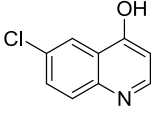
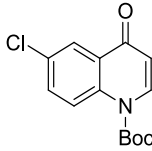
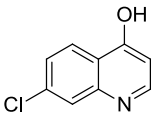
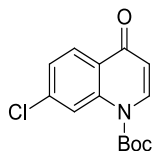
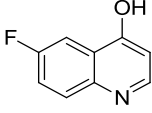
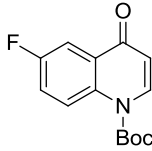
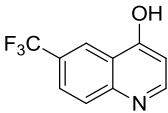
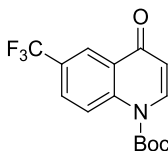
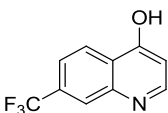
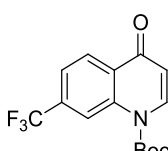
The substrates *tert*-butyl 4-oxoquinoline-1(4H)-carboxylate derivatives **4a-m** required for this study were next prepared in one step according to a reported procedure.<sup>209</sup> The *N*-Boc protection of 4-quinolinol derivatives was thus performed with di-*tert*-butyl dicarbonate (1.5 eq.), in the presence of triethylamine (1.5 eq.) and 5% DMAP in THF at room temperature for 2 h in 50-84% isolated yields (Table 1).

**Table 1.** preparation of *tert*-butyl 4-oxoquinoline-1(4H)-carboxylate derivatives



Entry	4-quinolinols	NO.	Substrates	yield (%)
1		<b>4a</b>		76
2		<b>4b</b>		72
3		<b>4c</b>		80
4		<b>4d</b>		80
5		<b>4e</b>		56

<sup>209</sup> Rosi, F.; Crucitti, G. C.; Lacovo, A.; Miele, G.; Pescatori, L.; Santo, R. D.; Costi, R. *Synth. Commun.* **2013**, *43*, 1063.

6		<b>4f</b>		80
7		<b>4g</b>		84
8		<b>4h</b>		83
9		<b>4i</b>		76
10		<b>4j</b>		60
11		<b>4k</b>		50
12		<b>4l</b>		68
13		<b>4m</b>		68

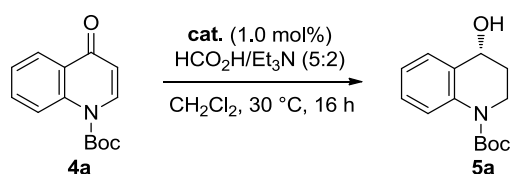
### 1.2.3 Optimisation of the reaction conditions

#### 1.2.3.1 Influence of the precatalyst

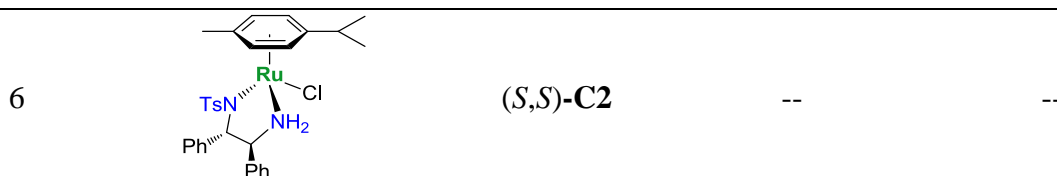
Our investigation of the ATH of 4-quinolone derivatives began with *tert*-butyl 4-oxoquinoline-1(4*H*)-carboxylate **4a** as the standard substrate for the optimization of the reaction parameters. We first examined the influence of different ruthenium and rhodium

complexes to the reaction that was carried out in dichloromethane at 30 °C with HCO<sub>2</sub>H/Et<sub>3</sub>N (5:2) azeotropic mixture as the hydrogen source. Under these conditions, the expected alcohol **5a** was obtained in 41-83% isolated yield with an excellent level of enantioselectivity (>99% ee) with the rhodium complexes **C86-89** (Table 2, entries 1–5). Full conversions were observed in all cases with these complexes and the lower yields of **5a** obtained with **C87-89** compared to **C86** are related to partial *in situ* cleavage of the Boc group. Of the above-mentioned rhodium complexes, **C86** provided the best results (83% yield, >99% ee, Table 2, entry 1), but lowering the catalyst loading to 0.5 mol% resulted in a decrease of the yield (55%, Table 2, entry 2).

**Table 2 Screening of precatalysts for the ATH of 4a<sup>a</sup>**



Entry	Cat.	yield <sup>[b]</sup> (%)	ee <sup>[c]</sup> (%)
1		83	>99
2 <sup>[e]</sup>	<b>(<i>R,R</i>)-C86</b>	55	>99
3		76	>99
4		67	>99
5		41	>99

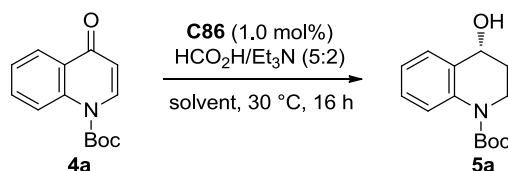


<sup>a</sup> Reaction conditions: **4a** (0.5 mmol), catalyst (1.0 mol%), HCO<sub>2</sub>H/Et<sub>3</sub>N (5:2) (170 μL, 4.0 equiv), CH<sub>2</sub>Cl<sub>2</sub> (0.5 mL), 30 °C. <sup>b</sup> Isolated yields. <sup>c</sup> Determined by SFC analysis using a chiral stationary phase.

### 1.2.3.2 Influence of the solvent

Pursuing the study with the tethered rhodium complex **C86** (Table 3), we investigated the influence of the solvent. We tried two non-polar solvents such as toluene and diethyl ether which gave 67% and 63% yields (Table 3, entries 2-3). Then we compared some polar solvents such as THF, CH<sub>3</sub>CN, DMF. However, the yields were even lower than with non-polar solvents (Table 3, entries 4-6). We also performed the reaction in greener solvents such as 2-MeTHF, dimethyl carbonate and TBME which led to 36-69% yields (Table 3, entries 7–9). Though all the solvents we tested gave excellent enantioselectivities (> 99%), CH<sub>2</sub>Cl<sub>2</sub> showed the most satisfying result with 83% yield.

**Table 3** Screening of solvents for the ATH of **4a**<sup>a</sup>



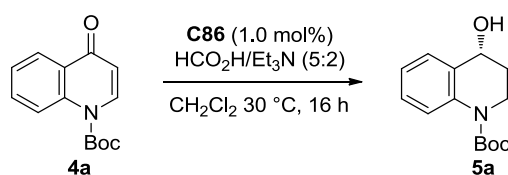
Entry	Solvent	yield <sup>[b]</sup> (%)	ee <sup>[c]</sup> (%)
1	CH <sub>2</sub> Cl <sub>2</sub>	83	>99
2	Toluene	67	>99
3	Et <sub>2</sub> O	63	>99
4	THF	59	>99
5	CH <sub>3</sub> CN	64	>99
6	DMF	22	>99
7	Me-THF	36	>99
8	DMC	63	>99
9	TBME	69	>99

<sup>a</sup> Reaction conditions: **4a** (0.5 mmol), **C86** (1.0 mol%), HCO<sub>2</sub>H/Et<sub>3</sub>N (5:2) (170 μL, 4.0 equiv), solvent (0.5 mL), 30 °C. <sup>b</sup> Isolated yields. <sup>c</sup> Determined by SFC analysis using a chiral stationary phase.

### 1.2.3.3 Influence of the amount of the HCO<sub>2</sub>H/Et<sub>3</sub>N azeotropic mixture

Using CH<sub>2</sub>Cl<sub>2</sub> as solvent, we then studied the effect of the amount of the HCO<sub>2</sub>H/Et<sub>3</sub>N (5:2) azeotropic mixture on the reaction. We screened the quantity of HCO<sub>2</sub>H/Et<sub>3</sub>N (5:2) from 2.0 equiv to 8.0 equiv and found the reaction to be sensitive to this parameter. The use of 4.0 equiv of HCO<sub>2</sub>H/Et<sub>3</sub>N (5:2) was the best option, since when lower or higher catalyst loadings were used, decreased yields were observed (Table 4, entries 1–6).

**Table 4 Screening of the amount of the HCO<sub>2</sub>H/Et<sub>3</sub>N<sup>a</sup>**



Entry	hydrogen source (equiv)	yield <sup>[b]</sup> (%)	ee <sup>[c]</sup> (%)
1	2.0	31	>99
2	3.0	70	>99
3	4.0	83	>99
4	5.0	76	>99
5	6.0	64	>99
6	8.0	66	>99

<sup>a</sup> Reaction conditions: **4a** (0.5 mmol), **C86** (1.0 mol%), HCO<sub>2</sub>H/Et<sub>3</sub>N (5:2) (170 μL, 4.0 equiv), CH<sub>2</sub>Cl<sub>2</sub> (0.5 mL), 30 °C. <sup>b</sup> Isolated yields. <sup>c</sup> Determined by SFC analysis using a chiral stationary phase.

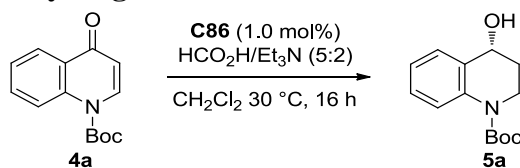
### 1.2.3.4 Influence of the hydrogen source

Trying to improve the yields, other hydrogen sources were evaluated as well but failed to afford better results or even the expected reduced products (Table 5, entries 1–5). Indeed, the use of a HCO<sub>2</sub>H/Et<sub>3</sub>N (1:1) azeotropic mixture instead of the (5:2) mixture furnished the corresponding alcohol in 51% yield (Table 5, entry 1) whereas with <sup>i</sup>PrOH/KOH no reduction occurred (Table 5, entry 2). Sodium formate failed to afford any conversion in CH<sub>2</sub>Cl<sub>2</sub> (Table 5, entry 3) but a 40% yield of **5a** was obtained in water using 20 mol% of CTAB as a surfactant (Table 5, entry 4). Finally, under the same conditions, no conversion was observed in the presence of ammonium formate (Table 5, entry 5). On the basis of the above screening, the optimized conditions were set as follows: **C86** (1.0 mol %) as the precatalyst, HCO<sub>2</sub>H/Et<sub>3</sub>N



(5:2) (4.0 equiv), CH<sub>2</sub>Cl<sub>2</sub> (1.0 M) at 30 °C.

**Table 5** Screening of other hydrogen sources<sup>a</sup>



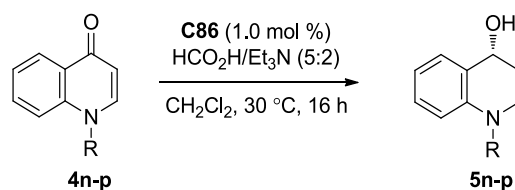
Entry	hydrogen source	yield <sup>[b]</sup> (%)	ee <sup>[c]</sup> (%)
1	HCO <sub>2</sub> H/Et <sub>3</sub> N (1:1)	51	99
2	<sup>t</sup> PrOH/KOH	--	--
3	HCO <sub>2</sub> Na	--	--
4	HCO <sub>2</sub> Na <sup>d</sup>	40	99
5	HCO <sub>2</sub> NH <sub>4</sub> <sup>d</sup>	--	--

<sup>a</sup> Reaction conditions: **4a** (0.5 mmol), **C86** (1.0 mol%), HCO<sub>2</sub>H/Et<sub>3</sub>N (5:2) (170 μL, 4 equiv), CH<sub>2</sub>Cl<sub>2</sub> (0.5 mL), 30 °C. <sup>b</sup> Isolated yields. <sup>c</sup> Determined by SFC analysis using a chiral stationary phase. <sup>d</sup> Water as solvent with 20 mol% of CTAB as a surfactant

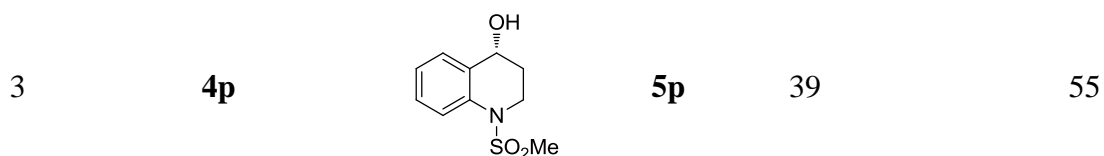
### 1.2.3.5 ATH of other *N*-protected substrates

Besides the *N*-boc protected substrates, we also synthesized other *N*-protected substrates such as *N*-methyl, *N*-benzyl and *N*-Ms derivatives. These compounds were subjected to the optimized ATH reaction conditions. However, *N*-methyl and *N*-benzyl substrates did not react under these conditions, and the *N*-Ms compound led to 39% yield and 55% ee. (Table 6, entries 1–3).

**Table 6.** ATH of other *N*-protected substrates<sup>a</sup>



Entry	substrate	product	NO.	yield (%) <sup>b</sup>	ee (%) <sup>c</sup>
1	<b>4n</b>		<b>5n</b>	--	--
2	<b>4o</b>		<b>5o</b>	--	--



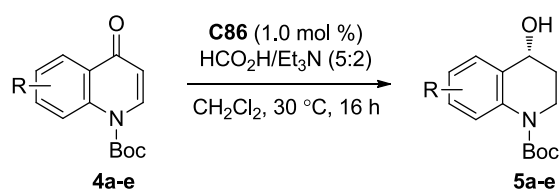
<sup>a</sup> Reaction conditions: **4** (0.5 mmol), (*R,R*)-**C86** (1.0 mol%), HCO<sub>2</sub>H/Et<sub>3</sub>N (5:2) (170 μL, 4 equiv), CH<sub>2</sub>Cl<sub>2</sub> (0.5 mL), 30 °C, 16 h. <sup>b</sup> Isolated yields. <sup>c</sup> Determined by SFC analysis using a chiral stationary phase.

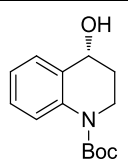
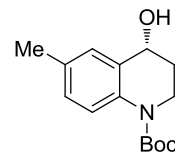
## 1.2.4 Substrate scope

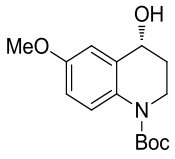
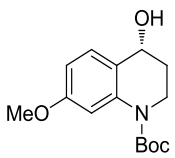
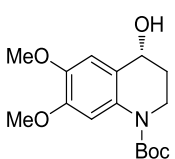
### 1.2.4.1 ATH of substrates bearing electron- donating substituents

With these optimized reaction conditions, the scope of the asymmetric transfer hydrogenation of a series of variously substituted 4-quinolone derivatives (**4b–m**) was evaluated. Notably, compounds **4a–m** having electron-donating or withdrawing groups on the aromatic ring remained reactive under these conditions leading to a uniformly excellent level of enantioselectivity (> 99% ee) with mainly good yields. The reaction was tolerant of methyl or methoxy electron-donating substituents on the aryl core and provided the corresponding alcohols **5a–m** in yields of 50-79% (Table 7, entries 2–4), but only 23% of the product **5e** was isolated when two methoxy groups were present (Table 7, entry 5).

**Table 7. ATH of substrates bearing electron-donating substituents<sup>a</sup>**



Entry	substrate	product	NO.	yield (%) <sup>b</sup>	ee (%) <sup>c</sup>
1	<b>4a</b>		<b>5a</b>	83	>99
2	<b>4b</b>		<b>5b</b>	79	>99

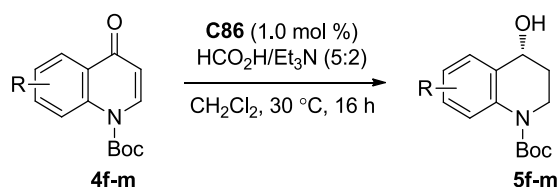
3	<b>4c</b>		<b>5c</b>	75	>99
4	<b>4d</b>		<b>5d</b>	50	99
5	<b>4e</b>		<b>5e</b>	23	97

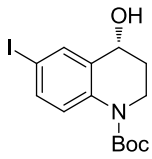
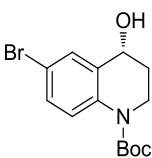
<sup>a</sup> Reaction conditions: **4** (0.5 mmol), (*R,R*)-**C86** (1.0 mol%), HCO<sub>2</sub>H/Et<sub>3</sub>N (5:2) (170 μL, 4 equiv), CH<sub>2</sub>Cl<sub>2</sub> (0.5 mL), 30 °C, 16 h. <sup>b</sup> Isolated yields. <sup>c</sup> Determined by SFC analysis using a chiral stationary phase.

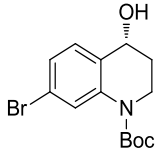
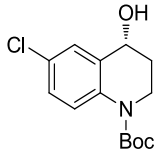
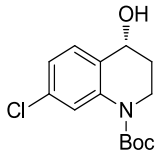
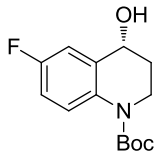
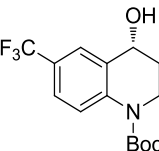
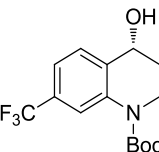
### 1.2.4.2 ATH of substrates bearing electron-withdrawing substituents

As for electron-withdrawing groups, the ATH reaction was amenable under the standard conditions to halogen substitution such as iodine, bromine, chlorine and fluorine, as well as a trifluoromethyl substituent. Alcohols **5f-m** displayed excellent enantioselectivities (up to > 99% ee) and moderate to good yields (64–73%) (Table 8, entries 1–8).

**Table 8. ATH of substrates bearing electron-withdrawing substituents<sup>a</sup>**



Entry	substrate	product	NO.	yield (%) <sup>b</sup>	ee (%) <sup>c</sup>
1	<b>4f</b>		<b>5f</b>	64	>99
2	<b>4g</b>		<b>5g</b>	73	99

3	<b>4h</b>		<b>5h</b>	67	99
4	<b>4i</b>		<b>5i</b>	67	>99
5	<b>4j</b>		<b>5j</b>	66	>99
6	<b>4k</b>		<b>5k</b>	73	>99
7	<b>4l</b>		<b>5l</b>	66	>99
8	<b>4m</b>		<b>5m</b>	67	>99

<sup>a</sup> Reaction conditions: **4** (0.5 mmol), (*R,R*)-**C86** (1.0 mol%), HCO<sub>2</sub>H/Et<sub>3</sub>N (5:2) (170 μL, 4.0 equiv), CH<sub>2</sub>Cl<sub>2</sub> (0.5 mL), 30 °C, 16 h. <sup>b</sup> Isolated yields. <sup>c</sup> Determined by SFC analysis using a chiral stationary phase.

### 1.2.5 Determination of the absolute configuration

The absolute configuration of alcohol **5f** was unambiguously assigned as (*R*) by X-ray crystallographic analysis (Figure 2), and by analogy, we conjectured that the remainder of the ATH products followed the same trend.

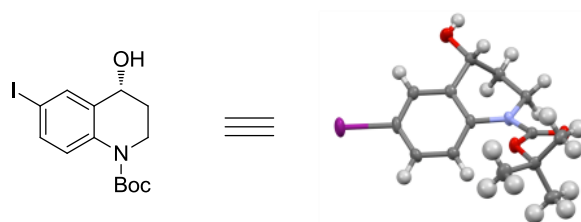


Figure 2. X-ray of **5f**

### 1.2.6 Scale up experiment

Of note, the reduction of **4a** could be conducted on a gram-scale with no detrimental effect on the enantioselectivity and the product **5a** was obtained with a comparable yield (81% yield, >99% ee), supporting the efficiency of the Rh-mediated ATH reaction (Scheme 127).



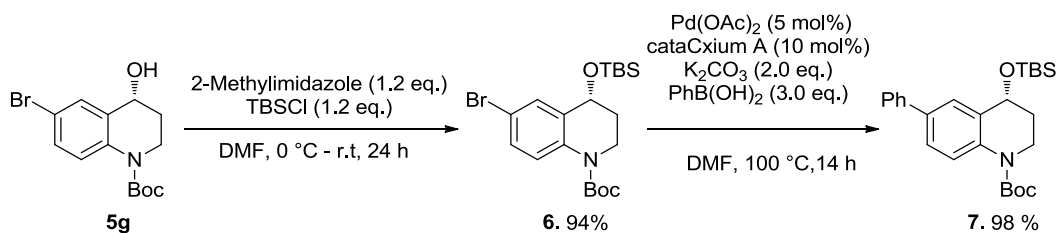
Scheme 127

### 1.2.7 Post-functionalization

Moreover, the reduced compounds **5** can serve as useful intermediates for further elaboration on either the aromatic ring or the heterocyclic counterpart. Thus, we performed post-functionalization reactions on the reduced compounds.

#### 1.2.7.1 Suzuki-Miyaura reaction

A Pd-catalyzed cross-coupling reaction was performed on the *O*-protected derivative **6**. Thus, after TBS protection of **5g**, a Suzuki-Miyaura reaction was carried out with Pd(OAc)<sub>2</sub>, cataCXium A as a ligand, K<sub>2</sub>CO<sub>3</sub> as a base and phenylboronic acid to deliver the corresponding product **7** in 98% yield (Scheme 128).

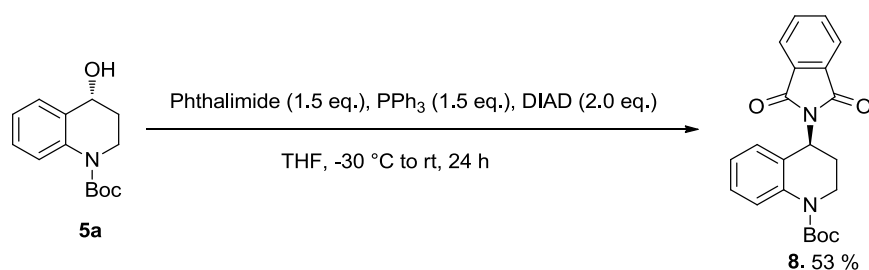


Scheme 128

#### 1.2.7.2 Mitsunobu reaction

A Mitsunobu reaction of **5a** afforded the introduction of a phthalimide substituent on the *N*-heterocycle to provide compound **8** in 53% yield by using PPh<sub>3</sub>, diisopropyl

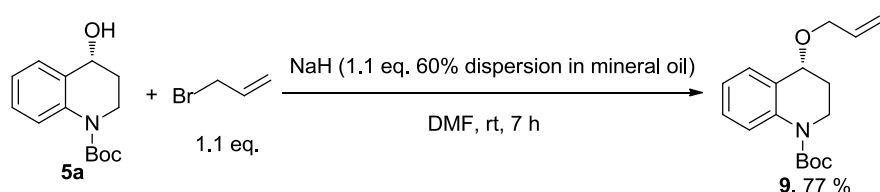
azodicarboxylate (DIAD) and phthalimide in THF (Scheme 129).



Scheme 129

### 1.2.7.3 O-Allylation

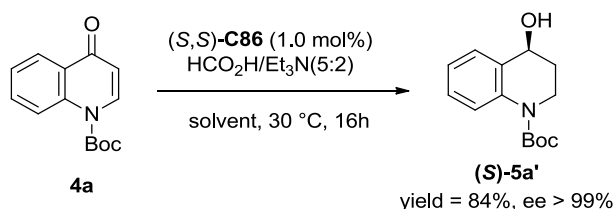
Finally, *O*-allylation of **5a** readily furnished compound **9** in 77% yield, which is prone to further functionalization such as e.g. a cross-metathesis reaction (Scheme 130).



Scheme 130

## 1.2.8 Synthesis of (*S*)-tert-butyl-4-hydroxy-3,4-dihydroquinoline-1(2*H*)-carboxylate

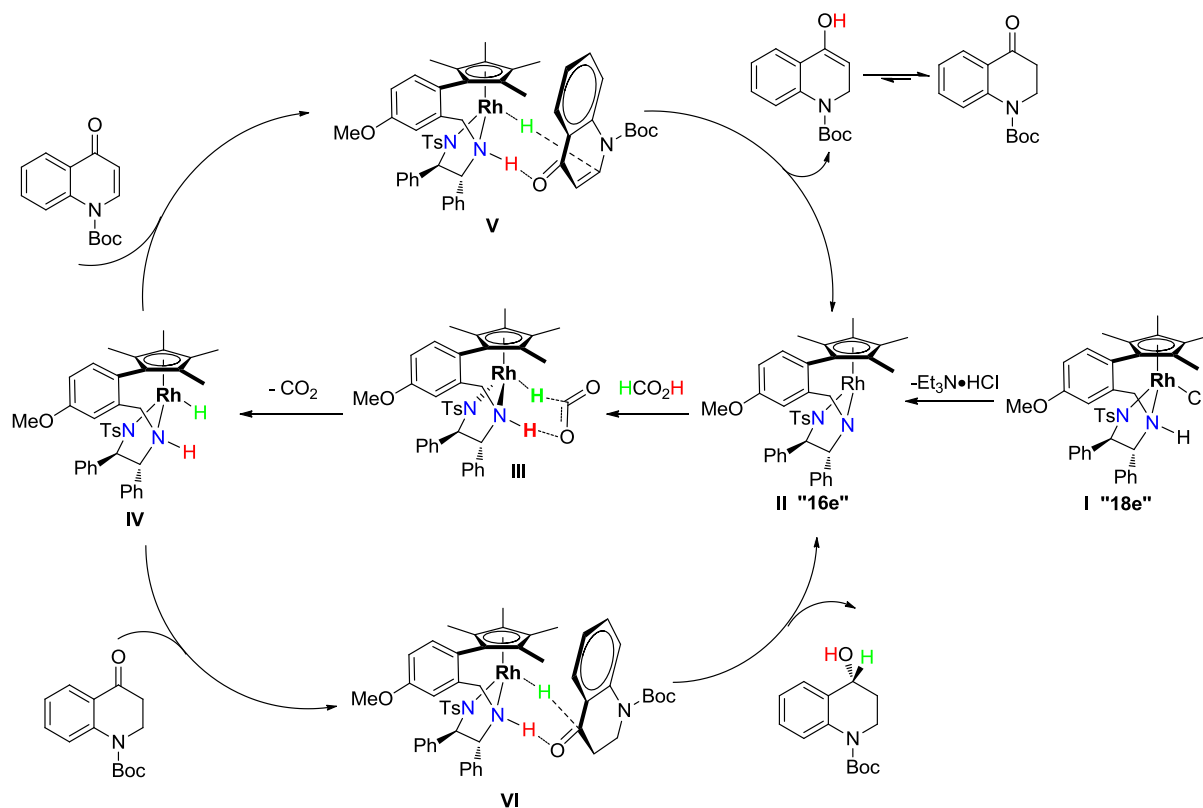
In addition, (*S*)-alcohol **5a'** could be prepared as well by using the (*S,S*)-enantiomer of complex **C86** instead of the (*R,R*)-isomer and the asymmetric reduction of **1a** with (*S,S*)- **C86** delivered (*S*)-**5a'** with comparable yield and ee as expected (Table 3, entry 2, 84% yield, > 99% ee) (Scheme 131).



Scheme 131

## 1.2.9 Mechanism

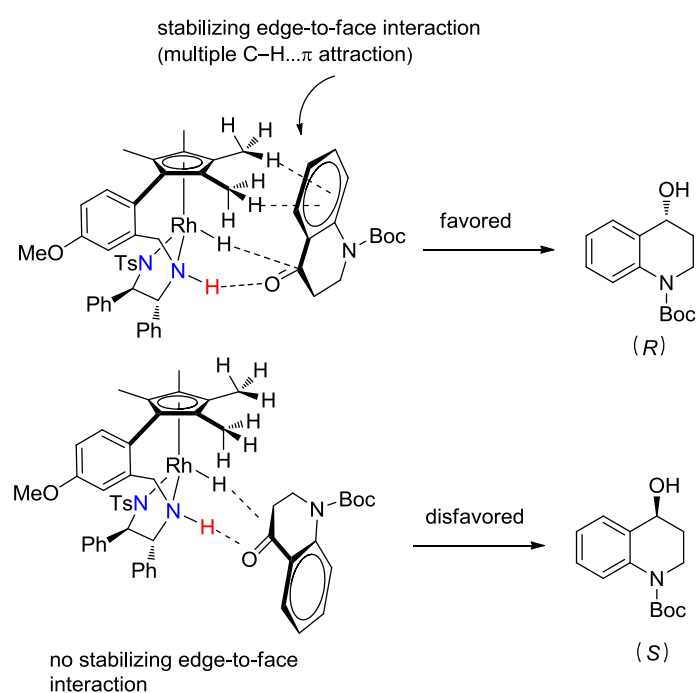
Based on previous studies,<sup>63</sup> a plausible mechanism for this reduction is given below (Scheme 132). The oxidation state of the rhodium does not change during the catalytic cycle and the 4-quinolone is reduced within the outer-sphere, without preliminary substrate coordination. First, a chiral unsaturated 16-electron amido rhodium complex **II** is formed by elimination of HCl from complex **I**. Then, the rhodium complex **II** readily reacts with HCOOH to give the corresponding formate complex **III**, which subsequently undergoes decarboxylation leading to the chiral hydrido-amine complex **IV** and CO<sub>2</sub>. This chiral hydrido rhodium complex **IV** readily reacts with the enone **1a** to provide of the C=C bond and regeneration of the amide complex **II**. The corresponding saturated ketone after reduction through transition state **V** showing N–H···O hydrogen-bonding interaction, Rh–H···C interaction, and C–H···π interaction between Cp\* ring and ketone aryl substituent. The resulting saturated ketone then react with complex **IV** to provide the optically active alcohol with regeneration of the amide complex **II** through transition state **VI**.



Scheme 132

### 1.2.10 Origin of enantioselectivity

Based on the configurations of hydrogenation products and the reported mechanism of rhodium catalyzed asymmetric hydrogenation reactions,<sup>210, 211</sup> the possible transition states for this ATH reaction are shown in Scheme 133. A well-established favorable edge-to-face interaction between the  $\eta^5$ -arene ligand and the aryl moiety of the 4-quinolone serves to stabilize the transition state. The transition state giving the *R* alcohol is energetically more favored than the one leading to the *S* alcohol because of the stabilizing edge-to-face interaction.



Scheme 133

### 1.3 Conclusion

In summary, we have demonstrated the ability of the in-house developed Rh(III)-complex **C86** to efficiently perform the operationally simple and practical asymmetric transfer hydrogenation of 4-quinolone derivatives. This reaction enables a straightforward access to the corresponding enantiomerically enriched alcohols with excellent levels of enantioselectivity (up to >99% ee). The reaction proceeds under mild conditions using

<sup>210</sup> Gridnev, I. D.; Yasutake, M.; Higashi, N. *J. Am. Chem. Soc.* **2001**, *123*, 5268.

<sup>211</sup> Gridnev, I. D.; Higashi, N.; Asakura, K.; Imamoto, T. *J. Am. Chem. Soc.* **2000**, *122*, 7183.



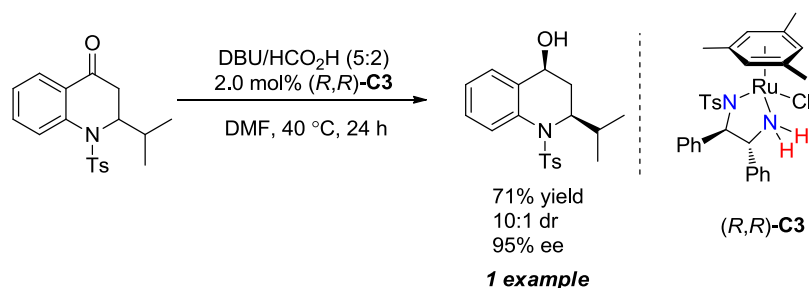
HCO<sub>2</sub>H/Et<sub>3</sub>N (5:2) as the hydrogen source. The efficient gram-scale asymmetric transfer hydrogenation of compound **4a** accounts for the usefulness of this method and furthermore, the various chiral alcohols **5** can be readily functionalized to access diversely substituted 1,2,3,4-tetrahydroquinoline-4-ol derivatives.<sup>241</sup>

## 2. Rhodium-Catalyzed Asymmetric Transfer Hydrogenation of 2-aryl-2,3-dihydroquinolin-4(1H)-one Derivatives

### 2.1 Introduction

As mentioned in the previous chapter, chiral benzylic alcohols are important building blocks for the synthesis of chemical materials, pharmaceuticals, and agrochemicals. Consequently, enantiopure 2-substituted tetrahydroquinolin-4-ols with two stereocentres are attractive targets due to their promising biological activities and wide-range use as synthetic intermediates for drug candidates (Figure 1).<sup>203</sup>

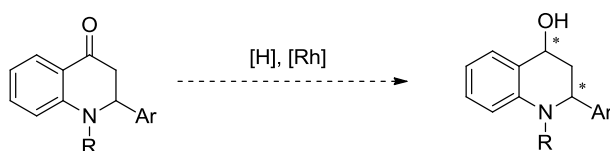
To the best of our knowledge, a single example to access such enantiomerically enriched 2-substituted tetrahydroquinolin-4-ol by using asymmetric transfer hydrogenation was reported. In 2017, Ruck *et al.* developed the ruthenium(II)-catalyzed asymmetric transfer hydrogenation of heterocyclic ketones with DBU and formic acid as hydrogen donor through dynamic kinetic resolution (Scheme 134).<sup>212</sup> Their conditions are suitable for 2-isopropyl-1-tosyl-2,3-dihydroquinolin-4(1H)-one as well. By using 2.0 mol% of the ruthenium complex **C3** with 5.0 equiv DBU/formic acid (5:2) at 40 °C in DMF, 2-isopropyl-1-tosyl-tetrahydroquinolin-4-ol was prepared in 71% yield with 10:1 diastereoselectivity and 95% enantioselectivity.



**Scheme 134**

*In this context, our project was focused on the asymmetric reduction of 2-aryl-2,3-dihydroquinolin-4(1H)-one derivatives (Scheme 135).*

<sup>212</sup> Ashley, E. R.; Sherer, E. C.; Pio, B.; Orr, R. K.; Ruck, R. T. *ACS Catal.* **2017**, *7*, 1446-1451.



Scheme 135

## 2.2 Results and discussion

### 2.2.1 Synthesis of 2-aryl-2,3-dihydroquinolin-4(1H)-ones

2-Aryl-2,3-dihydroquinolin-4(1H)-ones **10a-s** required for this study were prepared in two steps according to reported procedures.<sup>213</sup> The first step involved the reaction of 2-aminoacetophenone with benzaldehyde derivatives and proceeded in 99% conversion. After evaporation of the solvent, the crude intermediate products were submitted to the next step without further purification. With the assistance of  $\text{ZnCl}_2$ , the intermediate products cyclized to form the target substrates. 2-Aryl-2,3-dihydroquinolin-4(1H)-ones **10a-s** containing electron-donating and withdrawing groups on the aryl cores were synthesized in yields ranging from 35% to 77% (Figure 3).

<sup>213</sup> (a) Wang, J. F.; Liao, Y. X.; Kuo, P. Y.; Gau, Y. H.; Yang, D.Y. *Synlett*. **2006**, 17, 2791; (b) Lee, J. I.; Jung, H. J. *J. Korean. Chem. Soc.* **2007**, 51, 106.

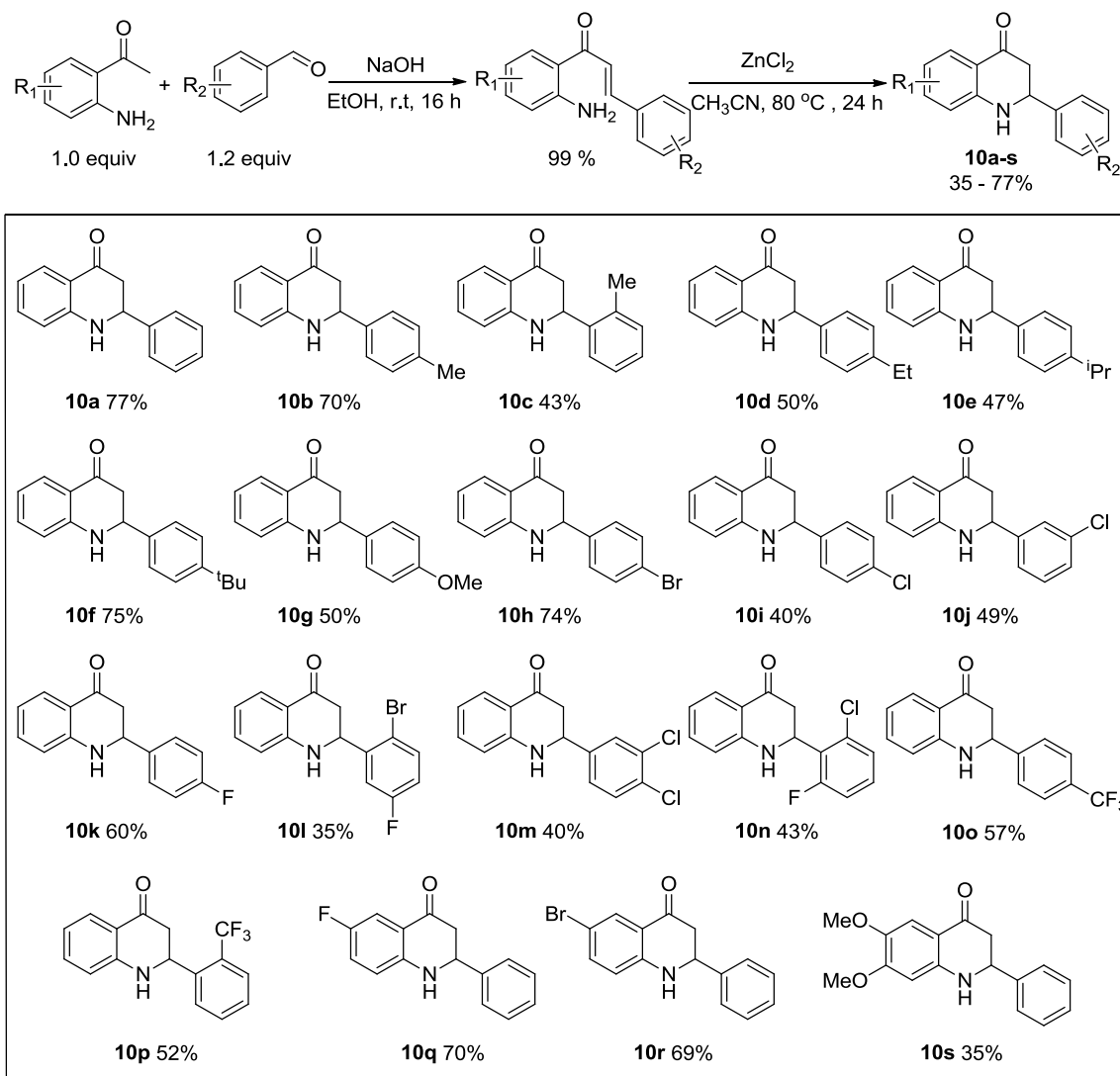


Figure 3. Preparation of 2-aryl-2,3-dihydroquinolin-4(1H)-ones

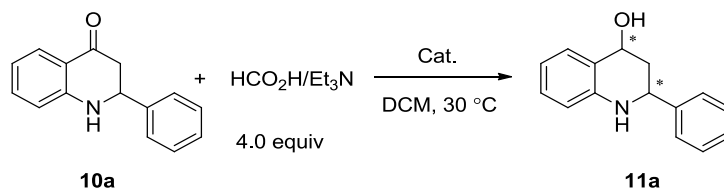
## 2.2.2 Optimisation of the reaction conditions with 2-phenyl-2,3-dihydroquinolin-4(1H)-one

### 2.2.2.1 Influence of the precatalyst

Our investigation of the ATH of 2-aryl-2,3-dihydroquinolin-4(1H)-ones began with 2-phenyl-2,3-dihydroquinolin-4(1H)-one **10a** as the standard substrate to optimize the reaction parameters. We first examined the ATH with the home-made Rh-complexes **C86-C89** in CH<sub>2</sub>Cl<sub>2</sub> at 30 °C with HCO<sub>2</sub>H/Et<sub>3</sub>N (5:2) azeotropic mixture as the hydrogen source. Under these conditions, the expected alcohol **11a** was obtained in 41-57% isolated yields (Table 9, entries 1–4) and Rh-complex **C86** was selected as the catalyst for this reaction because it led

to the best yield (57%) and enantioselectivity (94% ee) with a good diastereoselectivity (87% de) (Table 9, entry 1).

**Table 9 Screening of precatalysts for the ATH of 10a<sup>a</sup>**



Entry	Cat.	Solvent	yield <sup>[b]</sup> (%)	de <sup>[c]</sup> (%)	ee <sup>[d]</sup> (%)	
1		<b>C86</b>	CH <sub>2</sub> Cl <sub>2</sub>	57	87	94
2		<b>C87</b>	CH <sub>2</sub> Cl <sub>2</sub>	46	43	93
3		<b>C88</b>	CH <sub>2</sub> Cl <sub>2</sub>	41	73	92
4		<b>C89</b>	CH <sub>2</sub> Cl <sub>2</sub>	49	89	93

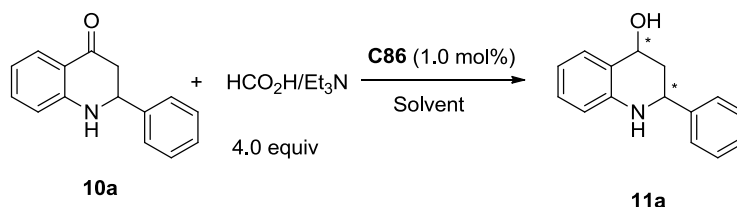
<sup>a</sup> Reaction conditions: **10a** (0.4 mmol), catalyst (1.0 mol%), HCO<sub>2</sub>H/Et<sub>3</sub>N (5:2) (136  $\mu$ L, 4.0 equiv), CH<sub>2</sub>Cl<sub>2</sub> (1.0 mL), 30 °C. <sup>b</sup> Isolated yields. <sup>c</sup> Determined by crude <sup>1</sup>H NMR. <sup>d</sup> Determined by SFC analysis using a chiral stationary phase.

### 2.2.2.2 Influence of the solvent

Pursuing the study with the selected tethered rhodium complex **C86**, we investigated the influence of the solvent and increased the reaction temperature to 50 °C to increase the yield (Table 10). Similar yield but with a low diastereoselectivity was obtained both in CH<sub>2</sub>Cl<sub>2</sub> and CH<sub>3</sub>OH (87% de, 8% de respectively) (Table 10, entries 1-2). CH<sub>3</sub>CN and DMF

gave the same excellent diastereoselectivities and enantioselectivities (Table 10, entries 3-4). Finally the use of THF led to 41% yield with 83% de and 99% ee (Table 10, entry 5).

**Table 10 Screening of solvents for the ATH of 10a<sup>a</sup>**



Entry	Solvent	yield <sup>[b]</sup> (%)	de <sup>[c]</sup> (%)	ee <sup>[d]</sup> (%)
1	CH <sub>2</sub> Cl <sub>2</sub>	57	87	94
2	CH <sub>3</sub> OH	56	8	99
3	CH <sub>3</sub> CN	51	99	99
4	DMF	36	99	99
5	THF	41	83	99

<sup>a</sup> Reaction conditions: **10a** (0.4 mmol), **C86** (1.0 mol%), HCO<sub>2</sub>H/Et<sub>3</sub>N (5:2) (136  $\mu$ L, 4.0 equiv), solvent (1.0 mL), 50  $^{\circ}$ C. <sup>b</sup> Isolated yields. <sup>c</sup> Determined by crude <sup>1</sup>H NMR. <sup>d</sup> Determined by SFC analysis using a chiral stationary phase.

From the results above, we envisage the reaction to proceed through a kinetic resolution. Therefore, for reactions giving the reduced product with a yield >50%, we measured the ee of the remaining starting material and found it to be 99% confirming the kinetic resolution process. Of note, the ATH product was found to be unstable during the purification by silica gel flash column. Consequently, we decided to protect the *N*-atom to optimize the reaction conditions.

### 2.2.3 Synthesis of 1-acetyl-2-aryl-2,3-dihydroquinolin-4(1H)-one derivatives

The 1-acetyl-2-aryl-2,3-dihydroquinolin-4(1H)-one derivatives **12** were prepared using established methods.<sup>214</sup> Compound **10** were dissolved in AcOH/Ac<sub>2</sub>O (1:1) and refluxed for 2 h to afford the desired substrates **12**. 1-Acetyl-2-aryl-2,3-dihydroquinolin-4(1H)-ones **12a-o** and **12q-t** substituted with both electron-donating and withdrawing groups were synthesized

<sup>214</sup> Singh, O.; Muthukrishnan, M.; Sundaravedivelu, M. *Synth. Commun.* **2006**, *36*, 943-950.

in isolated yields ranging from 35% to 88% (Figure 4). Compound **10p** (Figure 3) failed to afford the corresponding product **12p** under these conditions.

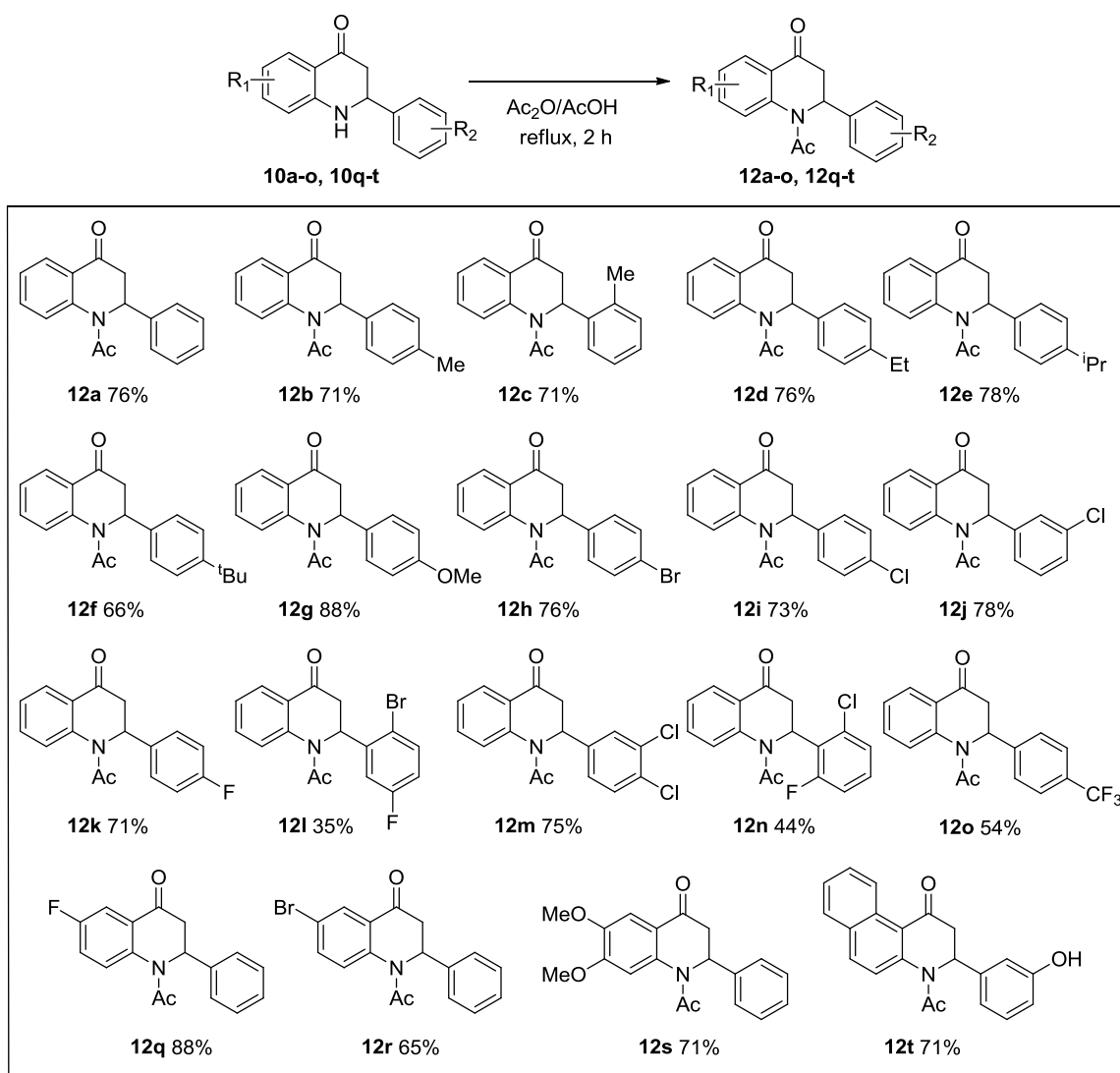


Figure 4. Preparation of 1-acetyl-2-aryl-2,3-dihydroquinolin-4(1H)-ones

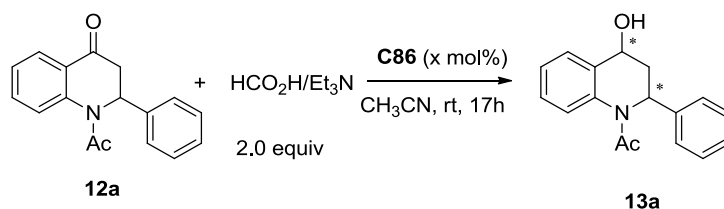
## 2.2.4 Optimisation of the reaction conditions with 1-acetyl-2-phenyl-2,3-dihydroquinolin-4(1H)-one

### 2.2.4.1 Influence of the catalyst loading

Rh-complex **C86** was selected because of its good catalytic performances for the ATH of 1-acetyl-2-phenyl-2,3-dihydroquinolin-4(1H)-one. The catalyst loading was varied from 0.01 mol% to 1 mol% using HCO<sub>2</sub>H/Et<sub>3</sub>N (5:2) azeotropic mixture as hydrogen donor in

acetonitrile. Table 11 shows that the reaction led to product **13a** with excellent diastereoselectivities (> 99%) in all cases except when 0.01 mol% of **C86** was used, for which no conversion was observed. With 1.0 mol% or 0.5 mol% of Rh-complex **C86**, we obtained more than 50% yields but not perfect enantioselectivities (Table 11, entries 1, 2). Reducing the catalyst loading to 0.1 mol% led to a lower yield of 29% but an excellent enantioselectivity of 99% ee (Table 11, entry 3). The use of 0.05 mol% of **C86** resulted in 15% yield with 99% ee (Table 11, entry 4), whereas 0.01 mol% of **C86** led to no conversion (Table 11, entry 5). From this study we chose to use a catalyst loading of 0.1 mol% for the next experiments.

**Table 11 Screening of catalyst loading<sup>a</sup>**



Entry	<b>C86</b> (x mol %)	yield <sup>[b]</sup> (%)	de <sup>[c]</sup> (%)	ee <sup>[d]</sup> (%)
1	1.0	56	>99	89
2	0.5	53	>99	96
3	0.1	29	>99	99
4	0.05	15	>99	99
5	0.01	0	--	--

<sup>a</sup> Reaction conditions: **12a** (0.4 mmol), **C86** (x mol%), HCO<sub>2</sub>H/Et<sub>3</sub>N (5:2) (68 μL, 2.0 equiv), CH<sub>3</sub>CN (1.0 mL), 30 °C. <sup>b</sup> Isolated yields. <sup>c</sup> Determined by crude <sup>1</sup>H NMR. <sup>d</sup> Determined by SFC analysis using a chiral stationary phase.

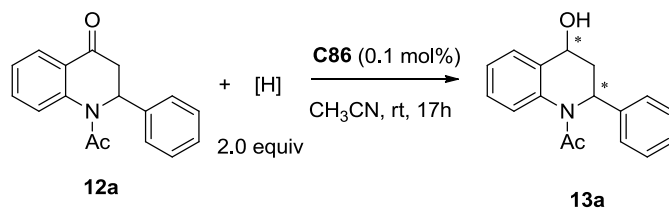
#### 2.2.4.2 Influence of the hydrogen source

Besides the HCO<sub>2</sub>H/Et<sub>3</sub>N (5:2) azeotropic mixture as hydrogen donor, we tried several other hydrogen sources shown in table 12 as well. The study was carried out with 0.1 mol% of **C86** as catalyst, CH<sub>3</sub>CN as solvent and a reaction time of 17 h. We obtained the best yield (50%), diastereoselectivity (>99% de) and enantioselectivity (99% ee) when HCOOH/DABCO (2:1) was used as hydrogen donor (Table 12, entry 2). We also tested HCOOH/DBU (2:1) which afforded 45% yield (Table 12, entry 3). Then we screened formates such as ammonium, sodium and calcium formates (Table 12, entries 4-6).



Ammonium and sodium formates led respectively to 20% and 37% yield, although calcium formate led to no conversion. Finally, we tested formic acid alone without a base, which gave no conversion neither (Table 12, entry 7). On the basis of the above screening, the optimized conditions were set as follows: **C86** (0.1 mol %) as the precatalyst, HCO<sub>2</sub>H/DABCO(2:1) (2.0 equiv) as the hydrogen donor, CH<sub>3</sub>CN (0.4 M) at room temperature.

**Table 12 Screening of hydrogen source <sup>a</sup>**

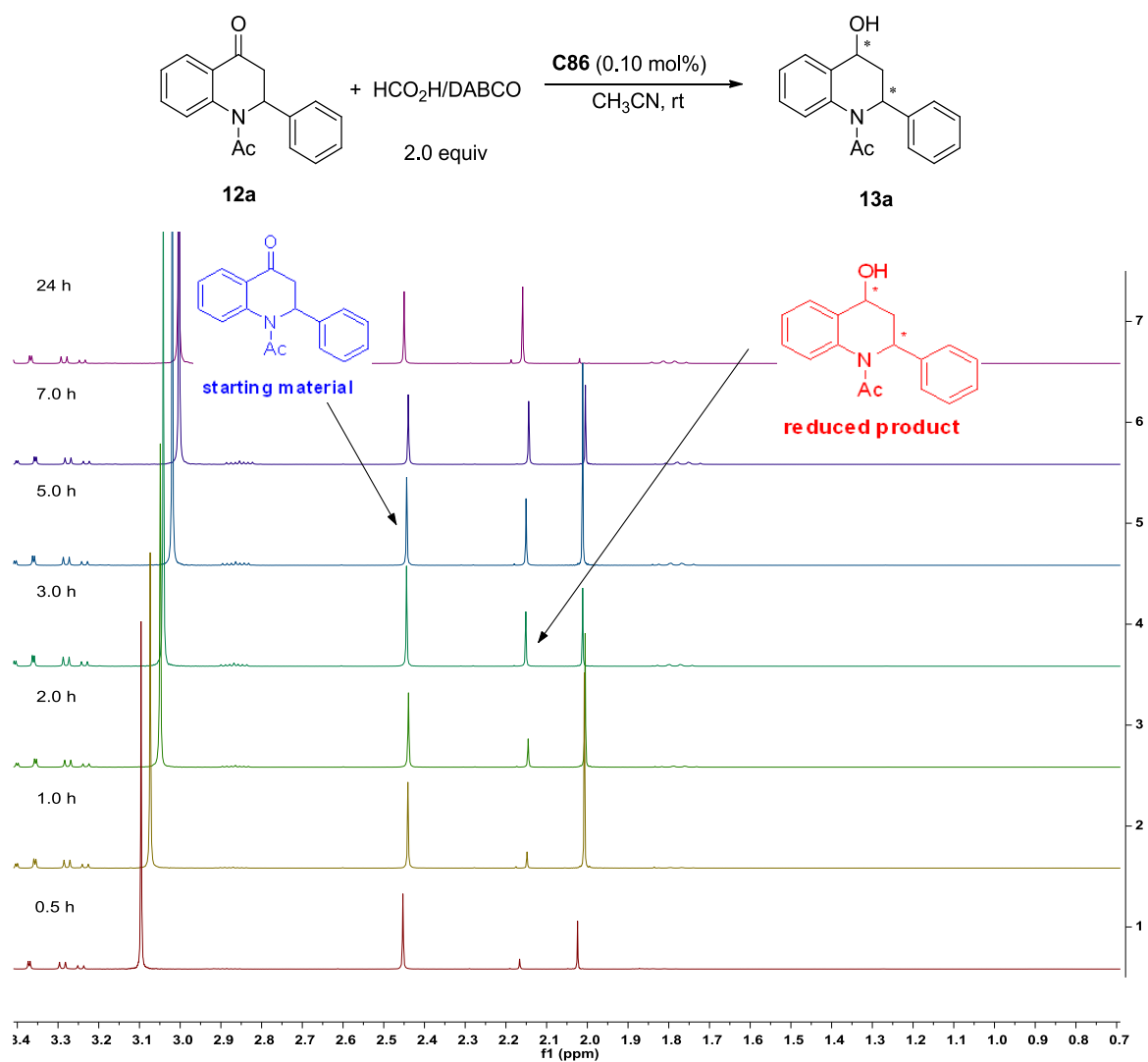


Entry	hydrogen source	yield <sup>[b]</sup> (%)	de <sup>[c]</sup> (%)	ee <sup>[d]</sup> (%)
1	HCO <sub>2</sub> H/Et <sub>3</sub> N(5:2) (2.0 eq)	29	>99	99
2	HCO <sub>2</sub> H/DABCO(2:1) (2.0 eq)	50	>99	99
3	HCO <sub>2</sub> H/DBU(2:1) (2.0 eq)	45	>99	96
4	HCOONH <sub>4</sub> (2.0 eq)	20	>99	99
5	HCOONa (2.0 eq)	37	>99	99
6	(HCOO) <sub>2</sub> Ca (1.0 eq)	0	--	--
7	HCOOH (2.0 eq)	0	--	--

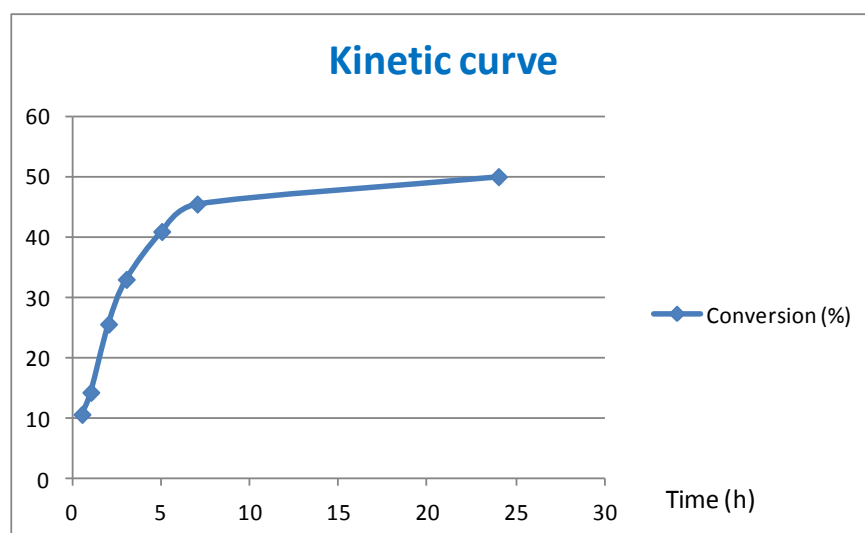
<sup>a</sup> Reaction conditions: **12a** (0.4 mmol), **C86** (0.1 mol%), [H] (2.0 equiv), CH<sub>3</sub>CN (1.0 mL), 30 °C. <sup>b</sup> Isolated yields. <sup>c</sup> Determined by crude <sup>1</sup>H NMR. <sup>d</sup> Determined by SFC analysis using a chiral stationary phase.

### 2.2.5 Kinetic experiment

To better understand the reaction process, we performed monitoring studies of the Rh-catalyzed asymmetric transfer hydrogenation of **12a** under the optimized conditions. We monitored the reaction by <sup>1</sup>H NMR and calculated the ratio between starting material and reduced products by the integration of the proton on the *N*-Ac of each compound (Figure 5a). As we can see from the curve, the reaction rate was fast in the beginning and decreased after a reaction time of 7 h. After 24 h, the conversion reached 50% (Figure 5b).



**a**



**b**

**Figure 5. kinetic experiment**

## 2.2.6 Substrate scope

### 2.2.6.1 ATH of substrates bearing electron-donating substituents

With these optimized reaction conditions, the scope of the kinetic resolution of a series of variously substituted 2-aryl-2,3-dihydroquinolin-4(1H)-one derivatives (**12b-s**) by Rh-catalyzed ATH was evaluated. As shown in Table 13, we first studied the ATH of substrates **12b-g** and **12s** bearing electron-donating substituents on the aromatic ring. Compounds bearing methyl, ethyl, isopropyl, tert-butyl and methoxy substituents on the different benzene core positions afforded the desired products (**13**) in good yields (48- 51%) with excellent enantiomeric excesses (95- > 99%). Compounds **12'** were obtained in 47-49% yields and 93- > 99% enantioselectivities. The absolute configurations of compounds **12a'**, **g'**, **h'**, **k'**, **o'** were attributed by comparison of their optical rotation values with those reported in the literature. By analogy, we conjectured that the remainder of the products **12'** followed the same trend.

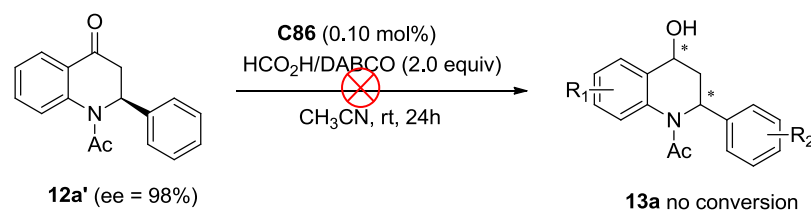
**Table 13** ATH of substrates bearing electron-donating substituents<sup>a</sup>

Entry	S	Time (h)	<b>12'</b> (NO.)	yield (%) <sup>e</sup>	ee (%) <sup>f</sup>	<b>13</b> (NO.)	yield (%) <sup>e</sup>	ee (%) <sup>f</sup>
1 <sup>b</sup>	<b>12a</b>	17		48	98		50	>99
2 <sup>b</sup>	<b>12b</b>	48		49	99		50	99

3 <sup>c</sup>	<b>12c</b>	17		49	>99		51	95
4 <sup>d</sup>	<b>12d</b>	17		47	>99		51	96
5 <sup>d</sup>	<b>12e</b>	17		49	>99		50	96
6 <sup>b</sup>	<b>12f</b>	48		49	>99		48	99
7 <sup>c</sup>	<b>12g</b>	17		49	>99		51	97
8 <sup>c</sup>	<b>12s</b>	17		48	93		48	>99

<sup>a</sup> Reaction conditions: **12** (0.4 mmol), **C86** (0.1-0.2 mol%), HCO<sub>2</sub>H/DABCO (2:1) (2.0 equiv), CH<sub>3</sub>CN (1.0 mL), rt. <sup>b</sup> **C86** (0.1 mol%). <sup>c</sup> **C86** (0.15 mol%). <sup>d</sup> **C86** (0.2 mol%). <sup>e</sup> Isolated yields. <sup>f</sup> Determined by SFC analysis using a chiral stationary phase.

When the ATH conditions were applied to the enantiomerically enriched ketone **12a'**, no conversion was observed after a reaction time of 24 h which demonstrated the efficiency of the kinetic resolution (Scheme 136).

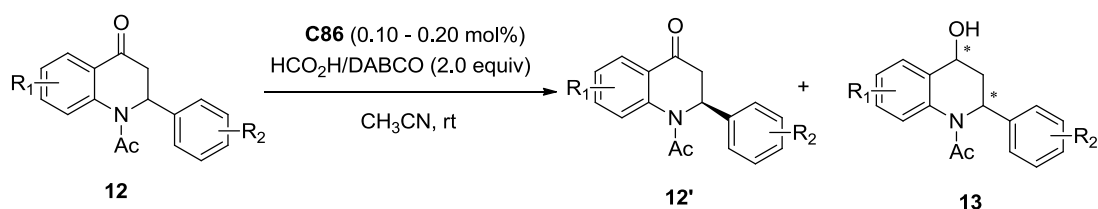


Scheme 136

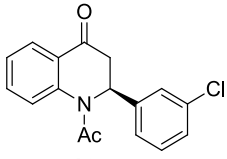
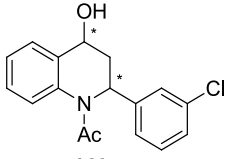
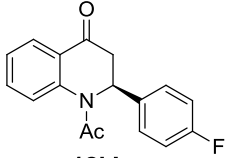
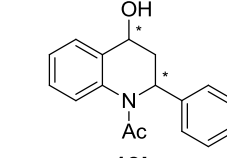
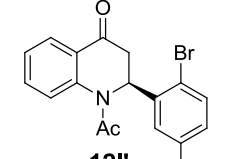
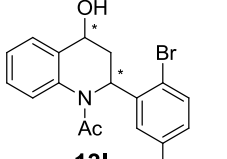
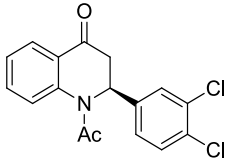
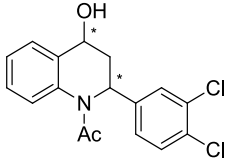
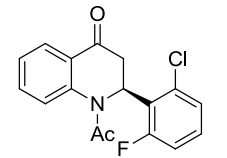
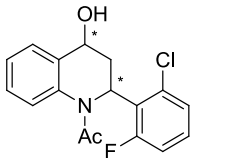
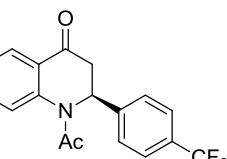
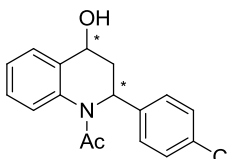
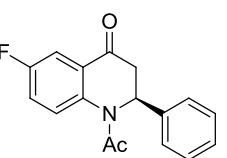
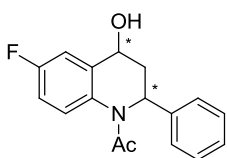
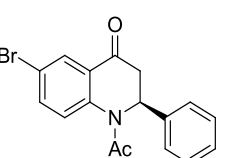
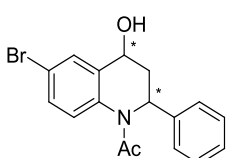
### 2.2.6.2 ATH of substrates bearing electron-withdrawing substituents<sup>a</sup>

As for electron-withdrawing groups, the ATH reaction was amenable under the standard conditions to halogen substitution such as bromine, chlorine and fluorine, as well as a trifluoromethyl substituent. They displayed good yields (up to 52%) with excellent enantioselectivities (up to > 99% ee) as well (Table 14, entries 1–9). For the substrate **12r**, we still observed > 99% enantioselectivity but 41% isolated yield of **13r**, whereas substrate **12r'** was obtained in 58% yield with 71% enantioselectivity (Table 14, entries 10). 44–50% yields with 98–> 99% ee were obtained for the remaining compound **12'**. We are currently working on the determination of the absolute configuration of products **12'** and **13**.

**Table 14** ATH of substrates bearing electron-withdrawing substituents



Entry	S	Time (h)	<b>12'</b> (NO.)	yield (%) <sup>e</sup>	ee (%) <sup>f</sup>	<b>13</b> (NO.)	yield (%) <sup>e</sup>	ee (%) <sup>f</sup>
1 <sup>c</sup>	<b>12h</b>	17		50	>99		50	98
2 <sup>c</sup>	<b>12i</b>	17		48	>99		50	97

3 <sup>c</sup>	<b>12j</b>	17		48	>99		51	96
			<b>12j'</b>			<b>13j</b>		
4 <sup>c</sup>	<b>12k</b>	24		49	98		51	97
			<b>12k'</b>			<b>13k</b>		
5 <sup>b</sup>	<b>12l</b>	17		46	>99		48	93
			<b>12l'</b>			<b>13l</b>		
6 <sup>c</sup>	<b>12m</b>	7		49	>99		51	96
			<b>12m'</b>			<b>13m</b>		
7 <sup>b</sup>	<b>12n</b>	7		44	>99		52	86
			<b>12n'</b>			<b>13n</b>		
8 <sup>c</sup>	<b>12o</b>	17		49	>99		49	96
			<b>12o'</b>			<b>13o</b>		
9 <sup>b</sup>	<b>12q</b>	48		48	99		50	97
			<b>12q'</b>			<b>13q</b>		
10 <sup>b</sup>	<b>12r</b>	48		58	71		41	>99
			<b>12r'</b>			<b>13r</b>		

<sup>a</sup> Reaction conditions: **12** (0.4 mmol), **C86** (0.1-0.2 mol%), HCO<sub>2</sub>H/DABCO (2:1) (2.0 equiv), CH<sub>3</sub>CN (1.0

mL), rt. <sup>b</sup> **C86** (0.1 mol%). <sup>c</sup> **C86** (0.15 mol%). <sup>d</sup> **C86** (0.2 mol%). <sup>e</sup> Isolated yields. <sup>f</sup> Determined by SFC analysis using a chiral stationary phase. <sup>g</sup> dr = 98.5:1.5

## 2.2.7 Kinetic resolution selectivity factor

The most commonly applied metric to assess the efficiency of a given kinetic resolution reaction is the selectivity factor (*s*). It is usually conveniently calculated using the reaction conversion (*c*) and the % enantiomeric excess (*ee*) of either the recovered substrate or the reaction product (eq. (1) or eq. (2), respectively) as originally outlined by Sih and co-workers<sup>215</sup> for enzymatic KRs, and Kagan and Fiaud<sup>216</sup> for general cases<sup>217</sup> (Scheme 137). In our case, we applied equation 1 to calculate the selectivity factors. From table 15, we can conclude that all the substrates gave high selectivity factors ranging from 145 to 1057, except in the case of **12n** which resulted in only 69 selectivity factor (Table 15, entry 14).

$$S = \frac{\ln[(1-C)(1-ee_{\text{substrate}})]}{\ln[(1-C)(1+ee_{\text{substrate}})]} \quad [1] \quad S = \frac{\ln[(1-C)(1+ee_{\text{product}})]}{\ln[(1-C)(1-ee_{\text{product}})]} \quad [2]$$

Scheme 137

Table 15 Selectivity factor for the ATH/KR

Entry	substrate	Selectivity factor
1	<b>12a</b>	922
2	<b>12b</b>	1057
3	<b>12c</b>	206
4	<b>12d</b>	259
5	<b>12e</b>	259
6	<b>12f</b>	1057
7	<b>12g</b>	348
8	<b>12h</b>	525
9	<b>12i</b>	348

<sup>215</sup> Chen, C.S.; Fujimoto, Y.; Girdaukas, G.; Sih, C. J. *J. Am. Chem. Soc.* **1982**, *104*, 7294.

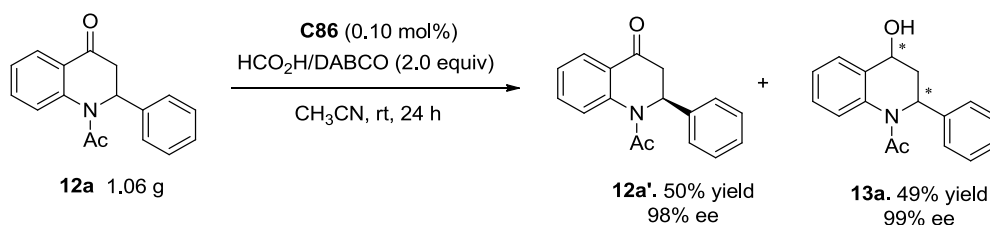
<sup>216</sup> Kagan, H.B.; Fiaud, J.-C.; *Topics in Stereochemistry*, **1988**, *18*, 249.

<sup>217</sup> Gawley, R.E. *J. Org. Chem.* **2006**, *71*, 2411.

10	<b>12j</b>	259
11	<b>12k</b>	303
12	<b>12l</b>	145
13	<b>12m</b>	259
14	<b>12n</b>	69
15	<b>12o</b>	259
16	<b>12q</b>	348
17	<b>12r</b>	425
18	<b>12s</b>	684

### 2.2.8 Scale-up experiment

The efficiency of this ATH was supported by a scale-up experiment. Under the standard conditions, a gram-scale reduction of **12a** delivered the desired product **13a** in 49% isolated yield with high enantioselectivity (99% ee), whereas **12a'** was obtained in 50% yield with 98% ee (Scheme 138).



Scheme 138

## 2.3 Conclusion

In summary, we have demonstrated the high catalytic efficiency of the in-house developed Rh(III)-complex **C86** in the operationally simple and practical asymmetric transfer hydrogenation of 2-aryl-2,3-dihydroquinolin-4(1H)-one derivatives through kinetic resolution. This reaction enables a straightforward access to the corresponding enantiomerically enriched 2-aryl-2,3-dihydroquinolin-4(1H)-ones with excellent levels of enantioselectivity (up to >99% ee) as well as the corresponding enantiomerically enriched alcohol products (up to >99% ee). The reaction proceeds under mild conditions at room temperature using HCO<sub>2</sub>H/DABCO (2:1)



as the hydrogen source. The efficient gram-scale asymmetric transfer hydrogenation of compound **12a** accounts for the usefulness of this method.

### 3. Rh-Mediated Asymmetric Transfer Hydrogenation of 3-Substituted Chromones: an Efficient Route to Enantioenriched cis 3-Hydroxymethyl Chroman-4-ol Derivatives through Dynamic Kinetic Resolution

#### 3.1 Introduction

##### 3.1.1 Biological interest of chromanoid and flavanoid derivatives

Chromanoids and flavanoids differ by the nature of the substituent on the oxygen heterocycle part (either alkyl or aryl substituent, respectively) and can be divided into different classes of compounds, such as chromones, flavones, chromanones, flavanones, chromanols, flavanols. They are found in a number of natural products and serve as key structural motifs thanks to their pharmacological and biological activities including antitumoral, antibacterial, antioxidant or antiestrogenic properties (Figure 6).<sup>218</sup> As such, identification of economical routes to access such compounds is highly desirable.

---

<sup>218</sup> (a) Ellis, G. P. *Chromenes, Chromanones, and Chromones*, Wiley, New York, **1977**. (b) Horton, D. A.; Bourne, G. T.; Smythe, M. L. *Chem. Rev.* **2003**, *103*, 893. (c) Gaspar, A.; Matos, M. J.; Garrido, J.; Uriarte, E.; Borges, F. *Chem. Rev.* **2014**, *114*, 4960. (d) Chandler, I. M.; McIntyre, C. R.; Simpson, T. J. *J. Chem. Soc. Perkin Trans. 1* **1992**, 2285. (e) Maiti, A.; Cuendet, M.; Croy, V. L.; Endringer, D. C.; Pezzuto, J. M.; Cushman, M. *J. Med. Chem.* **2007**, *50*, 2799. (f) Zhao, Z.; Ruan, J.; Jin, J.; Zou, J.; Zhou, D.; Fang, W.; Zeng, F. *J. Nat. Prod.* **2006**, *69*, 265. (g) Albrecht, U.; Lalk, M.; Langer, P. *Bioorg. Med. Chem.* **2005**, *13*, 1531. (h) Farmer, R. L.; Biddle, M. M.; Nibbs, A. E.; Huang, X.; Bergan, R. C.; Scheidt, K. A. *ACS Med. Chem. Lett.* **2010**, *1*, 400. (i) Picker, K.; Ritchie, E.; Taylor, W. C. *Aust. J. Chem.* **1976**, *29*, 2023; (j) Christopher, A.; Hu, Q.-Y.; Michael, K. G.; Julien, P. WO2008076336A2, **2008**; (k) Lommen, V.; Eugene, G. R.; William, L.; Gestel, R. V.; Elisabetha, J. F. EP0234656 A2, **1987**; (l) Pirotte, B.; Florence, X.; Goffin, E.; Lebrun, P. *ChemMedChem*, **2017**, *12*, 1810.

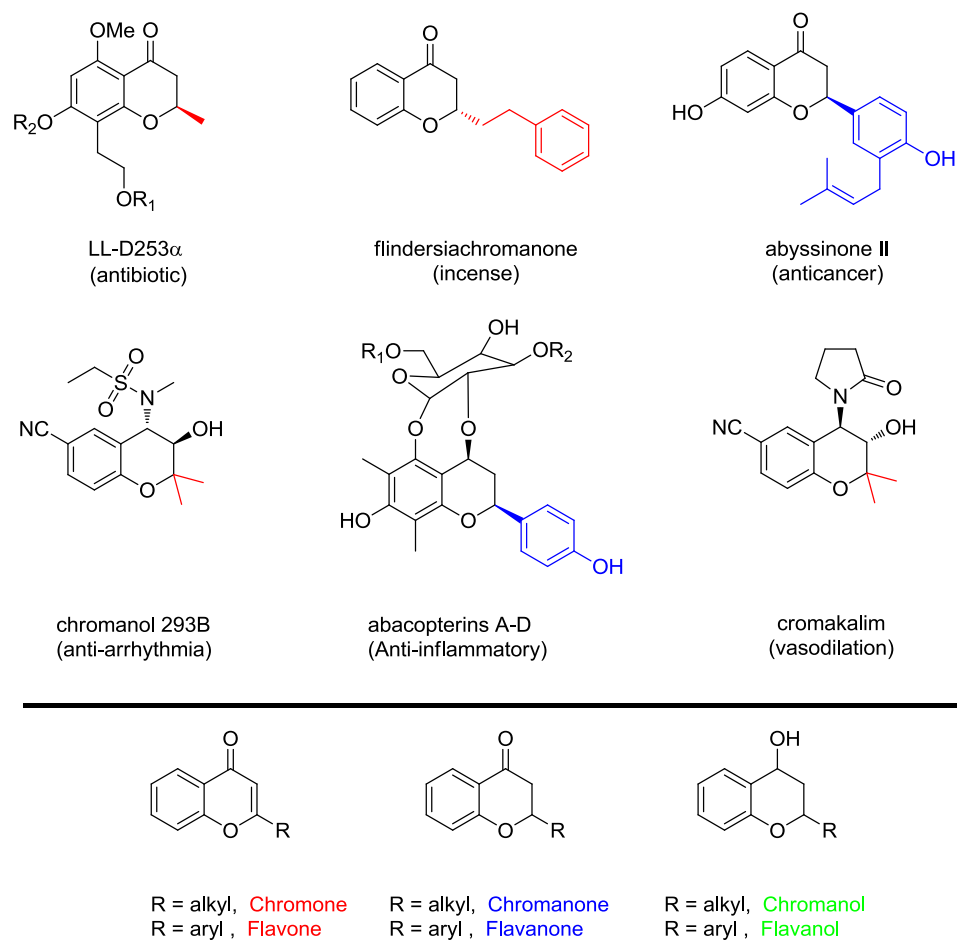
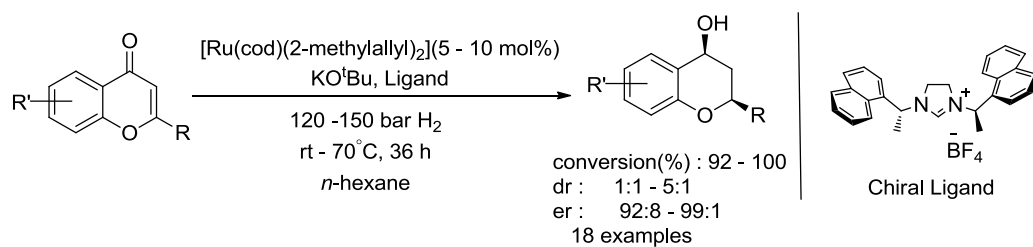


Figure 6

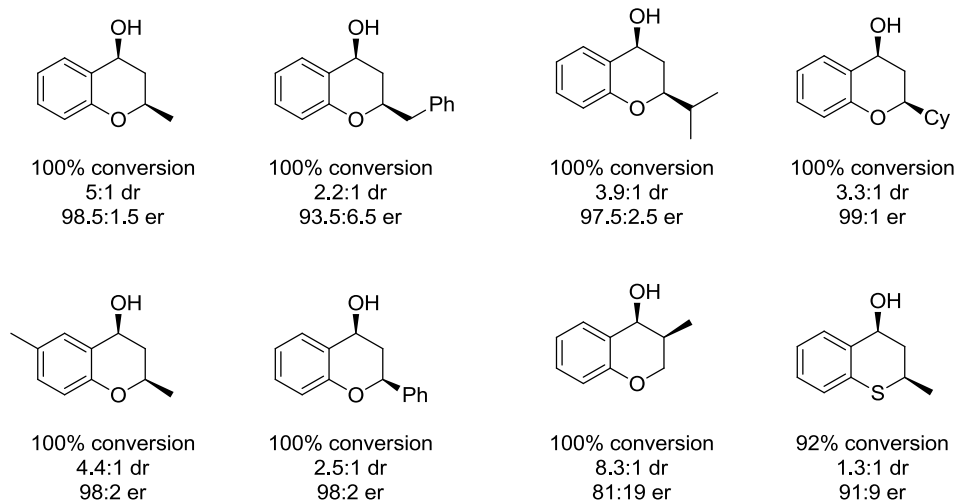
### 3.1.2 Different synthetic pathways to enantiomerically enriched chromanols and flavanols

Current methodologies mainly afford chiral chromanols and flavanols through the asymmetric (transfer) hydrogenation of chromones, chromanones, flavones or flavanones. In 2013, Glorius group developed an asymmetric hydrogenation of 2-substituted flavones and chromones using a chiral ruthenium–NHC complex, leading to the formation of chiral chromanols and flavanols.<sup>219</sup> Complete conversion and good enantioselectivities (up to 96% ee), but low diastereoselectivities were obtained under high hydrogen pressure (120–150 bar) (Scheme 139).

<sup>219</sup> Zhao, D.; Beiring, B.; Glorius, F. *Angew. Chem., Int. Ed.* **2013**, *52*, 8454.



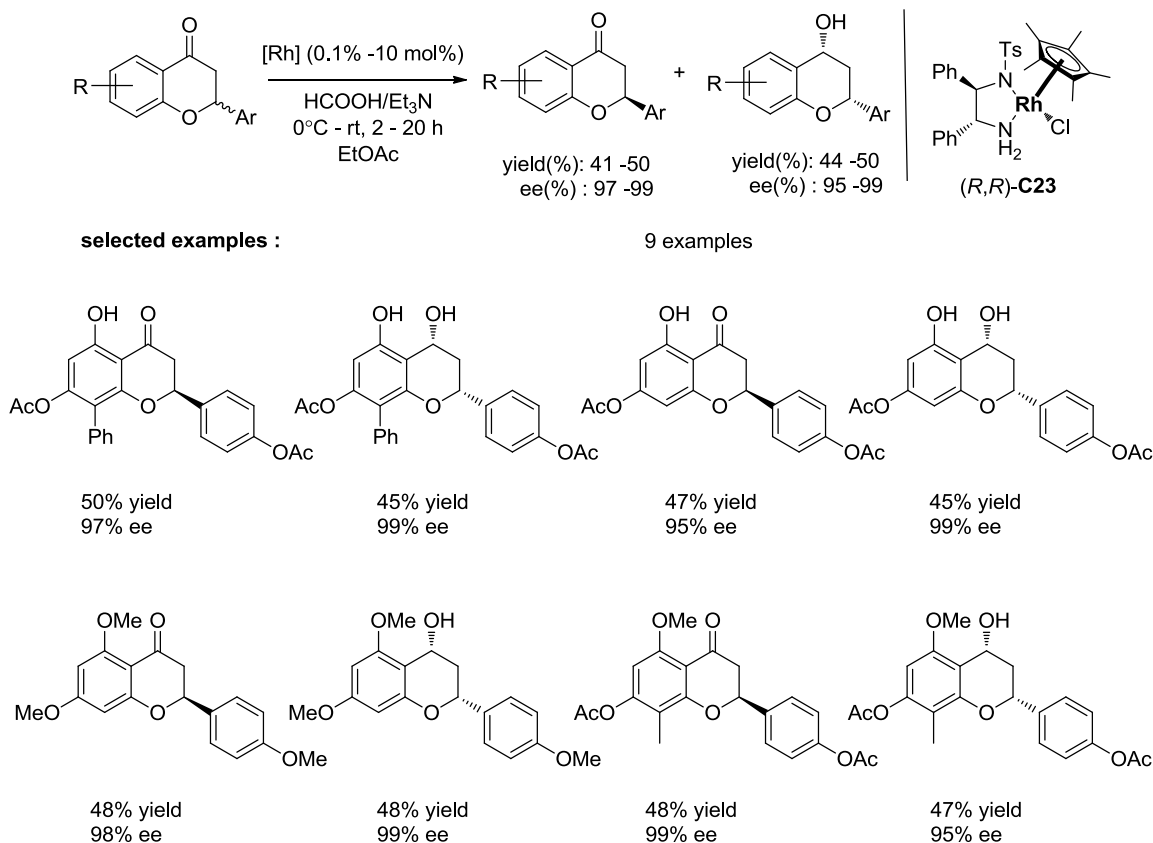
selected examples:



Scheme 139

The same year, Metz *et al.* reported a kinetic resolution of racemic flavanones through Rh(III)-catalyzed asymmetric transfer hydrogenation, using  $Et_3N/HCO_2H$  (3.6:1) as hydrogen donor and ethyl acetate as solvent. The reaction produced chiral flavanones and flavanols in high yields and with excellent enantioselectivities (up to 99% ee)<sup>220</sup> (Scheme 140).

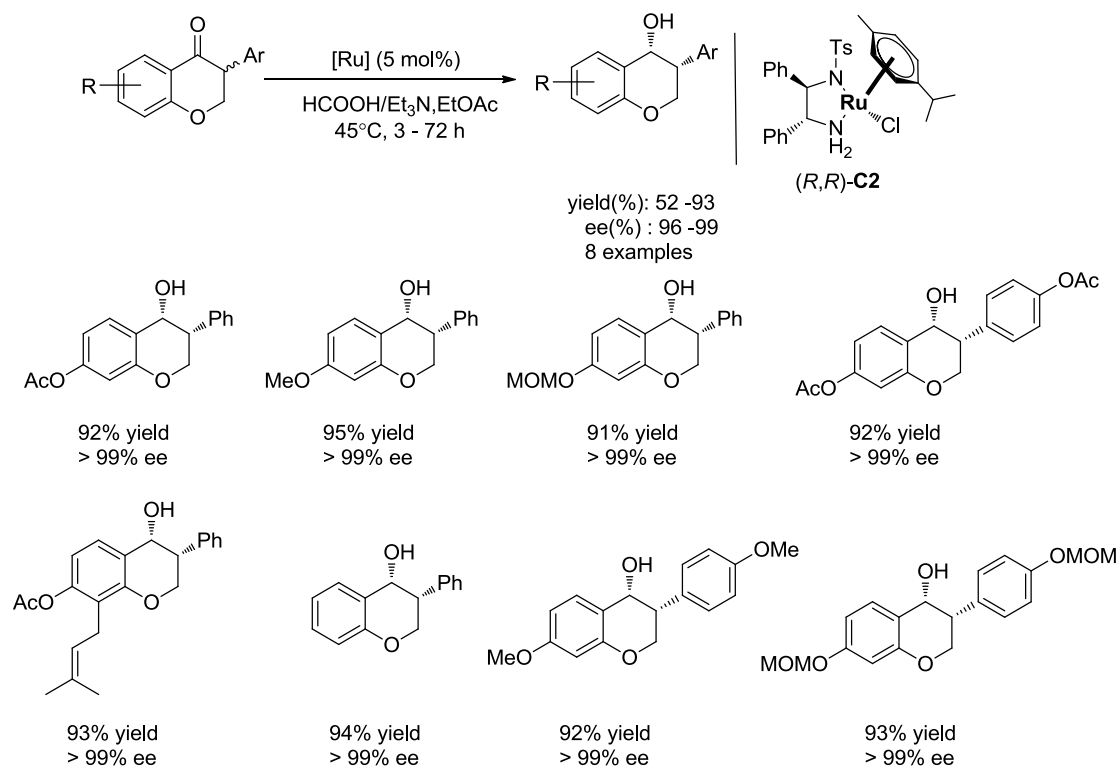
<sup>220</sup>Lemke, M. K.; Schwab, P.; Fischer, P.; Tischer, S.; Witt, M.; Noehringer, L.; Rogachev, V.; Jager, A.; Kataeva, O.; Frohlich, R.; Metz, P. *Angew. Chem., Int. Ed.* **2013**, *52*, 11651.



Scheme 140

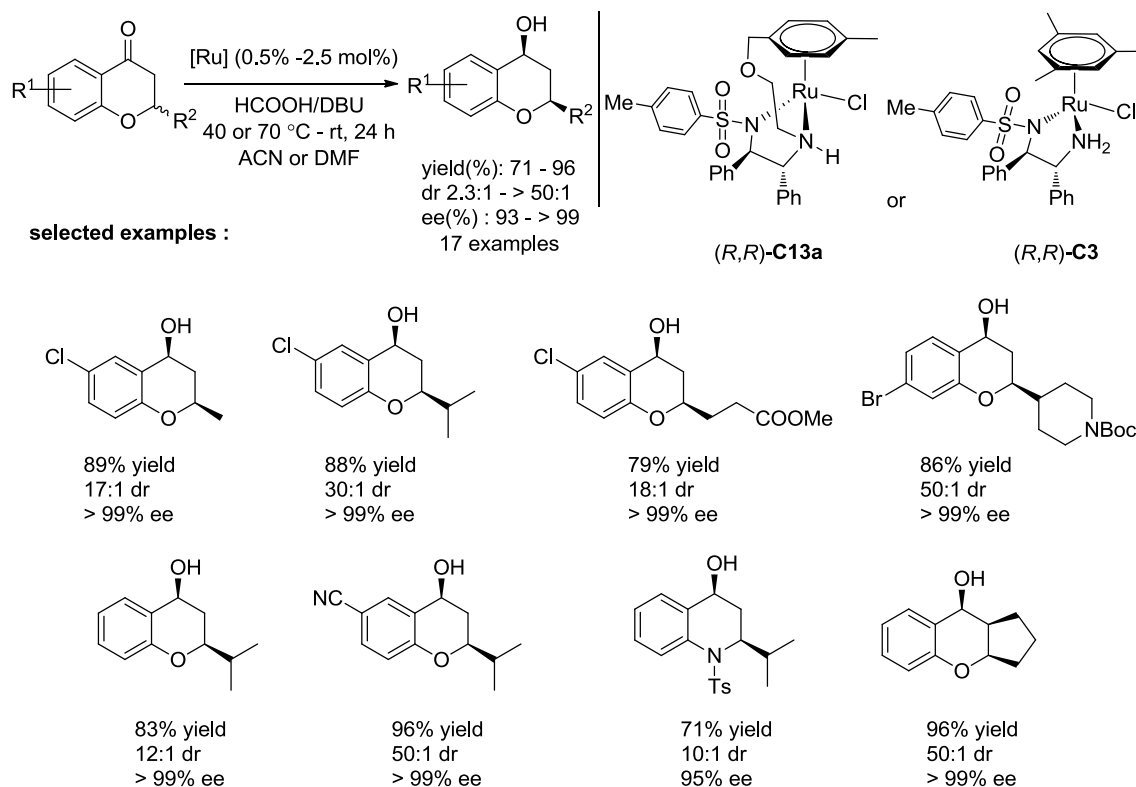
They later studied the asymmetric transfer hydrogenation of isoflavanones using the ruthenium complex  $[\text{RuCl}(p\text{-cym})((R,R)\text{-Ts-DPEN})]$  and  $\text{HCO}_2\text{H}/\text{Et}_3\text{N}$  (5:2) as the hydrogen donor. Under these conditions, the reaction proceeded with complete diastereoselectivity and excellent enantioselectivity through a dynamic kinetic resolution process. The isoflavanols were obtained as cis isomers in good yields (up to 93%)<sup>221</sup> (Scheme 141).

<sup>221</sup> Qin, T.; Metz, P. *Org. Lett.* **2017**, *19*, 2981.



Scheme 141

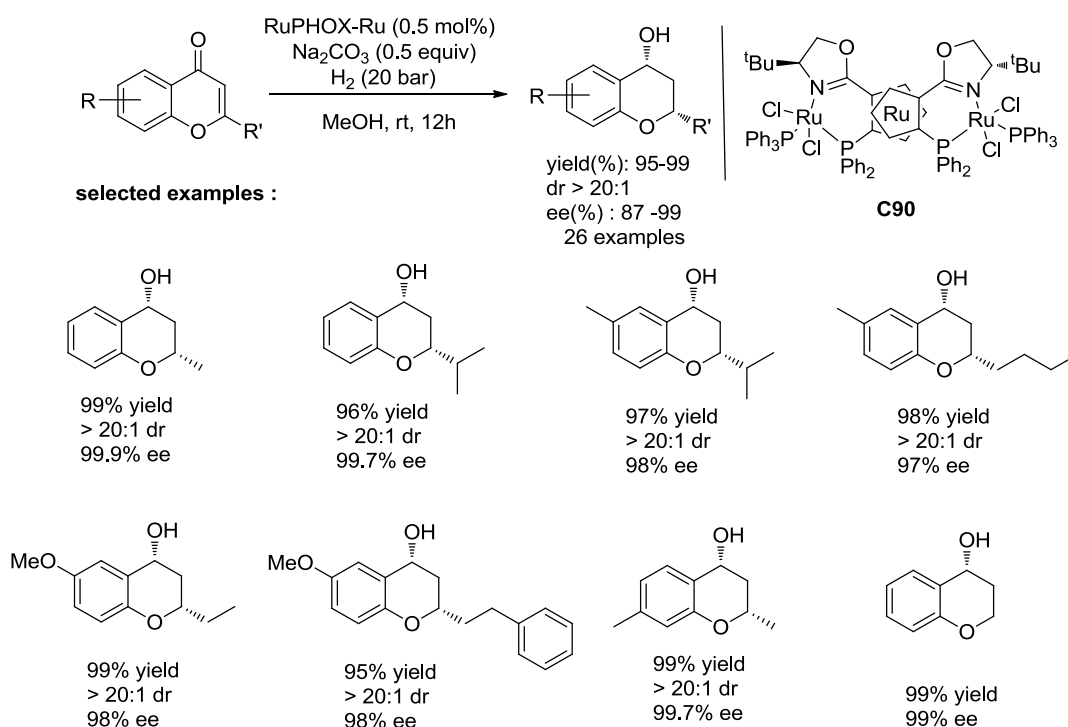
In 2017, Ruck *et al.* have developed a unique combination of base-catalyzed  $\beta$ -epimerization and ruthenium-catalyzed asymmetric transfer hydrogenation (ATH) that enables facile reductive dynamic kinetic resolution (DKR) of 2-substituted chromanones.<sup>212</sup> Torsional strain and novel CH–O sulfonamide hydrogen bonds have been shown to be important drivers of substrate preference and stereoselectivity. These efficient and practical reactions provide a wide range of synthetically useful chiral chromanols with good yields (71-96%), good diastereoselectivities (up to 50:1 dr) and excellent enantioselectivities (up to 99% ee) (Scheme 142).



Scheme 142

In 2018, Zhang *et al.* have developed a RuPHOX–Ru catalyzed asymmetric hydrogenation of chromones in methanol under 20 bar of H<sub>2</sub> for the synthesis of chiral chromanols and their derivatives.<sup>222</sup> Under the optimal reaction conditions, almost quantitative yields (95-99%), > 20:1 diastereoselectivities and up to 99.9% enantioselectivities were obtained (Scheme 143).

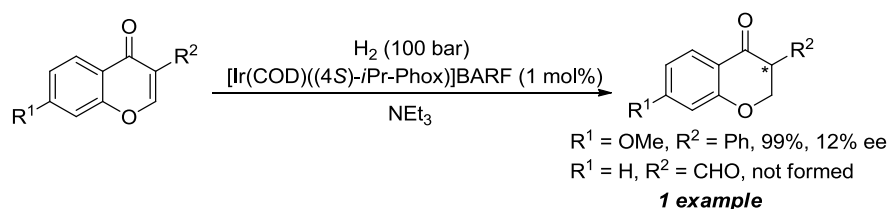
<sup>222</sup> Ma, Y.; Li, J.; Ye, J.; Liu, D.; Zhang, W. *Chem. Commun.*, **2018**, 54, 13571



Scheme 143

In this context, a straightforward synthesis of enantiomerically enriched 3-substituted chromanols relies on the asymmetric reduction of 3-substituted chromone derivatives. However, to the best of our knowledge, only two examples of such transformation were reported.

In 2011, Semeniuchenko *et al.* described the hydrogenation of electron deficient alkenes by using iridium complexes and a base as co-catalyst.<sup>223</sup> Whereas 7-methoxyisoflavone was reduced with [Ir(COD)((4*S*)-*i*Pr-Phox)]BARF and large excess of NEt<sub>3</sub> to the enantioenriched isoflavanol derivative (12% ee) in good yield, the reaction failed to afford the expected product in the case of 3-formylchromone (Scheme 144).



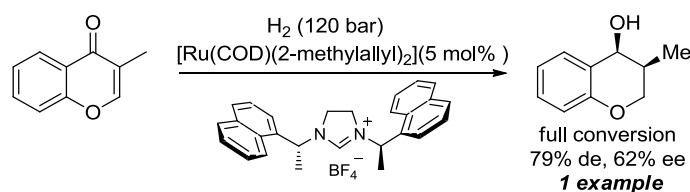
Scheme 144

On the other hand, Glorius *et al.* investigated the ruthenium-NHC catalyzed hydrogenation of flavones and chromones to stereoselectively access flavanones, flavanols,

<sup>223</sup> Semeniuchenko, V.; Exner, T. E.; Khilya, V.; Groth, U. *Appl. Organometal. Chem.* **2011**, *25*, 804.

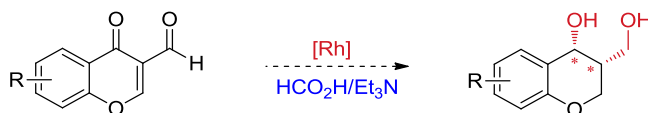


chromanones and chromanols. Whereas the asymmetric hydrogenation proceeded with moderate to good diastereoselectivities and high enantioselectivities for 2-substituted flavones and chromones (up to 67% de, up to 98% ee), a drop in enantioselectivity was observed with the 3-substituted regioisomer (79% de, 62% ee) (Scheme 145).



Scheme 145

As far as asymmetric transfer hydrogenation (ATH) of 3-substituted chromone derivatives is concerned, no example has been reported to date. As part of our ongoing studies directed toward the development of efficient methods for the asymmetric reduction of functionalized ketones, we investigated the first rhodium-catalyzed asymmetric transfer hydrogenation of 3-formylchromone derivatives that provided in a single operation the corresponding 3-hydroxymethyl chromanols through a dynamic kinetic resolution (DKR) process (Scheme 146).



Scheme 146

## 3.2 Results and discussion

### 3.2.1 Synthesis of 3-substituted chromones

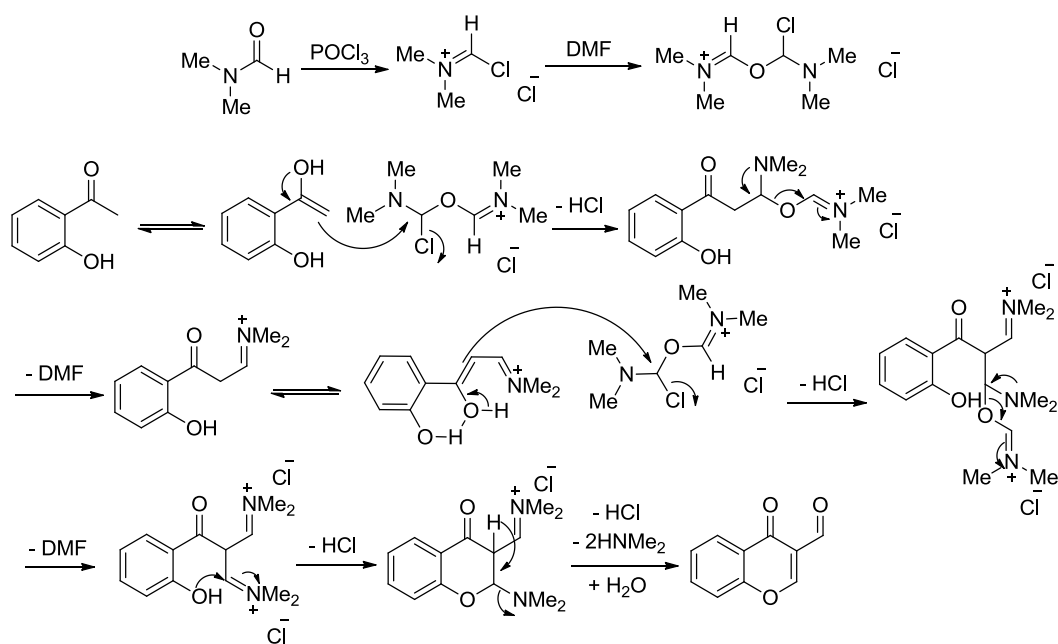
For this study, some commercially available 3-substituted chromones were used. We also synthesized 3-substituted chromones (**14c**, **i**, **j**) following reported procedure.<sup>224</sup> The desired compounds **14c**, **i**, **j**, were easily prepared in one step from the corresponding o-hydroxy-acetophenone (1.0 eq.) and phosphorous oxychloride (5.0 eq.) in DMF. The mixture was stirred at 0 °C for 30 minutes then at room temperature for 3–5 h giving the corresponding

<sup>224</sup> (a) China-Raju, B.; Nageswara-Rao, R.; Suman, P.; Yogeewari, P.; Sriram, D.; Shaik, T. B.; Kalivendi, S. V. *Bioorg. Med. Chem. Lett.* **2011**, *21*, 2855. (b) Su, W. K.; Li, Z. H.; Zhao, L. Y. *Org. Prep. Proced. Int.* **2007**, *39*, 495.

chromone derivatives with yields from 18% to 78% (Table 16).

**Table 16. preparation of 3-substituted chromones**

Entry	starting material	NO.	chromones	yield (%)
1		<b>14c</b>		51
2		<b>14i</b>		78
3		<b>14j</b>		58



**Scheme 147**

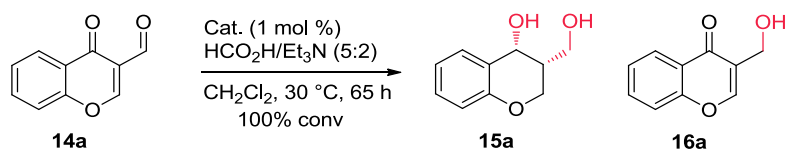
### 3.2.2 Optimisation of the reaction conditions

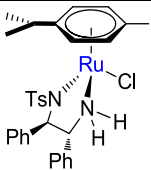
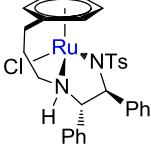
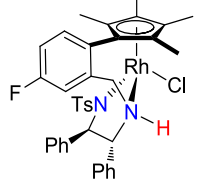
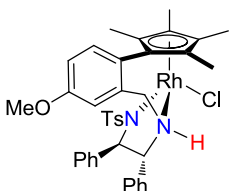
#### 3.2.2.1 Influence of the precatalyst

We first investigated the asymmetric transfer hydrogenation of 3-formylchromone **14a** to optimize the reaction conditions. When Noyori's ruthenium catalyst (*R,R*)-**C2** (1.0 mol%)

was used in the presence of 5.0 equiv of a HCO<sub>2</sub>H/Et<sub>3</sub>N (5:2) azeotropic mixture as the hydrogen source, in CH<sub>2</sub>Cl<sub>2</sub> at 30 °C, no traces of diol **15a** could be detected after 65 h of reaction and alcohol **16a** was exclusively isolated in 40% yield (Table 17, entry 1). Under otherwise identical conditions, the tethered ruthenium complex (*S,S*)-**C7** furnished the corresponding reduced compound **15a** with a moderate 44% yield, a diastereomeric ratio of 67:33 in favor of the *cis* compound and an enantioselectivity of 95% (Table 17, entry 2). Compound **15a** was produced with a lower yield by using the tethered rhodium complex (*R,R*)-**C88** although in this case a high dr was observed with an excellent ee value (28% yield, 96:4 dr, 99% ee, Table 17, entry 3). The reaction with the parent Rh complex (*R,R*)-**C86** resulted in a satisfying 62% yield with both high diastereo- and enantioselectivities (97:3 dr, 99% ee, Table 17, entry 4).

**Table 17. Screening of precatalysts for the ATH of 14a<sup>a</sup>**



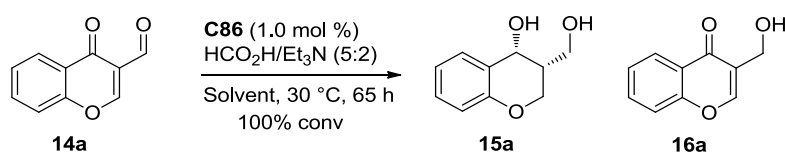
Entry	Cat.	yield <sup>[b]</sup> (%)	d.r. <sup>[c]</sup> (cis/trans)	ee <sub>cis</sub> <sup>[d]</sup> (%)
1	 ( <i>R,R</i> )- <b>C2</b>	-- <sup>e</sup>	--	--
2	 ( <i>S,S</i> )- <b>C7</b>	44	67:33	95
3	 ( <i>R,R</i> )- <b>C88</b>	28	96:4	99
4	 ( <i>R,R</i> )- <b>C86</b>	62	97:3	99

<sup>a</sup>Conditions: **14a** (0.5 mmol), Cat. (1.0 mol%), CH<sub>2</sub>Cl<sub>2</sub> (1.5 mL), HCO<sub>2</sub>H/Et<sub>3</sub>N (5:2) (212 μL), 30 °C. The reaction was monitored by TLC or <sup>1</sup>H NMR. <sup>b</sup>Isolated yield. <sup>c</sup>Determined by <sup>1</sup>H NMR of the crude after the ATH. <sup>d</sup>Determined by SFC analysis. <sup>e</sup>Compound **16a** was exclusively isolated in 40% yield.

### 3.2.2.2 Influence of the solvent

With these encouraging results in hand, and using complex (*R,R*)-**C86**, we then screened a variety of solvents. Non-polar solvents such as toluene and diethyl ether afforded lower yields (28% and 38%) with lower diastereoselectivities (Table 18, entries 2-3). Polar solvents such as CH<sub>3</sub>CN, dioxane, DMF, and 2-MeTHF were then investigated (Table 18, entries 4-7). Although a slightly better dr value was attained in CH<sub>3</sub>CN, the yield (56 %) was lower than in CH<sub>2</sub>Cl<sub>2</sub> (62 %) and none of the other solvents outperformed CH<sub>2</sub>Cl<sub>2</sub>. Consequently, CH<sub>2</sub>Cl<sub>2</sub> was selected as the solvent of choice for the ATH/DKR of **14a**.

**Table 18. Screening of solvents for the ATH of 14a<sup>a</sup>**



Entry	Solvent	yield <sup>[b]</sup> (%)	d.r. <sup>[c]</sup> (cis/trans)	ee <sub>cis</sub> <sup>[d]</sup> (%)
1	CH <sub>2</sub> Cl <sub>2</sub>	62	97:3	99
2	toluene	28	94:6	97
3	Et <sub>2</sub> O	38	91:9	99
4	CH <sub>3</sub> CN	56	98:2	98
5	dioxane	42	96:4	97
6	DMF	52	97:3	98
7	2-MeTHF	37	95:5	97

<sup>a</sup>Conditions: **14a** (0.5 mmol), **C86** (1.0 mol%), Solvent (1.5 mL), HCO<sub>2</sub>H/Et<sub>3</sub>N (5:2) (212 μL), 30 °C. The reaction was monitored by TLC or <sup>1</sup>H NMR. <sup>b</sup>Isolated yield. <sup>c</sup>Determined by <sup>1</sup>H NMR of the crude after the ATH. <sup>d</sup>Determined by SFC analysis.

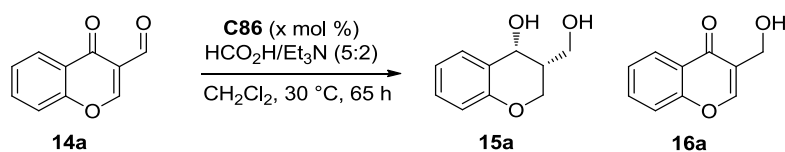
### 3.2.2.3 Influence of the hydrogen source

We tried to improve the yield of the reaction by testing other hydrogen sources such as sodium formate, calcium formate, sodium dihydrogen hypophosphite, ammonium formate, potassium hydroxide with isopropanol and HCO<sub>2</sub>H/Et<sub>3</sub>N (1:1) azeotropic mixture. However, none of these hydrogen sources allowed any conversion or formation of the expected diol **15a**. Consequently, we kept HCO<sub>2</sub>H/Et<sub>3</sub>N (5:2) azeotropic mixture as the hydrogen donor for this study.

### 3.2.2.4 Influence of the catalyst loading

We pursued the optimization of the reaction conditions by varying the catalyst loading. Identical results in terms of yield and stereoselectivity were obtained for the ATH/DKR of **14a** with S/C 100 and S/C 200 (Table 19, entries 1–2) but lowering to S/C 1000 had a detrimental effect on the yield of **15a** (Table 19, entry 3, 47% yield). A catalyst loading of S/C 10000 failed to afford the formation of the expected diol and only the product **16a** was observed (Table 19, entry 4).

**Table 19. Screening of catalyst loading for the ATH of 14a<sup>a</sup>**



Entry	S/C	yield <sup>[b]</sup> (%)	d.r. <sup>[c]</sup> (cis/trans)	ee <sub>cis</sub> <sup>[d]</sup> (%)
1	100	62	97:3	99
2	200	62	97:3	99
3	1000	47	99:1	99
4	10000	--	--	--

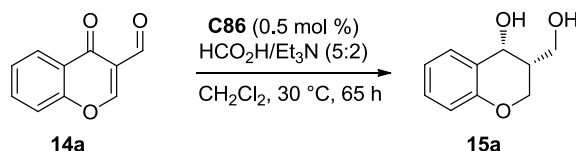
<sup>a</sup>Conditions: **14a** (0.5 mmol), **C86** (x mol%), CH<sub>2</sub>Cl<sub>2</sub> (1.5 mL), HCO<sub>2</sub>H/Et<sub>3</sub>N (5:2) (212 μL), 30 °C. The reaction was monitored by TLC or <sup>1</sup>H NMR. <sup>b</sup>Isolated yield. <sup>c</sup>Determined by <sup>1</sup>H NMR of the crude after the ATH. <sup>d</sup>Determined by SFC analysis.

### 3.2.2.5 Influence of the amount of the HCO<sub>2</sub>H/Et<sub>3</sub>N azeotropic mixture

We next studied the influence of the amount of the HCO<sub>2</sub>H/Et<sub>3</sub>N (5:2) mixture (Table

20). From the various tested conditions, from 3.0 equiv to 10.0 equiv HCO<sub>2</sub>H/Et<sub>3</sub>N (5:2), the best yield was attained by using 7.0 equiv of the hydrogen donor (74%, Table 20, entry 3).

**Table 20. Screening of the amount of the HCO<sub>2</sub>H/Et<sub>3</sub>N (5:2) mixture<sup>a</sup>**



Entry	FA/TEA (5:2) (equiv)	yield <sup>[b]</sup> (%)	d.r. <sup>[c]</sup> (cis/trans)	ee <sub>cis</sub> <sup>[d]</sup> (%)
1	3.0	26	90:10	98
2	5.0	62	97:3	99
3	7.0	74	97:3	99
4	10.0	67	98:2	99

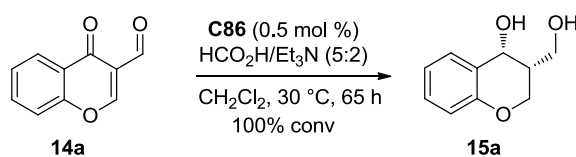
<sup>a</sup>Conditions: **14a** (0.5 mmol), **C86** (0.5 mol%), CH<sub>2</sub>Cl<sub>2</sub> (1.5 mL), HCO<sub>2</sub>H/Et<sub>3</sub>N (5:2), 30 °C. The reaction was monitored by TLC or <sup>1</sup>H NMR. <sup>b</sup>Isolated yield. <sup>c</sup>Determined by <sup>1</sup>H NMR of the crude after the ATH.

<sup>d</sup>Determined by SFC analysis.

### 3.2.2.6 Influence of the concentration

The last reaction parameter we considered was the concentration. We can conclude from Table 21 that when using CH<sub>2</sub>Cl<sub>2</sub> as a solvent, the more concentrated the reaction the higher the yield. Varying the amount of CH<sub>2</sub>Cl<sub>2</sub> from 2.0 mL to 0.5 mL increased the yields from 72% to 84% (Table 21, entries 1-4), whereas the neat reaction gave a less satisfying yield of 73% (Table 21, entry 5). So we found the optimum reaction concentration of 1.0 mol.L<sup>-1</sup> (0.5 ml CH<sub>2</sub>Cl<sub>2</sub>) afforded a good 84% yield. Based on the above screening, the optimized conditions were set as follows: **C86** (0.5 mol%) as the precatalyst, HCO<sub>2</sub>H/Et<sub>3</sub>N (5:2) (7.0 equiv) as the hydrogen donor, CH<sub>2</sub>Cl<sub>2</sub> (1.0 M) at 30 °C.

**Table 21. Screening of the amount of the HCO<sub>2</sub>H/Et<sub>3</sub>N (5:2) mixture<sup>a</sup>**



Entry	CH <sub>2</sub> Cl <sub>2</sub> (x mL)	yield <sup>[b]</sup> (%)	d.r. <sup>[c]</sup> (cis/trans)	ee <sub>cis</sub> <sup>[d]</sup> (%)
1	2.0	72	97:3	99
2	1.5	74	97:3	99
3	1.0	79	97:3	99
4	0.5	84	98:2	99
5	neat	73	98:2	99

<sup>a</sup>Conditions: **14a** (0.5 mmol), **C86** (0.5 mol%), CH<sub>2</sub>Cl<sub>2</sub> (x mL), HCO<sub>2</sub>H/Et<sub>3</sub>N (5:2) (446 μL), 30 °C. The reaction was monitored by TLC or <sup>1</sup>H NMR. <sup>b</sup>Isolated yield. <sup>c</sup>Determined by <sup>1</sup>H NMR of the crude after the ATH. <sup>d</sup>Determined by SFC analysis.

### 3.2.3 Kinetic experiment

To better understand the reaction process, a series of control experiments were conducted. We first performed monitoring studies of the Rh-catalyzed asymmetric transfer hydrogenation of **14a** under the optimized conditions (Figure 7). After 0.25 h of reaction, a complete consumption of the starting material was observed with formation of products **15a**, **16a** and **17a**. It should be noted that the diol resulting from the reduction of the ketone functional group of intermediate **16a** was not detected in this study. It appears that reduction of the aldehyde moiety and of the C=C bond was fast, yielding compounds **16a** and **17a** with a cumulative proportion of 80% as a mixture with **15a** after 0.25 h of reaction. The amount of intermediate **17a** then rapidly decreased, with only traces detected after 7 h and complete consumption was obtained after 48 h. It is worth noting that, when the reaction was quenched after 0.25 h, intermediate **17a** was found to be present as a racemic mixture. Suggesting, this reaction proceeded through a dynamic kinetic resolution.

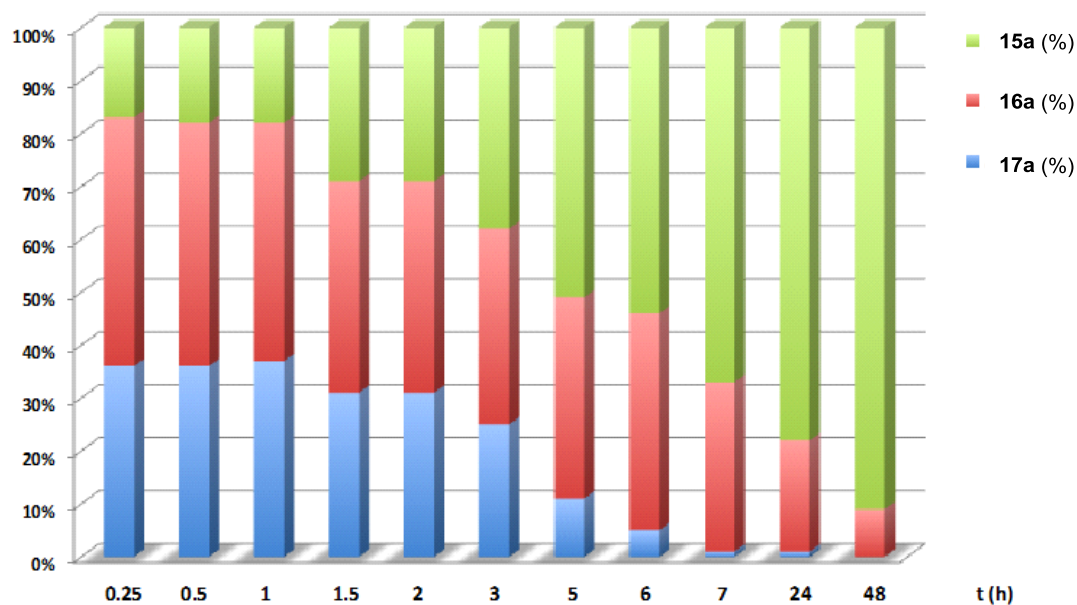
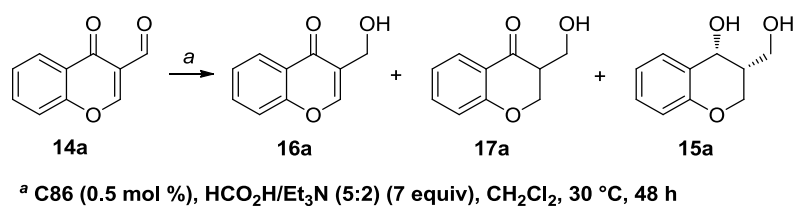


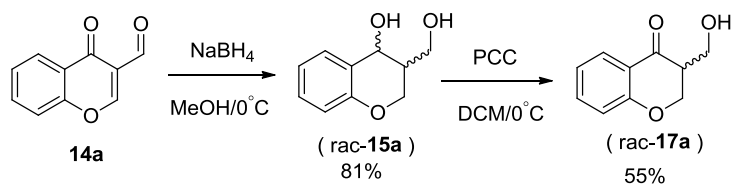
Figure 7. kinetic experiment

### 3.2.4 Dynamic kinetic experiment

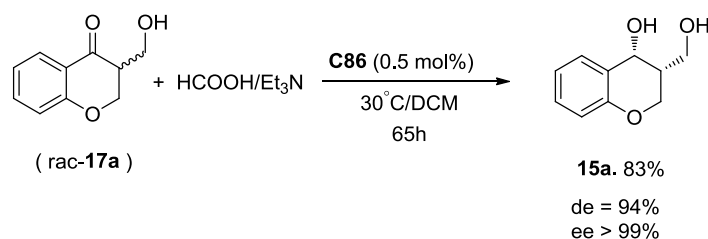
To confirm that the ATH of **14a** proceeded through a dynamic kinetic resolution, an authentic sample of racemic **17a** was prepared and subjected to the optimized reaction conditions. Reduction of **14a** with sodium borohydride in MeOH yielded the corresponding diol in 81% yield. The latter was then selectively oxidized to the desired hydroxy ketone in the presence of PCC in dichloromethane at 0 °C in 55% yield. Racemic **14a** was then reduced under the standard reaction conditions and we were pleased to find that racemic **17a** was converted to the expected product **15a** in the same yield (83%), diastereoselectivity (97:3 dr) and enantioselectivity (99% ee) than those obtained by using **14a** as the starting material, thus demonstrating that a DKR is occurring for this reaction (Scheme 148).



## a. Preparation of rac-17a



## b. Reduction of rac-17a under the standard conditions



Scheme 148

## 3.2.5 Substrate scope

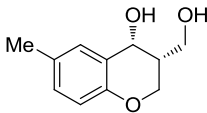
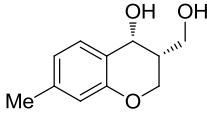
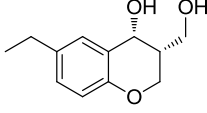
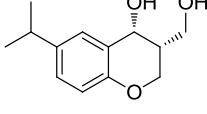
## 3.2.5.1 DKR/ATH of substrates bearing electron-donating substituents

With the defined optimized conditions in hand, we explored the substrate scope of the reaction with a series of 3-formyl chromones bearing various electron-donating or electron-withdrawing substituents on the phenyl ring. We first studied the asymmetric reduction of substrates having electron-donating substituents on the aromatic ring. Compounds bearing methyl, ethyl or isopropyl substituents on the benzene core at the *meta* or *para* positions afforded high levels of diastereoselectivities, from 97:3 or 98:2 dr, excellent ee values (> 99%) and good yields from 72% to 76%. (Table 22, entries 2–5)

Table 22. ATH of substrates bearing electron-donating substituents

O=C1C=CC(=O)C=C1c2ccccc2 (14a-e)  $\xrightarrow[100\% \text{ conv}]{\text{C86 (0.5 mol\%)}, \text{HCO}_2\text{H}/\text{Et}_3\text{N (5:2)}, \text{CH}_2\text{Cl}_2, 30^\circ\text{C}}$  OCC1C(O)C=CC(=O)C=C1c2ccccc2 (15a-e)

Entry	substrate	product	NO.	time (h)	yield (%) <sup>b</sup>	dr (cis/trans) <sup>c</sup>	ee <sub>cis</sub> (%) <sup>d</sup>
1	14a	<chem>OCC1C(O)C=CC(=O)C=C1c2ccccc2</chem>	15a	65	84	98:2	>99

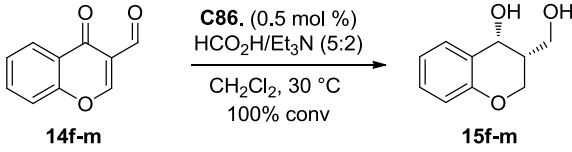
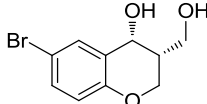
2	<b>14b</b>		<b>15b</b>	65	76	97:3	>99
3	<b>14c</b>		<b>15c</b>	65	72	97:3	>99
4	<b>14d</b>		<b>15d</b>	65	72	97:3	>99
5	<b>14e</b>		<b>15e</b>	65	75	97:3	>99

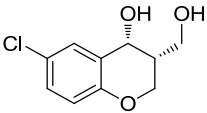
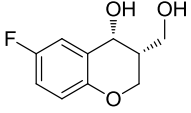
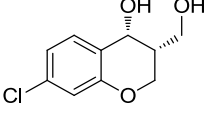
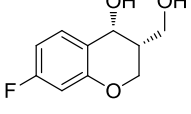
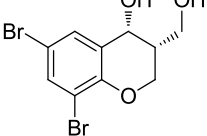
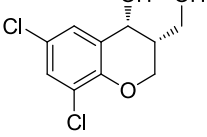
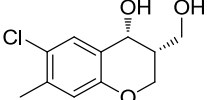
<sup>a</sup>Conditions: **14a-e** (0.75 mmol), **C86** (0.5 mol%), CH<sub>2</sub>Cl<sub>2</sub> (0.75 mL), HCO<sub>2</sub>H/Et<sub>3</sub>N (5:2) (446 μL), 30 °C. The reaction was monitored by TLC or <sup>1</sup>H NMR. <sup>b</sup>Isolated yield. <sup>c</sup>Determined by <sup>1</sup>H NMR of the crude after the ATH. <sup>d</sup>Determined by SFC analysis.

### 3.2.5.2 DKR/ATH of substrates bearing electron-withdrawing substituents

Substrates containing electron-withdrawing groups on the benzene ring such as bromo, chloro, fluoro substituents displayed good to high yields (74–92%), high levels of diastereocontrol (96:4 or 97:3 dr) and excellent enantioselectivities (> 99% ee) (Table 23, entries 1-5). Those with two-substituents on the benzene ring also gave good yields (80-88%), with good diastereoselectivities (92:8 to 98:2 dr) and excellent enantioselectivities (97% to > 99% ee) (Table 23, entries 6-8). We can also conclude from the table that with electron-withdrawing groups on the benzene ring the reaction time can be reduced to 24 h.

**Table 23. ATH of substrates bearing electron-withdrawing substituents**

							
Entry	substrate	product	NO.	time (h)	yield (%) <sup>b</sup>	dr (cis/trans) <sup>c</sup>	ee <sub>cis</sub> (%) <sup>d</sup>
1	<b>14f</b>		<b>15f</b>	24	85	96:4	>99

2	<b>14g</b>		<b>15g</b>	24	87	96:4	>99
3	<b>14h</b>		<b>15h</b>	24	83	96:4	>99
4	<b>14i</b>		<b>15i</b>	24	92	96:4	>99
5	<b>14j</b>		<b>15j</b>	24	74	97:3	>99
6	<b>14k</b>		<b>15k</b>	24	80	92:8	>99
7	<b>14l</b>		<b>15l</b>	24	87	94:6	97
8	<b>14m</b>		<b>15m</b>	65	88	98:2	>99

<sup>a</sup>Conditions: **14f-m** (0.75 mmol), **C86** (0.5 mol%), CH<sub>2</sub>Cl<sub>2</sub> (0.75 mL), HCO<sub>2</sub>H/Et<sub>3</sub>N (5:2) (446 μL), 30 °C. The reaction was monitored by TLC or <sup>1</sup>H NMR. <sup>b</sup>Isolated yield. <sup>c</sup>Determined by <sup>1</sup>H NMR of the crude after the ATH. <sup>d</sup>Determined by SFC analysis.

### 3.2.6 Determination of the absolute configuration

The absolute configurations of diols **15a** and **15g** were unambiguously assigned as (*R, R*) by X-ray crystallographic analysis (Figure 8). By analogy, we conjecture that the remainder of the ATH products **15** followed the same trend.

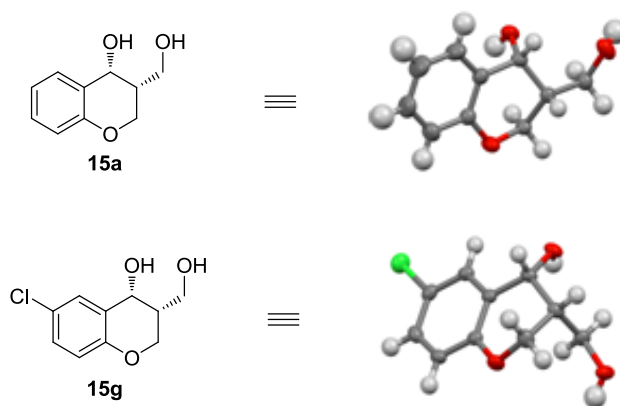
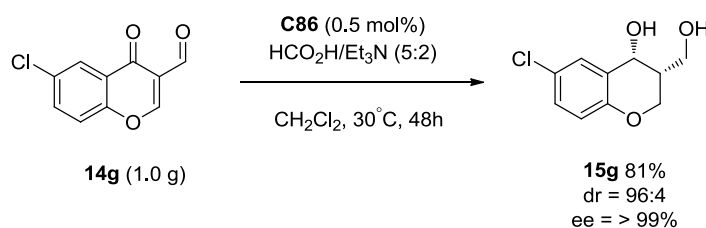


Figure 8. X-ray of 15a and 15g

### 3.2.7 Scale up experiment

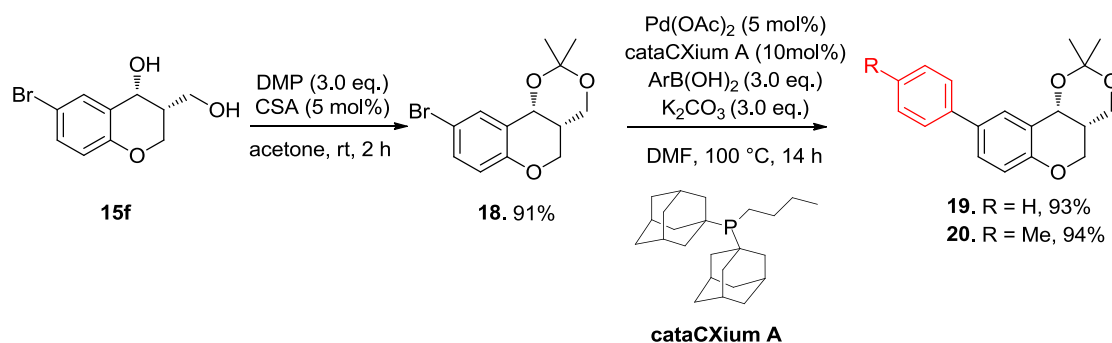
The efficiency of this ATH was supported by a scale-up experiment. Under the standard conditions, a gram-scale reduction of **14g** delivered the desired product **15g** in 81% yield with high diastereoselectivity (96:4 dr) and excellent enantioselectivity (> 99% ee) (Scheme 149).



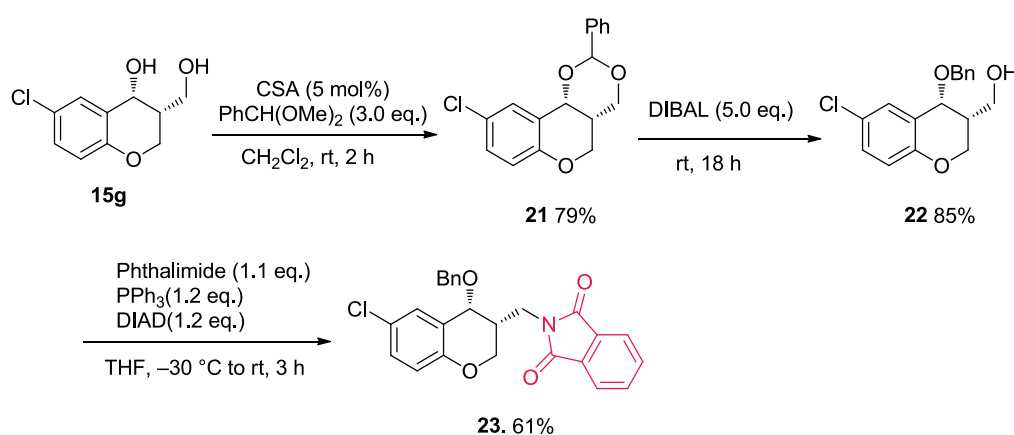
Scheme 149

### 3.2.8 Post-functionalization

In addition, the reduced compounds **2** can serve as useful intermediates for further elaboration on either the aromatic ring or the heterocyclic counterpart and post-functionalization reactions of compounds **15f** and **15g** were performed. After acetonide protection of **15f**, biaryl derivatives **19** and **20** were readily prepared in high yields through Suzuki-Miyaura coupling by using  $\text{Pd}(\text{OAc})_2$ , cataCXium A as a ligand,  $\text{K}_2\text{CO}_3$  as a base and phenyl- or 4-methoxyphenylboronic acid, respectively (Scheme 150).



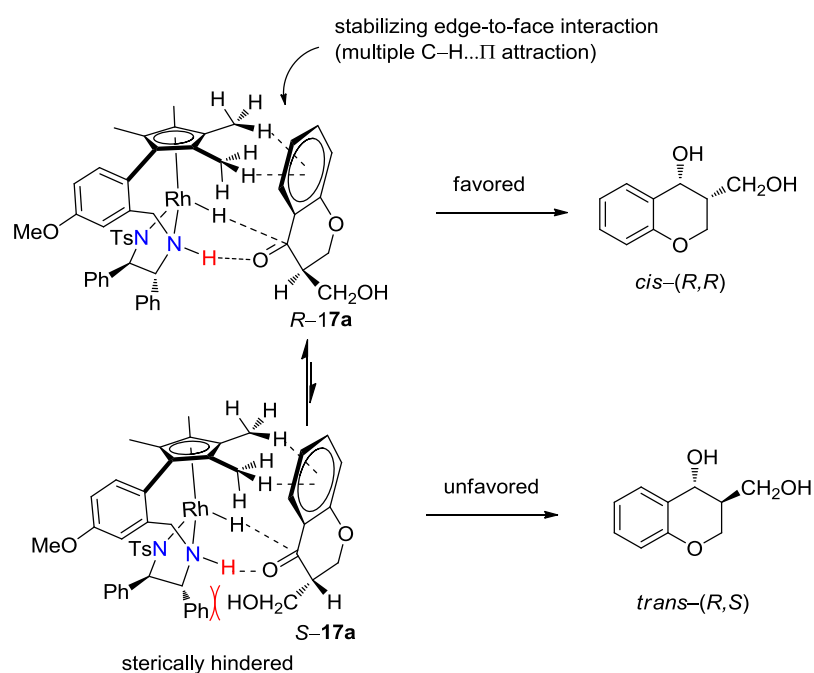
On the other hand, diol **15g** was readily converted into compound **23** in 3 steps via a Mitsunobu reaction. Protection of **15g** with 2,2-dimethoxypropane in the presence of catalytic CSA, gave the benzylidene acetal **21** in 79% yield. Treatment of the latter with an excess of DIBAL afforded the monoprotected diol **22** in 85% yield. Finally, the Mitsunobu reaction was carried out with DIAD, PPh<sub>3</sub> and phthalimide to furnish the substitution product **23** in 61% yield (Scheme 151).



### 3.2.9 Origin of the enantio- and diastereoselectivities

As discussed above, the ATH reaction proceeded through dynamic kinetic resolution and the partially reduced intermediate **17a** was found to be present as a racemic mixture in the reaction medium (Scheme 152). The enantio-control of the reaction would probably arise from the reduction of this intermediate, through a transition state in which the well-established edge to face arene/aryl interaction between the  $\eta^5$ -arene and the phenyl group of the ketone ensures a high enantiomeric excess with this stabilizing CH/ $\pi$  interaction. On

the other hand, the preferential formation of the *cis* isomer might be explained by a disfavorable steric interaction in the transition state leading to the *trans* isomer.



Scheme 152

### 3.3 conclusion

In summary, the operationally simple rhodium-catalyzed asymmetric transfer hydrogenation of 3-formyl chromones appears to be an efficient tool for the synthesis of *cis* 3-hydroxymethyl chromanol derivatives.<sup>225</sup> This method confers several advantages compared to the scarce examples of asymmetric hydrogenation. The in-house developed Rh(III)-complex enables the reduction under mild conditions using a low catalyst loading and HCO<sub>2</sub>H/Et<sub>3</sub>N (5:2) as the hydrogen source, delivering the reduced compounds in good yields and excellent diastereo- and enantioselectivities (up to 98:2 dr, up to >99% ee). Furthermore, the usefulness of this method was demonstrated by the efficient gram-scale asymmetric transfer hydrogenation of **14g**. Finally, the 3-hydroxymethyl chromanols produced in this study can serve as useful scaffolds for further functionalization to access diversely substituted chromanol derivatives.<sup>242</sup>

<sup>225</sup> He, B.; Phansavath, P.; Ratovelomanana-Vidal, V. *Org. Lett.* **2019**, *21*, 3276.

**PART C:**

**ATH of  $\alpha$ -methoxy  $\beta$ -ketoesters via  
dynamic kinetic resolution**





## Part C: ATH of $\alpha$ -methoxy $\beta$ -ketoesters via dynamic kinetic resolution

### 1. Rh(III)-Catalyzed Asymmetric Transfer Hydrogenation of $\alpha$ -Methoxy $\beta$ -Ketoesters through DKR in 2-MeTHF and Water: Toward a Greener Procedure

#### 1.1 Introduction

##### 1.1.1 Biological interest of 1,2- diol derivatives

Chiral 1,2-diols are important structural motifs found in a number of natural and biologically active molecules, such as macrocyclic natural product,<sup>226</sup> silymarin derivatives,<sup>227</sup>  $\alpha_{1A}$ -adrenoreceptor antagonist,<sup>228</sup> preventing epilepsy agent,<sup>229</sup> (*S,S*)-reboxetine,<sup>230</sup> selective norepinephrine reuptake inhibitors (sNRI),<sup>231</sup> carbohydrates, polyketides, or alkaloids,<sup>232</sup> and have found wide applications in organic synthesis either as chiral ligands or auxiliaries<sup>233</sup> (Figure 9).

<sup>226</sup> Aeluri, M.; Gaddam, J.; Trinath, D. V. K. S.; Chandrasekar, G.; Kitambi, S. S.; Arya, P. *Eur. J. Org. Chem.* **2013**, 3955.

<sup>227</sup> Zhuang, R.-X; Zhang, J.-K; Xi, J.-J; Zhao, Y.-M; Shao, Y.-D; Pan, X.-W; Fang, H.-Y; Cai, Z.-B; Liu S.-R; Wu, X.-M *Silybin 23-substituted derivative and preparation method and application of injection thereof*. CN106317033A, **2016**

<sup>228</sup> Romeiro, LAS; Fraga CAM; Lacerda, BEJ; Silva, CLM; Miranda, ALP; Eduardo, VT; Brito, FCF; Almeida, HCCC; NOËL, FG *Use of adrenergic n-phenylpiperazine antagonists, pharmaceutical compositions containing them, and methods of preparing them*. WO2005112538A2, **2005**

<sup>229</sup> Choi, Y.-M *Sulfamate derivative compound for use in preventing or treating epilepsy*. WO2015088271A1, **2015**

<sup>230</sup> Son, S.-M.; Lee, H.-K. *J. Org. Chem.* **2014**, *79*, 2666.

<sup>231</sup> Hudson, S.; Kiankarimi, M.; Eccles, W.; Dwight, W.; Mostofi, Y. S.; Genicot, M. J.; Fleck, B. A.; Gogas, K.; Aparicio, A.; Wang, H.; et al. *Bioorg. Med. Chem. Lett.* **2008**, *18*, 4491.

<sup>232</sup> Nicolaou, K. C.; Snyder, S. A. *Classics in Total Synthesis II*; Wiley-VCH: Weinheim, Germany, **2003**, and references therein.

<sup>233</sup> Seyden-Penn, J. In *Chiral Auxiliaries and Ligands in Asymmetric Synthesis*; Wiley-VCH: Weinheim, **1995**

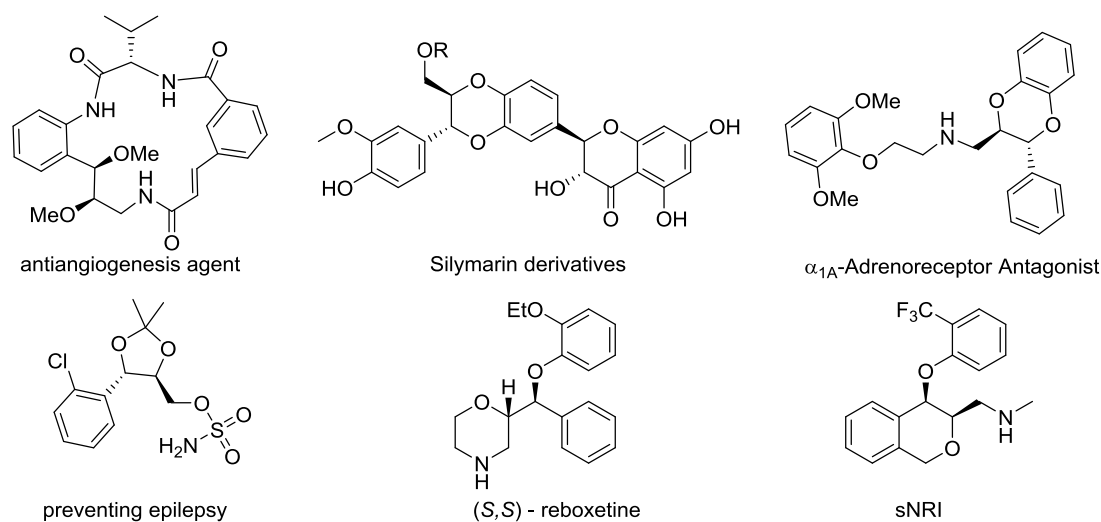
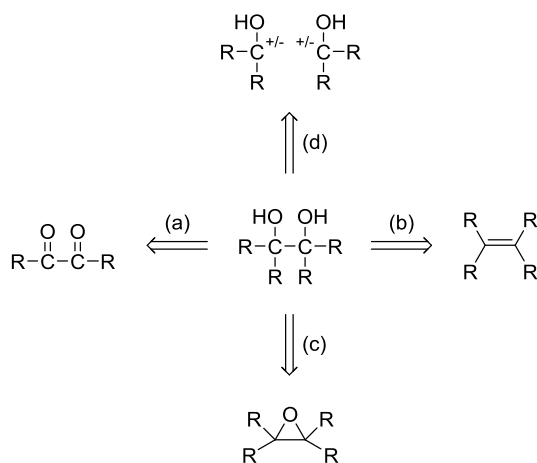


Figure 9

### 1.1.2 Different synthetic pathways for 1,2-diol derivatives

Several efficient approaches to access enantiomerically pure 1,2-diols are described in the literature.<sup>234,235</sup> These methods involve: (a) sequential reduction of a 1,2-diketone, (b) dihydroxylation reactions, (c) epoxide ring-opening, or (d) C-C bond formation reaction between two oxygen-bearing carbon atoms (Scheme 153).



Scheme 153

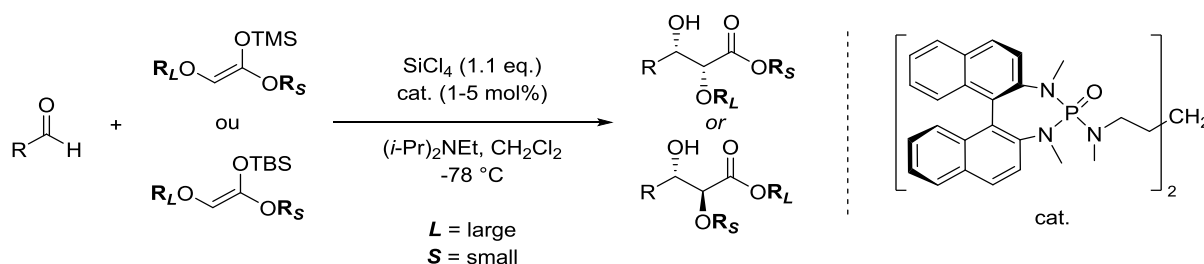
However, in most of the methods reported in the literature, the two hydroxy groups were not differentiated. Thus, the synthesis of monodifferentiated 1,2-diols remains a

<sup>234</sup> Ikariya, T.; Murata, K.; Noyori, R. *Org. Biomol. Chem.* **2006**, *4*, 393

<sup>235</sup> Haddad, Y. M. Y.; Henbest, H. B.; Husbands, J.; Mitchell, T. R. B. *Proc. Chem. Soc.* **1964**, 361.

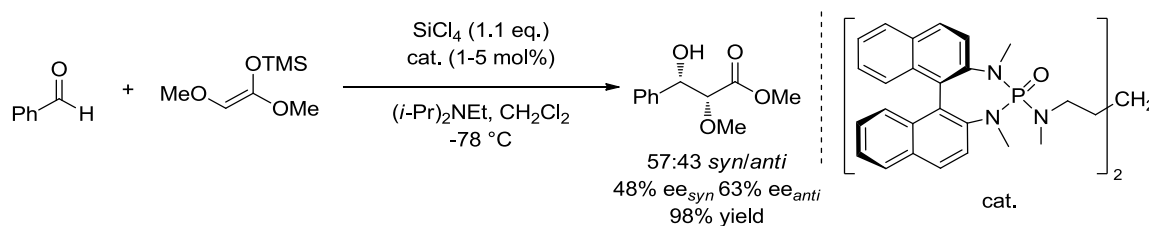
challenge. To our knowledge, only few examples of the preparation of this type of compounds have been described.

In 2008, Denmark *et al.* described a catalytic pathway for the preparation of stereodefined and monodifferentiated 1,2-diols via an enantioselective aldolization reaction between a glycolate-derived silyl ketene acetal and an aldehyde, in the presence of tetrachlorosilane and a catalytic amount of a chiral bisphosphoramidate (Scheme 154).<sup>236</sup>



Scheme 154

Interestingly, both *syn* and *anti* 1,2-diols can be obtained with the same catalyst system. However, this reaction requires a stoichiometric amount of tetrachlorosilane, and former conversion of the ester to a more reactive silyl ketene acetal, which considerably decreases the overall reaction efficiency. In addition, when the  $\alpha$ -alkoxy group is small, such as a methoxy group, the diastereoselectivity and enantioselectivity drop significantly (Scheme 155).<sup>237</sup>



Scheme 155

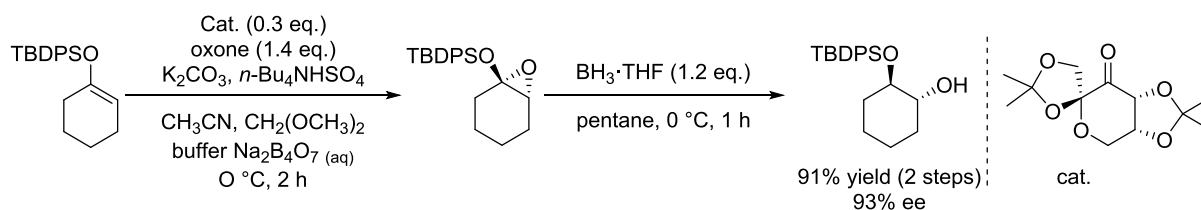
Myers *et al.*<sup>238</sup> reported the synthesis of enantiomerically enriched *trans* 1,2-diols monosilyl ether derivatives, with good isolated yields and good to excellent enantio- and

<sup>236</sup> Denmark, S. E.; Chung, W.-J. *Angew. Chem. Int. Ed.* **2008**, 47, 1890.

<sup>237</sup> Denmark, S. E.; Chung, W.-J. *J. Org. Chem.* **2008**, 73, 4582.

<sup>238</sup> Lim, S. M.; Hill, N.; Myers, A. G. *J. Am. Chem. Soc.* **2009**, 131, 5763.

diastereoselectivities (Scheme 156, 93% ee, 91% yield). This two-step sequence involves asymmetric Shi epoxidation and a regioselective epoxide opening.



**Scheme 156**

Despite the good results obtained, this synthetic route has certain disadvantages that limit its practicality, such as the use of a high catalyst loading (30 mol%) and an excess of reagents. Furthermore, this method remains essentially limited to cyclic silyl enol ethers.

Therefore, the development of new catalytic highly diastereo- and enantioselective methodologies to access optically active monodifferentiated 1,2-diols with a high level of selectivity and a high atom economy is still of major interest in organic synthesis. Our group and others have shown that dynamic kinetic resolution (DKR) combined with asymmetric hydrogenation catalyzed by ruthenium complexes has proven to be an effective synthetic tool for controlling two adjacent stereocentres in a single chemical operation.

*Based on our previous results on Ru-catalyzed DKR/ATH of  $\alpha$ -alkoxy  $\beta$ -keto esters and searching for more sustainable reaction conditions, we studied this reaction by using a new Rh tethered complex to evaluate the catalytic performances.*

## 1.2 Results and discussion

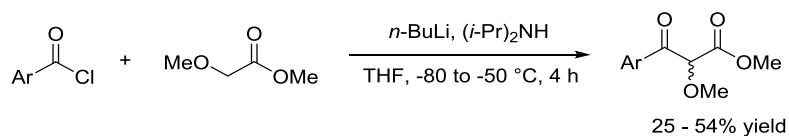
### 1.2.1 Synthesis of aryl $\alpha$ -methoxy $\beta$ -keto esters

For this study, we first prepared a series of  $\alpha$ -alkoxy-substituted  $\beta$ -ketoesters **24**. These compounds were synthesized in either one (Method A) or two (Method B) steps as described hereafter.

#### Method A :

This method involves addition of the lithioenolate of methyl methoxyacetate onto an

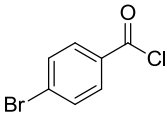
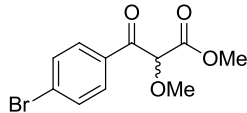
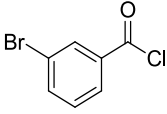
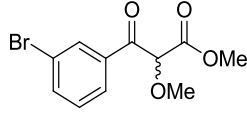
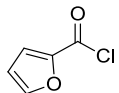
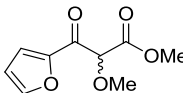
aryl acyl chloride, and afforded the desired ketoesters in 25–54% yields (Scheme 157 and Table 24).



Scheme 157

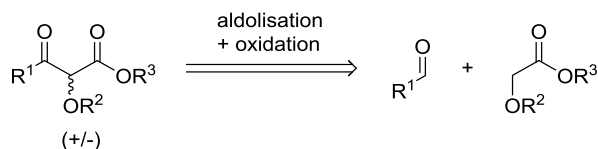
Table 24. Preparation of aryl  $\alpha$ -methoxy  $\beta$ -keto esters using method A

entry	Starting material	$\beta$ -ketoester	No.	Yields (%)
1			<b>24b</b>	38
2			<b>24c</b>	25
3			<b>24d</b>	54
4			<b>24e</b>	51
5			<b>24g</b>	43
6			<b>24h</b>	49

7			<b>24j</b>	26
8			<b>24k</b>	32
9			<b>24m</b>	29

**Method B:**

This two-step sequence involves an aldol reaction to give the corresponding  $\alpha$ -alkoxy- $\beta$ -ketoesters, followed by oxidation of the alcohol functional group to afford the desired  $\alpha$ -alkoxy- $\beta$ -ketoesters (Scheme 158).

**Scheme 158**

Following the above route, a series of  $\alpha$ -methoxy  $\beta$ -hydroxyesters were synthesized by aldol reaction between methyl methoxyacetate and a variety of aromatic aldehydes and subsequent oxidation of these compounds with 2-iodobenzoic acid (IBX) gave the corresponding  $\alpha$ -methoxy  $\beta$ -ketoesters in 26–63% yields over two steps (Scheme 155 and Table 25).

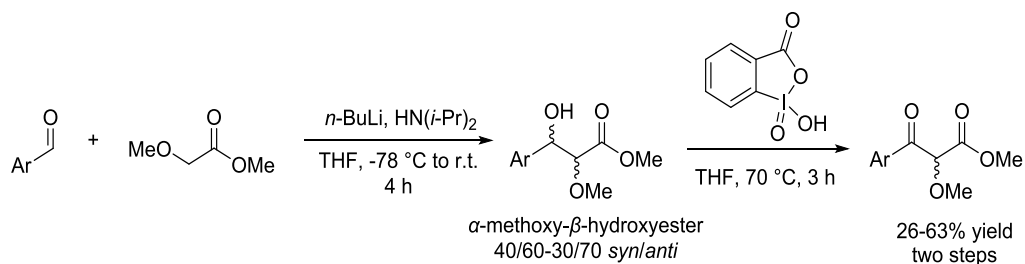
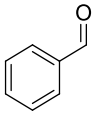
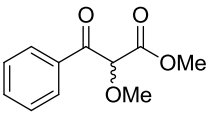
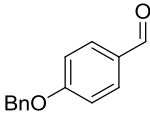
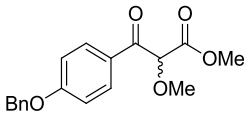
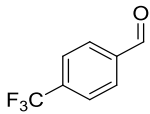
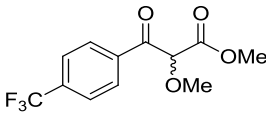
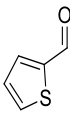
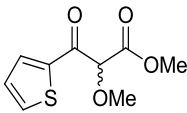
**Scheme 159**

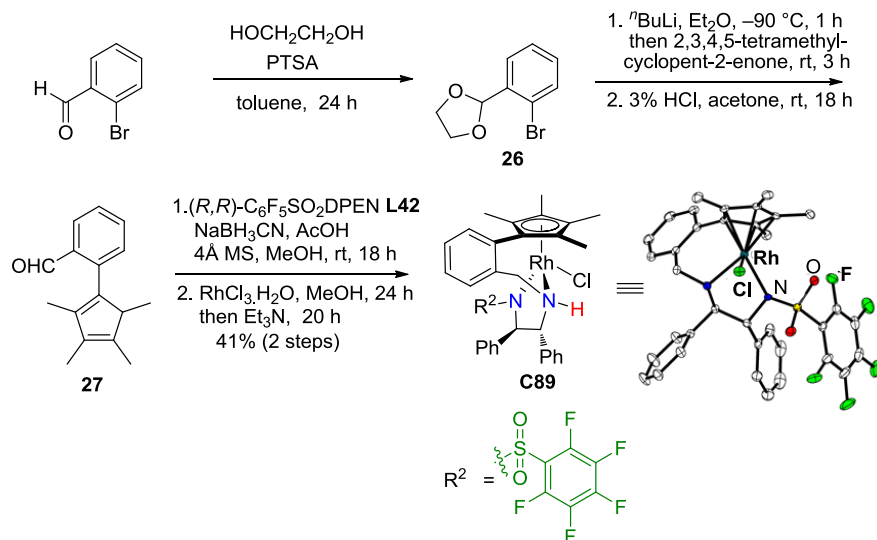
Table 25. Preparation of aryl  $\alpha$ -methoxy  $\beta$ -keto esters using method B

entry	Starting material	$\beta$ -ketoester	No.	Yields (%) 2 steps
1			<b>24a</b>	32
2			<b>24f</b>	36
3			<b>24i</b>	63
4			<b>24l</b>	26

### 1.2.2 Synthesis of a new Rh(III)-TsDPEN-based tethered complex

For this study, we have prepared and evaluated a new Rh(III)-TsDPEN-based tethered complex wherein the tosyl group has been replaced by a pentafluorobenzenesulfonyl substituent. This complex was prepared from 2-(2,3,4,5-tetramethylcyclopenta-1,3-dien-1-yl)benzaldehyde **27**, which was obtained by protection of 2-bromobenzaldehyde with glycol to 1,3-dioxolane derivative **26**, followed by treatment of compound **26** with  $n$ BuLi, and addition of 2,3,4,5-tetramethylcyclopent-2-enone to furnish the corresponding alcohol, which was then subjected to both deprotection of the aldehyde function and dehydration of the tertiary alcohol using 3% hydrochloric acid in acetone. Subsequent reductive amination using (*R,R*)-C<sub>6</sub>F<sub>5</sub>SO<sub>2</sub>DPEN **L42** in the presence of sodium cyanoborohydride then delivered the corresponding diamine. The targeted complex (*R,R*)-**C89** was then obtained through heating the latter in refluxing methanol in the presence of

rhodium(III) chloride followed by treatment with triethylamine. The new complex was isolated after flash chromatography as an orange solid and as a single diastereomer, whereas its structure was confirmed by X-ray crystallographic analysis (Scheme 160).



Scheme 160

### 1.2.3 Optimisation of the reaction conditions

#### 1.2.3.1 Influence of the precatalyst

In a previous study, our group reported that [(*S,S*)-TsDPEN-Ru(mesitylene)Cl] (*S,S*)-**C3** allowed high diastereoselectivities and excellent enantioselectivities in ATH/DKR of  $\alpha$ -alkoxy  $\beta$ -keto esters in favour of the *syn* 1,2-diol derivatives for a variety of substrates bearing diversely functionalized (hetero)aromatic and alkenyl moieties, and moderate to good enantio- and diastereo-inductions for alkyl and alkynyl substrates.<sup>239,240</sup>

Having in hand a family of in house- developed Rh(III)-complexes, we evaluated their catalytic properties for the ATH of  $\alpha$ -methoxy  $\beta$ -keto esters and compared their performances with readily available Ru(II)-complexes. We chose *rac*-**24a** as the standard substrate for this study and the ATH/DKR was run in dichloromethane at 30 °C with 0.5 mol% of the Rh or Ru complex and a HCO<sub>2</sub>H/Et<sub>3</sub>N (5:2) azeotropic mixture as the hydrogen source. Under these

<sup>239</sup> Monnereau, L.; Cartigny, D.; Scalone, M.; Ayad, T.; Ratovelomanana-Vidal, V. *Chem. Eur. J.* **2015**, *21*, 11799.

<sup>240</sup> Cartigny, D.; Püntener, K.; Ayad, T.; Scalone, M.; Ratovelomanana-Vidal, V. *Org. Lett.* **2010**, *12*, 3788.



conditions, commercially available oxo-tethered Ru(II) complex (*R,R*)-TsDENEb (*R,R*)-**C13a** afforded *syn* 1,2-diol **25a** with a good diastereoselectivity (85/15 dr, *syn/anti*) and an excellent enantioselectivity (99% ee) (Table 26, entry 1). Complex [(*S,S*)-teth-TsDPEN(RuCl)] (*S,S*)-**C7** also provided good yield (85%) and diastereoselection (70/30 dr, *syn/anti*), with a high level of enantioselectivity (97% ee) (Table 26, entry 2). Switching from tethered ruthenium to rhodium complexes allowed higher yields and diastereoselectivities whereas the enantioselectivities remained excellent and shorter reaction times were observed (Table 26, entries 3–9). When the reaction was carried out at 0 °C with complex (*R,R*)-**C86**, a longer reaction time was required with no improvement observed in terms of diastereoselectivity (88:12 dr) (Table 26, entry 4). Although all tested Rh complexes (*R,R*)-**C86-C89**, **C91**, (*R,R*)-**C11** showed comparable results in terms of yields and stereoselections (Table 26, entries 3-7 and 9), the newly prepared complex (*R,R*)-**C89** gave the highest yield (94%) and the best level of diastereoselectivity (93:7) in favor of the *syn* 1,2-diol **25a** (Table 26, entry 8). Therefore, rhodium complex (*R,R*)-**C89** was used for further screening of the reaction parameters.

Table 26. Influence of the precatalysts<sup>a</sup>

*rac*-**24a**  $\xrightarrow[\text{1 - 3 h}]{\text{Cat. (S/C = 200), HCO}_2\text{H/Et}_3\text{N (5:2), CH}_2\text{Cl}_2, 30\text{ }^\circ\text{C}}$  **25a**

Entry	Cat.	Time (h)	Yield (%) <sup>b</sup>	dr <sup>c</sup>	ee <sub>syn</sub> (%) <sup>d</sup>
1	 ( <i>R,R</i> )- <b>C13a</b>	20	85	85:15	99
2 <sup>e</sup>	 ( <i>S,S</i> )- <b>C7</b>	14	85	70:30	-97

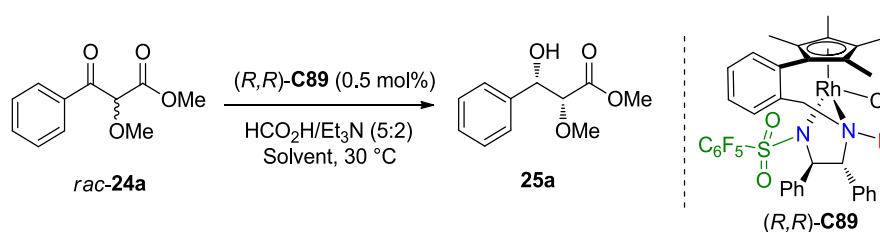
3		( <i>R,R</i> )-C86	1	91	91:9	99
4 <sup>f</sup>		( <i>R,R</i> )-C86	22	90	88:12	99
5		( <i>R,R</i> )-C87	1	89	91:9	99
6		( <i>R,R</i> )-C88	3	89	91:9	99
7		( <i>R,R</i> )-C91	3	92	89:11	99
8		( <i>R,R</i> )-C89	3	94	93:7	99
9		( <i>R,R</i> )-C11	1	89	91:9	99

<sup>a</sup> Reaction conditions: **24a** (0.8 mmol), [**Rh**] or [**Ru**] (0.5 mol%), HCO<sub>2</sub>H/Et<sub>3</sub>N (5:2) (2.0 equiv.), CH<sub>2</sub>Cl<sub>2</sub> (4.0 mL, 0.2 M), 30 °C, full conversion. <sup>b</sup> Isolated yield. <sup>c</sup> Determined by <sup>1</sup>HNMR of the crude product after the ATH reaction. <sup>d</sup> Determined by HPLC or SFC analysis using a chiral stationary phase.

### 1.2.3.2 Influence of the solvent

Using (*R,R*)-**C89** as a precatalyst, we pursued our study with the investigation of the solvent influence. The reaction was carried out at 30 °C with 0.5 mol% of complex (*R,R*)-**C89** in the presence of 2.0 equiv. of HCO<sub>2</sub>H/Et<sub>3</sub>N (5:2) as the hydrogen source. Complete conversions were observed for all the tested solvents except for acetonitrile and diisopropylether, which led to only 46% and 75% conversions, respectively (Table 27, entries 2 and 5). Toluene, isopropanol, ethyl acetate or dimethylcarbonate (DMC) gave comparable results as those obtained with dichloromethane in terms of yields or stereoselectivities (Table 27, entries 3, 4, 6, 10 vs entry 1). The reaction was also conducted in THF as a solvent at either 30 or 50 °C and a slight decrease of diastereoselectivity was observed at 50 °C. Therefore, the temperature was set at 30 °C for further optimization. (Table 27, entries 7 and 8) However, the best diastereoinductions were observed in THF and 2-MeTHF, and a high 97:3 diastereomeric ratio was attained in these solvents (Table 27, entries 7 and 9). Finally, under neat conditions, a lower 81:19 dr was obtained for the *syn* 1,2-diol **25a** (Table 27, entry 11). In view of these results, we privileged the use of 2-MeTHF as a green solvent for the remainder of the study and the optimized reaction conditions were set as follows: **24a** (0.8 mmol), complex (*R,R*)-**C89** (0.5 mol%), HCO<sub>2</sub>H/Et<sub>3</sub>N (5:2) (2.0 equiv.), 2-MeTHF (4.0 mL), 30 °C.

**Table 27. Influence of the solvent <sup>a</sup>**



Entry	Solvent	Time (h)	Conv. (%) <sup>b</sup>	Yield (%) <sup>c</sup>	dr <sup>b</sup>	ee <sub>syn</sub> (%) <sup>d</sup>
1	CH <sub>2</sub> Cl <sub>2</sub>	3	100	94	93:7	99
2	CH <sub>3</sub> CN	72	46.5	42	94:6	99

3	Toluene	6	100	88	95:5	99
4	<i>i</i> PrOH	6	100	87	94:6	99
5	<i>i</i> Pr <sub>2</sub> O	22	75	68	86:14	99
6	EtOAc	3	100	93	96:4	99
7	THF	10	100	95	97:3	99
8 <sup>e</sup>	THF	5	100	95	95:5	99
9	2-MeTHF	5	100	93	97:3	99
10	DMC <sup>f</sup>	3	100	92	95:5	99
11	neat	6	100	93	81:19	99

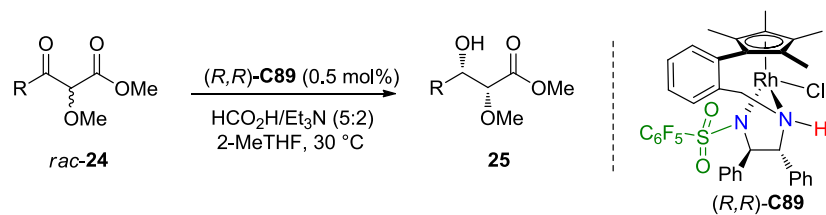
<sup>a</sup> Reaction conditions: **24a** (0.8 mmol), (*R,R*)-**C89** (0.5 mol%), HCO<sub>2</sub>H/Et<sub>3</sub>N (5:2) (2.0 equiv.), solvent (4.0 mL, 0.2 M), 30 °C, the reaction was traced by TLC. <sup>b</sup> Determined by <sup>1</sup>HNMR of the crude product after the ATH reaction. <sup>c</sup> Isolated yield. <sup>d</sup> Determined by HPLC or SFC analysis using a chiral stationary phase. <sup>e</sup> The reaction was carried out at 50 °C. <sup>f</sup> DMC = Dimethyl carbonate

## 1.2.4 Substrate scope in 2-MeTHF

### 1.2.4.1 DKR/ATH of substrates bearing electron-donating substituents

With these optimized conditions in hand, we then investigated the scope of the Rh-catalyzed ATH/DKR of  $\alpha$ -methoxy  $\beta$ -ketoesters with a series of variously substituted aryl ketones **24**. We first studied the asymmetric reduction of substrates **24b-g** having electron-donating substituents on the aromatic ring. Compounds bearing methyl, methoxy or benzyloxy substituents on the benzene core at the *ortho*, *meta* or *para* positions afforded high levels of diastereoselectivities, from 95:5 to 97:3 dr, with 88 to >99% ee values observed in all cases (Table 28, entries 2-7).

**Table 28. DKR/ATH of substrates bearing electron-donating substituents**<sup>a</sup>

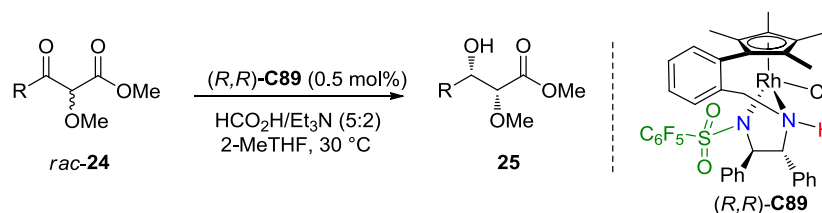
Part C: ATH of  $\alpha$ -methoxy  $\beta$ -ketoesters via dynamic kinetic resolution


Entry	Substrate	Product	Time (h)	Yield (%) <sup>b</sup>	dr ( <i>syn:anti</i> ) <sup>c</sup>	ee <sub>syn</sub> (%) <sup>d</sup>
1	<b>24a</b>	<b>25a</b>	5	93	97:3	99
2	<b>24b</b>	<b>25b</b>	7	80	97:3	>99
3	<b>24c</b>	<b>25c</b>	111	67	96:4	88
4	<b>24d</b>	<b>25d</b>	8	80	96:4	>99
5	<b>24e</b>	<b>25e</b>	45	82	96:4	>99
6	<b>24f</b>	<b>25f</b>	8	92	97:3	>99
7	<b>24g</b>	<b>25g</b>	14	83	95:5	99

<sup>a</sup> Reaction conditions: **24** (0.8 mmol),  $(R,R)\text{-C89}$  (0.5 mol%),  $\text{HCO}_2\text{H/Et}_3\text{N}$  (5:2) (2.0 equiv.), 2-MeTHF (4.0 mL, 0.2 M), 30 °C, the reaction was traced by TLC and  $^1\text{H NMR}$ . <sup>b</sup> Isolated yield. <sup>c</sup> Determined by  $^1\text{H NMR}$  of the crude product after the ATH reaction. <sup>d</sup> Determined by HPLC or SFC analysis using a chiral stationary phase.

## 1.2.4.2 DKR/ATH of substrates bearing electron-withdrawing substituents

Furthermore, substrates **24h-k** containing electron-withdrawing groups on the benzene ring such as fluoro, trifluoromethyl or bromo substituents, were investigated as well, and displayed good to high yields (68–82%), high levels of diastereocontrol (97:3 to 99:1 dr) and excellent enantioselectivities (>99% ee) (Table 29, entries 1–4).

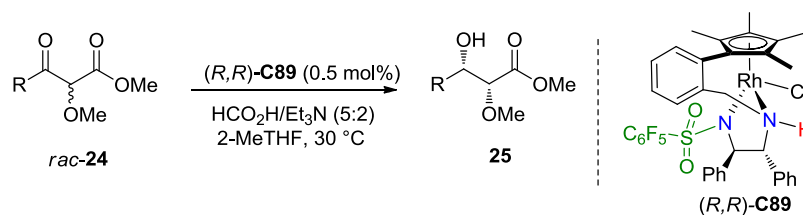
Table 29. DKR/ATH of substrates bearing electron-withdrawing substituents <sup>a</sup>

Entry	Substrate	Product	Time (h)	Yield (%) <sup>b</sup>	dr ( <i>syn:anti</i> ) <sup>c</sup>	ee <sub>syn</sub> (%) <sup>d</sup>
1	<b>24h</b>	<b>25h</b>	7	68	98:2	>99
2	<b>24i</b>	<b>25i</b>	8	80	97:3	>99
3	<b>24j</b>	<b>25j</b>	22	82	97:3	>99
4	<b>24k</b>	<b>25k</b>	8	68	99:1 <sup>d</sup>	>99

<sup>a</sup> Reaction conditions: **24** (0.8 mmol), **(R,R)-C89** (0.5 mol%), HCO<sub>2</sub>H/Et<sub>3</sub>N (5:2) (2.0 equiv.), 2-MeTHF (4.0 mL, 0.2 M), 30 °C, the reaction was traced by TLC and <sup>1</sup>H NMR. <sup>b</sup> Isolated yield. <sup>c</sup> Determined by <sup>1</sup>H NMR of the crude product after the ATH reaction. <sup>d</sup> Determined by HPLC or SFC analysis using a chiral stationary phase.

## 1.2.4.3 DKR/ATH of substrates bearing heteroaryl substituents

Interestingly, investigation of heteroaromatic substrates **24l-m** resulted in almost perfect diastereoselectivities (99:1 dr) and excellent *syn* enantioselectivities (Table 30, entries 1-2).

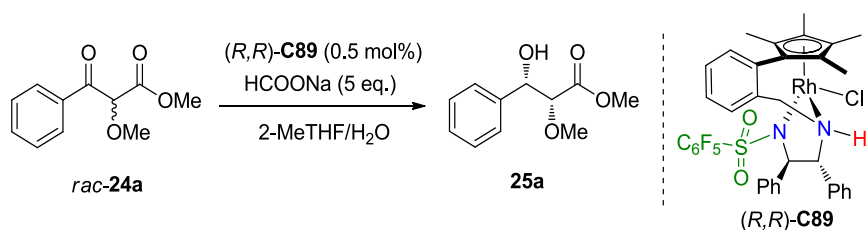
Table 30. DKR/ATH of substrates bearing heteroaryl substituents <sup>a</sup>

Entry	Substrate	Product	Time (h)	Yield (%) <sup>b</sup>	dr ( <i>syn:anti</i> ) <sup>c</sup>	ee <sub>syn</sub> (%) <sup>d</sup>	
1	<b>24l</b>		<b>25l</b>	14	91	>99:1	>99
2	<b>24m</b>		<b>25m</b>	10	86	99:1	>99

<sup>a</sup> Reaction conditions: **24** (0.8 mmol), (R,R)-C89 (0.5 mol%), HCO<sub>2</sub>H/Et<sub>3</sub>N (5:2) (2.0 equiv.), 2-MeTHF (4.0 mL, 0.2 M), 30 °C, the reaction was traced by TLC and <sup>1</sup>H NMR. <sup>b</sup> Isolated yield. <sup>c</sup> Determined by <sup>1</sup>H NMR of the crude product after the ATH reaction. <sup>d</sup> Determined by HPLC or SFC analysis using a chiral stationary phase.

## 1.2.5 Optimisation of the reaction conditions in water

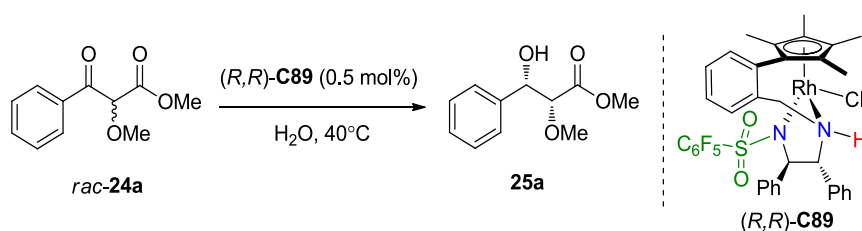
Aiming at ever greener procedures, we next sought to perform the reaction in aqueous media. First, we chose to use a 1:3 mixture of 2-MeTHF/H<sub>2</sub>O with sodium formate as the hydrogen source, however these conditions did not allow a complete conversion (58% yield) (Table 31, entry 1). Addition of 0.2 equiv of CTAB (cetyltrimethylammonium bromide) as a surfactant resulted in 82% yield of **25a** (Table 31, entry 2). A higher yield of 90% could be reached when switching the reaction temperature from 30 °C to 40 °C (Table 31, entry 3), whereas increasing the amount of water in the solvent mixture (from 2-MeTHF/H<sub>2</sub>O 1:3 to 1:6) had no significant effect (Table 31, entry 4).

Table 31. Optimisation of the reaction conditions in water <sup>a</sup>

Entry	2-MeTHF/H <sub>2</sub> O (V/V)	additive	Temp. °C	yield (%) <sup>b</sup>	dr ( <i>syn:anti</i> ) <sup>c</sup>	ee <sub>syn</sub> (%) <sup>d</sup>
1	1:3	--	30	58	99:1	99
2	1:3	CTAB	30	82	99:1	99
3	1:3	CTAB	40	90	98:2	99
4	1:6	CTAB	40	90	98:2	99

<sup>a</sup> Reaction conditions: **24a** (0.8 mmol), (*R,R*)-**C89** (0.5 mol%), HCO<sub>2</sub>Na (8.0 equiv.), 2-MeTHF/H<sub>2</sub>O (4.0 mL, 0.2 M), the reaction was traced by TLC and <sup>1</sup>H NMR. <sup>b</sup> Isolated yield. <sup>c</sup> Determined by <sup>1</sup>H NMR of the crude product after the ATH reaction. <sup>d</sup> Determined by HPLC or SFC analysis using a chiral stationary phase.

Since the reaction proceeded satisfyingly in the presence of water, we next performed the reaction in water alone as a solvent under otherwise identical conditions (Figure 10). In that case, a lower yield was obtained (84%), however, we found the amount of sodium formate to be essential for the asymmetric reduction, because decreasing the amount to 5.0 equiv provided a high yield of 92% whereas the use of 3 equiv afforded **25a** in only 83% yield. On the other hand, incomplete conversions were observed when SDS (sodium dodecyl sulfate) was used as a surfactant, or when ammonium formate acted as the hydrogen source. From these results, the optimized reaction conditions were set as follows: **25a**, (*R,R*)-**C89** (S/C 200), HCO<sub>2</sub>Na (5.0 equiv), H<sub>2</sub>O, CTAB (0.2 equiv), 40 °C.





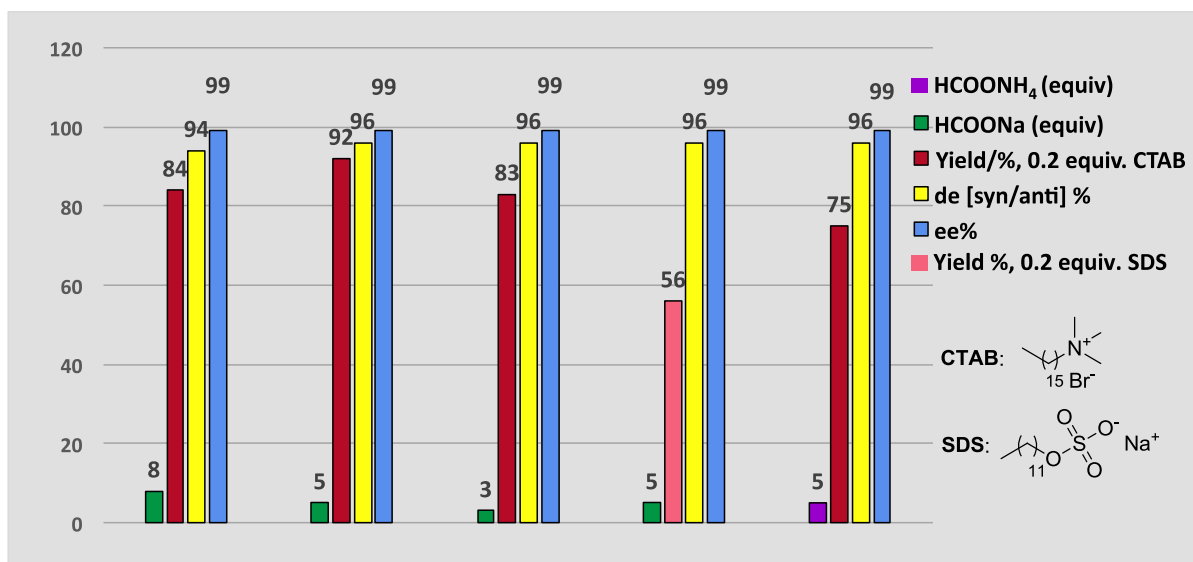


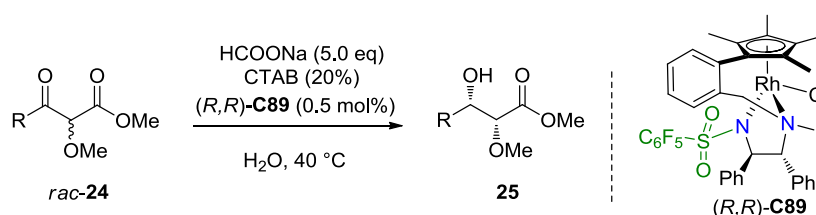
Figure 10. Optimization of the reaction conditions in water at 40 °C with (R,R)-C89

## 1.2.6 Substrate scope in water

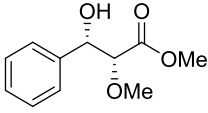
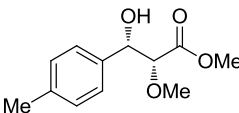
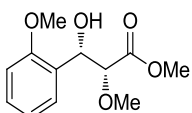
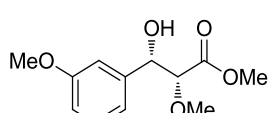
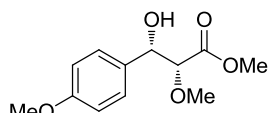
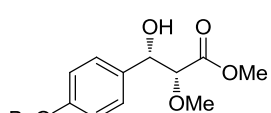
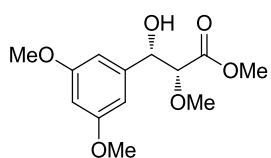
### 1.2.6.1 DKR/ATH of substrates bearing electron-donating substituents

With these optimized conditions in hand, we then investigated the scope of the Rh-catalyzed ATH/DKR of  $\alpha$ -methoxy  $\beta$ -ketoesters with a series of variously substituted aryl ketones **24b-m**. We first studied the asymmetric reduction of substrates **24b-g** having electron-donating substituents on the aromatic ring. Compounds bearing methyl, methoxy or benzyloxy substituents on the benzene core at the *ortho*, *meta* or *para* positions afforded high levels of diastereoselectivities, from 96:4 to 98:2 dr, with excellent ee values (> 99%) observed in all cases (Table 32, entries 2-6). Substrate **24g** with dimethoxy substituents on the benzene core also gave a good yield (80%), high diastereoselectivity (96:4) and good enantioselectivity (> 99%) (Table 32, entry 7).

Table 32. DKR/ATH of substrates bearing electron-donating substituents in water <sup>a</sup>



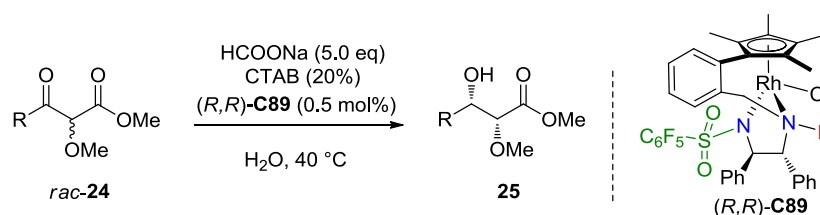
Entry	Substrate	Product	Time	Yield	dr	ee <sub>syn</sub>
-------	-----------	---------	------	-------	----	-------------------

				(h)	(%) <sup>b</sup>	( <i>syn:anti</i> ) <sup>c</sup>	(%) <sup>d</sup>
1	<b>24a</b>		<b>25a</b>	4	92	98:2	>99
2	<b>24b</b>		<b>25b</b>	6	84	97:3	>99
3	<b>24c</b>		<b>25c</b>	5	81	98:2	>99
4	<b>24d</b>		<b>25d</b>	6	83	97:3	>99
5	<b>24e</b>		<b>25e</b>	6	85	96:4	>99
6	<b>24f</b>		<b>25f</b>	24	93	98:2	>99
7	<b>24g</b>		<b>25g</b>	27	80	96:4	>99

<sup>a</sup> Reaction conditions: **24** (0.6 mmol), (*R,R*)-**C89** (0.5 mol%), HCO<sub>2</sub>Na (5.0 equiv), H<sub>2</sub>O (1.5 mL), CTAB (0.2 equiv), 40 °C, the reaction was traced by TLC and <sup>1</sup>H NMR. <sup>b</sup> Isolated yield. <sup>c</sup> Determined by <sup>1</sup>H NMR of the crude product after the ATH reaction. <sup>d</sup> Determined by HPLC or SFC analysis using a chiral stationary phase.

### 1.2.6.2 DKR/ATH of substrates bearing electron-withdrawing substituents

Substrates **24h–k** containing electron-withdrawing groups on the aryl ring such as fluoro, trifluoromethyl or bromo substituents, were investigated as well, and displayed good to high yields (73–97%), high levels of diastereocontrol (95:5 to 98:2 dr) and excellent enantioselectivities (> 99% ee) (Table 33).

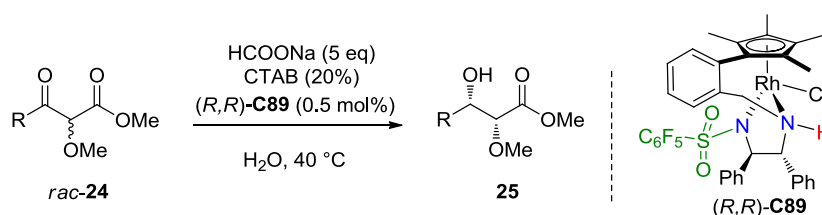
**Table 33. DKR/ATH of substrates bearing electron-withdrawing substituents in water<sup>a</sup>**

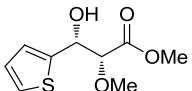
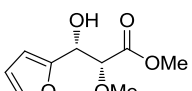
Entry	Substrate	Product	Time (h)	Yield (%) <sup>b</sup>	dr ( <i>syn:anti</i> ) <sup>c</sup>	ee <sub>syn</sub> (%) <sup>d</sup>	
1	<b>24h</b>		<b>25h</b>	6	73	98:2	>99
2	<b>24i</b>		<b>25i</b>	24	89	95:5	>99
3	<b>24j</b>		<b>25j</b>	4	82	96:4	>99
4	<b>24k</b>		<b>25k</b>	4	93	96:4	>99

<sup>a</sup> Reaction conditions: **24** (0.6 mmol), (*R,R*)-**C89** (0.5 mol%), HCO<sub>2</sub>Na (5.0 equiv), H<sub>2</sub>O (1.5 mL), CTAB (0.2 equiv), 40 °C, the reaction was traced by TLC and <sup>1</sup>H NMR. <sup>b</sup> Isolated yield. <sup>c</sup> Determined by <sup>1</sup>H NMR of the crude product after the ATH reaction. <sup>d</sup> Determined by HPLC or SFC analysis using a chiral stationary phase.

### 1.2.6.3 DKR/ATH of heteroaromatic substrates

Interestingly, investigation of heteroaromatic substrates **24k-l** resulted in good yields (88% and 98%), almost perfect *syn* diastereoselectivities (> 99:1 dr) and excellent enantioselectivities (> 99% ee) (Table 34).

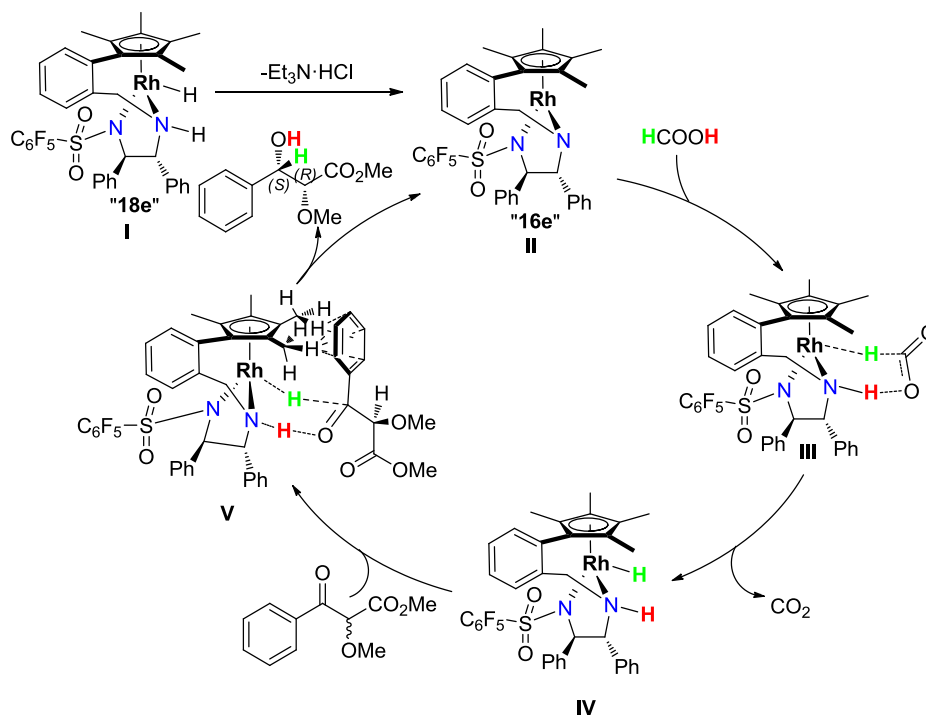
**Table 34. DKR/ATH of substrates bearing heteroaryl substituents in water<sup>a</sup>**

Entry	Substrate	Product	Time (h)	Yield (%) <sup>b</sup>	dr ( <i>syn:anti</i> ) <sup>c</sup>	<i>ee</i> <sub>syn</sub> (%) <sup>d</sup>	
1	<b>24l</b>		<b>25l</b>	6	88	>99:1	>99
2	<b>24m</b>		<b>25m</b>	4	98	>99:1	>99

<sup>a</sup> Reaction conditions: **24** (0.6 mmol), (*R,R*)-**C89** (0.5 mol%), HCO<sub>2</sub>Na (5.0 equiv), H<sub>2</sub>O (1.5 mL), CTAB (0.2 equiv), 40 °C, the reaction was traced by TLC and <sup>1</sup>H NMR. <sup>b</sup> Isolated yield. <sup>c</sup> Determined by <sup>1</sup>H NMR of the crude product after the ATH reaction. <sup>d</sup> Determined by HPLC or SFC analysis using a chiral stationary phase.

### 1.2.7 Mechanism

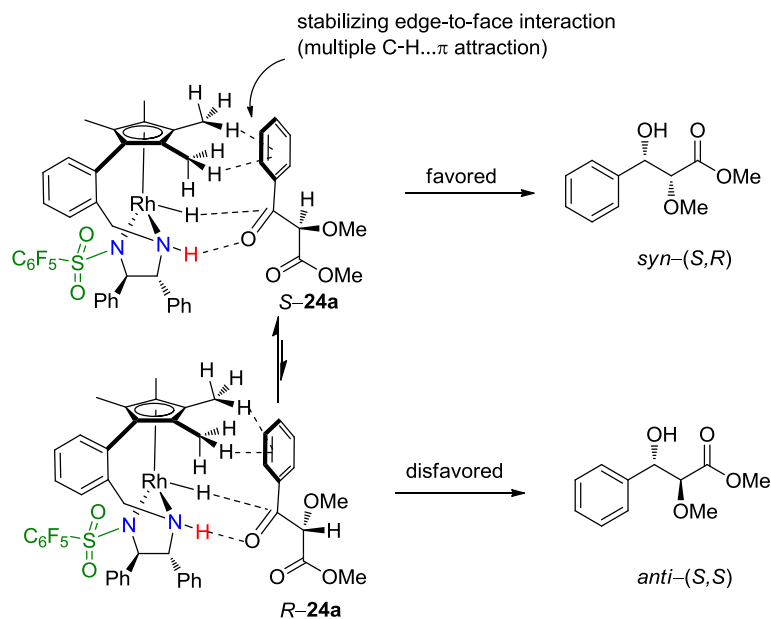
Based on the mechanism proposed for the ATH of ketones using Noyori's ruthenium complex,<sup>63</sup> we assumed the mechanism of these tethered rhodium complexes in the asymmetric transfer hydrogenation of ketones was as follows: first, a chiral unsaturated 16-electron amido rhodium complex **II** is formed by elimination of HCl from complex **I**. Then, the rhodium complex **II** readily reacts with HCOOH to give the corresponding formate complex **III**, which subsequently undergoes decarboxylation leading to the chiral hydrido-amine complex **IV** and CO<sub>2</sub>. This chiral hydrido rhodium complex **IV** readily reacts with ketonic substrates to provide optically active alcohols with regeneration of the amide complex **II** through transition state **V** showing N–H···O hydrogen-bonding interaction, Rh–H···C interaction, and C–H··· $\pi$  interaction between Cp\* ring and ketone aryl substituent (Scheme 161).



Scheme 161

### 1.2.8 Origin of enantioselectivity and diastereoselectivity

It is well-established that the enantiocontrol of the ATH reaction is governed by the attractive  $\text{CH}/\pi$  electrostatic interaction between the  $\eta^5$ -arene ligand and the ketone aryl group. Of the two transition states presenting this stabilizing edge-to-face interaction, the one leading to the *syn* isomer is favored because it does not show unfavorable steric interactions (Scheme 162).



Scheme 162

### 1.3 Conclusion

In summary, a new tethered Rh complex **C89** containing a penta-fluorobenzenesulfonyl diphenylethylenediamine ligand was prepared and characterized by X-ray crystallographic analysis. The novel fully characterized Rh-complex is not sensitive to water or air. Evaluation of the catalytic performances of this complex was carried out through DKR/ATH of  $\alpha$ -alkoxy  $\beta$ -keto esters.

A variety of enantioenriched monodifferentiated *syn* 1,2-diols was obtained with high yields (up to 93%), high levels of diastereoselectivities (up to > 99:1), and excellent ee values (up to > 99%) using this new complex with HCO<sub>2</sub>H/Et<sub>3</sub>N (5:2) at a low catalyst loading in an environmentally friendly solvent, 2-MeTHF.

This catalytic atom-economical ATH reaction proceeds equally well in water in high yields (up to 98%), high levels of diastereoselection (up to >99:1), and excellent ee values (up to >99%) through a dynamic kinetic resolution process.<sup>243</sup>



# **GENERAL CONCLUSION**



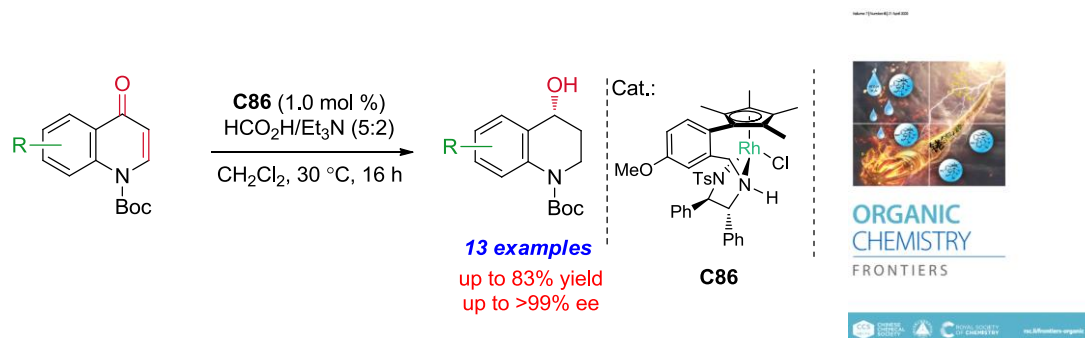




## General conclusion

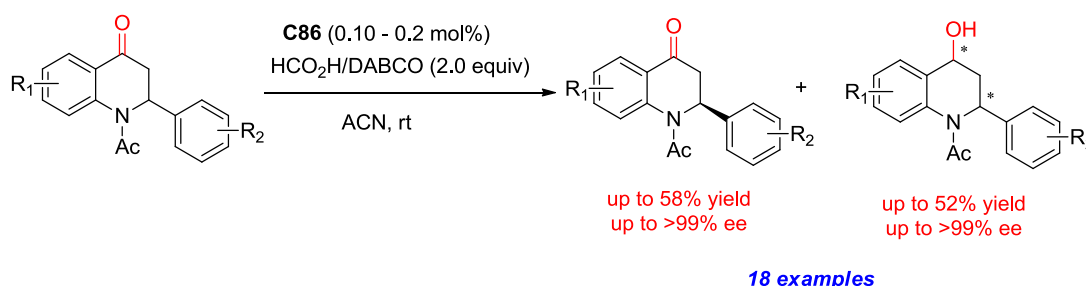
This manuscript presents the development of catalytic efficient methods to access enantioenriched functionalized alcohols such as chiral functionalized heterocycles and  $\alpha$ -methoxy  $\beta$ -hydroxyesters, using Rh-catalyzed asymmetric transfer hydrogenation (ATH) reactions combined or not with a dynamic kinetic resolution (DKR) process.

4-Quinolone derivatives were conveniently reduced to the corresponding 1,2,3,4-tetrahydroquinoline-4-ols with excellent enantioselectivities through Rh-catalyzed asymmetric transfer hydrogenation using  $\text{HCO}_2\text{H}/\text{Et}_3\text{N}$  (5:2) as the hydrogen source and the home-made complex **C86** under mild conditions (Scheme 163).<sup>241</sup>



**Scheme 163**

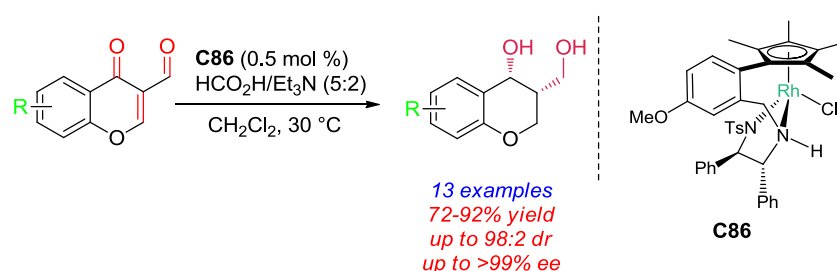
Then the home-made Rh complex **C86** was also successfully used in the asymmetric transfer hydrogenation of 2-aryl tetrahydro-4-quinolone derivatives through kinetic resolution. The reaction was catalyzed by 0.1 mol%-0.2 mol% of the Rh catalyst with  $\text{CH}_3\text{CN}$  as a solvent at room temperature. The chiral 2-aryl tetrahydro-4-quinolones and the corresponding alcohols were obtained with good isolated yields and high enantioselectivities (Scheme 164).



**Scheme 164**

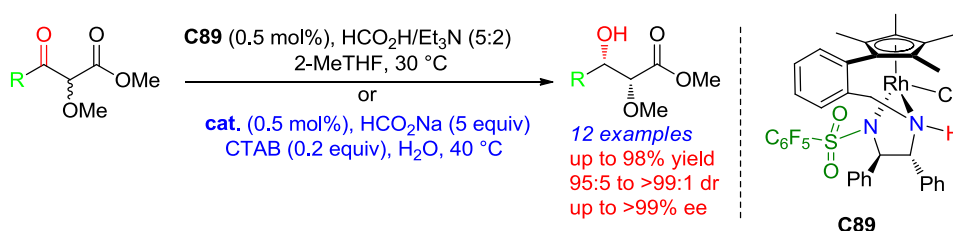
<sup>241</sup> He, B.; Phansavath, P.; Ratovelomanana-Vidal, V. *Org. Chem. Front.* **2020**, *7*, 975.

Moreover, the Rh-catalyst was successfully utilized to provide enantioenriched cis-3-(hydroxymethyl)-chroman-4-ol derivatives. The target compounds were prepared by asymmetric transfer hydrogenation of 3-formylchromones through a dynamic kinetic resolution process. The reaction proceeded under mild conditions using a low catalyst loading and HCO<sub>2</sub>H/Et<sub>3</sub>N (5:2) as the hydrogen source, delivering the reduced compounds in good yields, high diastereomeric ratios (up to 98:2 dr), and excellent enantioselectivities (up to >99% ee) (Scheme 165).<sup>242</sup>



Scheme 165

Finally, a new tethered Rh(III)/Cp\* complex **C89** containing a pentafluorobenzenesulfonyl-DPEN ligand was evaluated in the asymmetric transfer hydrogenation of  $\alpha$ -methoxy  $\beta$ -ketoesters. The reaction was efficiently carried out under sustainable reaction conditions in 2-MeTHF with formic acid/triethylamine or in water with sodium formate and accommodated a range of substrates. The corresponding syn  $\alpha$ -methoxy  $\beta$ -hydroxyesters were obtained with high diastereoselectivities (up to >99:1 dr) and excellent enantioinductions (up to >99:1 er) via a dynamic kinetic resolution process (Scheme 166)<sup>243</sup>.



Scheme 166

In all cases, the rhodium complexes developed in the laboratory have demonstrated efficient catalytic properties for the synthesis of chiral nitrogen- and oxygen containing

<sup>242</sup> He, B.; Phansavath, P.; Ratovelomanana-Vidal, V. *Org. Lett.* **2019**, *21*, 3276.

<sup>243</sup> He, B.; Zheng, L.-S.; Phansavath, P.; Ratovelomanana-Vidal, V. *ChemSusChem.* **2019**, *12*, 3032.

heterocycles and to access highly functionalized  $\alpha$ -methoxy  $\beta$ -hydroxy esters as well with excellent stereoselectivities.



# **EXPERIMENTAL PART**







## Experimental part

### 1. General informations

#### 1.1 Purification of solvents and reagents

All reactions were performed under an atmosphere of argon. Reaction vessels were oven-dried, cooled under vacuum and flushed with argon before use.

Petroleum ether, ethyl acetate and toluene used for column chromatography were distilled under reduced pressure. THF, Et<sub>2</sub>O, CH<sub>2</sub>H<sub>2</sub>, toluene and DMF were dried over alumina columns in a solvent purification apparatus (Innovative Technologies). HPLC grade methanol and ethanol, and reagent grade hexane and cyclohexane were purchased and used without further purification. Every reagent was either purified following the methods described in the literature,<sup>244</sup> or used without further purification.

#### 1.2 Chromatography

Reactions were monitored by thin layer chromatography (TLC) using commercial silica-gel plates (Merck 60 F254). Spots were detected with UV light (254 nm) and revealed with KMnO<sub>4</sub>, Kagi-Mosher or Ninhydrin stain.<sup>245</sup> VWR Silica Gel 60 (40-63 μm) was employed for flash column chromatography using Still's method.<sup>246</sup>

#### 1.3 Analysis

Proton nuclear magnetic resonance (<sup>1</sup>H NMR) spectra were recorded using a Bruker AVANCE 300 (300 MHz) or a Bruker AVANCE 400 (400 MHz). Chemical shifts are reported in delta (δ) units part per million (ppm) relative to residual protiated solvent (7.26 ppm for CDCl<sub>3</sub>, 2.50 ppm for *d*<sub>6</sub>-DMSO, 7.16 ppm for C<sub>6</sub>D<sub>6</sub>, 2.05 ppm for acetone-*d*<sub>6</sub>). Coupling constants are reported in Hertz (Hz). The following abbreviations are used: s = singlet, d = doublet, t = triplet, q = quartet, m = multiplet, brs = broad singlet, brd = broad doublet. Carbon-13 nuclear magnetic resonance (<sup>13</sup>C NMR) spectra were recorded using a Bruker

---

<sup>244</sup> Perrin, D. D.; Armarego, W. L. F. *Purification of laboratory chemicals*, Third Edition, Pergamon Press, Oxford, 1988.

<sup>245</sup> KMnO<sub>4</sub> : Purple solution composed of potassium permanganate (1.5 g), potassium carbonate (10 g), NaOH (1.25 mL, 10wt%) and water (200 mL). Kagi-Mosher solution : rose red solution composed of *p*-anisaldehyde (3.7 mL), concentrated sulfuric acid (5 mL) in ethanol (135 mL). Ninhydrin solution : pale yellow solution composed of ninhydrin (1.5 g), *n*-butanol (100 mL) and acetic acid (3.0 mL).

<sup>246</sup> Still, W.; Kahn, M.; Mitra, A. *J. Org. Chem.* **1978**, *43*, 2923

AVANCE 300 (101 MHz) or a Bruker AVANCE 400 (101 MHz). Chemical shifts are reported in delta ( $\delta$ ) units part per million (ppm) relative to the centre line of the triplet at 77.16 ppm for  $\text{CDCl}_3$ , the centre line of the septuplet at 39.52 ppm for  $d_6$ -DMSO, the centre line at 128.06 ppm for  $\text{C}_6\text{D}_6$ , the signal at 29.8 ppm for acetone- $d_6$ .  $^{13}\text{C}$  NMR experiments were routinely run with broadband decoupling. Fluorine-19 nuclear magnetic resonance ( $^{19}\text{F}$  NMR) was recorded using a Bruker AVANCE 300 (282 MHz) or a Bruker AVANCE 400 (376 MHz)

Mass spectra were recorded at the mass spectrometry laboratory in Chimie ParisTech using a Nermag R10-10C apparatus for chemical ionisation (CI) or electronic impact (EI), and API 3000 PE Sciex apparatus for electrospray (ESI) measurements. HRMS analyses were performed at the Sorbonne Université using a LTQ-Orbitrap (Thermo Fisher Scientific) apparatus.

Optical rotations were measured at 25 °C on a Perkin-Elmer 241 Polarimeter using a sodium lamp (589 nm) with spectrophotometric grade chloroform as a solvent.

Supercritical Fluid Chromatography (SFC) measurements were run on a Berger Instruments apparatus equipped with chiral stationary phase Daicel Chiralcel OD-H and Chiralpak IA, IC, ID, AD-H and AS-H columns. HPLC grade methanol or isopropanol were used as a polar modifier. High Performance Liquid Chromatography (HPLC) measurements were run on a Waters Instruments apparatus equipped with Chiralpak IA, IB, IC, ID, IE columns. HPLC grade hexane and isopropanol were used as eluents.

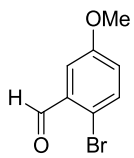
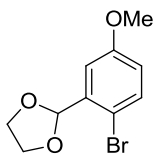
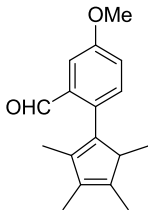
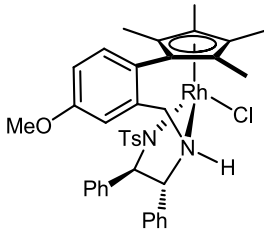
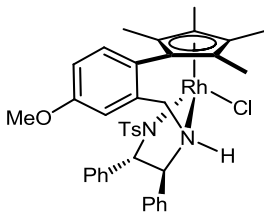
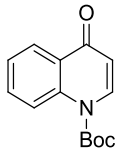
Melting point values were recorded on a Kofler bench.

X-ray diffraction studies were performed in the X-ray facility at the Sorbonne Université using a Bruker AXS Kapa-APEX II apparatus with a Cu source for absolute configuration determination.

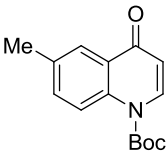
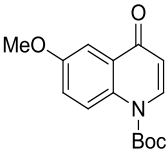
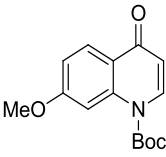
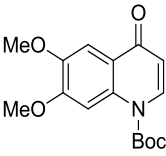
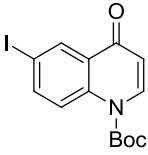
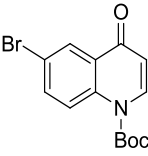
## **2. Description of the synthesized products**

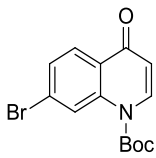
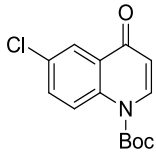
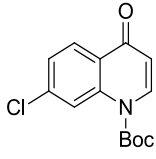
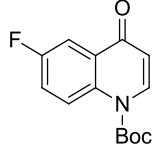
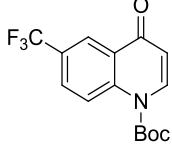
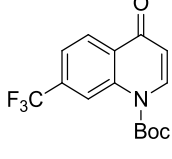
### **2.1 Index of the synthesized products**

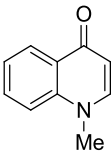
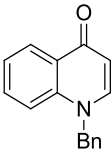
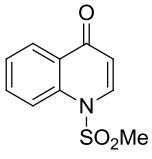
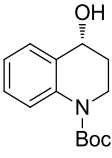
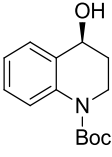
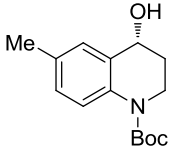
<b>No.</b>	<b>Structure</b>	<b>Page</b>
------------	------------------	-------------

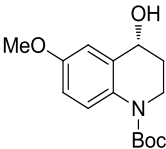
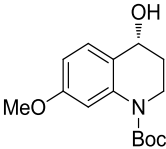
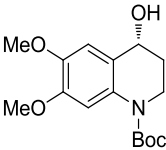
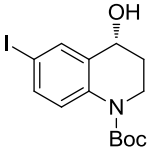
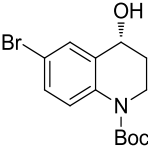
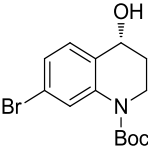
1		124
2		124
3		124
<i>(R,R)</i> -C86		124
<i>(S,S)</i> -C86		124
4g		125

Experimental part

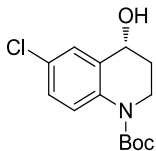
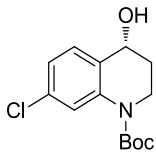
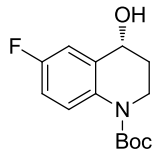
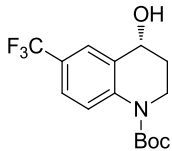
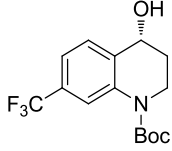
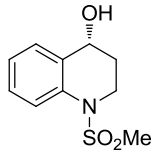
<p><b>4g</b></p>		<p>125</p>
<p><b>4h</b></p>		<p>125</p>
<p><b>4h</b></p>		<p>125</p>
<p><b>4i</b></p>		<p>125</p>
<p><b>4i</b></p>		<p>126</p>
<p><b>4j</b></p>		<p>126</p>

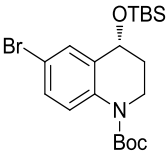
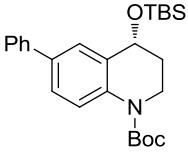
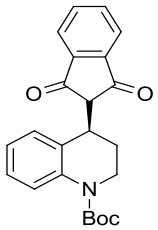
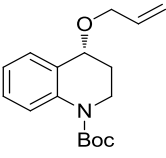
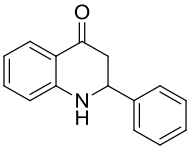
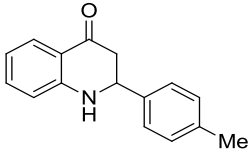
4j	 <chem>O=C1C=CC(=O)N1c2ccc(Br)cc2</chem>	126
4l	 <chem>O=C1C=CC(=O)N1c2ccc(Cl)cc2</chem>	126
4l	 <chem>O=C1C=CC(=O)N1c2ccc(Cl)cc2</chem>	126
4m	 <chem>O=C1C=CC(=O)N1c2ccc(F)cc2</chem>	126
4m	 <chem>O=C1C=CC(=O)N1c2ccc(C(F)(F)F)cc2</chem>	126
4n	 <chem>O=C1C=CC(=O)N1c2ccc(C(F)(F)F)cc2</chem>	126

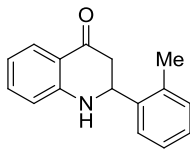
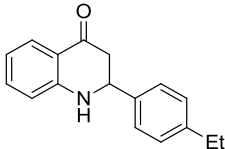
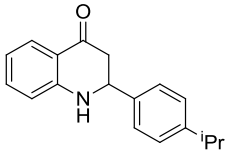
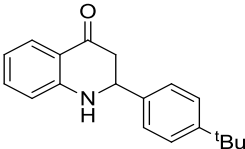
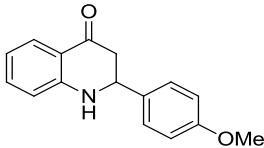
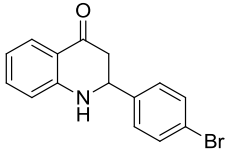
<p><b>4o</b></p>		<p>130</p>
<p><b>4p</b></p>		<p>130</p>
<p><b>4q</b></p>		<p>131</p>
<p><b>5a</b></p>		<p>131</p>
<p><b>5a'</b></p>		<p>135</p>
<p><b>5b</b></p>		<p>131</p>

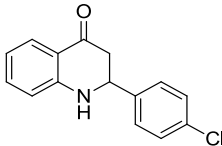
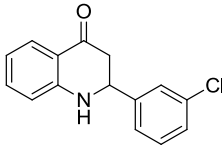
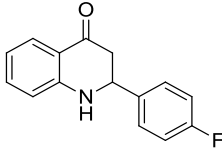
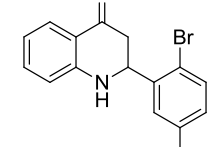
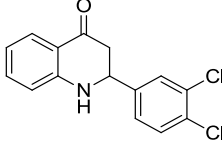
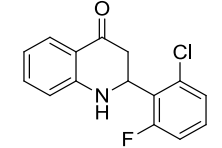
<b>5c</b>		132
<b>5d</b>		132
<b>5e</b>		132
<b>5f</b>		132
<b>5g</b>		132
<b>5h</b>		133

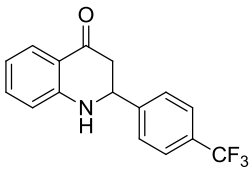
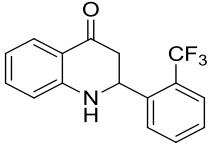
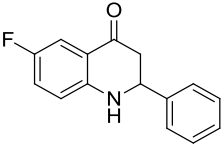
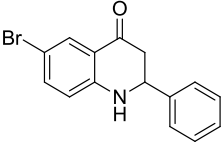
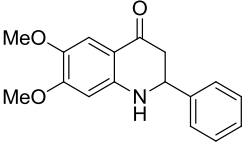
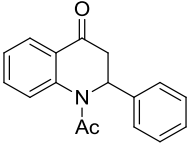


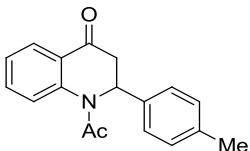
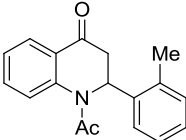
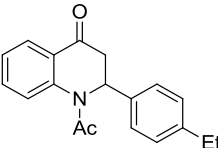
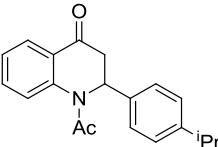
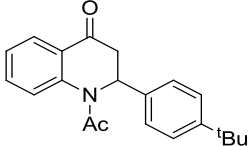
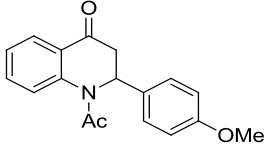
<p><b>5i</b></p>		<p>133</p>
<p><b>5j</b></p>		<p>133</p>
<p><b>5k</b></p>		<p>133</p>
<p><b>5l</b></p>		<p>133</p>
<p><b>5m</b></p>		<p>133</p>
<p><b>5p</b></p>		<p>131</p>

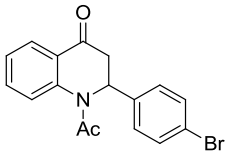
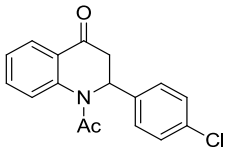
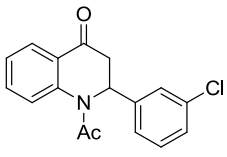
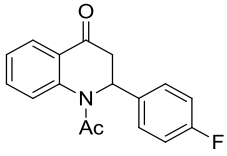
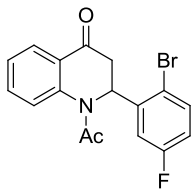
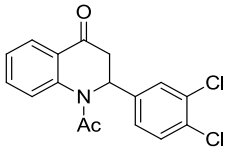
6		134
7		134
8		135
9		135
10a		141
10b		141

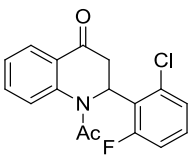
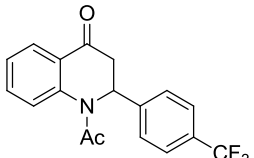
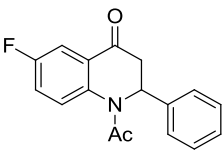
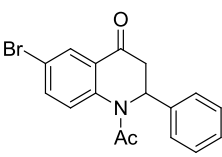
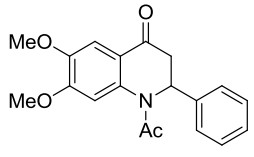
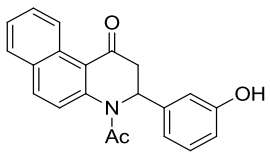
<p><b>10c</b></p>		<p>141</p>
<p><b>10d</b></p>		<p>141</p>
<p><b>10e</b></p>		<p>141</p>
<p><b>10f</b></p>		<p>141</p>
<p><b>10g</b></p>		<p>141</p>
<p><b>10h</b></p>		<p>141</p>

<b>10i</b>	 <chem>O=C1Nc2ccccc2C1c3ccc(Cl)cc3</chem>	141
<b>10j</b>	 <chem>O=C1Nc2ccccc2C1c3ccc(Cl)cc3</chem>	141
<b>10k</b>	 <chem>O=C1Nc2ccccc2C1c3ccc(F)cc3</chem>	141
<b>10l</b>	 <chem>O=C1Nc2ccccc2C1c3cc(F)ccc3Br</chem>	141
<b>10m</b>	 <chem>O=C1Nc2ccccc2C1c3cc(Cl)cc(Cl)c3</chem>	141
<b>10n</b>	 <chem>O=C1Nc2ccccc2C1c3cc(F)ccc3Cl</chem>	141

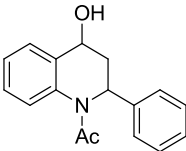
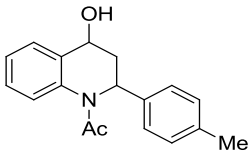
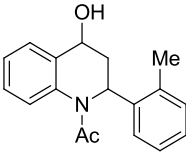
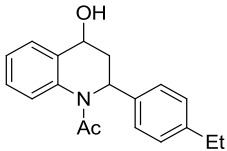
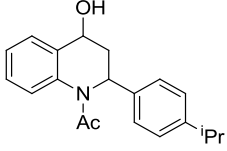
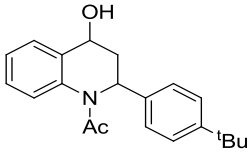
<p><b>10o</b></p>		<p>141</p>
<p><b>10p</b></p>		<p>141</p>
<p><b>10q</b></p>		<p>141</p>
<p><b>10r</b></p>		<p>141</p>
<p><b>10s</b></p>		<p>141</p>
<p><b>12a</b></p>		<p>144</p>

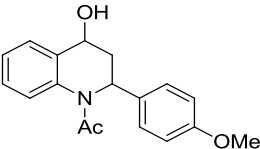
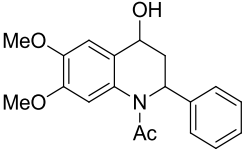
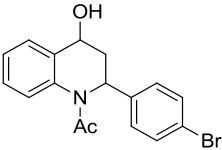
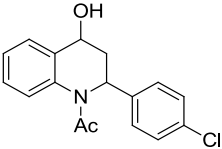
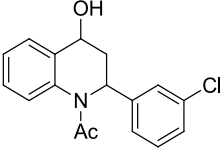
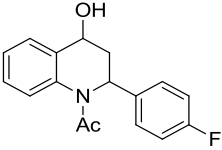
12b	 <chem>CC(=O)N1Cc2ccccc2C1c3ccc(C)cc3</chem>	144
12c	 <chem>CC(=O)N1Cc2ccccc2C1c3cccc(C)c3</chem>	144
12d	 <chem>CC(=O)N1Cc2ccccc2C1c3ccc(CC)cc3</chem>	144
12e	 <chem>CC(=O)N1Cc2ccccc2C1c3ccc(C(C)C)cc3</chem>	144
12f	 <chem>CC(=O)N1Cc2ccccc2C1c3ccc(C(C)(C)C)cc3</chem>	144
12g	 <chem>CC(=O)N1Cc2ccccc2C1c3ccc(OC)cc3</chem>	144

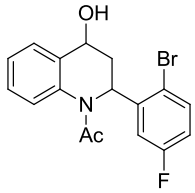
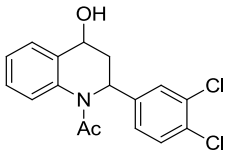
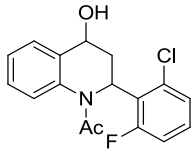
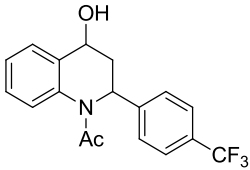
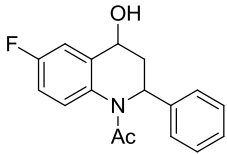
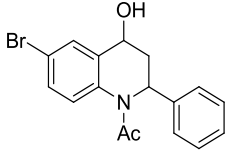
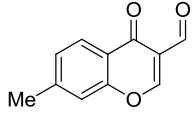
<p><b>12h</b></p>		<p>144</p>
<p><b>12i</b></p>		<p>144</p>
<p><b>12j</b></p>		<p>144</p>
<p><b>12k</b></p>		<p>144</p>
<p><b>12l</b></p>		<p>144</p>
<p><b>12m</b></p>		<p>144</p>

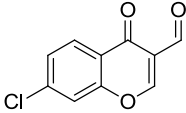
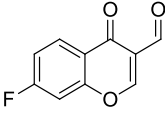
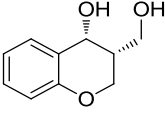
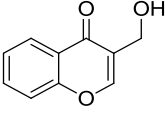
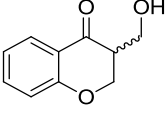
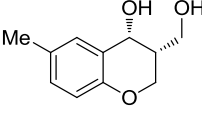
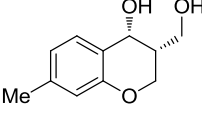
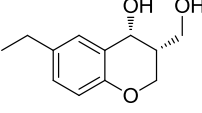
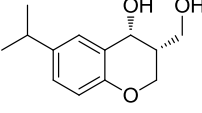
12n		144
12o		144
12q		144
12r		144
12s		144
12t		144

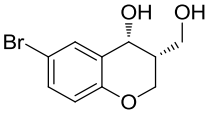
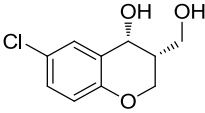
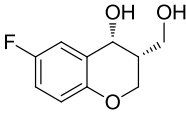
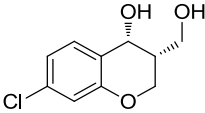
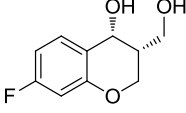
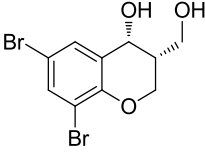


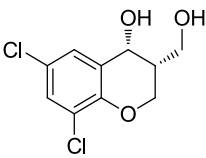
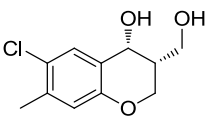
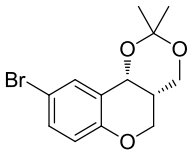
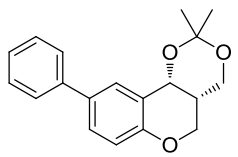
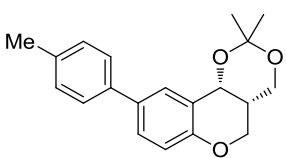
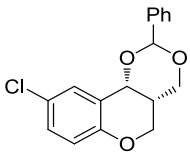
<p><b>13a</b></p>		<p>148</p>
<p><b>13b</b></p>		<p>148</p>
<p><b>13c</b></p>		<p>149</p>
<p><b>13d</b></p>		<p>149</p>
<p><b>13e</b></p>		<p>149</p>
<p><b>13f</b></p>		<p>149</p>

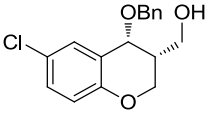
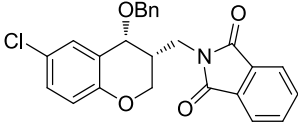
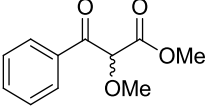
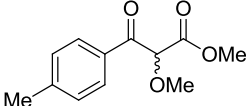
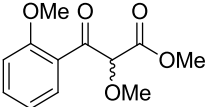
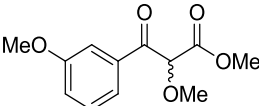
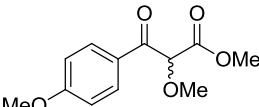
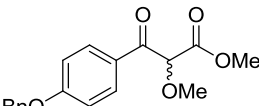
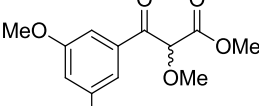
<b>13g</b>		149
<b>13s</b>		149
<b>13h</b>		150
<b>13i</b>		150
<b>13j</b>		151
<b>13k</b>		151

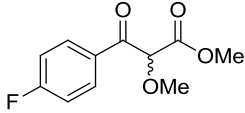
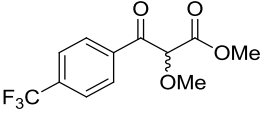
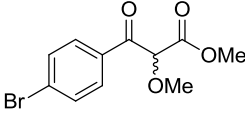
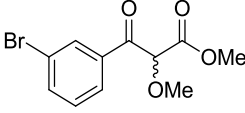
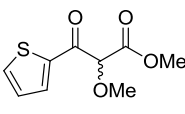
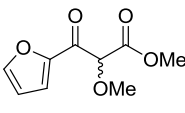
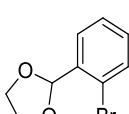
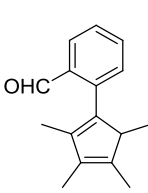
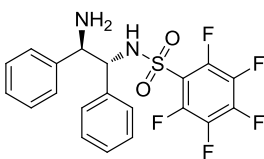
<p><b>13l</b></p>		<p>151</p>
<p><b>13m</b></p>		<p>151</p>
<p><b>13n</b></p>		<p>151</p>
<p><b>13o</b></p>		<p>151</p>
<p><b>13q</b></p>		<p>151</p>
<p><b>13r</b></p>		<p>151</p>
<p><b>14c</b></p>		<p>163</p>

14i		163
14j		163
15a		169
16a		169
17a		169
15b		171
15c		171
15d		171
15e		171

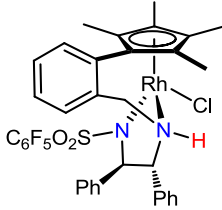
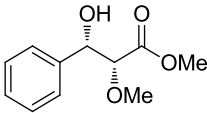
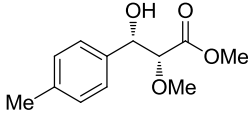
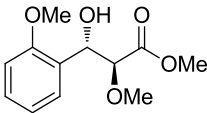
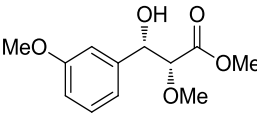
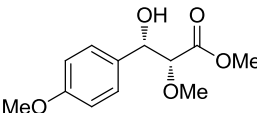
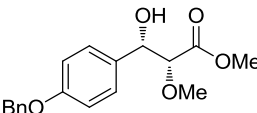
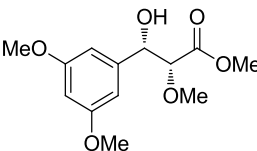
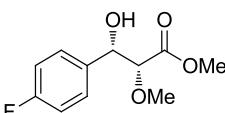
<p><b>15f</b></p>		<p>171</p>
<p><b>15g</b></p>		<p>172</p>
<p><b>15h</b></p>		<p>172</p>
<p><b>15i</b></p>		<p>172</p>
<p><b>15j</b></p>		<p>172</p>
<p><b>15k</b></p>		<p>172</p>

15l		172
15m		172
18		174
19		174
20		174
21		174

22		174
23		174
24a		182
24b		180
24c		180
24d		180
24e		180
24f		182
24g		180

24h		180
24i		182
24j		181
24k		181
24l		182
24m		181
26		183
27		183
L42		183



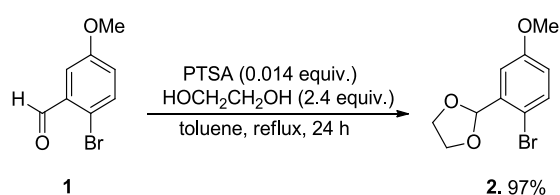
<p><b>(<i>R,R</i>)-C89</b></p>		<p>183</p>
<p><b>25a</b></p>		<p>188</p>
<p><b>25b</b></p>		<p>188</p>
<p><b>25c</b></p>		<p>188</p>
<p><b>25d</b></p>		<p>188</p>
<p><b>25e</b></p>		<p>188</p>
<p><b>25f</b></p>		<p>188</p>
<p><b>25g</b></p>		<p>188</p>
<p><b>25h</b></p>		<p>189</p>

25i		189
25j		189
25k		189
25l		190
25m		190

## 2.2 Description of the synthesis processes and detailed data

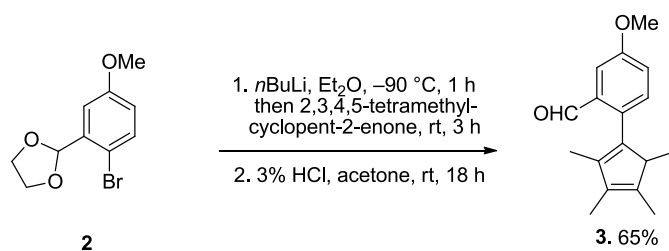
Synthesis of complexes (*R,R*)-**C86**<sup>208a</sup>, **C89**<sup>243</sup>:

**General procedure A:** synthesis of compounds **2**

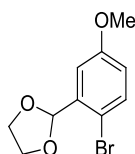


A mixture of 2-bromo-5-substituted-benzaldehyde **1** (1.0 equiv.), ethylene glycol (2.4 equiv.) and *p*-toluenesulfonic acid (0.014 equiv.) in toluene (0.5 mmol/mL) was refluxed in a Dean-Stark apparatus for 24 h. The cooled mixture was washed with H<sub>2</sub>O and brine. The organic layer was dried over MgSO<sub>4</sub>, filtered and concentrated. Purification of the residue by flash chromatography (SiO<sub>2</sub>, petroleum ether/EtOAc: 95/5) afforded **2** as a colorless oil.

**General procedure B:** synthesis of compounds **3**



To a solution of **2** (1.0 equiv.) in Et<sub>2</sub>O (0.55 mmol/mL) was added dropwise <sup>n</sup>BuLi (2.5 M in hexane, 1.05 equiv.) at -90 °C. After 1 h at this temperature, 2,3,4,5-tetramethylcyclopent-2-enone (1.05 equiv.) was added dropwise and the reaction was allowed to warm to rt and stirred for 3 h. Toluene and water (30 mL/30 mL) were added and the aqueous layer was extracted with toluene. The combined organic layers were washed with brine, dried over MgSO<sub>4</sub>, filtered and concentrated to afford the crude alcohol. THF (140 mL), acetone (18 mL) and 3% aqueous HCl solution (60 mL) were added and the mixture was stirred overnight at rt. Toluene was added, the organic layer was washed with H<sub>2</sub>O then brine, dried over MgSO<sub>4</sub>, filtered and concentrated. The crude residue was purified by flash chromatography (SiO<sub>2</sub>, petroleum ether/EtOAc: 98/2) to give **3** as a bright yellow oil.

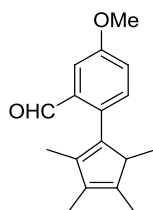
 2-(2-bromo-5-methoxyphenyl)-1,3-dioxolane (**2**)


Following the general procedure **A**, and starting from 2-bromo-5-methoxybenzaldehyde **1** (5.0 g, 23.2 mmol), compound **2** (6.1 g, quant. yield) was obtained as a colorless oil.

<sup>1</sup>H NMR (400 MHz, CDCl<sub>3</sub>): δ 7.44 (d, *J* = 8.8 Hz, 1H), 7.15 (d, *J* = 3.1 Hz, 1H), 6.78 (dd, *J* = 8.8, 3.1 Hz, 1H), 6.04 (s, 1H), 4.18–4.03 (m, 4H), 3.79 (s, 3H).

<sup>13</sup>C NMR (101 MHz, CDCl<sub>3</sub>): δ 158.9, 137.3, 133.6, 116.6, 113.1, 112.9, 102.4, 65.4 (2C), 55.5.

MS (DCI/NH<sub>3</sub>): *m/z* = 259 [M + H]<sup>+</sup>

 2-(1,3-dioxolan-2-yl)-4-methoxybenzaldehyde (**3**)


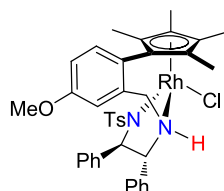
Following the general procedure **B**, and starting from **2** (6.0 g, 23.2 mmol), compound **3** (3.9 g, 65%) was obtained as a bright yellow oil.

**$^1\text{H}$  NMR** (400 MHz,  $\text{CDCl}_3$ ):  $\delta$  9.81 (br s, 1H), 7.44 (dd,  $J = 2.3, 0.8$  Hz, 1H), 7.15–7.14 (m, 2H), 3.88 (s, 1H), 3.87 (s, 3H), 1.92 (s, 3H), 1.85 (s, 3H), 1.71 (s, 3H), 0.93 (d,  $J = 7.7$  Hz, 3H).

**$^{13}\text{C}$  NMR** (101 MHz,  $\text{CDCl}_3$ ):  $\delta$  192.9, 158.3, 141.8 (2C), 138.2, 135.3, 134.5, 132.0, 121.8 (2C), 109.0, 55.5 (2C), 14.2, 12.3, 11.9, 11.0.

**MS** (DCI/ $\text{NH}_3$ ):  $m/z = 257$  [ $\text{M} + \text{H}$ ] $^+$ .

**Catalyst (*R,R*)-C84**



**Complex (*R,R*)-C84:** To a solution of compound **3a** (538 mg, 2.1 mmol) in dry MeOH (24 mL) was added (*R,R*)-TsDPEN (900 mg, 2.5 mmol) followed by the addition of 700 mg of molecular sieves (4 Å) and 2 drops of glacial acetic acid. The mixture was stirred at rt for 5 h then  $\text{NaBH}_3\text{CN}$  (170 mg, 2.7 mmol) was added and the reaction was stirred overnight at rt. After removal of the molecular sieves and evaporation of MeOH, the residue was dissolved in EtOAc (40 mL). The organic layer was washed with saturated  $\text{NaHCO}_3$  then brine, dried over  $\text{MgSO}_4$ , filtered and concentrated. Purification of the residue by flash chromatography ( $\text{SiO}_2$ , pentane/EtOAc: 9/1 to 8/2) afforded the diamine (786 mg, 60%) as a white solid. To a solution of the diamine (740 mg, 1.22 mmol) in MeOH (28 mL) was added  $\text{RhCl}_3 \cdot \text{H}_2\text{O}$  (255 mg, 1.22 mmol) and the reaction mixture was heated under reflux for 23 h.  $\text{Et}_3\text{N}$  (0.34 mL, 2.44 mmol) was then added and the mixture was refluxed for a further 20 h and concentrated. The residue was triturated with  $\text{H}_2\text{O}$  and the solid was filtered, washed with  $\text{H}_2\text{O}$  and dried under vacuum. Purification of the black solid by flash chromatography ( $\text{SiO}_2$ , EtOAc/cyclohexane: 1/1 to EtOAc/MeOH: 95/5) afforded (*R,R*)-C84 (455 mg, 50%) as an orange solid.<sup>168</sup> Mp: >260 °C (decomposition),  $R_f = 0.51$  ( $\text{CH}_2\text{Cl}_2/\text{MeOH} = 9/1$ , UV,  $\text{KMnO}_4$ ).  $[\alpha]_D^{25} = -154.4$  ( $c = 0.12$ ,  $\text{CHCl}_3$ ).

**IR** (neat): 2360, 2339, 1608, 1513, 1489, 1455, 1397, 1372, 1277, 1239, 1131, 1098, 1086, 1040, 1023, 940, 895, 812, 796, 766, 700, 682, 661, 646, 635, 622, 606  $\text{cm}^{-1}$ .

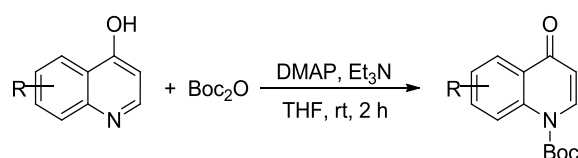
**$^1\text{H}$  NMR** (400 MHz,  $\text{CDCl}_3$ ):  $\delta$  7.37 (d,  $J = 8.5$  Hz, 1H), 7.27 (d,  $J = 8.6$  Hz, 2H), 7.19–7.16 (m, 3H), 7.02 (dd,  $J = 8.4, 2.5$  Hz, 1H), 6.73 (d,  $J = 8.0$  Hz, 2H), 6.70 (d,  $J = 7.3$  Hz, 2H), 6.59 (t,  $J = 7.8$  Hz, 2H), 6.48 (d,  $J = 7.4$  Hz, 2H), 6.42 (br d,  $J = 2.4$  Hz, 2H), 4.98 (d,  $J = 12.4$  Hz, 1H), 4.32 (d,  $J = 11.0$  Hz, 1H), 4.22 (dd,  $J = 14.0, 2.9$  Hz, 1H), 3.73 (s, 3H), 3.60 (d,  $J = 14.0$  Hz, 1H), 3.26 (t,  $J = 12.4$  Hz, 1H), 2.17 (s, 3H), 2.09 (s, 3H), 1.97 (s, 3H), 1.83 (s, 3H), 1.54 (s, 3H).

**$^{13}\text{C}$  NMR** (100 MHz,  $\text{CDCl}_3$ ):  $\delta$  160.2, 142.3, 139.0, 138.6, 137.5, 135.7, 131.2, 128.8, 128.7, 127.9, 127.7, 127.1, 126.2, 118.6, 117.0, 115.0, 106.4 (d,  $J_{\text{CRh}} = 6.6$  Hz), 99.2 (d,  $J_{\text{CRh}} = 6.6$  Hz), 97.0 (d,  $J_{\text{CRh}} = 8.8$  Hz), 88.7 (d,  $J_{\text{CRh}} = 9.5$  Hz), 80.6 (d,  $J_{\text{CRh}} = 8.0$  Hz), 75.9, 69.8, 55.5, 52.5, 21.3, 10.8, 10.7, 10.4, 8.3.

**HRMS** (ESI/ion trap):  $m/z$  [ $\text{M} - \text{Cl}$ ] $^+$  calcd for  $\text{C}_{38}\text{H}_{40}\text{N}_2\text{O}_3\text{RhS}$  707.1809, found 707.1813.

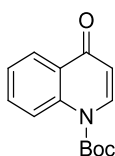
**General procedure for preparation of 4-quinolone derivatives (4a-m)**

**General procedure C<sup>209</sup>:**



A 100 mL round-bottom flask was charged with quinoline (3 mmol),  $\text{Boc}_2\text{O}$  (4.5 mmol, 1.5 equiv), DMAP (0.3 mmol, 0.1 equiv),  $\text{Et}_3\text{N}$  (4.5 mmol, 1.5 equiv), THF (15 mL). The mixture was stirred at room temperature for 2 h. The mixture was concentrated, and the residue was solubilized with ethyl acetate. The organic layer was washed with water and dried over anhydrous sodium sulfate. The solvent was evaporated, and the crude product was purified by chromatography on silica gel column (PE/EA = 2:1 as eluent).

Tert-butyl 4-oxoquinoline-1(4H)-carboxylate (**4a**)

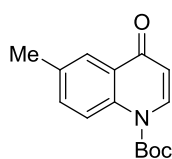


Following the above procedure, product **4a** was obtained as white solid, 7.5 g (76% yield), m.p. 80 °C.

<sup>1</sup>H NMR (400 MHz,  $\text{CDCl}_3$ )  $\delta$  8.58 (d,  $J = 8.8$  Hz, 1H), 8.37 (dd,  $J = 8.0, 1.5$  Hz, 1H), 8.30 (d,  $J = 8.5$  Hz, 1H), 7.65 (ddd,  $J = 8.9, 7.1, 1.8$  Hz, 1H), 7.42 (ddd,  $J = 8.0, 7.0, 1.0$  Hz, 1H), 6.25 (d,  $J = 8.5$  Hz, 1H), 1.67 (s, 9H).

<sup>13</sup>C NMR (101 MHz,  $\text{CDCl}_3$ )  $\delta$  179.1, 150.0, 138.8, 138.6, 132.7, 126.7, 126.5, 125.2, 120.0, 111.9, 86.6, 28.0.

Tert-butyl 6-methyl-4-oxoquinoline-1(4H)-carboxylate (**4b**)

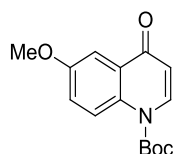


Following the above procedure, product **4b** was obtained as white solid, 563 mg (72% yield), m.p. 124 °C.

<sup>1</sup>H NMR (400 MHz,  $\text{CDCl}_3$ )  $\delta$  8.49 (d,  $J = 9.0$  Hz, 1H), 8.29 (d,  $J = 8.5$  Hz, 1H), 8.17 (dd,  $J = 1.6, 0.7$  Hz, 1H), 7.47 (ddd,  $J = 8.9, 2.3, 0.7$  Hz, 1H), 6.24 (d,  $J = 8.5$  Hz, 1H), 2.46 (s, 3H), 1.67 (s, 9H).

<sup>13</sup>C NMR (101 MHz,  $\text{CDCl}_3$ )  $\delta$  179.3, 150.1, 138.6, 136.6, 135.2, 134.0, 126.6, 126.1, 120.0, 111.8, 86.5, 28.1, 20.9.

Tert-butyl 6-methoxy-4-oxoquinoline-1(4H)-carboxylate (**4c**)

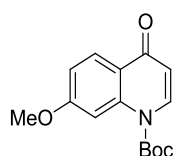


Following the above procedure, product **4c** was obtained as white solid, 1330 mg (80% yield), m.p. 114 °C.

$^1\text{H NMR}$  (400 MHz,  $\text{CDCl}_3$ )  $\delta$  8.55 (d,  $J = 9.5$  Hz, 1H), 8.29 (d,  $J = 8.4$  Hz, 1H), 7.77 (d,  $J = 3.1$  Hz, 1H), 7.25 (dd,  $J = 9.6, 3.2$  Hz, 1H), 6.25 (d,  $J = 8.4$  Hz, 1H), 3.92 (s, 3H), 1.67 (s, 9H).

$^{13}\text{C NMR}$  (101 MHz,  $\text{CDCl}_3$ )  $\delta$  178.7, 156.8, 149.9, 138.1, 132.9, 128.0, 122.4, 121.8, 111.0, 106.0, 86.4, 55.7, 28.0.

Tert-butyl 7-methoxy-4-oxoquinoline-1(4H)-carboxylate (**4d**)

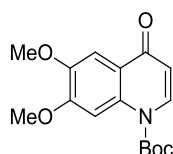


Following the above procedure, product **4d** was obtained as white solid, 1300 mg (80% yield), m.p. 123 °C.

$^1\text{H NMR}$  (400 MHz,  $\text{CDCl}_3$ )  $\delta$  8.30 (d,  $J = 9.0$  Hz, 1H), 8.26 (d,  $J = 8.5$  Hz, 1H), 8.17 (d,  $J = 2.4$  Hz, 1H), 7.00 (dd,  $J = 8.9, 2.4$  Hz, 1H), 6.20 (d,  $J = 8.6$  Hz, 1H), 3.91 (s, 3H), 1.68 (s, 9H).

$^{13}\text{C NMR}$  (101 MHz,  $\text{CDCl}_3$ )  $\delta$  178.6, 163.2, 150.1, 140.4, 138.5, 128.3, 120.8, 113.8, 112.0, 103.2, 86.5, 55.7, 28.0.

Tert-butyl 6,7-dimethoxy-4-oxoquinoline-1(4H)-carboxylate (**4e**)

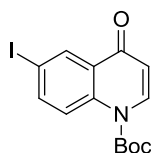


Following the above procedure, product **4e** was obtained as white solid, 1030 mg (78% yield), m.p. 154 °C.

$^1\text{H NMR}$  (400 MHz,  $\text{CDCl}_3$ )  $\delta$  8.29 (s, 1H), 8.28 (d,  $J = 8.5$  Hz, 1H), 7.75 (s, 1H), 6.23 (d,  $J = 8.4$  Hz, 1H), 4.00 (br, 6H), 1.68 (s, 9H).

$^{13}\text{C NMR}$  (101 MHz,  $\text{CDCl}_3$ )  $\delta$  178.1, 153.1, 150.1, 147.4, 137.8, 134.2, 121.1, 111.6, 105.9, 102.3, 86.5, 56.3, 56.2, 28.1.

Tert-butyl 6-iodo-4-oxoquinoline-1(4H)-carboxylate (**4f**)



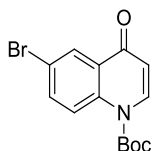
## Experimental part

Following the above procedure , product **4f** was obtained as white solid, 890 mg (80% yield), m.p. 178 °C.

**<sup>1</sup>H NMR** (400 MHz, CDCl<sub>3</sub>) δ 8.68 (t, *J* = 2.2 Hz, 1H), 8.37 (dd, *J* = 9.3, 1.3 Hz, 1H), 8.30 (dd, *J* = 8.5, 0.9 Hz, 1H), 7.90 (dt, *J* = 9.2, 2.0 Hz, 1H), 6.26 (dd, *J* = 8.6, 1.6 Hz, 1H), 1.67 (s, 9H).

**<sup>13</sup>C NMR** (101 MHz, CDCl<sub>3</sub>) δ 177.6, 149.6, 141.2, 139.0, 138.1, 135.4, 128.2, 122.2, 112.2, 90.1, 87.2, 28.1.

### Tert-butyl 6-bromo-4-oxoquinoline-1(4H)-carboxylate (**4g**)

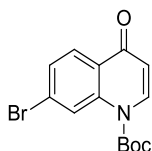


Following the above procedure , product **4g** was obtained as white solid, 1630 mg (84% yield), m.p. 166 °C.

**<sup>1</sup>H NMR** (400 MHz, CDCl<sub>3</sub>) δ 8.52 (d, *J* = 9.3 Hz, 1H), 8.49 (d, *J* = 2.5 Hz, 1H), 8.30 (d, *J* = 8.5 Hz, 1H), 7.72 (dd, *J* = 9.3, 2.6 Hz, 1H), 6.26 (d, *J* = 8.5 Hz, 1H), 1.67 (s, 9H).

**<sup>13</sup>C NMR** (101 MHz, CDCl<sub>3</sub>) δ 177.8, 149.7, 139.0, 137.5, 135.6, 129.2, 128.2, 122.2, 119.3, 112.2, 87.2, 28.1.

### Tert-butyl 7-bromo-4-oxoquinoline-1(4H)-carboxylate (**4h**)

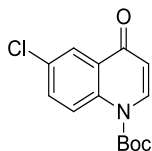


Following the above procedure , product **4h** was obtained as colourless solid, 800 mg (83% yield), m.p. 148 °C.

**<sup>1</sup>H NMR** (400 MHz, CDCl<sub>3</sub>) δ 8.87 (d, *J* = 1.8 Hz, 1H), 8.29 (d, *J* = 8.5 Hz, 1H), 8.22 (d, *J* = 8.5 Hz, 1H), 7.54 (dd, *J* = 8.6, 1.7 Hz, 1H), 6.25 (d, *J* = 8.6 Hz, 1H), 1.69 (s, 9H)

**<sup>13</sup>C NMR** (101 MHz, CDCl<sub>3</sub>) δ 178.4, 149.6, 139.2, 138.9, 128.7, 128.1, 127.8, 125.4, 123.15, 112.3, 87.3, 28.0.

### Tert-butyl 6-chloro-4-oxoquinoline-1(4H)-carboxylate (**4i**)



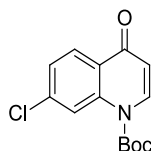
Following the above procedure , product **4i** was obtained as white solid, 640 mg (76% yield), m.p. 160 °C.

**<sup>1</sup>H NMR** (400 MHz, CDCl<sub>3</sub>) δ 8.60 (d, *J* = 9.5 Hz, 1H), 8.33 (d, *J* = 2.6 Hz, 1H), 8.31 (d, *J* = 8.6

Hz, 1H), 7.59 (dd,  $J = 9.4, 2.7$  Hz, 1H), 6.26 (d,  $J = 8.6$  Hz, 1H), 1.68 (s, 9H).

$^{13}\text{C}$  NMR (101 MHz,  $\text{CDCl}_3$ )  $\delta$  177.8, 149.6, 139.0, 137.0, 132.7, 131.4, 127.9, 125.9, 122.0, 112.0, 87.2, 28.0.

Tert-butyl 7-chloro-4-oxoquinoline-1(4H)-carboxylate (**4j**)

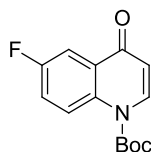


Following the above procedure, product **4j** was obtained as colourless solid, 1000 mg (60% yield), m.p. 126 °C.

$^1\text{H}$  NMR (400 MHz,  $\text{CDCl}_3$ )  $\delta$  8.66 (d,  $J = 1.9$  Hz, 1H), 8.26 (d,  $J = 7.2$  Hz, 1H), 8.24 (d,  $J = 7.1$  Hz, 1H), 7.34 (dd,  $J = 8.6, 1.9$  Hz, 1H), 6.20 (d,  $J = 8.5$  Hz, 1H), 1.66 (s, 9H).

$^{13}\text{C}$  NMR (101 MHz,  $\text{CDCl}_3$ )  $\delta$  178.2, 149.5, 139.2, 139.1, 138.9, 128.0, 125.8, 125.0, 120.1, 112.2, 87.2, 28.0.

Tert-butyl 6-fluoro-4-oxoquinoline-1(4H)-carboxylate (**4k**)



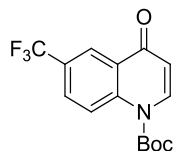
Following the above procedure, product **4k** was obtained as white solid, 400 mg (51% yield), m.p. 160 °C.

$^1\text{H}$  NMR (400 MHz,  $\text{CDCl}_3$ )  $\delta$  8.67 (dd,  $J = 9.6, 4.6$  Hz, 1H), 8.32 (d,  $J = 8.5$  Hz, 1H), 8.01 (dd,  $J = 8.6, 3.4$  Hz, 1H), 7.37 (ddd,  $J = 10.0, 7.3, 3.1$  Hz, 1H), 6.24 (d,  $J = 8.4$  Hz, 1H), 1.68 (s, 9H).

$^{13}\text{C}$  NMR (101 MHz,  $\text{CDCl}_3$ )  $\delta$  178.1, 159.7 (d,  $J = 247.8$  Hz), 149.7, 138.9, 135.0, 128.5 (d,  $J = 6.8$  Hz), 122.8 (d,  $J = 7.4$  Hz), 120.6 (d,  $J = 23.9$  Hz), 111.3 (d,  $J = 22.9$  Hz), 111.2, 87.0, 28.0.

$^{19}\text{F}$  NMR (282 MHz,  $\text{CDCl}_3$ )  $\delta$  -115.56 (q,  $J = 7.0$  Hz, 1F)

Tert-butyl 4-oxo-6-(trifluoromethyl)quinoline-1(4H)-carboxylate (**4l**)



Following the above procedure, product **4l** was obtained as white solid, 640 mg (68% yield), m.p. 158 °C.

$^1\text{H}$  NMR (400 MHz,  $\text{CDCl}_3$ )  $\delta$  8.75 (d,  $J = 9.2$  Hz, 1H), 8.67 (brs, 1H), 8.34 (d,  $J = 8.5$  Hz, 1H), 7.85 (dd,  $J = 9.3, 2.4$  Hz, 1H), 6.31 (d,  $J = 8.6$  Hz, 1H), 1.69 (s, 9H).

$^{13}\text{C}$  NMR (101 MHz,  $\text{CDCl}_3$ )  $\delta$  178.1, 149.6, 140.7, 139.4, 128.8 (d,  $J = 3.7$  Hz), 127.4 (q,  $J =$

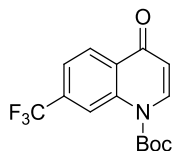


## Experimental part

33.7 Hz), 126.5, 124.4 (d,  $J = 4.3$  Hz), 123.8 (q,  $J = 272.2$  Hz), 121.2, 112.6, 87.6, 28.0.

$^{19}\text{F}$  NMR (282 MHz,  $\text{CDCl}_3$ )  $\delta$  -62.52 (s, 3F).

### Tert-butyl 4-oxo-7-(trifluoromethyl)quinoline-1(4H)-carboxylate (**4m**)



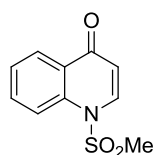
Following the above procedure, product **4m** was obtained as colourless solid, 640 mg (68% yield), m.p. 138 °C.

$^1\text{H}$  NMR (400 MHz,  $\text{CDCl}_3$ )  $\delta$  8.98 (s, 1H), 8.49 (d,  $J = 8.4$  Hz, 1H), 8.40 (d,  $J = 8.5$  Hz, 1H), 7.65 (dd,  $J = 8.4, 1.1$  Hz, 1H), 6.32 (d,  $J = 8.5$  Hz, 1H), 1.70 (s, 9H).

$^{13}\text{C}$  NMR (101 MHz,  $\text{CDCl}_3$ )  $\delta$  178.1, 149.6, 139.5, 138.4, 134.1 (q,  $J = 32.6$  Hz), 128.6, 127.8, 123.7 (q,  $J = 273.2$  Hz), 121.4 (d,  $J = 3.8$  Hz), 118.2 (q,  $J = 4.4$  Hz), 112.6, 87.8, 28.0.

$^{19}\text{F}$  NMR (282 MHz,  $\text{CDCl}_3$ )  $\delta$  -62.95 (s, 3F).

### 1-(methylsulfonyl)quinolin-4(1H)-one (**4n**)

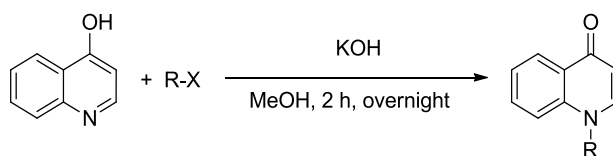


Following the above procedure, using  $\text{CH}_3\text{SO}_2\text{Cl}$  instead of  $\text{Boc}_2\text{O}$ , product **4n** was obtained as white solid, 320 mg (16% yield), m.p. 150 °C.

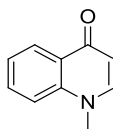
$^1\text{H}$  NMR (400 MHz,  $\text{CDCl}_3$ )  $\delta$  8.42 (dd,  $J = 8.0, 1.7$  Hz, 1H), 8.27 (d,  $J = 8.6$  Hz, 1H), 8.24 (d,  $J = 8.9$  Hz, 1H), 7.74 (ddd,  $J = 8.9, 7.1, 1.8$  Hz, 1H), 7.50 (ddd,  $J = 8.1, 7.1, 1.0$  Hz, 1H), 6.33 (d,  $J = 8.5$  Hz, 1H), 3.37 (s, 3H).

$^{13}\text{C}$  NMR (101 MHz,  $\text{CDCl}_3$ )  $\delta$  178.3, 137.4, 137.2, 133.5, 127.9, 126.6, 126.1, 117.6, 112.6, 41.2.

### General procedure D for preparation of 4-quinolone derivatives (**4o-p**)

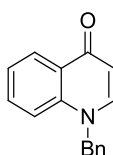


Alkyl halide (methyl iodide or benzyl bromide for 10 equiv) was added in one aliquot to a solution of a 4-quinolone compound (1 equiv), KOH (1.5 equiv) in methanol ( $c = 1.0$  M), and the mixture was stirred overnight at room temperature. After the precipitate was removed by filtration, the solvent was evaporated and the resulting residue was purified by flash chromatography column ( $\text{MeOH}/\text{CH}_2\text{Cl}_2$ : 0 ~ 5%, v/v).

1-methylquinolin-4(1H)-one (**4o**)

Following the above procedure, product **4o** was obtained as pale yellow solid, 320 mg (67% yield).

$^1\text{H NMR}$  (400 MHz,  $\text{CDCl}_3$ )  $\delta$  8.47 (dd,  $J = 8.2, 1.6$  Hz, 1H), 7.69 (ddd,  $J = 8.7, 7.1, 1.6$  Hz, 1H), 7.51 (d,  $J = 7.7$  Hz, 1H), 7.43 – 7.38 (m, 2H), 6.27 (d,  $J = 7.7$  Hz, 1H), 3.80 (s, 3H).

1-benzylquinolin-4(1H)-one (**4p**)

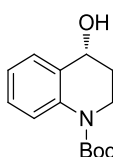
Following the above procedure, product **4p** was obtained as white solid, 533 mg (57% yield).

$^1\text{H NMR}$  (400 MHz,  $\text{CDCl}_3$ )  $\delta$  8.39 (dd,  $J = 8.0, 1.7$  Hz, 1H), 7.57 (d,  $J = 7.7$  Hz, 1H), 7.45 (ddd,  $J = 8.6, 7.1, 1.7$  Hz, 1H), 7.33 – 7.18 (m, 5H), 7.08 (d,  $J = 6.6$  Hz, 2H), 6.26 (d,  $J = 7.7$  Hz, 1H), 5.25 (s, 2H).

$^{13}\text{C NMR}$  (101 MHz,  $\text{CDCl}_3$ )  $\delta$  178.4, 143.8, 140.2, 135.2, 132.2, 129.3, 128.34, 127.4, 127.0, 126.1, 123.8, 116.2, 110.4, 56.5.

General procedure E for the synthesis of **5** via ATH

In a round-bottom tube charged with complex (*R,R*)-**C86** (5.0  $\mu\text{mol}$ , 0.01 equiv) was added under argon a solution of the ketone **4** (0.50 mmol, 1.0 equiv) in anhydrous  $\text{CH}_2\text{Cl}_2$  (0.5 mL), then  $\text{HCO}_2\text{H}/\text{NEt}_3$  (5:2) azeotropic mixture (170  $\mu\text{L}$ , 2.0 mmol, 4.0 equiv) was added dropwise. The mixture was stirred under argon at 30  $^\circ\text{C}$  for 16 h, then quenched with water (5.0 mL) and extracted with  $\text{CH}_2\text{Cl}_2$  (3\*15 mL). The combined organic phases were washed with brine, dried with  $\text{MgSO}_4$ , filtered and concentrated under vacuum. Purification of the residue by flash column chromatography (petroleum ether/ethyl acetate 2:1) afforded compound **2** and the enantiomeric excess was determined by SFC analysis.

*(R)*-tert-butyl 4-hydroxy-3,4-dihydroquinoline-1(2H)-carboxylate (**5a**)

White powder: 103 mg (83% yield),  $ee > 99\%$ , m.p. 85  $^\circ\text{C}$ ,  $[\alpha]_{\text{D}}^{25} = +33.0$  (c 0.96,  $\text{CHCl}_3$ ).

$^1\text{H NMR}$  (400 MHz,  $\text{CDCl}_3$ )  $\delta$  7.79 (d,  $J = 8.4$  Hz, 1H), 7.38 (dd,  $J = 7.6, 1.6$  Hz, 1H), 7.25 (ddd,

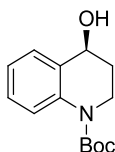
## Experimental part

$J = 8.6, 7.3, 1.7$  Hz, 1H), 7.07 (td,  $J = 7.5, 1.2$  Hz, 1H), 4.76 (q,  $J = 4.8$  Hz, 1H), 4.04 (ddd,  $J = 13.1, 5.5, 4.7$  Hz, 1H), 3.59 (ddd,  $J = 13.4, 9.8, 4.0$  Hz, 1H), 2.14 – 1.97 (m, 2H), 1.79 (d,  $J = 5.1$  Hz, 1H), 1.53 (s, 9H).

$^{13}\text{C NMR}$  (101 MHz,  $\text{CDCl}_3$ )  $\delta$  153.7, 137.9, 130.7, 128.3, 128.1, 123.8, 123.6, 81.3, 66.0, 40.6, 32.1, 28.5.

**SFC:** Chiralpak AS-H,  $\text{scCO}_2/\text{MeOH}$  98/2, 3.0 mL/min,  $P = 100$  bar,  $\lambda = 254$  nm,  $t_S = 5.30$  min,  $t_R = 6.31$  min.

### (*S*)-tert-butyl 4-hydroxy-3,4-dihydroquinoline-1(2H)-carboxylate (**5a'**)



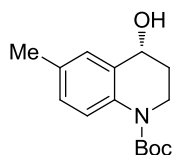
White powder: 103 mg (83% yield),  $ee > 99\%$ .

$^1\text{H NMR}$  (400 MHz,  $\text{CDCl}_3$ )  $\delta$  7.79 (d,  $J = 8.4$  Hz, 1H), 7.38 (dd,  $J = 7.6, 1.6$  Hz, 1H), 7.25 (ddd,  $J = 8.6, 7.3, 1.7$  Hz, 1H), 7.07 (td,  $J = 7.5, 1.2$  Hz, 1H), 4.76 (q,  $J = 4.8$  Hz, 1H), 4.04 (ddd,  $J = 13.1, 5.5, 4.7$  Hz, 1H), 3.59 (ddd,  $J = 13.4, 9.8, 4.0$  Hz, 1H), 2.14 – 1.97 (m, 2H), 1.79 (d,  $J = 5.1$  Hz, 1H), 1.53 (s, 9H).

$^{13}\text{C NMR}$  (101 MHz,  $\text{CDCl}_3$ )  $\delta$  153.7, 137.9, 130.7, 128.3, 128.1, 123.8, 123.6, 81.3, 66.0, 40.6, 32.1, 28.5.

**SFC:** Chiralpak AS-H,  $\text{scCO}_2/\text{MeOH}$  98/2, 3.0 mL/min,  $P = 100$  bar,  $\lambda = 254$  nm,  $t_S = 5.30$  min,  $t_R = 6.31$  min.

### (*R*)-tert-butyl 4-hydroxy-6-methyl-3,4-dihydroquinoline-1(2H)-carboxylate (**5b**)



White powder: 104 mg (79% yield),  $ee > 99\%$ , m.p. 111 °C,  $[\alpha]_D^{25} = +20.9$  (c 0.96,  $\text{CHCl}_3$ ).

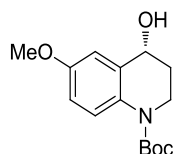
$^1\text{H NMR}$  (400 MHz,  $\text{CDCl}_3$ )  $\delta$  7.65 (d,  $J = 8.5$  Hz, 1H), 7.18 (br, 1H), 7.05 (dd,  $J = 8.5, 2.1$  Hz, 1H), 4.73 (q,  $J = 4.8$  Hz, 1H), 4.04 (dt,  $J = 13.1, 5.0$  Hz, 1H), 3.56 (ddd,  $J = 13.4, 9.9, 3.9$  Hz, 1H), 2.31 (s, 3H), 2.10 – 1.94 (m, 2H), 1.80 (d,  $J = 5.2$  Hz, 1H), 1.52 (s, 9H).

$^{13}\text{C NMR}$  (101 MHz,  $\text{CDCl}_3$ )  $\delta$  153.7, 135.3, 133.1, 130.5, 128.8, 128.7, 123.6, 81.1, 66.0, 40.6, 32.2, 28.5, 20.8.

**HRMS** (ESI/ion trap):  $m/z$   $[\text{M} + \text{Na}]^+$  calcd for  $\text{C}_{15}\text{H}_{21}\text{NNaO}_3$  286.1419, found 286.1415.

**SFC:** Chiralpak AS-H,  $\text{scCO}_2/\text{MeOH}$  95/5, 2.0 mL/min,  $P = 100$  bar,  $\lambda = 254$  nm,  $t_S = 3.91$  min,  $t_R = 4.61$  min.

### (*R*)-tert-butyl 4-hydroxy-6-methoxy-3,4-dihydroquinoline-1(2H)-carboxylate (**5c**)



Pale yellow powder: 105 mg (75% yield), *ee* > 99%, m.p. 111 °C,  $[\alpha]_D^{25} = +18.8$  (c 1.17, CHCl<sub>3</sub>).

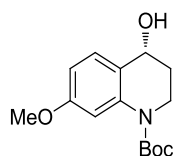
**<sup>1</sup>H NMR** (400 MHz, CDCl<sub>3</sub>) δ 7.65 (d, *J* = 9.1 Hz, 1H), 6.92 (d, *J* = 3.0 Hz, 1H), 6.80 (dd, *J* = 9.1, 3.0 Hz, 1H), 4.72 (q, *J* = 5.0 Hz, 1H), 3.99 (ddd, *J* = 13.1, 6.3, 4.3 Hz, 1H), 3.79 (s, 3H), 3.56 (ddd, *J* = 13.2, 9.5, 3.8 Hz, 1H), 2.09 (ddt, *J* = 14.0, 9.3, 4.5 Hz, 1H), 2.00 – 1.92 (m, 2H), 1.51 (s, 9H).

**<sup>13</sup>C NMR** (101 MHz, CDCl<sub>3</sub>) δ 155.8, 153.8, 132.1, 131.1, 125.2, 114.2, 112.2, 81.1, 66.2, 55.6, 40.8, 32.5, 28.5.

**HRMS** (ESI/ion trap): *m/z* [M + Na]<sup>+</sup> calcd for C<sub>15</sub>H<sub>21</sub>NNaO<sub>4</sub> 302.1368, found 302.1364.

**SFC**: Chiralpak AS-H, *sc*CO<sub>2</sub>/ MeOH 95/5, 2.0 mL/min, P = 100 bar, λ = 254 nm, *t*<sub>S</sub> = 4.66 min, *t*<sub>R</sub> = 5.73 min.

(*R*)-tert-butyl 4-hydroxy-7-methoxy-3,4-dihydroquinoline-1(2H)-carboxylate (**5d**)



Pale yellow powder: 70 mg (50% yield), *ee* = 99%, m.p. 95 °C,  $[\alpha]_D^{25} = +9.3$  (c 1.02, CHCl<sub>3</sub>).

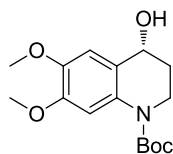
**<sup>1</sup>H NMR** (400 MHz, CDCl<sub>3</sub>) δ 7.45 (d, *J* = 2.5 Hz, 1H), 7.26 (d, *J* = 8.5 Hz, 1H), 6.65 (dd, *J* = 8.5, 2.6 Hz, 1H), 4.73 (q, *J* = 4.4 Hz, 1H), 4.08 (dt, *J* = 13.0, 4.8 Hz, 1H), 3.80 (s, 3H), 3.55 (ddd, *J* = 13.2, 7.9, 6.3 Hz, 1H), 2.03 – 1.98 (m, 2H), 1.76 (d, *J* = 4.6 Hz, 1H), 1.54 (s, 9H).

**<sup>13</sup>C NMR** (101 MHz, CDCl<sub>3</sub>) δ 159.3, 153.6, 139.1, 129.6, 123.0, 110.3, 108.4, 81.4, 65.6, 55.5, 40.5, 32.0, 28.5.

**HRMS** (ESI/ion trap): *m/z* [M + Na]<sup>+</sup> calcd for C<sub>15</sub>H<sub>21</sub>NNaO<sub>4</sub> 302.1368, found 302.1363.

**SFC**: Chiralpak IF, *sc*CO<sub>2</sub>/ MeOH 90/10, 2.0 mL/min, P = 100 bar, λ = 254 nm, *t*<sub>R</sub> = 7.45 min, *t*<sub>S</sub> = 9.38 min.

(*R*)-tert-butyl 4-hydroxy-6,7-dimethoxy-3,4-dihydroquinoline-1(2H)-carboxylate (**5e**)



White powder: 36 mg (23% yield), *ee* = 97%, m.p. 94 °C,  $[\alpha]_D^{25} = +30.7$  (c 0.57, CHCl<sub>3</sub>).

**<sup>1</sup>H NMR** (400 MHz, CDCl<sub>3</sub>) δ 7.40 (s, 1H), 6.86 (s, 1H), 4.70 (br, 1H), 4.06 (ddd, *J* = 13.1, 5.6, 3.9 Hz, 1H), 3.87 (s, 3H), 3.86 (s, 3H), 3.52 (ddd, *J* = 13.4, 10.3, 3.4 Hz, 1H), 2.11 – 1.93 (m,

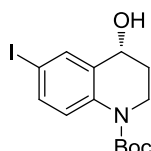
2H), 1.84 (brs, 1H), 1.53 (s, 9H).

$^{13}\text{C NMR}$  (101 MHz,  $\text{CDCl}_3$ )  $\delta$  153.6, 148.3, 145.6, 131.6, 122.4, 110.8, 107.5, 81.2, 65.8, 56.2, 56.1, 40.7, 32.6, 28.6.

**HRMS** (ESI/ion trap):  $m/z$   $[\text{M} + \text{Na}]^+$  calcd for  $\text{C}_{16}\text{H}_{23}\text{NNaO}_5$  332.1474, found 332.1469.

**SFC**: Chiralpak AS-H,  $sc\text{CO}_2$ / MeOH 97/3, 3.0 mL/min, P = 100 bar,  $\lambda$  = 254 nm,  $t_S$  = 5.09 min,  $t_R$  = 6.55 min.

(*R*)-tert-butyl 4-iodo-6-hydroxy-3,4-dihydroquinoline-1(2H)-carboxylate (**5f**)



White solid, 120 mg, 64% yield,  $ee > 99\%$ , m.p. 150 °C,  $[\alpha]_D^{25} = +4.7$  (c 0.94,  $\text{CHCl}_3$ ).

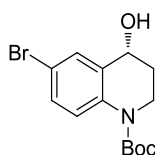
$^1\text{H NMR}$  (400 MHz,  $\text{CDCl}_3$ )  $\delta$  7.70 (d,  $J = 1.9$  Hz, 1H), 7.58 (d,  $J = 8.8$  Hz, 1H), 7.51 (dd,  $J = 8.9, 2.2$  Hz, 1H), 4.70 (q,  $J = 5.1$  Hz, 1H), 3.99 (ddd,  $J = 13.1, 6.2, 4.5$  Hz, 1H), 3.59 (ddd,  $J = 13.3, 9.5, 4.0$  Hz, 1H), 2.10 – 2.01 (m, 1H), 1.99 – 1.92 (m, 1H), 1.87 (d,  $J = 5.4$  Hz, 1H), 1.52 (s, 9H).

$^{13}\text{C NMR}$  (101 MHz,  $\text{CDCl}_3$ )  $\delta$  153.4, 137.6, 136.8, 136.8, 133.1, 125.6, 86.8, 81.8, 65.6, 40.7, 31.9, 28.4.

**HRMS** (ESI/ion trap):  $m/z$   $[\text{M} + \text{Na}]^+$  calcd for  $\text{C}_{14}\text{H}_{18}\text{INNaO}_3$  398.0229, found 398.0224.

**SFC**: Chiralpak AS-H,  $sc\text{CO}_2$ / MeOH 97/3, 3.0 mL/min, P = 100 bar,  $\lambda$  = 254 nm,  $t_S$  = 8.23 min,  $t_R$  = 9.72 min.

(*R*)-tert-butyl 6-bromo-4-hydroxy-3,4-dihydroquinoline-1(2H)-carboxylate (**5g**)



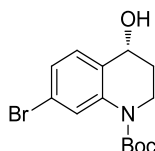
White solid, 120 mg, 73% yield,  $ee > 99\%$ , m.p. 131 °C,  $[\alpha]_D^{25} = +12$  (c 1.2,  $\text{CHCl}_3$ ).

$^1\text{H NMR}$  (400 MHz,  $\text{CDCl}_3$ )  $\delta$  7.69 (d,  $J = 8.9$  Hz, 1H), 7.52 (dd,  $J = 2.3, 0.5$  Hz, 1H), 7.33 (dd,  $J = 8.9, 2.3$  Hz, 1H), 4.71 (q,  $J = 5.1$  Hz, 1H), 3.98 (ddd,  $J = 13.0, 6.4, 4.5$  Hz, 1H), 3.59 (ddd,  $J = 13.2, 9.4, 4.0$  Hz, 1H), 2.07 (ddt,  $J = 13.8, 9.1, 4.5$  Hz, 1H), 2.00 – 1.91 (m, 2H), 1.52 (s, 9H).

$^{13}\text{C NMR}$  (101 MHz,  $\text{CDCl}_3$ )  $\delta$  153.5, 136.8, 133.0, 130.8, 130.7, 125.3, 116.2, 81.7, 65.6, 40.8, 32.0, 28.4.

**SFC**: Chiralpak AS-H,  $sc\text{CO}_2$ / MeOH 98/2, 2.0 mL/min, P = 100 bar,  $\lambda$  = 254 nm,  $t_R$  = 17.79 min,  $t_S$  = 21.42 min.

(*R*)-tert-butyl 7-bromo-4-hydroxy-3,4-dihydroquinoline-1(2H)-carboxylate (**5h**)



White solid, 110 mg, 67% yield, *ee* > 99%, m.p. 114 °C,  $[\alpha]_{\text{D}}^{25} = +5.7$  (c 1.04, CHCl<sub>3</sub>).

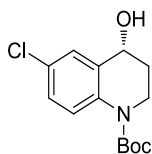
**<sup>1</sup>H NMR** (400 MHz, CDCl<sub>3</sub>)  $\delta$  8.05 (d, *J* = 1.9 Hz, 1H), 7.24 (d, *J* = 8.2 Hz, 1H), 7.18 (dd, *J* = 8.2, 1.9 Hz, 1H), 4.71 (q, *J* = 4.8 Hz, 1H), 4.01 (ddd, *J* = 13.1, 5.9, 4.5 Hz, 1H), 3.59 (ddd, *J* = 13.4, 9.6, 4.1 Hz, 1H), 2.10 – 1.93 (m, 2H), 1.83 (d, *J* = 5.2 Hz, 1H), 1.54 (s, 9H).

**<sup>13</sup>C NMR** (101 MHz, CDCl<sub>3</sub>)  $\delta$  153.3, 139.0, 129.6, 129.4, 126.3, 126.3, 121.6, 81.9, 65.6, 40.6, 31.7, 28.4.

**HRMS** (ESI/ion trap): *m/z* [M + Na]<sup>+</sup> calcd for C<sub>14</sub>H<sub>18</sub>BrNNaO<sub>3</sub> 350.0368, found 350.0362.

**SFC**: Chiralpak IF, *sc*CO<sub>2</sub>/ MeOH 90/10, 2.0 mL/min, P = 100 bar,  $\lambda$  = 254 nm, *t<sub>R</sub>* = 8.35 min, *t<sub>S</sub>* = 8.95 min.

(*R*)-tert-butyl 6-chloro-4-hydroxy-3,4-dihydroquinoline-1(2H)-carboxylate (**5i**)



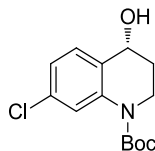
White solid, 95 mg, 67% yield, *ee* > 99%, m.p. 104 °C,  $[\alpha]_{\text{D}}^{25} = +19.5$  (c 1.06, CHCl<sub>3</sub>).

**<sup>1</sup>H NMR** (400 MHz, CDCl<sub>3</sub>)  $\delta$  7.70 (d, *J* = 8.9 Hz, 1H), 7.35 (d, *J* = 2.5 Hz, 1H), 7.16 (dd, *J* = 9.0, 2.6 Hz, 1H), 4.65 (q, *J* = 5.1 Hz, 1H), 3.93 (ddd, *J* = 13.0, 6.6, 4.5 Hz, 1H), 3.56 (ddd, *J* = 13.1, 9.2, 4.0 Hz, 1H), 2.49 (d, *J* = 5.1 Hz, 1H), 2.08 – 2.00 (m, 1H), 1.94 – 1.87 (m, 1H), 1.51 (s, 9H).

**<sup>13</sup>C NMR** (101 MHz, CDCl<sub>3</sub>)  $\delta$  153.6, 136.2, 132.6, 128.5, 127.8, 127.7, 125.0, 81.7, 65.6, 40.8, 32.0, 28.4.

**SFC**: Chiralpak AD-H, *sc*CO<sub>2</sub>/ MeOH 80/20, 2.0 mL/min, P = 100 bar,  $\lambda$  = 254 nm, *t<sub>R</sub>* = 3.77 min, *t<sub>S</sub>* = 5.75 min.

(*R*)-tert-butyl 7-chloro-4-hydroxy-3,4-dihydroquinoline-1(2H)-carboxylate (**5j**)



White solid, 94 mg, 66% yield, *ee* > 99%, m.p. 94 °C,  $[\alpha]_{\text{D}}^{25} = +12$  (c 0.94, CHCl<sub>3</sub>).

**<sup>1</sup>H NMR** (400 MHz, CDCl<sub>3</sub>)  $\delta$  7.88 (d, *J* = 2.1 Hz, 1H), 7.28 (d, *J* = 8.3 Hz, 1H), 7.01 (dd, *J* = 8.2, 2.1 Hz, 1H), 4.69 (br, 1H), 3.98 (ddd, *J* = 13.1, 5.9, 4.5 Hz, 1H), 3.57 (ddd, *J* = 13.4, 9.7, 4.1 Hz, 1H), 2.19 (brs, 1H), 2.06 – 1.91 (m, 2H), 1.53 (s, 9H).

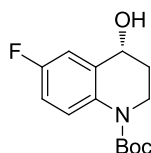
**<sup>13</sup>C NMR** (101 MHz, CDCl<sub>3</sub>)  $\delta$  153.6, 136.2, 132.6, 128.5, 127.8, 127.7, 125.0, 81.7, 65.6, 40.8,

## Experimental part

32.0, 28.4. 153.4, 138.8, 133.6, 129.4, 128.9, 123.4, 123.4, 81.9, 65.5, 40.6, 31.7, 28.4.

**SFC:** Chiralpak IF, *sc*CO<sub>2</sub>/ MeOH 90/10, 2.0 mL/min, P = 100 bar,  $\lambda$  = 254 nm,  $t_R$  = 7.97 min,  $t_S$  = 8.85 min.

(*R*)-tert-butyl 6-fluoro-4-hydroxy-3,4-dihydroquinoline-1(2H)-carboxylate (**5k**)



White solid, 97 mg, 73% yield, *ee* > 99%, m.p. 100 °C,  $[\alpha]_D^{25} = +26.5$  (c 0.99, CHCl<sub>3</sub>).

**<sup>1</sup>H NMR** (400 MHz, CDCl<sub>3</sub>)  $\delta$  7.72 (dd, *J* = 9.2, 5.1 Hz, 1H), 7.11 (dd, *J* = 8.8, 3.1 Hz, 1H), 6.94 (td, *J* = 8.6, 3.0 Hz, 1H), 4.72 (q, *J* = 5.4 Hz, 1H), 3.98 (ddd, *J* = 12.9, 6.6, 4.6 Hz, 1H), 3.59 (ddd, *J* = 13.0, 9.1, 4.0 Hz, 1H), 2.11 (ddt, *J* = 13.7, 9.2, 4.6 Hz, 1H), 2.00 – 1.90 (m, 2H), 1.52 (s, 9H).

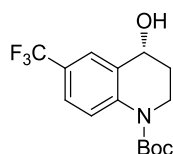
**<sup>13</sup>C NMR** (101 MHz, CDCl<sub>3</sub>)  $\delta$  158.9 (d, *J* = 243.4 Hz), 153.8, 133.7 (d, *J* = 2.8 Hz), 133.1 (d, *J* = 6.7 Hz), 125.5 (d, *J* = 7.8 Hz), 114.7 (d, *J* = 22.3 Hz), 114.0 (d, *J* = 22.6 Hz), 81.4, 65.8, 40.9, 32.4, 28.4.

**<sup>19</sup>F NMR** (282 MHz, CDCl<sub>3</sub>)  $\delta$  -119.37 (q, *J* = 7.4 Hz).

**HRMS** (ESI/ion trap): *m/z* [M + Na]<sup>+</sup> calcd for C<sub>14</sub>H<sub>18</sub>FNNaO<sub>3</sub> 290.1168, found 290.1166.

**SFC:** Chiralpak AD-H, *sc*CO<sub>2</sub>/ MeOH 80/20, 2.0 mL/min, P = 100 bar,  $\lambda$  = 254 nm,  $t_S$  = 2.55 min,  $t_R$  = 3.38 min.

(*R*)-tert-butyl 4-hydroxy-6-(trifluoromethyl)-3,4-dihydroquinoline-1(2H)-carboxylate (**5l**)



White solid, 105 mg, 66% yield, *ee* > 99%, m.p. 93 °C,  $[\alpha]_D^{25} = +36.1$  (c 1.18, CHCl<sub>3</sub>).

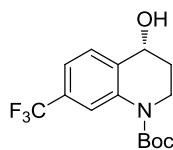
**<sup>1</sup>H NMR** (400 MHz, CDCl<sub>3</sub>)  $\delta$  7.97 (d, *J* = 8.8 Hz, 1H), 7.67 – 7.66 (brd, *J* = 1.8, 1H), 7.48 (dd, *J* = 8.9, 2.2 Hz, 1H), 4.79 (q, *J* = 5.2 Hz, 1H), 4.02 (ddd, *J* = 13.1, 6.4, 4.6 Hz, 1H), 3.66 (ddd, *J* = 13.2, 9.4, 4.1 Hz, 1H), 2.11 (ddt, *J* = 13.8, 9.2, 4.4 Hz, 1H), 2.05 – 1.96 (m, 1H), 1.91 (d, *J* = 5.4 Hz, 1H), 1.54 (s, 9H).

**<sup>13</sup>C NMR** (101 MHz, CDCl<sub>3</sub>)  $\delta$  153.5, 140.8, 130.9, 125.2 (d, *J* = 4.1 Hz), 124.9 (d, *J* = 4.3 Hz), 124.3 (q, *J* = 271.4 Hz), 123.5, 82.1, 65.8, 40.9, 31.8, 28.4.

**<sup>19</sup>F NMR** (282 MHz, CDCl<sub>3</sub>)  $\delta$  -62.10 (s, 3F).

**HRMS** (ESI/ion trap): *m/z* [M + Na]<sup>+</sup> calcd for C<sub>15</sub>H<sub>18</sub>F<sub>3</sub>NNaO<sub>3</sub> 340.1136, found 340.1131.

**SFC:** Chiralpak AD-H, *sc*CO<sub>2</sub>/ MeOH 80/20, 2.0 mL/min, P = 100 bar,  $\lambda$  = 254 nm,  $t_S$  = 2.46 min,  $t_R$  = 3.13 min.

**(R)-tert-butyl 4-hydroxy-7-(trifluoromethyl)-3,4-dihydroquinoline-1(2H)-carboxylate (5m)**

White solid, 106 mg, 67% yield, *ee* > 99%, m.p. 114 °C,  $[\alpha]_{\text{D}}^{25} = +31.7$  (c 1.0, CHCl<sub>3</sub>).

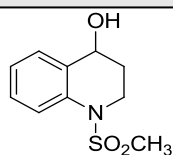
**<sup>1</sup>H NMR** (400 MHz, CDCl<sub>3</sub>)  $\delta$  8.11 (s, 1H), 7.51 (d, *J* = 8.0 Hz, 1H), 7.31 (ddd, *J* = 8.0, 1.8, 0.8 Hz, 1H), 4.79 (q, *J* = 5.2 Hz, 1H), 4.03 (ddd, *J* = 13.1, 6.6, 4.5 Hz, 1H), 3.64 (ddd, *J* = 13.2, 9.3, 4.0 Hz, 1H), 2.12 (ddt, *J* = 13.7, 9.1, 4.5 Hz, 1H), 2.00 (dddd, *J* = 13.7, 6.6, 5.6, 4.0 Hz, 1H), 1.88 (d, *J* = 5.4 Hz, 1H), 1.54 (s, 9H).

**<sup>13</sup>C NMR** (101 MHz, CDCl<sub>3</sub>)  $\delta$  153.4, 138.1, 134.1, 130.16 (q, *J* = 32.1 Hz), 128.5, 124.1 (q, *J* = 272.2 Hz), 120.8 (d, *J* = 4.5 Hz), 119.7 (d, *J* = 4.1 Hz), 82.2, 65.8, 40.7, 31.9, 28.4.

**<sup>19</sup>F NMR** (282 MHz, CDCl<sub>3</sub>)  $\delta$  -62.74 (s, 3F).

**HRMS** (ESI/ion trap): *m/z* [M + Na]<sup>+</sup> calcd for C<sub>15</sub>H<sub>18</sub>F<sub>3</sub>NNaO<sub>3</sub> 340.1136, found 340.1131.

**SFC**: Chiralpak IF, *sc*CO<sub>2</sub>/ <sup>i</sup>PrOH 97/3, 2.0 mL/min, P = 100 bar,  $\lambda$  = 254 nm, *t<sub>R</sub>* = 13.7 min, *t<sub>S</sub>* = 14.7 min.

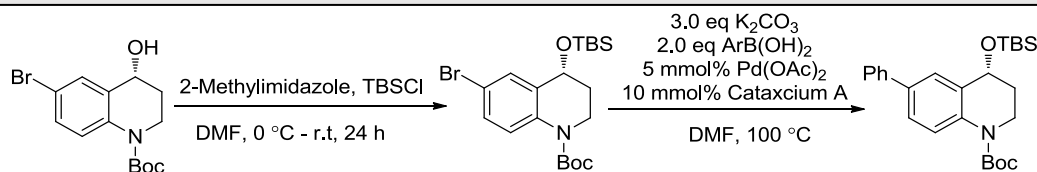
**(R)-1-(methylsulfonyl)-1,2,3,4-tetrahydroquinolin-4-ol (5p)**

White solid, 73 mg, 39% yield, *ee* = 55%, m.p. 46 °C.

**<sup>1</sup>H NMR** (400 MHz, CDCl<sub>3</sub>)  $\delta$  7.78 (d, *J* = 8.4 Hz, 1H), 7.40 (dd, *J* = 7.6, 1.7 Hz, 1H), 7.31 (ddd, *J* = 8.6, 7.4, 1.7 Hz, 1H), 7.15 (td, *J* = 7.5, 1.2 Hz, 1H), 4.83 (t, *J* = 4.1 Hz, 1H), 4.08 (dt, *J* = 13.0, 4.5 Hz, 1H), 3.76 (ddd, *J* = 13.0, 10.0, 4.6 Hz, 1H), 2.93 (s, 3H), 2.14 – 2.07 (m, 2H), 1.88 (br, 1H).

**<sup>13</sup>C NMR** (101 MHz, CDCl<sub>3</sub>)  $\delta$  136.4, 130.2, 129.8, 129.3, 124.6, 121.7, 65.3, 42.0, 38.3, 30.8.

**SFC**: Chiralpak AS-H, *sc*CO<sub>2</sub>/ MeOH 97/3, 3.0 mL/min, P = 100 bar,  $\lambda$  = 254 nm, *t<sub>R</sub>* = 4.04 min, *t<sub>S</sub>* = 5.14 min.

**Procedure F for the synthesis of compounds 7**

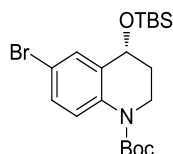
A solution of (R)-tert-butyl 6-bromo-4-hydroxy-3,4-dihydroquinoline-1(2H)-carboxylate **5g**



## Experimental part

(164 mg, 0.50 mmol) and imidazole (41 mg, 0.6 mmol) in DMF (1.0 mL) was added dropwise to a cooled (0 °C) solution of TBSCl (90 mg, 0.6 mmol) in DMF (0.2 mL) and the mixture stirred at 30 °C for 24 h. Water (10 ml) was added and the mixture was extracted with Et<sub>2</sub>O (3 x 20 mL). The organic extracts were combined, dried with MgSO<sub>4</sub>, and concentrated. The residue was purified by flash column chromatography to give pure (*R*)-tert-butyl-6-bromo-4-((tert-butyldimethylsilyl)oxy)-3,4-dihydroquinoline-1(2H)-carboxylate (207 mg, 94% yield). The latter compound (132 mg, 0.3 mmol) was placed in a round-bottom tube, and phenylboronic acid (73 mg, 0.6 mmol), K<sub>2</sub>CO<sub>3</sub> (124 mg, 0.9 mmol), Pd(OAc)<sub>2</sub> (3.4 mg, 0.015 mmol) and cataCXium A (10.7 mg, 0.03 mmol) were added. The tube was purged with argon three times and DMF (1.5 ml) was added. The reaction was heated at 100 °C overnight, quenched with water and extracted by CH<sub>2</sub>Cl<sub>2</sub> (3 x 5 mL). The combined organic layers were washed with brine (15 mL), dried over MgSO<sub>4</sub>, and concentrated under vacuum. The residue was purified by flash chromatography on silica gel (cyclohexane/EtOAc 20:1) to give pure **7** (129 mg, 98% yield) as a white solid.

(*R*)-tert-butyl-6-bromo-4-((tert-butyldimethylsilyl)oxy)-3,4-dihydroquinoline-1-(2H)-carboxylate (**6**)

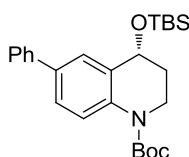


colorless liquid, 207 mg, 94% yield.

**<sup>1</sup>H NMR** (400 MHz, CDCl<sub>3</sub>) δ 7.61 (d, *J* = 8.9 Hz, 1H), 7.42 (dd, *J* = 2.5, 0.8 Hz, 1H), 7.30 (ddd, *J* = 8.9, 2.5, 0.6 Hz, 1H), 4.65 (dd, *J* = 7.8, 4.0 Hz, 1H), 3.78 (ddd, *J* = 12.7, 8.5, 5.5 Hz, 1H), 3.67 (ddd, *J* = 12.6, 6.7, 5.4 Hz, 1H), 2.12 – 2.00 (m, 1H), 1.91 – 1.77 (m, 1H), 1.52 (s, 9H), 0.93 (s, 9H), 0.15 (s, 3H), 0.13 (s, 3H).

**<sup>13</sup>C NMR** (101 MHz, CDCl<sub>3</sub>) δ 153.7, 136.2, 135.0, 130.2, 129.2, 125.3, 116.0, 81.4, 66.9, 41.5, 33.1, 28.5, 26.0, 18.3, -4.2, -4.4.

(*R*)-tert-butyl-4-((tert-butyldimethylsilyl)oxy)-6-phenyl-3,4-dihydroquinoline-1-(2H)-carboxylate (**7**)



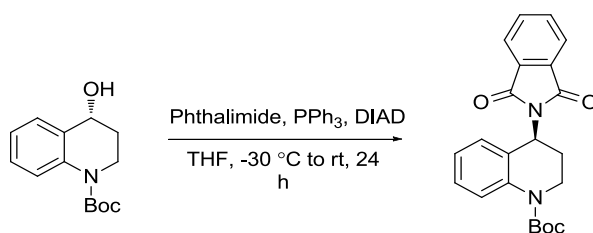
White solid, 129 mg, 98% yield, m.p. 85 °C, [α]<sub>D</sub><sup>25</sup> = +24.1 (c 1.19, CHCl<sub>3</sub>).

**<sup>1</sup>H NMR** (400 MHz, CDCl<sub>3</sub>) δ 7.85 (d, *J* = 8.6 Hz, 1H), 7.63 – 7.58 (m, 3H), 7.51 – 7.41 (m, 3H), 7.38 – 7.31 (m, 1H), 4.81 (dd, *J* = 7.4, 4.0 Hz, 1H), 3.94 – 3.85 (m, 1H), 3.82 – 3.72 (m, 1H), 2.20 – 2.07 (m, 1H), 2.03 – 1.89 (m, 1H), 1.58 (s, 9H), 0.98 (s, 9H), 0.21 (s, 3H), 0.18 (s, 3H).

**<sup>13</sup>C NMR** (101 MHz, CDCl<sub>3</sub>) δ 153.9, 141.0, 136.6, 135.7, 132.9, 128.9, 127.0, 126.8, 125.9, 125.2, 123.8, 81.1, 67.3, 41.6, 33.2, 28.5, 26.0, 18.3, -4.2, -4.4.

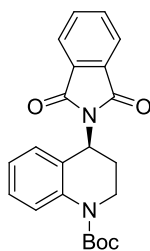
**HRMS** (ESI/ion trap): *m/z* [M + Na]<sup>+</sup> calcd for C<sub>26</sub>H<sub>37</sub>NNaO<sub>3</sub>Si 462.2440, found 462.2436.

### Procedure G for the synthesis of compounds 8



A solution of (*R*)-tert-butyl 4-hydroxy-3,4-dihydroquinoline-1(2H)-carboxylate **5a** (125 mg, 0.5 mmol) in THF (2 ml) was added to a mixture of PPh<sub>3</sub> (197 mg, 0.75 mmol) and phthalimide (100 mg, 0.75 mmol). The reaction mixture was allowed to stir for 10 min and then cooled to 0 °C. Once cooled, a solution of diisopropyl azodicarboxylate (DIAD) (202 mg, 1.0 mmol) in dry THF (1.0 ml) was added dropwise over a period of 5 min. The mixture was allowed to reach room temperature and stirred for 24 h. The reaction mixture was poured into water and extracted with CH<sub>2</sub>Cl<sub>2</sub>. The combined organic layers were washed with brine, dried over MgSO<sub>4</sub> and concentrated in vacuo. The residue was purified by flash column (PE/EA 10:1) to afford pure **8** (100 mg, 53% yield) as a white solid.

### (*S*)-tert-butyl 4-(1,3-dioxoisindolin-2-yl)-3,4-dihydroquinoline-1(2H)-carboxylate (**8**)



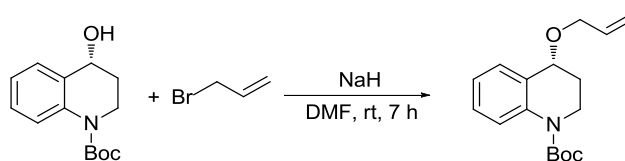
White solid, 100 mg, 53% yield, m.p. 166 °C,  $[\alpha]_D^{25} = -97.9$  (c 1.03, CHCl<sub>3</sub>).

**<sup>1</sup>H NMR** (400 MHz, CDCl<sub>3</sub>)  $\delta$  7.87 – 7.82 (m, 2H), 7.76 – 7.68 (m, 3H), 7.21 – 7.16 (m, 1H), 6.99 – 6.91 (m, 2H), 5.54 (t, *J* = 7.8 Hz, 1H), 4.17 (ddd, *J* = 13.1, 6.1, 4.2 Hz, 1H), 3.75 (ddd, *J* = 13.3, 9.7, 3.8 Hz, 1H), 2.58 – 2.49 (m, 1H), 2.30 – 2.22 (m, 1H), 1.55 (s, 9H).

**<sup>13</sup>C NMR** (101 MHz, CDCl<sub>3</sub>)  $\delta$  168.0, 153.7, 139.4, 134.3, 132.0, 127.4, 127.0, 126.2, 124.7, 123.9, 123.6, 81.3, 46.6, 43.3, 28.8, 28.5.

**HRMS** (ESI/ion trap): *m/z* [M + Na]<sup>+</sup> calcd for C<sub>22</sub>H<sub>22</sub>N<sub>2</sub>KO<sub>4</sub> 417.1217, found 417.1210.

### Procedure H for the synthesis of compounds 9

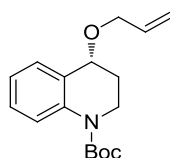


To a solution of (*R*)-tert-butyl 4-hydroxy-3,4-dihydroquinoline-1(2H)-carboxylate **5a** (125 mg, 0.5 mmol) in DMF (1.5 mL) was added NaH (60% dispersion in oil, 0.55 mmol, 22 mg) at

## Experimental part

room temperature. The mixture was stirred at the same temperature for 30 min then allyl bromide (0.55 mmol, 48  $\mu$ l) was added dropwise. After being stirred for 1 h, the reaction mixture was poured into water and extracted with  $\text{CH}_2\text{Cl}_2$ . The combined organic layers were washed with brine, dried over  $\text{MgSO}_4$  and concentrated in vacuo. The residue was purified by flash column chromatography (PE/EA 40:1) to afford pure **9** (111 mg, 77% yield) as a colorless liquid.

### (*R*)-tert-butyl 4-(allyloxy)-3,4-dihydroquinoline-1(2H)-carboxylate (**9**)



colorless liquid, 111 mg, 77% yield,  $[\alpha]_D^{25} = +39.7$  (c 0.75,  $\text{CHCl}_3$ ).

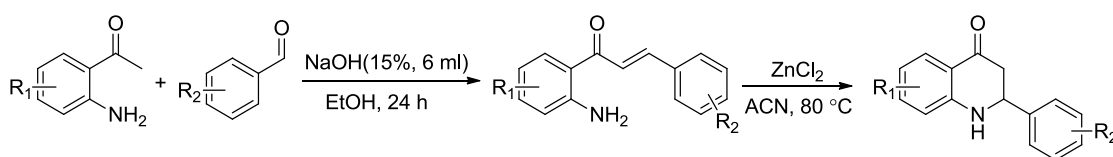
**$^1\text{H}$  NMR** (400 MHz,  $\text{CDCl}_3$ )  $\delta$  7.79 (d,  $J = 8.4$  Hz, 1H), 7.29 (dd,  $J = 7.6, 1.7$  Hz, 1H), 7.26 – 7.21 (m, 1H), 7.03 (td,  $J = 7.5, 1.1$  Hz, 1H), 5.96 (ddd,  $J = 22.8, 10.7, 5.6$  Hz, 1H), 5.31 (dq,  $J = 17.2, 1.7$  Hz, 1H), 5.20 (dq,  $J = 10.4, 1.5$  Hz, 1H), 4.43 (t,  $J = 4.4$  Hz, 1H), 4.09 (qdt,  $J = 12.7, 5.6, 1.5$  Hz, 2H), 3.93 (dt,  $J = 12.8, 5.2$  Hz, 1H), 3.66 (ddd,  $J = 12.7, 10.3, 4.4$  Hz, 1H), 2.15 – 2.08 (m, 1H), 2.00 – 1.94 (m, 1H), 1.53 (s, 9H).

**$^{13}\text{C}$  NMR** (101 MHz,  $\text{CDCl}_3$ )  $\delta$  153.9, 138.2, 135.1, 128.9, 128.0, 123.7, 123.0, 117.2, 81.1, 72.5, 69.4, 40.9, 28.9, 28.5.

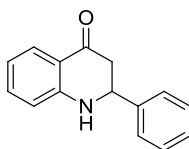
**HRMS** (ESI/ion trap):  $m/z$   $[\text{M} + \text{Na}]^+$  calcd for  $\text{C}_{17}\text{H}_{23}\text{NNaO}_3$  312.1576, found 312.1570.

## Substrates 10a-s

### General procedure I for preparing substrates 10a-s<sup>213</sup>



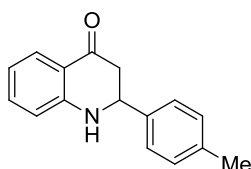
2'-Aminoacetophenone (20 mmol) and benzaldehyde (21 mmol) was dissolved in ethanol and a solution of sodium hydroxide (15%, 6 ml) was added under stirring. After 24 h the reaction mixture was neutralized with 10% HCl and diluted with water, then extracted by DCM. The combined organic layers were dried over  $\text{MgSO}_4$ , filtered, and evaporated under vacuum, then the crude product was used in the next step without further purification. The crude trans-2'-amino-chalcone and anhydrous zinc chloride (20 mmol) were dissolved in acetonitrile (60 ml), and the solution was heated to 80 °C for 24 hours. After evaporation of the solvent, the mixture was poured into sat.  $\text{NH}_4\text{Cl}$  (60 ml) and the aqueous phase was extracted with dichloromethane (70 ml  $\times$  3). The combined organic layers were dried over  $\text{MgSO}_4$ , filtered and evaporated under vacuum. The residue was first purified by flash column chromatography on silica gel (petroleum ether/ EtOAc = 4/1) then crystallized from n-hexane/EtOAc (9/1) to give the target product.

2-phenyl-2,3-dihydroquinolin-4(1H)-one (**10a**)

White solid, 17 g, 77% yield.

**<sup>1</sup>H NMR** (400 MHz, CDCl<sub>3</sub>) δ 7.87 (d, *J* = 7.9 Hz, 1H), 7.47 – 7.45 (m, 2H), 7.43 – 7.38 (m, 2H), 7.38 – 7.31 (m, 2H), 6.79 (t, *J* = 7.5 Hz, 1H), 6.72 (d, *J* = 8.2 Hz, 1H), 4.75 (dd, *J* = 13.7, 3.9 Hz, 1H), 4.54 (br, 1H), 2.88 (dd, *J* = 16.3, 13.7 Hz, 1H), 2.77 (ddd, *J* = 16.3, 3.9, 1.8 Hz, 1H).

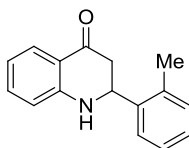
**<sup>13</sup>C NMR** (101 MHz, CDCl<sub>3</sub>) δ 193.4, 151.7, 141.1, 135.5, 129.1, 128.6, 127.7, 126.7, 119.1, 118.6, 116.1, 58.6, 46.5.

2-(p-tolyl)-2,3-dihydroquinolin-4(1H)-one (**10b**)

White solid, 3.0 g, 70% yield.

**<sup>1</sup>H NMR** (400 MHz, CDCl<sub>3</sub>) δ 7.87 (dd, *J* = 8.0, 1.6 Hz, 1H), 7.39 – 7.29 (m, 3H), 7.24 – 7.10 (m, 2H), 6.78 (ddd, *J* = 8.0, 7.1, 1.0 Hz, 1H), 6.70 (d, *J* = 8.2 Hz, 1H), 4.71 (dd, *J* = 13.8, 3.8 Hz, 1H), 4.50 (s, 1H), 2.87 (dd, *J* = 16.2, 13.8 Hz, 1H), 2.75 (ddd, *J* = 16.3, 3.8, 1.7 Hz, 1H), 2.37 (s, 3H).

**<sup>13</sup>C NMR** (101 MHz, CDCl<sub>3</sub>) δ 178.7, 156.8, 149.9, 138.1, 132.9, 128.0, 122.4, 121.8, 111.0, 106.0, 86.4, 55.7, 28.0.

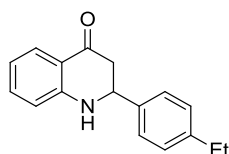
2-(o-tolyl)-2,3-dihydroquinolin-4(1H)-one (**10c**)

White solid, 2.0 g, 43% yield.

**<sup>1</sup>H NMR** (400 MHz, CDCl<sub>3</sub>) δ 7.96 (d, *J* = 7.8 Hz, 1H), 7.74 (d, *J* = 7.5 Hz, 1H), 7.49 – 7.19 (m, 4H), 6.87 (t, *J* = 7.5 Hz, 1H), 6.80 (d, *J* = 8.2 Hz, 1H), 5.09 (dd, *J* = 12.7, 4.9 Hz, 1H), 4.53 (br, 1H), 2.96 – 2.73 (m, 2H), 2.44 (s, 3H).

**<sup>13</sup>C NMR** (101 MHz, CDCl<sub>3</sub>) δ 193.5, 152.1, 139.2, 135.5, 135.2, 131.0, 128.1, 127.8, 126.9, 126.0, 119.1, 118.5, 116.1, 54.6, 45.3, 19.2.

2-(4-ethylphenyl)-2,3-dihydroquinolin-4(1H)-one (**10d**)

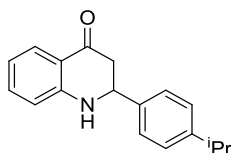


White solid, 2.5 g, 50% yield.

$^1\text{H NMR}$  (400 MHz,  $\text{CDCl}_3$ )  $\delta$  7.87 (dd,  $J = 7.9, 1.6$  Hz, 1H), 7.40 – 7.29 (m, 3H), 7.24 (d,  $J = 8.1$  Hz, 2H), 6.78 (ddd,  $J = 8.0, 7.1, 1.0$  Hz, 1H), 6.70 (d,  $J = 8.2$  Hz, 1H), 4.72 (dd,  $J = 13.8, 3.8$  Hz, 1H), 4.51 (br, 1H), 2.88 (dd,  $J = 16.2, 13.7$  Hz, 1H), 2.76 (ddd,  $J = 16.2, 3.8, 1.8$  Hz, 1H), 2.67 (q,  $J = 7.6$  Hz, 2H), 1.26 (t,  $J = 7.6$  Hz, 3H).

$^{13}\text{C NMR}$  (101 MHz,  $\text{CDCl}_3$ )  $\delta$  193.6, 151.7, 144.8, 138.4, 135.5, 128.6, 127.7, 126.8, 119.1, 118.5, 116.0, 58.4, 46.6, 28.7, 15.7.

2-(4-isopropylphenyl)-2,3-dihydroquinolin-4(1H)-one (**10e**)

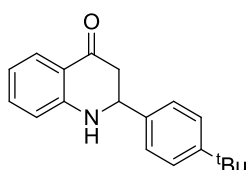


White solid, 2.5 g, 47% yield.

$^1\text{H NMR}$  (400 MHz,  $\text{CDCl}_3$ )  $\delta$  7.87 (dd,  $J = 7.9, 1.6$  Hz, 1H), 7.40 – 7.36 (m, 2H), 7.33 (ddd,  $J = 8.6, 7.1, 1.6$  Hz, 1H), 7.29 – 7.23 (m, 2H), 6.78 (ddd,  $J = 8.1, 7.1, 1.0$  Hz, 1H), 6.71 (d,  $J = 8.3$  Hz, 1H), 4.71 (dd,  $J = 13.8, 3.8$  Hz, 1H), 4.59 (br, 1H), 2.94 (hept,  $J = 6.9$  Hz, 1H), 2.87 (dd,  $J = 16.2, 13.7$  Hz, 1H), 2.75 (ddd,  $J = 16.2, 3.8, 1.7$  Hz, 1H), 1.27 (d,  $J = 7.0$  Hz, 6H).

$^{13}\text{C NMR}$  (101 MHz,  $\text{CDCl}_3$ )  $\delta$  193.6, 151.8, 149.3, 138.4, 135.4, 127.6, 127.1, 126.7, 119.0, 118.4, 116.0, 58.2, 46.5, 33.9, 24.1.

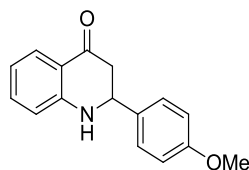
2-(4-(tert-butyl)phenyl)-2,3-dihydroquinolin-4(1H)-one (**10f**)



White solid, 4.5 g, 75% yield.

$^1\text{H NMR}$  (400 MHz,  $\text{CDCl}_3$ )  $\delta$  7.88 (dd,  $J = 7.9, 1.6$  Hz, 1H), 7.49 – 7.35 (m, 4H), 7.33 (ddd,  $J = 8.5, 7.1, 1.6$  Hz, 1H), 6.78 (t,  $J = 7.5$  Hz, 1H), 6.70 (d,  $J = 8.2$  Hz, 1H), 4.72 (dd,  $J = 13.7, 3.8$  Hz, 1H), 4.53 (br, 1H), 2.89 (dd,  $J = 16.1, 13.8$  Hz, 1H), 2.76 (dd,  $J = 16.2, 3.8$  Hz, 1H), 1.34 (s, 9H).

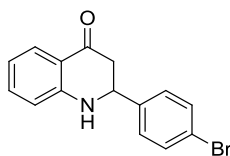
$^{13}\text{C NMR}$  (101 MHz,  $\text{CDCl}_3$ )  $\delta$  193.6, 151.7, 151.6, 138.0, 135.5, 127.7, 126.5, 126.0, 119.1, 118.4, 116.0, 58.2, 46.4, 34.7, 31.4.

2-(4-methoxyphenyl)-2,3-dihydroquinolin-4(1H)-one (**10g**)

White solid, 2.5 g, 50% yield.

$^1\text{H NMR}$  (400 MHz,  $\text{CDCl}_3$ )  $\delta$  7.88 (dd,  $J = 8.1, 1.5$  Hz, 1H), 7.41 – 7.32 (m, 3H), 6.99 – 6.91 (m, 2H), 6.79 (ddd,  $J = 8.0, 7.1, 1.1$  Hz, 1H), 6.73 (d,  $J = 8.3$  Hz, 1H), 4.69 (dd,  $J = 13.8, 3.7$  Hz, 1H), 4.57 (br, 1H), 3.84 (s, 3H), 2.86 (dd,  $J = 16.2, 13.8$  Hz, 1H), 2.73 (ddd,  $J = 16.3, 3.8, 1.0$  Hz, 1H).

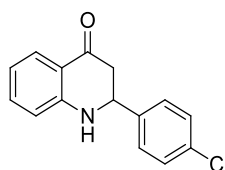
$^{13}\text{C NMR}$  (101 MHz,  $\text{CDCl}_3$ )  $\delta$  193.7, 159.7, 151.8, 135.5, 133.2, 127.9, 127.7, 119.0, 118.4, 116.0, 114.4, 58.0, 55.4, 46.6 .

2-(4-bromophenyl)-2,3-dihydroquinolin-4(1H)-one (**10h**)

White solid, 4.5 g, 74% yield.

$^1\text{H NMR}$  (400 MHz,  $\text{CDCl}_3$ )  $\delta$  7.84 (dd,  $J = 7.9, 1.6$  Hz, 1H), 7.55 – 7.46 (m, 2H), 7.39 – 7.29 (m, 3H), 6.79 (ddd,  $J = 8.1, 7.1, 1.0$  Hz, 1H), 6.74 (d,  $J = 8.2$  Hz, 1H), 4.69 (dd,  $J = 12.6, 4.8$  Hz, 1H), 4.61 (s, 1H), 2.92 – 2.61 (m, 2H).

$^{13}\text{C NMR}$  (101 MHz,  $\text{CDCl}_3$ )  $\delta$  192.9, 151.5, 140.2, 135.6, 132.2, 128.4, 127.7, 122.3, 119.1, 118.8, 116.1, 58.0, 46.4.

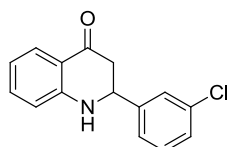
2-(4-chlorophenyl)-2,3-dihydroquinolin-4(1H)-one (**10i**)

White solid, 1.9 g, 40% yield.

$^1\text{H NMR}$  (400 MHz,  $\text{CDCl}_3$ )  $\delta$  7.85 (dd,  $J = 7.9, 1.6$  Hz, 1H), 7.45 – 7.32 (m, 5H), 6.80 (ddd,  $J = 8.0, 7.1, 1.0$  Hz, 1H), 6.73 (d,  $J = 8.2$  Hz, 1H), 4.72 (dd,  $J = 13.2, 4.3$  Hz, 1H), 4.57 (br, 1H), 2.81 (dd,  $J = 16.2, 13.1$  Hz, 1H), 2.73 (dd,  $J = 16.2, 4.3$  Hz, 1H).

$^{13}\text{C NMR}$  (101 MHz,  $\text{CDCl}_3$ )  $\delta$  193.0, 151.5, 139.6, 135.6, 134.3, 129.3, 128.1, 127.7, 119.1, 118.8, 116.1, 58.0, 46.5.

2-(3-chlorophenyl)-2,3-dihydroquinolin-4(1H)-one (**10j**)

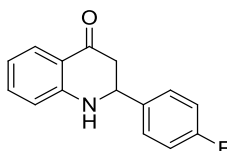


White solid, 2.5 g, 49% yield.

$^1\text{H NMR}$  (400 MHz,  $\text{CDCl}_3$ )  $\delta$  7.85 (d,  $J = 7.9$  Hz, 1H), 7.47 (s, 1H), 7.39 – 7.29 (m, 4H), 6.80 (t,  $J = 7.5$  Hz, 1H), 6.74 (d,  $J = 8.2$  Hz, 1H), 4.72 (dd,  $J = 13.1, 4.3$  Hz, 1H), 4.55 (br, 1H), 2.88 – 2.68 (m, 2H).

$^{13}\text{C NMR}$  (101 MHz,  $\text{CDCl}_3$ )  $\delta$  192.8, 151.4, 143.2, 135.6, 135.0, 130.4, 128.7, 127.7, 126.9, 125.0, 119.2, 118.9, 116.1, 58.1, 46.4.

2-(4-fluorophenyl)-2,3-dihydroquinolin-4(1H)-one (**10k**)



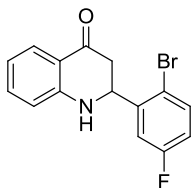
White solid, 3.0 g, 60% yield.

$^1\text{H NMR}$  (400 MHz,  $\text{CDCl}_3$ )  $\delta$  7.86 (dd,  $J = 8.0, 1.7$  Hz, 1H), 7.47 – 7.40 (m, 2H), 7.35 (ddd,  $J = 8.5, 7.1, 1.6$  Hz, 1H), 7.14 – 7.02 (m, 2H), 6.80 (ddd,  $J = 8.0, 7.1, 1.0$  Hz, 1H), 6.72 (d,  $J = 8.2$  Hz, 1H), 4.73 (dd,  $J = 13.5, 4.0$  Hz, 1H), 4.53 (br, 1H), 2.83 (dd,  $J = 16.2, 13.4$  Hz, 1H), 2.73 (ddd,  $J = 16.3, 4.0, 1.7$  Hz, 1H).

$^{13}\text{C NMR}$  (101 MHz,  $\text{CDCl}_3$ )  $\delta$  193.2, 162.7 (d,  $J = 247.0$  Hz), 151.6, 137.0 (d,  $J = 3.1$  Hz), 135.6, 128.4 (d,  $J = 8.2$  Hz), 127.7, 119.2, 118.7, 116.1 (d,  $J = 3.3$  Hz), 115.9, 58.0, 46.7.

$^{19}\text{F NMR}$  (282 MHz,  $\text{CDCl}_3$ )  $\delta$  -113.36 (tt,  $J = 9.0, 5.4$  Hz).

2-(2-bromo-5-fluorophenyl)-2,3-dihydroquinolin-4(1H)-one (**10l**)

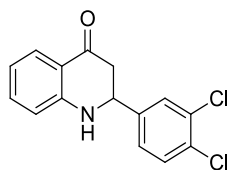


White solid, 1.5 g, 35% yield.

$^1\text{H NMR}$  (400 MHz,  $\text{CDCl}_3$ )  $\delta$  7.87 (dd,  $J = 8.0, 1.6$  Hz, 1H), 7.54 (dd,  $J = 8.8, 5.3$  Hz, 1H), 7.44 (dd,  $J = 9.5, 3.0$  Hz, 1H), 7.37 (ddd,  $J = 8.5, 7.1, 1.6$  Hz, 1H), 6.93 (ddd,  $J = 8.8, 7.6, 3.1$  Hz, 1H), 6.82 (ddd,  $J = 8.1, 7.1, 1.0$  Hz, 1H), 6.77 (d,  $J = 8.2$  Hz, 1H), 5.16 (ddd,  $J = 12.7, 3.9, 1.3$  Hz, 1H), 4.57 (br, 1H), 2.95 (dd,  $J = 16.3, 4.0$  Hz, 1H), 2.68 (dd,  $J = 16.3, 12.7$  Hz, 1H).

$^{13}\text{C NMR}$  (101 MHz,  $\text{CDCl}_3$ )  $\delta$  192.4, 162.4 (d,  $J = 248.2$  Hz), 151.4, 142.3 (d,  $J = 6.8$  Hz), 135.7, 134.7 (d,  $J = 7.8$  Hz), 127.7, 119.3, 119.1, 117.0 (d,  $J = 22.6$  Hz), 116.7 (d,  $J = 3.3$  Hz), 116.3, 115.2 (d,  $J = 24.3$  Hz), 57.0, 44.1.

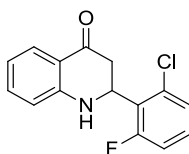
$^{19}\text{F NMR}$  (282 MHz,  $\text{CDCl}_3$ )  $\delta$  -112.33 (q,  $J = 7.6$  Hz).

2-(3,4-dichlorophenyl)-2,3-dihydroquinolin-4(1H)-one (**10m**)

White solid, 2.0 g, 40% yield.

**<sup>1</sup>H NMR** (400 MHz, CDCl<sub>3</sub>) δ 7.84 (dd, *J* = 8.0, 1.4 Hz, 1H), 7.57 (d, *J* = 2.1 Hz, 1H), 7.45 (d, *J* = 8.2 Hz, 1H), 7.36 (ddd, *J* = 8.3, 7.1, 1.6 Hz, 1H), 7.28 (dd, *J* = 8.3, 2.1 Hz, 1H), 6.81 (ddd, *J* = 8.0, 7.1, 1.0 Hz, 1H), 6.75 (d, *J* = 8.2 Hz, 1H), 4.70 (dd, *J* = 12.4, 5.0 Hz, 1H), 4.58 (br, 1H), 2.84 – 2.67 (m, 2H).

**<sup>13</sup>C NMR** (101 MHz, CDCl<sub>3</sub>) δ 192.5, 151.3, 141.4, 135.7, 133.2, 132.5, 131.1, 128.8, 127.7, 126.1, 119.2, 119.0, 116.2, 57.6, 46.4.

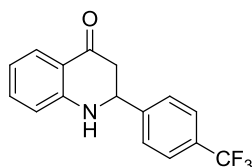
2-(2-chloro-6-fluorophenyl)-2,3-dihydroquinolin-4(1H)-one (**10n**)

White solid, 2.0 g, 40% yield.

**<sup>1</sup>H NMR** (400 MHz, CDCl<sub>3</sub>) δ 7.87 (dd, *J* = 8.0, 1.6 Hz, 1H), 7.31 (ddd, *J* = 8.5, 7.0, 1.6 Hz, 1H), 7.28 – 7.20 (m, 2H), 7.03 (ddd, *J* = 10.8, 7.9, 1.7 Hz, 1H), 6.77 (ddd, *J* = 7.9, 7.0, 1.0 Hz, 1H), 6.67 (d, *J* = 8.2 Hz, 1H), 5.41 (ddd, *J* = 14.2, 3.9, 1.3 Hz, 1H), 4.35 (br, 1H), 3.37 (dd, *J* = 16.1, 14.2 Hz, 1H), 2.71 (dd, *J* = 16.3, 3.8 Hz, 1H).

**<sup>13</sup>C NMR** (101 MHz, CDCl<sub>3</sub>) δ 193.1, 162.4 (d, *J* = 253.5 Hz), 151.5, 135.4, 134.9 (d, *J* = 6.4 Hz), 130.4 (d, *J* = 10.2 Hz), 127.8, 126.3 (d, *J* = 3.4 Hz), 125.1 (d, *J* = 13.8 Hz), 119.0, 118.5, 116.1, 115.8 (d, *J* = 23.0 Hz), 52.3, 41.7 (d, *J* = 3.0 Hz).

**<sup>19</sup>F NMR** (282 MHz, CDCl<sub>3</sub>) δ -107.59 (dd, *J* = 10.0, 4.5 Hz).

2-(4-(trifluoromethyl)phenyl)-2,3-dihydroquinolin-4(1H)-one (**10o**)

White solid, 3.3 g, 57% yield.

**<sup>1</sup>H NMR** (400 MHz, CDCl<sub>3</sub>) δ 7.85 (dd, *J* = 7.9, 1.6 Hz, 1H), 7.65 (d, *J* = 8.2 Hz, 2H), 7.58 (d, *J* = 8.2 Hz, 2H), 7.36 (ddd, *J* = 8.5, 7.1, 1.6 Hz, 1H), 6.81 (ddd, *J* = 8.1, 7.0, 1.0 Hz, 1H), 6.76 (d, *J* = 8.2 Hz, 1H), 4.81 (dd, *J* = 12.6, 4.7 Hz, 1H), 4.64 (br, 1H), 2.83 (dd, *J* = 16.2, 12.6 Hz, 1H), 2.76 (ddd, *J* = 16.2, 4.7, 1.6 Hz, 1H).

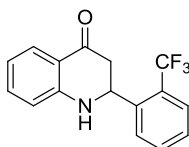


## Experimental part

$^{13}\text{C}$  NMR (101 MHz,  $\text{CDCl}_3$ )  $\delta$  192.6, 151.4, 145.2, 135.7, 130.8 (q,  $J = 32.5$  Hz), 127.7, 127.1, 126.1 (q,  $J = 3.8$  Hz), 124.0 (q,  $J = 272.4$  Hz), 119.2, 119.0, 116.2, 58.2, 46.4.

$^{19}\text{F}$  NMR (282 MHz,  $\text{CDCl}_3$ )  $\delta$  -62.58.

### 2-(2-(trifluoromethyl)phenyl)-2,3-dihydroquinolin-4(1H)-one (**10p**)



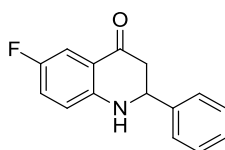
White solid, 3.0 g, 52% yield.

$^1\text{H}$  NMR (400 MHz,  $\text{CDCl}_3$ )  $\delta$  8.02 (d,  $J = 7.9$  Hz, 1H), 7.89 (dd,  $J = 8.0, 1.6$  Hz, 1H), 7.69 (d,  $J = 7.9$  Hz, 1H), 7.63 (t,  $J = 7.6$  Hz, 1H), 7.46 (t,  $J = 7.7$  Hz, 1H), 7.36 (ddd,  $J = 8.5, 7.1, 1.6$  Hz, 1H), 6.82 (t,  $J = 7.5$  Hz, 1H), 6.73 (d,  $J = 8.2$  Hz, 1H), 5.21 (t,  $J = 8.7$  Hz, 1H), 4.48 (br, 1H), 2.82 (d,  $J = 8.6$  Hz, 2H).

$^{13}\text{C}$  NMR (101 MHz,  $\text{CDCl}_3$ )  $\delta$  192.5, 151.6, 140.1, 135.6, 132.7, 128.5, 128.5, 128.00 (q,  $J = 30.2$  Hz), 127.8, 126.2 (q,  $J = 5.5$  Hz), 124.24 (q,  $J = 273.9$  Hz), 119.1, 119.0, 116.2, 53.9, 46.3.

$^{19}\text{F}$  NMR (282 MHz,  $\text{CDCl}_3$ )  $\delta$  -58.32.

### 6-fluoro-2-phenyl-2,3-dihydroquinolin-4(1H)-one (**10q**)



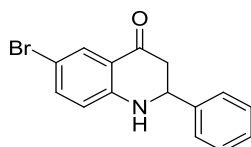
White solid, 1.0 g, 70% yield.

$^1\text{H}$  NMR (400 MHz,  $\text{CDCl}_3$ )  $\delta$  7.54 (dd,  $J = 8.8, 3.0$  Hz, 1H), 7.49 – 7.41 (m, 2H), 7.45 – 7.31 (m, 3H), 7.10 (ddd,  $J = 8.9, 7.8, 3.1$  Hz, 1H), 6.70 (dd,  $J = 8.9, 4.1$  Hz, 1H), 4.72 (dd,  $J = 13.6, 4.0$  Hz, 1H), 4.47 (br, 1H), 2.86 (dd,  $J = 16.4, 13.6$  Hz, 1H), 2.77 (dd,  $J = 16.4, 4.0$  Hz, 1H).

$^{13}\text{C}$  NMR (101 MHz,  $\text{CDCl}_3$ )  $\delta$  192.7, 156.1 (d,  $J = 238.9$  Hz), 148.3, 140.9, 129.2, 128.7, 126.8, 123.5 (d,  $J = 24.4$  Hz), 119.4 (d,  $J = 5.9$  Hz), 117.6 (d,  $J = 7.0$  Hz), 112.5 (d,  $J = 22.1$  Hz), 58.9, 46.3.

$^{19}\text{F}$  NMR (282 MHz,  $\text{CDCl}_3$ )  $\delta$  -125.59 (td,  $J = 8.5, 4.1$  Hz).

### 6-bromo-2-phenyl-2,3-dihydroquinolin-4(1H)-one (**10r**)



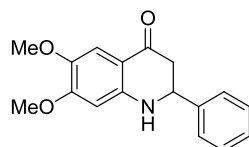
White solid, 900 mg, 69% yield.

$^1\text{H}$  NMR (400 MHz,  $\text{CDCl}_3$ )  $\delta$  7.97 (d,  $J = 2.4$  Hz, 1H), 7.50 – 7.30 (m, 6H), 6.63 (d,  $J = 8.7$  Hz,

1H), 4.72 (dd,  $J = 13.4, 4.1$  Hz, 1H), 4.60 (br, 1H), 2.86 (dd,  $J = 16.3, 13.4$  Hz, 1H), 2.76 (dd,  $J = 16.3, 3.9$  Hz, 1H).

$^{13}\text{C}$  NMR (101 MHz,  $\text{CDCl}_3$ )  $\delta$  192.1, 150.4, 140.6, 138.1, 130.1, 129.2, 128.8, 126.7, 120.3, 117.9, 110.8, 58.4, 46.1.

6,7-dimethoxy-2-phenyl-2,3-dihydroquinolin-4(1H)-one (**10s**)



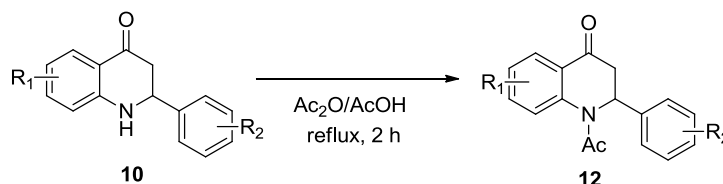
White solid, 1.5 g, 27% yield.

$^1\text{H}$  NMR (400 MHz,  $\text{CDCl}_3$ )  $\delta$  7.50 – 7.28 (m, 1H), 6.18 (s, 1H), 4.71 (dd,  $J = 13.5, 4.2$  Hz, 1H), 2.82 (dd,  $J = 16.3, 13.5$  Hz, 1H), 2.71 (dd,  $J = 16.3, 4.2$  Hz, 1H), 3.87 (s, 3H), 3.85 (s, 3H).

$^{13}\text{C}$  NMR (101 MHz,  $\text{CDCl}_3$ )  $\delta$  191.8, 156.2, 148.4, 143.2, 141.3, 129.1, 128.5, 126.8, 111.8, 108.0, 98.1, 59.4, 56.3, 56.2, 46.1.

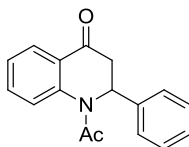
Substrates **12a-o**, **12q-t**

General procedure J for preparing substrates **12a-o**, **12q-t**<sup>214</sup>



Compound **10** (5.0 mmol) was dissolved in 20 ml of  $\text{AcOH}/\text{Ac}_2\text{O}$  (1:1) mixture and refluxed for 2 h. The solvent was removed under vacuum, and the residue was purified by flashcolumn chromatography on silica gel (petroleum ether/  $\text{EtOAc} = 4/1$ ) to afford the desired substrates **12**.

1-acetyl-2-phenyl-2,3-dihydroquinolin-4(1H)-one (**12a**)



White solid, 3.2 g, 76% yield, m.p. 174 °C.

$^1\text{H}$  NMR (400 MHz,  $\text{CDCl}_3$ )  $\delta$  7.92 (dd,  $J = 7.8, 1.7$  Hz, 1H), 7.46 (ddd,  $J = 8.2, 7.3, 1.7$  Hz, 1H), 7.26 (br, 1H), 7.23 – 7.11 (m, 6H), 6.47 (br, 1H), 3.37 (dd,  $J = 18.0, 2.0$  Hz, 1H), 3.24 (dd,  $J = 18.0, 5.9$  Hz, 1H), 2.43 (s, 3H).

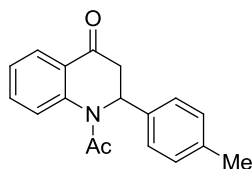
$^{13}\text{C}$  NMR (101 MHz,  $\text{CDCl}_3$ )  $\delta$  193.2, 170.2, 141.9, 138.1, 134.5, 128.7, 127.7, 127.4, 126.9,

## Experimental part

126.2, 125.6, 125.2, 54.8, 42.7, 23.5.

For the (*S*)-**12a**' enantiomer  $[\alpha]_D^{25} = -271.3$  ( $c = 1.25$ ,  $\text{CHCl}_3$ ) (lit: 247,  $[\alpha]_D^{20} = -219.1$  (0.66,  $\text{CHCl}_3$ )).

### 1-acetyl-2-(*p*-tolyl)-2,3-dihydroquinolin-4(1H)-one (**12b**)



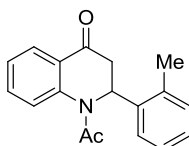
White solid, 1.0 g, 71% yield, m.p.196 °C.

**<sup>1</sup>H NMR** (400 MHz,  $\text{CDCl}_3$ )  $\delta$  7.92 (dd,  $J = 7.9, 1.7$  Hz, 1H), 7.46 (ddd,  $J = 8.2, 7.3, 1.7$  Hz, 1H), 7.29 (br, 1H), 7.16 (td,  $J = 7.8, 1.0$  Hz, 1H), 7.06 (d,  $J = 8.0$  Hz, 2H), 6.99 (d,  $J = 8.1$  Hz, 2H), 6.41 (br, 1H), 3.34 (dd,  $J = 18.0, 2.0$  Hz, 1H), 3.22 (dd,  $J = 17.9, 5.8$  Hz, 1H), 2.42 (s, 3H), 2.21 (s, 3H).

**<sup>13</sup>C NMR** (101 MHz,  $\text{CDCl}_3$ )  $\delta$  193.4, 170.2, 142.0, 137.4, 135.0, 134.5, 129.4, 127.4, 126.8, 126.2, 125.5, 125.2, 54.7, 42.8, 23.6, 21.1.

For the (*S*)-**12b**' enantiomer  $[\alpha]_D^{25} = -255.0$  ( $c = 1.59$ ,  $\text{CHCl}_3$ ).

### 1-acetyl-2-(*o*-tolyl)-2,3-dihydroquinolin-4(1H)-one (**12c**)



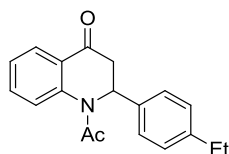
White solid, 1.0 g, 71% yield, m.p.138 °C.

**<sup>1</sup>H NMR** (400 MHz,  $\text{CDCl}_3$ )  $\delta$  7.97 (dd,  $J = 7.8, 1.5$  Hz, 1H), 7.42 (ddd,  $J = 8.1, 7.4, 1.7$  Hz, 1H), 7.22 (td,  $J = 7.6, 1.1$  Hz, 1H), 7.15 – 7.06 (m, 2H), 7.05 (td,  $J = 7.3, 1.3$  Hz, 1H), 6.90 (td,  $J = 7.7, 1.5$  Hz, 1H), 6.82 (d,  $J = 7.7$  Hz, 1H), 6.60 (d,  $J = 4.7$  Hz, 1H), 3.26 (dd,  $J = 18.2, 5.6$  Hz, 1H), 3.19 (dd,  $J = 18.2, 2.0$  Hz, 1H), 2.39 (s, 3H), 2.27 (s, 3H).

**<sup>13</sup>C NMR** (101 MHz,  $\text{CDCl}_3$ )  $\delta$  194.4, 169.4, 142.2, 137.4, 136.0, 134.5, 131.2, 128.0, 127.5, 127.2, 126.9, 126.4, 125.8, 125.6, 52.9, 43.2, 23.1, 19.8.

For the (*S*)-**12c**' enantiomer  $[\alpha]_D^{25} = -179.2$  ( $c = 1.07$ ,  $\text{CHCl}_3$ ).

### 1-acetyl-2-(4-ethylphenyl)-2,3-dihydroquinolin-4(1H)-one (**12d**)



<sup>247</sup> Lei, B.-L.; Ding, C.-H.; Yang, X.-F.; Wan, X.-L.; Hou, X.-L. *J. Am. Chem. Soc.* **2009**, *131*, 18250.

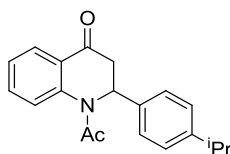
White solid, 1.1 g, 76% yield, m.p.196 °C.

**<sup>1</sup>H NMR** (400 MHz, CDCl<sub>3</sub>) δ 7.87 (dd, *J* = 7.9, 1.6 Hz, 1H), 7.40 – 7.29 (m, 3H), 7.24 (d, *J* = 8.1 Hz, 2H), 6.78 (ddd, *J* = 8.0, 7.1, 1.0 Hz, 1H), 6.70 (d, *J* = 8.2 Hz, 1H), 4.72 (dd, *J* = 13.8, 3.8 Hz, 1H), 4.51 (br, 1H), 2.88 (dd, *J* = 16.2, 13.7 Hz, 1H), 2.76 (ddd, *J* = 16.2, 3.8, 1.8 Hz, 1H), 2.67 (q, *J* = 7.6 Hz, 2H), 1.26 (t, *J* = 7.6 Hz, 3H).

**<sup>13</sup>C NMR** (101 MHz, CDCl<sub>3</sub>) δ 193.2, 170.1, 143.5, 141.9, 135.1, 134.4, 128.1, 127.2, 126.8, 126.0, 125.4, 125.2, 54.7, 42.7, 28.3, 23.5, 15.3.

For the (*S*)-**12d'** enantiomer  $[\alpha]_D^{25} = -239.7$  (*c* = 1.23, CHCl<sub>3</sub>).

1-acetyl-2-(4-isopropylphenyl)-2,3-dihydroquinolin-4(1H)-one (**12e**)



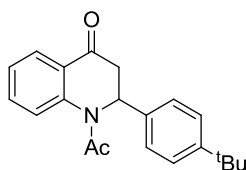
White solid, 1.2 g, 78% yield, m.p.70 °C.

**<sup>1</sup>H NMR** (400 MHz, CDCl<sub>3</sub>) δ 7.90 (dd, *J* = 7.8, 1.6 Hz, 1H), 7.43 (td, *J* = 7.8, 1.7 Hz, 1H), 7.32 (br, 1H), 7.16 – 7.03 (m, 3H), 7.02 (d, *J* = 8.4 Hz, 2H), 6.38 (br, 1H), 3.33 (dd, *J* = 17.9, 2.0 Hz, 1H), 3.22 (dd, *J* = 17.9, 5.8 Hz, 1H), 2.75 (hept, *J* = 6.9 Hz, 1H), 2.41 (s, 3H), 1.11 (d, *J* = 7.0 Hz, 6H).

**<sup>13</sup>C NMR** (101 MHz, CDCl<sub>3</sub>) δ 193.2, 170.1, 148.1, 141.9, 135.2, 134.4, 127.2, 126.7, 126.0, 125.3, 125.1, 54.8, 42.7, 33.5, 23.8, 23.8, 23.5.

For the (*S*)-**12e'** enantiomer  $[\alpha]_D^{25} = -227.9$  (*c* = 1.10, CHCl<sub>3</sub>).

1-acetyl-2-(4-(tert-butyl)phenyl)-2,3-dihydroquinolin-4(1H)-one (**12f**)



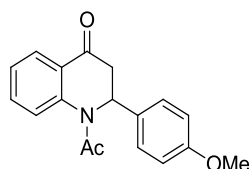
White solid, 2.1 g, 66% yield, m.p.146 °C.

**<sup>1</sup>H NMR** (400 MHz, CDCl<sub>3</sub>) δ 7.92 (dd, *J* = 7.8, 1.5 Hz, 1H), 7.46 (ddd, *J* = 8.2, 7.3, 1.7 Hz, 1H), 7.35 (br, 1H), 7.20 (d, *J* = 8.5 Hz, 2H), 7.14 (t, *J* = 7.9 Hz, 1H), 7.08 (d, *J* = 8.3 Hz, 2H), 6.38 (br, 1H), 3.34 (dd, *J* = 17.9, 2.0 Hz, 1H), 3.23 (dd, *J* = 17.9, 5.8 Hz, 1H), 2.42 (s, 3H), 1.20 (s, 9H).

**<sup>13</sup>C NMR** (101 MHz, CDCl<sub>3</sub>) δ 193.2, 170.2, 150.4, 142.0, 134.9, 134.4, 127.3, 126.5, 126.0, 125.6, 125.4, 125.2, 54.8, 42.8, 34.4, 31.2, 23.6.

For the (*S*)-**12f'** enantiomer  $[\alpha]_D^{25} = -171.9$  (*c* = 1.25, CHCl<sub>3</sub>).

1-acetyl-2-(4-methoxyphenyl)-2,3-dihydroquinolin-4(1H)-one (**12g**)



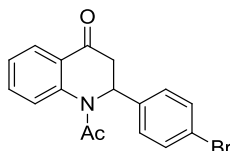
White solid, 1.3 g, 88% yield, m.p.122 °C.

**<sup>1</sup>H NMR** (400 MHz, CDCl<sub>3</sub>) δ 7.92 (d, *J* = 7.8 Hz, 1H), 7.44 (t, *J* = 7.7 Hz, 1H), 7.25 (br, 1H), 7.15 (t, *J* = 7.5 Hz, 1H), 7.08 (d, *J* = 8.8 Hz, 2H), 6.70 (d, *J* = 8.8 Hz, 2H), 6.40 (br, 1H), 3.68 (s, 3H), 3.31 (dd, *J* = 18.0, 1.9 Hz, 1H), 3.21 (dd, *J* = 17.9, 5.7 Hz, 1H), 2.41 (s, 3H).

**<sup>13</sup>C NMR** (101 MHz, CDCl<sub>3</sub>) δ 193.4, 170.1, 158.9, 141.8, 134.5, 130.0, 128.1, 127.3, 126.1, 125.5, 125.2, 114.0, 55.2, 42.8, 23.5.

For the (*S*)-**12g**' enantiomer  $[\alpha]_D^{25} = -233.1$  (*c* = 1.86, CHCl<sub>3</sub>) (lit:247,  $[\alpha]_D^{20} = -212.1$  (0.68, CHCl<sub>3</sub>)).

1-acetyl-2-(4-bromophenyl)-2,3-dihydroquinolin-4(1H)-one (**12h**)



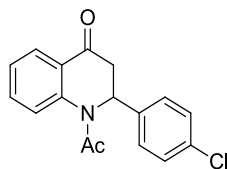
White solid, 1.3 g, 76% yield, m.p.174 °C.

**<sup>1</sup>H NMR** (400 MHz, CDCl<sub>3</sub>) δ 7.91 (d, *J* = 7.8 Hz, 1H), 7.46 (t, *J* = 7.8 Hz, 1H), 7.30 (d, *J* = 8.4 Hz, 2H), 7.25 – 7.12 (m, 2H), 7.04 (d, *J* = 8.5 Hz, 2H), 6.43 (br, 1H), 3.30 (dd, *J* = 18.1, 2.2 Hz, 1H), 3.22 (dd, *J* = 18.0, 5.6 Hz, 1H), 2.41 (s, 3H).

**<sup>13</sup>C NMR** (101 MHz, CDCl<sub>3</sub>) δ 192.8, 170.2, 141.6, 137.2, 134.7, 131.8, 128.6, 127.5, 126.0, 125.8, 125.1, 121.8, 54.2, 42.5, 23.4.

For the (*S*)-**12h**' enantiomer  $[\alpha]_D^{25} = -209.1$  (*c* = 1.94, CHCl<sub>3</sub>) (lit:247,  $[\alpha]_D^{20} = -199.2$  (0.77, CHCl<sub>3</sub>)).

1-acetyl-2-(4-chlorophenyl)-2,3-dihydroquinolin-4(1H)-one (**12i**)



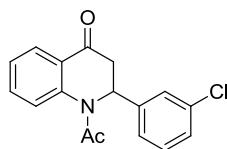
White solid, 1.1 g, 73% yield, m.p.194 °C.

**<sup>1</sup>H NMR** (400 MHz, CDCl<sub>3</sub>) δ 7.92 (dd, *J* = 7.9, 1.6 Hz, 1H), 7.47 (ddd, *J* = 8.2, 7.3, 1.7 Hz, 1H), 7.24 – 7.11 (m, 4H), 7.14 – 7.06 (m, 2H), 6.46 (br, 1H), 3.31 (dd, *J* = 18.0, 2.2 Hz, 1H), 3.23 (dd, *J* = 18.1, 5.6 Hz, 1H), 2.41 (s, 3H).

**<sup>13</sup>C NMR** (101 MHz, CDCl<sub>3</sub>) δ 192.9, 170.2, 141.7, 136.7, 134.7, 133.6, 128.9, 128.3, 127.5, 126.0, 125.8, 125.1, 54.2, 42.6, 23.4.

For the (*S*)-**12i**' enantiomer  $[\alpha]_D^{25} = -251.5$  ( $c = 1.18$ ,  $\text{CHCl}_3$ ).

1-acetyl-2-(3-chlorophenyl)-2,3-dihydroquinolin-4(1H)-one (**12j**)



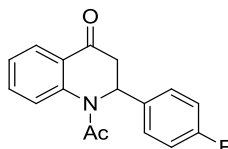
White solid, 2.5 g, 49% yield, m.p.152 °C.

**<sup>1</sup>H NMR** (400 MHz,  $\text{CDCl}_3$ )  $\delta$  7.93 (dd,  $J = 7.8, 1.7$  Hz, 1H), 7.48 (ddd,  $J = 8.2, 7.3, 1.7$  Hz, 1H), 7.25 (br, 1H), 7.21 – 7.15 (m, 2H), 7.14 – 7.08 (m, 2H), 7.07 – 7.01 (m, 1H), 6.47 (br, 1H), 3.32 (dd,  $J = 18.1, 2.1$  Hz, 1H), 3.23 (dd,  $J = 18.1, 5.7$  Hz, 1H), 2.42 (s, 3H).

**<sup>13</sup>C NMR** (101 MHz,  $\text{CDCl}_3$ )  $\delta$  192.7, 170.2, 141.7, 140.3, 134.9, 134.7, 130.0, 128.0, 127.6, 127.3, 126.0, 125.8, 125.2, 124.9, 54.2, 42.4, 23.4.

For the (*S*)-**12j**' enantiomer  $[\alpha]_D^{25} = -196.8$  ( $c = 1.50$ ,  $\text{CHCl}_3$ ).

1-acetyl-2-(4-fluorophenyl)-2,3-dihydroquinolin-4(1H)-one (**12k**)



White solid, 1.0 g, 71% yield, m.p.166 °C.

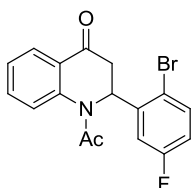
**<sup>1</sup>H NMR** (400 MHz,  $\text{CDCl}_3$ )  $\delta$  7.92 (dd,  $J = 7.9, 1.6$  Hz, 1H), 7.46 (ddd,  $J = 8.2, 7.3, 1.7$  Hz, 1H), 7.22 (br, 1H), 7.20 – 7.09 (m, 3H), 6.91 – 6.83 (m, 2H), 6.46 (br, 1H), 3.31 (dd,  $J = 18.0, 2.2$  Hz, 1H), 3.23 (dd,  $J = 18.0, 5.6$  Hz, 1H), 2.41 (s, 3H).

**<sup>13</sup>C NMR** (101 MHz,  $\text{CDCl}_3$ )  $\delta$  193.0, 170.2, 162.1 (d,  $J = 246.9$  Hz), 141.70, 134.6, 133.9 (d,  $J = 2.9$  Hz), 128.6 (d,  $J = 8.2$  Hz), 127.4, 126.0, 125.7, 125.1, 115.6 (d,  $J = 21.5$  Hz), 54.2, 42.7, 23.4.

**<sup>19</sup>F NMR** (282 MHz,  $\text{CDCl}_3$ )  $\delta$  -114.50.

For the (*S*)-**12k**' enantiomer  $[\alpha]_D^{25} = -246.0$  ( $c = 1.21$ ,  $\text{CHCl}_3$ ) (lit:247,  $[\alpha]_D^{20} = -261.7$  (0.59,  $\text{CHCl}_3$ )).

1-acetyl-2-(2-bromo-5-fluorophenyl)-2,3-dihydroquinolin-4(1H)-one (**12l**)



White solid, 660 mg, 35% yield, m.p.137 °C.

## Experimental part

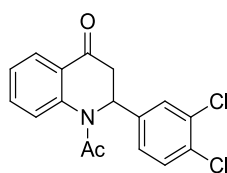
**<sup>1</sup>H NMR** (400 MHz, CDCl<sub>3</sub>) δ 7.94 (dt, *J* = 7.8, 1.1 Hz, 1H), 7.59 – 7.47 (m, 2H), 7.46 (dd, *J* = 8.7, 5.4 Hz, 1H), 7.28 – 7.19 (m, 1H), 6.75 (ddd, *J* = 8.7, 7.6, 2.9 Hz, 1H), 6.59 (ddd, *J* = 9.8, 2.9, 0.7 Hz, 1H), 6.38 (d, *J* = 6.4 Hz, 1H), 3.30 (dd, *J* = 18.1, 6.5 Hz, 1H), 3.20 (dd, *J* = 18.1, 1.9 Hz, 1H), 2.31 (s, 3H).

**<sup>13</sup>C NMR** (101 MHz, CDCl<sub>3</sub>) δ 192.4, 170.0, 161.6 (d, *J* = 247.8 Hz), 142.4, 139.8 (d, *J* = 6.8 Hz), 135.1 (d, *J* = 8.2 Hz), 135.0, 127.5, 126.0, 125.9, 124.8, 117.2 (d, *J* = 3.4 Hz), 116.5 (d, *J* = 22.2 Hz), 115.8 (d, *J* = 24.8 Hz), 55.6, 42.6, 23.4.

**<sup>19</sup>F NMR** (282 MHz, CDCl<sub>3</sub>) δ -113.01.

For the (*S*)-**12l'** enantiomer  $[\alpha]_D^{25} = -125.8$  (*c* = 1.60, CHCl<sub>3</sub>).

### 1-acetyl-2-(3,4-dichlorophenyl)-2,3-dihydroquinolin-4(1H)-one (**12m**)



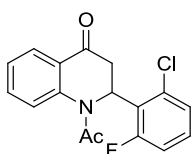
White solid, 1.0 g, 75% yield, m.p.149 °C.

**<sup>1</sup>H NMR** (400 MHz, CDCl<sub>3</sub>) δ 7.94 (dd, *J* = 7.9, 1.7 Hz, 1H), 7.51 (ddd, *J* = 8.0, 7.3, 1.7 Hz, 1H), 7.33 – 7.17 (m, 4H), 7.00 (ddd, *J* = 8.4, 2.3, 0.9 Hz, 1H), 6.48 (br, 1H), 3.58 – 3.12 (m, 2H), 2.44 (s, 3H).

**<sup>13</sup>C NMR** (101 MHz, CDCl<sub>3</sub>) δ 192.4, 170.2, 141.5, 138.6, 134.8, 133.1, 131.9, 130.6, 129.1, 127.6, 126.2, 126.0, 125.9, 125.1, 53.7, 42.3, 23.4.

For the (*S*)-**12m'** enantiomer  $[\alpha]_D^{25} = -210.8$  (*c* = 1.18, CHCl<sub>3</sub>).

### 1-acetyl-2-(2-chloro-6-fluorophenyl)-2,3-dihydroquinolin-4(1H)-one (**12n**)



White solid, 400 mg, 44% yield, m.p.183 °C.

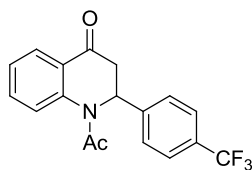
**<sup>1</sup>H NMR** (400 MHz, CDCl<sub>3</sub>) δ 7.97 (dd, *J* = 7.7, 1.6 Hz, 1H), 7.44 (td, *J* = 7.7, 1.6 Hz, 1H), 7.29 (ddd, *J* = 8.6, 7.2, 1.0 Hz, 1H), 7.19 (d, *J* = 7.9 Hz, 1H), 7.15 – 7.07 (m, 2H), 6.80 – 6.67 (m, 2H), 3.30 (dddd, *J* = 18.4, 6.5, 5.4, 0.8 Hz, 1H), 3.22 (dddd, *J* = 18.3, 5.5, 2.3, 0.7 Hz, 1H), 2.20 (s, 3H).

**<sup>13</sup>C NMR** (101 MHz, CDCl<sub>3</sub>) δ 193.4 (d, *J* = 5.7 Hz), 169.0, 161.8 (d, *J* = 249.9 Hz), 142.2, 136.2 (d, *J* = 6.9 Hz), 133.8, 129.9 (d, *J* = 10.5 Hz), 128.6, 127.2, 126.8, 126.5 (d, *J* = 3.2 Hz), 126.1, 123.6 (d, *J* = 14.8 Hz), 115.2 (d, *J* = 25.6 Hz), 52.0 (d, *J* = 2.0 Hz), 42.82 (d, *J* = 6.2 Hz), 22.7.

**<sup>19</sup>F NMR** (282 MHz, CDCl<sub>3</sub>) δ -108.91 (dd, *J* = 11.8, 5.8 Hz).

For the (*S*)-**12n'** enantiomer  $[\alpha]_D^{25} = -43.4$  ( $c = 1.60$ ,  $\text{CHCl}_3$ ).

1-acetyl-2-(4-(trifluoromethyl)phenyl)-2,3-dihydroquinolin-4(1H)-one (**12o**)



White solid, 900 mg, 54% yield, m.p.128 °C.

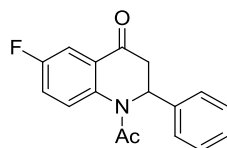
$^1\text{H NMR}$  (400 MHz,  $\text{CDCl}_3$ )  $\delta$  7.93 (dd,  $J = 8.0, 1.6$  Hz, 1H), 7.52 – 7.42 (m, 3H), 7.30 (dd,  $J = 8.1, 0.8$  Hz, 2H), 7.24 (br, 1H), 7.19 (td,  $J = 7.6, 1.0$  Hz, 1H), 6.55 (br, 1H), 3.37 (dd,  $J = 18.1, 2.1$  Hz, 1H), 3.28 (dd,  $J = 18.1, 5.7$  Hz, 1H), 2.43 (s, 3H).

$^{13}\text{C NMR}$  (101 MHz,  $\text{CDCl}_3$ )  $\delta$  192.6, 170.3, 142.3, 141.7, 134.8, 130.0 (q,  $J = 32.6$  Hz), 127.6, 127.3, 126.0, 125.7 (q,  $J = 3.8$  Hz), 125.1, 123.9 (q,  $J = 272.1$  Hz) 131.8, 128.6, 127.5, 126.0, 125.8, 125.1, 121.8, 54.4, 42.5, 23.4.

$^{19}\text{F NMR}$  (282 MHz,  $\text{CDCl}_3$ )  $\delta$  -62.73.

For the (*S*)-**12o'** enantiomer  $[\alpha]_D^{25} = -176.6$  ( $c = 1.17$ ,  $\text{CHCl}_3$ ) (lit: 247,  $[\alpha]_D^{20} = -176.1$  (0.78,  $\text{CHCl}_3$ )).

1-acetyl-6-fluoro-2-phenyl-2,3-dihydroquinolin-4(1H)-one (**12q**)



White solid, 700 mg, 88% yield, m.p.153 °C.

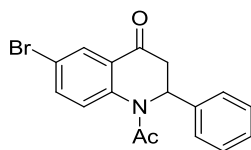
$^1\text{H NMR}$  (400 MHz,  $\text{CDCl}_3$ )  $\delta$  7.51 (dd,  $J = 8.3, 3.1$  Hz, 1H), 7.36 (br, 1H), 7.21 – 7.06 (m, 6H), 6.36 (br, 1H), 3.35 (dd,  $J = 18.0, 2.0$  Hz, 1H), 3.21 (dd,  $J = 18.0, 5.8$  Hz, 1H), 2.39 (s, 3H).

$^{13}\text{C NMR}$  (101 MHz,  $\text{CDCl}_3$ )  $\delta$  192.0, 169.9, 159.6 (d,  $J = 248.0$  Hz), 137.9, 137.7 (d,  $J = 40.9$  Hz), 128.7, 127.7, 127.4 (d,  $J = 6.5$  Hz), 127.2 (d,  $J = 7.3$  Hz), 126.6, 121.6 (d,  $J = 23.4$  Hz), 113.0 (d,  $J = 23.2$  Hz), 55.0, 42.2, 23.2.

$^{19}\text{F NMR}$  (282 MHz,  $\text{CDCl}_3$ )  $\delta$  -115.01.

For the (*S*)-**12q'** enantiomer  $[\alpha]_D^{25} = -212.2$  ( $c = 1.30$ ,  $\text{CHCl}_3$ ).

1-acetyl-6-bromo-2-phenyl-2,3-dihydroquinolin-4(1H)-one (**12r**)



White solid, 2.0 g, 65% yield, m.p.119 °C.



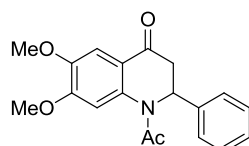
## Experimental part

**<sup>1</sup>H NMR** (400 MHz, CDCl<sub>3</sub>) δ 7.95 (d, *J* = 2.5 Hz, 1H), 7.49 (dd, *J* = 8.7, 2.5 Hz, 1H), 7.30 (s, 1H), 7.22 – 7.05 (m, 5H), 6.31 (br, 1H), 3.34 (dd, *J* = 17.9, 2.1 Hz, 1H), 3.20 (dd, *J* = 17.9, 5.8 Hz, 1H), 2.39 (s, 3H).

**<sup>13</sup>C NMR** (101 MHz, CDCl<sub>3</sub>) δ 191.5, 169.8, 140.6, 137.3, 137.0, 129.8, 128.7, 127.7, 126.9, 126.7, 126.5, 118.6, 55.0, 42.2, 23.3.

For the (*S*)-**12r'** enantiomer  $[\alpha]_D^{25} = -127.3$  (*c* = 1.30, CHCl<sub>3</sub>).

### 1-acetyl-6,7-dimethoxy-2-phenyl-2,3-dihydroquinolin-4(1H)-one (**12s**)



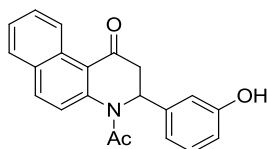
White solid, 800 mg, 71% yield, m.p. 182 °C.

**<sup>1</sup>H NMR** (400 MHz, CDCl<sub>3</sub>) δ 7.29 (s, 1H), 7.22 – 7.07 (m, 5H), 6.87 (br, 1H), 6.24 (br, 1H), 3.86 (s, 3H), 3.79 (s, 3H), 3.35 – 3.09 (m, 2H), 2.40 (s, 3H).

**<sup>13</sup>C NMR** (101 MHz, CDCl<sub>3</sub>) δ 191.6, 169.9, 153.9, 146.7, 138.0, 137.0, 128.6, 127.6, 126.6, 119.2, 107.6, 56.3, 56.0, 42.1, 23.7.

For the (*S*)-**12s'** enantiomer  $[\alpha]_D^{25} = -269.4$  (*c* = 0.87, CHCl<sub>3</sub>).

### 4-acetyl-3-(3-hydroxyphenyl)-3,4-dihydrobenzo[*f*]quinolin-1(2H)-one (**12t**)



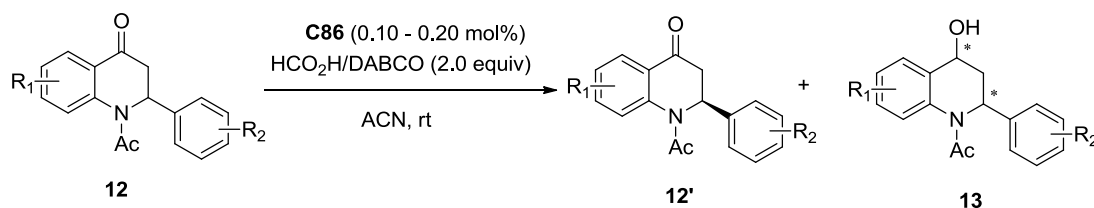
White solid, 800 mg, 71% yield.

**<sup>1</sup>H NMR** (400 MHz, CDCl<sub>3</sub>) δ 10.26 (s, 1H), 7.86 – 7.76 (m, 3H), 7.46 (ddd, *J* = 8.4, 6.9, 1.4 Hz, 1H), 7.39 (ddd, *J* = 8.1, 6.8, 1.2 Hz, 1H), 7.24 (dd, *J* = 8.5, 7.0 Hz, 2H), 6.99 (dddd, *J* = 9.1, 8.1, 2.0, 1.0 Hz, 2H), 6.92 (t, *J* = 2.1 Hz, 1H), 4.98 (d, *J* = 7.1 Hz, 1H), 3.23 (dd, *J* = 16.4, 7.6 Hz, 1H), 3.06 (d, *J* = 16.2 Hz, 1H), 2.21 (s, 3H).

**<sup>13</sup>C NMR** (101 MHz, CDCl<sub>3</sub>) δ 171.0, 169.2, 151.1, 143.5, 135.1, 131.4, 130.8, 129.9, 129.5, 128.8, 127.4, 124.5, 124.4, 122.7, 120.4, 120.1, 117.2, 38.6, 37.6, 21.1.

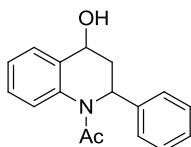
## ATH Products 13a-o, 13q-s

### General procedure K for the synthesis of 13 via ATH



In a round-bottom tube charged with complex (*R,R*)-**C86** (0.1-0.2 mol%) was added under argon a solution of the ketone **12** (0.40 mmol, 1.0 equiv) in anhydrous CH<sub>3</sub>CN (0.5 mL), then HCO<sub>2</sub>H/DABCO (2:1) mixture (2.0 equiv) was added dropwise. The mixture was stirred under argon at room temperature for 16 h, then the solution was concentrated under vacuum. Purification of the residue by flash column chromatography (acetone/petroleum ether 4:1) afforded compounds **12'** and **13** and the enantiomeric excesses were determined by SFC analysis.

1-(4-hydroxy-2-phenyl-3,4-dihydroquinolin-1(2H)-yl)ethanone (**13a**)



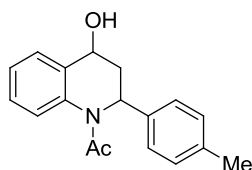
Colorless oil, 53 mg, 50% yield, *ee* > 99%,  $[\alpha]_{\text{D}}^{25} = +225.2$  (*c* = 1.60, CHCl<sub>3</sub>).

<sup>1</sup>H NMR (400 MHz, CDCl<sub>3</sub>) δ 7.59 (d, *J* = 7.9 Hz, 1H), 7.39 – 7.26 (m, 2H), 7.29 – 7.19 (m, 3H), 7.23 – 7.11 (m, 3H), 5.69 (br, 1H), 4.71 (dd, *J* = 11.3, 4.3 Hz, 1H), 2.83 (ddd, *J* = 12.8, 8.5, 4.4 Hz, 1H), 2.27 (br, 1H), 2.14 (s, 3H), 1.79 (q, *J* = 11.5 Hz, 1H).

<sup>13</sup>C NMR (101 MHz, CDCl<sub>3</sub>) δ 170.2, 143.0, 138.9, 136.3, 128.7, 127.5, 127.2, 126.4, 126.2, 125.6, 123.0, 66.1, 54.6, 43.9, 23.1.

HRMS (ESI/ion trap): *m/z* [M + H]<sup>+</sup> calcd for C<sub>17</sub>H<sub>18</sub>NO<sub>2</sub> 268.1338, found 268.1333.

1-(4-hydroxy-2-(*p*-tolyl)-3,4-dihydroquinolin-1(2H)-yl)ethanone (**13b**)



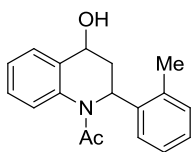
Colorless oil, 56 mg, 50% yield, *ee* = 99%,  $[\alpha]_{\text{D}}^{25} = +225.2$  (*c* = 1.60, CHCl<sub>3</sub>).

<sup>1</sup>H NMR (400 MHz, CDCl<sub>3</sub>) δ 7.59 (d, *J* = 7.0 Hz, 1H), 7.38 – 7.25 (m, 2H), 7.21 (br, 1H), 7.08 – 7.02 (m, 4H), 5.65 (br, 1H), 4.69 (dd, *J* = 11.3, 4.3 Hz, 1H), 2.80 (ddd, *J* = 12.8, 8.5, 4.5 Hz, 1H), 2.62 (br, 1H), 2.27 (s, 3H), 2.13 (s, 3H), 1.78 (q, *J* = 11.4 Hz, 1H).

<sup>13</sup>C NMR (101 MHz, CDCl<sub>3</sub>) δ 170.0, 139.9, 138.7, 136.7, 136.2, 129.2, 127.3, 126.3, 126.0, 125.4, 122.9, 65.9, 54.3, 43.8, 23.0, 21.0.

HRMS (ESI/ion trap): *m/z* [M + H]<sup>+</sup> calcd for C<sub>18</sub>H<sub>20</sub>NO<sub>2</sub> 282.1494, found 282.1490.

1-(4-hydroxy-2-(*o*-tolyl)-3,4-dihydroquinolin-1(2H)-yl)ethanone (**13c**)



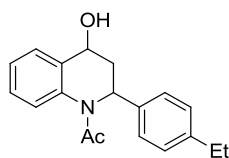
White solid, 57 mg, 51% yield, m.p.143 °C, *ee* = 95%,  $[\alpha]_D^{25} = +216.6$  (*c* = 1.63, CHCl<sub>3</sub>).

<sup>1</sup>H NMR (400 MHz, CDCl<sub>3</sub>) δ 7.59 (d, *J* = 7.4 Hz, 1H), 7.42 – 7.27 (m, 3H), 7.11 – 7.00 (m, 3H), 6.89 (br, 1H), 5.71 (br, 1H), 4.68 (dd, *J* = 11.9, 3.9 Hz, 1H), 2.76 (ddd, *J* = 12.2, 8.1, 4.0 Hz, 1H), 2.50 (s, 4H), 2.12 (s, 3H), 1.54 (td, *J* = 12.1, 11.0 Hz, 1H).

<sup>13</sup>C NMR (101 MHz, CDCl<sub>3</sub>) δ 170.2, 142.5, 139.0, 136.9, 134.8, 130.4, 127.4, 126.9, 126.6, 125.9, 125.3, 124.9, 122.6, 66.2, 52.3, 43.3, 23.2, 19.2.

HRMS (ESI/ion trap): *m/z* [M + H]<sup>+</sup> calcd for C<sub>18</sub>H<sub>20</sub>NO<sub>2</sub> 282.1494, found 282.1488.

1-(2-(4-ethylphenyl)-4-hydroxy-3,4-dihydroquinolin-1(2H)-yl)ethanone (**13d**)



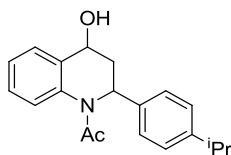
Light yellow solid, 60 mg, 51% yield, m.p.124 °C, *ee* = 96%,  $[\alpha]_D^{25} = +204.2$  (*c* = 1.10, CHCl<sub>3</sub>).

<sup>1</sup>H NMR (400 MHz, CDCl<sub>3</sub>) δ 7.59 (d, *J* = 7.8 Hz, 1H), 7.36 – 7.26 (m, 2H), 7.20 (br, 1H), 7.09 – 7.04 (m, 4H), 5.66 (br, 1H), 4.68 (dd, *J* = 11.4, 4.2 Hz, 1H), 2.83 – 2.77 (m, 2H), 2.57 (q, *J* = 7.6 Hz, 2H), 2.13 (s, 3H), 1.78 (q, *J* = 11.5 Hz, 1H), 1.18 (t, *J* = 7.6 Hz, 3H).

<sup>13</sup>C NMR (101 MHz, CDCl<sub>3</sub>) δ 170.2, 143.1, 140.2, 139.0, 136.3, 128.1, 127.4, 126.5, 126.1, 125.6, 123.0, 66.0, 54.4, 43.9, 28.5, 23.1, 15.5.

HRMS (ESI/ion trap): *m/z* [M + H]<sup>+</sup> calcd for C<sub>19</sub>H<sub>22</sub>NO<sub>2</sub> 296.1646, found 296.1651.

1-(4-hydroxy-2-(4-isopropylphenyl)-3,4-dihydroquinolin-1(2H)-yl)ethanone (**13e**)



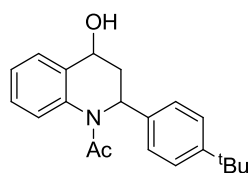
Colorless oil, 62 mg, 50% yield, *ee* = 96%,  $[\alpha]_D^{25} = +161.8$  (*c* = 1.55, CHCl<sub>3</sub>).

<sup>1</sup>H NMR (400 MHz, CDCl<sub>3</sub>) δ 7.58 (d, *J* = 7.7 Hz, 1H), 7.31 (tt, *J* = 6.9, 3.5 Hz, 2H), 7.21 (br, 1H), 7.08 (q, *J* = 8.4 Hz, 4H), 5.68 (br, 1H), 4.69 (dd, *J* = 11.4, 4.2 Hz, 1H), 2.91 – 2.74 (m, 2H), 2.62 (br, 1H), 2.13 (s, 3H), 1.79 (q, *J* = 11.6 Hz, 1H), 1.19 (d, *J* = 6.9 Hz, 6H).

<sup>13</sup>C NMR (101 MHz, CDCl<sub>3</sub>) δ 170.2, 147.7, 140.2, 139.0, 136.3, 127.4, 126.7, 126.4, 126.1, 125.6, 123.0, 66.1, 54.3, 43.9, 33.8, 24.0, 23.1.

**HRMS** (ESI/ion trap):  $m/z$   $[M + H]^+$  calcd for  $C_{20}H_{24}NO_2$  310.1807, found 310.1802.

1-(2-(4-(tert-butyl)phenyl)-4-hydroxy-3,4-dihydroquinolin-1(2H)-yl)ethanone (**13f**)



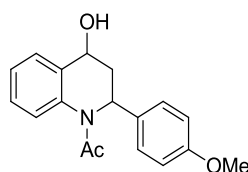
White solid, 62 mg, 48% yield,  $ee = 99\%$ ,  $[\alpha]_D^{25} = +198.9$  ( $c = 0.97$ ,  $CHCl_3$ ).

**$^1H$  NMR** (400 MHz,  $CDCl_3$ )  $\delta$  7.58 (d,  $J = 7.6$  Hz, 1H), 7.38 – 7.18 (m, 5H), 7.07 (d,  $J = 8.4$  Hz, 2H), 5.69 (br, 1H), 4.70 (dd,  $J = 11.3, 4.2$  Hz, 1H), 2.83 (ddd,  $J = 12.7, 8.6, 4.4$  Hz, 1H), 2.47 (br, 1H), 2.13 (s, 3H), 1.79 (q,  $J = 11.3$  Hz, 1H), 1.26 (s, 9H).

**$^{13}C$  NMR** (101 MHz,  $CDCl_3$ )  $\delta$  170.2, 149.9, 139.8, 138.9, 136.3, 127.4, 126.1, 125.6, 125.6, 123.0, 66.1, 54.2, 43.8, 34.5, 31.4, 23.2.

**HRMS** (ESI/ion trap):  $m/z$   $[M + H]^+$  calcd for  $C_{21}H_{26}NO_2$  324.1964, found 324.1959.

1-(4-hydroxy-2-(4-methoxyphenyl)-3,4-dihydroquinolin-1(2H)-yl)ethanone (**13g**)



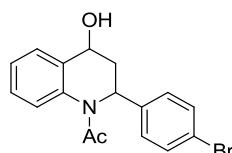
Colorless oil, 61 mg, 51% yield,  $ee = 97\%$ ,  $[\alpha]_D^{25} = +191.2$  ( $c = 1.30$ ,  $CHCl_3$ ).

**$^1H$  NMR** (400 MHz,  $CDCl_3$ )  $\delta$  7.64 – 7.55 (m, 1H), 7.37 – 7.25 (m, 2H), 7.18 (br, 1H), 7.11 – 7.02 (m, 2H), 6.81 – 6.72 (m, 2H), 5.65 (br, 1H), 4.69 (dd,  $J = 11.3, 4.2$  Hz, 1H), 3.74 (s, 3H), 2.80 (ddd,  $J = 12.8, 8.6, 4.5$  Hz, 1H), 2.47 (br, 1H), 2.12 (s, 3H), 1.78 (dd,  $J = 22.2, 11.5$  Hz, 1H).

**$^{13}C$  NMR** (101 MHz,  $CDCl_3$ )  $\delta$  170.1, 158.7, 138.8, 136.2, 135.1, 127.8, 127.4, 126.2, 125.6, 123.0, 114.0, 66.1, 55.4, 54.0, 43.9, 23.1.

**HRMS** (ESI/ion trap):  $m/z$   $[M + H]^+$  calcd for  $C_{18}H_{20}NO_3$  298.1443, found 298.1437.

1-(2-(4-bromophenyl)-4-hydroxy-3,4-dihydroquinolin-1(2H)-yl)ethanone (**13h**)



White solid, 69 mg, 50% yield, m.p. 78 °C,  $ee = 98\%$ ,  $[\alpha]_D^{25} = +163.8$  ( $c = 1.32$ ,  $CHCl_3$ ).

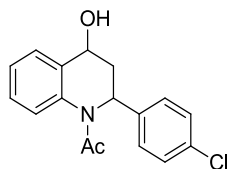
**$^1H$  NMR** (400 MHz,  $CDCl_3$ )  $\delta$  7.62 – 7.55 (m, 1H), 7.38 – 7.28 (m, 4H), 7.18 (br, 1H), 7.02 (d,  $J = 8.5$  Hz, 2H), 5.64 (br, 1H), 4.71 (dd,  $J = 11.4, 4.2$  Hz, 1H), 2.81 (ddd,  $J = 12.8, 8.6, 4.4$  Hz, 1H), 2.45 (br, 1H), 2.13 (s, 3H), 1.71 (q,  $J = 11.6$  Hz, 1H).

## Experimental part

$^{13}\text{C}$  NMR (101 MHz,  $\text{CDCl}_3$ )  $\delta$  170.2, 142.1, 138.7, 136.0, 131.8, 128.3, 127.6, 126.3, 125.4, 123.0, 121.0, 66.0, 54.2, 43.7, 23.1.

HRMS (ESI/ion trap):  $m/z$   $[\text{M} + \text{H}]^+$  calcd for  $\text{C}_{17}\text{H}_{17}\text{BrNO}_2$  346.0443, found 346.0437.

### 1-(2-(4-chlorophenyl)-4-hydroxy-3,4-dihydroquinolin-1(2H)-yl)ethanone (**13i**)



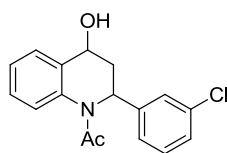
Colorless oil, 60 mg, 50% yield,  $ee = 97\%$ ,  $[\alpha]_{\text{D}}^{25} = +153.2$  ( $c = 0.95$ ,  $\text{CHCl}_3$ ).

$^1\text{H}$  NMR (400 MHz,  $\text{CDCl}_3$ )  $\delta$  7.62 – 7.56 (m, 1H), 7.33 (ddd,  $J = 6.8, 4.6, 1.7$  Hz, 2H), 7.20 (d,  $J = 8.5$  Hz, 3H), 7.07 (d,  $J = 8.5$  Hz, 2H), 5.65 (br, 1H), 4.71 (dd,  $J = 11.7, 4.0$  Hz, 1H), 2.81 (ddd,  $J = 12.3, 8.2, 3.8$  Hz, 1H), 2.58 (br, 1H), 2.13 (s, 3H), 1.72 (q,  $J = 11.2$  Hz, 1H).

$^{13}\text{C}$  NMR (101 MHz,  $\text{CDCl}_3$ )  $\delta$  170.2, 141.6, 138.8, 136.0, 132.9, 128.8, 127.9, 127.6, 126.3, 125.4, 123.0, 66.0, 54.1, 43.8, 23.1.

HRMS (ESI/ion trap):  $m/z$   $[\text{M} + \text{H}]^+$  calcd for  $\text{C}_{17}\text{H}_{17}\text{ClNO}_2$  302.0948, found 302.0944.

### 1-(2-(3-chlorophenyl)-4-hydroxy-3,4-dihydroquinolin-1(2H)-yl)ethanone (**13j**)



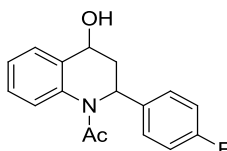
Colorless oil, 62 mg, 51% yield,  $ee = 96\%$ ,  $[\alpha]_{\text{D}}^{25} = +199.9$  ( $c = 1.80$ ,  $\text{CHCl}_3$ ).

$^1\text{H}$  NMR (400 MHz,  $\text{CDCl}_3$ )  $\delta$  7.59 (d,  $J = 7.7$  Hz, 1H), 7.39 – 7.29 (m, 2H), 7.22 (br, 1H), 7.18 – 7.10 (m, 3H), 7.07 – 6.98 (m, 1H), 5.63 (br, 1H), 4.69 (dt,  $J = 11.0, 5.1$  Hz, 1H), 2.85 (d,  $J = 6.2$  Hz, 1H), 2.80 (ddd,  $J = 12.7, 8.6, 4.4$  Hz, 1H), 2.14 (s, 3H), 1.69 (q,  $J = 11.8$  Hz, 1H).

$^{13}\text{C}$  NMR (101 MHz,  $\text{CDCl}_3$ )  $\delta$  170.3, 145.2, 138.8, 136.0, 134.4, 130.0, 127.6, 127.4, 126.6, 126.4, 125.4, 124.6, 123.0, 65.9, 54.3, 43.8, 23.1.

HRMS (ESI/ion trap):  $m/z$   $[\text{M} + \text{H}]^+$  calcd for  $\text{C}_{17}\text{H}_{17}\text{ClNO}_2$  302.0948, found 302.0944.

### 1-(2-(4-fluorophenyl)-4-hydroxy-3,4-dihydroquinolin-1(2H)-yl)ethanone (**13k**)



White solid, 62 mg, 51% yield, m.p. 158 °C,  $ee = 97\%$ ,  $[\alpha]_{\text{D}}^{25} = +203.2$  ( $c = 2.12$ ,  $\text{CHCl}_3$ ).

$^1\text{H}$  NMR (400 MHz,  $\text{CDCl}_3$ )  $\delta$  7.53 – 7.51 (m, 1H), 7.32 – 7.21 (m, 2H), 7.11 (br, 1H), 7.07 – 6.99 (m, 2H), 6.92 – 6.78 (m, 2H), 5.60 (br, 1H), 4.63 (dd,  $J = 11.4, 4.3$  Hz, 1H), 2.74 (ddd,  $J =$

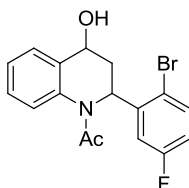
12.8, 8.6, 4.4 Hz, 1H), 2.45 (br, 1H), 2.05 (s, 3H), 1.66 (ddd,  $J = 12.6, 11.5, 10.0$  Hz, 1H).

$^{13}\text{C}$  NMR (101 MHz,  $\text{CDCl}_3$ )  $\delta$  170.2, 162.9 (d,  $J = 245.4$  Hz), 138.8 (2C), 136.1, 128.2 (d,  $J = 8.0$  Hz), 127.5, 126.3, 125.5, 123.0, 115.5 (d,  $J = 21.4$  Hz), 66.0, 54.0, 44.0, 23.1.

$^{19}\text{F}$  NMR (282 MHz,  $\text{CDCl}_3$ )  $\delta$  -115.53.

HRMS (ESI/ion trap):  $m/z$   $[\text{M} + \text{H}]^+$  calcd for  $\text{C}_{17}\text{H}_{16}\text{FNO}_2$  286.1243, found 286.1238.

1-(2-(2-bromo-5-fluorophenyl)-4-hydroxy-3,4-dihydroquinolin-1(2H)-yl)ethanone (**13l**)



Yellow solid, 70 mg, 48% yield, m.p. 174 °C,  $ee = 93\%$ ,  $[\alpha]_{\text{D}}^{25} = +198.5$  ( $c = 1.85$ ,  $\text{CHCl}_3$ ).

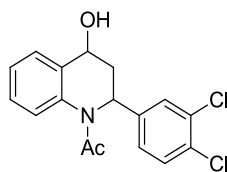
$^1\text{H}$  NMR (400 MHz,  $\text{CDCl}_3$ )  $\delta$  7.59 (d,  $J = 7.5$  Hz, 1H), 7.45 (dd,  $J = 8.6, 5.3$  Hz, 1H), 7.41 – 7.28 (m, 3H), 6.89 – 6.63 (m, 2H), 5.73 (br, 1H), 4.71 (dt,  $J = 10.7, 4.7$  Hz, 1H), 3.00 (ddd,  $J = 12.1, 8.0, 3.9$  Hz, 1H), 2.75 (br, 1H), 2.18 (s, 3H), 1.39 (q,  $J = 11.9$  Hz, 1H).

$^{13}\text{C}$  NMR (101 MHz,  $\text{CDCl}_3$ )  $\delta$  170.6, 162.4 (d,  $J = 247.1$  Hz), 145.6 (d,  $J = 6.6$  Hz), 138.9, 136.2, 134.3 (d,  $J = 7.9$  Hz), 127.6, 126.2, 124.9, 123.0, 116.1, 115.7 (d,  $J = 22.7$  Hz), 113.2 (d,  $J = 23.9$  Hz), 65.8, 55.7, 41.8, 23.1.

$^{19}\text{F}$  NMR (282 MHz,  $\text{CDCl}_3$ )  $\delta$  -113.39.

HRMS (ESI/ion trap):  $m/z$   $[\text{M} + \text{H}]^+$  calcd for  $\text{C}_{17}\text{H}_{16}\text{BrFNO}_2$  364.0348, found 364.0343.

1-(2-(3,4-dichlorophenyl)-4-hydroxy-3,4-dihydroquinolin-1(2H)-yl)ethanone (**13m**)



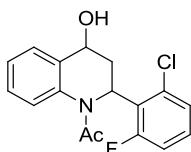
White solid, 69 mg, 51% yield, m.p. 94 °C,  $ee = 96\%$ ,  $[\alpha]_{\text{D}}^{25} = +114.8$  ( $c = 1.20$ ,  $\text{CHCl}_3$ ).

$^1\text{H}$  NMR (400 MHz,  $\text{CDCl}_3$ )  $\delta$  7.63 – 7.55 (m, 1H), 7.40 – 7.31 (m, 2H), 7.30 (d,  $J = 8.3$  Hz, 1H), 7.24 (d,  $J = 2.2$  Hz, 1H), 7.19 (br, 1H), 6.97 (dd,  $J = 8.3, 2.1$  Hz, 1H), 5.62 (t,  $J = 9.4$  Hz, 1H), 4.71 (dd,  $J = 11.3, 4.1$  Hz, 1H), 2.81 (ddd,  $J = 12.7, 8.6, 4.3$  Hz, 1H), 2.48 (br, 1H), 2.14 (s, 3H), 1.68 (dd,  $J = 22.7, 11.6$  Hz, 1H).

$^{13}\text{C}$  NMR (101 MHz,  $\text{CDCl}_3$ )  $\delta$  170.4, 143.4, 138.7, 135.8, 132.6, 131.2, 130.6, 128.6, 127.7, 126.5, 125.9, 125.3, 123.0, 65.8, 53.8, 43.6, 23.0.

HRMS (ESI/ion trap):  $m/z$   $[\text{M} + \text{H}]^+$  calcd for  $\text{C}_{17}\text{H}_{16}\text{Cl}_2\text{NO}_2$  336.0558, found 336.0554.

1-(2-(2-chloro-6-fluorophenyl)-4-hydroxy-3,4-dihydroquinolin-1(2H)-yl)ethanone (**13n**)



Colorless oil, 67 mg, 52% yield,  $ee = 86\%$ ,  $[\alpha]_D^{25} = +121.4$  ( $c = 1.09$ ,  $\text{CHCl}_3$ ).

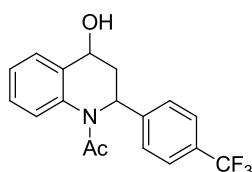
$^1\text{H NMR}$  (400 MHz,  $\text{CDCl}_3$ )  $\delta$  7.59 (d,  $J = 7.4$  Hz, 1H), 7.38 – 7.26 (m, 2H), 7.21 – 7.06 (m, 3H), 6.84 (ddd,  $J = 10.6, 8.0, 1.6$  Hz, 1H), 5.90 (dd,  $J = 12.5, 7.4$  Hz, 1H), 4.75 (dt,  $J = 10.9, 6.0$  Hz, 1H), 2.66 (ddd,  $J = 11.6, 7.4, 3.7$  Hz, 1H), 2.44 (d,  $J = 6.6$  Hz, 1H), 2.16 (s, 3H), 1.74 (q,  $J = 12.2$  Hz, 1H).

$^{13}\text{C NMR}$  (101 MHz,  $\text{CDCl}_3$ )  $\delta$  170.9, 161.0 (d,  $J = 250.8$  Hz), 137.8, 136.7, 134.2 (d,  $J = 5.8$  Hz), 128.7 (d,  $J = 9.7$  Hz), 127.8 (d,  $J = 15.3$  Hz), 127.0, 125.7 (d,  $J = 3.4$  Hz), 125.6, 122.4, 114.9 (d,  $J = 22.6$  Hz), 66.5, 52.3, 39.7, 23.4.

$^{19}\text{F NMR}$  (282 MHz,  $\text{CDCl}_3$ )  $\delta$  -111.87.

**HRMS** (ESI/ion trap):  $m/z$   $[\text{M} + \text{H}]^+$  calcd for  $\text{C}_{17}\text{H}_{16}\text{ClFNO}_2$  320.0854, found 320.0849.

1-(4-hydroxy-2-(4-(trifluoromethyl)phenyl)-3,4-dihydroquinolin-1(2H)-yl)ethanone (**13o**)



Colorless oil, 65 mg, 49% yield,  $ee = 96\%$ ,  $[\alpha]_D^{25} = +160.8$  ( $c = 1.57$ ,  $\text{CHCl}_3$ ).

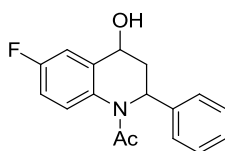
$^1\text{H NMR}$  (400 MHz,  $\text{CDCl}_3$ )  $\delta$  7.63 – 7.56 (m, 1H), 7.50 (d,  $J = 8.2$  Hz, 2H), 7.41 – 7.30 (m, 2H), 7.26 (d,  $J = 8.2$  Hz, 2H), 7.21 (br, 1H), 5.72 (t,  $J = 8.7$  Hz, 1H), 4.74 (dd,  $J = 11.5, 4.2$  Hz, 1H), 2.85 (ddd,  $J = 12.8, 8.6, 4.3$  Hz, 1H), 2.56 (br, 1H), 2.15 (s, 3H), 1.72 (q,  $J = 11.7$  Hz, 1H).

$^{13}\text{C NMR}$  (101 MHz,  $\text{CDCl}_3$ )  $\delta$  170.4, 147.1, 138.7, 136.0, 129.4 (q,  $J = 32.4$  Hz), 127.7, 126.8, 126.4, 125.7 (q,  $J = 3.9$  Hz), 125.3, 124.2 (q,  $J = 272.0$  Hz), 123.0, 66.0, 54.4, 43.8, 23.0.

$^{19}\text{F NMR}$  (282 MHz,  $\text{CDCl}_3$ )  $\delta$  -62.53.

**HRMS** (ESI/ion trap):  $m/z$   $[\text{M} + \text{H}]^+$  calcd for  $\text{C}_{18}\text{H}_{17}\text{F}_3\text{NO}_2$  336.1211, found 336.1207.

1-(6-fluoro-4-hydroxy-2-phenyl-3,4-dihydroquinolin-1(2H)-yl)ethanone (**13q**)



Colorless oil, 58 mg, 51% yield,  $ee = 97\%$ ,  $[\alpha]_D^{25} = +158.1$  ( $c = 1.60$ ,  $\text{CHCl}_3$ ).

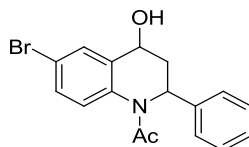
$^1\text{H NMR}$  (400 MHz,  $\text{CDCl}_3$ )  $\delta$  7.32 (d,  $J = 8.2$  Hz, 1H), 7.30 – 7.15 (m, 4H), 7.16 – 7.09 (m, 2H), 7.02 (td,  $J = 8.4, 3.1$  Hz, 1H), 5.67 (br, 1H), 4.65 (dt,  $J = 10.6, 4.6$  Hz, 1H), 2.89 – 2.68 (m, 2H), 2.11 (s, 3H), 1.81 – 1.68 (m, 1H).

$^{13}\text{C}$  NMR (101 MHz,  $\text{CDCl}_3$ )  $\delta$  170.2, 161.0 (d,  $J = 244.2$  Hz), 142.8, 141.8, 132.0, 128.7, 127.3, 127.0, 126.3, 114.0 (d,  $J = 23.3$  Hz), 110.6 (d,  $J = 24.2$  Hz), 65.7, 54.5, 43.6, 23.0.

$^{19}\text{F}$  NMR (282 MHz,  $\text{CDCl}_3$ )  $\delta$  -114.62.

HRMS (ESI/ion trap):  $m/z$   $[\text{M} + \text{H}]^+$  calcd for  $\text{C}_{17}\text{H}_{16}\text{FNO}_2$  286.1243, found 286.1239.

1-(6-bromo-4-hydroxy-2-phenyl-3,4-dihydroquinolin-1(2H)-yl)ethanone (**13r**)



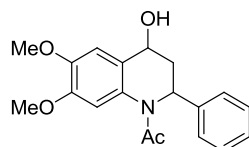
Light yellow solid, 57 mg, 41% yield, m.p. 112 °C,  $ee > 99\%$ ,  $[\alpha]_{\text{D}}^{25} = +154.4$  ( $c = 2.02$ ,  $\text{CHCl}_3$ ).

$^1\text{H}$  NMR (400 MHz,  $\text{CDCl}_3$ )  $\delta$  7.74 (s, 1H), 7.45 (dd,  $J = 8.4, 2.2$  Hz, 1H), 7.30 – 7.17 (m, 3H), 7.13 – 7.08 (m, 3H), 5.60 (br, 1H), 4.65 (dd,  $J = 11.5, 4.3$  Hz, 1H), 2.79 (ddd,  $J = 12.8, 8.5, 4.4$  Hz, 2H), 2.12 (s, 3H), 1.75 (td,  $J = 12.0, 10.0$  Hz, 1H).

$^{13}\text{C}$  NMR (101 MHz,  $\text{CDCl}_3$ )  $\delta$  170.0, 142.7, 140.9, 135.2, 130.5, 128.8, 127.4, 127.0, 126.6, 126.3, 119.8, 65.6, 54.8, 43.8, 23.1.

HRMS (ESI/ion trap):  $m/z$   $[\text{M} + \text{H}]^+$  calcd for  $\text{C}_{17}\text{H}_{17}\text{BrNO}_2$  346.0443, found 346.0437.

1-(4-hydroxy-6,7-dimethoxy-2-phenyl-3,4-dihydroquinolin-1(2H)-yl)ethanone (**13s**)



Light yellow solid, 63 mg, 48% yield, m.p. 129 °C,  $ee > 99\%$ ,  $[\alpha]_{\text{D}}^{25} = +176.0$  ( $c = 1.27$ ,  $\text{CHCl}_3$ ).

$^1\text{H}$  NMR (400 MHz,  $\text{CDCl}_3$ )  $\delta$  7.28 – 7.21 (m, 2H), 7.20 – 7.09 (m, 4H), 6.70 (br, 1H), 5.70 (br, 1H), 4.63 (dt,  $J = 10.7, 5.3$  Hz, 1H), 3.91 (s, 3H), 3.87 (s, 3H), 2.76 (ddd,  $J = 12.7, 8.3, 4.5$  Hz, 2H), 2.14 (s, 3H), 1.84 (br, 1H).

$^{13}\text{C}$  NMR (101 MHz,  $\text{CDCl}_3$ )  $\delta$  170.1, 147.9, 147.5, 142.8, 128.7, 127.2, 126.5, 109.7, 106.5, 65.7, 56.5, 56.2, 54.5, 43.7, 23.3.

HRMS (ESI/ion trap):  $m/z$   $[\text{M} + \text{H}]^+$  calcd for  $\text{C}_{19}\text{H}_{22}\text{NO}_4$  328.1549, found 328.1543.

Substrates **14c, i, j**

General procedure L for preparing  $\alpha,\alpha$ -dihalogeno  $\beta$ -keto esters or amides

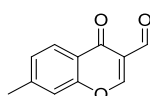
General procedure L:





To a solution of the o-hydroxy-acetophenone (8 mmol) in DMF (6.4 mL), was added dropwise phosphorous oxychloride (41 mmol) at 0 °C over 20–30 minutes. The mixture was stirred at 0 °C for 30 minutes then at room temperature for 3–5 h. Ice-cold water (30 mL) was added, and the mixture was extracted with CH<sub>2</sub>Cl<sub>2</sub>. The combined organic layers were dried (MgSO<sub>4</sub>), the solvent was evaporated under vacuum, and the crude product was purified by flash chromatography on silica gel (cyclohexane/EtOAc = 3:1) to give the desired product.

7-Methyl-4-oxochroman-3-carbaldehyde (**14c**)

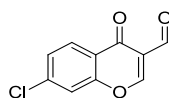


Following the above procedure, product **12f** was obtained as yellow solid, 767 mg (51% yield), m.p. 182 °C.

<sup>1</sup>H NMR (400 MHz, CDCl<sub>3</sub>) δ 10.38 (s, 1H), 8.51 (s, 1H), 8.17 (d, *J* = 8.0 Hz, 1H), 7.32-7.30 (m, 2H), 2.52 (s, 3H).

<sup>13</sup>C NMR (101 MHz, CDCl<sub>3</sub>) δ 188.9, 176.0, 160.6, 156.5, 146.7, 128.2, 126.0, 123.1, 120.4, 118.5, 22.06.

7-Chloro-4-oxochroman-3-carbaldehyde (**14i**)

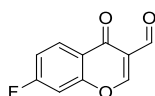


Following the above procedure, product **12f** was obtained as yellow solid, 1.3 g (78% yield), m.p. 189 °C.

<sup>1</sup>H NMR (400 MHz, CDCl<sub>3</sub>) δ 10.36 (s, 1H), 8.51 (s, 1H), 8.24 (d, *J* = 8.5 Hz, 1H), 7.57 (d, *J* = 1.9 Hz, 1H), 7.48 (dd, *J* = 8.5, 1.9 Hz, 1H).

<sup>13</sup>C NMR (101 MHz, CDCl<sub>3</sub>) δ 188.3, 175.3, 160.7, 156.4, 141.2, 127.6, 123.9, 120.6, 118.9.

7-Fluoro-4-oxochroman-3-carbaldehyde (**14j**)



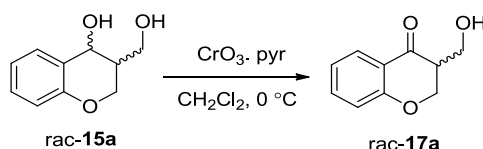
Following the above procedure, product **12f** was obtained as yellow solid, 900 mg (58% yield), m.p. 141 °C.

**<sup>1</sup>H NMR** (400 MHz, CDCl<sub>3</sub>)  $\delta$  10.39 (s, 1H), 8.54 (s, 1H), 8.35 (dd,  $J = 9.5, 6.1$  Hz, 1H), 7.28-7.24 (m, 2H), 2.52 (s, 3H).

**<sup>13</sup>C NMR** (101 MHz, CDCl<sub>3</sub>)  $\delta$  188.4, 175.1, 166.3 (d,  $J = 257.9$  Hz), 160.8, 157.3 (d,  $J = 13.3$  Hz), 128.9 (d,  $J = 10.6$  Hz), 122.2, 120.5, 115.5 (d,  $J = 22.6$  Hz), 105.7 (d,  $J = 25.6$  Hz); **<sup>19</sup>F NMR** (282 MHz, CDCl<sub>3</sub>)  $\delta$  -100.19 (q,  $J = 7.6$  Hz).

**<sup>19</sup>F NMR** (282 MHz, CDCl<sub>3</sub>)  $\delta$  -100.19 (q,  $J = 7.6$  Hz, 1F).

### Preparation of compound rac-17a



To a solution of the diol rac-**15a** (1.0 g, 5.6 mmol) in CH<sub>2</sub>Cl<sub>2</sub> (30 mL), was added PCC (2.75 g, 12.8 mmol) at 0°C over 1 h. The reaction mixture was filtered, and the solid was rinsed with CH<sub>2</sub>Cl<sub>2</sub>. The filtrate was concentrated under vacuum and the crude product was purified by flash chromatography on silica gel (cyclohexane/EtOAc= 2/1) to give rac-**17a** as a yellow oil (400 mg, 40%).

**<sup>1</sup>H NMR** (400 MHz, CDCl<sub>3</sub>)  $\delta$  7.80 (dd,  $J = 7.9, 1.7$  Hz, 1H), 7.46-7.36 (br, 1H), 6.99-6.87 (m, 2H), 4.52 (dd,  $J = 11.4, 5.2$  Hz, 1H), 4.35 (t,  $J = 11.4$ , 1H), 3.96-3.81 (m, 2H), 2.94 (dq,  $J = 11.0, 5.5$  Hz, 1H), 2.69 (br, 1H).

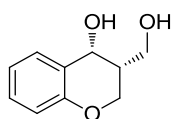
**<sup>13</sup>C NMR** (101 MHz, CDCl<sub>3</sub>)  $\delta$  194.4, 162.0, 136.4, 127.2, 121.6, 120.9, 118.0, 68.7, 59.3, 47.9.

**HPLC:** Chiralpak IE, Hexane : *i*PrOH = 95 : 5, 1.0 mL/min,  $\lambda = 215$  nm,  $t_1 = 30.91$  min,  $t_2 = 34.19$  min.

### General procedure M for the synthesis of 15a-m by ATH.

In a round-bottom tube charged with formylchromone **14** (0.75 mmol, 1.0 equiv) was added a solution of the Rh complex (*R,R*)-**C86** (750  $\mu$ L,  $5 \cdot 10^{-3}$  mol.L<sup>-1</sup>, 0.5 mol%), and the mixture was stirred under air for 10 minutes. HCOOH/Et<sub>3</sub>N (5:2) azeotropic mixture (446  $\mu$ L, 5.25 mmol, 7.0 equiv) was added and the tube was placed under an atmosphere of argon. The reaction mixture was stirred at 30 °C for 24 or 65 h, then quenched with sat. aq. NaHCO<sub>3</sub> and extracted with CH<sub>2</sub>Cl<sub>2</sub>. The combined organic phase was dried (MgSO<sub>4</sub>), filtered and concentrated under vacuum. The diastereomeric ratio was determined by <sup>1</sup>H NMR analysis of the crude product. After filtration of the crude product on silica gel (petroleum ether/ethyl acetate), the enantiomeric excess was determined by SFC analysis (CHIRALPAK IA or AD-H column).

### (3*R*,4*R*)-3-(Hydroxymethyl)chroman-4-ol (**15a**)



White powder: 113 mg, 84% yield, dr (*cis/trans*) = 98/2 (*cis/trans*), ee<sub>*cis*</sub> = 99%, m.p. 88 °C,

## Experimental part

$[\alpha]_D^{20} = +12.8$  (c 1.0, MeOH).

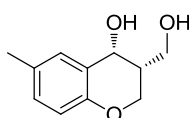
**$^1\text{H NMR}$**  (400 MHz,  $\text{CDCl}_3$ )  $\delta$  7.29–7.27 (m, 1H), 7.24–7.20 (m, 1H), 6.93 (t,  $J = 7.4$  Hz, 1H), 6.86 (d,  $J = 8.2$  Hz, 1H), 4.86 (br, 1H), 4.21–4.15 (m, 2H), 3.95–3.83 (m, 2H), 2.66–2.62 (m, 2H), 2.24–2.17 (m, 1H).

**$^{13}\text{C NMR}$**  (101 MHz,  $\text{CDCl}_3$ )  $\delta$  154.4, 130.1, 130.1, 123.9, 120.8, 117.1, 66.1, 63.6, 61.7, 39.7.

**SFC:** Chiralpak AD-H,  $sc\text{CO}_2$ /  $i\text{PrOH}$  90/10, 3.0 mL/min,  $P = 150$  bar,  $\lambda = 215$  nm,  $t_R$  [*cis*-(3*R*,4*R*)] = 8.88 min (major),  $t_R$  [*cis*-(3*S*,4*S*)] = 10.31 min,  $t_R$  [*trans*] = 11.40 min,  $t_R$  [*trans*] = 12.68 min.

**HRMS** (ESI/ion trap):  $m/z$  [ $M + \text{Na}$ ] $^+$  calcd for  $\text{C}_{10}\text{H}_{12}\text{NaO}_3$  203.0684, found 203.0680.

### (3*R*,4*R*)-3-(Hydroxymethyl)-6-methylchroman-4-ol (**15b**)



White powder: 110 mg, 76% yield, dr (*cis/trans*) = 97/3 (*cis/trans*),  $ee_{cis} = 99\%$ , m.p. 122 °C,  $[\alpha]_D^{20} = +10.3$  (c 1.0, MeOH).

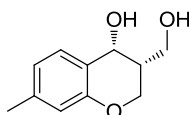
**$^1\text{H NMR}$**  (400 MHz,  $\text{CDCl}_3$ )  $\delta$  7.09 (br, 1H), 7.05–7.02 (br, 1H), 6.76 (d,  $J = 8.3$  Hz, 1H), 4.84 (t,  $J = 3.9$  Hz, 1H), 4.20–4.14 (m, 2H), 3.99–3.86 (m, 2H), 2.42–2.39 (m, 1H), 2.39 (d,  $J = 4.4$  Hz, 1H), 2.28 (s, 3H), 2.25–2.17 (m, 1H).

**$^{13}\text{C NMR}$**  (101 MHz,  $\text{CDCl}_3$ )  $\delta$  152.2, 130.9, 130.1, 130.0, 123.5, 116.8, 66.3, 63.5, 61.8, 39.7, 20.5.

**SFC:** Chiralpak AD-H,  $sc\text{CO}_2$ / MeOH 90/10, 3.0 mL/min,  $P = 150$  bar,  $\lambda = 215$  nm,  $t_R$  [*cis*-(3*R*,4*R*)] = 14.06 min (major),  $t_R$  [*trans*] = 17.29 min,  $t_R$  [*trans*] = 18.69 min,  $t_R$  [*cis*-(3*S*,4*S*)] = 27.16 min.

**HRMS** (ESI/ion trap):  $m/z$  [ $M + \text{Na}$ ] $^+$  calcd for  $\text{C}_{11}\text{H}_{14}\text{NaO}_3$  217.0841, found 217.0837.

### (3*R*,4*R*)-3-(Hydroxymethyl)-7-methylchroman-4-ol (**15c**)



White powder: 105 mg, 72% yield, dr (*cis/trans*) = 97/3 (*cis/trans*),  $ee_{cis} = 99\%$ , m.p. 114 °C,  $[\alpha]_D^{20} = +10.4$  (c 1.0, MeOH).

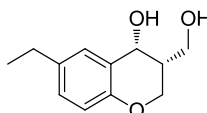
**$^1\text{H NMR}$**  (400 MHz,  $\text{CDCl}_3$ )  $\delta$  7.16 (d,  $J = 7.7$  Hz, 1H), 6.75 (d,  $J = 7.7$  Hz, 1H), 6.68 (s, 1H), 4.85 (br, 1H), 4.20–4.15 (m, 2H), 3.97–3.84 (m, 2H), 2.53 (dd,  $J = 6.8, 4.4$  Hz, 1H), 2.39 (d,  $J = 4.2$  Hz, 1H), 2.30 (s, 3H), 2.22–2.15 (m, 1H);

**$^{13}\text{C NMR}$**  (101 MHz,  $\text{CDCl}_3$ )  $\delta$  154.3, 140.5, 129.8, 121.9, 121.1, 117.4, 66.2, 63.6, 62.0, 39.8, 21.4.

**SFC:** Chiralpak AD-H, *scCO*<sub>2</sub>/ MeOH 93/7, 4.0 mL/min, P = 150 bar,  $\lambda$  = 215 nm,  $t_R$  [*trans*] = 24.45 min,  $t_R$  [*cis*-(3*S*,4*S*)] = 33.10 min,  $t_R$  [*cis*-(3*R*,4*R*)] = 35.20 min (major),  $t_R$  [*trans*] = 40.73 min.

**HRMS** (ESI/ion trap):  $m/z$  [M + Na]<sup>+</sup> calcd for C<sub>11</sub>H<sub>14</sub>NaO<sub>3</sub> 217.0841, found 217.0837.

(3*R*,4*R*)-6-Ethyl-3-(hydroxymethyl)chroman-4-ol (**15d**)



White powder: 113 mg, 72% yield, dr (*cis/trans*) = 98/2 (*cis/trans*), ee<sub>*cis*</sub> = 99%, m.p. 101 °C,  $[\alpha]_D^{20}$  = +8.5(c 1.0, MeOH).

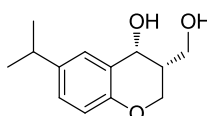
**<sup>1</sup>H NMR** (400 MHz, CDCl<sub>3</sub>)  $\delta$  7.09-7.04 (m, 2H), 6.77 (d,  $J$  = 8.3 Hz, 1H), 4.81 (br s, 1H), 4.14-4.09 (m, 2H), 3.91-3.80 (m, 2H), 2.87 (br s, 2H), 2.57 (q,  $J$  = 7.6 Hz, 2H), 2.18-2.15 (m, 1H), 1.20 (t,  $J$  = 7.5 Hz, 3H).

**<sup>13</sup>C NMR** (101 MHz, CDCl<sub>3</sub>)  $\delta$  152.3, 136.6, 129.7, 129.1, 123.5, 116.9, 66.2, 63.6, 61.7, 39.8, 28.0, 15.9.

**SFC:** Chiralpak AD-H, *scCO*<sub>2</sub>/ MeOH 90/10, 3.0 mL/min, P = 150 bar,  $\lambda$  = 215 nm,  $t_R$  [*cis*-(3*R*,4*R*)] = 11.87 min (major),  $t_R$  [*trans*] = 14.00 min,  $t_R$  [*trans*] = 16.11 min,  $t_R$  [*cis*-(3*S*,4*S*)] = 19.19 min.

**HRMS** (ESI/ion trap):  $m/z$  [M + Na]<sup>+</sup> calcd for C<sub>12</sub>H<sub>16</sub>NaO<sub>3</sub> 231.0997, found 231.0992.

(3*R*,4*R*)-3-(Hydroxymethyl)-6-isopropylchroman-4-ol (**15e**)



White powder: 125 mg, 75% yield, dr (*cis/trans*) = 97/3 (*cis/trans*), ee<sub>*cis*</sub> = 99%, m.p. 107 °C,  $[\alpha]_D^{20}$  = +8.3(c 1.0, MeOH).

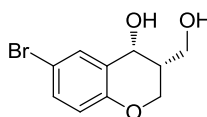
**<sup>1</sup>H NMR** (400 MHz, CDCl<sub>3</sub>)  $\delta$  7.14-7.09 (m, 2H), 6.80 (d,  $J$  = 8.4 Hz, 1H), 4.87 (m, 1H), 4.20-4.17 (m, 2H), 4.01-3.87 (m, 2H), 2.85 (hept,  $J$  = 7.0 Hz, 1H), 2.51-2.31 (m, 2H), 2.26-2.17 (m, 1H), 1.23 (d,  $J$  = 6.9 Hz, 6H).

**<sup>13</sup>C NMR** (101 MHz, CDCl<sub>3</sub>)  $\delta$  152.4, 141.4, 128.4, 127.6, 123.5, 117.0, 66.6, 63.6, 62.0, 39.8, 33.4, 24.4, 24.2.

**SFC:** Chiralpak IA, *scCO*<sub>2</sub>/ *i*PrOH 93/7, 3.0 mL/min, P = 150 bar,  $\lambda$  = 215 nm,  $t_R$  [*cis*-(3*R*,4*R*)] = 17.13 min (major),  $t_R$  [*cis*-(3*S*,4*S*)] = 18.90 min,  $t_R$  [*trans*] = 20.99 min,  $t_R$  [*trans*] = 22.82 min.

**HRMS** (ESI/ion trap):  $m/z$  [M + Na]<sup>+</sup> calcd for C<sub>13</sub>H<sub>18</sub>NaO<sub>3</sub> 245.1154, found 245.1149.

(3*R*,4*R*)-6-Bromo-3-(hydroxymethyl)chroman-4-ol (**15f**)



White powder: 165 mg, 85% yield, dr (*cis/trans*) = 96/4 (*cis/trans*), ee<sub>*cis*</sub> = 99%, m.p. 104 °C,  $[\alpha]_{\text{D}}^{20} = +5.2$  (c 1.0, MeOH).

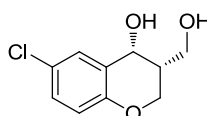
<sup>1</sup>H NMR (400 MHz, CDCl<sub>3</sub>) δ 7.43 (d, *J* = 2.5 Hz, 1H), 7.30 (dd, *J* = 8.8, 2.5 Hz, 1H), 6.75 (dd, *J* = 8.8, 1.6 Hz, 1H), 4.86 (br s, 1H), 4.28-4.15 (m, 2H), 3.99-3.87 (m, 2H), 2.57 (d, *J* = 4.3 Hz, 1H), 2.28-2.19 (m, 2H).

<sup>13</sup>C NMR (101 MHz, CDCl<sub>3</sub>) δ 153.5, 132.9, 132.5, 125.9, 119.0, 112.7, 65.9, 64.0, 61.7, 39.4.

SFC: Chiralpak AD-H, *sc*CO<sub>2</sub>/ MeOH 90/10, 3.0 mL/min, P = 150 bar, λ = 215 nm, t<sub>R</sub> [*cis*-(3*R*,4*R*)] = 27.92 min (major), t<sub>R</sub> [*trans*] = 31.51 min, t<sub>R</sub> [*trans*] = 45.61 min, t<sub>R</sub> [*cis*-(3*S*,4*S*)] = 50.26 min.

HRMS (ESI/ion trap): *m/z* [M + Na]<sup>+</sup> calcd for C<sub>10</sub>H<sub>11</sub>BrNaO<sub>3</sub> 280.9787, found 280.9792.

(3*R*,4*R*)-6-Chloro-3-(hydroxymethyl)chroman-4-ol (**15g**)



White powder: 140 mg, 87% yield, dr (*cis/trans*) = 96/4 (*cis/trans*), ee<sub>*cis*</sub> = 99%, m.p. 99 °C,  $[\alpha]_{\text{D}}^{20} = +8.2$  (c 1.0, MeOH).

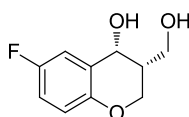
<sup>1</sup>H NMR (400 MHz, CDCl<sub>3</sub>) δ 7.28 (d, *J* = 2.6 Hz, 1H), 7.17 (dd, *J* = 8.8, 2.6 Hz, 1H), 6.79 (d, *J* = 8.8 Hz, 1H), 4.85 (t, *J* = 3.9 Hz, 1H), 4.23-4.14 (m, 2H), 3.97-3.85 (m, 2H), 2.70 (d, *J* = 4.4 Hz, 1H), 2.38 (dd, *J* = 6.3, 4.4 Hz, 1H), 2.26-2.17 (m, 1H).

<sup>13</sup>C NMR (101 MHz, CDCl<sub>3</sub>) δ 153.0, 130.1, 129.5, 125.5, 125.3, 118.6, 66.0, 64.0, 61.7, 39.4.

SFC: Chiralpak AD-H, *sc*CO<sub>2</sub>/ MeOH 90/10, 3.0 mL/min, P = 150 bar, λ = 215 nm, t<sub>R</sub> [*cis*-(3*R*,4*R*)] = 21.53 min (major), t<sub>R</sub> [*trans*] = 24.15 min, t<sub>R</sub> [*trans*] = 33.19 min, t<sub>R</sub> [*cis*-(3*S*,4*S*)] = 39.51 min.

HRMS (ESI/ion trap): *m/z* [M + Na]<sup>+</sup> calcd for C<sub>10</sub>H<sub>11</sub>ClNaO<sub>3</sub> 237.0294, found 237.0297.

(3*R*,4*R*)-6-Fluoro-3-(hydroxymethyl)chroman-4-ol (**15h**)



White powder: 123 mg, 83% yield, dr (*cis/trans*) = 96/4 (*cis/trans*), ee<sub>*cis*</sub> = 99%, m.p. 98 °C,  $[\alpha]_{\text{D}}^{20} = +12.7$  (c 1.0, MeOH).

**<sup>1</sup>H NMR** (400 MHz, CDCl<sub>3</sub>) δ 7.02 (dd, *J* = 8.5, 3.1 Hz, 1H), 6.93 (td, *J* = 8.5, 3.1 Hz, 1H), 6.80 (dd, *J* = 9.0, 4.6 Hz, 1H), 4.86 (t, *J* = 4.2 Hz, 1H), 4.21-4.13 (m, 2H), 3.99-3.87 (m, 2H), 2.64 (d, *J* = 4.6 Hz, 1H), 2.34-2.32 (m, 1H), 2.28-2.20 (m, 1H).

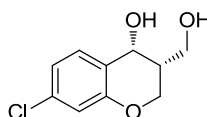
**<sup>13</sup>C NMR** (101 MHz, CDCl<sub>3</sub>) δ 157.0 (d, *J* = 238.9 Hz), 150.4, 124.7 (d, *J* = 6.9 Hz), 118.2 (d, *J* = 7.8 Hz), 117.0 (d, *J* = 23.3 Hz), 115.6 (d, *J* = 22.6 Hz), 66.1, 64.0, 61.7, 39.5.

**<sup>19</sup>F NMR** (282 MHz, CDCl<sub>3</sub>) δ -123.37 (q, *J* = 7.5 Hz)

**SFC:** Chiralpak AD-H, *sc*CO<sub>2</sub>/ MeOH 90/10, 3.0 mL/min, P = 150 bar, λ = 215 nm, *t<sub>R</sub>* [*cis*-(3*R*,4*R*)] = 10.77 min (major), *t<sub>R</sub>* [*trans*] = 12.55 min, *t<sub>R</sub>* [*trans*] = 13.92 min, *t<sub>R</sub>* [*cis*-(3*S*,4*S*)] = 18.29 min.

**HRMS** (ESI/ion trap): *m/z* [M + Na]<sup>+</sup> calcd for C<sub>10</sub>H<sub>11</sub>FNao<sub>3</sub> 221.0590, found 221.0585.

**(3*R*,4*R*)-7-Chloro-3-(hydroxymethyl)chroman-4-ol (15j)**



White powder: 123 mg, 83% yield, dr (*cis/trans*) = 96/4 (*cis/trans*), ee<sub>*cis*</sub> = 99%, m.p. 85 °C, [α]<sub>D</sub><sup>20</sup> = +10.6 (c 1.0, MeOH).

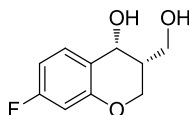
**<sup>1</sup>H NMR** (400 MHz, CDCl<sub>3</sub>) δ 7.02 (dd, *J* = 8.5, 3.1 Hz, 1H), 6.93 (td, *J* = 8.5, 3.1 Hz, 1H), 6.80 (dd, *J* = 9.0, 4.6 Hz, 1H), 4.86 (t, *J* = 4.2 Hz, 1H), 4.21-4.13 (m, 2H), 3.99-3.87 (m, 2H), 2.64 (d, *J* = 4.6 Hz, 1H), 2.34-2.32 (m, 1H), 2.28-2.20 (m, 1H).

**<sup>13</sup>C NMR** (101 MHz, CDCl<sub>3</sub>) δ 157.0 (d, *J* = 238.9 Hz), 150.4, 124.7 (d, *J* = 6.9 Hz), 118.2 (d, *J* = 7.8 Hz), 117.0 (d, *J* = 23.3 Hz), 115.6 (d, *J* = 22.6 Hz), 66.1, 64.0, 61.7, 39.5.

**SFC:** Chiralpak AD-H, *sc*CO<sub>2</sub>/ MeOH 90/10, 4.0 mL/min, P = 150 bar, λ = 215 nm, *t<sub>R</sub>* [*trans*] = 17.52 min, *t<sub>R</sub>* [*cis*-(3*S*,4*S*)] = 23.05 min, *t<sub>R</sub>* [*cis*-(3*R*,4*R*)] = 31.57 min (major), *t<sub>R</sub>* [*trans*] = 37.27 min.

**HRMS** (ESI/ion trap): *m/z* [M + Na]<sup>+</sup> calcd for C<sub>10</sub>H<sub>11</sub>ClNaO<sub>3</sub> 237.0294, found 237.0297.

**(3*R*,4*R*)-7-Fluoro-3-(hydroxymethyl)chroman-4-ol (15k)**



White powder: 123 mg, 83% yield, dr (*cis/trans*) = 97/3 (*cis/trans*), ee<sub>*cis*</sub> = 99%, m.p. 78 °C, [α]<sub>D</sub><sup>20</sup> = +13.1 (c 1.0, MeOH).

**<sup>1</sup>H NMR** (400 MHz, CDCl<sub>3</sub>) δ 7.23 (dd, *J* = 8.5, 6.5 Hz, 1H), 6.64 (td, *J* = 8.3, 2.5 Hz, 1H), 6.56 (dd, *J* = 10.2, 2.5 Hz, 1H), 4.84 (br s, 1H), 4.21-4.14 (m, 2H), 3.96-3.83 (m, 2H), 2.68 (br s, 1H), 2.58 (br s, 1H), 2.22-2.15 (m, 1H).

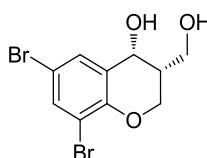
**<sup>13</sup>C NMR** (101 MHz, CDCl<sub>3</sub>) δ 163.6 (d, *J* = 246.4 Hz), 155.7 (d, *J* = 12.4 Hz), 131.3 (d, *J* = 10.1 Hz), 120.1, 108.3 (d, *J* = 22.0 Hz), 104.2 (d, *J* = 24.5 Hz), 65.8, 63.8, 61.8, 39.5.

$^{19}\text{F}$  NMR (282 MHz,  $\text{CDCl}_3$ )  $\delta$  -111.08 (q,  $J$  = 8.2 Hz).

**SFC:** Chiralpak AD-H,  $sc\text{CO}_2$ / MeOH 90/10, 3.0 mL/min,  $P$  = 150 bar,  $\lambda$  = 215 nm,  $t_R$  [*trans*] = 10.24 min,  $t_R$  [*cis*-(3*R*,4*R*)] = 12.77 min (major),  $t_R$  [*cis*-(3*S*,4*S*)] = 14.24 min,  $t_R$  [*trans*] = 15.32 min.

**HRMS** (ESI/ion trap):  $m/z$  [ $M + \text{Na}$ ] $^+$  calcd for  $\text{C}_{10}\text{H}_{11}\text{FNaO}_3$  221.0590, found 221.0585.

(3*R*,4*R*)-6,8-Dibromo-3-(hydroxymethyl)chroman-4-ol (**15l**)



White powder: 135 mg, 80% yield, dr (*cis/trans*) = 92/8 (*cis/trans*),  $ee_{cis}$  = 94%, m.p. 139 °C,  $[\alpha]_D^{20}$  = +6.8 (c 1.0, MeOH).

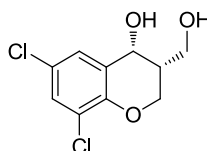
$^1\text{H}$  NMR (400 MHz,  $\text{CDCl}_3$ )  $\delta$  7.60 (d,  $J$  = 2.4 Hz, 1H), 7.39 (d,  $J$  = 2.4 Hz, 1H), 4.86 (br s, 1H), 4.36-4.25 (m, 2H), 3.99-3.86 (m, 2H), 2.85 (d,  $J$  = 4.3 Hz, 1H), 2.30-2.22 (m, 2H).

$^{13}\text{C}$  NMR (101 MHz,  $\text{CDCl}_3$ )  $\delta$  150.4, 135.7, 131.8, 126.9, 112.6, 111.8, 65.9, 64.9, 61.4, 39.1.

**SFC:** Chiralpak AD-H,  $sc\text{CO}_2$ / *i*PrOH 92/8, 5.0 mL/min,  $P$  = 150 bar,  $\lambda$  = 215 nm,  $t_R$  [*cis*-(3*R*,4*R*)] = 23.58 min (major),  $t_R$  [*cis*-(3*S*,4*S*)] = 24.95 min,  $t_R$  [*trans*] = 30.07 min,  $t_R$  [*trans*] = 33.20 min.

**HRMS** (ESI/ion trap):  $m/z$  [ $M + \text{Na}$ ] $^+$  calcd for  $\text{C}_{10}\text{H}_{10}\text{Br}_2\text{NaO}_3$  358.8894, found 358.8897.

(3*R*,4*R*)-6,8-Dichloro-3-(hydroxymethyl)chroman-4-ol (**15m**)



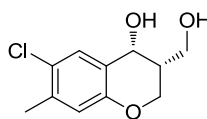
White powder: 162 mg, 87% yield, dr (*cis/trans*) = 93/7 (*cis/trans*),  $ee_{cis}$  = 97%, m.p. 85 °C,  $[\alpha]_D^{20}$  = +8.5 (c 1.0, MeOH).

$^1\text{H}$  NMR (400 MHz,  $\text{CDCl}_3$ )  $\delta$  7.31 (d,  $J$  = 2.5 Hz, 1H), 7.21 (d,  $J$  = 2.5 Hz, 1H), 4.86 (t,  $J$  = 4.0 Hz, 1H), 4.36-4.21 (m, 2H), 3.99-3.86 (m, 2H), 2.93 (d,  $J$  = 4.4 Hz, 1H), 2.36 (dd,  $J$  = 6.1, 4.3 Hz, 1H), 2.29-2.21 (m, 1H).

$^{13}\text{C}$  NMR (101 MHz,  $\text{CDCl}_3$ )  $\delta$  148.9, 130.1, 128.2, 126.3, 125.2, 122.5, 65.6, 64.6, 61.2, 39.1.

**SFC:** Chiralpak AD-H,  $sc\text{CO}_2$ / MeOH 90/10, 4.0 mL/min,  $P$  = 150 bar,  $\lambda$  = 215 nm,  $t_R$  [*trans*] = 17.07 min,  $t_R$  [*cis*-(3*R*,4*R*)] = 20.08 min (major),  $t_R$  [*cis*-(3*S*,4*S*)] = 32.92 min,  $t_R$  [*trans*] = 45.00 min..

**HRMS** (ESI/ion trap):  $m/z$  [ $M + \text{Na}$ ] $^+$  calcd for  $\text{C}_{10}\text{H}_{10}\text{Cl}_2\text{NaO}_3$  270.9905, found 270.9900.

**(3*R*,4*R*)-6-Chloro-3-(hydroxymethyl)-7-methylchroman-4-ol (15n)**

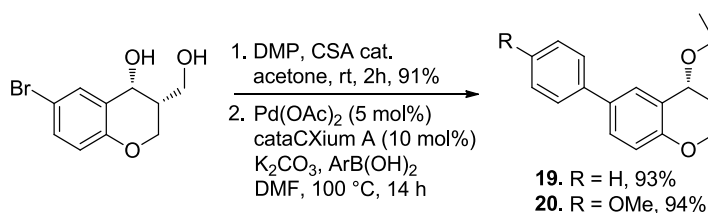
White powder: 150 mg, 88% yield, dr (*cis/trans*) = 98/2 (*cis/trans*),  $ee_{cis}$  = 99%, m.p. 136 °C,  $[\alpha]_D^{20}$  = +9.5 (c 1.0, MeOH).

<sup>1</sup>H NMR (400 MHz, CDCl<sub>3</sub>) δ 7.26 (s, 1H), 6.74 (s, 1H), 4.84 (br s, 1H), 4.22-4.14 (m, 2H), 3.99-3.87 (m, 2H), 2.31-2.18 (m, 6H).

<sup>13</sup>C NMR (101 MHz, CDCl<sub>3</sub>) δ 152.8, 138.1, 129.8, 125.9, 123.0, 119.2, 65.8, 63.9, 61.8, 39.6, 20.2.

SFC: Chiralpak AD-H, *sc*CO<sub>2</sub>/ MeOH 90/10, 3.0 mL/min, P = 150 bar, λ = 215 nm,  $t_R$  [*cis*-(3*R*,4*R*)] = 29.37 min (major),  $t_R$  [*trans*] = 31.49 min,  $t_R$  [*trans*] = 34.44 min,  $t_R$  [*cis*-(3*S*,4*S*)] = 44.49 min.

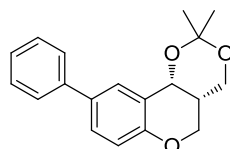
HRMS (ESI/ion trap):  $m/z$  [M + Na]<sup>+</sup> calcd for C<sub>11</sub>H<sub>13</sub>ClNaO<sub>3</sub> 251.0451, found 251.0446.

**General procedure N for the synthesis of compounds 19 and 20.**

To a solution of **15f** (258 mg, 1.0 mmol) in acetone (5 mL), were added 2,2-dimethoxypropane (367 μL, 3.0 mmol) and camphorosulfonic acid (12 mg, 0.05 mmol). The mixture was stirred at rt for 2 h, then quenched with sat. aq. NaHCO<sub>3</sub> and extracted with CH<sub>2</sub>Cl<sub>2</sub>. The combined organic phase was dried over MgSO<sub>4</sub>, filtered and concentrated. The crude mixture was purified by flash chromatography (silica gel, cyclohexane/EtOAc 4:1) to give the corresponding acetal (267 mg, 90%) as a white solid. A round-bottom tube was charged with the previous acetal (89 mg, 0.3 mmol, 1.0 equiv), arylboronic acid (0.6 mmol, 2.0 equiv), K<sub>2</sub>CO<sub>3</sub> (0.9 mmol, 3.0 equiv), Pd(OAc)<sub>2</sub> (5 mol%, 3.4 mg) and cataCXium A (10 mol%, 11 mg). The system was degazed 3 times and placed under an argon atmosphere. DMF (1.5 mL) was added and the mixture was heated at 100 °C overnight. Water was then added and the mixture was extracted with CH<sub>2</sub>Cl<sub>2</sub>. The combined organic phase was washed with brine, dried (MgSO<sub>4</sub>), filtered and concentrated under vacuum. The crude product was purified by flash chromatography on silica gel (cyclohexane/EtOAc 4:1) to give the desired product **19** or **20**.

**(4*aS*,10*bR*)-2,2-dimethyl-9-phenyl-4,4*a*,5,10*b*-tetrahydro-[1,3]dioxino[5,4-*c*]chromene (19)**





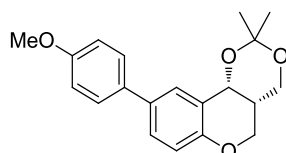
Following the above procedure, product **19** was obtained as white solid, 110 mg (93% yield),  $[\alpha]_{\text{D}}^{20} = -33.3$  (c 1.05,  $\text{CHCl}_3$ ).

$^1\text{H NMR}$  (400 MHz,  $\text{CDCl}_3$ )  $\delta$  7.57 – 7.53 (m, 2H), 7.48 – 7.39 (m, 4H), 7.32 – 7.26 (m, 1H), 6.94 (d,  $J = 8.4$  Hz, 1H), 4.96 (br s, 1H), 4.62 (dd,  $J = 12.4, 10.6$  Hz, 1H), 4.36 (dd,  $J = 12.4, 4.0$  Hz, 1H), 4.17 (ddd,  $J = 10.7, 4.1, 1.5$  Hz, 1H), 3.79 (dd,  $J = 12.5, 1.6$  Hz, 1H), 2.08 – 2.02 (m, 1H), 1.66 (s, 3H), 1.44 (s, 3H).

$^{13}\text{C NMR}$  (101 MHz,  $\text{CDCl}_3$ )  $\delta$  154.8, 140.8, 134.0, 129.8, 129.0, 128.8, 126.9, 126.8, 121.6, 117.5, 99.3, 64.5, 64.0, 60.4, 32.4, 29.7, 19.5.

HRMS (ESI/ion trap):  $m/z$   $[\text{M} + \text{H}]^+$  calcd for  $\text{C}_{19}\text{H}_{21}\text{O}_3$  297.1491, found 297.1485.

(4a*S*,10b*R*)-9-(4-methoxyphenyl)-2,2-dimethyl-4,4a,5,10b-tetrahydro-[1,3]dioxino[5,4-*c*]chromene (**20**)



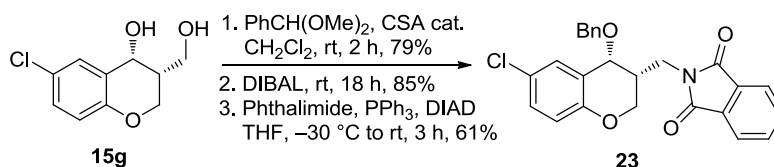
Following the above procedure, product **20** was obtained as white solid, 92 mg (94% yield),  $[\alpha]_{\text{D}}^{20} = -46.8$  (c 0.56,  $\text{CHCl}_3$ ).

$^1\text{H NMR}$  (400 MHz,  $\text{CDCl}_3$ )  $\delta$  7.49-7.46 (m, 2H), 7.48-7.39 (m, 2H), 6.97 – 6.91 (m, 3H), 4.94 (br, 1H), 4.61 (t,  $J = 11.5$  Hz, 1H), 4.35 (dd,  $J = 12.4, 3.8$  Hz, 1H), 4.18 – 4.14 (m, 1H), 3.84 (s, 3H), 3.78 (d,  $J = 12.4$  Hz, 1H), 2.07 – 2.02 (m, 1H), 1.66 (s, 3H), 1.44 (s, 3H).

$^{13}\text{C NMR}$  (101 MHz,  $\text{CDCl}_3$ )  $\delta$  158.8, 154.3, 133.7, 133.5, 129.3, 128.6, 127.9, 121.6, 117.4, 114.2, 99.3, 64.5, 64.0, 60.4, 55.5, 32.4, 29.7, 19.5.

HRMS (ESI/ion trap):  $m/z$   $[\text{M} + \text{H}]^+$  calcd for  $\text{C}_{10}\text{H}_{23}\text{O}_4$  327.1596, found 327.1591.

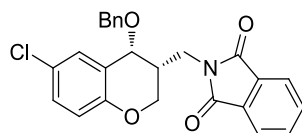
**Procedure O for the synthesis of compound 23.**



To a solution of diol **15g** (214mg, 1 mmol) in  $\text{CH}_2\text{Cl}_2$  (5.0 mL) was added camphorsulfonic acid (12 mg, 0.05 mmol), and benzaldehyde dimethyl acetal (450  $\mu\text{l}$ , 3 mmol) was added dropwise at rt over 2 h. The mixture was concentrated under vacuum and the crude product was purified by flash chromatography on silica gel (cyclohexane/ $\text{EtOAc}$  5:1) to give the corresponding acetal (240 mg, 79%). To a cooled ( $-78$  °C) solution of the previous acetal (220 mg, 0.72 mmol) in  $\text{CH}_2\text{Cl}_2$  (5.0 mL) was added dropwise over 5 min  $i\text{-Bu}_2\text{AlH}$  (3.6 mL,

3.6mmol, 1.0 M in toluene) and the solution was warmed to room temperature and stirred for 18 h. The reaction mixture was cooled to 0 °C and MeOH (2.0 mL) was added. Sat. aq. sodium potassium tartrate (20 mL) was added and the mixture was stirred for 2 h. The organic layer was separated, and the aqueous layer was extracted with CH<sub>2</sub>Cl<sub>2</sub>. The combined organic layers were dried over MgSO<sub>4</sub>, filtered, and concentrated in vacuo. The crude product was purified by flash column chromatography (cyclohexane/EtOAc 3:1) to afford the corresponding ((3R,4R)-4-(benzyloxy)-6-chlorochroman-3-yl)methanol (165 mg, 85%). To a solution of ((3R,4R)-4-(benzyloxy)-6-chlorochroman-3-yl)methanol (135 mg, 0.5 mmol), PPh<sub>3</sub> (157 mg, 0.6 mmol) and phthalimide (80 mg, 0.55 mmol) in THF (3.4 mL), was added diisopropyl azodicarboxylate (DIAD) (123 mg, 0.6 mmol) in THF (1.2 mL) -30 °C. The mixture was warmed to rt and stirred for a further 1 h. Then the solvent was evaporated to provide the crude product which was purified by flash chromatography (cyclohexane/EtOAc 3:1) to give **23** as a white solid (133 mg, 61%).

2-(((3R,4R)-4-(benzyloxy)-6-chlorochroman-3-yl)methyl)isoindoline-1,3-dione (**23**)



Following the above procedure, product **23** was obtained as white solid, 133 mg (61% yield),  $[\alpha]_D^{20} = +122.9$  (c 1.08, CHCl<sub>3</sub>).

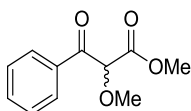
**<sup>1</sup>H NMR** (400 MHz, CDCl<sub>3</sub>)  $\delta$  7.90 – 7.82 (m, 2H), 7.75 – 7.70 (m, 2H), 7.43 – 7.27 (m, 5H), 7.19 – 7.16 (m, 2H), 6.80 (d,  $J = 8.3$  Hz, 1H), 4.69 (d,  $J = 11.3$  Hz, 1H), 4.64 (d,  $J = 11.3$  Hz, 1H), 4.47 (d,  $J = 3.2$  Hz, 1H), 4.35 (t,  $J = 10.7$  Hz, 1H), 4.14 (dd,  $J = 10.9, 3.6$  Hz, 1H), 3.96 (dd,  $J = 14.1, 5.0$  Hz, 1H), 3.87 (dd,  $J = 14.1, 8.4$  Hz, 1H), 2.60 – 2.50 (m, 1H).

**<sup>13</sup>C NMR** (101 MHz, CDCl<sub>3</sub>)  $\delta$  168.5, 153.1, 138.0, 134.2, 132.1, 130.0, 129.7, 128.6, 128.0, 127.9, 124.5, 123.5, 122.2, 118.5, 71.4, 70.3, 64.4, 36.9, 36.0.

**HRMS** (ESI/ion trap):  $m/z$   $[M + H]^+$  calcd for C<sub>25</sub>H<sub>21</sub>ClNO<sub>4</sub> 434.1159, found 434.1154.

**Substrates:  $\alpha$ -methoxyl- $\beta$ -keto esters (24a-m)**

Methyl 2-methoxy-3-oxo-3-phenylpropanoate (**24a**)

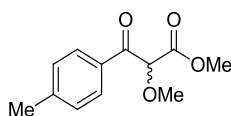


**<sup>1</sup>H NMR** (400 MHz, CDCl<sub>3</sub>)  $\delta$  8.08 – 8.05 (m, 2H), 7.63 – 7.58 (m, 1H), 7.50 – 7.46 (m, 2H), 4.95 (s, 1H), 3.78 (s, 3H), 3.53 (s, 3H).

**<sup>13</sup>C NMR** (101 MHz, CDCl<sub>3</sub>)  $\delta$  192.5, 168.1, 134.2, 134.1, 129.5 (2C), 128.8 (2C), 85.2, 58.8, 52.9.

**MS** (ESI) = 209  $[M + H]^+$

Methyl 2-methoxy-3-oxo-3-(p-tolyl)propanoate (**24b**)

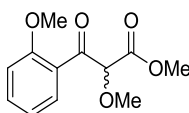


**<sup>1</sup>H NMR** (400 MHz, CDCl<sub>3</sub>) δ 7.97 (d, *J* = 8.1 Hz, 2H), 7.27 (d, *J* = 8.1 Hz, 2H), 4.93 (s, 1H), 3.76 (s, 3H), 3.52 (s, 3H), 2.41 (s, 3H).

**<sup>13</sup>C NMR** (101 MHz, CDCl<sub>3</sub>) δ 192.0, 168.2, 145.2, 131.7, 129.6 (2C), 129.5 (2C), 85.1, 58.7, 52.8, 21.8.

**MS** (ESI) = 223 [M + H]<sup>+</sup>

Methyl 2-methoxy-3-(2-methoxyphenyl)-3-oxopropanoate (**24c**)

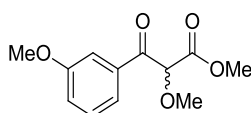


**<sup>1</sup>H NMR** (400 MHz, CDCl<sub>3</sub>) δ 7.79 (dd, *J* = 7.7, 1.7 Hz, 1H), 7.55 – 7.46 (m, 1H), 7.07 – 7.01 (m, 1H), 6.96 (d, *J* = 8.4 Hz, 1H), 5.06 (s, 1H), 3.88 (s, 3H), 3.75 (s, 3H), 3.50 (s, 3H).

**<sup>13</sup>C NMR** (101 MHz, CDCl<sub>3</sub>) δ 194.3, 167.8, 158.9, 134.7, 131.2, 125.5, 121.2, 111.7, 86.6, 59.3, 55.4, 52.4.

**MS** (ESI) = 239 [M + H]<sup>+</sup>

Methyl 2-methoxy-3-(3-methoxyphenyl)-3-oxopropanoate (**24d**)

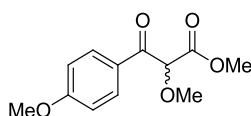


**<sup>1</sup>H NMR** (400 MHz, CDCl<sub>3</sub>) δ 7.67 (ddd, *J* = 7.7, 1.6, 1.0 Hz, 1H), 7.57 (dd, *J* = 2.5, 1.6 Hz, 1H), 7.40 – 7.35 (m, 1H), 7.15 (ddd, *J* = 8.3, 2.7, 1.0 Hz, 1H), 4.95 (s, 1H), 3.85 (s, 3H), 3.77 (s, 3H), 3.53 (s, 3H).

**<sup>13</sup>C NMR** (101 MHz, CDCl<sub>3</sub>) δ 192.3, 168.1, 160.0, 135.5, 129.8, 122.2, 121.0, 113.4, 85.1, 58.8, 55.6, 52.9.

**MS** (ESI) = 239 [M + H]<sup>+</sup>

Methyl 2-methoxy-3-(4-methoxyphenyl)-3-oxopropanoate (**24e**)



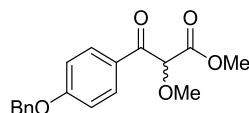
**<sup>1</sup>H NMR** (400 MHz, CDCl<sub>3</sub>) δ 8.07 (d, *J* = 8.9 Hz, 2H), 6.93 (d, *J* = 8.7 Hz, 2H), 4.90 (s, 1H),

3.87 (s, 3H), 3.76 (s, 3H), 3.51 (s, 3H).

$^{13}\text{C}$  NMR (101 MHz,  $\text{CDCl}_3$ )  $\delta$  190.8, 168.3, 164.4, 132.0 (2C), 127.2, 114.0 (2C), 85.3, 58.6, 55.6, 52.7

MS (ESI) = 239  $[\text{M} + \text{H}]^+$

Methyl 3-(4-(benzyloxy)phenyl)-2-methoxy-3-oxopropanoate (**24f**)

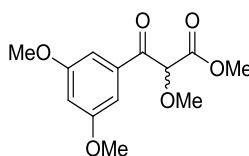


$^1\text{H}$  NMR (400 MHz,  $\text{CDCl}_3$ )  $\delta$  8.07 (d,  $J = 9.0$  Hz, 2H), 7.43 – 7.32 (m, 5H), 7.01 (d,  $J = 9.0$  Hz, 2H), 5.13 (s, 2H), 4.90 (s, 1H), 3.76 (s, 3H), 3.51 (s, 3H).

$^{13}\text{C}$  NMR (101 MHz,  $\text{CDCl}_3$ )  $\delta$  190.9, 168.3, 163.5, 136.1, 132.1 (2C), 128.8 (2C), 128.4, 127.6 (2C), 127.4, 114.9 (2C), 85.3, 70.3, 58.7, 52.8.

MS (ESI) = 315  $[\text{M} + \text{H}]^+$

Methyl 3-(3,5-dimethoxyphenyl)-2-methoxy-3-oxopropanoate (**24g**)

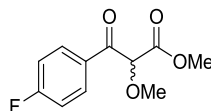


$^1\text{H}$  NMR (400 MHz,  $\text{CDCl}_3$ )  $\delta$  7.21 (d,  $J = 2.3$  Hz, 2H), 6.68 (t,  $J = 2.3$  Hz, 1H), 4.92 (s, 1H), 3.82 (s, 6H), 3.77 (s, 3H), 3.53 (s, 3H).

$^{13}\text{C}$  NMR (101 MHz,  $\text{CDCl}_3$ )  $\delta$  192.1, 168.0, 161.0 (2C), 135.9, 107.1 (2C), 106.9, 85.0, 58.8, 55.7 (2C), 52.9.

MS (ESI) = 269  $[\text{M} + \text{H}]^+$

Methyl 3-(4-fluorophenyl)-2-methoxy-3-oxopropanoate (**24h**)

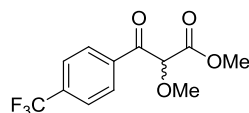


$^1\text{H}$  NMR (400 MHz,  $\text{CDCl}_3$ )  $\delta$  8.15 – 8.09 (m, 2H), 7.17 – 7.10 (m, 2H), 4.88 (s, 1H), 3.77 (s, 3H), 3.52 (s, 3H).

$^{13}\text{C}$  NMR (101 MHz,  $\text{CDCl}_3$ )  $\delta$  190.8, 167.9, 166.2 (d,  $J_{\text{CF}} = 256.6$  Hz), 132.3 (d,  $J_{\text{CF}} = 9.5$  Hz, 2C), 130.4 (d,  $J_{\text{CF}} = 26.2$  Hz), 115.9 (d,  $J_{\text{CF}} = 21.9$  Hz, 2C), 85.3, 58.7, 52.8.

MS (ESI) = 227  $[\text{M} + \text{H}]^+$

Methyl 2-methoxy-3-oxo-3-(4-(trifluoromethyl)phenyl)propanoate (**24i**)

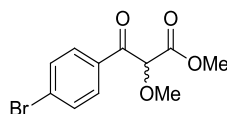


**$^1\text{H NMR}$**  (400 MHz,  $\text{CDCl}_3$ )  $\delta$  8.19 – 8.17 (m, 2H), 7.75 – 7.71 (m, 2H), 4.91 (s, 1H), 3.78 (s, 3H), 3.54 (s, 3H).

**$^{13}\text{C NMR}$**  (75 MHz,  $\text{CDCl}_3$ )  $\delta$  191.8, 167.7, 136.8, 135.3 (q,  $J_{\text{CF}} = 32.9$  Hz), 130.0 (2C), 125.9 (q,  $J_{\text{CF}} = 3.5$  Hz, 2C), 123.4 (q,  $J_{\text{CF}} = 272.7$  Hz), 85.6, 59.1, 53.1.

**MS** (ESI) = 294  $[\text{M} + \text{NH}_4]^+$

Methyl 3-(4-bromophenyl)-2-methoxy-3-oxopropanoate (**24j**)

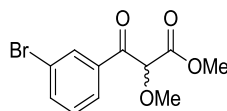


**$^1\text{H NMR}$**  (400 MHz,  $\text{CDCl}_3$ )  $\delta$  7.96 – 7.92 (m, 2H), 7.63 – 7.59 (m, 2H), 4.87 (s, 1H), 3.77 (s, 3H), 3.52 (s, 3H).

**$^{13}\text{C NMR}$**  (101 MHz,  $\text{CDCl}_3$ )  $\delta$  191.6, 167.9, 132.8, 132.2 (2C), 131.1 (2C), 129.6, 85.5, 58.9, 53.0.

**MS** (ESI) = 304  $[\text{M} + \text{NH}_4]^+$

Methyl 3-(3-bromophenyl)-2-methoxy-3-oxopropanoate (**24k**)

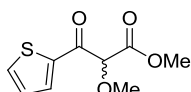


**$^1\text{H NMR}$**  (400 MHz,  $\text{CDCl}_3$ )  $\delta$  8.18 (t,  $J = 1.7$  Hz, 1H), 8.02 – 7.99 (m, 1H), 7.72 (ddd,  $J = 8.0, 2.0, 1.0$  Hz, 1H), 7.34 (t,  $J = 7.9$  Hz, 1H), 4.89 (s, 1H), 3.78 (s, 3H), 3.53 (s, 3H).

**$^{13}\text{C NMR}$**  (101 MHz,  $\text{CDCl}_3$ )  $\delta$  191.3, 167.8, 137.0, 135.8, 132.4, 130.4, 128.2, 123.1, 85.2, 59.0, 53.0.

**MS** (ESI) = 304  $[\text{M} + \text{NH}_4]^+$

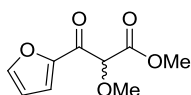
Methyl 2-methoxy-3-oxo-3-(thiophen-2-yl)propanoate (**24l**)



**$^1\text{H NMR}$**  (400 MHz,  $\text{CDCl}_3$ )  $\delta$  8.05 (dd,  $J = 3.9, 1.1$  Hz, 1H), 7.73 (dd,  $J = 4.9, 1.1$  Hz, 1H), 7.15 (dd,  $J = 4.9, 3.9$  Hz, 1H), 4.80 (s, 1H), 3.78 (s, 3H), 3.54 (s, 3H).

**$^{13}\text{C NMR}$**  (101 MHz,  $\text{CDCl}_3$ )  $\delta$  185.5, 167.5, 140.1, 135.6, 135.1, 128.5, 85.7, 58.7, 52.9.

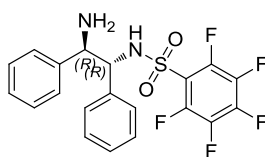
**MS** (ESI) = 215  $[\text{M} + \text{H}]^+$

methyl 3-(furan-2-yl)-2-methoxy-3-oxopropanoate (**24m**)

$^1\text{H NMR}$  (400 MHz,  $\text{CDCl}_3$ )  $\delta$  7.67 (dd,  $J = 1.6, 0.7$  Hz, 1H), 7.50 – 7.48 (m, 1H), 6.58 (dd,  $J = 3.6, 1.7$  Hz, 1H), 4.81 (s, 1H), 3.78 (s, 3H), 3.53 (s, 3H).

$^{13}\text{C NMR}$  (101 MHz,  $\text{CDCl}_3$ )  $\delta$  180.8, 167.5, 150.1, 147.9, 121.2, 112.8, 84.4, 59.0, 52.9.

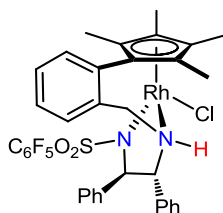
$\text{MS (ESI)} = 199 [\text{M} + \text{H}]^+$

*N*-(2-Amino-1,2-diphenyl-ethyl)-2,3,4,5,6-pentamethyl-benzene sulfonamide (**L42**)

(*R,R*)-DPEN (0.5 g, 2.4 mmol) was dissolved in dichloromethane (20 mL) and the solution was cooled to 0 °C when triethylamine (0.4 mL, 2.88 mmol) was added followed by 2,3,4,5,6-pentamethylbenzenesulfonyl chloride (0.64 g, 2.4 mmol) in dichloromethane (5 mL). The reaction was allowed to stay at rt and was stirred overnight. The mixture was washed with water (10 mL) and then the organic phase was separated, dried over dried  $\text{MgSO}_4$  and evaporated under reduced pressure to afford the crude product which was purified by silica gel chromatography (1:1 % v/v ethyl acetate/hexane) to afford the product **L42** as a white solid (0.68 g, 64%). The analytical data were identical to those reported in the literature.<sup>248</sup>

$^1\text{H NMR}$  (400 MHz,  $\text{CDCl}_3$ )  $\delta$  7.39 – 7.16 (m, 11H), 4.70 (d,  $J = 3.5$  Hz, 1H), 4.39 (d,  $J = 3.5$  Hz, 1H), 2.42 (brs, 2H).

$^{19}\text{F NMR}$  (376 MHz,  $\text{CDCl}_3$ )  $\delta$  -135.43 (dp,  $J = 18.1, 7.0$  Hz), -147.68 (tt,  $J = 21.1, 6.2$  Hz), -159.49 (tt,  $J = 21.5, 6.0$  Hz).

Catalyst (*R,R*)-**C89**

To a solution of compound **27** (271 mg, 1.2 mmol) in dry MeOH (24 mL) was added (*R,R*)- $\text{C}_6\text{F}_5\text{SO}_2\text{DPEN}$  **L42** (442 mg, 1.0 mmol) followed by the addition of 500 mg of molecular sieves (4 Å) and 1 drops of glacial acetic acid. The mixture was stirred at rt for 20 h, then  $\text{NaBH}_3\text{CN}$  (81.7 mg, 1.3 mmol) was added, and the reaction was stirred at rt for 18 h. After removal of the molecular sieves and evaporation of MeOH, the residue was dissolved in EtOAc (20 mL). The organic layer was washed with saturated  $\text{NaHCO}_3$  and then brine, dried over

<sup>248</sup> Martins, J. E. D.; Wills, M. *Tetrahedron* **2009**, *65*, 5782.

MgSO<sub>4</sub>, filtered, and concentrated. Purification of the residue by flash chromatography (SiO<sub>2</sub>, pentane/EtOAc = 9/1 to 8/2) afforded the diamine (465 mg, 71%) as a white solid. To a solution of the diamine (440 mg, 0.674 mmol) in MeOH (15 mL) was added RhCl<sub>3</sub> · H<sub>2</sub>O (177 mg, 0.674 mmol), and the reaction mixture was heated under reflux using an oil bath for 22 h. Et<sub>3</sub>N (190 μL, 1.348 mmol) was then added, and the mixture was refluxed for a further 20 h and concentrated. The residue was triturated with H<sub>2</sub>O, and the solid was filtered, washed with H<sub>2</sub>O, and dried under vacuum. Purification of the black solid by flash chromatography (SiO<sub>2</sub>, EtOAc/Petrol ether = 1 : 1 – 2 : 1) afforded (*R,R*)-**C90** (311 mg, 58.5%) as an orange solid.  $[\alpha]_{25}^D = -41.4^\circ$  ( $c = 1.0$ , CHCl<sub>3</sub>).

<sup>1</sup>H NMR (400 MHz, CDCl<sub>3</sub>) δ 7.57 – 7.35 (m, 4H), 7.23 – 7.14 (m, 3H), 6.94 – 6.70 (m, 7H), 5.00 (d,  $J = 12.3$  Hz, 1H), 4.45 (d,  $J = 11.0$  Hz, 1H), 4.22 (dd,  $J = 13.9, 2.8$  Hz, 1H), 3.72 (d,  $J = 14.1$  Hz, 1H), 3.39 – 3.31 (m, 1H), 2.01 (s, 3H), 1.96 (s, 3H), 1.89 (s, 3H), 1.48 (s, 3H).

<sup>13</sup>C NMR (101 MHz, CDCl<sub>3</sub>) δ 145.2 (m, br), 142.7 (m, br), 140.2 (m, br), 138.3, 138.1 (m, br), 135.7 (m, br), 135.5, 134.9, 131.7, 130.0, 129.9, 129.1, 128.0, 127.3, 127.1, 126.6, 121.3 (t,  $J_{CF} = 15.5$  Hz), 107.7 (d,  $J_{CRh} = 6.5$  Hz), 100.8 (d,  $J_{CRh} = 7.0$  Hz), 97.4 (d,  $J_{CRh} = 9.3$  Hz), 90.0 (d,  $J_{CRh} = 9.1$  Hz), 79.8 (d,  $J_{CRh} = 9.2$  Hz), 76.8, 75.5, 69.0, 52.1, 10.6, 10.4, 10.2, 8.1.

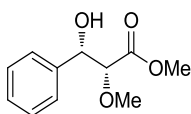
<sup>19</sup>F NMR (376 MHz, CDCl<sub>3</sub>) δ 135.9 (d,  $J = 22.5$  Hz), 154.0 (t,  $J = 21.0$  Hz), 163.7 (t,  $J = 19.5$  Hz).

HRMS (ESI):  $m/z$  [M+H]<sup>+</sup> calcd for C<sub>36</sub>H<sub>32</sub>ClF<sub>5</sub>N<sub>2</sub>O<sub>2</sub>RhS: 789.0848, found 789.1256.

**Typical procedure P for rhodium complex (*R,R*)-**C89**-catalyzed ATH of  $\alpha$ -methoxyl- $\beta$ -keto esters **24****

A round-bottomed tube equipped with a balloon of argon was charged with the corresponding  $\alpha$ -methoxyl- $\beta$ -keto esters **24** (0.8 mmol) and the rhodium complex (*R,R*)-**C89** (0.0040 mmol, 0.5 mol%). The solids were subjected to three vacuum/argon cycles before anhydrous 2-MeTHF (4.0 mL) was added. The mixture was stirred at room temperature for 3–5 min, and the tube was transferred into 30 °C oil bath, before the HCO<sub>2</sub>H/Et<sub>3</sub>N (5:2) azeotropic mixture (134 μL, 1.6 mmol, 2.0 equiv) was added dropwise. After complete consumption of the starting material (monitored by TLC or <sup>1</sup>H NMR), the reaction mixture was evaporated under vacuum, followed by quenched with sat. aq NaHCO<sub>3</sub>, extracted with CH<sub>2</sub>Cl<sub>2</sub>, the combined organic layers were washed with brine, dried (MgSO<sub>4</sub>), filtrated and concentrated under vacuum. The conversion and diastereomeric ratio were determined by <sup>1</sup>H NMR analysis of the crude product. After purification of the crude product, the enantiomeric excess was determined by SFC or HPLC analysis (Chiralcel OD-H or Chiralpak IA, IB, IC or AD-H column).

Methyl (2*R*,3*S*)-3-hydroxy-2-methoxy-3-phenylpropanoate (**25a**)



Pale yellow oil, 116 mg, 92% yield, *syn* : *anti* = 98 : 2,  $ee_{syn} >99\%$ ;

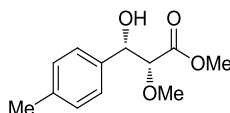
<sup>1</sup>H NMR (400 MHz, CDCl<sub>3</sub>) δ 7.38 – 7.28 (m, 5H), 4.92 (t,  $J = 5.3$  Hz, 1H), 3.91 (d,  $J = 5.6$  Hz, 1H), 3.65 (s, 3H), 3.42 (s, 3H), 2.95 (d,  $J = 5.1$  Hz, 1H).

$^{13}\text{C}$  NMR (101 MHz,  $\text{CDCl}_3$ )  $\delta$  170.8, 139.2, 128.4, 128.3, 126.6, 85.4, 74.8, 59.0, 52.1.

MS (ESI):  $m/z = 228$   $[\text{M} + \text{NH}_4]^+$

HPLC : Chiralpak IC, Hexane : EtOH = 90 : 10, 0.7 mL/min,  $\lambda = 215$  nm,  $t_R$  [*anti*] = 11.22 min,  $t_R$  [*anti*] = 12.45 min,  $t_R$  [*syn*] = 14.02 min,  $t_R$  [*syn*] = 16.43 min.

Methyl (2*R*,3*S*)-3-hydroxy-2-methoxy-3-(*p*-tolyl)propanoate (**25b**)



Pale yellow oil, 113 mg, 84% yield, *syn* : *anti* = 97 : 3,  $ee_{syn} > 99\%$ ;

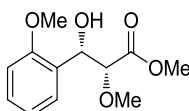
$^1\text{H}$  NMR (400 MHz,  $\text{CDCl}_3$ )  $\delta$  7.30-7.25 (m, 2H), 7.21 – 7.16 (m, 2H), 4.90 (t,  $J = 5.3$  Hz, 1H), 3.91 (d,  $J = 5.6$  Hz, 1H), 3.68 (s, 3H), 3.45 (s, 3H), 2.96 (d,  $J = 5.0$  Hz, 1H), 2.37 (s, 3H).

$^{13}\text{C}$  NMR (101 MHz,  $\text{CDCl}_3$ )  $\delta$  170.9, 138.0, 136.2, 129.2, 126.5, 85.4, 74.6, 59.0, 52.1, 21.3..

ESI ( $m/z$ ) = 242  $[\text{M} + \text{NH}_4]^+$

HPLC : Chiralpak IC, Hexane : EtOH = 90 : 10, 1.0 mL/min,  $\lambda = 215$  nm,  $t_R$  [*anti*] = 8.85 min,  $t_R$  [*anti*] = 10.34 min,  $t_R$  [*syn*] = 11.73 min,  $t_R$  [*syn*] = 13.32 min.

Methyl (2*S*,3*S*)-3-hydroxy-2-methoxy-3-(2-methoxyphenyl)propanoate (**25c**)



Pale yellow oil, 117 mg, 81% yield, *syn* : *anti* = 98 : 2,  $ee_{syn} = 88\%$ ;

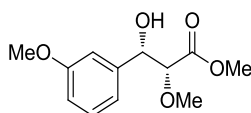
$^1\text{H}$  NMR (400 MHz,  $\text{CDCl}_3$ )  $\delta$  7.36 – 7.33 (m, 1H), 7.30 – 7.25 (m, 1H), 6.96 (td,  $J = 7.5, 1.1$  Hz, 1H), 6.89 (dd,  $J = 8.3, 1.0$  Hz, 1H), 5.19 (t,  $J = 5.9$  Hz, 1H), 4.18 (d,  $J = 5.4$  Hz, 1H), 3.87 (s, 3H), 3.64 (s, 3H), 3.38 (s, 3H), 3.24 (d,  $J = 6.4$  Hz, 1H).

$^{13}\text{C}$  NMR (101 MHz,  $\text{CDCl}_3$ )  $\delta$  170.9, 156.5, 129.1, 128.0, 127.2, 120.8, 110.4, 83.2, 71.1, 58.5, 55.5, 51.8.

MS (ESI):  $m/z = 258$   $[\text{M} + \text{NH}_4]^+$

HPLC : Chiralpak IC, Hexane : EtOH = 90 : 10, 0.7 mL/min,  $\lambda = 215$  nm,  $t_R$  [*anti*] = 42.09 min,  $t_R$  [*anti*] = 47.84 min,  $t_R$  [*syn*] = 18.08 min,  $t_R$  [*syn*] = 30.20 min.

Methyl (2*R*,3*S*)-3-hydroxy-2-methoxy-3-(3-methoxyphenyl)propanoate (**25d**)





## Experimental part

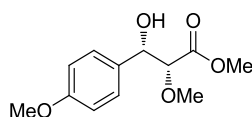
Pale yellow oil, 120 mg, 83% yield, *syn* : *anti* = 97 : 3, *ee*<sub>syn</sub> >99%;

**<sup>1</sup>H NMR** (400 MHz, CDCl<sub>3</sub>) δ 7.25 (t, *J* = 8.0 Hz, 1H), 6.95 – 6.91 (m, 2H), 6.84 (ddd, *J* = 8.2, 2.6, 1.0 Hz, 1H), 4.90 (t, *J* = 5.3 Hz, 1H), 3.90 (d, *J* = 5.4 Hz, 1H), 3.81 (s, 3H), 3.67 (s, 3H), 3.41 (s, 3H), 2.95 (d, *J* = 5.2 Hz, 1H).

**<sup>13</sup>C NMR** (101 MHz, CDCl<sub>3</sub>) δ 170.9, 159.8, 140.9, 129.5, 118.8, 113.9, 112.0, 85.3, 74.7, 59.1, 55.4, 52.2.

**MS** (ESI): *m/z* = 258 [M + NH<sub>4</sub>]<sup>+</sup>

### Methyl (2*R*,3*S*)-3-hydroxy-2-methoxy-3-(4-methoxyphenyl)propanoate (**25e**)



Pale yellow oil, 123 mg, 85% yield, *syn* : *anti* = 96 : 4, *ee*<sub>syn</sub> >99%;

**<sup>1</sup>H NMR** (400 MHz, CDCl<sub>3</sub>) δ 7.30 – 7.27 (m, 2H), 6.89 – 6.86 (m, 2H), 4.89 – 4.81 (m, 1H), 3.86 (d, *J* = 6.0 Hz, 1H), 3.80 (s, 3H), 3.63 (s, 3H), 3.43 (s, 3H), 2.93 (d, *J* = 4.6 Hz, 1H).

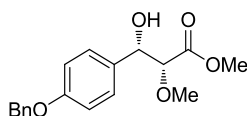
**<sup>13</sup>C NMR** (101 MHz, CDCl<sub>3</sub>) δ 170.9, 159.6, 131.1, 128.0, 113.9, 85.6, 74.5, 59.0, 55.4, 52.1.

**MS** (ESI): *m/z* = 258 [M + NH<sub>4</sub>]<sup>+</sup>

**SFC** : Chiralpak IC, Hexane : EtOH = 90 : 10, 0.7 mL/min, λ = 215 nm, *t*<sub>R</sub> [*anti*] = 19.62 min, *t*<sub>R</sub> [*anti*] = 23.98 min, *t*<sub>R</sub> [*syn*-(*S,S*)] = 25.90 min, *t*<sub>R</sub> [*syn*-(*R,R*)] = 30.61 min.

**SFC** : Chiralpak IA, Hexane : EtOH = 90 : 10, 0.7 mL/min, λ = 215 nm, *t*<sub>R</sub> [*anti*] = 20.06 min, *t*<sub>R</sub> [*anti*] = 23.11 min, *t*<sub>R</sub> [*syn*] = 26.70 min, *t*<sub>R</sub> [*syn*] = 28.94 min.

### Methyl (2*R*,3*S*)-3-(4-(benzyloxy)phenyl)-3-hydroxy-2-methoxypropanoate (**25f**)



White solid, 177 mg, 93% yield, *syn* : *anti* = 98 : 2, *ee*<sub>syn</sub> >99%;

**<sup>1</sup>H NMR** (400 MHz, CDCl<sub>3</sub>) δ 7.44 – 7.36 (m, 4H), 7.35 – 7.27 (m, 3H), 6.97 – 6.93 (m, 2H), 5.06 (s, 2H), 4.89 – 4.83 (m, 1H), 3.87 (d, *J* = 5.9 Hz, 1H), 3.63 (s, 3H), 3.43 (s, 3H), 2.92 (t, *J* = 3.7 Hz, 1H).

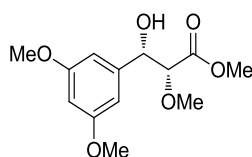
**<sup>13</sup>C NMR** (101 MHz, CDCl<sub>3</sub>) δ 170.9, 158.9, 137.0, 131.4, 128.7, 128.1, 128.0, 127.6, 114.9, 85.6, 74.5, 70.1, 59.0, 52.1.

**MS** (ESI): *m/z* = 334 [M + NH<sub>4</sub>]<sup>+</sup>

**HPLC** : Chiralpak IE, Hexane : EtOH = 90 : 10, 1.0 mL/min, λ = 215 nm, *t*<sub>R</sub> [*anti*] = 23.64 min,

$t_R$  [*anti*] = 25.13 min,  $t_R$  [*syn*] = 34.62 min,  $t_R$  [*syn*] = 37.23 min.

Methyl (2*R*,3*S*)-3-(3,5-dimethoxyphenyl)-3-hydroxy-2-methoxypropanoate (**25g**)



Pale yellow oil, 130 mg, 80% yield, *syn* : *anti* = 96 : 4,  $ee_{syn}$  >99%;

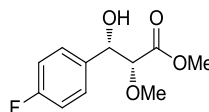
$^1\text{H NMR}$  (400 MHz,  $\text{CDCl}_3$ )  $\delta$  6.53 (d,  $J$  = 2.2 Hz, 2H), 6.40 (t,  $J$  = 2.3 Hz, 1H), 4.86 (t,  $J$  = 5.0 Hz, 1H), 3.89 (d,  $J$  = 5.2 Hz, 1H), 3.79 (s, 6H), 3.69 (s, 3H), 3.42 (s, 3H), 2.91 (d,  $J$  = 5.1 Hz, 1H).

$^{13}\text{C NMR}$  (101 MHz,  $\text{CDCl}_3$ )  $\delta$  170.8, 160.8, 141.8, 104.4, 100.2, 85.1, 74.6, 59.0, 55.4, 52.1.

**MS** (ESI):  $m/z$  = 288 [ $\text{M} + \text{NH}_4$ ] $^+$

**HPLC** : Chiralpak IA, Hexane : EtOH = 90 : 10, 1.0 mL/min,  $\lambda$  = 215 nm,  $t_R$  [*anti*] = 19.29 min,  $t_R$  [*anti*] = 22.84 min,  $t_R$  [*syn*] = 28.83 min,  $t_R$  [*syn*] = 35.40 min.

Methyl (2*R*,3*S*)-3-(4-fluorophenyl)-3-hydroxy-2-methoxypropanoate (**25h**)



Pale yellow oil, 100 mg, 73% yield, *syn* : *anti* = 98 : 2,  $ee_{syn}$  >99%;

$^1\text{H NMR}$  (400 MHz,  $\text{CDCl}_3$ )  $\delta$  7.36 – 7.32 (m, 2H), 7.07 – 7.01 (m, 2H), 4.89 (t,  $J$  = 5.2 Hz, 1H), 3.85 (d,  $J$  = 5.8 Hz, 1H), 3.65 (s, 3H), 3.48 – 3.40 (m, 3H), 3.00 – 2.96 (m, 1H).

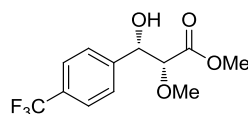
$^{13}\text{C NMR}$  (101 MHz,  $\text{CDCl}_3$ )  $\delta$  170.7, 162.7 (d,  $J_{CF}$  = 246.4 Hz), 134.9, 128.4 (d,  $J_{CF}$  = 8.2 Hz), 115.4 (d,  $J_{CF}$  = 21.5 Hz), 85.3, 74.2, 59.0, 52.2.

$^{19}\text{F NMR}$  (376 MHz,  $\text{CDCl}_3$ )  $\delta$  -114.0.

**MS** (ESI):  $m/z$  = 246 [ $\text{M} + \text{NH}_4$ ] $^+$

**HPLC** : Chiralpak IE, Hexane : EtOH = 90 : 10, 1.0 mL/min,  $\lambda$  = 215 nm,  $t_R$  [*anti*] = 9.05 min,  $t_R$  [*anti*] = 9.88 min,  $t_R$  [*syn*] = 12.28 min,  $t_R$  [*syn*] = 13.74 min.

Methyl (2*R*,3*S*)-3-hydroxy-2-methoxy-3-(4-(trifluoromethyl)phenyl)propanoate (**25i**)



Pale yellow oil, 148 mg, 89% yield, *syn* : *anti* = 95 : 5,  $ee_{syn}$  >99%;

$^1\text{H NMR}$  (400 MHz,  $\text{CDCl}_3$ )  $\delta$  7.62 (d,  $J$  = 8.2 Hz, 2H), 7.49 (d,  $J$  = 8.4 Hz, 2H), 4.99 (t,  $J$  = 5.3 Hz, 1H), 3.90 (d,  $J$  = 5.1 Hz, 1H), 3.69 (s, 3H), 3.42 (s, 3H), 3.06 (d,  $J$  = 5.6 Hz, 1H).

## Experimental part

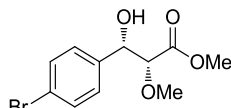
$^{13}\text{C}$  NMR (101 MHz,  $\text{CDCl}_3$ )  $\delta$  170.6, 143.4, 130.5 (q,  $J = 32.4$  Hz), 127.0, 125.39 (q,  $J = 3.8$  Hz), 124.2 (q,  $J = 274$  Hz), 84.7, 74.2, 59.2, 52.3.

$^{19}\text{F}$  NMR (376 MHz,  $\text{CDCl}_3$ )  $\delta$  -62.59.

MS (ESI):  $m/z = 296$   $[\text{M} + \text{NH}_4]^+$

HPLC : Chiralpak IB, Hexane : EtOH = 90 : 10, 1.0 mL/min,  $\lambda = 215$  nm,  $t_R$  [*anti*] = 7.32 min,  $t_R$  [*anti*] = 8.35 min,  $t_R$  [*syn*] = 9.28 min,  $t_R$  [*syn*] = 10.17 min.

### Methyl (2*R*,3*S*)-3-(4-bromophenyl)-3-hydroxy-2-methoxypropanoate (**25j**)



White solid, 168 mg, 97% yield, *syn* : *anti* = 96 : 4,  $ee_{syn} >99\%$ ;

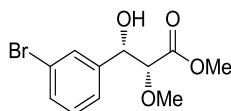
$^1\text{H}$  NMR (400 MHz,  $\text{CDCl}_3$ )  $\delta$  7.48 (d,  $J = 8.4$  Hz, 2H), 7.24 (d,  $J = 8.4$  Hz, 2H), 4.88 (t,  $J = 5.3$  Hz, 1H), 3.85 (d,  $J = 5.4$  Hz, 1H), 3.67 (s, 3H), 3.42 (s, 3H), 3.01 – 2.98 (br, 1H).

$^{13}\text{C}$  NMR (101 MHz,  $\text{CDCl}_3$ )  $\delta$  170.6, 138.3, 131.6, 128.3, 122.2, 85.0, 74.2, 59.1, 52.2.

MS (ESI):  $m/z = 306$   $[\text{M} + \text{NH}_4]^+$

HPLC : Chiralpak IA, Hexane : EtOH = 90 : 10, 0.7 mL/min,  $\lambda = 215$  nm,  $t_R$  [*anti*] = 16.14 min,  $t_R$  [*anti*] = 17.61 min,  $t_R$  [*syn*] = 19.73 min,  $t_R$  [*syn*] = 22.02 min.

### Methyl (2*R*,3*S*)-3-(3-bromophenyl)-3-hydroxy-2-methoxypropanoate (**25k**)



Pale yellow oil, 161mg, 93% yield, *syn* : *anti* = 96 : 4,  $ee_{syn} >99\%$ ;

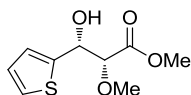
$^1\text{H}$  NMR (400 MHz,  $\text{CDCl}_3$ )  $\delta$  7.54 (m, 1H), 7.44 (m,  $J = 7.8$  Hz, 1H), 7.28 (m, 1H), 7.22 (t,  $J = 7.8$  Hz, 1H), 4.89 (t,  $J = 5.3$  Hz, 1H), 3.87 (d,  $J = 5.3$  Hz, 1H), 3.69 (s, 3H), 3.42 (s, 3H), 3.00 (d,  $J = 5.4$  Hz, 1H).

$^{13}\text{C}$  NMR (101 MHz,  $\text{CDCl}_3$ )  $\delta$  170.6, 141.7, 131.4, 130.0, 129.7, 125.2, 122.6, 84.9, 74.1, 59.1, 52.3.

MS (ESI):  $m/z = 306$   $[\text{M} + \text{NH}_4]^+$

HPLC : Chiralpak IE, Hexane : EtOH = 90 : 10, 1.0 mL/min,  $\lambda = 215$  nm,  $t_R$  [*anti*] = 8.78 min,  $t_R$  [*anti*] = 10.08 min,  $t_R$  [*syn*] = 12.43 min,  $t_R$  [*syn*] = 13.45 min.

### Methyl (2*R*,3*R*)-3-hydroxy-2-methoxy-3-(thiophen-2-yl)propanoate (**25l**)



Pale yellow oil, 114 mg, 88% yield, *syn* : *anti* > 99 : 1, *ee<sub>syn</sub>* >99%;

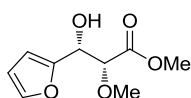
**<sup>1</sup>H NMR** (400 MHz, CDCl<sub>3</sub>) δ 7.29 (dd, *J* = 5.0, 1.2 Hz, 1H), 7.03 (m, 1H), 6.97 (dd, *J* = 5.0, 3.5 Hz, 1H), 5.22 (dd, *J* = 6.5, 4.6 Hz, 1H), 3.96 (d, *J* = 4.6 Hz, 1H), 3.74 (s, 3H), 3.51 (s, 3H), 2.98 (d, *J* = 6.5 Hz, 1H).

**<sup>13</sup>C NMR** (101 MHz, CDCl<sub>3</sub>) δ 170.6, 142.6, 126.6, 125.9, 125.6, 84.6, 71.0, 59.3, 52.4..

**MS** (ESI): *m/z* = 234 [M + NH<sub>4</sub>]<sup>+</sup>

**HPLC** : Chiralpak IC, Hexane : EtOH = 90 : 10, 1.0 mL/min, λ = 215 nm, *t<sub>R</sub>* [*anti*] = 9.19 min, *t<sub>R</sub>* [*anti*] = 10.44 min, *t<sub>R</sub>* [*syn*] = 12.43 min, *t<sub>R</sub>* [*syn*] = 13.75 min.

Methyl (2*R*,3*R*)-3-(furan-2-yl)-3-hydroxy-2-methoxypropanoate (**25m**)



Pale yellow oil, 169 mg, 98% yield, *syn* : *anti* = 99 : 1, *ee<sub>syn</sub>* >99%;

**<sup>1</sup>H NMR** (400 MHz, CDCl<sub>3</sub>) δ 7.39 (t, *J* = 1.3 Hz, 1H), 6.35 (d, *J* = 1.4 Hz, 2H), 4.97 (dd, *J* = 7.2, 4.9 Hz, 1H), 4.13 (d, *J* = 4.9 Hz, 1H), 3.74 (s, 3H), 3.47 (s, 3H), 2.90 (d, *J* = 7.2 Hz, 1H).

**<sup>13</sup>C NMR** (101 MHz, CDCl<sub>3</sub>) δ 170.6, 152.4, 142.5, 110.5, 107.9, 82.4, 69.0, 59.2, 52.4.

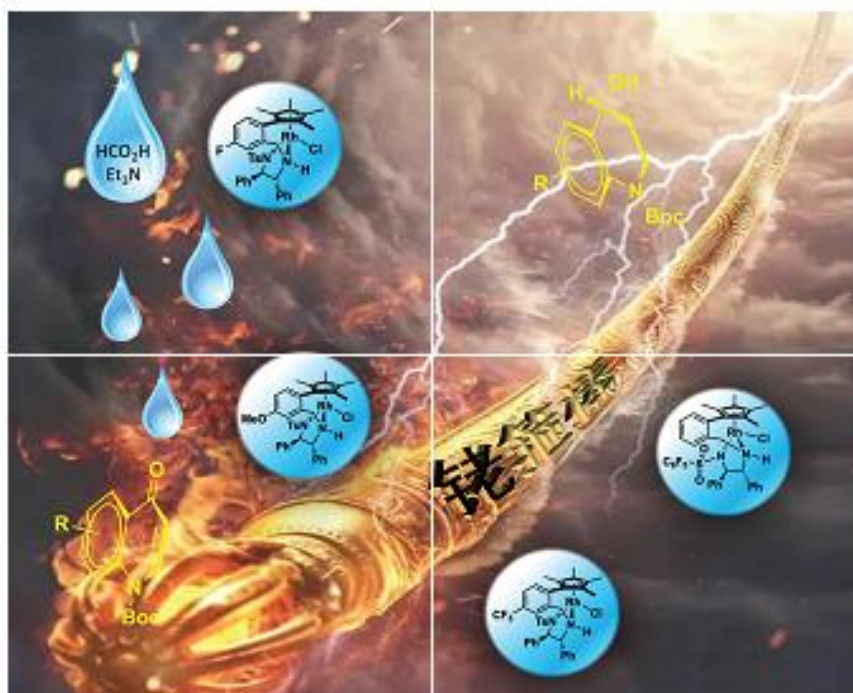
**MS** (ESI): *m/z* = 218 [M + NH<sub>4</sub>]<sup>+</sup>

**HPLC** : Chiralpak IC, Hexane : EtOH = 90 : 10, 1.0 mL/min, λ = 215 nm, *t<sub>R</sub>* [*anti*] = 16.46 min, *t<sub>R</sub>* [*anti*] = 24.59 min, *t<sub>R</sub>* [*syn*] = 19.70 min, *t<sub>R</sub>* [*syn*] = 22.54 min.

# **PUBLICATIONS**



Volume 7 | Number 8 | 21 April 2020



# ORGANIC CHEMISTRY

## FRONTIERS



CHINESE  
CHEMICAL  
SOCIETY



ROYAL SOCIETY  
OF CHEMISTRY

[rsc.li/frontiers-organic](https://rsc.li/frontiers-organic)

## RESEARCH ARTICLE



## Rhodium-catalyzed asymmetric transfer hydrogenation of 4-quinolone derivatives†

Cite this: *Org. Chem. Front.*, 2020, **7**, 975Received 20th December 2019,  
Accepted 24th January 2020

DOI: 10.1039/c9qo01514k

rsc.li/frontiers-organic

Bin He, Phannarath Phansavath<sup>ID</sup>\* and Virginie Ratovelomanana-Vidal<sup>ID</sup>\*

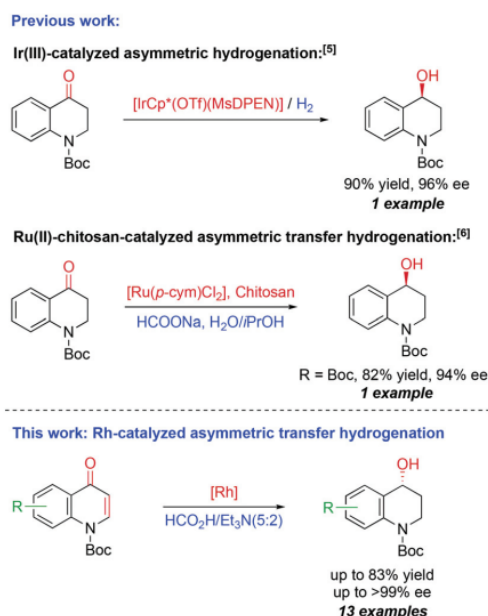
4-Quinolone derivatives were conveniently reduced to the corresponding 1,2,3,4-tetrahydroquinoline-4-ols with excellent enantioselectivities through asymmetric transfer hydrogenation using a tethered rhodium complex and formic acid/triethylamine as the hydride source.

Chiral benzylic alcohols and their derivatives are important building blocks for the synthesis of chemical materials, pharmaceuticals, and agrochemicals, as the hydroxyl group can be easily functionalized, giving access to versatile intermediates. Consequently, significant efforts have been displayed to develop efficient and atom-economical stereoselective processes to obtain such compounds.<sup>1</sup> Among these, enantiopure tetrahydroquinoline-4-ols are attractive targets due to their promising biological activities and wide-ranging use as synthetic intermediates for drug candidates.<sup>2</sup> Accordingly, quests for efficient routes to access these scaffolds are still underway. Although various methods allow the synthesis of enantiomerically enriched tetrahydroquinoline-4-ols, this motif can be conveniently prepared from the corresponding ketone through (*S*)-methyl-CBS-catalyzed reduction,<sup>2</sup> enzymatic reduction<sup>3</sup> or asymmetric (transfer) hydrogenation.<sup>4</sup> For the latter approach, only scarce examples have been reported (Scheme 1). Ohkuma *et al.* described the asymmetric hydrogenation of *tert*-butyl 4-oxo-3,4-dihydroquinoline-1(2*H*)-carboxylate in 90% yield and 96% ee using [IrCp\*(OTf)(MsDPEN)] complex at 60 °C under 15 atm of hydrogen.<sup>5</sup> Szöllösi *et al.* disclosed a single example of ruthenium(II)-catalyzed asymmetric transfer hydrogenation of the same substrate using the chitosan biopolymer as a ligand and sodium formate as the hydrogen source. The reaction proceeded in 82% yield with 94% ee in 168 h.<sup>6</sup> However, as far as asymmetric transfer hydrogenation (ATH) of *tert*-butyl 4-oxoquinoline-1(4*H*)-carboxylate is concerned, no example has been reported to the best of our knowledge.

As part of our ongoing studies directed toward the development of efficient methods for the asymmetric reduction of functionalized ketones,<sup>7</sup> we report herein the first rhodium-catalyzed asymmetric transfer hydrogenation of 4-quinolone

derivatives which provided the corresponding alcohols with excellent levels of enantioselectivity.

Our investigation of the ATH of 4-quinolone derivatives began with *tert*-butyl 4-oxoquinoline-1(4*H*)-carboxylate **1a** as the standard substrate for the optimization of the reaction parameters (Table 1). The reduction was carried out at 30 °C in dichloromethane, using 1.0 mol% of Rh(III) or Ru(II) complexes in the presence of HCO<sub>2</sub>H/Et<sub>3</sub>N (5 : 2) azeotropic mixture as the hydrogen source. Under these conditions, the expected alcohol **2a** was obtained in 41–83% yield with an excellent level of enantioselectivity (>99% ee) with the rhodium complexes **3a–3d**<sup>8</sup> (Table 1, entries 1–4). Full conversions were

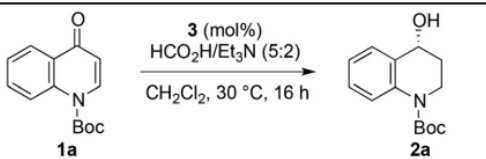


**Scheme 1** Asymmetric reduction of *tert*-butyl 4-oxo-3,4-dihydroquinoline-1(2*H*)-carboxylate and *tert*-butyl 4-oxoquinoline-1(4*H*)-carboxylate derivatives.

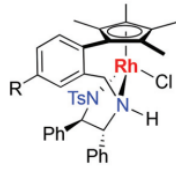
PSL University, Chimie ParisTech, CNRS, Institute of Chemistry for Life and Health Sciences, CSB2D team, 75005 Paris, France. E-mail: virginie.vidal@chimieparitech.psl.eu

† Electronic supplementary information (ESI) available: Experimental details, compound characterization, NMR and SFC spectra. CCDC 1973001. For ESI and crystallographic data in CIF or other electronic format see DOI: 10.1039/c9qo01514k

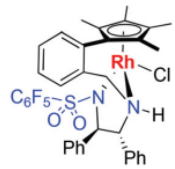


Table 1 Screening of precatalysts for the ATH of **1a**<sup>a</sup>


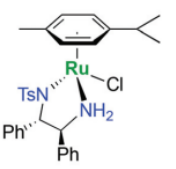
**1a**  $\xrightarrow[CH_2Cl_2, 30\text{ }^\circ C, 16\text{ h}]{\text{3 (1.0 mol\%)}, HCO_2H/Et_3N (5:2)}$  **2a**



**3a**: R = OMe



**3b**: R = Me

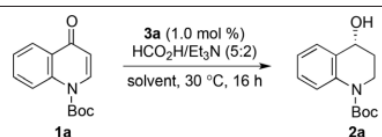


**3c**: R = F

Entry	Precatalyst (mol%)	Yield <sup>b</sup> (%)	ee <sup>c</sup> (%)
1	<b>3a</b> (1.0)	83	>99
2	<b>3b</b> (1.0)	76	>99
3	<b>3c</b> (1.0)	67	>99
4	<b>3d</b> (1.0)	41	>99
5	<b>3e</b> (1.0)	–	–
6	<b>3a</b> (0.5)	55	>99

<sup>a</sup> Reaction conditions: **1a** (0.5 mmol), complex **3**, HCO<sub>2</sub>H/Et<sub>3</sub>N (5 : 2) (170 μL, 4 equiv.), CH<sub>2</sub>Cl<sub>2</sub> (0.5 mL), 30 °C. <sup>b</sup> Isolated yields. <sup>c</sup> Determined by SFC analysis using a chiral stationary phase.

observed in all cases with these complexes and the lower yields of **2a** obtained with **3b–3d** compared to **3a** are related to partial *in situ* cleavage of the Boc group. On the other hand, the ruthenium-catalyzed reaction with **3e**<sup>9</sup> led to no conversion (Table 1, entry 5). Of the above-mentioned complexes, **3a** provided the best results (83% yield, >99% ee, Table 1, entry 1), but lowering the catalyst loading to 0.5 mol% resulted in a decrease of the yield (55%, Table 1, entry 6). Pursuing the study with the tethered rhodium complex **3a** (Table 2), we found that the ATH of **1a** was best achieved in CH<sub>2</sub>Cl<sub>2</sub>, as all the other explored solvents (Me-THF, THF, toluene, Et<sub>2</sub>O, DMF, CH<sub>3</sub>CN, DMC, TBME) gave lower yields even though the enantioselectivity was maintained (Table 2, entries 1–9). We then studied the effect of the amount of the HCO<sub>2</sub>H/Et<sub>3</sub>N (5 : 2) azeotropic mixture on the reaction. The use of 4.0 equiv. of HCO<sub>2</sub>H/Et<sub>3</sub>N (5 : 2) was the best option, since when lower or higher loadings were used, decreased yields were observed (Table 2, entries 10–14). Other hydrogen sources were evaluated as well but failed to afford better results or even the expected reduced product at all (Table 2, entries 15–19). Indeed, the use of a HCO<sub>2</sub>H/Et<sub>3</sub>N (1 : 1) azeotropic mixture instead of the (5 : 2) mixture furnished the corresponding alcohol in only 51% yield (Table 2, entry 15) whereas with *i*PrOH/KOH no reduction occurred (Table 2, entry 16). Sodium formate failed to afford any conversion in CH<sub>2</sub>Cl<sub>2</sub> (Table 2, entry 17) but a 40% yield of **2a** was obtained in water using 20 mol% of CTAB as a surfactant (Table 2, entry 18). Finally,

Table 2 Optimization of the reaction conditions for the ATH of **1a** with complex **3a**<sup>a</sup>


**1a**  $\xrightarrow[\text{solvent}, 30\text{ }^\circ C, 16\text{ h}]{\text{3a (1.0 mol\%)}, HCO_2H/Et_3N (5:2)}$  **2a**

Entry	Hydride source (equiv.)	Solvent	Yield <sup>b</sup> (%)	ee <sup>c</sup> (%)
1	HCO <sub>2</sub> H/Et <sub>3</sub> N (5 : 2) (4.0)	CH <sub>2</sub> Cl <sub>2</sub>	83	>99
2	HCO <sub>2</sub> H/Et <sub>3</sub> N (5 : 2) (4.0)	Me-THF	36	>99
3	HCO <sub>2</sub> H/Et <sub>3</sub> N (5 : 2) (4.0)	THF	59	>99
4	HCO <sub>2</sub> H/Et <sub>3</sub> N (5 : 2) (4.0)	Toluene	67	>99
5	HCO <sub>2</sub> H/Et <sub>3</sub> N (5 : 2) (4.0)	Et <sub>2</sub> O	63	>99
6	HCO <sub>2</sub> H/Et <sub>3</sub> N (5 : 2) (4.0)	DMF	22	>99
7	HCO <sub>2</sub> H/Et <sub>3</sub> N (5 : 2) (4.0)	CH <sub>3</sub> CN	64	>99
8	HCO <sub>2</sub> H/Et <sub>3</sub> N (5 : 2) (4.0)	DMC	63	>99
9	HCO <sub>2</sub> H/Et <sub>3</sub> N (5 : 2) (4.0)	TBME	69	>99
10	HCO <sub>2</sub> H/Et <sub>3</sub> N (5 : 2) (2.0)	CH <sub>2</sub> Cl <sub>2</sub>	31	>99
11	HCO <sub>2</sub> H/Et <sub>3</sub> N (5 : 2) (3.0)	CH <sub>2</sub> Cl <sub>2</sub>	70	>99
12	HCO <sub>2</sub> H/Et <sub>3</sub> N (5 : 2) (5.0)	CH <sub>2</sub> Cl <sub>2</sub>	76	>99
13	HCO <sub>2</sub> H/Et <sub>3</sub> N (5 : 2) (6.0)	CH <sub>2</sub> Cl <sub>2</sub>	64	>99
14	HCO <sub>2</sub> H/Et <sub>3</sub> N (5 : 2) (8.0)	CH <sub>2</sub> Cl <sub>2</sub>	66	>99
15	HCO <sub>2</sub> H/Et <sub>3</sub> N (1 : 1) (4.0)	CH <sub>2</sub> Cl <sub>2</sub>	51	99
16	<i>i</i> PrOH/KOH (4.0)	<i>i</i> PrOH	–	–
17	HCO <sub>2</sub> Na (4.0)	CH <sub>2</sub> Cl <sub>2</sub>	–	–
18	HCO <sub>2</sub> Na (4.0)	H <sub>2</sub> O/CTAB (20%)	40	99
19	HCO <sub>2</sub> NH <sub>4</sub> (4.0)	H <sub>2</sub> O/CTAB (20%)	–	–

<sup>a</sup> Reaction conditions: **1a** (0.5 mmol), **3a** (1.0 mol%), hydride source, solvent (0.5 mL), 30 °C. <sup>b</sup> Isolated yields. <sup>c</sup> Determined by SFC analysis using a chiral stationary phase.

under the same conditions, no conversion was observed in the presence of ammonium formate (Table 2, entry 19). It should be noted that under 10 bar of hydrogen pressure and in the presence of silver triflate in MeOH at 30 °C, full conversion was achieved after 24 h and the reaction led mainly to reduction of the C=C bond only (with 5% of the product resulting from reduction of both C=C and C=O bonds). On the basis of the above screening, the optimized conditions were set as follows: **3a** (1.0 mol%) as the precatalyst, HCO<sub>2</sub>H/Et<sub>3</sub>N (5 : 2) (4.0 equiv.), CH<sub>2</sub>Cl<sub>2</sub> (1.0 M) at 30 °C. With these optimized reaction conditions, the scope of the asymmetric transfer hydrogenation of a series of variously substituted 4-quinolone derivatives was evaluated (Table 3). Notably, compounds **1a–1m** having electron donating or withdrawing groups on the aromatic ring remained reactive under these conditions leading to a uniformly excellent level of enantioselectivity with mainly good yields. The reaction was tolerant of methyl or methoxy electron-donating substituents on the aryl core (Table 3, entries 3–5), but only 23% of the product was isolated when two methoxy groups were present (Table 3, entry 6). As for electron-withdrawing groups, the ATH was amenable under the standard conditions to halogen substitution such as iodine, bromine, chlorine and fluorine, as well as a trifluoromethyl substituent (Table 3, entries 7–14). Other protections of the nitrogen atom such as Bn, Me and Ms groups were tested and gave either lower conversions and enantioselectivities or no reaction.

Table 3 Substrate scope of the ATH of 4-quinolone derivatives<sup>a</sup>

Entry	ATH product 2	Yield <sup>b</sup> (%)	ee <sup>c</sup> (%)
1	( <i>R</i> )-2a	83	>99
2 <sup>d</sup>	( <i>S</i> )-2b	84	>99
3	( <i>R</i> )-2b	79	>99
4	( <i>R</i> )-2c	75	>99
5	( <i>R</i> )-2d	50	99
6	( <i>R</i> )-2e	23	97
7	( <i>R</i> )-2f	64	>99
8	( <i>R</i> )-2g	73	99
9	( <i>R</i> )-2h	67	99
10	( <i>R</i> )-2i	67	>99
11	( <i>R</i> )-2j	66	>99

Table 3 (Contd.)

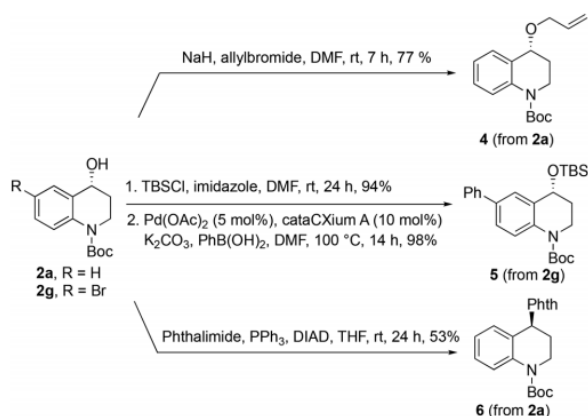
Entry	ATH product 2	Yield <sup>b</sup> (%)	ee <sup>c</sup> (%)
12	( <i>R</i> )-2k	73	>99
13	( <i>R</i> )-2l	66	>99
14	( <i>R</i> )-2m	67	>99

X-ray structure of **2f**

<sup>a</sup> Reaction conditions: **1a** (0.5 mmol), (*R,R*)-**3a** (1.0 mol%), HCO<sub>2</sub>H/Et<sub>3</sub>N (5:2) (170 μL, 4 equiv.), CH<sub>2</sub>Cl<sub>2</sub> (0.5 mL), 30 °C, 16 h. <sup>b</sup> Isolated yields. <sup>c</sup> Determined by SFC analysis using a chiral stationary phase. <sup>d</sup> Reaction carried out with (*S,S*)-**3a**.

The absolute configuration of alcohol **2f** was unambiguously assigned as (*R*) by X-ray crystallographic analysis, and by analogy, we conjectured that the remainder of the ATH products followed the same trend. Of note, the reduction of **1a** could be conducted on a gram-scale with no detrimental effect on the enantioselectivity and the product **2a** was obtained with a comparable yield (81% yield, >99% ee), supporting the efficiency of the Rh-mediated ATH reaction. In addition, (*S*)-alcohols **2** could be prepared as well by using the (*S,S*)-enantiomer of complex **3a** instead of the (*R,R*)-isomer and the asymmetric reduction of **1a** with (*S,S*)-**3a** delivered (*S*)-**2a** with comparable yield and ee as expected (Table 3, entry 2, 84% yield, 99% ee). Moreover, the reduced compounds **2** can serve as useful intermediates for further elaboration on either the aromatic ring or the heterocyclic counterpart (Scheme 2). Thus, *O*-allylation of **2a** readily furnished compound **4**, which is prone to further functionalization such as *e.g.* a cross-metathesis reaction.

A Pd-catalyzed cross-coupling reaction was performed on **2g**, which after *O*-silylation was subjected to a Suzuki–Miyaura reaction with Pd(OAc)<sub>2</sub>, cataCXium A as a ligand, K<sub>2</sub>CO<sub>3</sub> as a base and phenylboronic acid to deliver the corresponding product **5** in 98% yield. Finally, a Mitsunobu reaction of **2a**



Scheme 2 Post-functionalization reactions.

afforded the introduction of a phthalimide substituent on the N-heterocycle.

## Conclusions

In summary, we have demonstrated the ability of the in-house developed Rh(III)-complex **3a** to efficiently perform the operationally simple and practical asymmetric transfer hydrogenation of 4-quinolone derivatives. This reaction enables a straightforward access to the corresponding enantiomerically enriched alcohols with excellent levels of enantioselectivity (up to >99% ee). The reaction proceeds under mild conditions using HCO<sub>2</sub>H/Et<sub>3</sub>N (5 : 2) as the hydrogen source. The efficient gram-scale asymmetric transfer hydrogenation of compound **1a** accounts for the usefulness of this method and furthermore, the various chiral alcohols **2** can be readily functionalized to access diversely substituted 1,2,3,4-tetrahydroquinoline-4-ols derivatives.

## Experimental

Typical procedure for the asymmetric transfer hydrogenation of **1a**: in a round-bottom tube charged with complex (*R,R*)-**3a** (5.0 μmol, 0.01 equiv.) was added under argon a solution of the ketone **1a** (0.50 mmol, 1.0 equiv.) in anhydrous CH<sub>2</sub>Cl<sub>2</sub> (0.5 mL), then HCO<sub>2</sub>H/NEt<sub>3</sub> (5 : 2) azeotropic mixture (170 μL, 2.0 mmol, 4.0 equiv.) was added dropwise. The mixture was stirred under argon at 30 °C for 16 h, then quenched with water (5.0 mL) and extracted with CH<sub>2</sub>Cl<sub>2</sub> (3 × 15 mL). The combined organic phases were washed with brine, dried with MgSO<sub>4</sub>, filtered and concentrated under vacuum. Purification of the residue by flash column chromatography (petroleum ether/ethyl acetate 2 : 1) afforded compound **2a** and the enantiomeric excess was determined by SFC analysis (Chiralpak AS-H).

## Conflicts of interest

There are no conflicts to declare.

## Acknowledgements

This work was supported by the Ministère de l'Éducation Nationale, de l'Enseignement Supérieur et de la Recherche (MENESR) and the Centre National de la Recherche Scientifique (CNRS). We gratefully acknowledge the China Scholarship Council (CSC) for a grant to B. H. We thank J. Forté for the X-ray analysis (Sorbonne Université, Paris).

## Notes and references

- (a) A. Bartoszewicz, N. Ahlsten and B. Martín-Matute, Enantioselective Synthesis of Alcohols and Amines by Iridium-Catalyzed Hydrogenation, Transfer Hydrogenation, and Related Processes, *Chem. – Eur. J.*, 2013, **19**, 7274; (b) Y. Ahn, S.-B. Ko, M.-J. Kim and J. Park, Racemization catalysts for the dynamic kinetic resolution of alcohols and amines, *Coord. Chem. Rev.*, 2008, **252**, 647.
- H. I. Mosberg, L. Yeomans, A. A. Harland, A. M. Bender, K. Sobczyk-Kojiro, J. P. Anand, M. J. Clark, E. M. Jutkiewicz and J. R. Traynor, Opioid Peptidomimetics: Leads for the Design of Bioavailable Mixed Efficacy  $\mu$  Opioid Receptor (MOR) Agonist/ $\delta$  Opioid Receptor (DOR) Antagonist Ligands, *J. Med. Chem.*, 2013, **56**, 2139.
- A. S. Rowan, T. S. Moody, R. M. Howard, T. J. Underwood, I. R. Miskelly, Y. He and B. Wang, Preparative access to medicinal chemistry related chiral alcohols using carbonyl reductase technology, *Tetrahedron: Asymmetry*, 2013, **24**, 1369.
- For selected reviews on asymmetric (transfer) hydrogenation of ketones, see: (a) R. Noyori and S. Hashiguchi, Asymmetric Transfer Hydrogenation Catalyzed by Chiral Ruthenium Complexes, *Acc. Chem. Res.*, 1997, **30**, 97; (b) M. J. Palmer and M. Wills, Asymmetric transfer hydrogenation of C=O and C=N bonds, *Tetrahedron: Asymmetry*, 1999, **10**, 2045; (c) K. Everaere, A. Mortreux and J.-F. Carpentier, Ruthenium (II)-Catalyzed Asymmetric Transfer Hydrogenation of Carbonyl Compounds with 2-Propanol and Ephedrine-Type Ligands, *Adv. Synth. Catal.*, 2003, **345**, 67; (d) S. Gladiali and E. Alberico, Asymmetric transfer hydrogenation: chiral ligands and applications, *Chem. Soc. Rev.*, 2006, **35**, 226; (e) J. S. M. Samec, J.-E. Bäckvall, P. G. Andersson and P. Brandt, Mechanistic aspects of transition metal-catalyzed hydrogen transfer reactions, *Chem. Soc. Rev.*, 2006, **35**, 237; (f) T. Ikariya and A. J. Blacker, Asymmetric Transfer Hydrogenation of Ketones with Bifunctional Transition Metal-Based Molecular Catalysts, *Acc. Chem. Res.*, 2007, **40**, 1300; (g) A. J. Blacker, Enantioselective Transfer Hydrogenation, in *Handbook of Homogeneous Hydrogenation*, ed. J. G. de Vries and C. J. Elsevier, Wiley-VCH, Weinheim, 2007, pp. 1215–1244; (h) F. Foubelo, C. Nájera and M. Yus, Catalytic asymmetric transfer hydrogenation of ketones: recent advances, *Tetrahedron: Asymmetry*, 2015, **26**, 769; (i) D. Wang and D. Astruc, The Golden Age of Transfer Hydrogenation, *Chem. Rev.*, 2015, **115**, 6621;



- (j) P.-G. Echeverria, T. Ayad, P. Phansavath and V. Ratovelomanana-Vidal, Recent Developments in Asymmetric Hydrogenation and Transfer Hydrogenation of Ketones and Imines through Dynamic Kinetic Resolution, *Synthesis*, 2016, **48**, 2523.
- 5 N. Utsumi, K. Tsutsumi, M. Watanabe, K. Murata, N. Arai, N. Kurono and T. Ohkuma, Asymmetric Hydrogenation of Aromatic Heterocyclic Ketones Catalyzed by The MsDPEN-Cp\*Ir(III) Complex, *Heterocycles*, 2010, **80**, 141.
- 6 V. J. Kolcsár, F. Fülöp and G. Szöllösi, Ruthenium(II)-Chitosan, an Enantioselective Catalyst for the Transfer Hydrogenation of *N*-Heterocyclic Ketones, *ChemCatChem*, 2019, **11**, 2725.
- 7 (a) L.-S. Zheng, C. Féraud, P. Phansavath and V. Ratovelomanana-Vidal, Rhodium-mediated asymmetric transfer hydrogenation: a diastereo- and enantioselective synthesis of *syn*- $\alpha$ -amido  $\beta$ -hydroxy esters, *Chem. Commun.*, 2018, **54**, 283; (b) L.-S. Zheng, P. Phansavath and V. Ratovelomanana-Vidal, Ruthenium-catalyzed dynamic kinetic asymmetric transfer hydrogenation: stereoselective access to *syn* 2-(1,2,3,4-tetrahydro-1-isoquinolyl)ethanol derivatives, *Org. Chem. Front.*, 2018, **5**, 1366; (c) L.-S. Zheng, P. Phansavath and V. Ratovelomanana-Vidal, Synthesis of Enantioenriched  $\alpha,\alpha$ -Dichloro- and  $\alpha,\alpha$ -Difluoro- $\beta$ -Hydroxy Esters and Amides by Ruthenium-Catalyzed Asymmetric Transfer Hydrogenation, *Org. Lett.*, 2018, **20**, 5107; (d) B. He, P. Phansavath and V. Ratovelomanana-Vidal, Rh-Mediated Asymmetric-Transfer Hydrogenation of 3-Substituted Chromones: A Route to Enantioenriched *cis*-3-(Hydroxymethyl)chroman-4-ol Derivatives through Dynamic Kinetic Resolution, *Org. Lett.*, 2019, **21**, 3276.
- 8 (a) P.-G. Echeverria, C. Féraud, P. Phansavath and V. Ratovelomanana-Vidal, Synthesis, characterization and use of a new tethered Rh(III) complex in asymmetric transfer hydrogenation of ketones, *Catal. Commun.*, 2015, **62**, 95; (b) L.-S. Zheng, Q. Llopis, P.-G. Echeverria, C. Féraud, G. Guillamot, P. Phansavath and V. Ratovelomanana-Vidal, Asymmetric Transfer Hydrogenation of (Hetero)arylketones with Tethered Rh(III)-*N*-(*p*-Tolylsulfonyl)-1,2-diphenylethylene-1,2-diamine Complexes: Scope and Limitations, *J. Org. Chem.*, 2017, **82**, 5607; (c) B. He, L.-S. Zheng, P. Phansavath and V. Ratovelomanana-Vidal, Rh<sup>III</sup>-Catalyzed Asymmetric Transfer Hydrogenation of  $\alpha$ -Methoxy  $\beta$ -Ketoesters through DKR in Water: Toward a Greener Procedure, *ChemSusChem*, 2019, **12**, 3032.
- 9 (a) K.-J. Haack, S. Hashiguchi, A. Fujii, T. Ikariya and R. Noyori, The Catalyst Precursor, Catalyst, and Intermediate in the Ru<sup>II</sup>-Promoted Asymmetric Hydrogen Transfer between Alcohols and Ketones, *Angew. Chem., Int. Ed. Engl.*, 1997, **36**, 285; (b) K. Matsumura, S. Hashiguchi, T. Ikariya and R. Noyori, Asymmetric Transfer Hydrogenation of  $\alpha,\beta$ -Acetylenic Ketones, *J. Am. Chem. Soc.*, 1997, **119**, 8738.

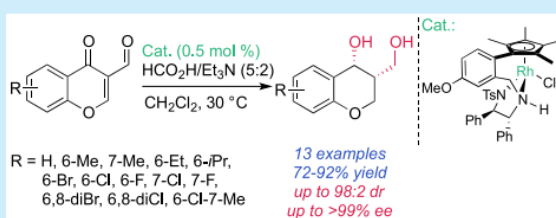
# Rh-Mediated Asymmetric-Transfer Hydrogenation of 3-Substituted Chromones: A Route to Enantioenriched *cis*-3-(Hydroxymethyl)chroman-4-ol Derivatives through Dynamic Kinetic Resolution

Bin He, Phannarath Phansavath,\* and Virginie Ratovelomanana-Vidal\*<sup>†</sup>

PSL University, Chimie ParisTech, CNRS, Institute of Chemistry for Life and Health Sciences, CSB2D Team, 75005 Paris, France

**S** Supporting Information

**ABSTRACT:** Enantioenriched *cis*-3-(hydroxymethyl)-chroman-4-ol derivatives were conveniently prepared by rhodium-catalyzed asymmetric transfer hydrogenation of 3-formylchromones through a dynamic kinetic resolution process. The reaction proceeded under mild conditions using a low catalyst loading and HCO<sub>2</sub>H/Et<sub>3</sub>N (5:2) as the hydrogen source, delivering the reduced compounds in good yields, high diastereomeric ratio (up to 98:2 dr), and excellent enantioselectivities (up to >99% ee).



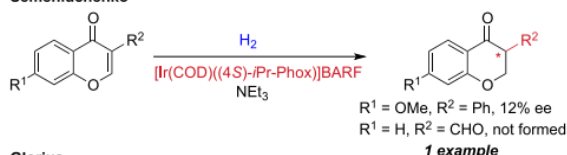
Chromanoids and their derivatives found in a number of natural products are relevant targets and serve as key structural motifs thanks to their pharmacological and biological activities including antitumoral, antibacterial, antioxidant, or antiestrogenic properties.<sup>1</sup> As such, identification of economical routes to access such compounds is highly desirable. In this context, a straightforward synthesis to enantiomerically enriched 3-substituted chromanols relies on the asymmetric reduction of 3-substituted chroman-4-one derivatives. However, to the best of our knowledge, only two examples of such transformations were reported (Scheme 1). Semeniuchenko et al. described the hydrogenation of electron-deficient alkenes by using iridium complexes and a base as co-catalyst.<sup>2</sup> Whereas 7-methoxyisoflavone was reduced with [Ir(COD)((4*S*)-*i*Pr-Phox)]BARF and a large excess of NEt<sub>3</sub> to the enantioenriched isoflavanol derivative (12% ee) in good yield, the reaction failed to afford the expected product in the case of 3-formylchromone. On the other hand, Glorius et al. investigated the ruthenium–NHC-catalyzed hydrogenation of flavones and chromones to stereoselectively access flavanones, flavanols, chromanones, and chromanols.<sup>3</sup> Whereas the asymmetric hydrogenation proceeded with moderate to good diastereoselectivities and high enantioselectivities for 2-substituted alkenes and chromones (up to 67% de, up to 98% ee), a drop in enantioselectivity was observed with the 3-substituted regioisomer (79% de, 62% ee).

As far as asymmetric transfer hydrogenation (ATH)<sup>4,5</sup> of 3-substituted chromone derivatives is concerned, no example has been reported to date. As part of our ongoing studies directed toward the development of efficient methods for the asymmetric reduction of functionalized ketones,<sup>6</sup> we report herein the first rhodium-catalyzed asymmetric transfer hydrogenation of 3-formylchromone derivatives that provides in a single operation the corresponding 3-(hydroxymethyl)chromanols in good

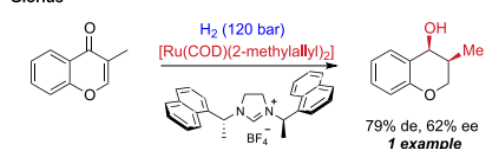
## Scheme 1. Asymmetric Reduction of 3-Substituted Chromones

Previous work: asymmetric hydrogenation

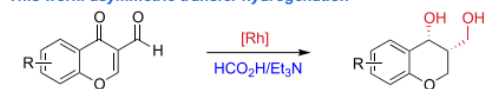
Semeniuchenko



Glorius



This work: asymmetric transfer hydrogenation



yields and with excellent levels of diastereo- and enantioselectivity through a dynamic kinetic resolution (DKR)<sup>7</sup> process.

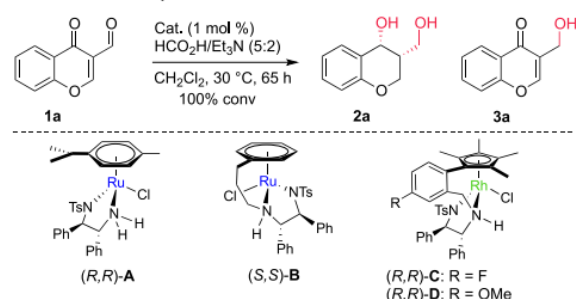
We first investigated the asymmetric transfer hydrogenation of 3-formylchromone **1a** to optimize the reaction conditions. When Noyori's ruthenium catalyst (*R,R*)-**A**<sup>8</sup> (1 mol %) was used in the presence of 5 equiv of a HCO<sub>2</sub>H/Et<sub>3</sub>N (5:2) azeotropic mixture as the hydrogen source, in CH<sub>2</sub>Cl<sub>2</sub> at 30 °C, no traces of diol **2a** could be detected after 65 h of reaction, and alcohol **3a**

Received: March 21, 2019

Published: April 15, 2019

was exclusively isolated in 40% yield (Table 1, entry 1). Under otherwise identical conditions, the tethered ruthenium complex

**Table 1. Screening of Catalysts and Solvent Effect for the ATH of 3-Formylchromone 1a<sup>a</sup>**



entry	cat.	solvent	yield of 2a <sup>b</sup> (%)	dr <sup>c</sup>	ee <sup>d</sup> (%)
1	( <i>R,R</i> )-A	CH <sub>2</sub> Cl <sub>2</sub>	<sup>e</sup>		
2	( <i>S,S</i> )-B	CH <sub>2</sub> Cl <sub>2</sub>	44	67:33	-95
3	( <i>R,R</i> )-C	CH <sub>2</sub> Cl <sub>2</sub>	28	96:4	99
4	( <i>R,R</i> )-D	CH <sub>2</sub> Cl <sub>2</sub>	62	97:3	99
5	( <i>R,R</i> )-D	CH <sub>3</sub> CN	56	98:2	98
6	( <i>R,R</i> )-D	dioxane	42	96:4	97
7	( <i>R,R</i> )-D	2-MeTHF	37	95:5	97
8	( <i>R,R</i> )-D	toluene	28	94:6	97
9	( <i>R,R</i> )-D	Et <sub>2</sub> O	38	91:9	99
10	( <i>R,R</i> )-D	DMF	52	97:3	98

<sup>a</sup>Conditions: 1a (0.5 mmol), cat. (1 mol %), CH<sub>2</sub>Cl<sub>2</sub> (1.5 mL), HCO<sub>2</sub>H/Et<sub>3</sub>N (5:2) (212 μL), 30 °C. The reaction was monitored by TLC or <sup>1</sup>H NMR. <sup>b</sup>Isolated yield of 2a. With the exception of entry 2, compound 3a was formed in all cases. <sup>c</sup>Determined by <sup>1</sup>H NMR of the crude after the ATH. <sup>d</sup>Determined by SFC analysis. <sup>e</sup>Compound 3a was exclusively isolated in 40% yield.

(*S,S*)-B<sup>9</sup> furnished the corresponding reduced compound 2a with a moderate 44% yield, a diastereomeric ratio of 67:33 in favor of the *cis* compound, and an enantioselectivity of 95% ee (Table 1, entry 2).

Compound 2a was produced with a lower yield by using the tethered rhodium complex (*R,R*)-C,<sup>10</sup> although in this case a high dr was observed with an excellent ee (28% yield, 96:4 dr, 99% ee, Table 1, entry 3). The reaction with the parent Rh complex (*R,R*)-D<sup>10,11</sup> resulted in a satisfying 62% yield with both high diastereo- and enantioselectivities (97:3 dr, 99% ee, Table 1, entry 4). With these encouraging results in hand, and using complex (*R,R*)-D, we then screened a variety of solvents, such as CH<sub>3</sub>CN, dioxane, 2-MeTHF, toluene, Et<sub>2</sub>O, and DMF (Table 1, entries 5–10). Although a slightly better dr value was attained in CH<sub>3</sub>CN, the yield was lower than in CH<sub>2</sub>Cl<sub>2</sub>, and none of the tested solvents outperformed the latter. Consequently, CH<sub>2</sub>Cl<sub>2</sub> was selected as the solvent of choice for the ATH/DKR of 1a. We pursued the optimization of the reaction conditions by varying the catalyst loading, the concentration, and the amount and nature of the hydrogen source (Table 2).

Identical results in terms of yield and stereoselectivity were obtained for the ATH/DKR of 1a with S/C 100 and S/C 200 (Table 2, entries 1 and 2), but lowering to S/C 1000 and S/C 10000 had a detrimental effect on the yield of 2a with no formation of the expected diol in the latter case (Table 2, entries 3 and 4). Maintaining the catalyst loading to S/C 200, we next studied the influence of the amount of the HCO<sub>2</sub>H/Et<sub>3</sub>N (5:2) mixture. From the various tested conditions, the best yield was

**Table 2. Optimization of the Reaction Parameters<sup>a</sup>**

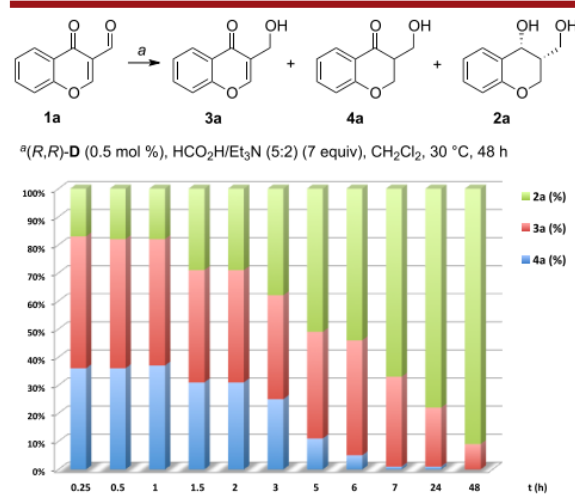
entry	S/C	conc (M)	FA/TEA (5:2) (equiv)	yield <sup>b</sup> (%)	dr <sup>c</sup>	ee <sup>d</sup> (%)
1	100	0.33	5	62	97:3	99
2	200	0.33	5	62	97:3	99
3	1000	0.33	5	47	99:1	99
4	10000	0.33	5			
5	200	0.33	3	26	90:10	98
6	200	0.33	7	74	97:3	99
7	200	0.33	10	67	98:2	99
8	200	0.25	7	72	97:3	99
9	200	0.5	7	79	97:3	99
10	200	1.0	7	84	98:2	99
11	200	neat	7	73	98:2	99

<sup>a</sup>Conditions: The reaction was carried out on 1a (0.5 mmol) with (*R,R*)-D and HCO<sub>2</sub>H/Et<sub>3</sub>N (5:2) as the hydrogen source. <sup>b</sup>Isolated yield. <sup>c</sup>Determined by <sup>1</sup>H NMR of the crude after the ATH. <sup>d</sup>Determined by SFC analysis.

attained by using 7 equiv of the hydride donor (74%, Table 2, entry 6 vs entries 2, 5, and 7).

Other hydrogen-donor sources such as HCO<sub>2</sub>Na, HCO<sub>2</sub>NH<sub>4</sub>, (HCO<sub>2</sub>)<sub>2</sub>Ca, NaH<sub>2</sub>PO<sub>2</sub>·H<sub>2</sub>O, and KOH/*i*-PrOH were evaluated as well (not shown in Table 2). With these reagents, however, the reaction led to either no conversion or reduction only of the aldehyde functional group to afford alcohol 3a. Besides, switching the HCO<sub>2</sub>H/Et<sub>3</sub>N ratio from 5:2 to 1:1 resulted in the formation of compound 3a only (not shown in Table 2). The last reaction parameter we considered was the concentration and we found the optimum reaction concentration of 1.0 mol·L<sup>-1</sup> afforded a good 84% yield (Table 2, entry 10 vs 6, 8, and 9), whereas the neat reaction gave a less satisfying result (Table 2, entry 11). On the basis of the above screening, the optimized conditions were set as follows: (*R,R*)-D (0.5 mol %) as the precatalyst, HCO<sub>2</sub>H/Et<sub>3</sub>N (5:2) (7.0 equiv), CH<sub>2</sub>Cl<sub>2</sub> (1.0 M) at 30 °C.

To better understand the reaction process, a series of control experiments were conducted. We first performed monitoring studies of the Rh-catalyzed asymmetric transfer hydrogenation of 1a under the optimized conditions (Figure 1). After 0.25 h of



**Figure 1.** Monitoring studies of the ATH/DKR of 1a (proportions were determined by <sup>1</sup>H NMR).



Table 3. Substrate Scope of the ATH/DKR of 3-Formylchromone Derivatives<sup>a</sup>

entry/product	time (h)	yield (%) <sup>b</sup>	dr <sup>c</sup>	ee (%) <sup>d</sup>	entry/product	time (h)	yield (%) <sup>b</sup>	dr <sup>c</sup>	ee (%) <sup>d</sup>
1/2a	65	84	98:2	>99	8/2h	24	83	96:4	>99
2/2b	65	76	97:3	>99	9/2i	24	92	96:4	>99
3/2c	65	72	97:3	>99	10/2j	24	74	97:3	>99
4/2d	65	72	97:3	>99	11/2k	24	80	92:8	>99
5/2e	65	75	97:3	>99	12/2l	24	87	94:6	97
6/2f	24	85	96:4	>99	13/2m	65	88	98:2	>99
7/2g	24	87	96:4	>99					

<sup>a</sup>Conditions: **1a–m** (0.75 mmol), (*R,R*)-**D** (0.5 mol %), CH<sub>2</sub>Cl<sub>2</sub> (0.75 mL), HCO<sub>2</sub>H/Et<sub>3</sub>N (5:2) (446 μL), 30 °C. The reaction was monitored by TLC or <sup>1</sup>H NMR. <sup>b</sup>Isolated yield. <sup>c</sup>Determined by <sup>1</sup>H NMR of the crude after the ATH. <sup>d</sup>Determined by SFC analysis.

reaction, a complete consumption of the starting material was observed with formation of products **2a**, **3a**, and **4a**. It should be noted that the diol resulting from the reduction of the ketone functional group of intermediate **3a** was not detected in this study. It appears that reduction of the aldehyde moiety and of the C=C bond was fast, yielding compounds **3a** and **4a** with a cumulative proportion of 80% as a mixture with **2a** after 0.25 h of reaction. The amount of intermediate **4a** then rapidly decreased, with only traces detected after 7 h, and complete consumption was obtained after 48 h. It is worth noting that when the reaction was quenched after 0.25 h, intermediate **4a** was found to be present as a racemic mixture. To confirm that the ATH of **1a** proceeded through a dynamic kinetic resolution, an authentic sample of racemic **4a** was prepared (see the [Supporting Information](#)) and subjected to the optimized reaction conditions.

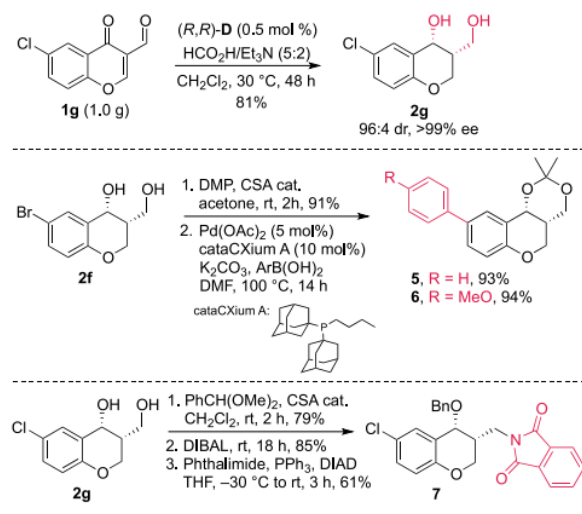
In this control experiment, the ATH of (±)-**4a** afforded the diol **2a** in 83% yield, with a high level of diastereo- and

enantioinduction (97:3 dr, > 99% ee), thus supporting a DKR process.

With these optimized conditions in hand, we explored the substrate scope of the reaction with a series of 3-formylchromones **1a–m** bearing various electron-donating or electron-withdrawing substituents on the phenyl ring (Table 3). All substrates afforded the suitable *cis*-diols in good yields with high dr values and excellent enantioselectivities (Table 3, entries 1–13). The absolute configurations of diols **2a** and **2g** were unambiguously assigned as (*R,R*) by X-ray crystallographic analysis. By analogy, we conjecture that the remainder of the ATH products **2** followed the same trend.

The efficiency of this ATH was supported by a scale-up experiment. Under the standard conditions, a gram-scale reduction of **1g** delivered the desired product **2g** in 81% yield with high dr and ee values (Scheme 2). In addition, the postfunctionalization of compounds **2f** and **2g** was performed. After acetonide protection of **2f**, biaryl derivatives **5** and **6** were readily prepared in high yields through Suzuki–Miyaura

## Scheme 2. Scale-up Experiment and Post-functionalization Reactions



coupling by using  $\text{Pd}(\text{OAc})_2$ , cataCXium A as a ligand,  $\text{K}_2\text{CO}_3$  as a base, and phenyl- or 4-methoxyphenylboronic acid, respectively. Finally, diol **2g** was readily converted into protected amino alcohol **7** in three steps via a Mitsunobu reaction.

In summary, the operationally simple rhodium-catalyzed asymmetric transfer hydrogenation of 3-formylchromones appears to be an efficient tool for the synthesis of *cis*-3-(hydroxymethyl)chromanol derivatives. This method confers several advantages compared to the scarce examples of asymmetric hydrogenation. The in-house developed Rh(III) complex enables the reduction under mild conditions using a low catalyst loading and  $\text{HCO}_2\text{H}/\text{Et}_3\text{N}$  (5:2) as the hydrogen source, delivering the reduced compounds in good yields and excellent diastereo- and enantioselectivities (up to 98:2 dr, up to >99% ee). Furthermore, the usefulness of this method was demonstrated by the efficient gram-scale asymmetric transfer hydrogenation of **1g**. Finally, the 3-(hydroxymethyl)chromanols produced in this study can serve as useful scaffolds for further functionalization to access diversely substituted chromanol derivatives.

## ■ ASSOCIATED CONTENT

### Supporting Information

The Supporting Information is available free of charge on the ACS Publications website at DOI: 10.1021/acs.orglett.9b01002.

Experimental procedures, compound characterization data, NMR spectra, and SCF data for all new compounds (PDF)

### Accession Codes

CCDC 1896174–1896175 contain the supplementary crystallographic data for this paper. These data can be obtained free of charge via [www.ccdc.cam.ac.uk/data\\_request/cif](http://www.ccdc.cam.ac.uk/data_request/cif), or by emailing [data\\_request@ccdc.cam.ac.uk](mailto:data_request@ccdc.cam.ac.uk), or by contacting The Cambridge Crystallographic Data Centre, 12 Union Road, Cambridge CB2 1EZ, UK; fax: +44 1223 336033.

## ■ AUTHOR INFORMATION

### Corresponding Authors

\*E-mail: [phannarath.phansavath@chimieparistech.psl.eu](mailto:phannarath.phansavath@chimieparistech.psl.eu)

\*E-mail: [virginie.vidal@chimieparistech.psl.eu](mailto:virginie.vidal@chimieparistech.psl.eu)

### ORCID

Virginie Ratovelomanana-Vidal: 0000-0003-1167-1195

### Notes

The authors declare no competing financial interest.

## ■ ACKNOWLEDGMENTS

This work was supported by the Ministère de l'Éducation Nationale, de l'Enseignement Supérieur et de la Recherche (MENESR), and the Centre National de la Recherche Scientifique (CNRS). We gratefully acknowledge the China Scholarship Council (CSC) for a grant to B.H. We thank G. Gontard for the X-ray analysis (Sorbonne Université, Paris).

## ■ REFERENCES

- (a) Ellis, G. P. *Chromenes, Chromanones, and Chromones*; Wiley: New York, 1977. (b) Horton, D. A.; Bourne, G. T.; Smythe, M. L. *Chem. Rev.* **2003**, *103*, 893. (c) Gaspar, A.; Matos, M. J.; Garrido, J.; Uriarte, E.; Borges, F. *Chem. Rev.* **2014**, *114*, 4960. (d) Chandler, I. M.; McIntyre, C. R.; Simpson, T. J. *J. Chem. Soc., Perkin Trans. 1* **1992**, 2285. (e) Maiti, A.; Cuendet, M.; Croy, V. L.; Endringer, D. C.; Pezzuto, J. M.; Cushman, M. J. *Med. Chem.* **2007**, *50*, 2799. (f) Zhao, Z.; Ruan, J.; Jin, J.; Zou, J.; Zhou, D.; Fang, W.; Zeng, F. *J. Nat. Prod.* **2006**, *69*, 265. (g) Albrecht, U.; Lalk, M.; Langer, P. *Bioorg. Med. Chem.* **2005**, *13*, 1531. (h) Farmer, R. L.; Biddle, M. M.; Nibbs, A. E.; Huang, X.; Bergan, R. C.; Scheidt, K. A. *ACS Med. Chem. Lett.* **2010**, *1*, 400.
- (2) Semeniuchenko, V.; Exner, T. E.; Khilya, V.; Groth, U. *Appl. Organomet. Chem.* **2011**, *25*, 804.
- (3) Zhao, D.; Beiring, B.; Glorius, F. *Angew. Chem., Int. Ed.* **2013**, *52*, 8454.
- (4) For selected reviews on ATH, see: (a) Noyori, R.; Hashiguchi, S. *Acc. Chem. Res.* **1997**, *30*, 97. (b) Palmer, M. J.; Wills, M. *Tetrahedron: Asymmetry* **1999**, *10*, 2045. (c) Everaere, K.; Mortreux, A.; Carpentier, J.-F. *Adv. Synth. Catal.* **2003**, *345*, 67. (d) Gladiali, S.; Alberico, E. *Chem. Soc. Rev.* **2006**, *35*, 226. (e) Samec, J. S. M.; Bäckvall, J.-E.; Andersson, P. G.; Brandt, P. *Chem. Soc. Rev.* **2006**, *35*, 237. (f) Ikariya, T.; Blacker, A. J. *Acc. Chem. Res.* **2007**, *40*, 1300. (g) Blacker, A. J. In *Handbook of Homogeneous Hydrogenation*; de Vries, J. G., Elsevier, C. J., Ed.; Wiley-VCH: Weinheim, 2007; p 1215. (h) Foubelo, F.; Nájera, C.; Yus, M. *Tetrahedron: Asymmetry* **2015**, *26*, 769. (i) Wang, D.; Astruc, D. *Chem. Rev.* **2015**, *115*, 6621. (j) Ayad, T.; Phansavath, P.; Ratovelomanana-Vidal, V. *Chem. Rec.* **2016**, *16*, 2754.
- (5) For a Ru-catalyzed enantioselective synthesis of isoflavanones by DKR, see: Qin, T.; Metz, P. *Org. Lett.* **2017**, *19*, 2981.
- (6) (a) Echeverria, P.-G.; Cornil, J.; Féraud, C.; Guérinot, A.; Cossy, J.; Phansavath, P.; Ratovelomanana-Vidal, V. *RSC Adv.* **2015**, *5*, 56815. (b) Monnereau, L.; Cartigny, D.; Scalone, M.; Ayad, T.; Ratovelomanana-Vidal, V. *Chem. - Eur. J.* **2015**, *21*, 11799. (c) Perez, M.; Echeverria, P.-G.; Martinez-Arripe, E.; Ez Zoubir, M.; Touati, R.; Zhang, Z.; Genet, J.-P.; Phansavath, P.; Ayad, T.; Ratovelomanana-Vidal, V. *Eur. J. Org. Chem.* **2015**, *2015*, 5949. (d) Zheng, L.-S.; Féraud, C.; Phansavath, P.; Ratovelomanana-Vidal, V. *Chem. Commun.* **2018**, *54*, 283. (e) Zheng, L.-S.; Phansavath, P.; Ratovelomanana-Vidal, V. *Org. Chem. Front.* **2018**, *5*, 1366. (f) Zheng, L.-S.; Phansavath, P.; Ratovelomanana-Vidal, V. *Org. Lett.* **2018**, *20*, 5107.
- (7) For selected reviews on DKR, see: (a) Noyori, R.; Tokunaga, M.; Kitamura, M. *Bull. Chem. Soc. Jpn.* **1995**, *68*, 36. (b) Caddick, S.; Jenkins, K. *Chem. Soc. Rev.* **1996**, *25*, 447. (c) Ward, R. S. *Tetrahedron: Asymmetry* **1995**, *6*, 1475. (d) Ratovelomanana-Vidal, V.; Genêt, J.-P. *Can. J. Chem.* **2000**, *78*, 846. (e) Huerta, F. F.; Minidis, A. B. E.; Bäckvall, J.-E. *Chem. Soc. Rev.* **2001**, *30*, 321. (f) Pàmies, O.; Bäckvall, J.-E. *Chem. Rev.* **2003**, *103*, 3247. (g) Pellissier, H. *Tetrahedron* **2003**, *59*,



8291. (h) Pellissier, H. *Tetrahedron* **2008**, *64*, 1563. (i) Pellissier, H. *Tetrahedron* **2011**, *67*, 3769. (j) Hamada, Y. *Chem. Rec.* **2014**, *14*, 235. (k) Foubelo, F.; Nájera, C.; Yus, M. *Tetrahedron: Asymmetry* **2015**, *26*, 769. (l) Echeverria, P.-G.; Ayad, T.; Phansavath, P.; Ratovelomanana-Vidal, V. *Synthesis* **2016**, *48*, 2523.

(8) (a) Haack, K.-J.; Hashiguchi, S.; Fujii, A.; Ikariya, T.; Noyori, R. *Angew. Chem., Int. Ed. Engl.* **1997**, *36*, 285. (b) Matsumura, K.; Hashiguchi, S.; Ikariya, T.; Noyori, R. *J. Am. Chem. Soc.* **1997**, *119*, 8738.

(9) (a) Hannedouche, J.; Clarkson, G. J.; Wills, M. J. *J. Am. Chem. Soc.* **2004**, *126*, 986. (b) Cheung, F. K. K.; Hayes, A. M.; Hannedouche, J.; Yim, A. S. Y.; Wills, M. J. *Org. Chem.* **2005**, *70*, 3188.

(10) Zheng, L.-S.; Llopis, Q.; Echeverria, P.-G.; Férard, C.; Guillamot, G.; Phansavath, P.; Ratovelomanana-Vidal, V. *J. Org. Chem.* **2017**, *82*, 5607.

(11) Echeverria, P.; Férard, C.; Phansavath, P.; Ratovelomanana-Vidal, V. *Catal. Commun.* **2015**, *62*, 95.

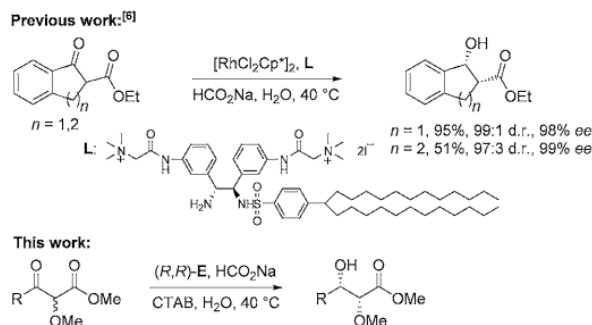
# Rh<sup>III</sup>-Catalyzed Asymmetric Transfer Hydrogenation of $\alpha$ -Methoxy $\beta$ -Ketoesters through DKR in Water: Toward a Greener Procedure

Bin He<sup>+</sup>, Long-Sheng Zheng<sup>+</sup>, Phannarath Phansavath,<sup>\*</sup> and Virginie Ratovelomanana-Vidal<sup>\*,[a]</sup>

The asymmetric reduction of  $\alpha$ -methoxy  $\beta$ -ketoesters through transfer hydrogenation with a new rhodium(III) complex was developed. The reaction was efficient in 2-MeTHF with formic acid/triethylamine or in water with sodium formate. The corresponding *syn*  $\alpha$ -methoxy  $\beta$ -hydroxyesters were obtained with high diastereoselectivities and excellent levels of enantioselectivity through a dynamic kinetic resolution process.

Although numerous methods are available for the enantioselective preparation of 1,2-diol derivatives,<sup>[1]</sup> most of them do not allow differentiation of the two hydroxyl functions, and only few examples of the preparation of monodifferentiated diols have been described.<sup>[2]</sup> A straightforward and atom-economical access to such compounds involves the asymmetric reduction through dynamic kinetic resolution (DKR)<sup>[3]</sup> of racemic  $\alpha$ -alkoxy  $\beta$ -ketoester derivatives. In this context, we have reported in a previous work the asymmetric transfer hydrogenation (ATH)<sup>[4]</sup> of these compounds through DKR to access the corresponding enantiomerically enriched *syn*  $\alpha$ -alkoxy  $\beta$ -hydroxyesters directly<sup>[5]</sup> by using ruthenium complexes in CH<sub>2</sub>Cl<sub>2</sub> and a 5:2 mixture of formic acid/triethylamine as the hydrogen source. In search of a greener approach, we decided to investigate this reaction in more ecofriendly solvents, and water appeared as the solvent of choice for this transformation. As far as rhodium-catalyzed ATH through DKR in water is concerned, to the best of our knowledge, only two examples were previously disclosed (Scheme 1).<sup>[6]</sup>

In these instances, the reaction was performed on bicyclic  $\beta$ -ketoesters with a Rh catalyst formed from a chiral double-chain surfactant-type ligand giving high enantio- and diastereoselectivities but moderate yield for the six-membered  $\beta$ -hydroxyester. Herein we report an environmentally sustainable



Scheme 1. Rhodium-catalyzed ATH/DKR in water.

procedure for the ATH/DKR of  $\alpha$ -alkoxy  $\beta$ -ketoesters in water involving a new rhodium complex (Scheme 1). In line with the 12 principles of green chemistry,<sup>[7]</sup> one key point of our ATH/DKR process was to use an easy-to-handle and air-stable complex that would operate under environmentally sound conditions. As part of our ongoing studies aimed at developing efficient catalysts for the asymmetric reduction of unsaturated compounds, we recently developed a series of tethered rhodium complexes (*R,R*)-A–(*R,R*)-D<sup>[8]</sup> analogous to a complex developed by Wills and co-workers,<sup>[9]</sup> which we chose to evaluate in this study. Additionally, we prepared a new *N*-pentafluorophenylsulfonyl-DPEN-based (DPEN = diphenylethylenediamine) tethered Rh<sup>III</sup> complex (*R,R*)-E (see the Supporting Information; Figures 1 and 2).<sup>[10]</sup>

We first examined the catalytic activity of complexes (*R,R*)-A–(*R,R*)-E in the asymmetric reduction of methyl-2-methoxy-3-

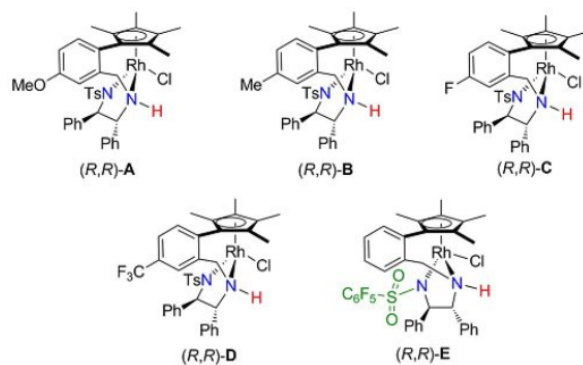


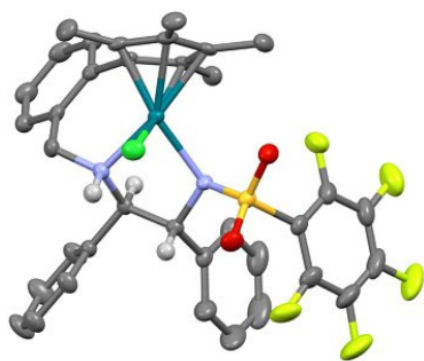
Figure 1. Rhodium complexes used in this study.

[a] B. He,<sup>+</sup> L.-S. Zheng,<sup>+</sup> Dr. P. Phansavath, Dr. V. Ratovelomanana-Vidal  
Chimie ParisTech, CNRS,  
i-CLeHS (Institute of Chemistry for Life & Health Sciences), CSB2D team  
PSL Research University  
75005 Paris (France)  
E-mail: phannarath.phansavath@chimieparistech.psl.eu  
virginie.vidal@chimieparistech.psl.eu

[†] These authors contributed equally to this work.

Supporting Information and the ORCID identification number(s) for the author(s) of this article can be found under:  
<https://doi.org/10.1002/cssc.201900358>.

This publication is part of a Special Issue on "Sustainable Organic Synthesis".  
Please visit the issue at <http://doi.org/10.1002/cssc.v12.13>



**Figure 2.** X-ray crystallographic structure of (*R,R*)-E (hydrogen atoms are omitted for clarity).

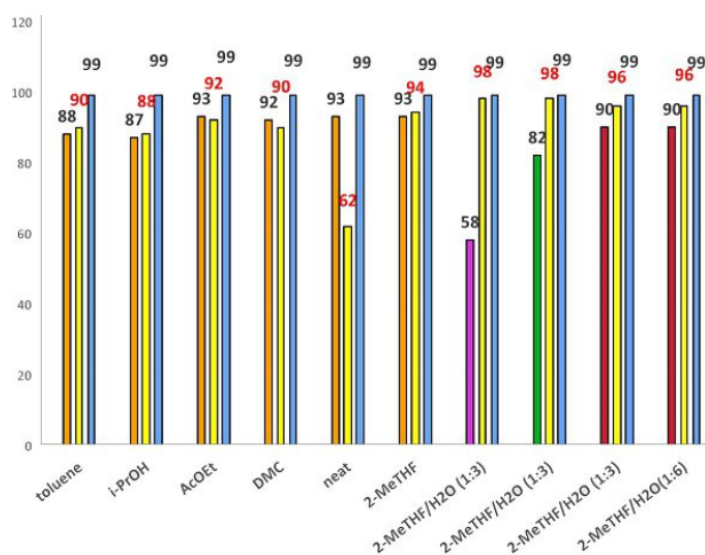
oxo-3-phenylpropanoate (*rac*-1a). The ATH/DKR of *rac*-1a was initially performed in CH<sub>2</sub>Cl<sub>2</sub> at 30 °C with 0.5 mol% of the Rh complexes (*R,R*)-A–(*R,R*)-E and a HCO<sub>2</sub>H/Et<sub>3</sub>N (5:2) azeotropic mixture as the hydrogen source (Table 1). Under these conditions, high yields (89–94%) and diastereoselectivities [88:12 to 93:7 diastereomeric ratio (d.r.)] were observed for the corresponding *syn* α-methoxy β-hydroxyester 2a, which was obtained with an excellent enantioselectivity [99% enantiomeric excess (*ee*)]. If the reaction was performed at 0 °C with complex (*R,R*)-A, a longer reaction time was required, but no improvement was observed in terms of diastereoselectivity (88:12 d.r.; Table 1, entry 2).

Although all tested rhodium complexes (*R,R*)-A–(*R,R*)-E showed comparable results in terms of yields and stereoselection, the newly prepared complex (*R,R*)-E gave the highest yield (94%) and the best level of diastereoselectivity (93:7 d.r.) in favor of the *syn* 1,2-diol 2a (Table 1, entry 6). Therefore, (*R,R*)-E was used for further screening of the reaction parameters, and the influence of greener solvents was next investigated (Figure 3). The results obtained in toluene, *i*PrOH, AcOEt, and dimethyl carbonate (DMC) matched those previously observed in CH<sub>2</sub>Cl<sub>2</sub> in terms of yields but not for the diastereomeric excess (*de*) values, which were higher (88–90 vs. 86% *de* in CH<sub>2</sub>Cl<sub>2</sub>). The neat reaction resulted in high yield and enantiomeric excess but a lower diastereoselectivity (62% *de*). Interestingly, the use of the ecofriendly solvent 2-MeTHF resulted in a high diastereoselectivity (94% *de*), affording a satisfying 93% yield of 2a. Aiming at ever greener procedures, we next sought to perform the reaction in aqueous media and chose to use a 1:3 mixture of 2-MeTHF/H<sub>2</sub>O with sodium formate as the hydrogen source. These conditions did not allow a complete conversion (58% yield), but addition of 0.2 equiv. of CTAB (cetyltrimethylammonium bromide) as a surfactant resulted in 82% yield of 2a. A higher yield of 90% could be reached upon switching the reaction temperature from 30 to 40 °C, whereas increasing the amount of water in the solvent mixture (from 2-MeTHF/H<sub>2</sub>O 1:3 to 1:6) had no significant effect.

**Table 1.** Precatalyst screening.<sup>[a]</sup>

Entry	Cat.	t [h]	Yield <sup>[b]</sup> [%]	d.r. <sup>[c]</sup> ( <i>syn/anti</i> )	<i>ee</i> <sub>syn</sub> <sup>[d]</sup> [%]
1	( <i>R,R</i> )-A	1	91	91:9	99
2 <sup>[e]</sup>	( <i>R,R</i> )-A	22	90	88:12	99
3	( <i>R,R</i> )-B	1	89	91:9	99
4	( <i>R,R</i> )-C	3	89	91:9	99
5	( <i>R,R</i> )-D	3	92	89:11	99
6	( <i>R,R</i> )-E	3	94	93:7	> 99

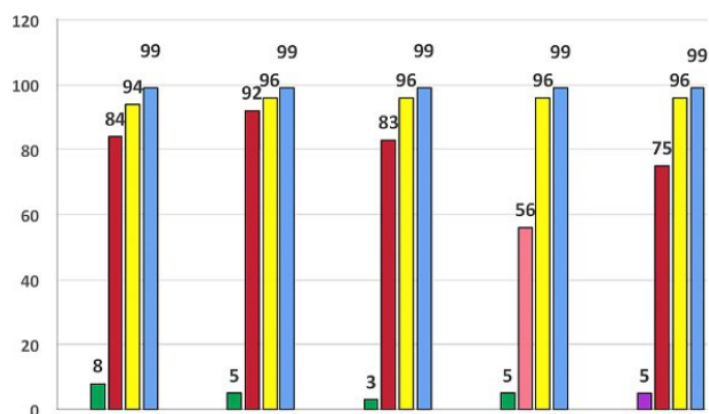
[a] Conditions: 1a (0.8 mmol), [Rh] complex (0.5 mol%), HCO<sub>2</sub>H/Et<sub>3</sub>N (5:2) (134 μL, 2 equiv.), CH<sub>2</sub>Cl<sub>2</sub> (4.0 mL), 30 °C, full conversion. [b] Isolated yields. [c] Determined by <sup>1</sup>H NMR spectroscopy of the crude product after the ATH reaction. [d] Determined by HPLC analysis with a chiral stationary phase. [e] The reaction was performed at 0 °C.



**Figure 3.** Optimization of the reaction conditions for the ATH of 1a with (*R,R*)-E. Reaction conditions: 1a (0.8 mmol), (*R,R*)-E (0.5 mol%), HCO<sub>2</sub>H/Et<sub>3</sub>N 5:2 (2 equiv.) or HCO<sub>2</sub>Na (8 equiv.), solvent (4.0 mL), 30 or 40 °C, 3–40 h. ■, *de* (*syn/anti*) [%]; ■, yield [%] for HCOOH/Et<sub>3</sub>N (2 equiv.), no surfactant, 30 °C; ■, yield [%] for HCOONa (8 equiv.), CTAB (0.2 equiv.), 30 °C; ■, yield [%] for HCOONa (8 equiv.), CTAB (0.2 equiv.), 40 °C; ■, yield [%] for HCOONa (8 equiv.), no surfactant, 30 °C; ■, *ee* [%].

We next performed the reaction in water alone as a solvent under otherwise identical conditions (Figure 4). In that case, a lower yield was obtained (84%); however, we found the amount of sodium formate to be essential for the asymmetric reduction because decreasing the amount to 5 equiv. provided a high yield of 92% whereas the use of 3 equiv. afforded 2a in only 83% yield (Figure 4). It should be noted that lowering the catalyst loading to 0.25 mol% resulted only in longer reaction times with no beneficial impact on the stereoselectivity of the reduction. However, incomplete conversions were observed if sodium dodecyl sulfate (SDS) was used as a surfactant or if ammonium formate acted as the hydrogen source. From these results, 2-MeTHF and water were selected as greener solvents for





**Figure 4.** Optimization of the reaction conditions in water at 40 °C with (R,R)-E. ■: HCOONH<sub>4</sub> [equiv.]; ■: HCOONa [equiv.]; ■: yield [%] with CTAB (0.2 equiv.); ■: de (syn/anti) [%]; ■: ee [%]; ■: yield [%] with SDS (0.2 equiv.).

the remainder of the study, and the optimized reaction conditions were set as follows: **2a**, (R,R)-E (*S/C* = 200), HCO<sub>2</sub>H/Et<sub>3</sub>N = 5:2 (2.0 equiv.), 2-MeTHF, 30 °C; or **2a**, (R,R)-E (*S/C* = 200), HCO<sub>2</sub>Na (5.0 equiv.), H<sub>2</sub>O, CTAB (0.2 equiv.), 40 °C. With these optimized conditions in hand, we then investigated the scope of the Rh-catalyzed ATH/DKR of  $\alpha$ -methoxy  $\beta$ -ketoesters with a series of substituted aryl ketones **1b–1m**. We first studied the asymmetric reduction of substrates **1b–1f** bearing electron-donating substituents on the aromatic ring. Compounds bearing methyl, methoxy, or benzyloxy substituents on the benzene core at the *meta* or *para* positions afforded high levels of diastereoselectivities, from 95:5 to 98:2 d.r., with excellent *ee* values observed in all cases (Table 2, entries 2–6). Substrates **1g–1j** containing electron-withdrawing groups on the benzene ring, such as fluoro, trifluoromethyl, or bromo substituents, were investigated as well and displayed good-to-high yields (68–97%), high levels of diastereocontrol (95:5 to 99:1 d.r.), and excellent enantioselectivities (>99% *ee*; Table 2, entries 7–10). Interestingly, investigation of the heteroaromatic substrates **1k–1l** resulted in almost perfect diastereoselectivities (99:1 to >99:1 d.r.) and excellent enantioselectivities (>99% *ee*; Table 2, entries 11 and 12). To complete the substrate scope, the sterically demanding compound **1m** bearing an *ortho*-substituted phenyl group was submitted to the ATH conditions and delivered the *syn* alcohol in good yield, high diastereoselectivity, and good enantioselectivity in water, whereas the reaction was sluggish in 2-MeTHF and gave a lower yield (Table 2, entry 13). This study showed that constant high levels of stereoselectivity were observed both in water in an open flask and in 2-MeTHF, whereas higher yields were achieved in water in several instances (Table 2, entries 7–10, 12, and 13). It should be noted that the methyl protecting group of compounds **2** could be removed to provide the corresponding *syn*-1,2-diols.<sup>[2a]</sup>

Finally, a scale-up experiment performed on compound **1a** (1.25 g, 6.0 mmol) in water delivered the reduced  $\alpha$ -methoxy  $\beta$ -hydroxyester **2a** in 88% yield and with the same high level

of stereoselectivity as on a 0.6 mmol scale, demonstrating the usefulness of the procedure.

In conclusion, we have prepared a new rhodium catalyst having an electron-deficient diamine ligand carrying a pentafluorobenzenesulfonyl substituent. The new fully characterized Rh complex is not sensitive to water or air, convenient to handle, and was efficiently used for the ATH of  $\alpha$ -methoxy  $\beta$ -ketoesters with either HCO<sub>2</sub>H/Et<sub>3</sub>N (5:2) at a low catalyst loading in an environmentally sound solvent (2-MeTHF) or with HCO<sub>2</sub>Na in water in an open flask. This catalytic atom-economical ATH reaction proceeds in water through a dynamic kinetic resolution process, affording monodifferentiated  $\beta$ -hydroxyester derivatives in high yields (up to 98%) with high levels of diastereoselectivity (up to >99:1 d.r.) and excellent *ee* values (up to >99%).

## Experimental Section

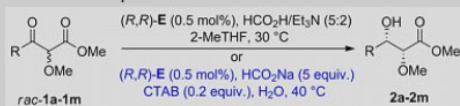
**General procedure for the ATH of 1a–1m in 2-MeTHF:** A round-bottomed tube equipped with a balloon of argon was charged with  $\alpha$ -methoxy  $\beta$ -keto ester **1** (0.8 mmol) and the rhodium complex (R,R)-E (4.0  $\mu$ mol, 0.5 mol%). The solids were subjected to three vacuum/argon cycles before anhydrous 2-MeTHF (4.0 mL) was added. The mixture was stirred at RT for 3–5 min, and the tube was transferred into a 30 °C oil bath before the HCO<sub>2</sub>H/Et<sub>3</sub>N (5:2) azeotropic mixture (134  $\mu$ L, 1.6 mmol, 2.0 equiv.) was added dropwise. After complete consumption of the starting material [monitored by thin layer chromatography (TLC) or <sup>1</sup>H NMR spectroscopy], the reaction mixture was concentrated under vacuum, quenched with sat. NaHCO<sub>3</sub>, and extracted with CH<sub>2</sub>Cl<sub>2</sub>. The combined organic layers were washed with brine, dried (MgSO<sub>4</sub>), filtered, and concentrated under vacuum. The conversion and diastereomeric ratio were determined by <sup>1</sup>H NMR spectroscopic analysis of the crude product. After filtration of the crude product on silica gel, the enantiomeric excess was determined by HPLC analysis (CHIRALPAK IA, IB, IC, or IE column).

**General procedure for the ATH of 1a–1m in water:** A round-bottomed tube was charged with  $\alpha$ -methoxy  $\beta$ -keto ester **1** (0.6 mmol), sodium formate (3.0 mmol), CTAB (0.12 mmol, 20 mol%), the rhodium complex (R,R)-E (3.0  $\mu$ mol, 0.5 mol%), and water (1.5 mL), and the mixture was stirred at 40 °C. After complete consumption of the starting material (monitored by TLC), the reaction mixture was extracted with 2-MeTHF, and the combined organic layers were washed with brine, dried (MgSO<sub>4</sub>), filtered, and concentrated under vacuum. The conversion and diastereomeric ratio were determined by <sup>1</sup>H NMR spectroscopic analysis of the crude product. After filtration of the crude product on silica gel, the enantiomeric excess was determined by HPLC analysis (CHIRALPAK IA, IB, IC, or IE column).

## Acknowledgements

This work was supported by the Ministère de l'Éducation Nationale, de l'Enseignement Supérieur et de la Recherche (MENESR) and the Centre National de la Recherche Scientifique (CNRS). We acknowledge the China Scholarship Council (CSC) for a grant to B.H. and L.-S.Z.. We thank C. Féraud for technical assistance. We

Table 2. Substrate scope.



Entry	ATH product <sup>[a,b]</sup>	t [h]	Yield <sup>[c]</sup> [%]	d.r. <sup>[d]</sup> (syn/anti)	ee <sub>syn</sub> <sup>[e]</sup> [%]
1		5 <sup>[a]</sup> 4 <sup>[b]</sup>	93 <sup>[a]</sup> 92 <sup>[b]</sup>	97:3 <sup>[a]</sup> 98:2 <sup>[b]</sup>	99 <sup>[a]</sup> > 99 <sup>[b]</sup>
2		7 <sup>[a]</sup> 6 <sup>[b]</sup>	80 <sup>[a]</sup> 84 <sup>[b]</sup>	97:3 <sup>[a]</sup> 97:3 <sup>[b]</sup>	> 99 <sup>[a]</sup> > 99 <sup>[b]</sup>
3		8 <sup>[a]</sup> 6 <sup>[b]</sup>	80 <sup>[a]</sup> 83 <sup>[b]</sup>	96:4 <sup>[a]</sup> 97:3 <sup>[b]</sup>	> 99 <sup>[a]</sup> > 99 <sup>[b]</sup>
4		45 <sup>[a]</sup> 6 <sup>[b]</sup>	82 <sup>[a]</sup> 85 <sup>[b]</sup>	96:4 <sup>[a]</sup> 96:4 <sup>[b]</sup>	> 99 <sup>[a]</sup> > 99 <sup>[b]</sup>
5		8 <sup>[a]</sup> 24 <sup>[b]</sup>	92 <sup>[a]</sup> 93 <sup>[b]</sup>	97:3 <sup>[a]</sup> 98:2 <sup>[b]</sup>	> 99 <sup>[a]</sup> > 99 <sup>[b]</sup>
6		14 <sup>[a]</sup> 24 <sup>[b]</sup>	83 <sup>[a]</sup> 80 <sup>[b]</sup>	95:5 <sup>[a]</sup> 96:4 <sup>[b]</sup>	99 <sup>[a]</sup> > 99 <sup>[b]</sup>
7		7 <sup>[a]</sup> 6 <sup>[b]</sup>	68 <sup>[a]</sup> 73 <sup>[b]</sup>	98:2 <sup>[a]</sup> 98:2 <sup>[b]</sup>	> 99 <sup>[a]</sup> > 99 <sup>[b]</sup>
8		8 <sup>[a]</sup> 24 <sup>[b]</sup>	80 <sup>[a]</sup> 89 <sup>[b]</sup>	97:3 <sup>[a]</sup> 95:5 <sup>[b]</sup>	> 99 <sup>[a]</sup> > 99 <sup>[b]</sup>
9		22 <sup>[a]</sup> 4 <sup>[b]</sup>	82 <sup>[a]</sup> 97 <sup>[b]</sup>	97:3 <sup>[a]</sup> 96:4 <sup>[b]</sup>	> 99 <sup>[a]</sup> > 99 <sup>[b]</sup>
10		8 <sup>[a]</sup> 4 <sup>[b]</sup>	68 <sup>[a]</sup> 92 <sup>[b]</sup>	99:1 <sup>[a]</sup> 96:4 <sup>[b]</sup>	> 99 <sup>[a]</sup> > 99 <sup>[b]</sup>
11		14 <sup>[a]</sup> 6 <sup>[b]</sup>	91 <sup>[a]</sup> 88 <sup>[b]</sup>	> 99:1 <sup>[a]</sup> > 99:1 <sup>[b]</sup>	> 99 <sup>[a]</sup> > 99 <sup>[b]</sup>
12		10 <sup>[a]</sup> 4 <sup>[b]</sup>	86 <sup>[a]</sup> 98 <sup>[b]</sup>	99:1 <sup>[a]</sup> > 99:1 <sup>[b]</sup>	> 99 <sup>[a]</sup> > 99 <sup>[b]</sup>
13		111 <sup>[a]</sup> 5 <sup>[b]</sup>	67 <sup>[a]</sup> 81 <sup>[b]</sup>	96:4 <sup>[a]</sup> 98:2 <sup>[b]</sup>	88 <sup>[a]</sup> 88 <sup>[b]</sup>

[a] Conditions A: **1** (0.8 mmol), (R,R)-E (0.5 mol%), HCO<sub>2</sub>H/Et<sub>3</sub>N (5:2, 134 μL, 2 equiv.), 2-MeTHF (4.0 mL), 30 °C, full conversion. [b] Conditions B: **1** (0.6 mmol), (R,R)-E (0.5 mol%), HCO<sub>2</sub>Na (5.0 equiv.), H<sub>2</sub>O (1.5 mL), CTAB (0.2 equiv.), 40 °C, full conversion. [c] Isolated yields. [d] Determined by <sup>1</sup>H NMR spectroscopy of the crude product after the ATH reaction. [e] Determined by HPLC analysis with a chiral stationary phase.

are grateful to G. Gontard for the X-ray analysis (Sorbonne Université, Paris), to M.-N. Rager for the NMR analysis (Chimie ParisTech, Paris) and to C. Fosse for the mass spectrometry analysis (Chimie ParisTech, Paris).

## Conflict of interest

The authors declare no conflict of interest.

**Keywords:** asymmetric catalysis • hydrogen transfer • reduction • rhodium • water

- [1] a) H. C. Kolb, M. S. VanNieuwenhze, K. B. Sharpless, *Chem. Rev.* **1994**, *94*, 2483; b) Y. Shi, *Acc. Chem. Res.* **2004**, *37*, 488; c) T. Ikariya, K. Murata, R. Noyori, *Org. Biomol. Chem.* **2006**, *4*, 393; d) G. Guillena, C. Nájera, D. Ramón, *Tetrahedron: Asymmetry* **2007**, *18*, 2249; e) F. Tanaka, C. F. Barbas III in *Enantioselective Organocatalysis, Reaction and Experimental Procedures* (Ed.: P. I. Dalko), Wiley-VCH, Weinheim, **2007**, pp. 19–55; f) P. Jiao, M. Kawasaki, H. Yamamoto, *Angew. Chem. Int. Ed.* **2009**, *48*, 3333; *Angew. Chem.* **2009**, *121*, 3383.
- [2] a) R. Noyori, M. Tokunaga, W.-J. Chung, *Angew. Chem. Int. Ed.* **2008**, *47*, 1890; *Angew. Chem.* **2008**, *120*, 1916; b) S. E. Denmark, W.-J. Chung, *J. Org. Chem.* **2008**, *73*, 4582; c) S. M. Lim, N. Hill, A. G. Myers, *J. Am. Chem. Soc.* **2009**, *131*, 5763; d) K. M. Steward, J. S. Johnson, *Org. Lett.* **2010**, *12*, 2864; e) S.-M. Son, H.-K. Lee, *J. Org. Chem.* **2013**, *78*, 8396; f) S.-M. Son, H.-K. Lee, *J. Org. Chem.* **2014**, *79*, 2666; g) N. Alnafta, J. P. Schmidt, C. L. Nesbitt, C. S. P. McElean, *Org. Lett.* **2016**, *18*, 6520; h) L. Fang, S. Liu, L. Han, H. Li, F. Zhao, *Organometallics* **2017**, *36*, 1217.
- [3] a) R. Noyori, M. Tokunaga, M. Kitamura, *Bull. Chem. Soc. Jpn.* **1995**, *68*, 36; b) S. Caddick, K. Jenkins, *Chem. Soc. Rev.* **1996**, *25*, 447; c) R. S. Ward, *Tetrahedron: Asymmetry* **1995**, *6*, 1475; d) R. Stürmer, *Angew. Chem. Int. Ed. Engl.* **1997**, *36*, 1173; *Angew. Chem.* **1997**, *109*, 1221; e) M. T. El Ghiani, J. M. J. Williams, *Curr. Opin. Chem. Biol.* **1999**, *3*, 11; f) V. Ratovelomanana-Vidal, J.-P. Genêt, *Can. J. Chem.* **2000**, *78*, 846; g) F. F. Huerta, A. B. E. Minidis, J.-E. Bäckvall, *Chem. Soc. Rev.* **2001**, *30*, 321; h) K. Faber, *Chem. Eur. J.* **2001**, *7*, 5004; i) O. Pàmies, J.-E. Bäckvall, *Chem. Rev.* **2003**, *103*, 3247; j) H. Pellissier, *Tetrahedron* **2003**, *59*, 8291; k) N. J. Turner, *Curr. Opin. Chem. Biol.* **2004**, *8*, 114; l) E. Vedejs, M. Jure, *Angew. Chem. Int. Ed.* **2005**, *44*, 3974; *Angew. Chem.* **2005**, *117*, 4040; m) B. Martín-Matute, J.-E. Bäckvall, *Curr. Opin. Chem. Biol.* **2007**, *11*, 226; n) H. Pellissier, *Tetrahedron* **2008**, *64*, 1563; o) H. Pellissier, *Tetrahedron* **2011**, *67*, 3769; p) P.-G. Echeverria, T. Ayad, P. Phansavath, V. Ratovelomanana-Vidal, *Synthesis* **2016**, *48*, 2523.
- [4] a) G. Zassinovich, G. Mestroni, S. Gladiali, *Chem. Rev.* **1992**, *92*, 1051; b) C. F. de Graauw, J. A. Peters, H. van Bekkum, J. Huskens, *Synthesis* **1994**, 1007; c) R. Noyori, S. Hashiguchi, *Acc. Chem. Res.* **1997**, *30*, 97; d) M. J. Palmer, M. Wills, *Tetrahedron: Asymmetry* **1999**, *10*, 2045; e) O. Pàmies, J.-E. Bäckvall, *Chem. Eur. J.* **2001**, *7*, 5052; f) K. Everaere, A. Mor-treux, J.-F. Carpentier, *Adv. Synth. Catal.* **2003**, *345*, 67; g) S. Gladiali, E. Alberico, *Chem. Soc. Rev.* **2006**, *35*, 226; h) J. S. M. Samec, J.-E. Bäckvall, P. G. Andersson, P. Brandt, *Chem. Soc. Rev.* **2006**, *35*, 237; i) T. Ikariya, A. J. Blacker, *Acc. Chem. Res.* **2007**, *40*, 1300; j) A. J. Blacker in *Handbook of Homogeneous Hydrogenation* (Eds.: J. G. de Vries, C. J. Elsevier), Wiley-VCH, Weinheim, **2007**, pp. 1215–1244; k) C. Wang, X. Wu, J. Xiao, *Chem. Asian J.* **2008**, *3*, 1750; l) T. Ikariya, *Bull. Chem. Soc. Jpn.* **2011**, *84*, 1; m) A. Bartoszewicz, N. Ahlsten, B. Martín-Matute, *Chem. Eur. J.* **2013**, *19*, 7274; n) T. Slagbrand, H. Lundberg, H. Adolfsson, *Chem. Eur. J.* **2014**, *20*, 16102; o) B. Štefane, F. Požgan, *Catal. Rev.* **2014**, *56*, 82; p) D. Wang, D. Astruc, *Chem. Rev.* **2015**, *115*, 6621; q) F. Foubelo, C. Nájera, M. Yus, *Tetrahedron: Asymmetry* **2015**, *26*, 769; r) T. Ayad, P. Phansavath, V. Ratovelomanana-Vidal, *Chem. Rec.* **2016**, *16*, 2754; s) A. Matsunami, Y. Kayaki, *Tetrahedron Lett.* **2018**, *59*, 504.
- [5] a) D. Cartigny, K. Püntener, T. Ayad, M. Scalone, V. Ratovelomanana-Vidal, *Org. Lett.* **2010**, *12*, 3788; b) L. Monnerau, D. Cartigny, M. Scalone, T. Ayad, V. Ratovelomanana-Vidal, *Chem. Eur. J.* **2015**, *21*, 11799.
- [6] J. Li, Z. Lin, Q. Huang, Q. Wang, L. Tang, J. Zhu, J. Deng, *Green Chem.* **2017**, *19*, 5367.
- [7] a) M. E. Eissen, J. O. Metzger, E. Schmidt, U. Schneidewind, *Angew. Chem. Int. Ed.* **2002**, *41*, 414; *Angew. Chem.* **2002**, *114*, 402; b) P. T. Anastas, J. C. Warner, *Green Chemistry: Theory and Practice*, Oxford University Press, New York, **1998**, p. 15.

- [8] a) P.-G. Echeverría, C. Féraud, P. Phansavath, V. Ratovelomanana-Vidal, *Catal. Commun.* **2015**, *62*, 95; b) L.-S. Zheng, Q. Llopis, P.-G. Echeverría, C. Féraud, G. Guillamot, P. Phansavath, V. Ratovelomanana-Vidal, *J. Org. Chem.* **2017**, *82*, 5607; c) L.-S. Zheng, C. Féraud, P. Phansavath, V. Ratovelomanana-Vidal, *Chem. Commun.* **2018**, *54*, 283.
- [9] D. S. Matharu, D. J. Morris, A. M. Kawamoto, G. J. Clarkson, M. Wills, *Org. Lett.* **2005**, *7*, 5489.
- [10] CCDC 1894366 contains the supplementary crystallographic data for this paper. These data can be obtained free of charge from The Cambridge Crystallographic Data Centre.

---

Manuscript received: February 5, 2019  
Revised manuscript received: March 15, 2019  
Accepted manuscript online: March 18, 2019  
Version of record online: April 18, 2019







## RÉSUMÉ

---

Ce manuscrit présente le développement de méthodes catalytiques efficaces pour accéder à des alcools fonctionnalisés énantioenrichis tels que des alpha-méthoxy beta-hydroxyesters et des hétérocycles fonctionnalisés chiraux, en utilisant des réactions de transfert d'hydrogène asymétrique (ATH) catalysées par le Rh, combinées à un processus de dédoublement cinétique dynamique (DKR). Les dérivés de la 4-quinolone ont été réduits en 1,2,3,4-tétrahydroquinoline-4-ols correspondants avec d'excellentes énantiosélectivités via une réaction de transfert d'hydrogène asymétrique catalysée par un complexe de rhodium en présence d'un mélange azéotropique HCO<sub>2</sub>H/Et<sub>3</sub>N (5:2) comme source d'hydrogène. Le complexe de Rh développé au laboratoire a également été utilisé avec succès pour le transfert d'hydrogène asymétrique de dérivés de 2-aryl tétrahydro-4-quinolones par dédoublement cinétique. Le même complexe de rhodium a également permis la synthèse des dérivés de cis-3-(hydroxyméthyl)-chroman-4-ol énantioenrichis. Les composés ciblés ont été préparés par transfert d'hydrogène asymétrique catalysé au rhodium de 3-formylchromones par un processus de dédoublement cinétique dynamique. La réaction s'effectue dans des conditions douces en utilisant un faible taux catalytique et le mélange azéotropique HCO<sub>2</sub>H/Et<sub>3</sub>N (5:2) comme source d'hydrogène, ce qui a permis d'obtenir les composés réduits avec de bons rendements, des rapports diastéromériques élevés (jusqu'à 98:2 dr) et d'excellentes énantiosélectivités (jusqu'à >99% ee). Enfin, un nouveau complexe Rh(III)/Cp\* contenant un ligand pentafluorobenzènesulfonyl-DPEN a été évalué dans la réaction de transfert d'hydrogène asymétrique des alpha-méthoxy beta-cétoesters. La réaction est conduite dans solvants plus « verts » aussi bien dans le 2-MeTHF en présence du mélange acide formique/triéthylamine que dans de l'eau en utilisant du formiate de sodium et tolère une grande variété de substrats. Les syn alpha-méthoxy beta-hydroxyesters correspondants ont été obtenus avec des diastéroselectivités élevées (jusqu'à >99:1 rd) et d'excellentes énantiosélectivités (jusqu'à >99:1 re) via un processus de dédoublement cinétique dynamique. Dans tous les cas, le complexe de rhodium développé au laboratoire a montré des propriétés catalytiques performantes aussi bien pour la synthèse d'hétérocycles chiraux azotés et oxygénés que pour accéder à des beta-hydroxy esters alpha-substitués hautement fonctionnalisés avec d'excellentes stéréosélectivités.

## MOTS CLÉS

---

catalyse asymétrique, transfert d'hydrogène, synthèse multi-étapes, dédoublement cinétique dynamique, métaux de transition, hétérocycles

## ABSTRACT

---

This manuscript presents the development of catalytic efficient methods to access enantioenriched functionalized alcohols such as alpha-methoxy beta-hydroxyesters and chiral functionalized heterocycles, using Rh-catalyzed asymmetric transfer hydrogenation (ATH) reactions combined with a dynamic kinetic resolution (DKR) process. 4-Quinolone derivatives were conveniently reduced to the corresponding 1,2,3,4-tetrahydroquinoline-4-ols with excellent enantioselectivities through Rh-catalyzed asymmetric transfer hydrogenation with HCO<sub>2</sub>H/Et<sub>3</sub>N (5:2) as the hydrogen source. The home-made Rh complex was also successfully used in the asymmetric transfer hydrogenation of 2-aryl tetrahydro-4-quinolone derivatives through kinetic resolution. Moreover, The Rh-catalyst was successfully utilized to provide enantioenriched cis-3-(hydroxymethyl)-chroman-4-ol derivatives. The target compounds were prepared by asymmetric transfer hydrogenation of 3-formylchromones through a dynamic kinetic resolution process. The reaction proceeded under mild conditions using a low catalyst loading and HCO<sub>2</sub>H/Et<sub>3</sub>N (5:2) as the hydrogen source, delivering the reduced compounds in good yields, high diastereomeric ratios (up to 98:2 dr), and excellent enantioselectivities (up to >99% ee). Finally, a new tethered Rh(III)/Cp\* complex containing a pentafluorobenzenesulfonyl-DPEN ligand was evaluated in the asymmetric transfer hydrogenation of alpha-methoxy beta-ketoesters. The reaction was efficiently carried out under sustainable reaction conditions in 2-MeTHF with formic acid/triethylamine or in water with sodium formate and accommodated a range of substrates. The corresponding syn alpha-methoxy beta-hydroxyesters were obtained with high diastereoselectivities (up to >99:1 dr) and excellent enantioinductions (up to >99:1 er) via a dynamic kinetic resolution process. In all cases, the rhodium complex developed in the laboratory has demonstrated efficient catalytic properties for the synthesis of chiral nitrogen- and oxygen containing heterocycles and to access highly functionalized alpha-substituted beta-hydroxy esters as well with excellent stereoselectivities.

## KEYWORDS

---

asymmetric catalysis, transfer hydrogenation, multi-step synthesis, dynamic kinetic resolution, transition metals, heterocycles